

DETAILED AND SIMPLIFIED CHEMICAL KINETICS  
OF AVIATION FUELS AND SURROGATES

VALENTINI MARKAKI  
DIPL.CHEM., MSc

THESIS SUBMITTED FOR  
THE DEGREE OF DOCTOR OF PHILOSOPHY  
AND FOR THE  
DIPLOMA OF MEMBERSHIP OF THE IMPERIAL COLLEGE LONDON

MECHANICAL ENGINEERING DEPARTMENT  
IMPERIAL COLLEGE LONDON

SEPTEMBER 2009



*Στον Αλέξανδρο*



## Abstract

The chemistries of aviation fuels are invariably complex due to large hydrocarbon molecules. There are also large variations for a given fuel type. Furthermore, flow timescales encountered in high performance propulsion devices increasingly lead to difficulties associated with kinetically controlled or influenced phenomena such as flame stability, extinction and re-light. Current indications also suggest that fuel sources will become significantly more diverse in the future and may, for example, encompass Fischer-Tropsch and/or bio-derived components. The combustion properties of such fuels can vary significantly from those in current use and this work outlines a route towards surrogate fuel mechanisms of sufficient accuracy and generality to support the development of practical devices.

A reaction class based route to the derivation of detailed chemical kinetic mechanisms for alkyl-substituted aromatics is outlined and applied to the cyclopentadiene/indene, benzene/naphthalene, toluene/1-methyl naphthalene systems. Work has also been extended to the *n*-propyl benzene system as well. These reaction classes were applied to model the oxidation of the above fuels with encouraging results. Important reaction channels during oxidation were identified and specifically, the methyl groups on aromatic rings have been identified as important in the context of radical scavenging. Furthermore, 1-methyl naphthalene may also be used to modulate sooting tendencies in aviation and Diesel surrogates. Results obtained from chemical kinetic modelling of cyclopentadiene, toluene, *n*-propyl benzene, naphthalene and 1-methyl naphthalene oxidation in shock tubes, jet-stirred and plug-flow reactors at various sets of representative stoichiometries and temperatures are reported.



## **Acknowledgements**

First of all, I would like to thank my supervisor, Professor R. P. Lindstedt for his guidance and support through this four-year period, which made it possible to complete this work.

I am grateful to the Air Force Office of Scientific Research (AFOSR) for providing the financial support for this work. I would also like to express my gratitude for the financial support provided by the Flame SOFC and the European Office of Aerospace Research and Development (EOARD). In particular, the interest of Dr. J. Tishkoff and Dr. S. Surampudi is gratefully acknowledged.

I would like to thank Dr. R. K. Robinson who provided many of the thermochemical data and reaction rates that were utilised in this work. Many thanks to Ms Serena Dalrymple for her continuous support. Special thanks to Drs. F. Cerru, H.C Ozarovsky, K. Gkagkas and Miss K. Vogiatzaki for the great time we had together.

I will always be thankful to my parents and family who have always been there for me and supported me during my studies. Finally, thank you Alexandros for being there for me and for your continuous support and encouragement throughout the good and difficult times. You are an inspiration to me!





# Contents

LIST OF FIGURES	12
LIST OF TABLES	23
NOMENCLATURE	24
<b>CHAPTER 1</b>	<b>26</b>
INTRODUCTION	26
1.1 <i>Background</i>	26
1.2 <i>Types and Chemistries of Aviation Fuels</i>	29
1.3 <i>Mechanism Construction and Status</i>	31
1.4 <i>Mathematical Description of Reactors</i>	32
1.4.1 <i>Spatially Homogeneous Reactors</i>	33
1.5 <i>Present Contribution</i>	38
1.6 <i>Thesis Outline</i>	39
<b>CHAPTER 2</b>	<b>41</b>
CHEMICAL KINETICS	41
2.1 <i>Rate Laws and Orders of Reactions</i>	41
2.2 <i>Temperature Dependence of Rate Constants</i>	43
2.3 <i>Pressure Dependence of Rate Constants</i>	44
2.4 <i>Thermodynamics and Reaction Kinetics</i>	45
2.5 <i>Radical Reactions</i>	46
2.6 <i>Collision Theory</i>	47
<b>CHAPTER 3</b>	<b>49</b>
CYCLOPENTADIENE	49
3.1 <i>Introduction</i>	49
3.2 <i>Modelling Approach</i>	54
3.3 <i>Oxidation of Cyclopentadiene</i>	59
3.4 <i>Reaction Rate Analysis for Cyclopentadiene Oxidation</i>	63
3.5 <i>Pyrolysis of Cyclopentadiene</i>	70
3.6 <i>Reaction Rate Analysis for Cyclopentadiene Pyrolysis</i>	77
3.7 <i>Conclusions</i>	80

<b>CHAPTER 4</b>	84
TOLUENE	84
4.1 <i>Introduction</i>	84
4.2 <i>Modelling Approach and Mechanism Updates</i>	88
4.3 <i>Thermal Decomposition</i>	91
4.4 <i>Time Resolved OH Concentrations during Oxidation</i>	94
4.5 <i>Ignition Delay Times</i>	98
4.6 <i>Thermal Decomposition Paths</i>	101
4.7 <i>Oxidation Paths</i>	105
4.8 <i>Conclusions</i>	108
<b>CHAPTER 5</b>	110
N-PROPYL BENZENE	110
5.1 <i>Introduction</i>	110
5.2 <i>Modelling Approach</i>	113
5.3 <i>Oxidation at Atmospheric Pressure</i>	114
5.4 <i>Rate Analysis for Fuel Oxidation at Atmospheric Pressure</i>	120
5.5 <i>Oxidation at High Pressures</i>	125
5.6 <i>Rate Analysis for Fuel Oxidations at High Pressures</i>	132
5.7 <i>N-Propyl benzene Ignition Delay Times</i>	137
5.8 <i>Rate Analysis for Auto-ignition of N-Propyl benzene</i>	139
5.9 <i>Conclusions</i>	142
<b>CHAPTER 6</b>	144
NAPHTHALENE	144
6.1 <i>Introduction</i>	144
6.2 <i>Modelling Approach</i>	145
6.3 <i>Oxidation of Naphthalene and Reaction Analysis</i>	146
6.4 <i>Conclusions</i>	152
<b>CHAPTER 7</b>	153
1-METHYL NAPHTHALENE	153
7.1 <i>Introduction</i>	153
7.2 <i>Modelling Approach</i>	154
7.3 <i>Oxidation in Jet-Stirred Reactors</i>	154
7.4 <i>Fuel Lean Mixtures</i>	162
7.5 <i>Fuel Rich Mixtures</i>	169
7.6 <i>Oxidation in Turbulent Flow Reactors</i>	172
7.7 <i>Further Analysis of Reaction Paths</i>	179
7.8 <i>Conclusions</i>	184

<b>CHAPTER 8</b>	185
CONCLUSIONS AND FUTURE WORK	185
8.1 <i>Conclusions</i>	185
8.2 <i>Suggestions for Future Work</i>	188
REFERENCES	190
APPENDIX A	215
<i>Reaction Mechanisms</i>	215
APPENDIX B	267
<i>Thermodynamic Properties</i>	267

## List of Figures

- Figure 1.1 Chemical composition of typical aviation fuels [8] 28
- Figure 1.2 Chromatogram of a fuel sample. a) naphthalene, b) methyl naphthalene, c) ethyl naphthalenes, d) C<sub>3</sub>-naphthalenes, e) diphenylamine, f) C<sub>4</sub>-naphthalenes, g) phenanthrene, h) anthracene, i) methyl anthracene [9] 30
- Figure 1.3 Hierarchical construction of a detailed chemical mechanism for jet fuels 31
- Figure 1.4 The Princeton turbulent flow reactor [23] 35
- Figure 1.5 Single pulse shock tube wave diagram and pressure trace. Shock waves are discontinuities through the gas. The contact surface separates the driver and the shocked gas. The image is adopted from Tsand and Lifshitz [29]. 36
- Figure 1.6 Jet stirred reactor. Image adopted from Dagaut *et al.* [32] A, external tube; B, convergent cone; C, injectors; D, spherical quartz reactor; E, divergent cone; F, sampling sonic probe and thermocouple probe; G, capillary surrounded by the preheating resistor [32]. 38
- Figure 3.1 Arrhenius plot of the reaction rates proposed for the reaction  $C_5H_6 = C_5H_5 + H$ . The solid line indicates the rate determination of Zhong and Bozzelli [51], the dashed line indicates the rate determination of Roy *et al.* [48] and the dashed dotted line indicates the rate determination of Colket *et al.* [49] 50
- Figure 3.2 Arrhenius plot of the reaction rates of the critical pathway  $C_5H_5 + HO_2 = C_5H_5O + OH$ . The solid line indicates the rate used here which was derived using RRKM/ME theory [15] and the dotted line indicates the previously used rate adopted from Zhong and Bozzelli [51]. Units are kmol, m<sup>3</sup>, s, K. 57
- Figure 3.3 Arrhenius plot of the reaction rates of the critical pathway  $C_5H_5 + HO_2 = C_5H_4O + H_2O$ . The solid line indicates the rate used here which was derived using RRKM/ME theory [15] and the dotted line indicates the previously used rate adopted from Zhong and Bozzelli [51]. Units are kmol, m<sup>3</sup>, s, K. 58

- Figure 3.4 Concentration profiles during cyclopentadiene oxidation in a plug flow reactor for  $\Phi = 1.03$ ,  $P = 1$  atm,  $T = 1198$  K, initial fuel concentration 2243 ppm (Case 1 – see Table 3.1). Circles are measurements [20] and the solid line the current simulation 60
- Figure 3.5 Concentration profiles during cyclopentadiene oxidation in a plug flow reactor for  $\Phi = 1.03$ ,  $P = 1$  atm,  $T = 1198$  K, initial fuel concentration 2243 ppm (Case 1 – see Table 3.1). Circles are measurements [20] and the solid line the current simulation 60
- Figure 3.6 Concentration profiles during cyclopentadiene oxidation in a plug flow reactor for  $\Phi = 1.03$ ,  $P = 1$  atm,  $T = 1148$  K, initial fuel concentration 1050 ppm (Case 2 – see Table 3.1). Circles are measurements [20] and the solid line the current simulation 61
- Figure 3.7 Concentration profiles during cyclopentadiene oxidation in a plug flow reactor for  $\Phi = 1.03$ ,  $P = 1$  atm,  $T = 1148$  K, initial fuel concentration 1050 ppm (Case 2 – see Table 3.1). Circles are measurements [20] and the solid line the current simulation 61
- Figure 3.8 Concentration profiles during cyclopentadiene oxidation in a plug flow reactor for  $\Phi = 1.61$ ,  $P = 1$  atm,  $T = 1153$  K, initial fuel concentration 2070 ppm (Case 3 – see Table 3.1). Circles are measurements [20] and the solid line the current simulation 62
- Figure 3.9 Concentration profiles during cyclopentadiene oxidation in a plug flow reactor for  $\Phi = 1.61$ ,  $P = 1$  atm,  $T = 1153$  K, initial fuel concentration 2070 ppm (Case 3 – see Table 3.1). Circles are measurements [20] and the solid line the current simulation 62
- Figure 3.10 Major cyclopentadiene consumption pathways in a plug flow reactor for  $\Phi = 1.03$ ,  $T = 1148$  K, initial fuel concentration of 1051 ppm. 64
- Figure 3.11 Major indene formation channels in a turbulent flow reactor for  $\Phi = 1.03$ ,  $P = 1$  atm,  $T = 1148$  K and cyclopentadiene concentration of 1051 ppm. 67
- Figure 3.12 Concentration profiles during cyclopentadiene pyrolysis in a plug flow reactor at  $P = 1$  atm,  $T = 1147$  K, initial fuel concentration 2083 ppm (Case 1 – see Table 3.2). Circles are measurements [20] and the solid line the current simulation 72

- Figure 3.13 Concentration profiles during cyclopentadiene pyrolysis in a plug flow reactor at  $P = 1$  atm,  $T = 1147$  K, initial fuel concentration 2083 ppm (Case 1 – see Table 3.2). Circles are measurements [20] and the solid line the current simulation 72
- Figure 3.14 Concentration profiles during cyclopentadiene pyrolysis in a plug flow reactor at  $P = 1$  atm,  $T = 1148$  K, initial fuel concentration 1044 ppm (Case 2 – see Table 3.2). Circles are measurements [20] and the solid line the current simulation 73
- Figure 3.15 Concentration profiles during cyclopentadiene pyrolysis in a plug flow reactor at  $P = 1$  atm,  $T = 1148$  K, initial fuel concentration 1044 ppm (Case 2 – see Table 3.2). Circles are measurements [20] and the solid line the current simulation 73
- Figure 3.16 Concentration profiles during cyclopentadiene pyrolysis in a plug flow reactor at  $P = 1$  atm,  $T = 1147$  K, initial fuel concentration 3081 ppm (Case 3 – see Table 3.2). Circles are measurements [20] and the solid line the current simulation 74
- Figure 3.17 Concentration profiles during cyclopentadiene pyrolysis in a plug flow reactor at  $P = 1$  atm,  $T = 1147$  K, initial fuel concentration 3081 ppm (Case 3 – see Table 3.2). Circles are measurements [20] and the solid line the current simulation 74
- Figure 3.18 Concentration profiles during cyclopentadiene pyrolysis in a plug flow reactor at  $P = 1$  atm,  $T = 1106$  K, initial fuel concentration 2094 ppm (Case 4 – see Table 3.2). Circles are measurements [20] and the solid line the current simulation 75
- Figure 3.19 Concentration profiles during cyclopentadiene pyrolysis in a plug flow reactor at  $P = 1$  atm,  $T = 1202$  K, initial fuel concentration 2077 ppm (Case 5 – see Table 3.2). Circles are measurements [20] and the solid line the current simulation 76
- Figure 3.20 Concentration profiles during cyclopentadiene pyrolysis a plug flow reactor at  $P = 1$  atm,  $T = 1202$  K, initial fuel concentration 2077 ppm (Case 5 – see Table 3.2). Circles are measurements [20] and the solid line the current simulation 76
- Figure 4.1 Schematic representation of electronic states of the two benzoperoxy radicals. 90

- Figure 4.2 Hydrogen radical concentration against time for toluene thermal decomposition with an initial fuel concentration of 2.0 ppm,  $T = 1515$  K and  $P = 1.85$  bar. The solid line indicates the current computations and the circles indicate the experimental data from Braun-Unkhoff *et al.* [27]. 92
- Figure 4.3 Hydrogen radical concentration against time for toluene thermal decomposition with an initial fuel concentration of 2.8 ppm,  $T = 1655$  K and  $P = 1.89$  bar. The solid line indicates the current computations and the circles indicate the experimental data from Braun-Unkhoff *et al.* [27]. 93
- Figure 4.4 Hydrogen radical concentration against time for toluene thermal decomposition with an initial fuel concentration of 3.0 ppm,  $T = 1585$  K and  $P = 1.93$  bar. The solid line indicates the current computations and the circles indicate the experimental data from Braun-Unkhoff *et al.* [27]. 93
- Figure 4.5 Hydrogen radical concentration against time for toluene thermal decomposition with an initial fuel concentration of 19.3 ppm,  $T = 1555$  K and  $P = 1.92$  bar. The solid line indicates the current computations and the circles indicate the experimental data from Braun-Unkhoff *et al.* [27]. 94
- Figure 4.6 Time resolved OH radical concentrations obtained in Toluene/Oxygen/Argon mixtures in a shock tube with  $\Phi = 1$  (0.1% toluene, 0.9% oxygen),  $T = 1689$  K and  $P = 1.79$  atm. The circles indicate the measurements from Vasudevan *et al.* [25] and the solid line indicates the current simulation. 95
- Figure 4.7 Sensitivity analysis of time resolved OH radical concentrations obtained in Toluene/Oxygen/Argon mixtures in shock tube with  $\Phi = 1$  (0.1% toluene, 0.9% oxygen),  $T = 1689$  K and  $P = 1.79$  atm. The circles indicate the measurements from Vasudevan *et al.* [25], the solid line indicates the current model, the dashed line indicates the current model with the rate of Sun *et al.* [94] for the reaction  $O + H_2 \rightarrow OH + H$  and the dashed dotted line indicates the current model in the absence of the  $C_5H_5 + C_2H_2 \rightarrow C_7H_7$  reaction. 96

- Figure 4.8 Time resolved  $OH$  radical concentrations obtained in Toluene/Oxygen/Argon mixtures in a shock tube with  $\Phi = 1$  (0.025% toluene, 0.225% oxygen),  $T = 1648$  K and  $P = 2.03$  atm. The circles indicate the measurements from Vasudevan *et al.* [25] and the solid line indicates the current simulation. 97
- Figure 4.9 Ignition delay times of toluene with  $\Phi = 1$  (0.1% toluene, 0.9% oxygen, 99% argon) and  $P = 1$  atm. Symbols indicate measurements from Vasudevan *et al.* [25] and the solid line indicates the current computations. 99
- Figure 4.10 Ignition delay times for toluene mole fractions of  $2 \times 10^{-4} - 1 \times 10^{-2}$  with  $\Phi = 1$  (toluene/oxygen/argon),  $T = 1600$  K and  $P = 1$  atm. The solid squares indicate the measurements from Vasudevan *et al.* [25], the open circles indicate experimental data from Burcat *et al.* [24] and the solid line indicates the current computations. 99
- Figure 4.11 Ignition delay times for toluene obtained in a shock tube with  $\Phi = 1$  (0.497%  $C_7H_8$ , 4.48%  $O_2$ , 95.023%  $Ar$ ) and  $P = 2.28$  atm. The circles indicate experimental data from Burcat *et al.* [24] and the solid line indicates the current computations. 100
- Figure 4.12 Predicted toluene thermal decomposition pathways corresponding to the study of Braun-Unkloff *et al.* [27] with an initial fuel concentration of 2.0 ppm,  $T = 1515$  K and  $P = 1.85$  bar. 104
- Figure 5.1 Concentration profiles of intermediate species during  $n$ -propyl benzene oxidation in a jet-stirred reactor with  $\Phi = 0.5$ ,  $P = 1$  atm,  $T = 900 - 1200$  K. The circles are measurements [104] and the solid line the current simulation. 115
- Figure 5.2 Concentration profiles of intermediate species during  $n$ -propyl benzene oxidation in a jet-stirred reactor with  $\Phi = 0.5$ ,  $P = 1$  atm,  $T = 900 - 1200$  K. The circles are measurements [104] and the solid line the current simulation. 115
- Figure 5.3 Concentration profiles of intermediate species during  $n$ -propyl benzene oxidation in a jet-stirred reactor with  $\Phi = 0.5$ ,  $P = 1$  atm,  $T = 900 - 1200$  K. The circles are measurements [104] and the solid line the current simulation. 116



- Figure 5.4 Concentration profiles of intermediate species during *n*-propyl benzene oxidation in a jet-stirred reactor with  $\Phi = 1.0$ ,  $P = 1$  atm,  $T = 950 - 1250$  K. The circles are measurements [104] and the solid line the current simulation. 116
- Figure 5.5 Concentration profiles of intermediate species during *n*-propyl benzene oxidation in a jet-stirred reactor with  $\Phi = 1.0$ ,  $P = 1$  atm,  $T = 950 - 1250$  K. The circles are measurements [104] and the solid line the current simulation. 117
- Figure 5.6 Concentration profiles of intermediate species during *n*-propyl benzene oxidation in a jet-stirred reactor with  $\Phi = 1.0$ ,  $P = 1$  atm,  $T = 950 - 1250$  K. The circles are measurements [104] and the solid line the current simulation. 117
- Figure 5.7 Concentration profiles of intermediate species during *n*-propyl benzene oxidation in a jet-stirred reactor with  $\Phi = 1.5$ ,  $P = 1$  atm,  $T = 950 - 1250$  K. The circles are measurements [104] and the solid line the current simulation. 118
- Figure 5.8 Concentration profiles of intermediate species during *n*-propyl benzene oxidation in a jet-stirred reactor with  $\Phi = 1.5$ ,  $P = 1$  atm,  $T = 950 - 1250$  K. The circles are measurements [104] and the solid line the current simulation. 118
- Figure 5.9 Concentration profiles of intermediate species during *n*-propyl benzene oxidation in a jet-stirred reactor with  $\Phi = 1.5$ ,  $P = 1$  atm,  $T = 950 - 1250$  K. The circles are measurements [104] and the solid line the current simulation. 119
- Figure 5.10 Major *n*-propyl benzene decomposition routes for  $\Phi = 1.5$ ,  $T = 1050$  K and  $P = 1$  atm in a jet-stirred reactor 123
- Figure 5.11 Benzyl radical consumption paths for  $\Phi = 1.5$ ,  $T = 1050$  K and  $P = 1$  atm in a jet-stirred reactor 123
- Figure 5.12 *N*-Propyl benzene oxidation for  $\Phi = 1.5$ ,  $T = 1050$  K and  $P = 1$  atm in a jet stirred reactor 124
- Figure 5.13 Concentration profiles of intermediate species during *n*-propyl benzene oxidation in a jet-stirred reactor with  $\Phi = 0.5$ ,  $P = 10$  atm,  $T = 900 - 1200$  K. The circles are measurements [113] and the solid lines the current computations. 126

- Figure 5.14 Concentration profiles of intermediate species during *n*-propyl benzene oxidation in a jet-stirred reactor with  $\Phi = 0.5$ ,  $P = 10$  atm,  $T = 900 - 1200$  K. The circles are measurements [113] and the solid lines the current computations. 126
- Figure 5.15 Concentration profiles of intermediate species during *n*-propyl benzene oxidation in a jet-stirred reactor with  $\Phi = 0.5$ ,  $P = 10$  atm,  $T = 900 - 1200$  K. The circles are measurements [113] and the solid lines current computations. 127
- Figure 5.16 Concentration profiles of intermediate species during *n*-propyl benzene oxidation in a jet-stirred reactor with  $\Phi = 1.0$ ,  $P = 10$  atm,  $T = 900 - 1200$  K. The circles are measurements [113] and the solid lines the current computations. 127
- Figure 5.17 Concentration profiles of intermediate species during *n*-propyl benzene oxidation in a jet-stirred reactor with  $\Phi = 1.0$ ,  $P = 10$  atm,  $T = 900 - 1200$  K. The circles are measurements [113] and the solid lines the current computations. 128
- Figure 5.18 Concentration profiles of intermediate species during *n*-propyl benzene oxidation in a jet-stirred reactor with  $\Phi = 1.0$ ,  $P = 10$  atm,  $T = 900 - 1200$  K. The circles are measurements [113] and the solid lines the current computations. 128
- Figure 5.19 Concentration profiles of intermediate species during *n*-propyl benzene oxidation in a jet-stirred reactor with  $\Phi = 1.5$ ,  $P = 10$  atm,  $T = 900 - 1200$  K. The circles are measurements [113] and the solid lines the current computations. 129
- Figure 5.20 Concentration profiles of intermediate species during *n*-propyl benzene oxidation in a jet-stirred reactor with  $\Phi = 1.5$ ,  $P = 10$  atm,  $T = 900 - 1200$  K. The circles are measurements [113] and the solid lines the current computations. 129
- Figure 5.21 Concentration profiles of intermediate species during *n*-propyl benzene oxidation in a jet-stirred reactor with  $\Phi = 1.5$ ,  $P = 10$  atm,  $T = 900 - 1200$  K. The circles are measurements [113] and the solid lines the current computations. 130
- Figure 5.22 Concentration profiles of intermediate species during *n*-propyl benzene oxidation in a jet-stirred reactor with  $\Phi = 2.0$ ,  $P = 10$  atm,  $T$

- = 900 - 1200 K. The circles are measurements [113] and the solid lines the current computations. 130
- Figure 5.23 Concentration profiles of intermediate species during *n*-propyl benzene oxidation in a jet-stirred reactor with  $\Phi = 2.0$ ,  $P = 10$  atm,  $T = 900 - 1200$  K. The circles are measurements [113] and the solid lines the current computations. 131
- Figure 5.24 Concentration profiles of intermediate species during *n*-propyl benzene oxidation in a jet-stirred reactor with  $\Phi = 2.0$ ,  $P = 10$  atm,  $T = 900 - 1200$  K. The circles are measurements [113] and the solid lines the current computations. 131
- Figure 5.25 Benzyl radical consumption paths for  $\Phi = 1.5$ ,  $T = 1050$  K and  $P = 10$  atm in a jet-stirred reactor 135
- Figure 5.26 *N*-propyl benzene oxidation for  $\Phi = 1.5$ ,  $T = 1050$  K and  $P = 10$  atm in a jet-stirred reactor 136
- Figure 5.27 Ignition delay times of *n*-propyl benzene at  $P = 5$  atm,  $0.71 < \Phi < 1.18$ . The circles are the measurements [116] and the solid line is the current simulation 138
- Figure 5.28 Reaction pathways for the oxidation of *n*-propyl benzene in a shock tube at  $T = 1448$  K,  $\Phi = 1.026$  and  $P = 5.06$  bar 141
- Figure 6.1 Concentration profiles of major species during naphthalene oxidation in a plug flow reactor for  $\Phi = 1.1$ ,  $T = 1197$  and  $P = 1$  atm. The solid lines indicate the current computations and the circles indicate the measurements [23]. 148
- Figure 6.2 Concentration profiles of major species during naphthalene oxidation in a plug flow reactor for  $\Phi = 1.1$ ,  $T = 1197$  and  $P = 1$  atm. The solid lines indicate the current computations and the circles indicate the measurements [23]. 148
- Figure 6.3 Concentration profiles of major species during naphthalene oxidation in a plug flow reactor for  $\Phi = 1.1$ ,  $T = 1197$  and  $P = 1$  atm. The solid lines indicate the current computations and the circles indicate the measurements [23]. 149
- Figure 6.4 Naphthalene and indene oxidation pathways 149
- Figure 7.1 Concentration profiles of intermediate species during 1-methyl naphthalene oxidation in a jet-stirred reactor with  $\Phi = 0.5$ ,  $P = 1$  atm

- and  $T = 1097 - 1290$  K. Circles are experimental data [33] and the solid lines the current simulations. 156
- Figure 7.2 Concentration profiles of intermediate species during 1-methyl naphthalene oxidation in a jet-stirred reactor with  $\Phi = 0.5$ ,  $P = 1$  atm and  $T = 1097 - 1290$  K. Circles are experimental data [33] and the solid lines the current simulations. 156
- Figure 7.3 Concentration profiles of intermediate species during 1-methyl naphthalene oxidation in a jet-stirred reactor with  $\Phi = 0.5$ ,  $P = 1$  atm and  $T = 1097 - 1290$  K. Circles are experimental data [33] and the solid lines the current simulations. 157
- Figure 7.4 Concentration profiles of intermediate species during 1-methyl naphthalene oxidation in a jet-stirred reactor with  $\Phi = 0.5$ ,  $P = 1$  atm and  $T = 1097 - 1290$  K. Circles are experimental data [33] and the solid lines the current simulations. 157
- Figure 7.5 Concentration profiles of intermediate species during 1-methyl naphthalene oxidation in jet-stirred reactor.  $\Phi = 1.0$ ,  $P = 1$  atm and  $T = 1094 - 1400$  K. Circles are experimental data [33] and the solid lines the current simulations. 158
- Figure 7.6 Concentration profiles of intermediate species during 1-methyl naphthalene oxidation in jet-stirred reactor.  $\Phi = 1.0$ ,  $P = 1$  atm and  $T = 1094 - 1400$  K. Circles are experimental data [33] and the solid lines the current simulations. 158
- Figure 7.7 Concentration profiles of intermediate species during 1-methyl naphthalene oxidation in jet-stirred reactor.  $\Phi = 1.0$ ,  $P = 1$  atm and  $T = 1094 - 1400$  K. Circles are experimental data [33] and the solid lines the current simulations. 159
- Figure 7.8 Concentration profiles of intermediate species during 1-methyl naphthalene oxidation in jet-stirred reactor.  $\Phi = 1.0$ ,  $P = 1$  atm and  $T = 1094 - 1400$  K. Circles are experimental data [33] and the solid lines the current simulations. 159
- Figure 7.9 Concentration profiles of intermediate species during 1-methyl naphthalene oxidation in jet-stirred reactor.  $\Phi = 1.5$ ,  $P = 1$  atm and  $T = 1147 - 1440$  K. Circles are experimental data [33] and the solid lines the current simulations. 160

- Figure 7.10 Concentration profiles of intermediate species during 1-methyl naphthalene oxidation in jet-stirred reactor.  $\Phi = 1.5$ ,  $P = 1$  atm and  $T = 1147 - 1440$  K. Circles are experimental data [33] and the solid lines the current simulations. 160
- Figure 7.11 Concentration profiles of intermediate species during 1-methyl naphthalene oxidation in jet-stirred reactor.  $\Phi = 1.5$ ,  $P = 1$  atm and  $T = 1147 - 1440$  K. Circles are experimental data [33] and the solid lines the current simulations. 161
- Figure 7.12 Concentration profiles of intermediate species during 1-methyl naphthalene oxidation in jet-stirred reactor.  $\Phi = 1.5$ ,  $P = 1$  atm and  $T = 1147 - 1440$  K. Circles are experimental data [33] and the solid lines the current simulations. 161
- Figure 7.13 Major 1-methyl naphthalene decomposition pathways. 165
- Figure 7.14 Major 1-methyl naphthalene formation pathways. 166
- Figure 7.15 Naphthalene formation pathways 166
- Figure 7.16 Major indene formation pathways 167
- Figure 7.17 Concentration profiles of major species during 1-methyl naphthalene oxidation in a flow reactor ( $\Phi = 1.0$ ,  $P = 1$  atm,  $T = 1169$  K). Circles indicate measurements [23] and solid lines the current computations. 173
- Figure 7.18 Concentration profiles of major species during 1-methyl naphthalene oxidation in a flow reactor ( $\Phi = 1.0$ ,  $P = 1$  atm,  $T = 1169$  K). Circles indicate measurements [23] and solid lines the current computations. 173
- Figure 7.19 Concentration profiles of major species during 1-methyl naphthalene oxidation in a flow reactor ( $\Phi = 1.0$ ,  $P = 1$  atm,  $T = 1169$  K). Circles indicate measurements [23] and solid lines the current computations. 174
- Figure 7.20 Concentration profiles of major species during 1-methyl naphthalene oxidation in a flow reactor ( $\Phi = 1.0$ ,  $P = 1$  atm,  $T = 1169$  K). Circles indicate measurements [23] and solid lines the current computations. 174
- Figure 7.21 Concentration profiles of major species during 1-methyl naphthalene oxidation in a flow reactor ( $\Phi = 1.5$ ,  $P = 1$  atm,  $T = 1166$  K). Circles indicate measurements [23] and solid lines the current computations. 175
- Figure 7.22 Concentration profiles of major species during 1-methyl naphthalene oxidation in a flow reactor ( $\Phi = 1.5$ ,  $P = 1$  atm,  $T = 1166$  K). Circles indicate measurements [23] and solid lines the current computations. 175

- Figure 7.23 Concentration profiles of major species during 1-methyl naphthalene oxidation in a flow reactor ( $\Phi = 1.5$ ,  $P = 1$  atm,  $T = 1166$  K). Circles indicate measurements [23] and solid lines the current computations. 176
- Figure 7.24 Concentration profiles of major species during 1-methyl naphthalene oxidation in a flow reactor ( $\Phi = 1.5$ ,  $P = 1$  atm,  $T = 1166$  K). Circles indicate measurements [23] and solid lines the current computations. 176
- Figure 7.25 Concentration profiles of major species during 1-methyl naphthalene oxidation in a flow reactor ( $\Phi = 1.5$ ,  $P = 1$  atm,  $T = 1198$  K). Circles indicate measurements [23] and solid lines the current computations. 177
- Figure 7.26 Concentration profiles of major species during 1-methyl naphthalene oxidation in a flow reactor ( $\Phi = 1.5$ ,  $P = 1$  atm,  $T = 1198$  K). Circles indicate measurements [23] and solid lines the current computations. 177
- Figure 7.27 Concentration profiles of major species during 1-methyl naphthalene oxidation in a flow reactor ( $\Phi = 1.5$ ,  $P = 1$  atm,  $T = 1198$  K). Circles indicate measurements [23] and solid lines the current computations. 178
- Figure 7.28 Concentration profiles of major species during 1-methyl naphthalene oxidation in a flow reactor ( $\Phi = 1.5$ ,  $P = 1$  atm,  $T = 1198$  K). Circles indicate measurements [23] and solid lines the current computations. 178
- Figure 7.29 Major 1-methyl naphthalene decomposition pathways under plug flow reactor conditions 183

**List of Tables**

Table 2.1 Reaction steps in the H <sub>2</sub> /O <sub>2</sub> mechanism	47
Table 3.1 Experimental and modelling conditions for cyclopentadiene oxidation in a flow reactor. (The experimental time shifts correspond to time shifting performed on modelling computations performed by Butler [55]).	59
Table 3.2 Experimental and modelling conditions for cyclopentadiene pyrolysis in a flow reactor	71
Table 4.1 Experimental and modelling conditions for toluene thermal decomposition	91
Table 5.1 Experimental and modelling conditions for the oxidation of <i>n</i> -propyl benzene in a jet-stirred reactor at P = 1 atm. The species concentrations correspond to mole fractions	114
Table 5.2 Experimental and modelling conditions for the oxidation of <i>n</i> -propyl benzene in a jet-stirred reactor at P = 10 atm. The species concentrations correspond to mole fractions	125
Table 5.3 Experimental and modelling conditions for <i>n</i> -propyl benzene ignition delay times in a shock tube	137
Table 7.1 Experimental and modelling conditions for the oxidation of 1-methyl naphthalene in a jet-stirred reactor. The species concentrations correspond to mole fractions.	155
Table 7.2 Experimental and modelling conditions for the oxidation of 1-methyl naphthalene in a turbulent flow reactor.	172

## Nomenclature

### Symbols

$A$	Temperature Independent Constant / Pre-Exponential Factor
$A^*$	Excited Molecule
$[A]_o$	Initial Concentration of A
$[A]_t$	Concentration at Time t
A, B, C,...	Species Involved in the Reaction
a, b, c,...	Reaction Orders with Respect to the Species A, B, C,...
$\Delta G^\circ$	Standard Gibbs Energy Change
$\Delta H^\circ_T$	Standard Enthalpy of Reaction at Temperature T
$\Delta S^\circ_T$	Standard Entropy of Reaction at Temperature T
$E_a$	Activation Energy
h	Mixture Enthalpy
$h_k$	Specific Enthalpy of Species k
$K_{eq}$	Equilibrium Constant
$k_f$	Forward Rate Constant
$k_r$	Reverse Rate Constant
m	Mass Flow Rate through a Reactor
$M_k$	Molar Mass Fraction of Species k
$\bar{M}$	Mean Molecular Weight
$p^\circ$	Standard Pressure
R	Universal Gas Constant
$R_k$	Species Formation Source Term
T	Temperature of the Mixture
u	Stream Wise Velocity
$V_R$	Reactor Volume
$x_k$	Mole Fraction of Species k
x	Distance Along the Reactor
$Y_k$	Mass Fraction



**Greek Symbols**

$\Xi_j$	Stoichiometric Coefficient for Species in Reaction j
$\Phi_i$	Molar Concentration of Species i
$\xi_j^i$	Concentration Dependence for Species i in Reaction j
$\tau$	Residence Time
$\rho$	Fluid Density

# Chapter 1

## Introduction

### 1.1 Background

The increase in global fuel consumption over the last century has resulted in major socioeconomic and environmental challenges. Transportation and, to an increased extent, aviation, is one of the major fuel consumption sectors. This leads to the need for new engines with new operating systems that will comply with the environmental and energy saving directives. The new aircraft engines are expected to perform with maximum combustion efficiency as well as providing stability and low emissions. Aromatic hydrocarbons and, to a much lesser extent, polycyclic aromatic hydrocarbons (PAH) are major components of current aviation fuels.

It is already known that aromatic compounds, apart from being responsible for soot and pollutant formation, also have carcinogenic and mutagenic properties [1-3]. They also contribute to the detection of aircrafts due to the associated infrared signals produced. The aromatic components of aviation fuels can also reduce the life cycle of the combustor as it increases the radiative heat transfer to the combustor walls [4]. Hence, research needs to be focussed on the energy saving aspect, on pollution reduction and on the optimisation of the combustor behaviour through good knowledge of the chemistry of aromatic fuel components.

The term “aviation fuel” generally implies a fuel whose energy can be used for propulsive purposes. A typical aviation fuel such as kerosene consists of various classes of hydrocarbon compounds, which exhibit different behaviours in respect of refining processes and crude oil feedstocks [5]. The chemical composition of typical aviation fuels can be found in Figure 1.1.

An aviation fuel can be determined by operational need and used either for commercial or military service. The fuels were developed to have good combustion characteristics combined with good physical properties such as low temperature

fluidity. The blends need to consist of storable hydrocarbon compounds. In the 1940's, the U.S. Air Force used 'wide-cut' fuel, which was available in large quantities at that time. Wide-cut fuels were highly volatile and were replaced by kerosene fuels in the 1970's (Jet A, Jet A-1 and JP-8) for safety reasons [6].

However, the complexity of the jet fuels does not allow direct simulation of their combustion behaviour. They contain thousands of chemical compounds and their composition also alters with time. Recent scientific advances regarding chemical modelling have provided important insight that is complementary to experimental studies. Such detailed fuel modelling provides a very important tool in understanding and controlling soot growth and predicting the overall behaviour of the fuel. It is a necessity to represent fuel mixtures with compositions functionally similar to commercial aviation fuels. These mixtures are called surrogates and they can be characterized accurately. With such models, it is also feasible to study the combustion process in connection with the chemical composition and the fuel properties [6]. In addition to that, the use of a surrogate fuel with a controlled composition facilitates the development of computational codes for combustor design.

A surrogate aviation fuel can reproduce physical and chemical properties of a commercial aviation fuel such as heat capacity, enthalpy, viscosity, rates of reaction of specific ignition and oxidation behaviours. Surrogate mixtures can be reproduced computationally and experimentally. A physical surrogate is a mixture that can reproduce physical properties such as density, heat capacity, volatility and a chemical surrogate is a mixture with a chemical class composition that matches the one of the real jet fuel and can reproduce chemical properties such as reaction rates, ignition and sooting behaviour. A surrogate mixture that has the same chemical and physical properties as the real fuel is characterized as a comprehensive surrogate and can be expected to match diverse aspects of the real fuel behaviour such the evaporation process and the sooting tendency [7].

The current work evaluates the use of a reaction class based concept for the generation of chemical mechanisms for surrogate fuels. In the past, reaction classes for higher aromatics, such as naphthalene and indene, have been defined based on similarities with the oxidation of cyclopentadiene and benzene. These were subsequently applied to model the oxidation of toluene, 1-methyl naphthalene, naphthalene and *n*-propyl benzene with encouraging results. The current work

extends past efforts related to the aforementioned systems. The compounds have been identified as important in the context of a range of surrogate fuel compositions from gasoline to aviation fuels. Specifically, the methyl groups, or the alkyl branches in general, on aromatic rings (e.g. xylenes and tri-methyl benzenes) have been identified as important in the context of ignition properties and 1-methyl naphthalene may also be used to modulate sooting tendencies in aviation and Diesel surrogates. These systems therefore constitute a natural starting point for the evaluation of the current approach.

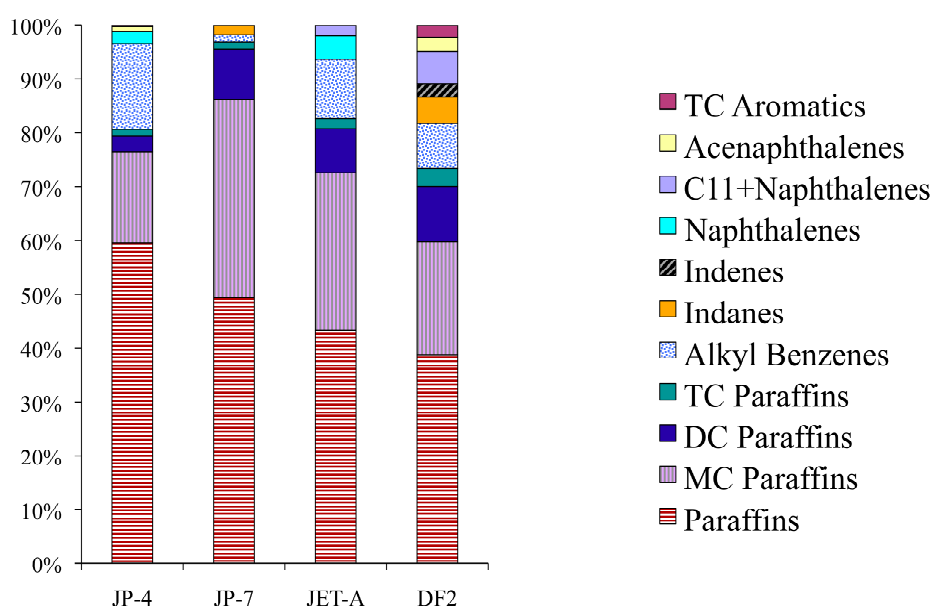


Figure 1.1 Chemical composition of typical aviation fuels [8]

## 1.2 Types and Chemistries of Aviation Fuels

Aviation fuel is a mixture of hydrocarbons whose size is restricted by properties such as the freezing point and distillation. A kerosene type jet fuel comprises two major classes; the paraffins and the aromatics. The molecules typically feature 7 to 16 carbon atoms. Paraffin compounds are defined as all the saturated compounds with a straight chain, branched or cyclic structures and are the dominant components of the fuel and comprise around 80% of the total. Aromatics constitute the other major class of chemical compounds. Aromatics promote soot formation and are thus potentially responsible for the reduction of the combustor life due to the increased radiative transfer to the combustor wall. Hence, large concentrations are not desirable and a typical aviation fuel comprises 10-20% of aromatic compounds per volume. Aromaticity is defined by the planar ring structure of the molecule where the C-C bonds are shared equally with all the atoms around the ring and each carbon atom has a p orbital. Although the aromatic molecules exhibit high volumetric heating values, they result in low heat release per unit weight due to the lower  $H/C$  ratios compared to saturated compounds.

The evaluation of the burning quality of an aviation fuel, which depends on the chemical class composition, may be determined via UV spectrophotometric analysis of the concentration of the naphthalene compounds and a chromatographic analysis of the total aromatics. An example of a chromatograph of a fuel sample is shown in Figure 1.2. The development of these chemical analysis methods facilitates the measurement and identification of the intermediates and products of the oxidation and hence the influence of temperature and pressure effects.

The composition of the jet fuel is restricted by the boiling point and freezing point of the chemical components. As the carbon number increases, the boiling point increases when the compounds belong to the same class. But if the compounds with the same carbon number belong to different classes, then the boiling point increases by going from paraffins to cycloparaffins and then aromatics. Similarly, the freezing point increases with the carbon number with the difference that aromatics and normal paraffins freeze at higher temperatures than other hydrocarbons due to their shape that facilitates packing into crystalline structure.

Another critical factor is fuel density. The energy content per unit weight increases from aromatics to cycloparaffins and then paraffins whereas the energy content per unit volume increases in the reverse order.

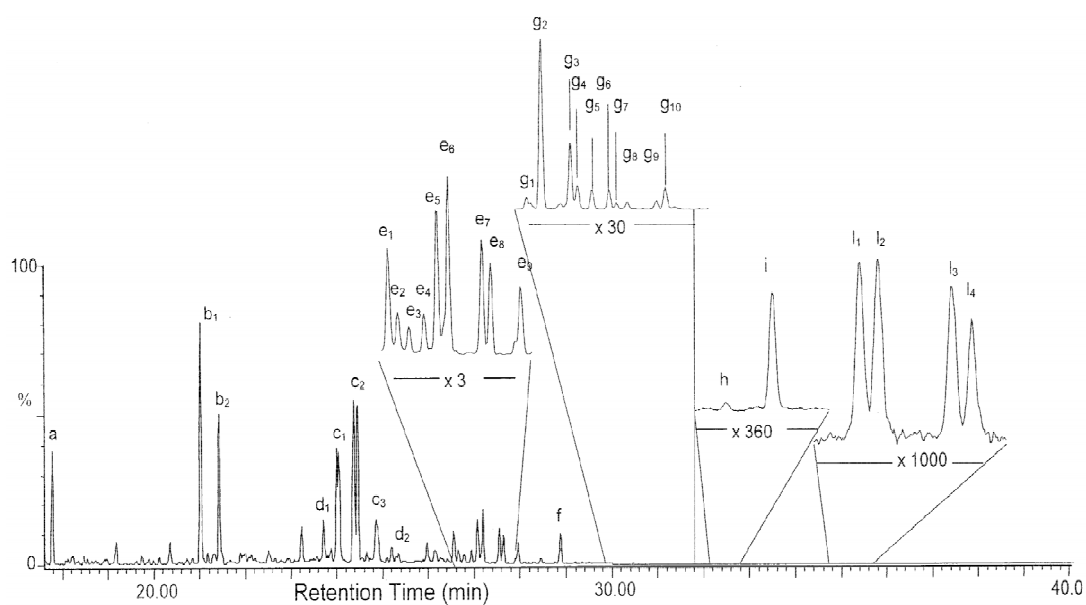


Figure 1.2 Chromatogram of a fuel sample. a) naphthalene, b) methyl naphthalene, c) ethyl naphthalenes, d) C<sub>3</sub>-naphthalenes, e) diphenylamine, f) C<sub>4</sub>-naphthalenes, g) phenanthrene, h) anthracene, i) methyl anthracene [9]

### 1.3 Mechanism Construction and Status

A detailed chemical mechanism comprises a series of elementary chemical reaction steps that involve chemical species that describe oxidation and pyrolytic processes associated with thermochemical and transport property data. The construction of such a mechanism can start from the simplest hydrogen/oxygen submechanism involving common sub-elements of more complex molecules that compose an aviation fuel [10]. The scheme can be expanded with the implementation of new steps and species with increasing molecular weight and complexity. The hierarchical detailed chemical mechanism construction approach is illustrated in Figure 1.3.

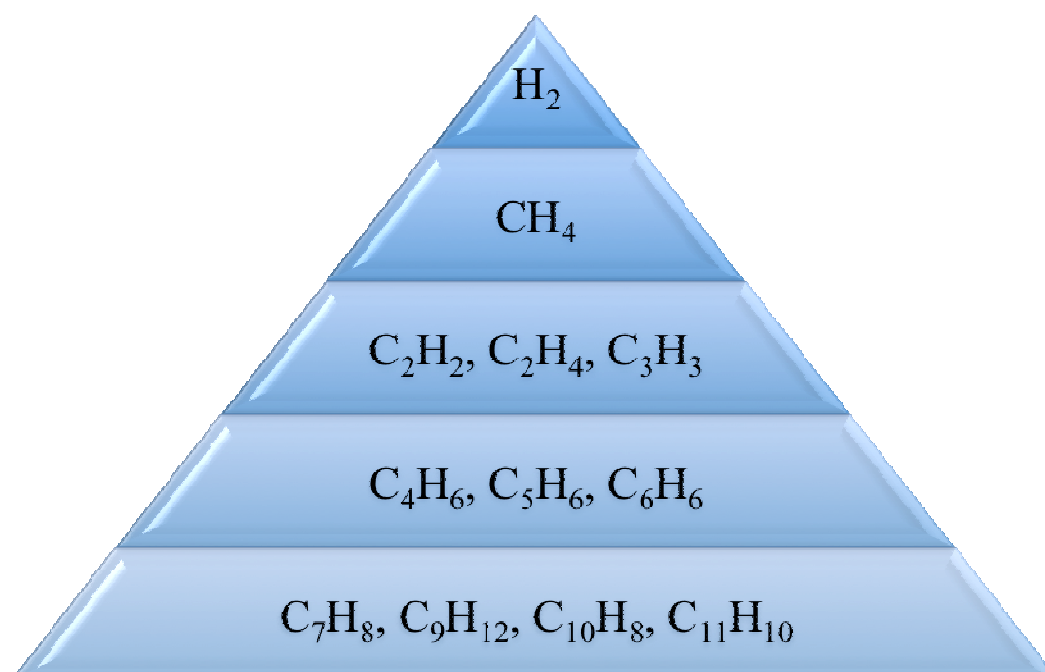


Figure 1.3 Hierarchical construction of a detailed chemical mechanism for jet fuels

The construction of a chemical mechanism is a very complex task that can be simplified with the identification of principal reaction pathways and reaction classes combined with major intermediate species that are formed through oxidation or pyrolysis of higher hydrocarbon molecules. Some reactions have been studied experimentally under combustion conditions and can be implemented directly in the relevant mechanism. These reactions can also be utilised as template reaction steps for the estimation of relevant chemical routes and reaction rates of higher

hydrocarbons by making adjustments based on molecular properties. Moreover, when experimental data for reaction rates are not available, other ways of determining new steps and reaction rates are through the application of collision theory [11], quantum mechanical methods [12] and semi-empirical methods [13].

Once the model is constructed, it has to be evaluated under as wide a range of conditions as possible, including data from shock tubes, jet-stirred reactors and plug flow reactors for a variety of temperatures, pressures and equivalence ratios.

Reaction rates that have been determined with the aforementioned methods are utilised in the present work. The reaction steps are reversible with the reverse rates computed from equilibrium constants. The thermodynamic data utilised in the present work were obtained from Burcat and Ruscic [14] and Robinson [15]. The detailed chemical mechanism and the thermodynamic data contained in the present work are presented in Table A.1 (see Appendix A) and Table B.3 (see Appendix B). The enthalpy of formation and entropy computed at 298 K for each specie are presented in Table B.2 of Appendix B in combination with the molecular structure of each species.

## **1.4 Mathematical Description of Reactors**

The developed detailed mechanism was evaluated for a wide range of combustion conditions featuring different devices such as shock tubes, jet-stirred reactors and flow reactors. The mathematical description of these reactors is presented below. A detailed discussion regarding the governing equations is available in the literature [16-19].



### 1.4.1 Spatially Homogeneous Reactors

Devices such as shock tubes, jet-stirred reactors and plug flow reactors or more specifically the princeton turbulent flow reactor utilized for chemical modelling in this study are assumed to take into account kinetic and thermodynamic data while neglecting heat and transport effects. When spatial transport effects are removed, the conservation equations become a set of ordinary differential equations for the species concentrations and temperature with time as the single independent variable.

Plug flow reactors are characterized by high flow rates with negligible circulation where the complete and rapid mixing between the fuel and the oxidizer occurs at the inlet end of the reactor. Combustion typically takes place at atmospheric pressure and in a temperature range of 900-1300 K. The governing equations for spatially homogenous adiabatic reactors and isobaric flow are shown below:

$$\text{Conservation of Species} \quad \rho \frac{dY_k}{dt} = R_k M_k \quad (1.1)$$

$$\text{Conservation of Enthalpy} \quad \rho \frac{dh}{dt} = -\sum_{k=1}^{n_{sp}} h_k R_k M_k \quad (1.2)$$

$$\text{Equation of State} \quad P = \frac{\rho RT}{M} \quad (1.3)$$

$$\text{Mean molecular weight} \quad \bar{M} = \sum_{k=1}^{n_{sp}} x_k M_k \quad (1.4)$$

$$\text{Species formation Source Term} \quad R_k = \sum_{j=1}^{n_{reac}} \Xi_{jk} \left[ k_j^f \prod_{i=1}^{n_{sp}} \Phi_i^{s_{ji}^f} - k_j^r \prod_{i=1}^{n_{sp}} \Phi_i^{s_{ji}^r} \right] \quad (1.5)$$

In the above equations,  $\rho$  indicates the fluid density,  $h$  is the mixture enthalpy,  $h_k$  is the specific enthalpy of the species  $k$ ,  $Y_k$  is the mass fraction and  $M_k$  the molar

mass fraction of species  $k$  respectively,  $R$  is the universal gas constant,  $T$  is the temperature of the mixture,  $\bar{M}$  is the mean molecular weight,  $x_k$  is the mole fraction of species  $k$  and  $R_k$  is the species formation source term. In the species source term equation  $\bar{\nu}$  is the stoichiometric coefficient for species in reaction  $j$ ,  $\Phi$  is the molar concentration of species  $i$ ,  $k_j^f$  and  $k_j^r$  are the forward and reverse rate constants for reaction  $j$  and  $\zeta$  is the concentration dependence for species  $i$  in reaction  $j$ .

Plug flow reactors provide information on species profiles over time and are very useful in determining important details of a reaction mechanism. They are excellent tools for the examination of combustion phenomena as they examine the pure steady state temperature dependent chemistry from the effects that are characteristic of flames such as diffusive and radiative heat transfer, turbulence and wall quenching that complicate the understanding of the kinetic data [20]. In this study, data obtained from the princeton turbulent flow reactor were utilized and compared against predictions that were computed under the relevant set of conditions. The test section of a princeton turbulent flow reactor is cylindrical, wide-diameter (10 cm) quartz tube of 1 meter length that is heater-insulated (see Figure 1.4). Through this tube, a dilute mixture of fuel vapor and oxygen flow are injected in a hot nitrogen carrier gas. A stainless steel, water-cooled sampling probe measures the local reaction temperature and collects gas samples along the centerline of the quartz test section and by performing gas chromatography and mass spectroscopy the concentrations of species are measured and unknown species are also identified when necessary [21, 22]. However, the vapor pressures of some oxygenated species are low and are responsible for some condensation effects on the sampling probe that lead to significant scatter in the species profiles analysed through gas chromatography [22]. According to Shaddix *et al.* [22] and Butler and Glassman [23], the uncertainty in the calibration factors for aliphatic species is approximately  $\pm 5\%$ , for monocyclic aromatics is  $\pm 10\%$  and  $\pm 20\%$  for larger aromatics. Added to this,  $\pm 5\%$  is the uncertainty for the oxygen measurement and  $10\%$  in the nominal equivalence ratio. Moreover, there is also the uncertainty of the thermocouple temperature which lies at the range of 10 K. Due to velocity profile variabilities there is an uncertainty of  $\pm 15\%$  [23].

Plug flow reactors and shock tubes are computed using a numerical method based on the work of Jones and Lindstedt [17]. The equations relevant to shock

tubes are identical to those solved by a flow reactor. In a shock tube simulation it is assumed that the pressure remains constant after the arrival of the shock wave. Shock tube temperatures typically vary from 1000 K to 3000 K and provide significant information for high temperature reaction rates. For a plug-flow reactor, if the data are reported as a function of distance, the trivial transformation  $(d/dt) = u(d/dx)$  is used, where  $u$  is the flow velocity and  $x$  is the distance along the reactor. Plug-flow reactors vary spatially but are steady in time, whereas shock tubes are considered to be homogeneous in space but varying in time [10].

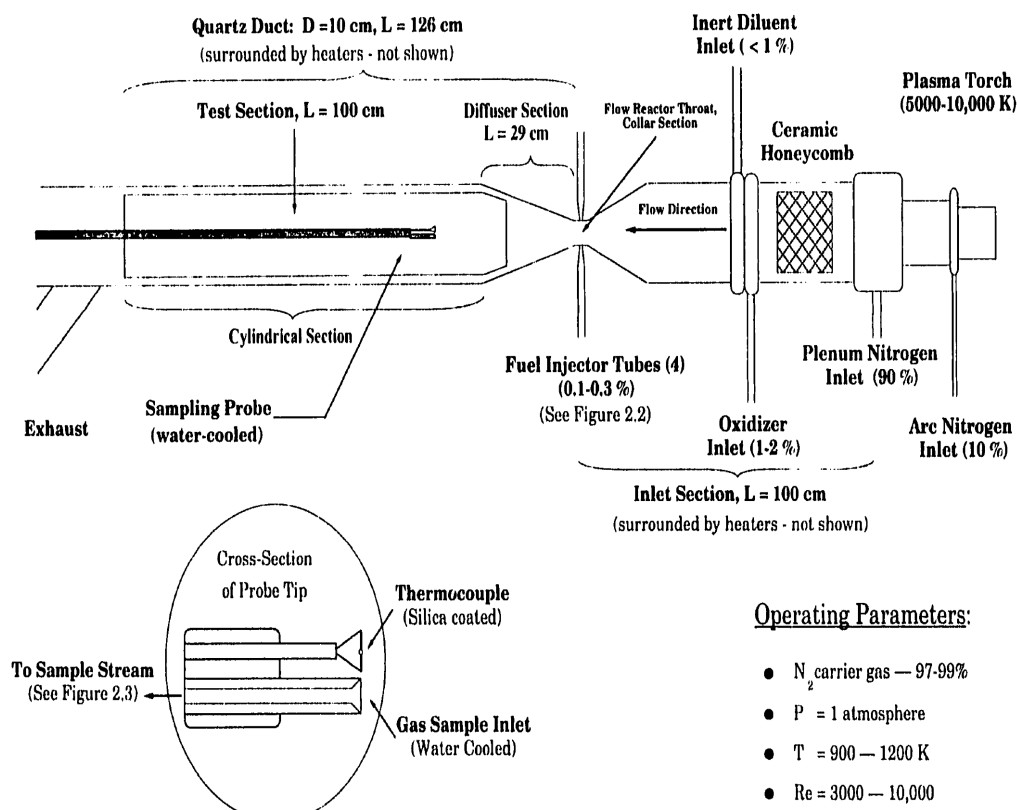


Figure 1.4 The Princeton turbulent flow reactor [24]

Shock tubes were utilized and described in earlier studies of Burcat [25], Vasudevan *et al.* [26], Rao and Skinner [27], Braun-Unkhoff *et al.* [28], Davidson *et al.* [29]. Shock tubes are considered as extremely simple experimental devices and a schematic representation adopted from Tsang and Lifshitz [30] illustrates the physical process that occurs in a shock tube and can be seen in Figure 1.5. According to Belford and Strehlow [31], the shock tubes can be used for a wide

range of temperatures (500 K to 12,000 K) and small testing times ( $10^{-6}$  to  $10^{-3}$  sec). The shock tube is considered as a long tube divided in two sections of different pressures by a membrane that disappears instantaneously. This leads to the generation of a shock wave to the low pressure section and a temperature increase on the test gas due to collisions. The incident shock wave after reflection from the end wall, produces a further increase at the temperature of the gas. The use of the shock tube is mostly preferred from kineticists as it is easier to deduce kinetic data, rate coefficients at high temperatures and also monitor the molecule or radical concentrations during the short reaction time that occurs in a shock tube [32]. Measurements within the shock tube are performed using atomic resonance absorption spectroscopy (ARAS), ring dye laser spectroscopy and laser photolysis. In the study of Belford and Strehlow [31], the significance of nonidealities in shock tube behaviour was discussed and it was found that this happens due to the formation of a boundary layer and its interactions. This is responsible for misinterpretation of the measurements. Errors in the reaction temperature can lead to erroneous rate constants at a factor of 1.25 uncertainty at room temperature and atmospheric chemistry [31, 33]. Uncertainties of the order of  $\pm 3\%$  were estimated in the study of Vasudevan *et al.* [26] who measured the concentrations of the OH radical under shock tube conditions using ring dye laser.

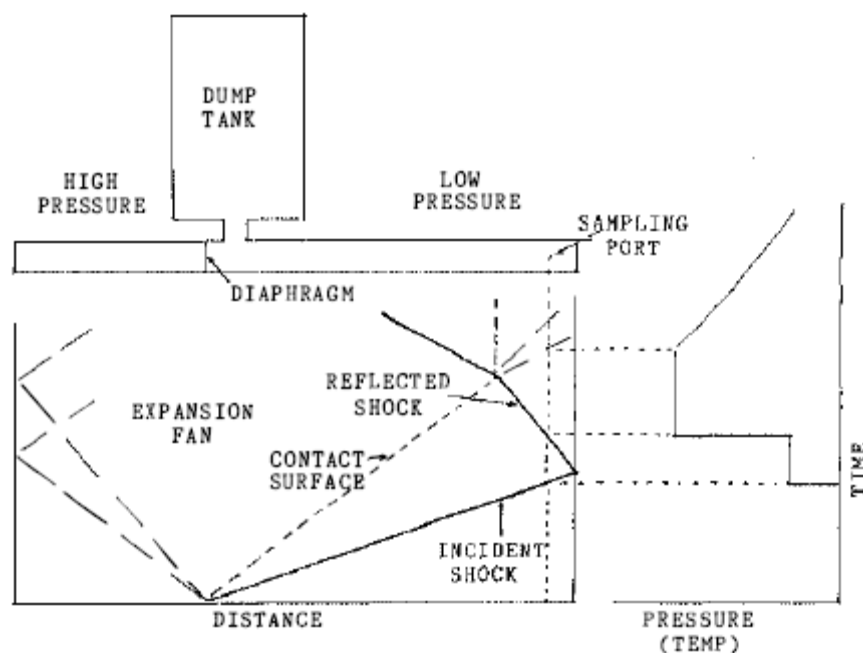


Figure 1.5 Single pulse shock tube wave diagram and pressure trace. Shock waves are discontinuities through the gas. The contact surface separates the driver and the shocked gas. The image is adopted from Tsand and Lifshitz [30].

Jet stirred reactors are computed using a numerical method based on the work of Jones and Lindstedt [17]. Stirred reactors operate under highly turbulent conditions to achieve spatial homogeneity within the reactor. The mixing is assumed instantaneous. The mixing region is spatially homogeneous and diffusion phenomena can be neglected. Jet stirred reactors generally operate at temperature below 1200 K and in a pressure range of 1-20 atm. The governing equations for a jet stirred reactor are shown below:

$$\text{Conservation of Species} \quad \frac{dY_k}{dt} = \frac{1}{\tau} (Y_k^* - Y_k) + \frac{R_k M_k}{\rho} \quad (1.6)$$

$$\text{Conservation of Enthalpy} \quad \frac{dh}{dt} = \frac{1}{\tau} \sum_{k=1}^{n_{sp}} Y_k^* (h_k^* - h_k) - \frac{1}{\rho} \sum_{k=1}^{n_{sp}} h_k R_k M_k \quad (1.7)$$

$$\text{Nominal Residence Time} \quad \tau = \frac{\rho V_R}{m} \quad (1.8)$$

In the above equations the superscript \* indicates the inlet conditions,  $\tau$  is the nominal residence time,  $V_R$  is the reactor volume and  $m$  is the mass flow rate through the reactor.

Jet stirred reactors were described on previous studies of Dagaut *et al.* [34] and more recent studies of Mati *et al.* [35]. According to these studies, the reactor is made from fused silica sphere of 42 mm diameter with 4 nozzles of 1mm diameter for the admission of the reactants. The fuel is diluted with a nitrogen flow in order to avoid the pyrolysis before the injection into the reactor. In order to reduce heat release and the temperature gradient, all the reactants are preheated before the injection inside the reactor. The fuel vapors and oxygen are diluted by a flow of nitrogen and mixed at the entrance of the injectors. The pressure is constant in time. Samples of the reacting mixtures are obtained at steady temperature and residence time with a low-pressure fused-silica sonic probe. Gas chromatography and mass spectrometry are utilized for the analysis of the samples. Jet stirred reactors result in small uncertainties in the measurements obtained in different experiments. More specifically, the measurements performed by Mati *et al.* [35] in jet stirred reactor, show a good repeatability of carbon balance of the range of  $\pm 10\%$ . A good

repeatability of the measurements and the carbon balance was also achieved in the study of Dagaut *et al.* [36] for the oxidation of *n*-propyl benzene.

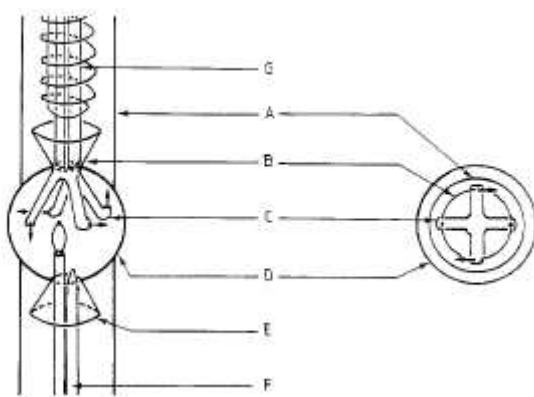


Figure 1.6 Jet stirred reactor. Image adopted from Dagaut *et al.* [34] A, external tube; B, convergent cone; C, injectors; D, spherical quartz reactor; E, divergent cone; F, sampling sonic probe and thermocouple probe; G, capillary surrounded by the preheating resistor [34].

## 1.5 Present Contribution

The current work evaluates the use of a reaction class based concept for the generation of chemical mechanisms for surrogate fuels. Reaction classes for higher aromatics, such as naphthalene and indene, have been defined based on similarities with the oxidation of cyclopentadiene and benzene. The developed mechanisms were subsequently applied to model the oxidation of toluene, *a*-methyl naphthalene and *n*-propyl benzene with encouraging results. The current work extends past efforts related to the aforementioned systems. The compounds have been identified as important in the context of a range of surrogate fuel compositions from gasoline to aviation fuels. Specifically, the methyl groups on aromatic rings (e.g. xylenes and tri-methyl benzenes) have been identified as important in the context of radical scavenging and *a*-methyl naphthalene may be used to modulate sooting tendencies

in aviation and Diesel surrogates. These systems therefore constitute a natural starting point for the evaluation of the current approach.

## 1.6 Thesis Outline

The structure of the thesis reflects the complexity of the aviation fuels by developing the fuel components starting from simpler constituents. Chapter 2 describes basic chemical rate laws and the equations that govern the chemical model. Moreover, it is shown that gas phase reactions are grouped into different categories depending on radical generation or elimination processes.

In Chapter 3 the combustion of cyclopentadiene is discussed. Pyrolysis and oxidation cases at various fuel mixture equivalence ratios are presented and analysed. Intermediate species concentrations are predicted and presented. New reaction rates are applied and evaluated. Important reaction steps are identified and problematic pathways are also highlighted.

In Chapter 4 the combustion of toluene is discussed. Toluene is the simplest alkylated benzene compound. The pyrolysis and oxidation of toluene under shock tube conditions is presented. Principal paths are identified and reaction rate updates are applied. Reaction classes are also identified and constitute the framework for the development of larger alkylated aromatic compounds.

In Chapter 5 the combustion of *n*-propyl benzene is discussed. An updated chemical mechanism based on toluene and propane analogies is tested, analysed and presented. The oxidation of *n*-propyl benzene is performed under jet-stirred reactor conditions for low and high pressures and concentration profiles of important species are presented. The toluene and propane analogies are evaluated and extended reaction classes are identified that can be applied on larger alkyl substituted aromatic compounds which form part of real and surrogate fuel formulations.

In Chapter 6 the combustion of naphthalene is discussed. Naphthalene represents the first step in the aromatic growth process. A naphthalene model based on benzene analogies is further developed, updated and validated under plug flow

reactor conditions. Chemical pathways that play significant role in the aromatic growth are identified.

In Chapter 7 the combustion of 1-methyl naphthalene is discussed. 1-Methyl naphthalene is the bicyclic analog of toluene and its chemical model is based on structural similarities with the latter. The model for the oxidation of 1-methyl naphthalene is tested over a range of jet-stirred reactor conditions. A variety of fuel mixture equivalence ratios are also tested under plug flow reactor conditions. Main decomposition channels are identified and important reaction routes for the formation of significant intermediate species are also presented.

In Chapter 8, the conclusions of the present work are presented, highlighting the critical improvements or discrepancies encountered with the current models. Suggestions for future work are also made.



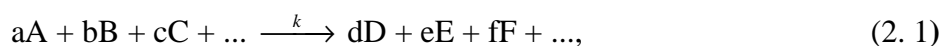
## Chapter 2

### Chemical Kinetics

When two or more molecules collide and produce one or more new chemical species then a chemical reaction has occurred. In order for a chemical reaction to occur, an energy that is equal or greater than the energy needed for the breakage of bonds and the formation of new bonds is required. The energy differs according to the nature of the atoms or molecules and their stereochemical structure. The basic laws of chemical kinetics as applied in the current work are discussed briefly below.

#### 2.1 Rate Laws and Orders of Reactions

The rate of the reaction depends on a variety of factors such as temperature, pressure, concentration of the reactants and products and whether a catalyst is present or not. The changes in the rates of reaction due to these factors can provide an important insight into what might happen on the molecular level. The definition of the rate law for a reaction is the time rate of change in concentration of one of the reactants or products [37]. For a general case a chemical reaction described by the equation



where A, B, C, ... indicate the species involved in the reaction, the reaction rate that describes the consumption of the species A can be expressed as

$$\frac{d[A]}{dt} = -k[A]^a[B]^b[C]^c \dots \quad (2.2)$$

where  $a, b, c, \dots$  are reaction orders with respect to the species A, B, C, ... and  $k$  is the rate coefficient of the reaction. The overall reaction order is defined by the sum of all the exponents. In some cases, the concentrations of some of the species are in excess and do not change noticeably (e.g. [B] and [C]) during the reaction. Hence, an effective rate coefficient can be produced by their concentrations and the rate coefficient  $k_{\text{exp}} = k[B]^b[C]^c$  and obtain the following simplified equation

$$\frac{d[A]}{dt} = -k_{\text{exp}}[A]^\alpha \quad (2.3)$$

For first order reactions  $\alpha = 1$  and equation (2.3) yields a first-order behaviour

$$\ln \frac{[A]_t}{[A]_0} = -k_{\text{exp}}(t - t_0) \quad (2.4)$$

where  $[A]_0$  denotes the initial concentration of A and  $[A]_t$  the concentration at time  $t$ . For  $t_0 = 0$  and exponentiating both sides of equation (2.4)

$$[A(t)] = [A(0)\exp(-kt)] \quad (2.5)$$

For second order ( $\alpha = 2$ ) and third order ( $\alpha = 3$ ) reactions the equations describing the temporal behaviour is shown below

$$\frac{1}{[A]_t} - \frac{1}{[A]_0} = -k_{\text{exp}}(t - t_0) \quad (2.6)$$

$$\frac{1}{[A]_t^2} - \frac{1}{[A]_0^2} = -2k_{\text{exp}}(t - t_0) \quad (2.7)$$

A logarithmic plot of the concentrations against time leads to linear dependences with a slope  $-k_{\text{exp}}$  for the first order reactions, similarly a plot of  $1/[A]_t$

against time for second order reactions leads to linear dependencies with a slope  $k_{\text{exp}}$ .

## 2.2 Temperature Dependence of Rate Constants

The temperature dependency constitutes another factor that provides a basis for understanding reactions on a molecular level. Rate coefficients for chemical reactions often depend strongly and in a nonlinear way on the temperature. Arrhenius [38] described this relationship with a formula subsequently called the Arrhenius Rate Law,

$$k = A \exp\left(-\frac{E_{\alpha}}{RT}\right) \quad (2.8)$$

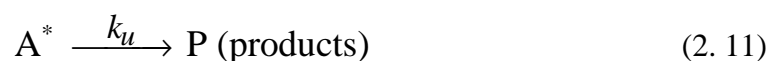
where  $A$  is a temperature independent constant or else called pre-exponential factor and  $E_{\alpha}$  is the activation energy. In some cases, a modified temperature dependence of the pre-exponential factor, provides a better fit to experimental data of computations.

$$k = AT^b \exp\left(-\frac{E_{\alpha}}{RT}\right) \quad (2.9)$$

The pre-exponential factor  $A$  is proportional to the number of collisions per unit volume and shows the fraction of collisions that have enough energy to proceed to reaction. The activation energy  $E_{\alpha}$  defines the energy barrier that the reactant species need to overcome in order to produce new species (products). It actually represents the bond energies in the molecule but it can also be smaller if new bonds are formed simultaneously with the breaking of old bonds.

### 2.3 Pressure Dependence of Rate Constants

For some dissociation and recombination reactions it is apparent that there is a pressure dependency which shows that these steps are not elementary. The steps follow a sequence of reactions that in some cases can be described with the Lindemann model [39], which states that a unimolecular decomposition is likely to occur when there is enough energy in the molecule to break the bond. So it is essential to add energy to the molecule through collisions with other molecules (M). The collisions may achieve the required excitation of the molecular vibrations so that the molecule can proceed to decomposition or it may deactivate the molecule through a second collision.



where  $A^*$  denotes the excited molecule and  $k_a$ ,  $k_{-a}$  and  $k_u$  are the rate coefficients of activation, deactivation and unimolecular reactions respectively. If the rate laws are applied to the above reactions

$$\frac{d[A^*]}{dt} = k_a [A][M] - k_{-a} [A^*][M] - k_u [A^*] \quad (2.12)$$

$$\frac{d[P]}{dt} = k_u [A^*] \quad (2.13)$$

Since  $A^*$  is an intermediate in the mechanism it is useful to assume that  $A^*$  is in steady state so the net rate equation of  $A^*$  production (2.12) is equal to zero. Hence, by solving the rate equations for  $A^*$  and P the following equation is obtained.

$$\frac{d[P]}{dt} = \frac{k_u k_a [A][M]}{k_{-a} [M] + k_u} \quad (2.14)$$

Under low-pressure conditions, the concentration of M is very low so the production rate becomes second order and takes into account both the species A and the collision partner. Under high-pressure conditions, the concentration of M is large so that the production rate becomes first order.

$$\frac{d[\text{P}]}{dt} = k_a [\text{A}][\text{M}] \quad (2.15)$$

$$\frac{d[\text{P}]}{dt} = \frac{k_u k_a}{k_{-a}} [\text{A}] = k_\infty [\text{A}] \quad (2.16)$$

## 2.4 Thermodynamics and Reaction Kinetics

All reaction in the mechanism are reversible and the equilibrium is dynamic. The reaction rates in both forward and reverse directions are equal at equilibrium and for a typical reaction (2.17) the following applies:



The relationships that apply at equilibrium are

$$\frac{r_f}{r_r} = \frac{k_f [\text{A}]_{eq} [\text{B}]_{eq}}{k_r [\text{C}]_{eq} [\text{D}]_{eq}} = 1 \quad (2.18)$$

$$\frac{k_f}{k_r} = \frac{[\text{C}]_{eq} [\text{D}]_{eq}}{[\text{A}]_{eq} [\text{B}]_{eq}} \quad (2.19)$$

$$\frac{k_f}{k_r} = K_{eq} \quad (2.20)$$

where  $r_f$  and  $r_r$  are the rates of the forward and reverse reactions. The subscript *eq* refers to equilibrium and  $K_{eq}$  is the equilibrium constant. Some times it is easier to

measure the rate in one direction and then, via the equilibrium constant, calculate the value of the reverse rate (2. 22). This may be the case for recombination reactions (2. 21)



$$k_{-2} = \frac{K_{eq}}{k_2} \quad (2. 22)$$

In order to calculate the reverse reaction rate, it is necessary to know  $K_{eq}$ . The equilibrium constant can be converted using  $K_{eq} = K_p/p^0(RT)^{-1}$ , where  $p^0$  is a standard pressure, and the standard Gibbs energy change  $\Delta G^0$

$$\Delta G^0 = -RT \ln \frac{K_p}{p^0} \quad (2. 23)$$

$$\Delta G^0 = \Delta H^0 - T\Delta S^0 \quad (2. 24)$$

it is obtained that

$$k_{-2} = (k_2 RT) \exp\left(\frac{-\Delta H_T^0}{RT}\right) \exp\left(\frac{\Delta S_T^0}{R}\right) \quad (2. 25)$$

where  $\Delta H_T^0$  and  $\Delta S_T^0$  are the standard enthalpy and entropy of reaction at temperature T.

## 2.5 Radical Reactions

Many gas-phase reactions proceed via a so-called chain mechanism where the links of the chain, the elementary reactions, are repeated over and over again. Such a mechanism involves free radical carriers, molecules, or atoms with one or more unpaired electrons and it consists of at least three steps [37]. The first is the *initiation* step that creates the radicals that carry the chain. This step is generally slow and usually involves thermal or photochemical dissociations of a relatively

stable reactant to form free radicals. Then, the mechanism proceeds via the *chain propagation* step, where a reactive species reacts with a stable species forming another reactive species, the *chain branching* step, where a reactive species reacts with a stable species forming two reactive species, and the *termination* step where the chain is broken by consuming the chain carrying radicals. An example of the above steps is shown in Table 2.1 which depicts some of the important  $H_2/O_2$  reaction steps.

	Reaction	Reaction Type
1	$H_2 + O_2 = 2OH$	Initiation
2	$OH + H_2 = H + H_2O$	Chain Propagation
3	$H + O_2 = OH + O$	Chain Branching
4	$H + O_2 + M = HO_2 + M$ $HO_2 + OH = H_2O + O_2$	Termination

Table 2.1 Reaction steps in the  $H_2/O_2$  mechanism

## 2.6 Collision Theory

In chemical kinetics it is well known that some reactions occur faster or slower than others and some have strong temperature dependencies while some do not have any. Hence, it is necessary to understand the physical meaning and magnitude of the assigned rate coefficient and its temperature dependence. As mentioned earlier, it is possible to estimate reaction rates using the collision theory.

According to this theory [40], it is assumed that the molecules are hard and structureless spheres. There is no interaction between them until they come into contact. Their dimensions remain the same even after collision and the closest distance equals to the sum of their radii. In order for the reaction to occur, an energy barrier which is expressed by an electron rearrangement needs to be overcome. All vibrational, translational and rotational motions of the molecules seemed of lesser

importance in the first instance and were neglected. In a gas temperature T, the molecules (A, B) follow a Maxwell distribution of speed with a mean value of

$$\bar{u} = (8k_A T / \pi\mu)^{\frac{1}{2}} \quad (2.26)$$

where  $\mu$  is the reduced mass,  $m_A m_B / (m_A + m_B)$  and  $k_A$  is known as the Boltzmann constant. Hence

$$Z_{AB} = C_A C_B \pi d^2 (8k_A T / \pi\mu)^{\frac{1}{2}} \quad (2.27)$$

where  $Z_{AB}$  is the collision number or collision frequency and represents the collision rate per unit volume for unit concentrations of A and B. Only the molecules that have sufficient kinetic energy will react in order to overcome an energy barrier  $E^0$ . Thus the rate of reaction is expressed by

$$k = Z \exp\left(\frac{-E^0}{RT}\right) \quad (2.28)$$

where  $Z = Z_{AB}/C_A C_B$  the collision frequency factor,  $E^0$  is the activation energy, R is the Avogadro constant and T is the temperature.



## Chapter 3

### Cyclopentadiene

#### 3.1 Introduction

The study of the chemical kinetics of aromatic hydrocarbons in combustion processes has become a main focus of combustion research. Apart from the environmental impact caused by soot formation, polyaromatic compounds have a biological impact on human health. However, detailed chemical models are often tentative. There is a limited amount of elementary reaction rate data in the literature, which is mostly focussed on single ring molecules, such as benzene and toluene. It is apparent that the benzene submechanism plays a significant role in soot formation and soot reduction processes. Benzene oxidizes to the phenoxy radical which decomposes to the cyclopentadienyl radical and  $CO$ . The cyclopentadienyl radical is subject to ring opening and forms a transition point between aromatic and aliphatic compounds [23].

Cyclopentadiene is thus an important intermediate species in combustion of single ring aromatics. The potential importance of the cyclopentadienyl radical in PAH growth has also been noted due to delocalised reactivity. The contribution of the cyclopentadienyl radical to the formation of aromatics has been reported in various studies [41-47]. Hence, an adequate knowledge of the cyclopentadienyl combustion chemistry is essential for the accurate modelling of the aromatic components of the aviation fuels.

The pyrolysis of cyclopentadiene has been extensively studied behind reflected shock waves [23, 48-52], but there is only one oxidation study in a plug flow reactor performed by Butler and Glassman [23]. It is generally agreed that the cyclopentadiene consumption under pyrolytic conditions begins with  $CH$  fission leading to the formation of the cyclopentadienyl radical plus a hydrogen atom (832).

However, there are significant differences in reaction rates obtained in the different studies.



Roy *et al.* [50] studied the pyrolysis of cyclopentadiene in argon mixtures over a pressure range of 0.7 to 5.6 bar and obtained a rate constant of  $k_{832} = 4.0 \times 10^{14} \exp(-322 \text{ kJ mol}^{-1}/RT) \text{ s}^{-1}$  for which they concluded that there was no pressure dependence. Kern *et al.* [52] studied cyclopentadiene pyrolysis at reduced pressures in the range 100-450 Torr and proposed a barrier of 351 kJ/mol for the *CH* fission. Colket *et al.* [51] proposed a rate constant of  $k_{832} = 2 \times 10^{15} \exp(-339 \text{ kJ mol}^{-1}/RT) \text{ s}^{-1}$  for a range of slightly higher pressures than the study of Roy *et al.* [50]. Zhong and Bozzelli [53] suggested a rate of  $k_{832} = 5.96 \times 10^{14} \exp(-314 \text{ kJ mol}^{-1}/RT) \text{ s}^{-1}$ , which was calculated using the Rice-Ramsperger Kassel (QRRK) approach at atmospheric pressure and a temperature range of 900-1300K. Comparison of the proposed rate constants above against temperature is shown in Figure 3.1.

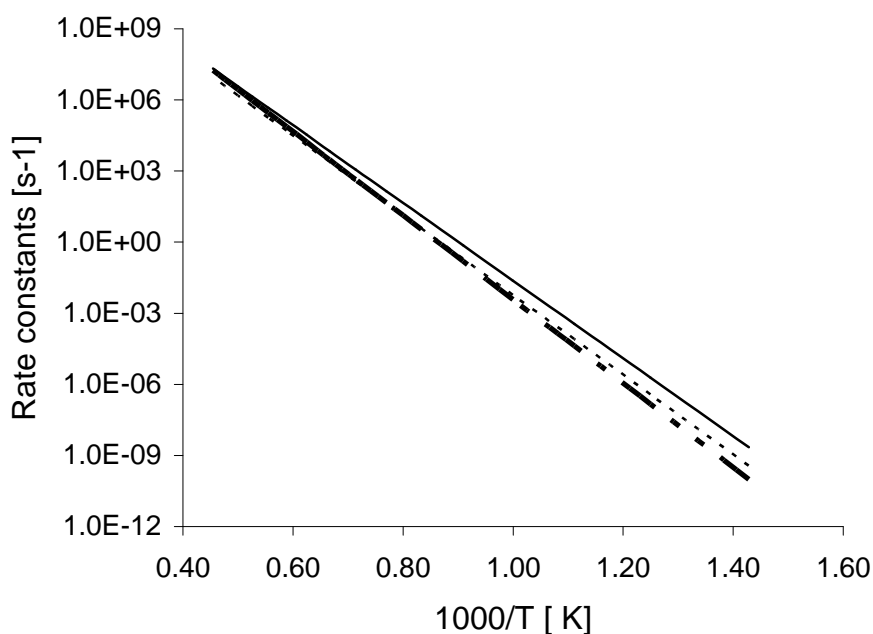


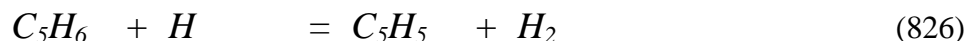
Figure 3.1 Arrhenius plot of the reaction rates proposed for the reaction  $C_5H_6 = C_5H_5 + H$ . The solid line indicates the rate determination of Zhong and Bozzelli [53], the dashed line indicates the rate determination of Roy *et al.* [50] and the dashed dotted line indicates the rate determination of Colket *et al.* [51]

In a recent study, Roy *et al.* [49] studied the reverse reaction, which involves the cyclopentadienyl recombination with a hydrogen atom (-832), behind reflected shock waves and a rate constant of  $k_{-833}=2.6 \times 10^{11} \text{ m}^3 \text{ kmol}^{-1} \text{ s}^{-1}$  was obtained at a pressure of 2 bar. Hence, in combination with previous study of the same group, an equilibrium constant  $K_c(T)$  for reaction (832) was calculated.



Moreover, data for the enthalpy of formation of the  $C_5H_5$  were obtained. Zhong and Bozzelli [53] have also proposed a high-pressure limit rate constant for reaction (-832):  $k_{-832}=3.2 \times 10^{11} \text{ m}^3 \text{ kmol}^{-1} \text{ s}^{-1}$ . The rate proposed was tested against the data of Lovell *et al.* [54] at 1 atm and 1100 K and there were discrepancies of about a factor of 2 between the model and measurements.

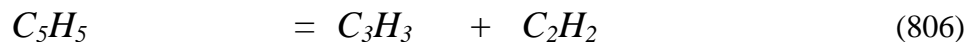
The  $H$  abstraction leading to the formation of the cyclopentadienyl radical and molecular hydrogen is another important reaction channel for the decomposition of cyclopentadiene.



Roy *et al.* [50] studied reaction (826) and obtained a rate constant of  $k_{826}=2.8 \times 10^{10} \exp(-9.45 \text{ kJ mol}^{-1}/RT) \text{ m}^3 \text{ kmol}^{-1} \text{ s}^{-1}$ . On the other hand Emdee *et al.* [55] have proposed a rate constant of  $k_3=2.19 \times 10^5 \times T^{1.77} \exp(-125 \text{ kJ mol}^{-1}/RT) \text{ m}^3 \text{ kmol}^{-1} \text{ s}^{-1}$ . Moskaleva and Lin [56] studied the reaction between hydrogen and cyclopentadiene at the modified Gaussian-2 level of theory and provided potential energy surfaces and reaction rates for the channel. The TST and RRKM calculations performed produced a rate constant for reaction channel (826) of  $k_{826}=3.03 \times 10^5 T^{1.71} \exp(-117 \text{ kJ mol}^{-1}/T) \text{ m}^3 \text{ kmol}^{-1} \text{ s}^{-1}$  valid for a temperature range  $1000 \text{ K} \leq T \leq 3000 \text{ K}$ . The study showed that the abstraction rate constant does not have any pressure dependency, but a positive temperature dependence. Moskaleva and Lin [56] also showed that apart from hydrogen abstraction, hydrogen addition to the cyclopentadiene ring should also be included.

The  $CH$  fission leading to the cyclopentadienyl radical is followed by  $C-C$  breakage and the formation of acetylene and the propargyl radical (806). Studies

have shown that this reaction is a multi-step process which leads to a stable intermediate and then a ring opening producing open chain radicals followed by the C-C fission for the formation of the final products [57].



Roy *et al.* [50] performed computations for reaction channel (806) and optimized the geometries of the cyclopentadienyl radical and of all the intermediates, the transition states and products at the UHF/6-31G\* level. According to their study, the cyclic  $C_5H_5$  decay is initiated by a 1,2-*H* transfer followed by a ring opening and isomerization to a number of straight chain radicals that lead to the formation of acetylene and propargyl radical. However, application of the proposed rate resulted in an over-prediction of acetylene concentration by a factor of three. Hence, they reduced the rate constant by a factor of three and achieved a good agreement with measurements. In addition to this study, Moskaleva and Lin [56] estimated the barrier heights of the 1,2 hydrogen transfer in the cyclopentadienyl radical (274.88 kJ/mol), ring opening (317.14 kJ/mol) and C-C breakage (317.14 kJ/mol), which are in agreement with values proposed by Roy *et al.* [50], which were obtained using a lower level computations [57]. Kern *et al.* [52] also obtained a rate constant for reaction (806) using Rice-Ramsperger-Kassel-Marcus (RRKM) computations. The 1,2-*H* migration was identified as the rate-limiting step with a barrier of 258.98 kJ/mol. The result is in contrast to Roy *et al.* [50] who proposed the ring opening as the rate limiting step. Kern *et al.* [52] also showed that there is a 10-fold reaction-path-degeneracy that arises from a facile pseudorotation in this Jahn-Teller molecule.

Cyclopentadiene, apart from the unimolecular decomposition leading to the formation of acetylene and propargyl radical which contribute to PAH growth, can also recombine with itself or its radical leading to the formation of naphthalene or indene [42, 58]. There are a number of studies that have exploited this potential formation mechanism. Melius *et al.* [42] studied the recombination of two cyclopentadienyl radicals that lead to the formation of naphthalene via a nine step mechanism that goes through the formation of hydrofulvalene and involves a three-membered ring closing and opening of resonance-stabilized radicals. Kislov and

Mebel [59] showed that at low temperatures naphthalene was the major product whereas at high temperatures fulvalene was the dominant one. Lu *et al.* [60] extended the mechanism of PAH growth of naphthalene formation from cyclopentadienyl recombination as proposed by Melius *et al.* [42] to compounds that contain four six-membered rings.

Marinov *et al.* [58] developed a chemical kinetic model for the formation of the polyaromatic hydrocarbons and the predicted species concentrations were compared against measurements obtained from rich sooting methane and ethane flames that were stabilized over a porous burner. They proposed that the cyclopentadienyl radical recombines to itself to the formation of naphthalene involving two hydrogen atom ejections. In the same study, a rate constant and an activation energy barrier was suggested based on the assumption that the rate limiting step of the  $C_5H_5$  recombination is the 34 kJ/mol barrier that accounts for the ejection of the first hydrogen atom of the bicyclopentadienyl adduct. However, Lindstedt *et al.* [61] and Lindstedt and Rizos [62] questioned the global reaction rate proposed by Marinov *et al.* [58], as computations that were performed showed that the naphthalene levels were 35 times higher than the measurements. Hence, an alternative two-step reaction featuring stabilization of  $C_5H_5-C_5H_4$  with a barrier of 34kJ/mol and the frequency factor of the global step proposed by Marinov *et al.* [58] was proposed [61]. The barrier utilized follows the recommendations of Melius *et al.* [42]. Moreover, McEnally and Pfefferle [63] performed experimental work with  $^{13}C$ -labeled aromatic compounds and showed that the labelled cyclopentadienyl moieties do not contribute to second ring formation.

The potential role of the cyclopentadienyl moieties in PAH growth was also studied by Mulholland and co-workers [64] using experimental analysis in a laminar flow reactor and the result suggest that indene, naphthalene and benzene are major products of cyclopentadiene pyrolysis. Apart from the cyclopentadienyl radical route to naphthalene, recombination has also been proposed as route to other aromatics. The importance of such reaction for PAH growth was extensively studied by Violi and co-workers [65-67], who proposed a two-step molecule-radical addition reaction mechanism followed by rearrangement. Wang *et al.* [41] applied this molecule radical mechanism in order to produce new pathways for the formation of indene and naphthalene during cyclopentadienyl pyrolysis. Four new reaction pathways for aromatic growth from cyclopentadiene pyrolysis were

proposed leading to naphthalene, indene and benzene via intramolecular addition, *C-H*  $\beta$ -scission and *C-C*  $\beta$ -scission. Density functional theory calculations were performed to calculate transition states, energy barriers for isomerizations,  $\beta$ -scission and dissociation reactions. Indene was mainly formed by intramolecular addition of the cyclopentadiene to cyclopentadienyl via a resonantly stabilised cyclopentadiene-cyclopentadienyl dimer.

Kislov and Mebel [68] also studied indene formation via the combination of cyclopentadiene and the cyclopentadienyl radical and showed that at temperatures relevant to combustion, indene was found to be the major product (>50%). The mechanism suggested, combined with their computed tests, was in agreement with experimental data for cyclopentadienyl pyrolysis that showed both naphthalene and indene as major products.

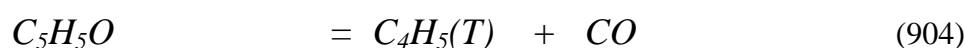
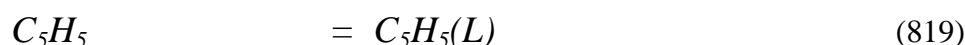
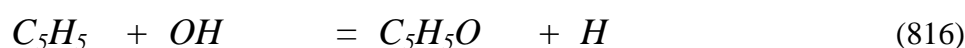
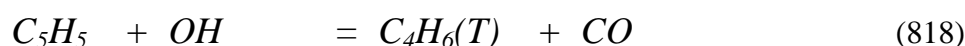
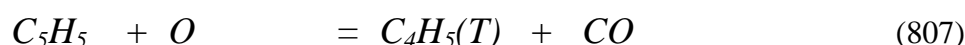
Another reaction route that involves the cyclopentadienyl radical features its combination with the methyl radical to the formation of fulvene ( $C_5H_4CH_2$ ), which latter isomerizes to benzene. Moskaleva *et al.* [69] studied this reaction route and showed that the combination of these two radicals produce an intermediate specie ( $C_5H_5CH_3$ ) that proceeds to the formation of  $C_5H_4CH_3$  and hydrogen atom. The hydrogen elimination occurs from the ring since the *C-H* bond is weaker than the relative one of the methyl group. The second hydrogen atom elimination comes from  $C_5H_4CH_3$  leading to the formation of fulvene. The reaction channel was also studied by Melius *et al.* [42] who underlined the importance of hydrogen migration around the cyclopentadienyl moiety in providing resonance-stabilized radicals and in further ring formation. These findings are also supported by a more recent study of Lindstedt and Rizos [62].

### 3.2 Modelling Approach

The starting point for the current work stems from previous studies related to the chemistry of aromatics [61, 62] as mentioned above, the oxidation of fine carbon based particles [70] and an earlier study by Zhong and Bozzelli [53].

The developed mechanism was validated under plug flow reactor conditions obtained by Butler [20]. Rates were analysed for both fuel lean and rich conditions

for temperatures varying from 1100 to 1200 K. The studies identified possible reaction channels featuring  $O$ ,  $OH$ ,  $HO_2$  and  $O_2$  though estimates of the rates of reaction proved problematic in some cases. Moreover, reaction rates for isomerization reactions, or thermal dissociation of oxygenated  $C_5$  species were also updated using PES determined via DFT and composite quantum mechanical computations [15]. Both RRKM/ME and VTST approach were used to derive estimates of the rate constants [15]. The rates of consumption and productions were also calculated for each species. The thermochemical data were obtained from literature sources [71] and when not available, were calculated with quantum mechanical methods using Gaussian-03 [15]. The reaction mechanism used here consists of 1431 reversible reactions involving 269 species with reverse rates computed via equilibrium constants.





Selected comparisons of the reaction rates of critical pathways such as (817) and (811) are shown in Figure 3.2 and Figure 3.3. It can be seen that the rate of reaction (811) which was derived using the RRKM/ME theory and VTST by Robinson [15] is slower than the one proposed by Zhong and Bozelli [53] for temperatures over 1000 K and the rate of reaction (817) is faster than the rate proposed by Zhong and Bozelli [53].



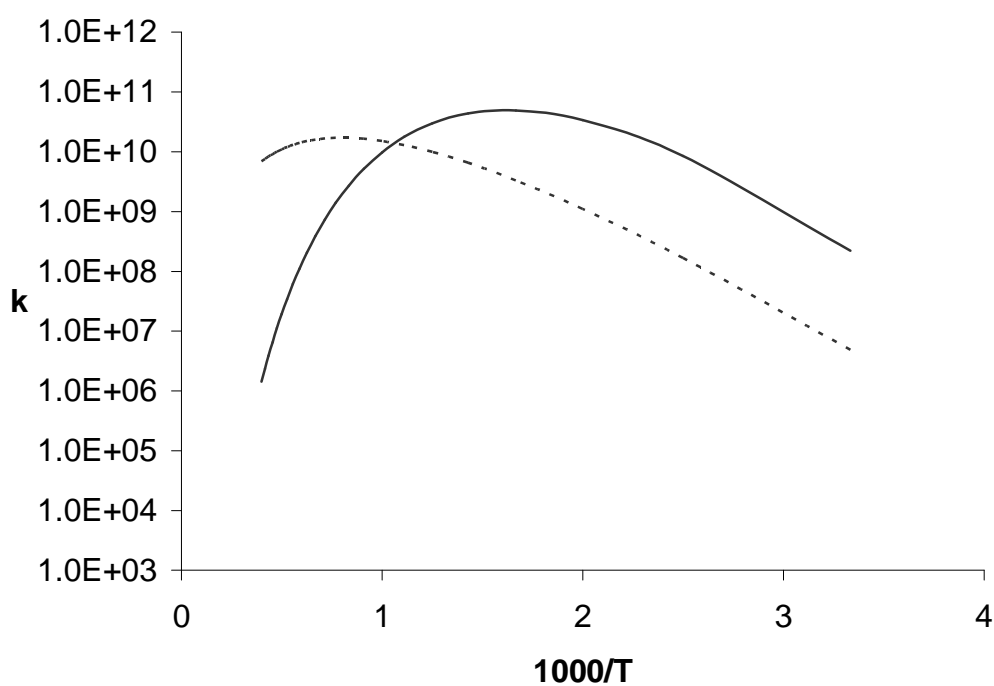


Figure 3.2 Arrhenius plot of the reaction rates of the critical pathway  $C_5H_5 + HO_2 = C_5H_5O + OH$ . The solid line indicates the rate used here which was derived using RRKM/ME theory [15] and the dotted line indicates the previously used rate adopted from Zhong and Bozelli [53]. Units are  $\text{kmol}, \text{m}^3, \text{s}, \text{K}$ .

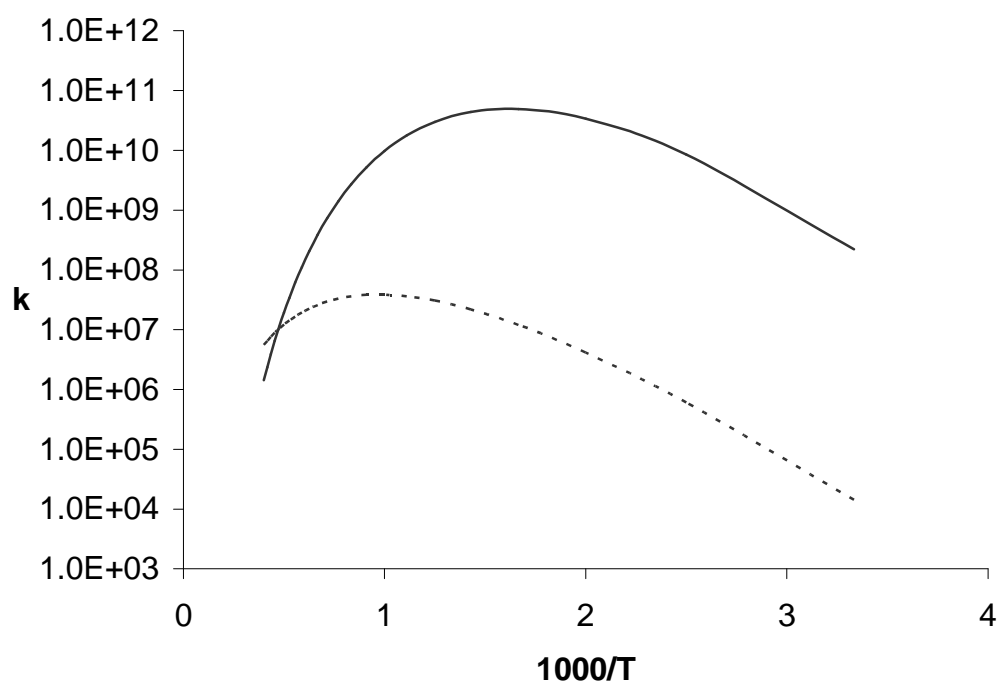


Figure 3.3 Arrhenius plot of the reaction rates of the critical pathway  $C_5H_5 + HO_2 = C_5H_4O + H_2O$ . The solid line indicates the rate used here which was derived using RRKM/ME theory [15] and the dotted line indicates the previously used rate adopted from Zhong and Bozelli [53]. Units are  $\text{kmol}, \text{m}^3, \text{s}, \text{K}$ .

### 3.3 Oxidation of Cyclopentadiene

The oxidation of cyclopentadiene was studied under plug flow reactor conditions obtained from Butler [20]. Three oxidation cases were computed for stoichiometric and rich fuel mixtures at atmospheric pressure utilizing nitrogen as the carrier gas. The conditions are presented in Table 3.1.

Case	$\Phi$	T init (K)	Initial Fuel (ppm)	Initial Oxygen (ppm)	Modelling Time Shift (msec)	Experimental Time Shift (msec)
1	1.03	1198	2243	14128	20	36
2	1.03	1148	1051	6618	50	123
3	1.61	1153	2070	8363	20	50

Table 3.1 Experimental and modelling conditions for cyclopentadiene oxidation in a flow reactor. (The experimental time shifts correspond to time shifting performed on modelling computations performed by Butler [20]).

Major species concentrations are predicted and compared to measurements as shown in Figure 3.4 to Figure 3.9. It can be seen that there is reasonably good agreement. However, surface chemistry interfering with the gas phase chemistry was identified as a problem by Butler [20] and some caution is hence required. Moreover, during the experimental studies, measurements showed an initial discontinuous drop in the fuel concentration at the first data point that was due to the recirculation zone in the diffuser and surface chemistry near the throat of the reactor [20]. Because of this, a time shift of the predictions is necessary in order to capture more accurately the species profiles.

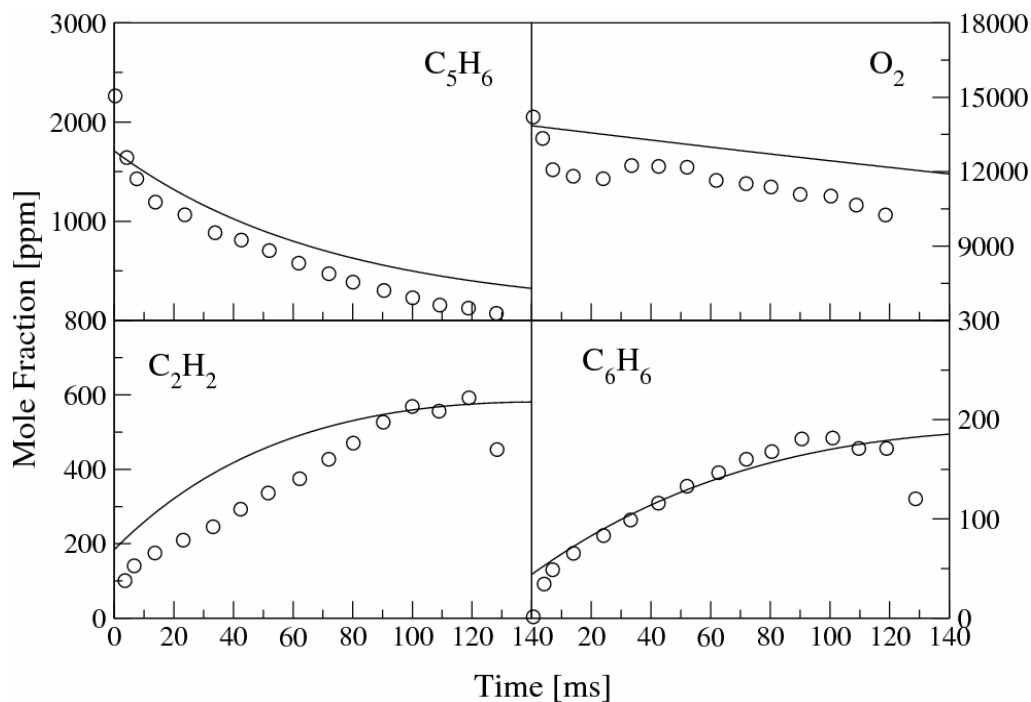


Figure 3.4 Concentration profiles during cyclopentadiene oxidation in a plug flow reactor for  $\Phi = 1.03$ ,  $P = 1$  atm,  $T = 1198$  K, initial fuel concentration 2243 ppm (Case 1 – see Table 3.1). Circles are measurements [20] and the solid line the current simulation

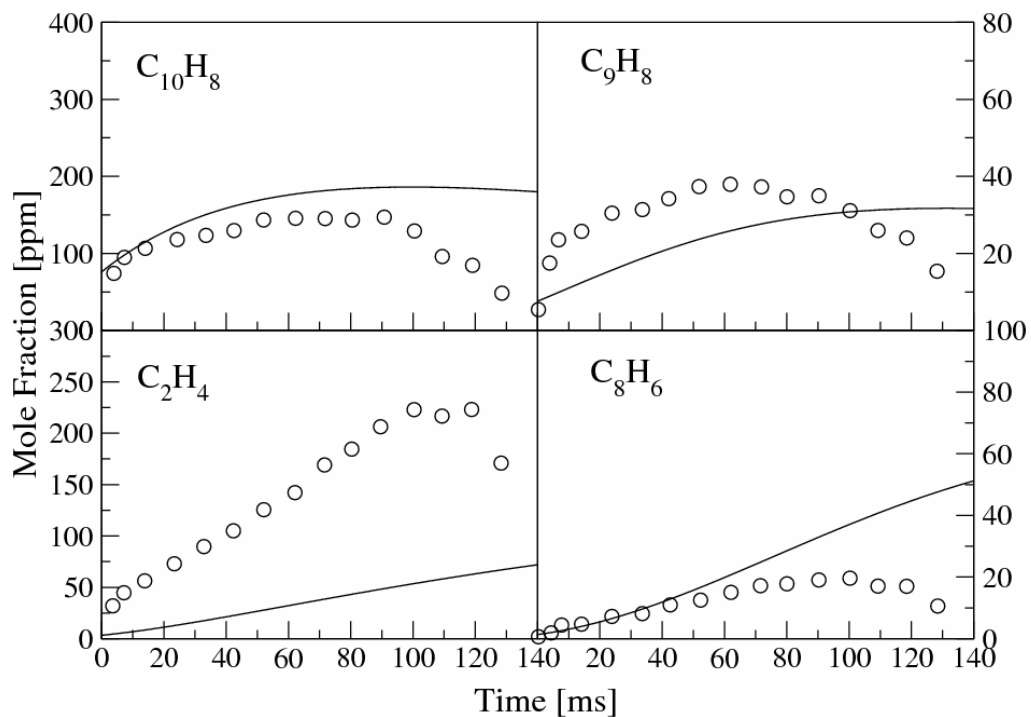


Figure 3.5 Concentration profiles during cyclopentadiene oxidation in a plug flow reactor for  $\Phi = 1.03$ ,  $P = 1$  atm,  $T = 1198$  K, initial fuel concentration 2243 ppm (Case 1 – see Table 3.1). Circles are measurements [20] and the solid line the current simulation

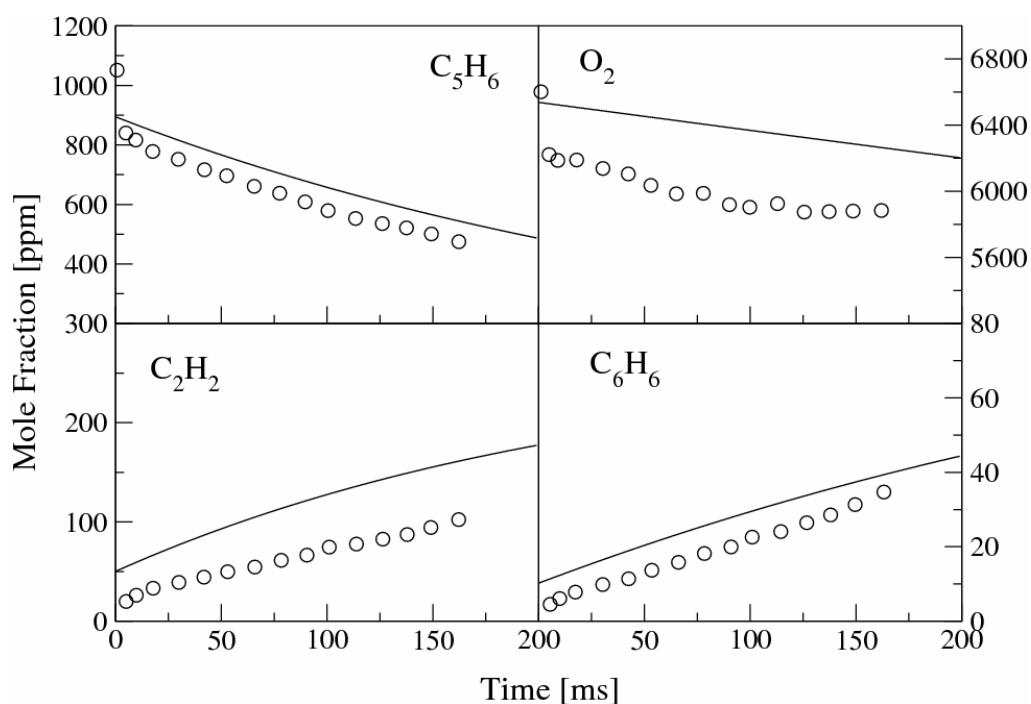


Figure 3.6 Concentration profiles during cyclopentadiene oxidation in a plug flow reactor for  $\Phi = 1.03$ ,  $P = 1$  atm,  $T = 1148$  K, initial fuel concentration 1050 ppm (Case 2 – see Table 3.1). Circles are measurements [20] and the solid line the current simulation

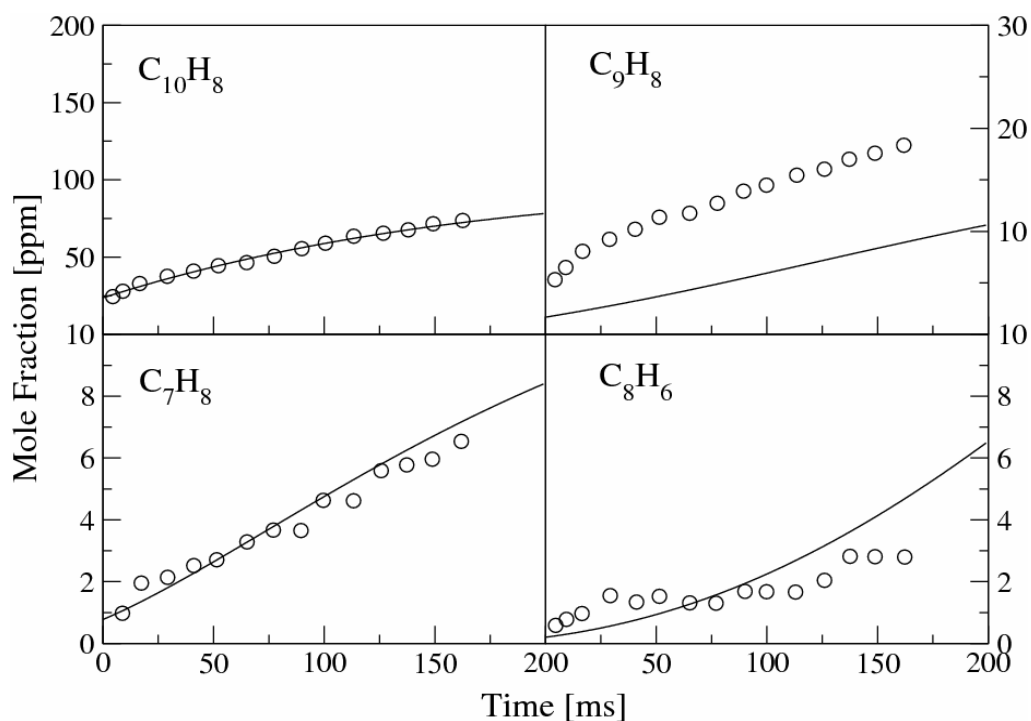


Figure 3.7 Concentration profiles during cyclopentadiene oxidation in a plug flow reactor for  $\Phi = 1.03$ ,  $P = 1$  atm,  $T = 1148$  K, initial fuel concentration 1050 ppm (Case 2 – see Table 3.1). Circles are measurements [20] and the solid line the current simulation

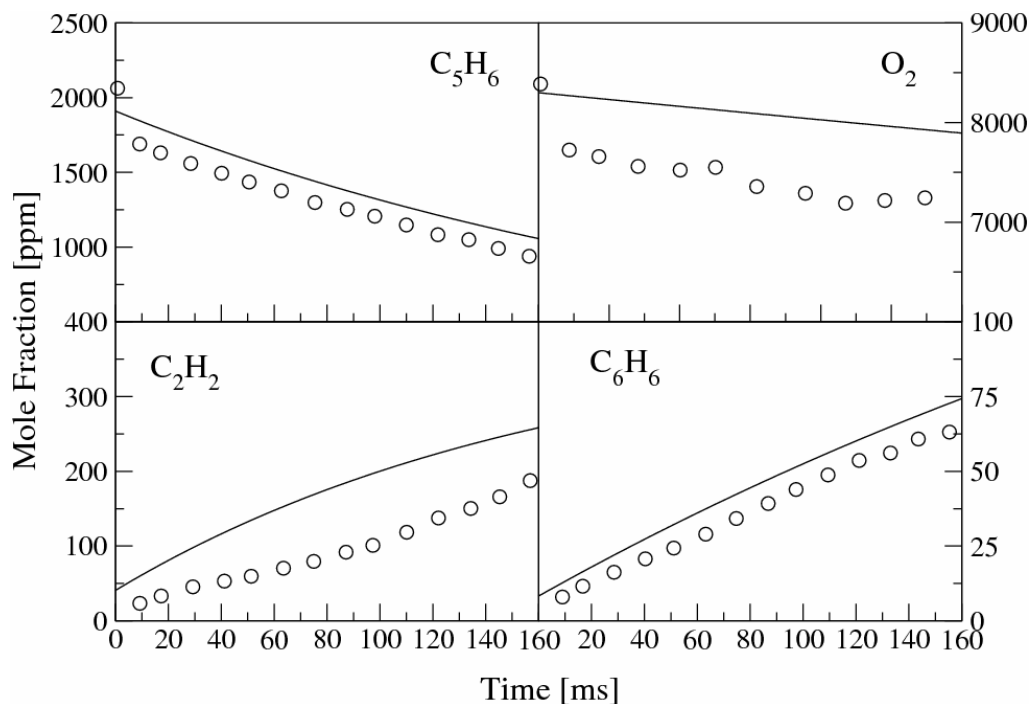


Figure 3.8 Concentration profiles during cyclopentadiene oxidation in a plug flow reactor for  $\Phi = 1.61$ ,  $P = 1$  atm,  $T = 1153$  K, initial fuel concentration 2070 ppm (Case 3 – see Table 3.1). Circles are measurements [20] and the solid line the current simulation

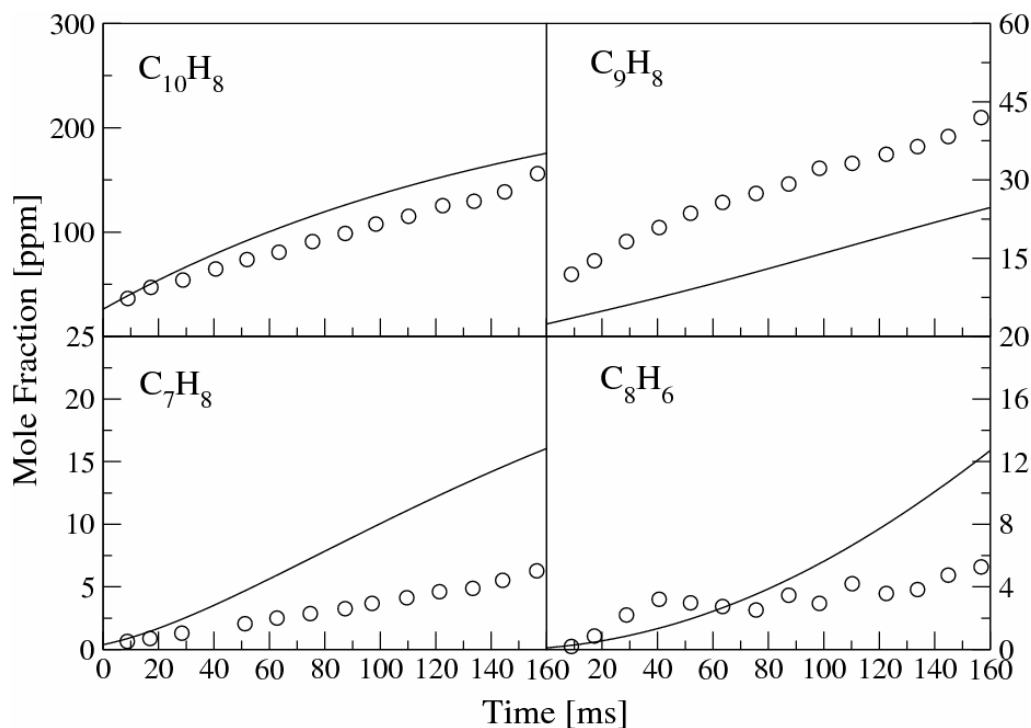
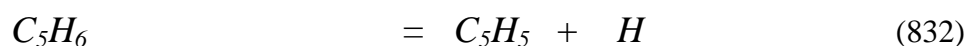
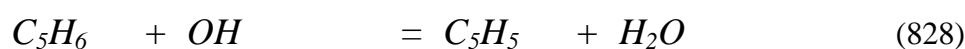
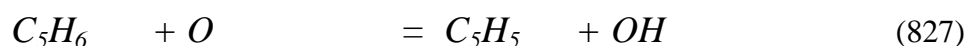


Figure 3.9 Concentration profiles during cyclopentadiene oxidation in a plug flow reactor for  $\Phi = 1.61$ ,  $P = 1$  atm,  $T = 1153$  K, initial fuel concentration 2070 ppm (Case 3 – see Table 3.1). Circles are measurements [20] and the solid line the current simulation

### 3.4 Reaction Rate Analysis for Cyclopentadiene Oxidation

A reaction rate analysis was performed for a stoichiometric fuel mixture with  $\Phi = 1.03$  at  $T = 1148$  K,  $P = 1$  atm and an initial fuel concentration of 1051 ppm. The fuel is consumed via four major channels that involve hydrogen abstraction via  $H$ ,  $O$  and  $OH$  radicals and thermal decomposition.



Reaction (826) is responsible for 35% of the total fuel consumption and is assigned with a rate proposed by Robinson [15]. The channel is of major importance as small perturbations to the reaction rate causes big differences at the fuel consumption profile. Approximately 25% of the fuel decay proceeds via reaction (828) that was assigned a rate proposed by Rizos [72]. A rate discussed by Leung and Lindstedt [73] is used for reaction (827), which consumes a further 10%. Reaction (832) is responsible for 12% of the total fuel consumption and was assigned a rate proposed by Kern *et al.* [52].

Approximately 86% of the fuel consumption leads to the cyclopentadienyl radical. The consumption of  $C_5H_5$  follows two major routes as shown in Figure 3.10. The  $C_5H_5$  recombination pathway leading to  $C_{10}H_9F$  (813) is responsible for 33% of the consumption and was assigned a rate proposed by Lindstedt *et al.* [61]. The second major consumption channel (33%) occurs via thermal decomposition of the cyclopentadienyl radical via C-C scission leading to acetylene and the propargyl radical (806). The channel is of significant importance and affects the temporal evolution of the acetylene concentration profile. A rate of Kern *et al.* [52] was also evaluated, but found to lead to an overproduction of acetylene by 50%. Hence an adjustment by a factor of 2 was applied leading to more reasonable acetylene profiles.

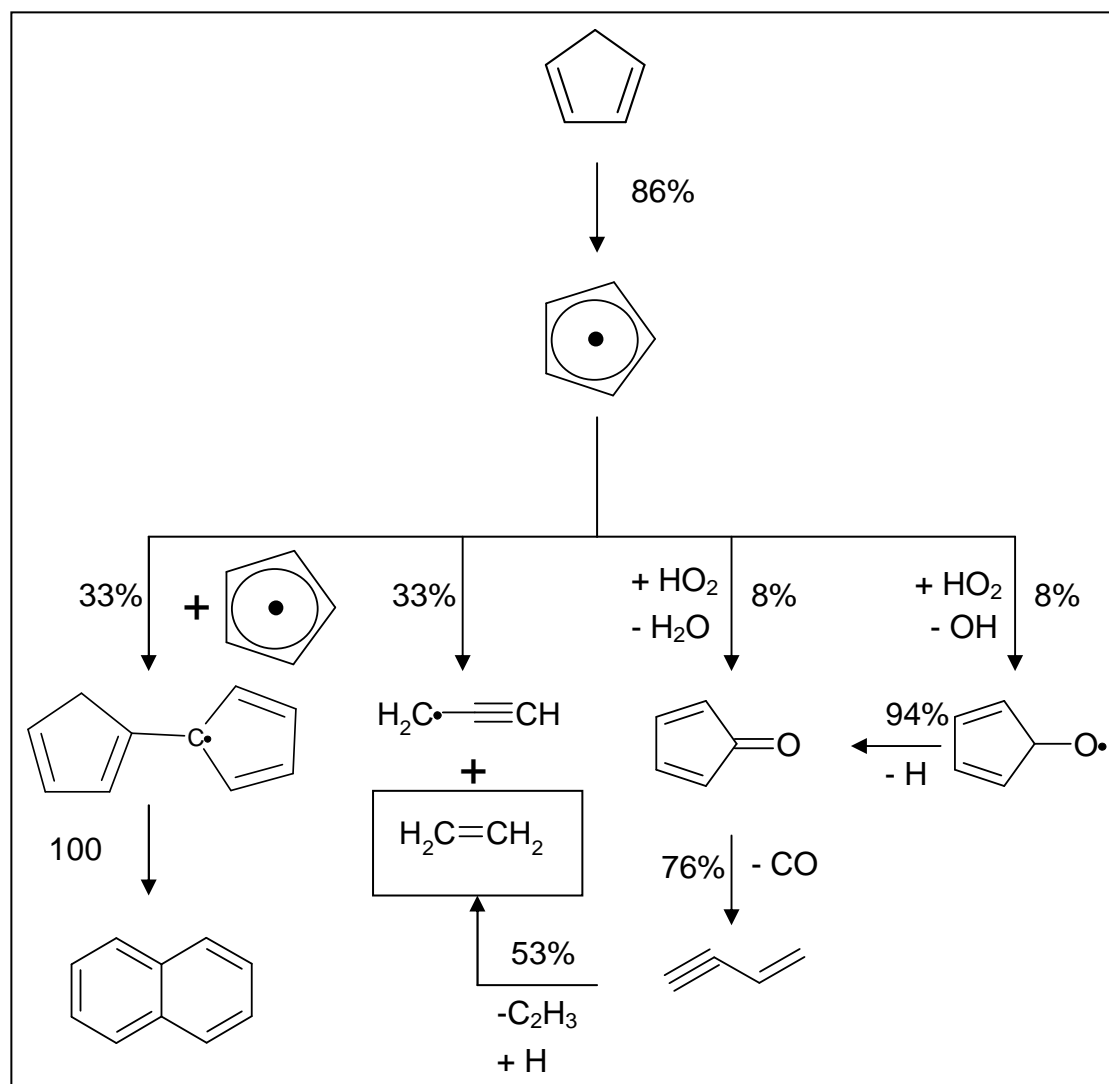
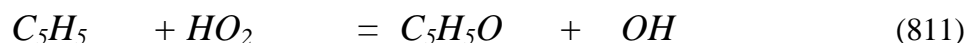
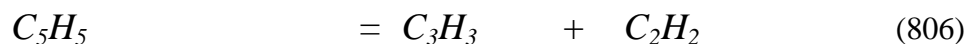


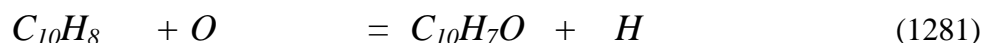
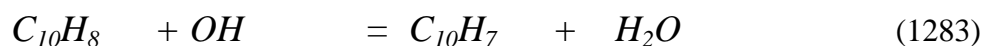
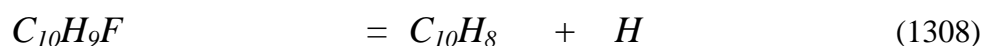
Figure 3.10 Major cyclopentadiene consumption pathways in a plug flow reactor for  $\Phi = 1.03$ ,  $T = 1148 \text{ K}$ , initial fuel concentration of 1051 ppm.



The oxidation channels featuring  $HO_2$  attack leading to the formation of  $C_5H_4O$  (817) and  $C_5H_5O$  (811) are each responsible for 8% of the  $C_5H_5$  consumption.

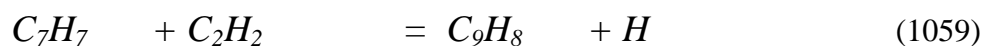


The  $C_{10}H_9F$  is a precursor to naphthalene, which subsequently is formed via hydrogen thermal dissociation (1308). Naphthalene decomposes through two major reaction channels that involve hydrogen abstraction (1283) via  $OH$  (49%) and oxygen addition (1281) forming  $C_{10}H_7O$  (39%) that utilize rates adopted from the kinetics of benzene and adjusted according to molecular weight differences.

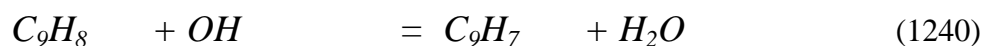
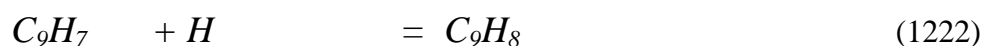
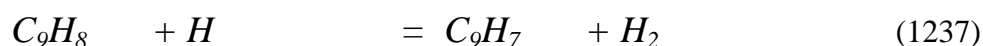


Indene is formed predominantly (48%) through acetylene recombination with the benzyl radical (1059). The rate assigned to this channel was adopted from Colket *et al.* [74]. An additional 44% of the indene formation comes from the recombination of cyclopentadiene and cyclopentadienyl radical (831) with the simultaneous abstraction of a methyl radical. The reaction channels was studied extensively by Wang *et al.* [41], who proposed possible intermediate routes for the naphthalene and indene formation via  $C_5H_6$  and  $C_5H_5$  recombination.

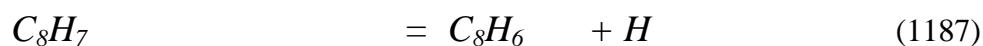
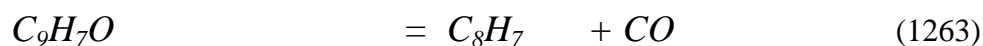
In this study it is assumed that the recombination of these two species does not stabilize to the formation of the CPD-CPDyl intermediate but to a bridged intermediate specie with the radical on the bridged atom. The highest energy barrier (177.11 kJ/mol) that occurs from the conversion of this bridged specie to the final indene molecule through other intermediate routes, as discussed by Wang *et al.* [41], is used as the activation energy of the global step (see Figure 3.11).



Indene decomposes solely to the indenyl radical via three major reaction routes. Reaction (1237) is responsible for 59% of the indene consumption, (1222) for 21% and (1240) 12% respectively. Reaction rates utilized for these three indenyl consumption routes are adopted from suggestions of Potter [75] based on the kinetics of cyclopentadiene with reaction rates proposed by Lindstedt and Rizos [62] and Rizos [72].



Approximately 63% of the total indenyl radical comes from indene and 23% is produced via CO expulsion of the  $C_{10}H_7O$ , which is one of the major products of the naphthalene decay. The indenyl radical is the precursor of phenylacetylene via the formation of  $C_9H_7O$ . The indenyl radical oxidizes to  $C_9H_7O$  (83%) via  $HO_2$  reaction. The reaction rate utilized for this channel was obtained from Lindstedt *et al.* [70]. The  $C_9H_7O$  decomposes to  $C_8H_7$  (100%) via CO thermal expulsion followed by hydrogen thermal dissociation of the  $C_8H_7$  to the formation of phenylacetylene.



Phenylacetylene is consumed via four major reaction pathways that predominantly feature oxygen attacks. The displacement of the chain via oxygen attack is responsible for 33% of the phenylacetylene consumption (1163) and the step features a rate suggested by Lindstedt *et al.* [61]. The second major channel

(22%) involves hydrogen abstraction via  $OH$  (1154). A rate adopted by Frenklach *et al.* [76] was assigned to this channel.

Moreover, reactions (1162) and (1151) involve hydrogen abstraction/oxygen addition and consume 12% and 11% of styrene, respectively. Rates applied to these channels were adopted from Potter [75].

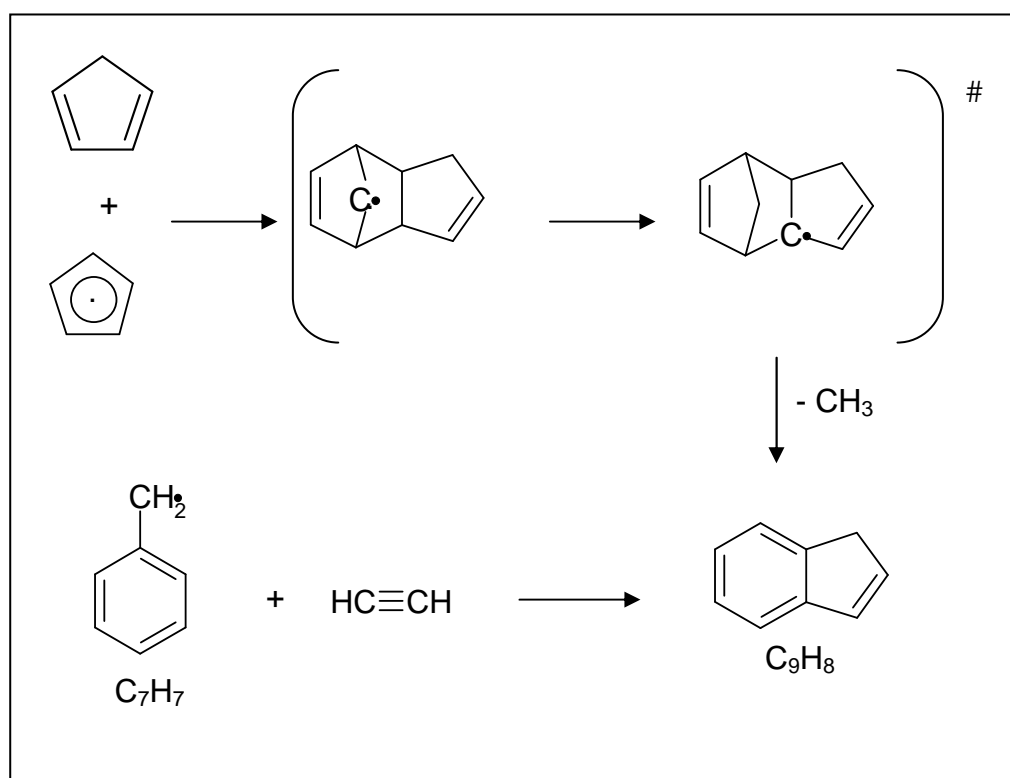
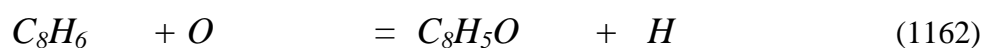
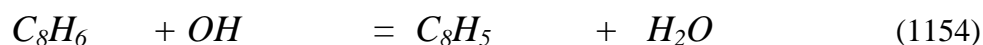
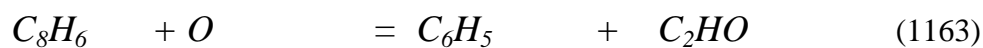
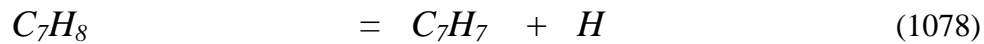
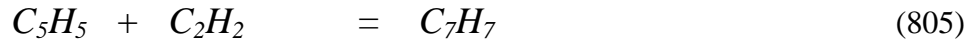


Figure 3.11 Major indene formation channels in a turbulent flow reactor for  $\Phi = 1.03$ ,  $P = 1$  atm,  $T = 1148$  K and cyclopentadiene concentration of 1051 ppm.

Toluene is formed from the benzyl radical, with the formation of benzyl radical controlled via one major reaction. The recombination of the cyclopentadienyl radical with acetylene is responsible for 84% of the total benzyl radical pool. The rate for the channel was adopted from Colket and Seery [77].

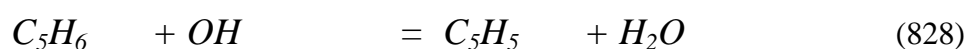


Approximately 22% of toluene leads to the formation of benzene through a chain displacement reaction via hydrogen. However, benzene is predominantly formed (94%) through isomerisation reaction from fulvene (980). The isomerization of  $C_6H_6(F)$  to benzene is assigned a rate proposed by Marinov *et al.* [78]. Fulvene is mostly produced via isomerization reactions from  $C_6H_6(S)$  (43%) and  $C_6H_6(B)$  (26%) and via thermal hydrogen dissociation (26%) from  $C_5H_4CH_3$ . The methyl cyclopentadienyl radical is formed via recombination of the methyl radical with  $C_5H_5$  (93%) and was assigned a rate adopted from suggestions of Lindstedt *et al.* [61].

Acetylene is predominantly formed (77%) by the thermal decomposition of the cyclopentadienyl radical.



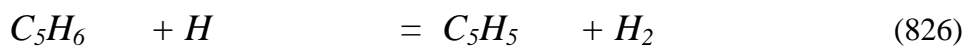
A reaction rate analysis was also performed for a fuel rich mixture with  $\Phi = 1.61$  at  $T = 1153$  K,  $P = 1$  atm and initial fuel concentration of 2070 ppm. The fuel consumption follows the same routes as in the stoichiometric case. However, the impact of reaction (826) increases by 4% and the impact of reactions (828) and (837) reduces by 4-5% compared to the stoichiometric case.



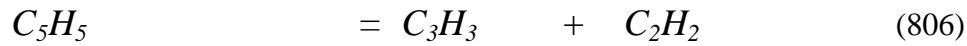
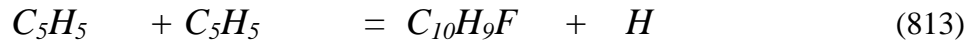
The cyclopentadienyl radical follows two major consumption under fuel rich conditions, as was the case for the stoichiometric conditions. In the latter case, 38% of the  $C_5H_5$  recombines with itself leading to  $C_{10}H_9F$  and 26% thermally decomposes acetylene and the propargyl radical. The reactions featuring  $HO_2$  attack and leading to formation of  $C_5H_5O$  and  $C_5H_4O$  perform similarly to the stoichiometric case and found to be responsible for 8% of total cyclopentadienyl consumption.

The naphthalene, indene, styrene, toluene, butadiene and acetylene formation and consumption routes follow the same behaviour as in stoichiometric mixtures with a perturbation of order 4-6% for each of the steps.

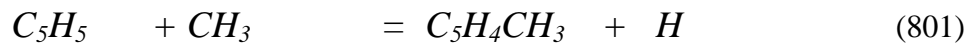
Apart from the rate analysis performed for a temperature range of 1149 – 1153 K, a test was also performed for a stoichiometric fuel mixture oxidation (Case 1 - Table 3.1) at the temperature of  $T = 1198$  K in order to identify important pathways of the fuel decomposition. Reactions (826) and (828) are found to be dominant contributing 33% and 27% to the fuel consumption. Moreover, reaction (827) is responsible for 12% of the total fuel consumption at higher temperatures.



Moreover, it should be highlighted that once the cyclopentadienyl radical is formed, its consumption is controlled by two dominant reaction channels that are identical to the  $C_5H_5$  consumption route for rich mixtures, with the difference that the role of these reactions (813) and (806) is now reversed. The impact of reaction (806) increases from 32% at stoichiometric fuel mixtures and  $T = 1149$  K and 26% for rich mixtures of the same temperature, to 34% for stoichiometric mixtures at a temperature of  $T = 1198$  K. Whereas the contribution of the cyclopentadienyl recombination reaction falls from 38% for rich mixtures or 33% at stoichiometric mixtures of  $T = 1150$  K, to 24% at stoichiometric mixtures and higher temperatures. Accordingly, the more the temperature increases, the more the thermal decomposition of the  $C_5H_5$  dominates consumption.



The increased impact of the thermal decomposition route of the  $C_5H_5$ , is responsible for the excessive propargyl radical and acetylene. The propargyl radical pool follows a recombination route that produces benzene. Hence, as expected, the benzene concentration is increased by 62% at the temperature of  $T = 1198$  K compared to the  $T = 1150$  K cases (see Figure 3.4 and Figure 3.6). Moreover, the concentration of benzene is affected by the increased contribution of reaction (801) leading to  $C_5H_4CH_3$ , which is the precursor to fulvene.



The formation and consumption routes of the rest intermediate species such as indene, phenylacetylene, toluene follow the same behaviour as in lower temperatures.

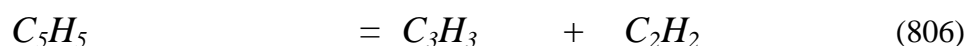
### 3.5 Pyrolysis of Cyclopentadiene

The pyrolysis of cyclopentadiene was studied under plug flow reactor conditions corresponding to the experimental studies of Butler [20]. Five pyrolysis cases were computed and concentrations of the reactants and intermediate species were compared to measurements of Butler [20]. The evolution of the species concentrations over time are presented in Figure 3.12 to Figure 3.20. The concentration of the fuel varies from 1000 to 3000 ppm and the temperature varies from 1100 to 1200 K (see Table 3.2). Due to the absence of oxygen, the consumption is slower and especially the fuel profile follows an approximately linear trend.

Case	T init (K)	Initial Fuel (ppm)
1	1147	2083
2	1148	1044
3	1147	3081
4	1106	2094
5	1202	2077

Table 3.2 Experimental and modelling conditions for cyclopentadiene pyrolysis in a flow reactor

It must be highlighted that the computations performed for the cyclopentadiene pyrolysis utilising the current chemical model caused overproduction of acetylene and benzene and showed corresponding discrepancies due to the impact of reaction (806). More specifically, the rate of Kern *et al.* [52] used in the oxidation cases was responsible for a 133% increase of the computed acetylene concentrations and 200% increase of the benzene concentration as compared to the rate proposed by Robinson [15]. Hence, for the pyrolysis cases only, a modification to the rate of reaction (806) was applied and the rate suggested by Robinson [15] was adopted.



As can be seen from the comparisons between the predicted species concentration profiles and the measurements obtained by Butler [20] there is a reasonably good agreement. The model captures the fuel profile very well indicating that the initiation reactions are satisfactory. The acetylene profiles show an overprediction that applies to all the tested cases at the temperature range of  $T = 1100 - 1150$  K. Good agreement is obtained for the benzene and naphthalene species showing that the steps leading to their formation and consumption are also well represented

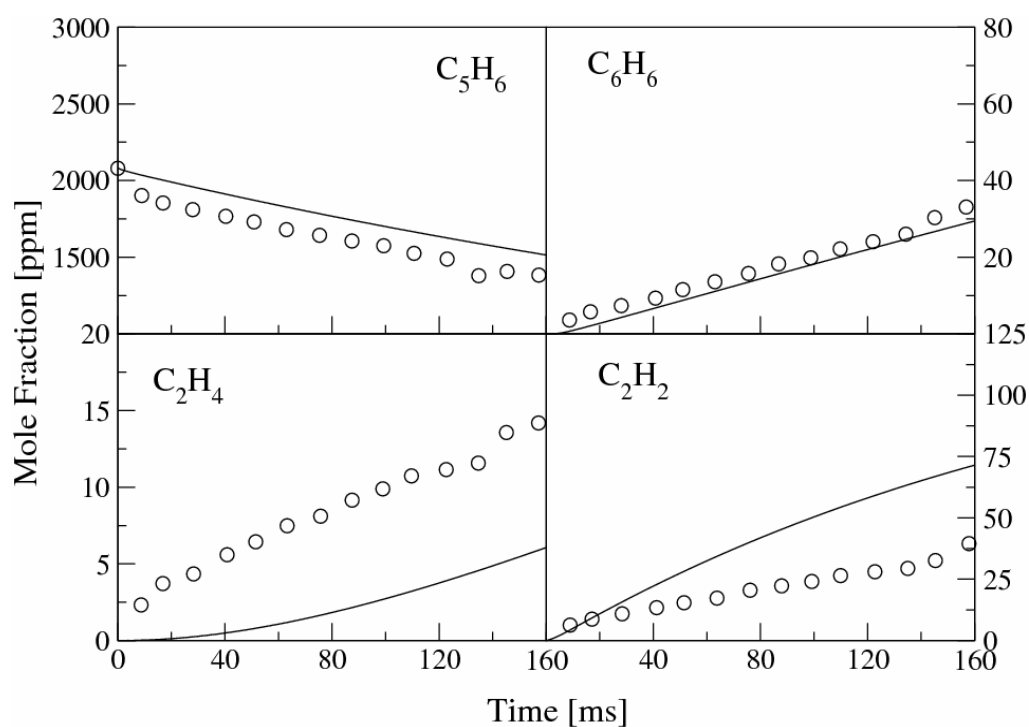


Figure 3.12 Concentration profiles during cyclopentadiene pyrolysis in a plug flow reactor at  $P = 1$  atm,  $T = 1147$  K, initial fuel concentration 2083 ppm (Case 1 – see Table 3.2). Circles are measurements [20] and the solid line the current simulation

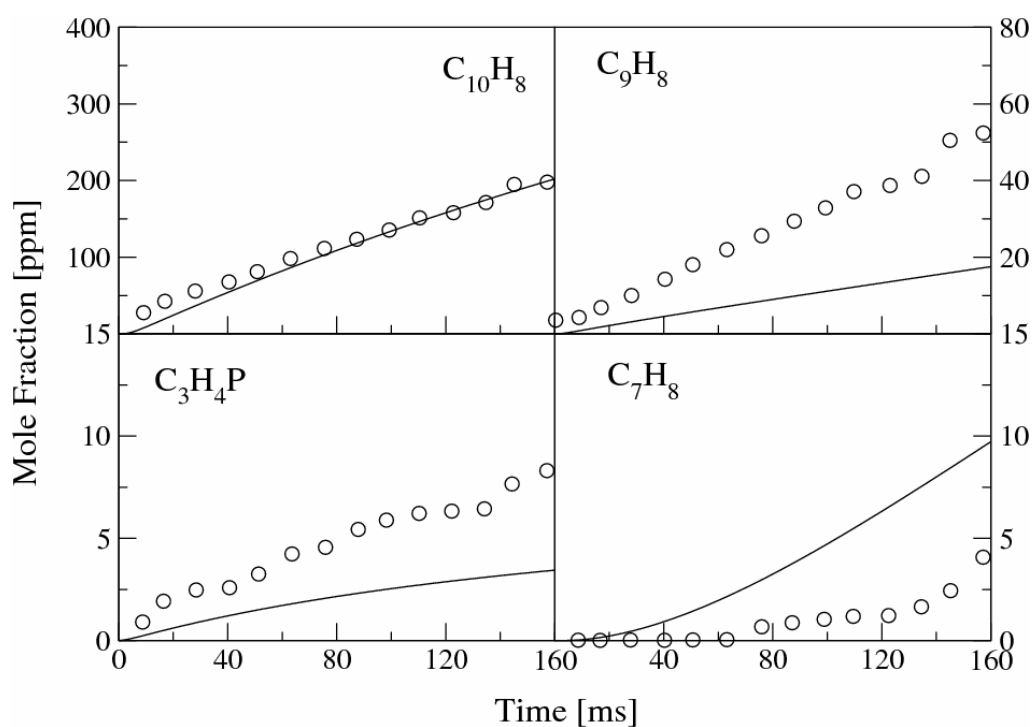


Figure 3.13 Concentration profiles during cyclopentadiene pyrolysis in a plug flow reactor at  $P = 1$  atm,  $T = 1147$  K, initial fuel concentration 2083 ppm (Case 1 – see Table 3.2). Circles are measurements [20] and the solid line the current simulation



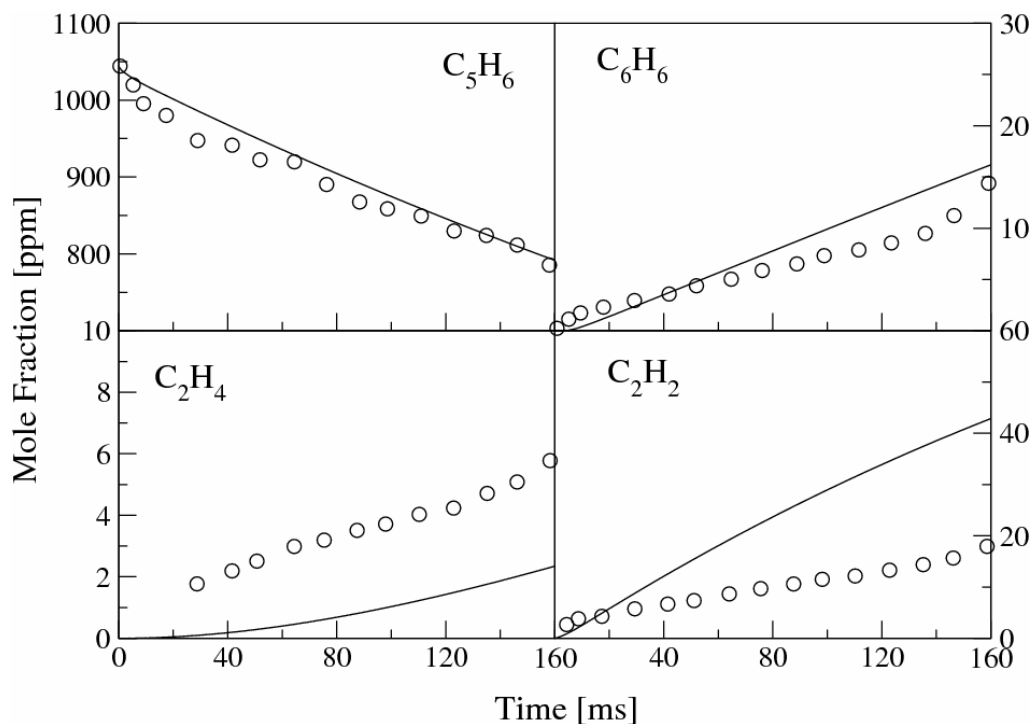


Figure 3.14 Concentration profiles during cyclopentadiene pyrolysis in a plug flow reactor at  $P = 1$  atm,  $T = 1148$  K, initial fuel concentration 1044 ppm (Case 2 – see Table 3.2). Circles are measurements [20] and the solid line the current simulation

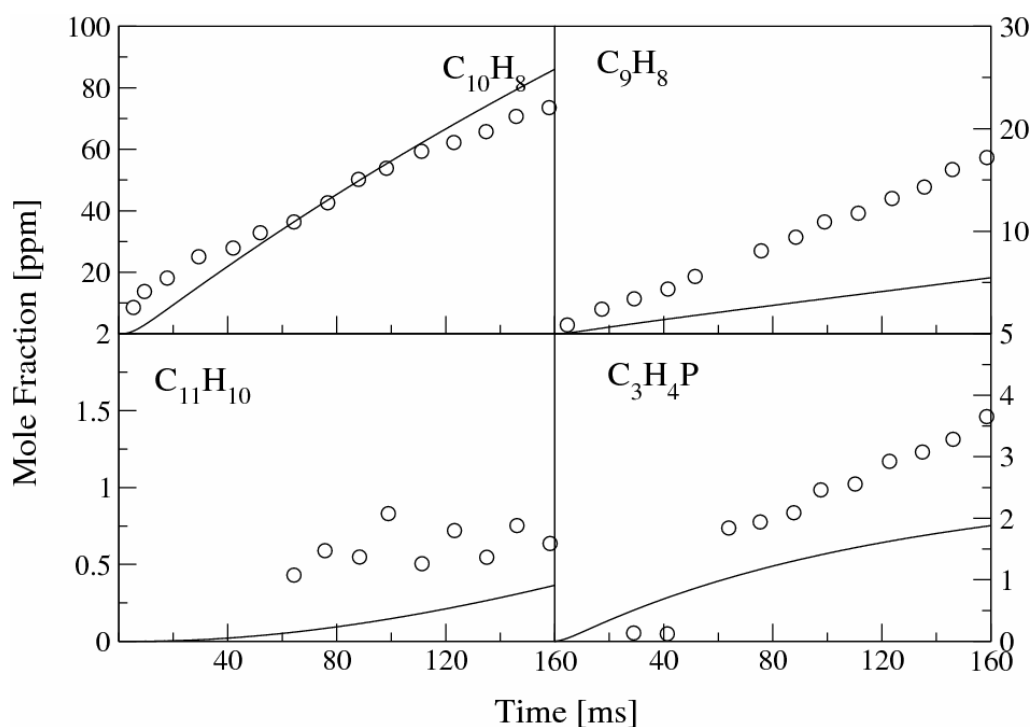


Figure 3.15 Concentration profiles during cyclopentadiene pyrolysis in a plug flow reactor at  $P = 1$  atm,  $T = 1148$  K, initial fuel concentration 1044 ppm (Case 2 – see Table 3.2). Circles are measurements [20] and the solid line the current simulation

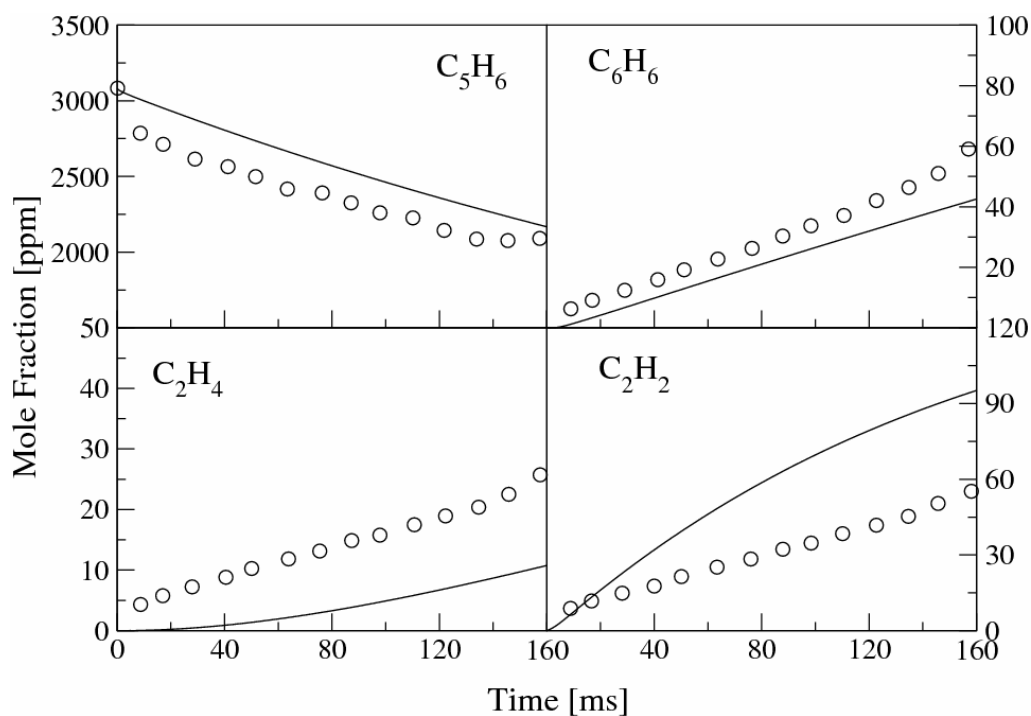


Figure 3.16 Concentration profiles during cyclopentadiene pyrolysis in a plug flow reactor at  $P = 1$  atm,  $T = 1147$  K, initial fuel concentration 3081 ppm (Case 3 – see Table 3.2). Circles are measurements [20] and the solid line the current simulation

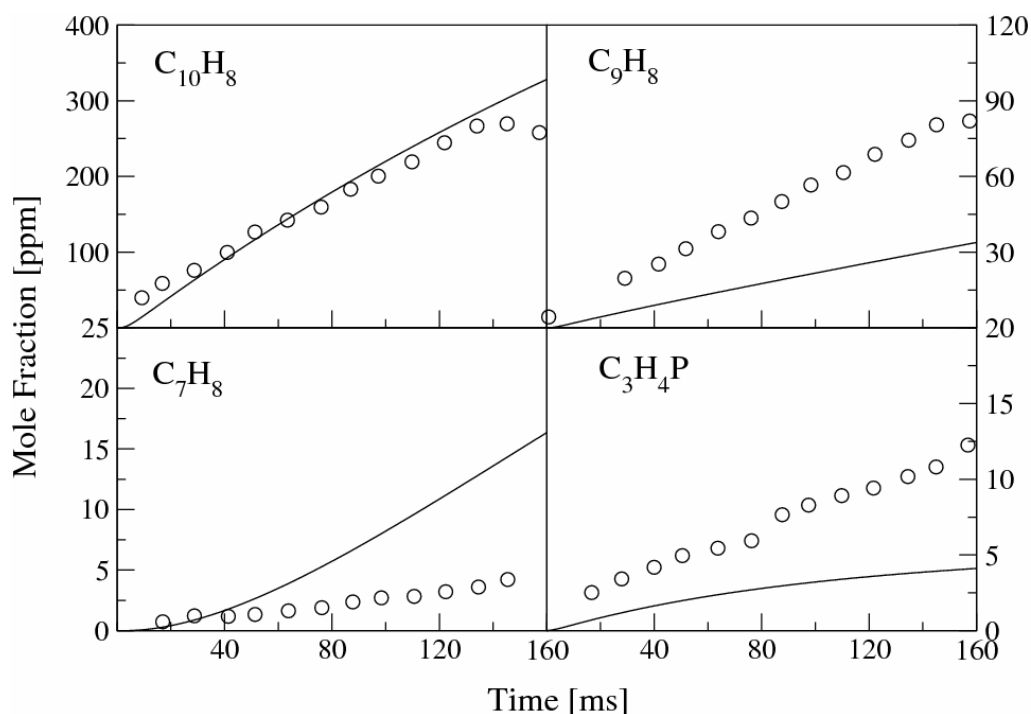


Figure 3.17 Concentration profiles during cyclopentadiene pyrolysis in a plug flow reactor at  $P = 1$  atm,  $T = 1147$  K, initial fuel concentration 3081 ppm (Case 3 – see Table 3.2). Circles are measurements [20] and the solid line the current simulation

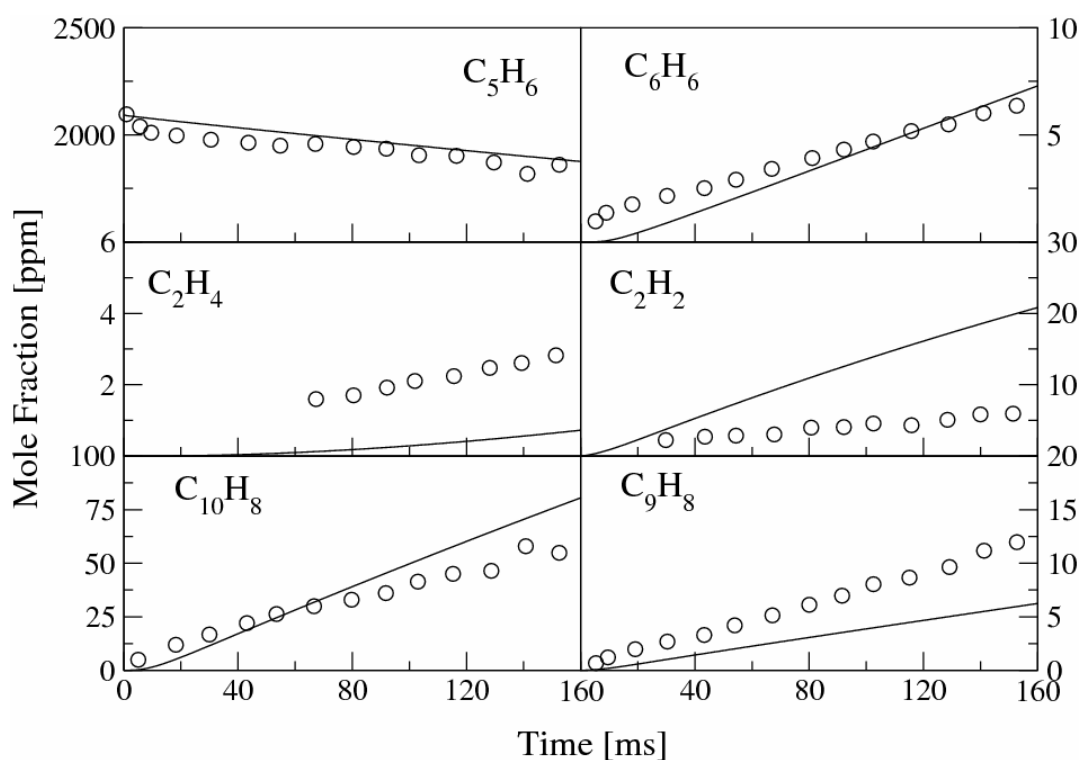


Figure 3.18 Concentration profiles during cyclopentadiene pyrolysis in a plug flow reactor at  $P = 1$  atm,  $T = 1106$  K, initial fuel concentration 2094 ppm (Case 4 – see Table 3.2). Circles are measurements [20] and the solid line the current simulation

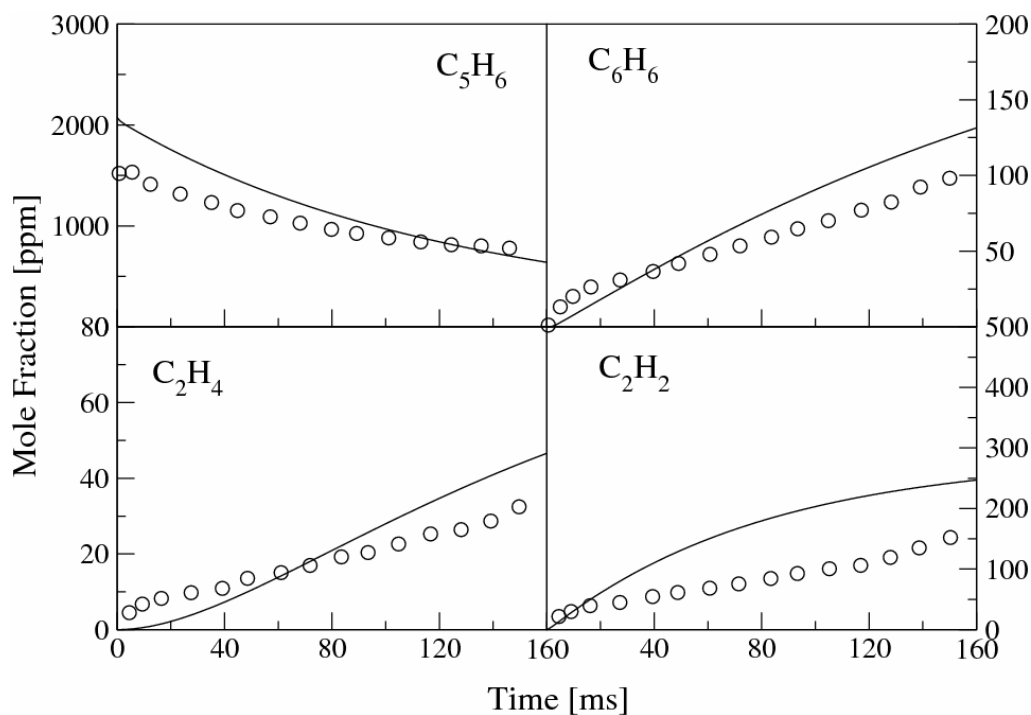


Figure 3.19 Concentration profiles during cyclopentadiene pyrolysis in a plug flow reactor at  $P = 1$  atm,  $T = 1202$  K, initial fuel concentration 2077 ppm (Case 5 – see Table 3.2). Circles are measurements [20] and the solid line the current simulation

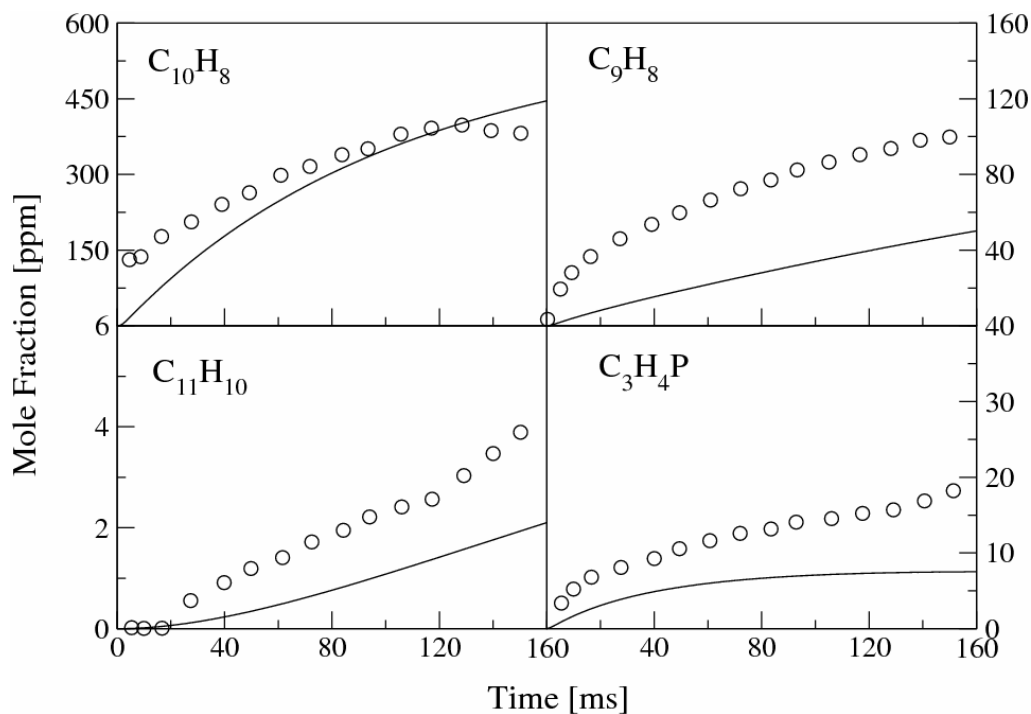
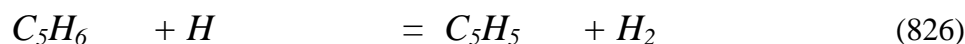


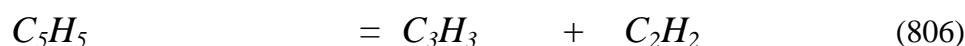
Figure 3.20 Concentration profiles during cyclopentadiene pyrolysis a plug flow reactor at  $P = 1$  atm,  $T = 1202$  K, initial fuel concentration 2077 ppm (Case 5 – see Table 3.2). Circles are measurements [20] and the solid line the current simulation

### 3.6 Reaction Rate Analysis for Cyclopentadiene Pyrolysis

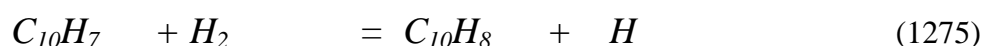
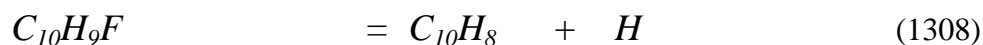
A reaction rate analysis was performed for the thermal decomposition of cyclopentadiene at atmospheric pressure, a temperature of  $T = 1147$  K and initial fuel concentration of 2083 ppm. The consumption is slower due to the absence of oxygen and the decomposition is controlled by the generation of radicals such as  $H$ ,  $CH_3$ . The fuel decomposes via one major channel (74%) that involves hydrogen abstraction via  $H$  atom attack leading to the formation of cyclopentadiene and molecular hydrogen (826). An additional 15% of the  $C_5H_6$  decomposes via thermal dissociation producing a hydrogen atom (832).



The cyclopentadienyl radical recombines with itself (82%) leading to the formation of  $C_{10}H_9F$ . Reaction (806) is responsible for not more than 9% of the total consumption of  $C_5H_5$ .

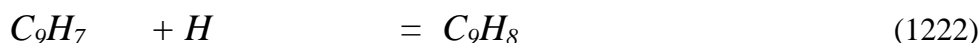
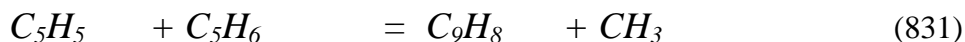


The  $C_{10}H_9F$  lead to the naphthalene formation via reaction (1308). Naphthalene forms naphthyl radical via hydrogen abstraction (-1275) that is responsible for 86% of the total naphthalene consumption.

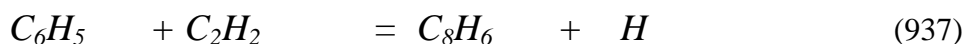


Indene is formed predominantly via recombination of  $C_5H_5$  and  $C_5H_6$  (831) with simultaneous methyl radical abstraction (72%). This is in contrast to the oxidation case, where indene is formed approximately 60% via acetylene addition to

the benzyl radical (1059) and only 30% by  $C_5H_6$  and  $C_5H_5$  recombination. During pyrolysis, the acetylene addition to the benzyl radical (1059) accounts for no more than 10% of the total indene formation. An additional 18% of indene is produced via hydrogen recombination with the indenyl radical (1222).

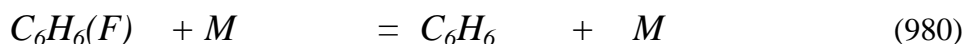
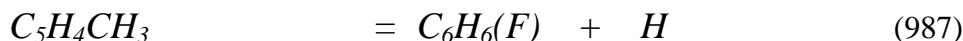
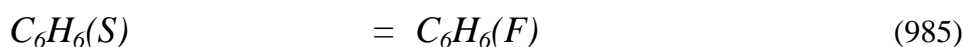
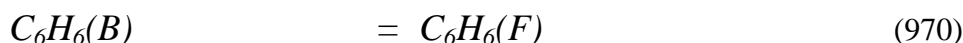


Styrene was not observed experimentally during pyrolysis. Phenyl acetylene is predominantly formed via  $C_6H_5$ . Approximately 53% of  $C_8H_6$  is formed via acetylene recombination with the phenyl radical (937) that was assigned a rate from Richter *et al.* [79]. An additional 22% is formed via acetylene recombination with  $C_6H_4$  (937), which is produced 100% via hydrogen abstraction with  $H$  attack from phenyl radical. A rate proposed by Potter [75] was applied to reaction (1160).

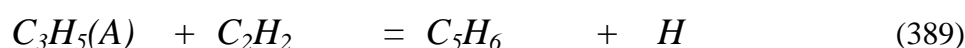
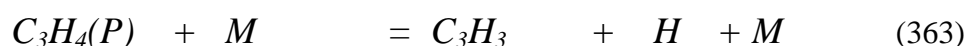


Toluene is another important intermediate species. It is produced via the benzyl radical (100%), which is formed (95%) via acetylene recombination with the cyclopentadienyl radical.

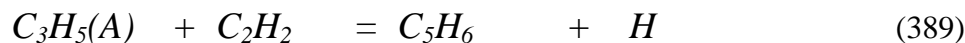
Benzene is produced via isomerization (980) from fulvene, with the latter produced via three major reaction channels. The channels involve hydrogen thermal dissociation from  $C_5H_4CH_3$  (987) (31%) and isomerization reactions via  $C_6H_6(B)$  (970) (23%) and  $C_6H_6(S)$  (985) (40%). The latter species stem from propargyl radical recombination.



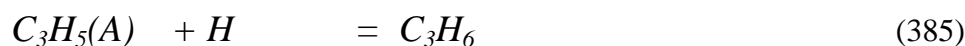
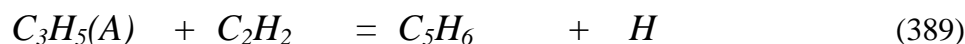
The propargyl radical is responsible for 42% of the  $C_3H_4(P)$  formation via reaction (363) that utilizes a rate proposed by Leung and Lindstedt [73]. Moreover, 57% of  $C_3H_4(P)$  is formed via a sequence of reactions through  $C_3H_5(A) \rightarrow C_3H_4(A) \rightarrow C_3H_4(P)$ . The  $C_3H_5(A)$  radical is essentially (98%) produced by reaction (389) and approximately 90% of  $C_3H_4(P)$  decomposes to the methyl radical and acetylene.



Reaction (389) is responsible for 41% of the total acetylene formation, which highlights one more time the significant role of this step in the  $C_5H_6$  thermal decomposition and production of major species. The dominant acetylene formation channel is via thermal decomposition of the cyclopentadienyl radical (54%).



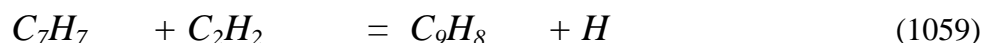
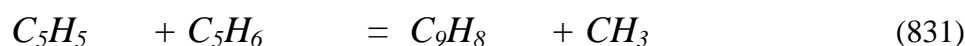
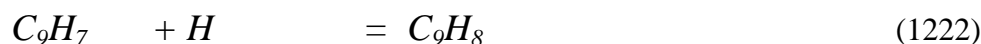
The impact of reaction (389) is significant for the formation of ethylene through  $C_3H_6$  (95%) via the reaction route shown below.



A reaction rate analysis was also performed for the thermal decomposition of  $C_5H_6$  at the higher temperatures of 1202 K, where the fuel follows the same two decomposition pathways as at 1147 K, but the thermal dissociation channels increase in importance relative to abstraction or recombination reactions. Hence, the thermal  $C-H$  scission of  $C_5H_6$  increases from 15% to 25% of the total fuel

consumption and the abstraction reactions via atomic hydrogen reduce from 74% to 62%. The  $C_5H_5$  decomposition is controlled via a second channel that involves the thermal C-C rupture leading to the production of  $C_2H_2$  and  $C_3H_3$  (16%), in combination with the  $C_5H_5$  recombination leading to the formation of  $C_{10}H_9F$  (72%).

The formation route to indene is interesting. As the temperature rises, the impact of the different indene formation channels changes substantially. At 1202 K three reaction steps control the formation of indene. The hydrogen recombination (1222) with the indenyl radical constitutes the major indene formation channel by 42%, compared to 18% at lower temperatures. The recombination of cyclopentadiene with cyclopentadienyl radical shows a reduction to 36%, while the step is the dominant indene formation channel (72%) at 1147 K. On the other hand, reaction (1059), which involves the recombination of acetylene with the benzyl radical, shows an increase from 10% to 23% at higher temperatures.



The formation of major intermediate species follow the same behaviour as at lower temperatures.

### 3.7 Conclusions

The objective of this chapter was to reveal important pathways that proceed through cyclopentadiene and to highlight the importance of the cyclopentadienyl radical in the growth of higher aromatics. Three cases for the oxidation of cyclopentadiene in nitrogen bath were studied stoichiometric and rich mixtures with fuel concentrations varying from 1051 – 2243 ppm in a temperature range of 1148 – 1198 K. Moreover, five pyrolyses cases were also studied for the same range of fuel concentrations and for a temperature range of 1147 - 1202 K. The computed levels

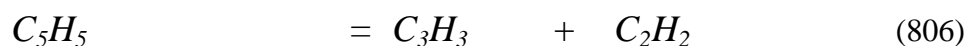


that describe the evolution of the reactants and intermediate species were compared against measurements obtained by Butler [20].

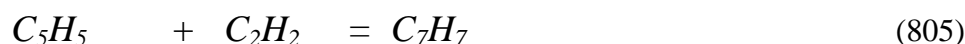
Due to catalytic effects from the surface chemistry that occurred in the reactor during the oxidation experiments, a steep initial drop in the fuel concentration was apparent and a time shift to the computations performed here was necessary. From the computations performed, it is shown that species such as naphthalene, toluene, benzene and acetylene reached the end of the reactor in high and detectable concentrations, a fact that shows that these species are hard to oxidize and play important role in soot growth. Cyclopentadiene converts to the cyclopentadienyl radical via hydrogen abstraction reaction by  $H$ ,  $OH$ ,  $O$  radicals. The formed cyclopentadienyl radical subsequently follows two competing major consumption pathways that involve its recombination leading to the formation of  $C_{10}H_9F$  and the thermal decomposition to the formation of acetylene and the propargyl radical. As the temperature rises, the thermal decomposition of  $C_5H_5$  becomes dominant. In rich mixtures and low temperatures around 1147 K, the recombination channel becomes dominant over the thermal decomposition channel. Two more  $C_5H_5$  decomposition channels appear to play a significant role during the oxidation of stoichiometric mixtures at low temperatures. The channels involve the cyclopentadienyl oxidation via  $HO_2$  attack, leading to the formation of  $C_5$  oxygenated species such as  $C_5H_5O$  and  $C_5H_4O$ . It was predicted that as the temperature rises, the concentration of acetylene and benzene rises due to the increased impact of  $C_5H_5$  thermal decomposition leading to the production of  $C_2H_2$  and  $C_3H_3$ . The latter specie is associated with benzene formation. The cyclopentadienyl radical is precursor to naphthalene and at low temperatures high concentrations of  $C_{10}H_8$  are predicted.

The modelling studies of the pyrolysis of cyclopentadiene show a reasonably good agreement. However, errors in prediction of some of the intermediate species are obvious. Due to the absence of oxygen, the fuel concentration profile follows a smooth linear trend compared to the initial drop in the fuel concentration for the oxidation cases. The model that was utilised in the simulation of the oxidation cases was responsible for the excessive species concentration predictions during pyrolysis. For this reason, a modification was applied to the reaction rate of the cyclopentadienyl thermal decomposition (806) and a slower rate proposed by Robinson [15] was utilised. This lead to improved agreement between the predictions and the measurements for benzene and naphthalene and for the fuel

concentration profile. The excellent concentration predictions of benzene, that is mostly controlled by the production of the propargyl radical, and the excellent computed naphthalene concentration predictions show that the rate adjustment of the  $C_5H_5$  thermal decomposition is well justified. However, the persistent overprediction of acetylene suggests that the acetylene concentrations and decomposition route is not controlled only by the thermal decomposition of the cyclopentadienyl radical. The hydrogen attack to the cyclopentadiene (-389) that leads to C-C rupture and produces  $C_3H_5(A)$  and  $C_2H_2$  plays a very important role under pyrolytic conditions. The reaction rate utilized for this channel was adopted from Rizos [72].



Toluene is also somewhat overpredicted and this is due to excessive  $C_7H_7$  overproduction via acetylene recombination reaction with the cyclopentadienyl radical (805). The rate applied to this channel was adopted by suggestions of Colket and Seery [77]. This channel is also the main acetylene consumption channel and contributes 82% under pyrolysis and 50% under oxidation conditions. The acetylene and toluene concentrations also depend on reaction (1059) that constitutes one of the major consumption paths for these species respectively.



The acetylene recombination channel with the benzyl radical (1059) is one of the major indene production channels and contributes up to 60% under oxidation conditions and 20% during pyrolysis depending on the temperature applied. The second important indene production channel is the  $C_5H_6$  recombination with  $C_5H_5$  (831) here utilizing the rate of Wang *et al.* [41]. The channel is also the main production channel for the methyl radical leading to methane production. Methane, as well as indene, are underpredicted a fact that shows that revised kinetics should be considered.



These five channels (806), (389), (805),(1059) and (831) that are highlighted are in need of further investigation.

## Chapter 4

### Toluene

#### 4.1 Introduction

The ability to predict the combustion and growth of monosubstituted single ring or polycyclic aromatics is of key importance for aviation fuels for environmental reasons. Alkylated benzenes are also a significant hydrocarbon class in gasoline and diesel fuels, hence the knowledge of the combustion chemistry of these hydrocarbons is necessary. Toluene is the simplest alkylated benzene and its chemistry constitutes the framework for the development of mechanisms describing other alkylated benzenes. It is also important due to its ability to promote soot formation.

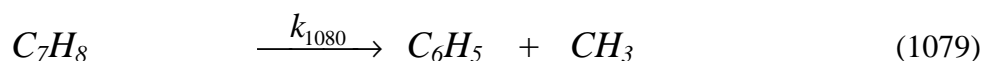
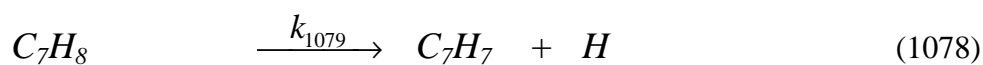
There has been much previous work on model development for toluene, as well as experimental studies on toluene oxidation and thermal decomposition. Emdee *et al.* [55] developed a model for high temperature toluene oxidation utilizing previous benzene and toluene schemes and validated it with flow reactor experiments at temperatures from 1100 to 1200 K at atmospheric pressure. Klotz *et al.* [80] updated the Emdee *et al.* [55] model and validated it against toluene-butane fuel blends. Dagaut *et al.* [81] developed a model that describes toluene oxidation and validated it against jet-stirred reactor at a temperature range of 1000 – 1375 K and equivalence ratios of from 0.5 - 1.5. Lindstedt and Maurice [82] developed a comprehensive toluene mechanism and validated it against experimental data from plug flow reactors, shock tubes, counterflow diffusion flames and premixed flames. Moreover, Sivaramakrishnan *et al.* [83] developed a detailed chemical model based on an earlier literature model for toluene oxidation and validated it against shock tube experimental data at temperature in the region 1200 - 1500 K over a wide pressure range (25 – 610 bar) and for stoichiometries of  $\Phi = 1$  and  $\Phi = 5$ .

A number of experimental studies reported in the literature describe the toluene oxidation or thermal decomposition. Ignition delay times in argon mixtures were measured by Burcat *et al.* [25] for toluene concentration of 0.5 to 1.5 % , 4.48 to 13.45 % oxygen, temperature in the range of 1339 - 1797 K and with reflected shock pressures of 1.95 to 8.85 atm. More recent studies on toluene oxidation were performed by Vasudevan *et al.* [26] and Davidson and co-workers [29]. Vasudevan *et al.* [26] measured ignition delay times and *OH* radical concentrations in toluene/ $O_2$ /*Ar* mixtures behind reflected shock waves at high temperatures (1400 - 2000 K) and low pressures (1 - 4 atm) for equivalence ratios of 0.5 - 1.875 with toluene concentrations of 0.025 - 0.5%. The measured toluene ignition delay times were compared with the models of Pitz *et al.* [84], Dagaut *et al.* [81] and Lindstedt and Maurice [82]. At low to moderate temperatures, the data agrees with the model of Dagaut *et al.* [81] and Pitz *et al.* [84] whereas at higher temperatures the model by Dagaut *et al.* [81] shows a better agreement with measurements. The measurements of ignition delay times against fuel concentration shows that the ignition time falls as the fuel concentration increases and this trend is also supported by Burcat *et al.* [25]. The Lindstedt and Maurice [82] model captures the trend of the experimental model but with lower ignition delay times. The Pitz *et al.* [84] and Dagaut *et al.* [81] models can predict the ignition delays at low fuel concentrations but show a significant disagreement at high fuel concentrations.

Davidson *et al.* [29] measured *OH* concentrations and ignition delay times in a shock tube for toluene/air at of low temperatures (855 - 1269 K) and high pressures (14 - 59 atm) for equivalence ratios of 0.5 and 1 in synthetic air. Their ignition delays were validated against the models of Pitz *et al.* [84] and Dagaut *et al.* [81]. The model of Dagaut *et al.* [81] predicts ten times longer ignition delays than the experiments of Davidson *et al.* [29] and the model of Pitz *et al.* [84] predicts ignition delay times two times longer that the measurements. However, for  $\Phi = 0.5$  the model of Pitz *et al.* [84] captures the data very well.

The toluene initiation reactions have been the target of several studies. Pamidimukkala *et al.* [85] performed shock tube studies with time-of-flight mass spectrometry and laser schlieren densitometry for a temperature range of 1550 - 2000 K and pressures of 0.2 - 0.5 atm. Their study supports the dominance of *C-C* scission in toluene dissociation leading to the production of methyl and phenyl

radicals (1079) against the *C-H* scission leading to the benzyl radical and the hydrogen atom (1078). A rate constant was also suggested.



In addition, it was suggested that the stability of the benzyl radical leads to a partial equilibrium, whereas the unstable phenyl radical makes reaction (1079) irreversible and hence a major route in the thermal dissociation of toluene. Colket and Seery [77] performed shock tube studies for temperature range of 1100 - 2700 K and suggested that (1079) always controls the distribution of products from toluene dissociation.

Rao and Skinner [27] monitored the formation of hydrogen atoms under pyrolytic conditions behind shock waves in argon mixtures at a total pressure of 0.4 atm and for a temperature range of 1450 - 1790 K. Rate constants for the two major toluene dissociation channels were proposed and it was concluded that the hydrogen abstraction reaction (1078) is the only important initiation step. The study was also supported by Muller-Markgraf and Troe [86], who studied the benzyl radical absorption during its decay behind shock waves. Added to this, Brouwer *et al.* [87], utilising UV spectroscopy to study the toluene thermal decomposition, highlighted the dominance of the hydrogen abstraction dissociation channel with a branching ratio of  $k_{1078} / k_{1079} = 10$ .

Braun-Unkhoff [28] monitored the formation of the hydrogen atom during thermal decomposition in the temperature range of 1300-1800 K, pressures of 1.5 - 7.8 bar in argon mixtures and highlighted the importance of  $CH_3$  formation (1079) for the product distribution. The results also suggested that the hydrogen abstraction from toluene leading to the formation of benzyl radical is important.

Rate constants were proposed in the above studies for the two dissociation channels. For the *C-H* bond scission, Rao and Skinner [27] assigned an energy barrier of 360 kJ/mole, Braun-Unkhoff *et al.* [28] assigned a value of 374 kJ/mole and Brouwer *et al.* [87] a value of 369 kJ/mole. Later shock tube studies by Hippler and Troe [88] revised the *C-H* bond scission dissociation channel and assigned a

new rate with a barrier of 360 kJ/mole over a temperature range of 1200-1500 K and a value of 356 kJ/mole in a flow system over a temperature range of 913-1143 K.

Eng *et al.* [89] investigated the thermal decomposition of toluene at temperatures in the range 1350 - 1900 K and for pressures from 0.1 to 2.0 bar. It was suggested that toluene dissociation proceeds mainly via (1078) for which a rate constant was determined based on *H*-atom detection via calibrated atomic resonance absorption spectroscopy. The reaction showed no pressure dependence at lower temperatures, whereas at the highest temperature a slight pressure dependence was observed. Moreover, Eng *et al.* [89] defined a branching ratio  $k_{1078} / (k_{1078} + k_{1079})$  for toluene decomposition that is affected by temperature and pressure.

A more recent study of the thermal decomposition of toluene was performed by Oehlschlaeger *et al.* [90], who investigated the contribution of the two dissociation channels in shock wave experiments over a temperature range of 1400 - 1780 K and at a pressure of 1.5 bar. The benzyl radical absorption at 266 nm was monitored during toluene decomposition in argon mixtures and the rates for the two channels were determined. Moreover, it was suggested that the branching ratio  $k_{1078} / (k_{1078} + k_{1079})$  between the two channels varied from 0.8 at 1450 K to 0.6 at 1800 K. The findings were compared to previous studies and it was found that the overall decomposition rate agrees with a deviation of less than 30% from the results of Braun-Unkhoff *et al.* [28] and Eng *et al.* [89] and, hence, is faster than the values proposed by Pamidimukkala *et al.* [85] and Rao and Skinner [27]. The branching ratio is in good agreement with Eng *et al.* [89], but in disagreement with Pamidimukkala *et al.* [85] and Braun-Unkhoff *et al.* [28]. Moreover, the *H*-atom measurements performed in the study of Braun-Unkhoff *et al.* [28] are in agreement with the findings of Eng *et al.* [89].

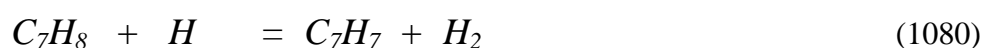
In the present study, the comprehensively validated detailed mechanism developed by Lindstedt and Maurice [82], with subsequent developments by Potter [75], was used as a starting point for the re-evaluation of the toluene chemistry in light of recent studies. The toluene sub-mechanism features 103 elementary reactions and 23 species. Further analysis was performed and improvements were made by considering new reaction steps and species. A full listing can be found in Table A.1 and the heats of formation can be found in Table B.1.

## 4.2 Modelling Approach and Mechanism Updates

The complete mechanism was validated and analysed against data and conditions corresponding to i) shock tube data for toluene pyrolysis [28] and ii) shock tube data for toluene oxidation [25, 26]. The rates of toluene pyrolysis were analysed at conditions corresponding to shock tube experiments of Braun-Unkloff *et al.* [28]. Moreover, the toluene sub-mechanism was analysed at conditions corresponding to toluene oxidation in argon mixtures behind reflected shock waves of Vasudevan *et al.* [26] and Burcat *et al.* [25]. The validation and analysis of the current model was performed in order to analyse the principal reaction paths and to evaluate new reaction steps and reaction rate updates.

All the elementary reaction steps are assumed reversible with the reverse rates computed via chemical equilibrium. The thermodynamic data was obtained from literature sources [71] and, when not available, were calculated via quantum mechanical methods using Gaussian-03 by Robinson [15].

The following decomposition pathways were updated using the reaction rates determined by Oehlschlaeger *et al.* [90].



Another addition involves the thermal decomposition of the benzylperoxy radical (1131). The reaction rate was adjusted to the reverse rate of the corresponding dissociation reaction of the phenylperoxy radical (1006) from DiNaro *et al.* [91].





Reaction (1131) was tested under the shock tube conditions of Davidson *et al.* [29] and was found to play a significant role in the evaluation of the *OH* profile and reduced the ignition delay time by approximately 22% as compared to the starting mechanism. However, the current model still fails to capture the low temperature (< 1269 K) ignition data. In the current study the following reaction path was also considered.



Reaction (R1) was found to be the rate-limiting step of the three-step reaction sequence. Due to lack of accurate pathway information, the global step given by reaction (1130) was added to the scheme with a rate and barrier based on suggestions of Hunter *et al.* [92] with the relative isomerization  $C_2H_5OO = C_2H_4OOH$  as a reference for estimation purposes.



The three-step reaction pathway (1061, R1, R2) follows the study of Zellner and Ewig [93], Walch [94] and Clothier *et al.* [95] for the arguably related sequence (R3,R5,R6 or R3, R4)



The reaction of methyl with molecular oxygen producing the methylperoxy radical leads either, via decomposition, to the methoxy radical and atomic oxygen (R4) or, via isomerization, to  $CH_2OOH$  (R5). The later step is potentially important

pathway under radical depleted conditions e.g. during ignition. The activation energy for the transition state (R4) is found to be 243 kJ/mole whereas the activation energy for the transition state (R5) is only 160 kJ/mole. Hence the production of  $CH_2O + OH$  occurs with smaller activation barrier and dominates over (R4) at temperatures below 2800 K. The two different channels for the  $CH_3OO$  decomposition come from different electronic states. The species can exist either in the  $X\ 3\Sigma_g^-$  ground state (R4), where the closest 2p orbital of the oxygen is double occupied from the electrons and 1,3-hydrogen migration is not possible, or in the  $1\Delta_g$  state (R5) where the same 2p orbital of the oxygen is singly occupied and hydrogen migration is favourable [94]. A schematic representation of the the ground and excited state of the oxygen atom on the benzylperoxy radical is shown in Figure 4.1.

According to Clothier *et al.* [95] the activation energy of reactions (R3-R4) is calculated to be approximately 121 kJ/mol less than the value estimated by Zellner and Ewig [93]. It is obvious that the above analogy is in need of refinement and that the current rates are subject to uncertainties. However, the pathway increases in significance under lower temperature conditions and further work is desirable.

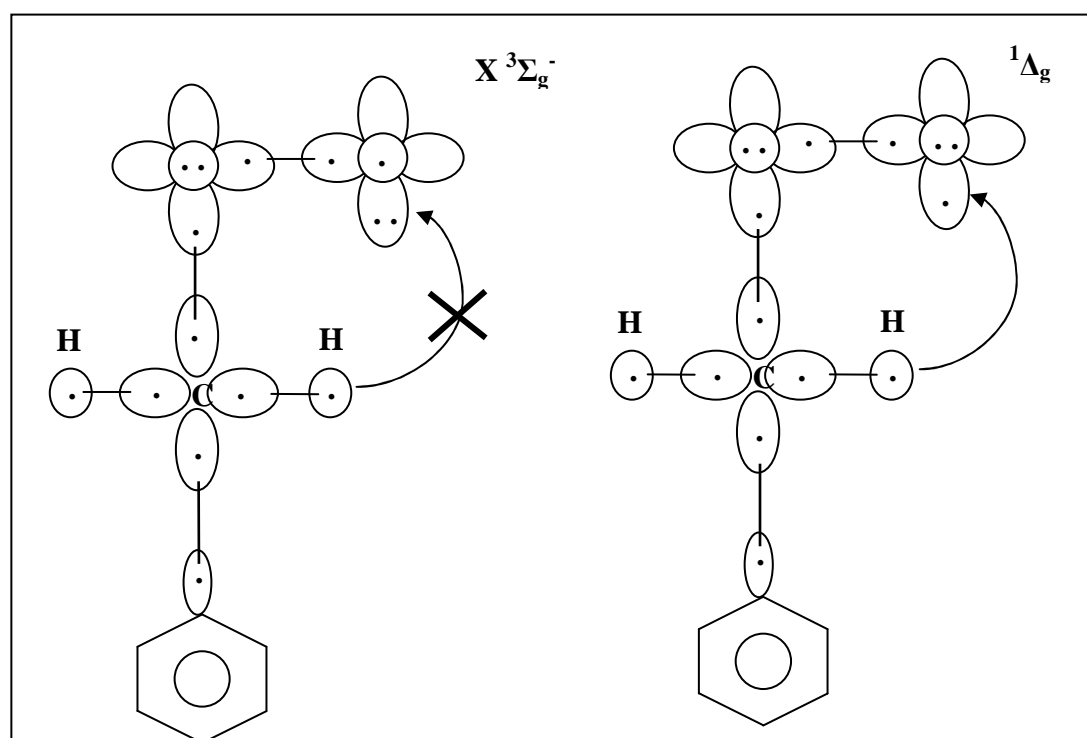
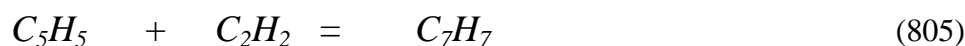


Figure 4.1 Schematic representation of electronic states of the two benzylperoxy radicals.

Another reaction step (805) that plays a significant role in both toluene pyrolysis and oxidation processes was added with a rate adopted from Colket and Seery [77]. A rate from Muller-Markgraf and Troe [86] was also tested for the reverse reaction. However, it was found to lead to an increase in ignition delays of approximately 20% and was not utilized here.



### 4.3 Thermal Decomposition

The thermal decomposition of toluene in shock tubes was studied at conditions corresponding to experiments performed by Braun-Unkhoff *et al.* [28] in order to evaluate the branching ratio of the main toluene decomposition reaction channels and to monitor the temporal evolution of the hydrogen radical. Braun-Unkhoff *et al.* [28] studied the thermal decomposition in argon mixtures and measured  $H$  profiles at fuel concentrations of 2 - 19.3 ppm, temperatures of 1515 - 1655 K and pressures of 1.89 - 1.93 bar (Table 4.1). Moreover, an attempt was made to model the experimental profiles by utilising a ten-step reaction scheme to which adjustments had to be made in order to achieve the appropriate fit to the profiles. The analysis in this study is similar to that by Lindstedt and Maurice [82] and was performed to assess the consistency with the revised principal reaction paths mention in Section 4.2.

	$C_7H_8$ (ppm)	T [K]	P [bar]
1	2.0	1515	1.85
2	2.8	1655	1.89
3	3.0	1585	1.93
4	19.3	1555	1.92

Table 4.1 Experimental and modelling conditions for toluene thermal decomposition

The computed hydrogen profiles for all the experimental conditions (Table 4.1) are shown in Figure 4.2 to Figure 4.5. The modelled hydrogen profiles are reasonably well captured and show that the adopted branching ratio from Oehlschlaeger *et al.* [90] is satisfactory.

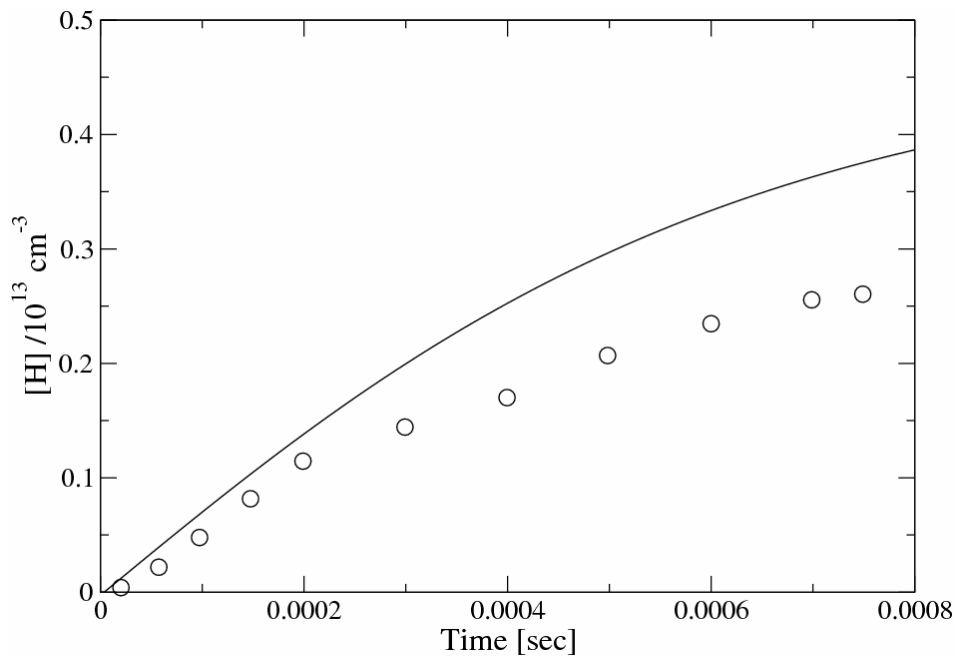


Figure 4.2 Hydrogen radical concentration against time for toluene thermal decomposition with an initial fuel concentration of 2.0 ppm,  $T = 1515$  K and  $P = 1.85$  bar. The solid line indicates the current computations and the circles indicate the experimental data from Braun-Unkloff *et al.* [28].

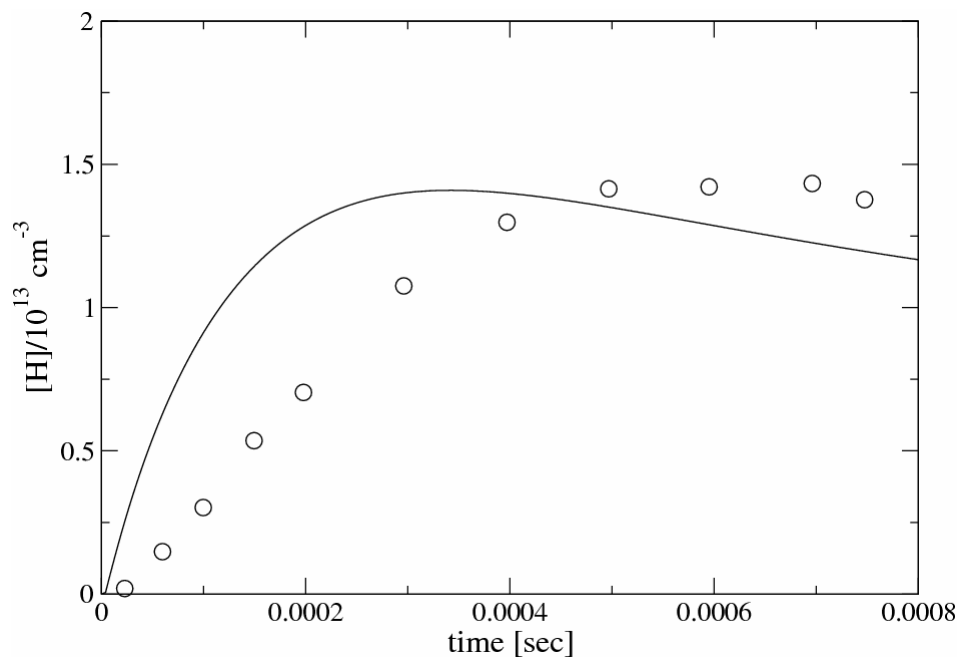


Figure 4.3 Hydrogen radical concentration against time for toluene thermal decomposition with an initial fuel concentration of 2.8 ppm,  $T = 1655$  K and  $P = 1.89$  bar. The solid line indicates the current computations and the circles indicate the experimental data from Braun-Unkhoff *et al.* [28].

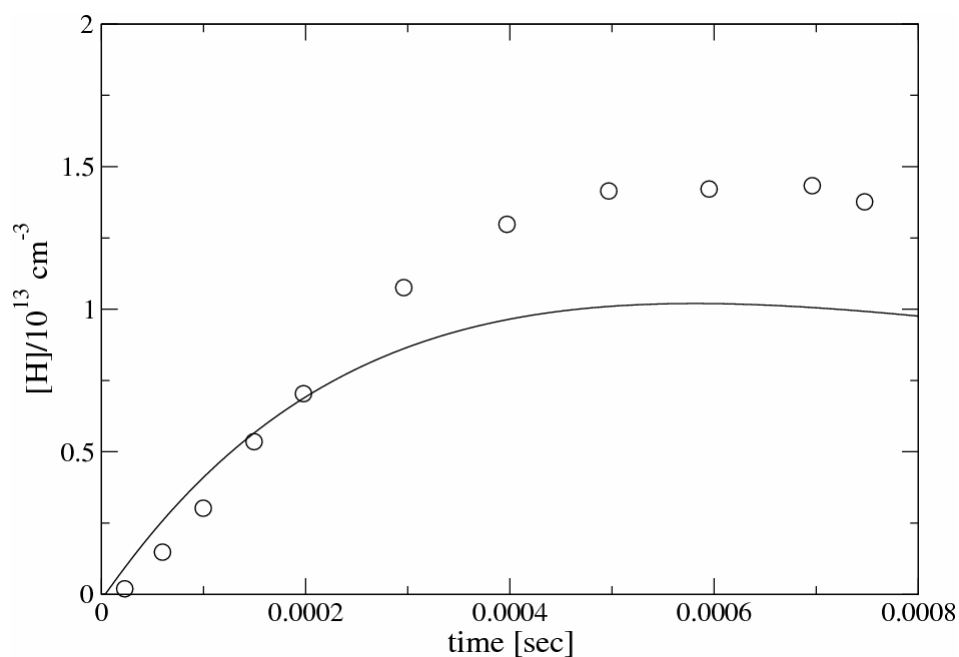


Figure 4.4 Hydrogen radical concentration against time for toluene thermal decomposition with an initial fuel concentration of 3.0 ppm,  $T = 1585$  K and  $P = 1.93$  bar. The solid line indicates the current computations and the circles indicate the experimental data from Braun-Unkhoff *et al.* [28].

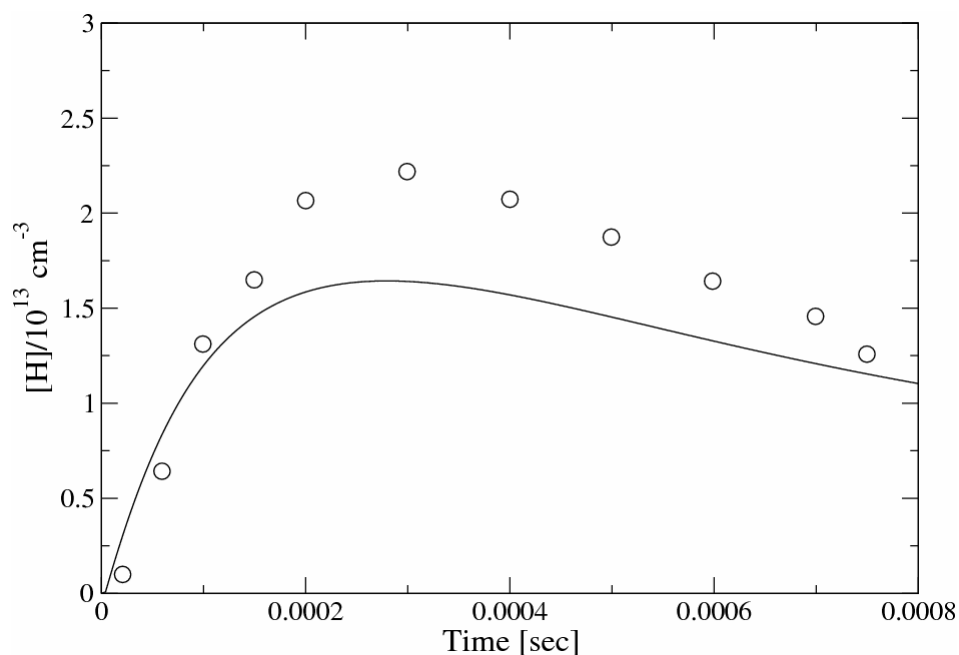


Figure 4.5 Hydrogen radical concentration against time for toluene thermal decomposition with an initial fuel concentration of 19.3 ppm,  $T = 1555$  K and  $P = 1.92$  bar. The solid line indicates the current computations and the circles indicate the experimental data from Braun-Unkhoff *et al.* [28].

#### 4.4 Time Resolved OH Concentrations during Oxidation

The data used to validate the toluene mechanism under oxidation conditions at high temperatures was obtained from Vasudevan *et al.* [26], who monitored the time resolved *OH* radical concentration profiles in toluene/ $O_2$ /*Ar* mixtures in shock tubes. Vasudevan *et al.* [26] measured *OH* concentration profiles over a wide range of conditions. The study provides unique time-resolved data of a complementary nature to the pyrolysis experiments discussed above. In the present work, computations were performed corresponding to data with a temperature of 1689 K and pressure of 1.79 atm ( $\Phi = 1$ , 0.1%  $C_7H_8$ , 0.9%  $O_2$ , 99% *Ar*). The computed profile is shown in Figure 4.6 along with the experimental data of Vasudevan *et al.* [26].

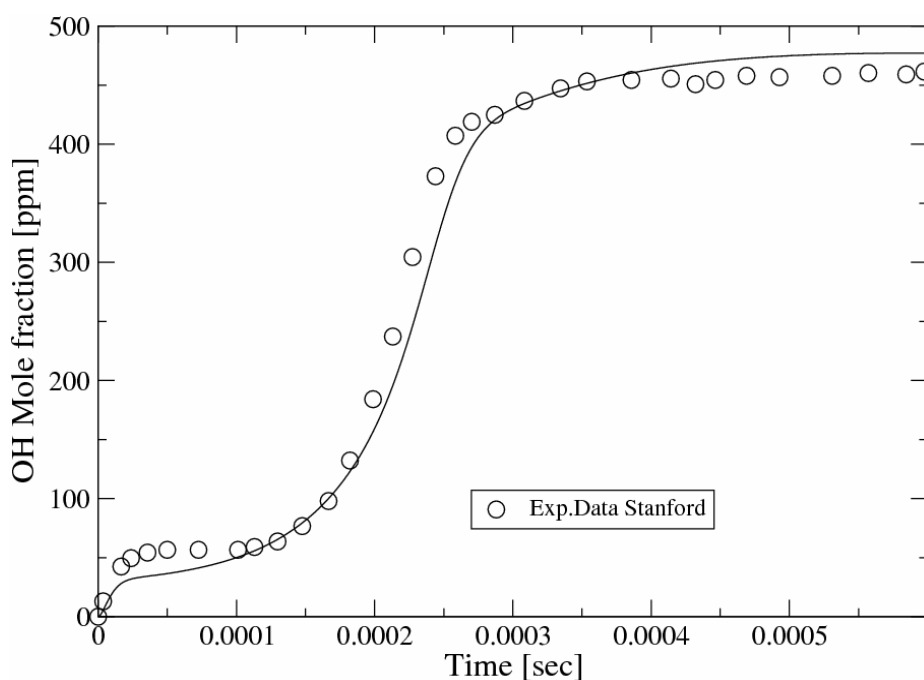


Figure 4.6 Time resolved OH radical concentrations obtained in Toluene/Oxygen/Argon mixtures in a shock tube with  $\Phi = 1$  (0.1% toluene, 0.9% oxygen),  $T = 1689$  K and  $P = 1.79$  atm. The circles indicate the measurements from Vasudevan *et al.* [26] and the solid line indicates the current simulation.

There is excellent agreement between the measurements and the current toluene model. The *OH* profile can be divided in three regions; the first shows the rapid increase in the *OH* concentration due to toluene decomposition, the second where *OH* rises, indicating the presence and impact of the chain branching reactions and the third where the *OH* production is close to zero [26].

A sensitivity analysis was also performed and the current model shows that the *OH* profile is sensitive to the chain branching reaction:  $O + H_2 \rightarrow OH + H$ . The rate of Sun *et al.* [96] adopted from Baulch *et al.* [97] was tested to this reaction step with the current scheme (Figure 4.7) and the current toluene model fails to capture the *OH* slope and delays the onset of ignition approximately 17% compared to the rate of Li *et al.* [98] adopted from Sutherland *et al.* [99]. A further analysis has been presented by Gkagkas and Lindstedt [100]. It was also shown that the reaction step is responsible for 12% of the *OH* radical production. In addition, the chain branching step  $H + O_2 \rightarrow OH + O$  is significant. The step is responsible for 67% of the *OH* production and has been studied extensively in the past [101-103].

Moreover, the added reaction (805) plays significant role in the  $OH$  evolution as shown in Figure 4.7. The absence of this reaction step causes a delay in the  $OH$  ignition by 20%.



Another sample of a  $OH$  concentration profile versus time is shown in Figure 4.8 for a stoichiometric 250 ppm toluene mixture at  $T = 1648$  K and  $P = 2.03$  atm.

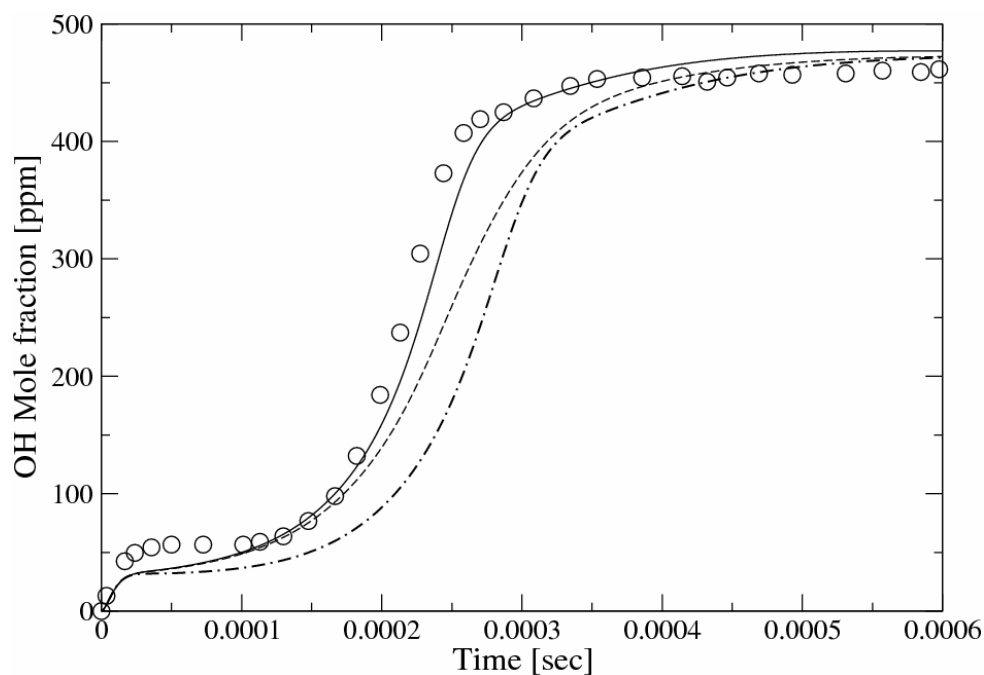


Figure 4.7 Sensitivity analysis of time resolved  $OH$  radical concentrations obtained in Toluene/Oxygen/Argon mixtures in shock tube with  $\Phi = 1$  (0.1% toluene, 0.9% oxygen),  $T = 1689$  K and  $P = 1.79$  atm. The circles indicate the measurements from Vasudevan *et al.* [26], the solid line indicates the current model, the dashed line indicates the current model with the rate of Sun *et al.* [96] for the reaction  $O + H_2 \rightarrow OH + H$  and the dashed dotted line indicates the current model in the absence of the  $C_5H_5 + C_2H_2 \rightarrow C_7H_7$  reaction.



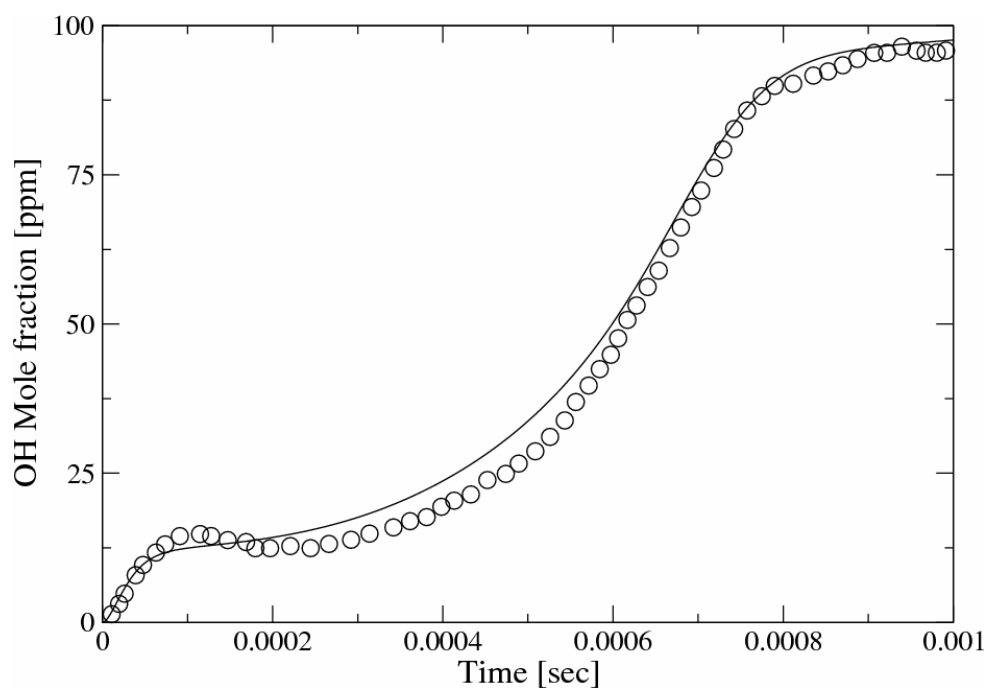


Figure 4.8 Time resolved *OH* radical concentrations obtained in Toluene/Oxygen/Argon mixtures in a shock tube with  $\Phi = 1$  (0.025% toluene, 0.225% oxygen),  $T = 1648$  K and  $P = 2.03$  atm. The circles indicate the measurements from Vasudevan *et al.* [26] and the solid line indicates the current simulation.

## 4.5 Ignition Delay Times

Ignition delay times were measured by Vasudevan *et al.* [26] in toluene/ $O_2$ /Ar mixtures for a temperature range 1510 – 1818 K with  $\Phi = 1$  (0.1% toluene, 0.9% oxygen, 99% argon) and a pressure of 1 atm. Vasudevan *et al.* [26] defined the ignition delay time as the time needed for the  $OH$  radical concentration to reach 50% of the peak value by setting as zero the time of the arrival of the reflected shock.

Ignition delay times were also measured by Vasudevan *et al.* [26] for different fuel mole fractions varying from  $2 \times 10^{-4}$  –  $2 \times 10^{-2}$  with  $\Phi = 1$ , at a temperature of 1600 K and a pressure of 1 atm. Variations of the ignition delay times with temperature and fuel concentrations are presented in Figure 4.9 and Figure 4.10. Experimental data by Burcat *et al.* [25] are also shown in Figure 4.10 for higher fuel concentrations. As is evident in Figure 4.9, the current toluene model agrees well with the measurements and at higher temperatures follows the experimental data closely.

The fuel concentration dependence on ignition delay times for the two experimental data sets (see Figure 4.10) shows that the ignition time falls as the fuel concentration increases. The model arguably performs well.

Ignition delay times were also measured by Burcat *et al.* [25] for toluene/oxygen/argon mixtures for a temperature range of 1379 – 1785 K, pressures of 1.96 – 2.81 atm for a stoichiometric mixture (0.497%  $C_7H_8$ , 4.48%  $O_2$ , 95.023% Ar). The comparison between the model and the experimental data is shown in Figure 4.11.

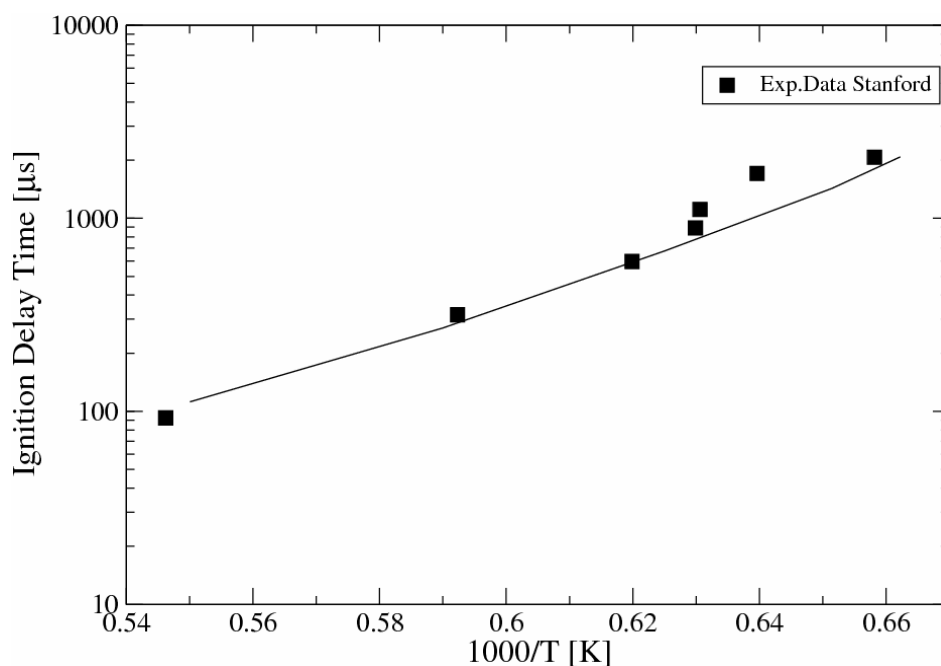


Figure 4.9 Ignition delay times of toluene with  $\Phi = 1$  (0.1% toluene, 0.9% oxygen, 99% argon) and  $P = 1$  atm. Symbols indicate measurements from Vasudevan *et al.* [26] and the solid line indicates the current computations.

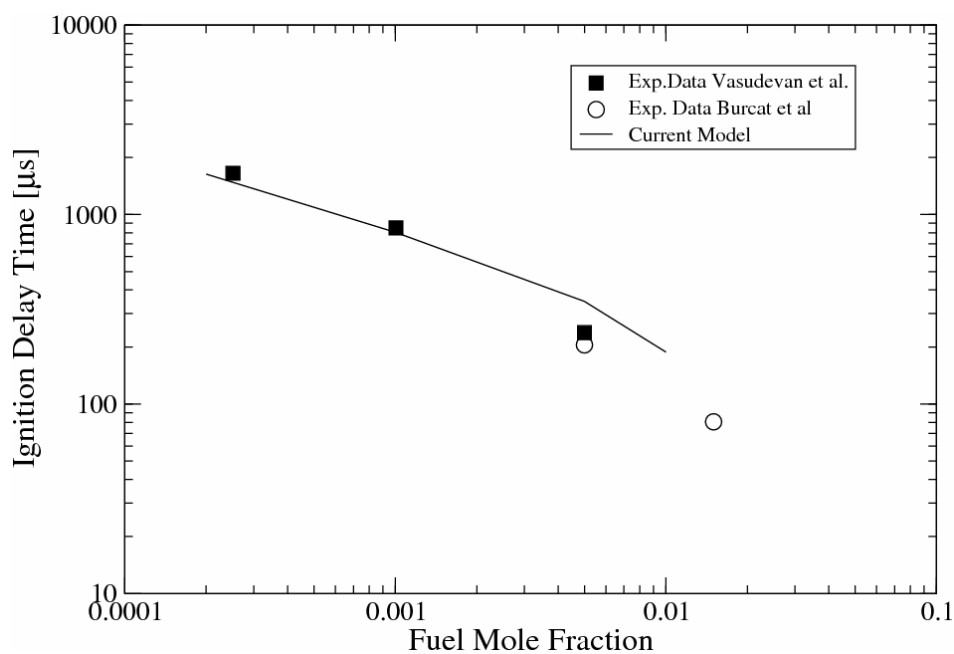


Figure 4.10 Ignition delay times for toluene mole fractions of  $2 \times 10^{-4} - 1 \times 10^{-2}$  with  $\Phi = 1$  (toluene/oxygen/argon),  $T = 1600$  K and  $P = 1$  atm. The solid squares indicate the measurements from Vasudevan *et al.* [26], the open circles indicate experimental data from Burcat *et al.* [25] and the solid line indicates the current computations.

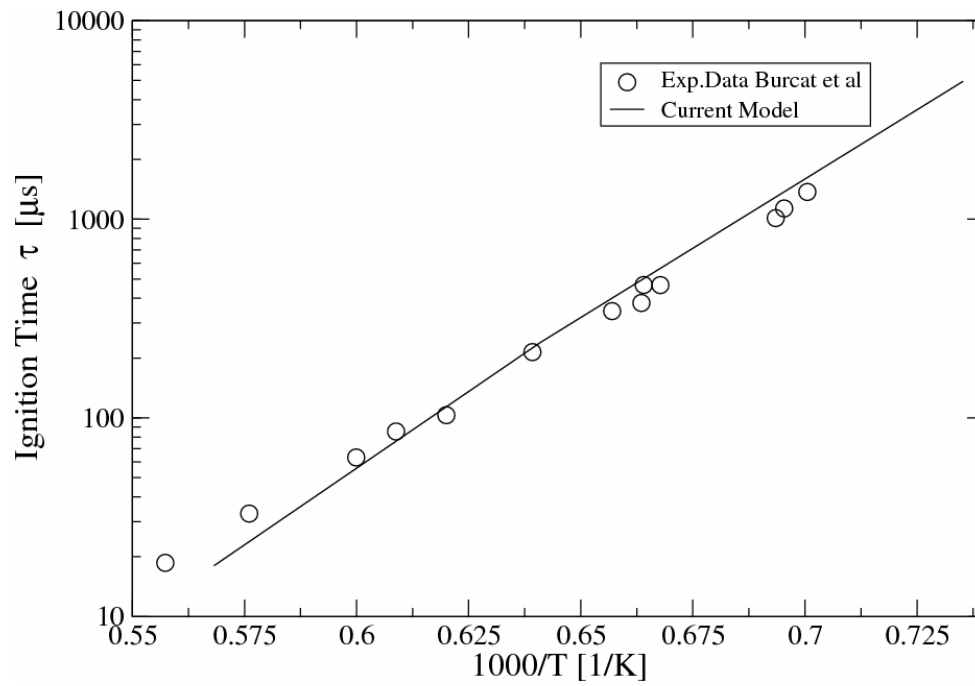
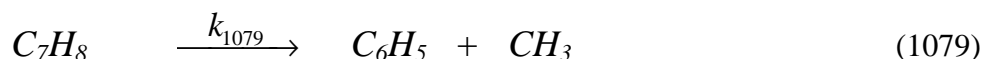
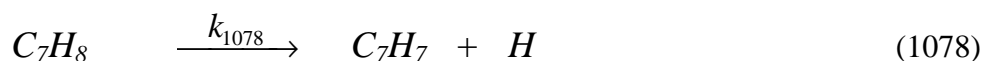


Figure 4.11 Ignition delay times for toluene obtained in a shock tube with  $\Phi = 1$  (0.497%  $C_7H_8$ , 4.48%  $O_2$ , 95.023%  $Ar$ ) and  $P = 2.28$  atm. The circles indicate experimental data from Burcat *et al.* [25] and the solid line indicates the current computations.

## 4.6 Thermal Decomposition Paths

A reaction rate analysis was performed for the toluene thermal decomposition in shock tubes at the experimental conditions of Braun-Unkloff *et al.* [28], as discussed above, and the major reaction pathways were determined.

For the case of a toluene concentration of 2 ppm at 1515 K and 1.85 bar, the toluene decomposition is controlled by two major reaction channels. The C-H fission to the formation of benzyl radical and atomic hydrogen (1078) is responsible for 67% of the fuel decomposition. The reaction channel that proceeds via C-C scission to the formation of phenyl and methyl radical, accounts for 27% of the toluene decomposition. Rates determined by Oehlschlaeger *et al.* [90] were applied to these channels.

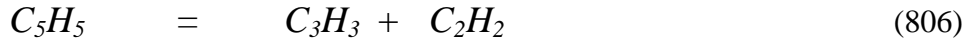


The current findings highlight the dominance of reaction (1078) in agreement with studies of Muller-Markgraf and Troe [86], Brouwer *et al.* [87], Rao and Skinner [27] and Hippler [88]. There is, however, a disagreement with Pamidimukkala *et al.* [85] who proposed reaction (1079) as the main decomposition channel. As shown in the work by Oehlschlaeger *et al.* [90], the overall decomposition rate agrees with Braun-Unkloff [28], Eng *et al.* [89] and Luther *et al.* [104] with a deviation of less than 30%. Recommendations of Pamidimukkala *et al.* [85] and Rao and Skinner [27] are significantly slower.

The benzyl radical decomposes (90%) via reaction (805) featuring the rate of Colket and Seery [77] leading to the cyclopentadienyl radical and acetylene.



The cyclopentadienyl radical leads to the formation of the propargyl radical and acetylene (60%) or isomerizes to the linear form of  $C_5H_5(L)$  (38%) .



Both decomposition channels (806) and (819) were assigned rate constants computed from potential energy surfaces using variable transition state theory and Rice-Ramsperger-Kassel-Marcus/master equation approaches [15]. A faster rate of Kern *et al.* [52] was also tested but lead to overproduction of the hydrogen atom by 20%.

The other main product of the toluene thermal decomposition, the phenyl radical, undergoes isomerization to the linear  $C_6H_5(B)$  or undergoes hydrogen fission reactions that follow a route from  $C_6H_5 \rightarrow C_6H_4 \rightarrow C_6H_4L \rightarrow C_6H_3 \rightarrow C_6H_2$  and both channels lead to the formation of acetylene via 1,3-butadiyne. A schematic representation of the toluene thermal decomposition for 2.0 ppm of fuel at 1515 K and 1.85 bar is shown in Figure 4.12.

The temporal evolution of the hydrogen radical is controlled predominantly by reaction (1078), which accounts for 92% of the production.



The concentration of the hydrogen radical is also sensitive to reactions (1080), (928), (929) and (1081) which are responsible for 27%, 23%, 12% and 11% of the consumption respectively. The rates for reactions (1080) and (1081) were adopted from Oehlschlaeger *et al.* [90]. The rate for the hydrogen assisted hydrogen abstraction reaction (928) was adopted from Leung and Lindstedt [73]. The benzene formation reaction via hydrogen addition to the phenyl radical (929) was assigned a rate proposed by Baulch *et al.* [101].



The impact of reaction (1080) on the hydrogen profile was also noted by Braun-Unkhoff *et al.* [28], who considered it in the context of a bringing agreement between their measured and computed hydrogen profiles. The rates proposed by Braun-Unkhoff *et al.* [28] and Baulch *et al.* [101] were tested for reaction (1080), but caused an increase of the hydrogen concentration ~20% compared to the rate proposed by Oehlschlaeger *et al.* [90]

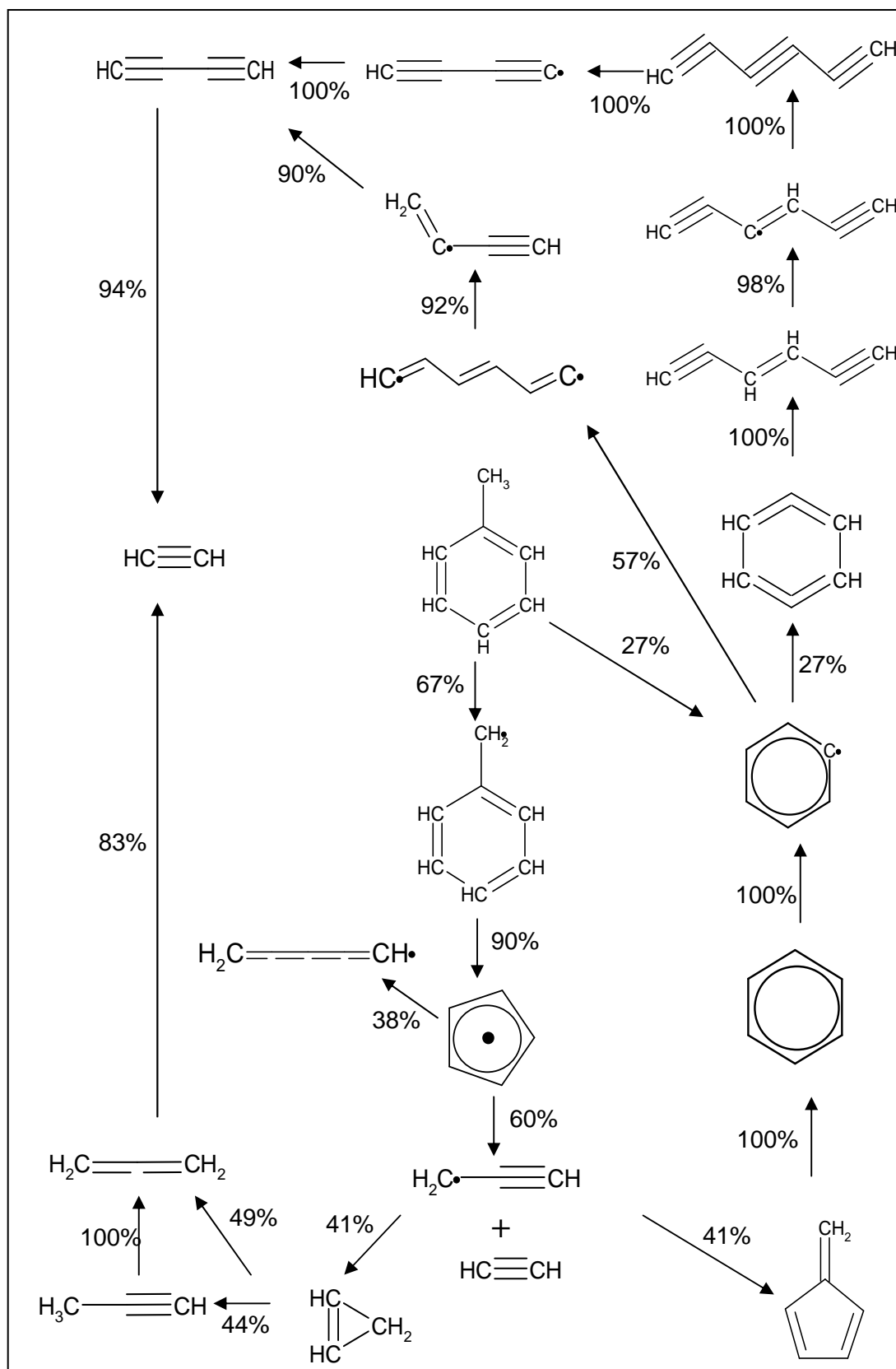


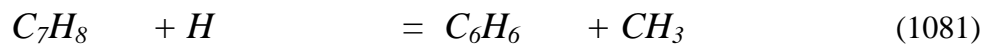
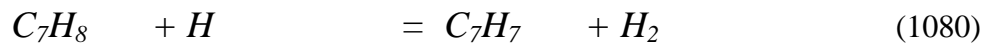
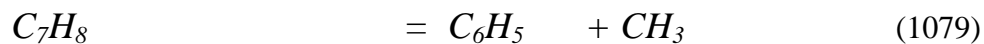
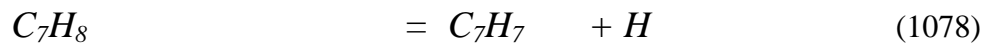
Figure 4.12 Predicted toluene thermal decomposition pathways corresponding to the study of Braun-Unkloff *et al.* [28] with an initial fuel concentration of 2.0 ppm,  $T = 1515$  K and  $P = 1.85$  bar.



## 4.7 Oxidation Paths

The reaction paths for toluene oxidation under shock tube conditions were analysed at the conditions of Vasudevan *et al.* [26], who measured the temporal evolution of the *OH* radical for a stoichiometric mixture of 0.1% toluene and 0.9% oxygen in argon mixture at 1689 K and 1.79 atm.

The overall toluene decomposition is mainly controlled by four reactions as discussed above. These include the two main thermal decomposition pathways leading to the formation of benzyl (1078) and the phenyl radical (1079) which are each responsible for 18% of the fuel consumption and two hydrogen assisted hydrogen abstraction reactions (1080) and (1081) leading to the formation of benzyl (29%) and phenyl radicals (10%) respectively. The rates of these four steps were adopted from Oehlschlaeger *et al.* [90].

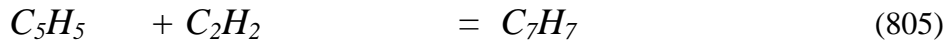


According to the temporal evolution of the *OH* radical concentration, the fuel decomposition follows three stages. The first region where initiation reactions occur and the fuel is decomposed, the second region where ignition occurs due to chain branching reactions and the third region with zero net *OH* production. These regions for the specific test case considered, are separated for times up to 100  $\mu$ s, 250  $\mu$ s and 800  $\mu$ s. Hence, the contribution of each decomposition step varies with time. Although reaction (1078) plays a significant role in the overall fuel consumption, it is predicted that it is responsible for 20% of the fuel decomposition in the first stage, with no impact on the subsequent stages of the fuel oxidation process. Reaction (1079) is responsible for 19%, 12% and 14% of the fuel decomposition over the three stages.

The contribution of reaction (1080) to the fuel consumption increases over time from 27% in the first region to 45% in the second and third regions

respectively. The reaction consumes the reactive H radical and leads to the formation of the less reactive benzyl radical and molecular hydrogen. It must be noted that reactions that consume reactive radicals during fuel oxidation, can be inhibit ignition. However, as it is shown above under fuel pyrolysis conditions, this reaction step is necessary for the consumption of the hydrogen radical. Reaction (1081) follows an increasing impact on the fuel consumption as the time passes from 9% at the first stage to 15% up to the end of the fuel decomposition.

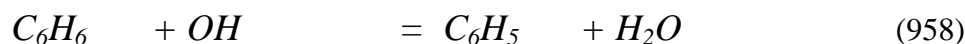
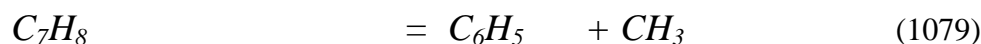
The benzyl radical produced from reactions (1078) and (1080), undergoes thermal dissociation that leads to the production of the cyclopentadienyl radical and acetylene via reaction (805) which accounts for 80% of the benzyl consumption. The rate of Colket and Seery [77] was applied to this step.



Benzene is mostly produced (50%) via reaction (1081) and consumed (38%) via reaction (959) for which a rate from Leung and Lindstedt [73] was adopted. A rate of Leung and Lindstedt was also assigned to reaction (956) which is responsible for 30% of the benzene consumption. The production of the phenoxy radical and the hydrogen atom via oxygen attack on benzene is responsible for 28% of the consumption of the latter with a rate adopted from DiNaro *et al.* [91].



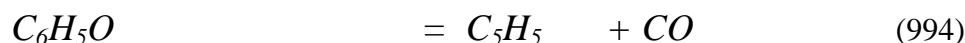
The phenyl radical is initially produced (75%) from the thermal decomposition of toluene via reaction (1079). As time passes and most of the fuel is consumed, secondary reactions occur and the phenyl radical pool is produced via reactions (958) and (956) that were assigned rates from Leung and Lindstedt [73]. The contribution of reaction (958) to the phenyl production remains the same up to 800  $\mu$ s (47%), but reaction (956) is responsible for between 38% and 48 % of the production.



The consumption of the phenyl radical proceeds mainly (54%) via reaction (934) featuring molecular oxygen attack on the phenyl radical leading to the phenoxy radical and an oxygen atom. A rate from Frank *et al.* [105] was adopted for this step. In addition, a hydrogen atom is abstracted from the ring (18%) via hydrogen attack (928) that leads to the production of  $C_6H_4$  and molecular hydrogen. The rate assigned to reaction (928) was obtained from Leung and Lindstedt [73]. Approximately 12% of the phenyl radical consumption occurs via reaction (935) which involves molecular oxygen addition to the phenyl radical leading to the formation of the phenyl peroxy radical.



The phenoxy radical is mainly produced (58%) from reaction (934) and then decomposed (83%) to cyclopentadienyl and carbon monoxide (994) and 15% of its concentration is responsible for the formation of phenol (995). The rate for the carbon monoxide abstraction was adopted from Leung and Lindstedt [73] and the rate for the phenol formation was adopted from DiNaro *et al.* [91].

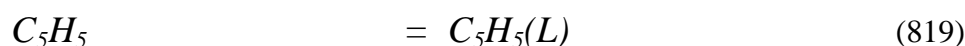
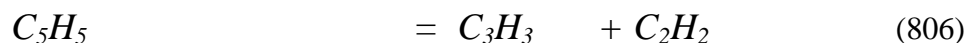


The consumption of  $C_6H_4$  follows the reaction route  $C_6H_4 \rightarrow C_6H_4L \rightarrow C_6H_3 \rightarrow C_6H_2 \rightarrow C_4H_2 \rightarrow C_4H_2O \rightarrow C_2H_2$  to end up forming acetylene. The phenylperoxy radical decays via two thermal pathways (1006, 1010) and leads to

the formation of reactive radicals which are responsible for 68% and 22% of the consumption. Both decomposition steps were assigned the rates of DiNaro *et al.* [91]. The *p*-benzoquinone that is formed via (1010) is decomposed to acetylene via the formation of  $C_6H_3O_3$  and  $C_5H_5O$ .



The cyclopentadienyl radical, which is produced via benzyl radical decomposition or via the phenyl radical degradation route, is decomposed via four main reaction pathways. Approximately 30% is thermally decomposed leading to the formation of acetylene and the propargyl radical and 29% reacts with the oxygen atom leading to carbon monoxide and  $C_4H_5(T)$ . Moreover, 15% isomerizes to a linear structure and 13% recombines with hydrogen forming cyclopentadiene. Rates for reactions (806), (807) and (819) were calculated by Robinson [15] from potential energy surfaces determined using variable transition state theory and Rice-Ramsperger-Kassel-Marcus/master equation approaches. A rate from Kern *et al.* [52] was applied to the hydrogen recombination reaction (832).



## 4.8 Conclusions

In the current chapter a detailed chemical reaction analysis of the toluene chemistry was presented for a reasonably wide range of conditions. The chemical sub-model was evaluated under shock tube conditions and analyzed for both

pyrolysis and oxidation cases. New reaction rates were evaluated their impact was analysed.

The *H* atom profiles show generally good agreement with measurements under pyrolytic conditions. Under oxidation conditions and at high temperatures, the current toluene chemistry captures the temporal evolution of the *OH* radical in excellent agreement with the measurements. The major toluene consumption pathways were identified by performing reaction path analysis. Ignition delay times for stoichiometric toluene mixtures were also computed and showed good agreement with the experimental data sets of Vasudevan *et al.* (2005) and Burcat *et al.* (1986).

The results are encouraging and suggest that the current reaction class based approach can be applied also to other methyl substituted aromatic fuel compounds that form part of real and surrogate fuel formulations.

## Chapter 5

### *N*-Propyl Benzene

#### 5.1 Introduction

Previous studies of the oxidation of *n*-alkyl benzenes have highlighted that after the side chain removal, the fuels follow the same oxidation route as that of benzene. Benzene has been studied extensively, but can not represent more complex aromatic fuels that are present in commercial blends. *N*-propyl benzene is potentially a good candidate representing the mono alkylated and mono cyclic aromatic component of fuels such as gasoline, diesel and kerosene [36]. The current work was focused on determining the process of the side chain removal and the steps that characterize it. Three routes were found (i) homolysis – direct cleavage of the side chain followed by the oxidation of the remaining radical, (ii) displacement of the alkyl side chain by a radical species and (iii) abstraction of a hydrogen atom from the alkyl group [106-109].

Due to the analogy between the alkyl benzenes and alkanes regarding atomic hydrogen abstraction by another radical, reactions were proposed for the *n*-propyl benzene chemistry based on the propane chemistry. Moreover, this analogy between alkanes and normal alkyl benzenes can be used to the understanding and the prediction of the behaviour of *n*-propyl benzene.

#### *Abstraction route*

*N*-propyl benzene has three primary, two secondary and two benzylic hydrogen atoms. According to the hydrogen carbon bonding rules, the benzylic bond is the weakest as compared to the primary and secondary, thus it is easier to abstract a hydrogen atom from the benzyl carbon atom. The benzylic bond strength

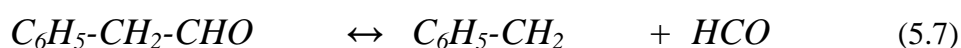
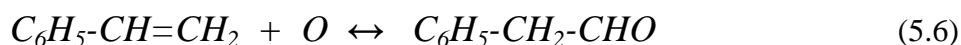
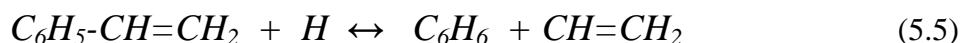
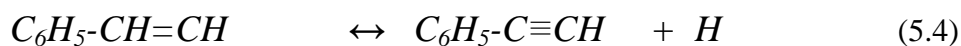
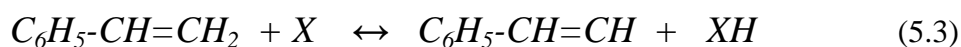
is 368 kJ/mol, the secondary and primary are 397 kJ/mol and 410 kJ/mol respectively. Moreover, the benzylic *C-H* bond strength is less than the *C-H* bonds of the other two sites due to the resonance of the resulting benzyl radical. From the bond strengths, it is easy to say that the benzylic hydrogen atom abstraction is the dominant abstraction reaction [108, 109].

Alkyl benzenes are characterized by resonance which is responsible for the promotion of the benzylic hydrogen abstraction. However, it is not possible for any other oxidation to occur to the benzylic radical as it is stereochemically hindered [110]. The radical species that play the role of the abstractor are predominantly *H*, *O* and *OH*. For the benzylic hydrogen abstraction, the reactions that occur are the following:

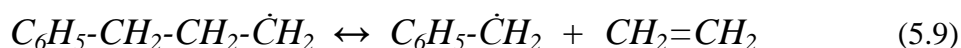


where  $X = H, O$  and  $OH$

The resulting benzylic radical will undergo a beta scission to form styrene and the methyl radical (5.1) - (5.2). Hence, the early appearance of styrene shows that the above step is quite significant for the fuel breakdown route. Styrene can be further decomposed to  $C_6H_5CH\dot{C}H$ , benzene or react with oxygen leading to the formation of oxygenated species [108].

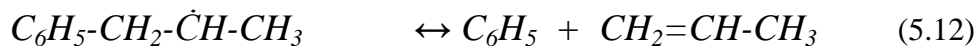


The primary hydrogen abstraction is as follows:



The resulting benzyl radical has three possible routes for its further oxidation; (i) toluene formation via hydrogen addition, (ii) benzaldehyde formation via oxygen addition or (iii) alkyl radical recombination to the benzyl side producing alkyl benzene with a prolonged chain. The alkyl radical for the latter case could be species such as  $CH_3$ ,  $C_2H_5$  and  $C_3H_7$ . Ethylene appears in large quantities in experimental studies of *n*-propyl benzene oxidation showing that the primary hydrogen atom abstraction is a significant path for the fuel oxidation [109].

Since significant quantities of products from primary and benzylic hydrogen abstraction are measured, it is expected that secondary hydrogen abstractions occur due to the fact that the secondary hydrogen carbon bond strength is between the two other cases.



Apart from the two products of reactions (5.11) - (5.12), isomerization (5.13) or phenyl shift (5.14) may also occur. Hydrogen shift from the benzylic to the secondary carbon atom is possible, producing the  $\alpha$ -phenyl propyl radical, the product of benzyl hydrogen abstraction; the oxidation of the latter leads to styrene. Instead of a hydrogen shift, it is also possible for the phenyl group to be transferred to the beta-carbon atom (5.14) [111]. The product of the phenyl shift (5.14) will lead to styrene production.

#### *Displacement of the alkyl group*

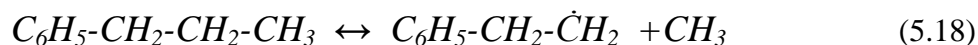
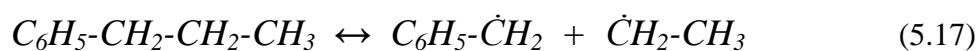
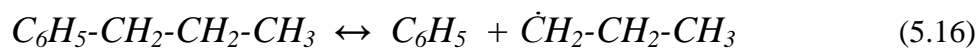
The displacement of the propyl group by a radical species (e.s. a hydrogen atom) produces benzene and the propyl radical. The detection of propylene in the products suggests strong evidence that the displacement reaction occurs.





### Homolysis

The homolysis reaction route involves carbon-carbon cleavage. There are three possible routes for this.



The homolysis route is known to have large activation energies, hence it will only be an important path at high temperatures. The benzylic C-C bond is weaker than the other two in the chain and its breakage is expected to occur faster.

In this study, the oxidation steps of *n*-propyl benzene were analysed and the fuel breakdown was predicted for two different pressures and different stoichiometries. The chemical reaction model was derived from analogies with propane and toluene chemistries. The rates adopted for the reactions steps were also based on the kinetics of propane and toluene and validation was performed with data obtained in jet stirred and shock tube reactors.

## 5.2 Modelling Approach

The updated *n*-propyl benzene reaction mechanism used here consists of 1683 reversible reactions involving 269 species. The reverse rates were computed via equilibrium constants. The rates of consumption and production were also calculated for each species. The thermochemical data are obtained from literature sources [71] and, when not available, were calculated with quantum mechanical methods using Gaussian-03 [15].

### 5.3 Oxidation at Atmospheric Pressure

The oxidation of *n*-propyl benzene was studied under Jet Stirred Reactor (JSR) conditions at atmospheric pressure and validated utilizing measurements obtained by Dagaut *et al.* [36]. Three different stoichiometries ( $\Phi = 0.5, 1.0$  and  $1.5$ ) were analyzed for a temperature range of  $900 - 1250$  K (Table 5.1). Concentration profiles of all major species were computed at a mean residence time of  $\tau = 70$  ms and significant pathways for the fuel breakdown were identified. Comparisons between the simulations and experimental data sets from Dagaut *et al.* [36] are shown in Figure 5.1 to Figure 5.9.

$\Phi$	P(atm)	T (K)	$X_{O_2}$	$X_{C_9H_{12}}$
0.5	1.0	900-1200	0.024	0.001
1.0	1.0	950-1250	0.012	0.001
1.5	1.0	950-1250	0.008	0.001

Table 5.1 Experimental and modelling conditions for the oxidation of *n*-propyl benzene in a jet-stirred reactor at  $P = 1$  atm. The species concentrations correspond to mole fractions

The overall species evolution profiles as a function of temperature are well reproduced by the current *n*-propyl benzene chemistry. The major species that were measured by Dagaut *et al.* [36] apart from  $O_2$ ,  $CO$  and  $CO_2$ , were ethyl benzene ( $C_8H_{10}$ ), styrene ( $C_8H_8$ ), toluene ( $C_7H_8$ ), benzene ( $C_6H_6$ ), acetylene ( $C_2H_2$ ), ethylene ( $C_2H_4$ ), methane ( $CH_4$ ) and formaldehyde ( $CH_2O$ ). The fuel decay is very well captured for all the three tested equivalence ratios and as the stoichiometry increases a better agreement between the model and the measurements is achieved for all the intermediate major species. The agreement between the predictions and the measurements of the fuel decay shows that the *n*-propyl benzene submechanism is adequate.

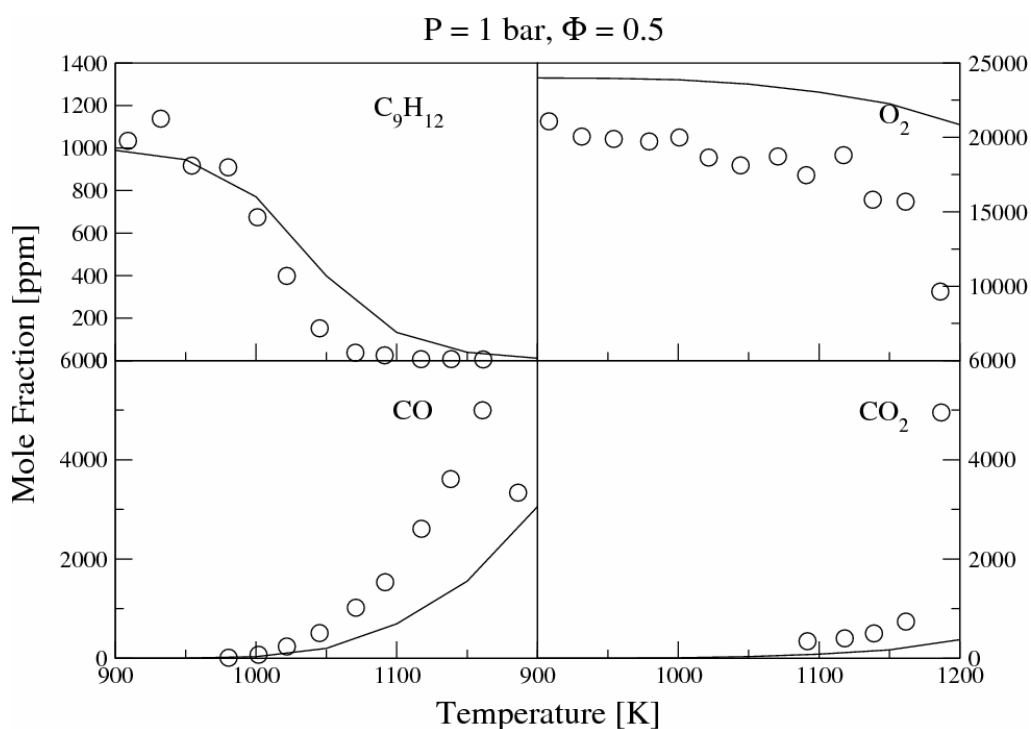


Figure 5.1 Concentration profiles of intermediate species during *n*-propyl benzene oxidation in a jet-stirred reactor with  $\Phi = 0.5$ ,  $P = 1$  atm,  $T = 900 - 1200$  K. The circles are measurements [36] and the solid line the current simulation.

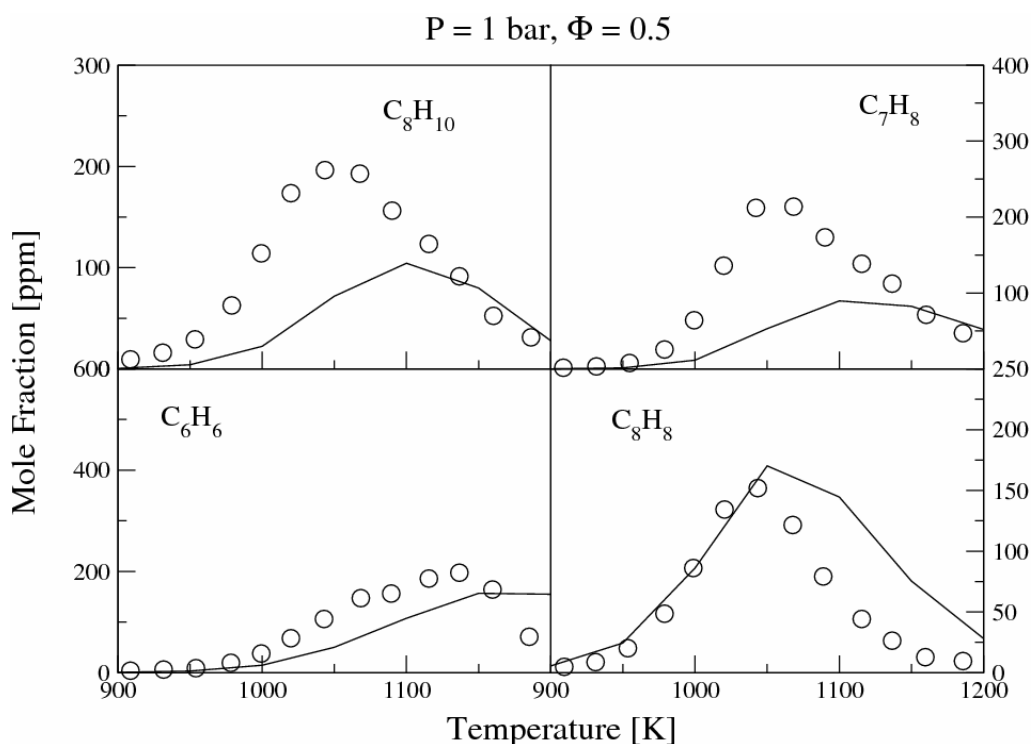


Figure 5.2 Concentration profiles of intermediate species during *n*-propyl benzene oxidation in a jet-stirred reactor with  $\Phi = 0.5$ ,  $P = 1$  atm,  $T = 900 - 1200$  K. The circles are measurements [36] and the solid line the current simulation.

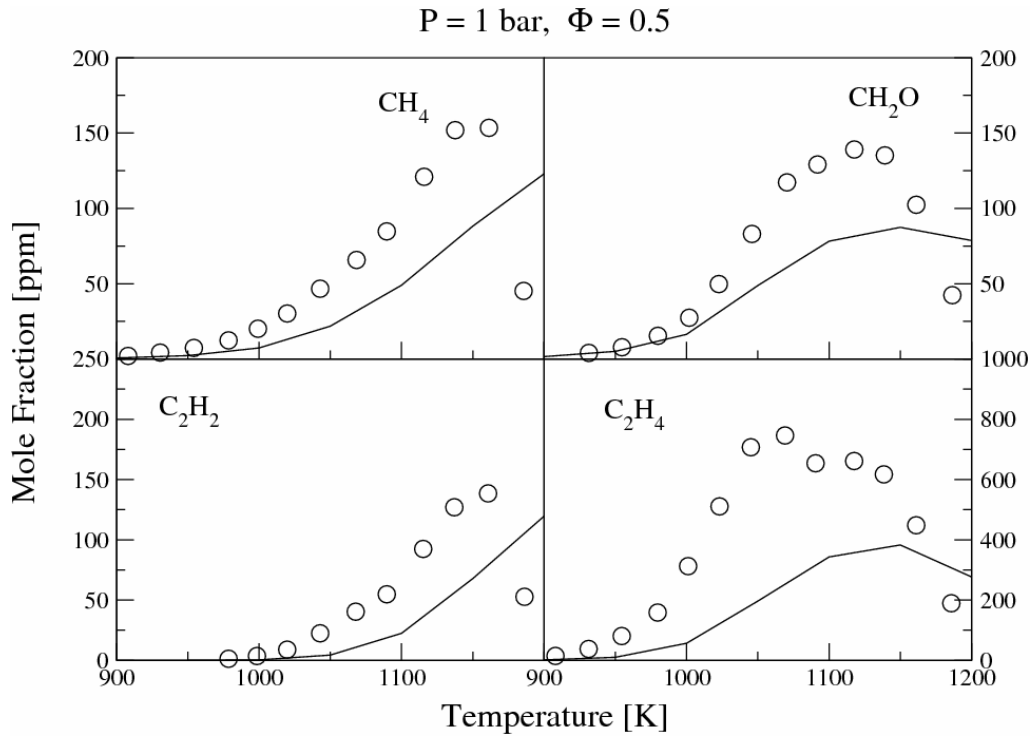


Figure 5.3 Concentration profiles of intermediate species during *n*-propyl benzene oxidation in a jet-stirred reactor with  $\Phi = 0.5$ ,  $P = 1 \text{ atm}$ ,  $T = 900 - 1200 \text{ K}$ . The circles are measurements [36] and the solid line the current simulation.

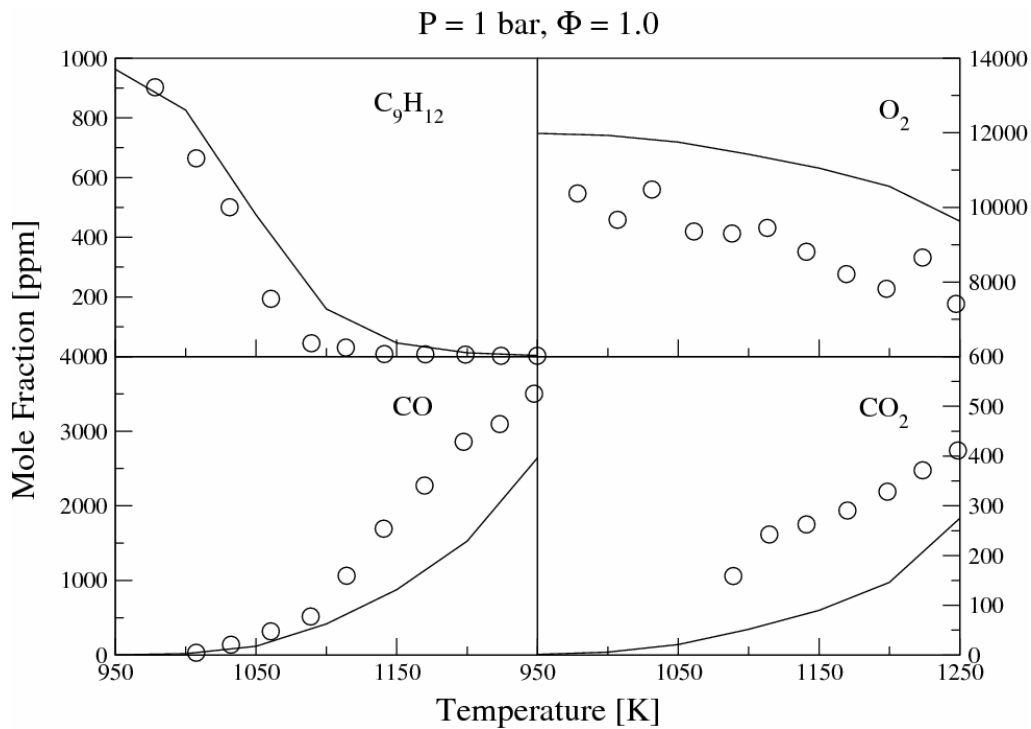


Figure 5.4 Concentration profiles of intermediate species during *n*-propyl benzene oxidation in a jet-stirred reactor with  $\Phi = 1.0$ ,  $P = 1 \text{ atm}$ ,  $T = 950 - 1250 \text{ K}$ . The circles are measurements [36] and the solid line the current simulation.

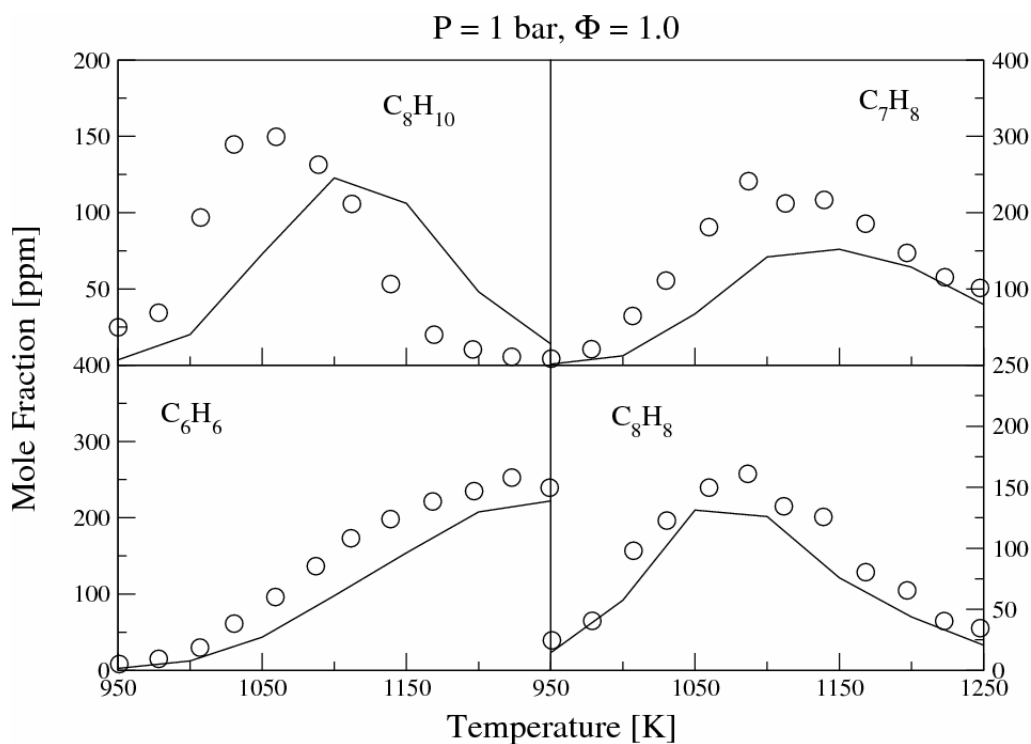


Figure 5.5 Concentration profiles of intermediate species during *n*-propyl benzene oxidation in a jet-stirred reactor with  $\Phi = 1.0$ ,  $P = 1$  atm,  $T = 950 - 1250$  K. The circles are measurements [36] and the solid line the current simulation.

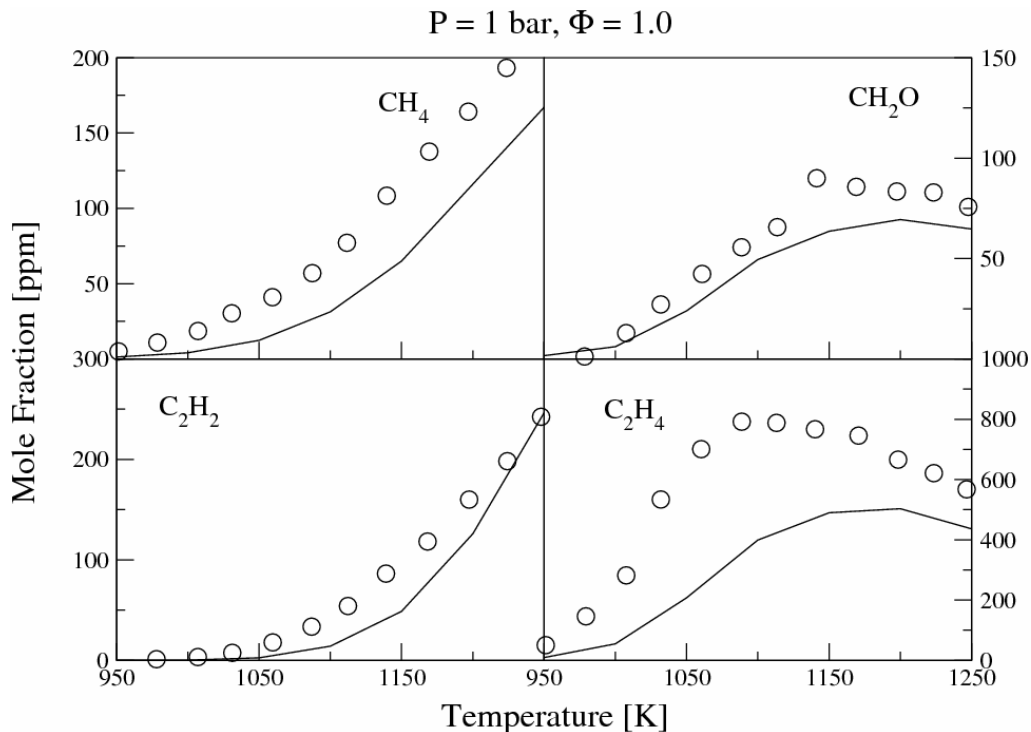


Figure 5.6 Concentration profiles of intermediate species during *n*-propyl benzene oxidation in a jet-stirred reactor with  $\Phi = 1.0$ ,  $P = 1$  atm,  $T = 950 - 1250$  K. The circles are measurements [36] and the solid line the current simulation.

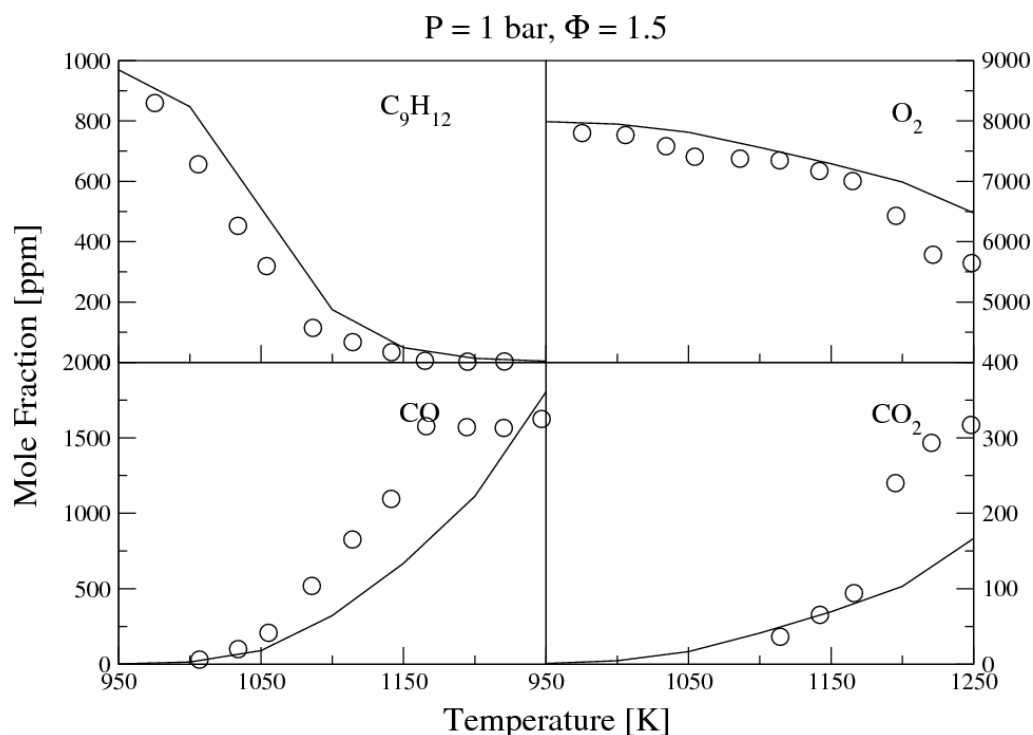


Figure 5.7 Concentration profiles of intermediate species during *n*-propyl benzene oxidation in a jet-stirred reactor with  $\Phi = 1.5$ ,  $P = 1 \text{ atm}$ ,  $T = 950 - 1250 \text{ K}$ . The circles are measurements [36] and the solid line the current simulation.

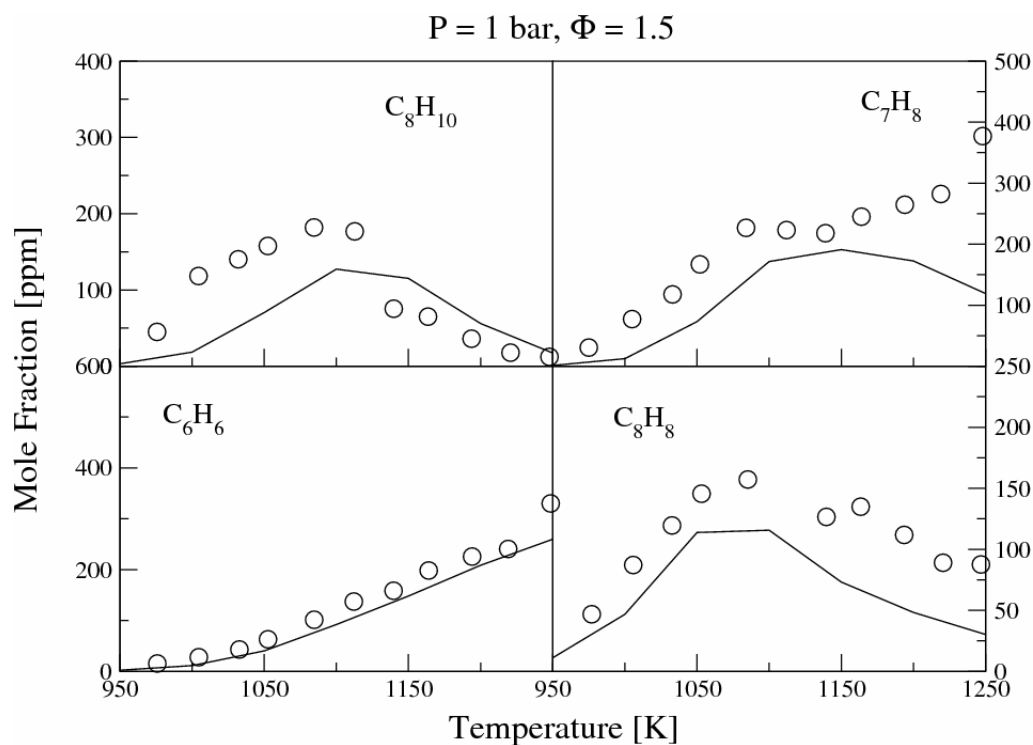


Figure 5.8 Concentration profiles of intermediate species during *n*-propyl benzene oxidation in a jet-stirred reactor with  $\Phi = 1.5$ ,  $P = 1 \text{ atm}$ ,  $T = 950 - 1250 \text{ K}$ . The circles are measurements [36] and the solid line the current simulation.

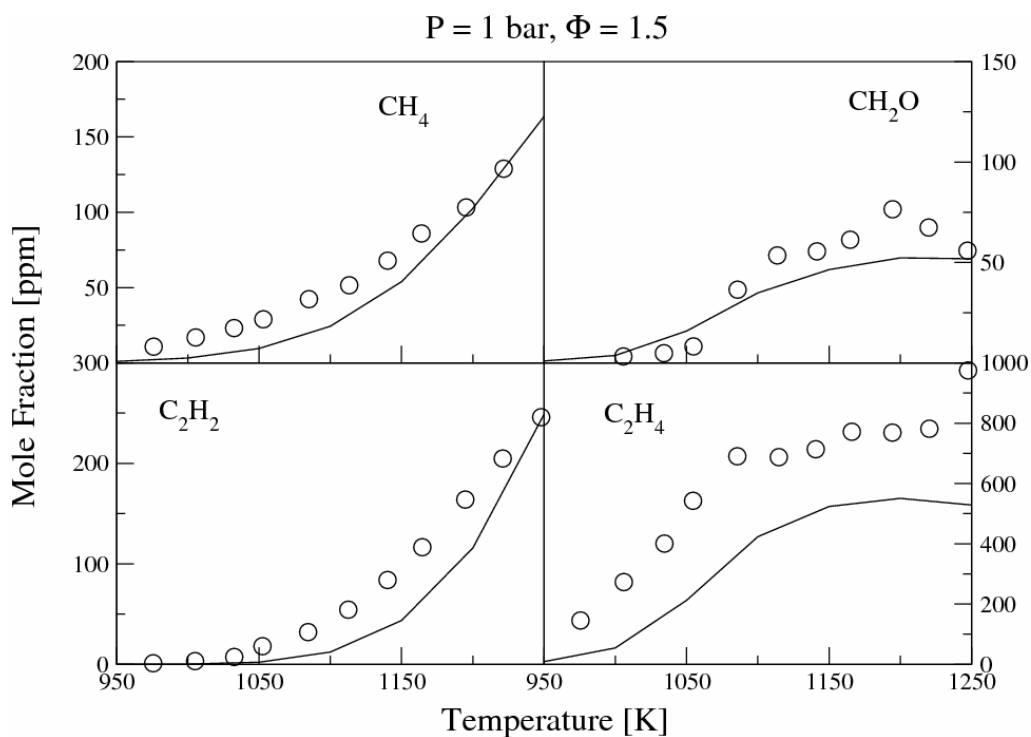


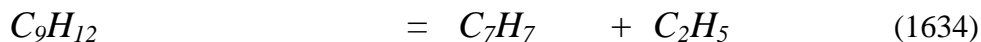
Figure 5.9 Concentration profiles of intermediate species during *n*-propyl benzene oxidation in a jet-stirred reactor with  $\Phi = 1.5$ ,  $P = 1 \text{ atm}$ ,  $T = 950 - 1250 \text{ K}$ . The circles are measurements [36] and the solid line the current simulation.

## 5.4 Rate Analysis for Fuel Oxidation at Atmospheric Pressure

A reaction rate analysis was performed for a fuel rich mixture ( $\Phi = 1.5$ ) tested under oxidation conditions in jet-stirred reactor at a temperature of 1050 K and at atmospheric pressure.

Computations show that the fuel decomposes predominantly (35%) by homolytic fission at the secondary carbon atom of the branch leading to the formation of benzyl and ethyl radicals. An additional 10% of the fuel is consumed via hydrogen abstraction reaction with hydrogen atom attack on the ‘benzylic’ (primary) carbon atom of the branch forming 1-propyl benzyl radical (1600). The kinetics of reaction (1634) was estimated according to the approach of Dean [13]. The same approach was applied to the C-C homolytic steps that occur either at the primary or at the tertiary carbon atom to estimate their kinetics. The rate utilized for reaction (1600) was based on suggestions of Dagaut *et al.* [36].

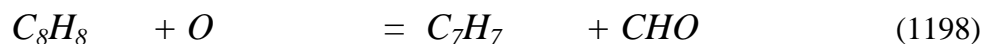
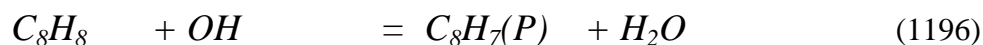
Approximately 23% of the total fuel consumption leads to the formation of the 1-propyl benzyl radical via hydrogen atom abstraction with  $H$ ,  $O$  and  $OH$  radicals. The primary homolytic reaction which occurs via C-C scission leading to the phenyl and propyl radicals corresponds to 8% of the total fuel consumption with a rate assigned based on the approach of Dean [13]. Approximately 16% of the total fuel concentration is decomposed via hydrogen abstraction reactions leading to the formation of the 2-propyl benzyl radical in comparison to 8% of the fuel that leads to 3-propyl benzyl radical (Figure 5.10).



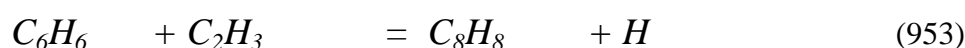
The 1-propyl benzyl radical decomposes (100%) to styrene via methyl radical abstraction with a rate adopted by Dagaut *et al.* [36]. The step also constitutes the major styrene formation pathway. Once styrene was formed, five major routes were detected that contribute to its decay. Reaction (1196) was assigned a rate proposed by Maurice [112] and contributes 21% to the consumption of styrene. The formed  $C_8H_7(P)$  recycles back to styrene (78%). The formation of the benzyl radical and



CHO (1198) constitutes the second major consumption pathway (18%) with a reaction rate suggested by Potter [75].



Reactions (953), (920) and (1199) make approximately equal contributions to the styrene consumption at 13, 12 and 10% respectively.



The major product of the fuel decay, the benzyl radical, recombines with a hydrogen atom leading to the formation of toluene and contributes (35%) to the total rate of formation. The recombination step is the major toluene formation channel (90%) and was assigned a rate from Oehlschlaeger *et al.* [90]. Approximately 34% of the benzyl radical reacts with the methyl radical and forms ethyl benzene with rate proposed by Lindstedt *et al.* [61]. The reaction step represents the major ethyl benzene formation channel (97%). Moreover, 20% of the benzyl radical recombines leading to  $C_{14}H_{14}$  with a reaction rate obtained from Oehlschlaeger *et al.* [90]. The major benzyl consumption steps are shown in Figure 5.11.

Ethyl benzene is consumed via two major steps. The displacement of the ethyl branch via a hydrogen atom is responsible for 50% of the ethyl benzene consumption. The second major channel occurs via hydrogen atom abstraction to the formation of ethylbenzyl radical (34%) which essentially recycles back to ethyl benzene (95%).



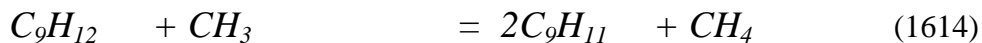
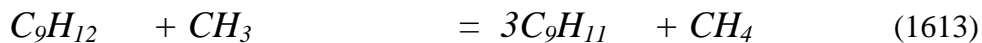
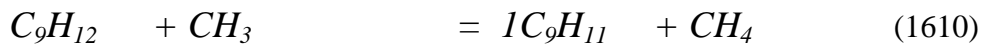
Benzene is decomposed via oxygen atom addition and hydrogen abstraction (957) leading to  $C_6H_5O$  (58%) with a rate adopted from DiNaro *et al.* [91] and 34% to the phenyl radical via  $OH$  attack (959) with a rate of Leung *et al.* [73]. Oxygen addition to the phenyl radical leads to the production of  $C_6H_5O$  (57%) and  $C_6H_5OO$  (42%). The latter products are responsible for cyclopentadienyl radical production by 70% and 25% respectively.



As mentioned above, the major fuel consumption pathway produces benzyl and ethyl radicals and also constitutes the major ethyl radical formation step (96%). The ethyl radical is consumed via hydrogen abstraction (95%) leading to the formation of ethylene (76%).

Acetylene is another important specie produced during propyl benzene oxidation. The main channel is via the thermal decomposition of the cyclopentadienyl radical (41%), which features an adjusted reaction rate proposed by Kern *et al.* [52]. An additional 28% of the acetylene production occurs via methyl abstraction from the  $C_3H_5(S)$  that is formed through the following reaction route  $C_9H_{12} \leftrightarrow 2C_9H_{11} \leftrightarrow C_3H_6 \leftrightarrow C_3H_5(S) \leftrightarrow C_2H_2$ .

Methane is formed via reaction routes directly linked to the fuel and involves hydrogen abstraction via methyl radical attack. The hydrogen abstraction reactions lead to the formation of  $1C_9H_{11}$  and  $3C_9H_{11}$  with each of these contributing 20% to the methane production. It must be noted that the relative methane production channel that produces  $2C_9H_{11}$  is responsible for not more than 3% of the methane production. The rates assigned to the following reactions are based on the kinetics of propane suggested by Tsang [113].



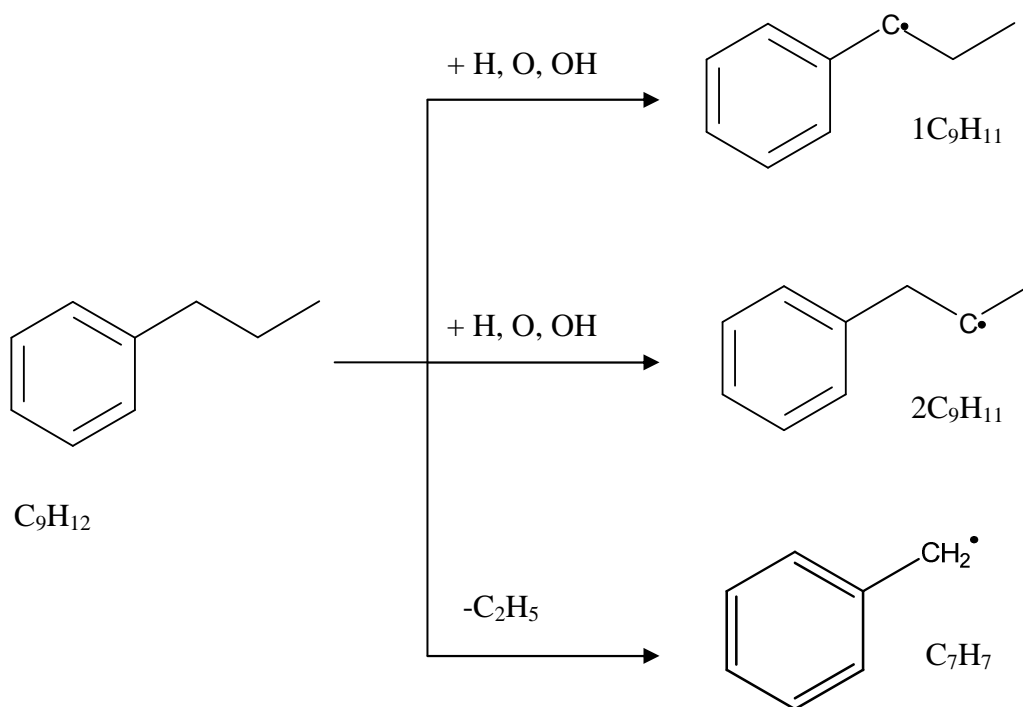


Figure 5.10 Major *n*-propyl benzene decomposition routes for  $\Phi = 1.5$ ,  $T = 1050 \text{ K}$  and  $P = 1 \text{ atm}$  in a jet-stirred reactor

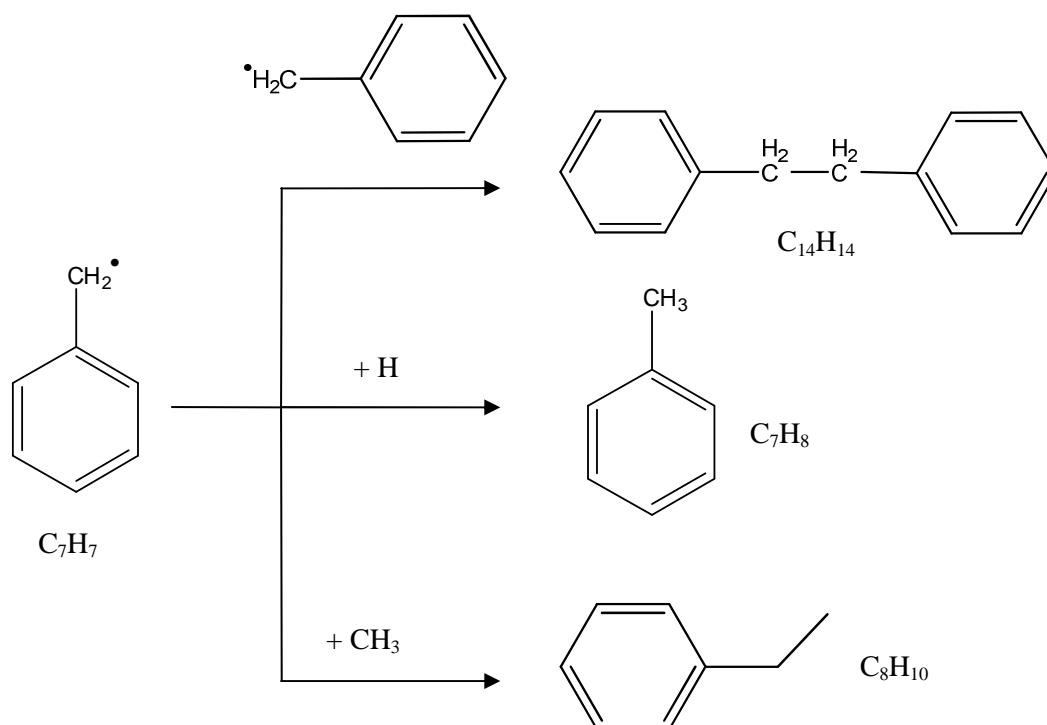


Figure 5.11 Benzyl radical consumption paths for  $\Phi = 1.5$ ,  $T = 1050 \text{ K}$  and  $P = 1 \text{ atm}$  in a jet-stirred reactor

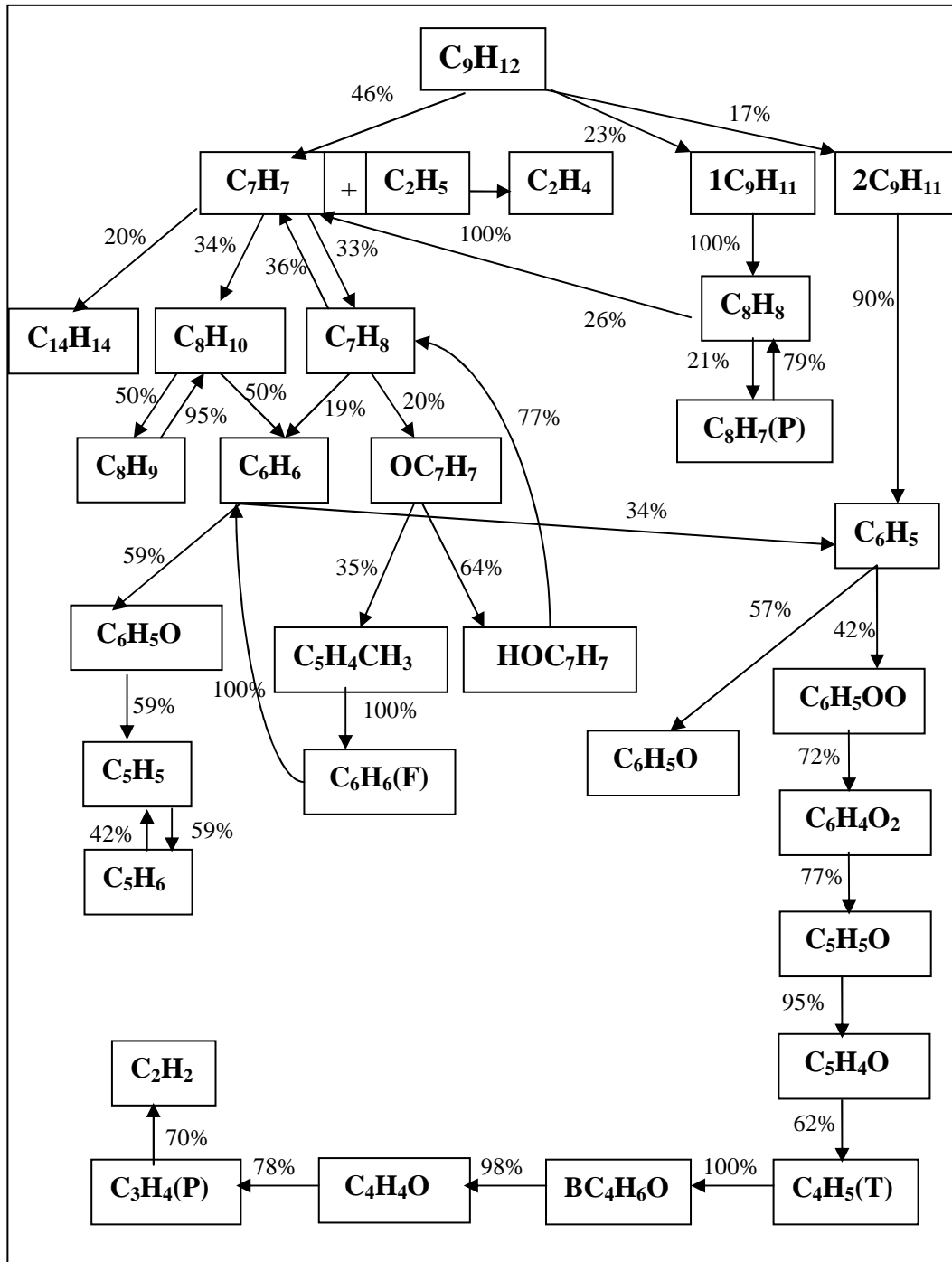


Figure 5.12 *N*-Propyl benzene oxidation for  $\Phi = 1.5$ ,  $T = 1050$  K and  $P = 1$  atm in a jet stirred reactor

## 5.5 Oxidation at High Pressures

The oxidation of *n*-propyl benzene was also studied under Jet Stirred Reactor (JSR) conditions at a pressure of 10 atm and validated utilizing measurements obtained by Dagaut *et al.* [114]. The stoichiometries tested were 0.5, 1.0, 1.5 and 2.0 for a temperature range of 900 – 1200 K. Concentrations of the major species are predicted at a residence time of  $\tau = 0.5$  sec. The conditions tested are summarized in Table 5.2. Comparisons between the simulations and experimental data sets from Dagaut *et al.* [114] are shown in Figure 5.13 to Figure 5.24.

$\Phi$	P(atm)	T (K)	$X_{O_2}$	$X_{C_9H_{12}}$
0.5	10.0	900-1200	0.024	0.001
1.0	10.0	900-1200	0.012	0.001
1.5	10.0	900-1200	0.008	0.001
2.0	10.0	900-1200	0.006	0.001

Table 5.2 Experimental and modelling conditions for the oxidation of *n*-propyl benzene in a jet-stirred reactor at P = 10 atm. The species concentrations correspond to mole fractions

The computed species profiles for all the equivalence ratios are reasonably well reproduced when compared to the measurements. Predictions in this study are shown on a normal scale compared to the logarithmic variant often used in other studies in order to highlight both agreement and discrepancies in the fuel decay and species formation at high pressures. The *n*-propyl benzene submechanism that involves the thermal scission at either of the three carbon atoms of the branch plays a pivotal role in the evolution of the rest of the major species. The reaction rates applied to these three steps were initially based on the propane chemistry and found to result in slow ignition and underproduction of the species concentrations. Hence, an adjustment according to that of the Dean [13] theory was applied to the channels and was shown to perform better and arguably to satisfactory predictions.

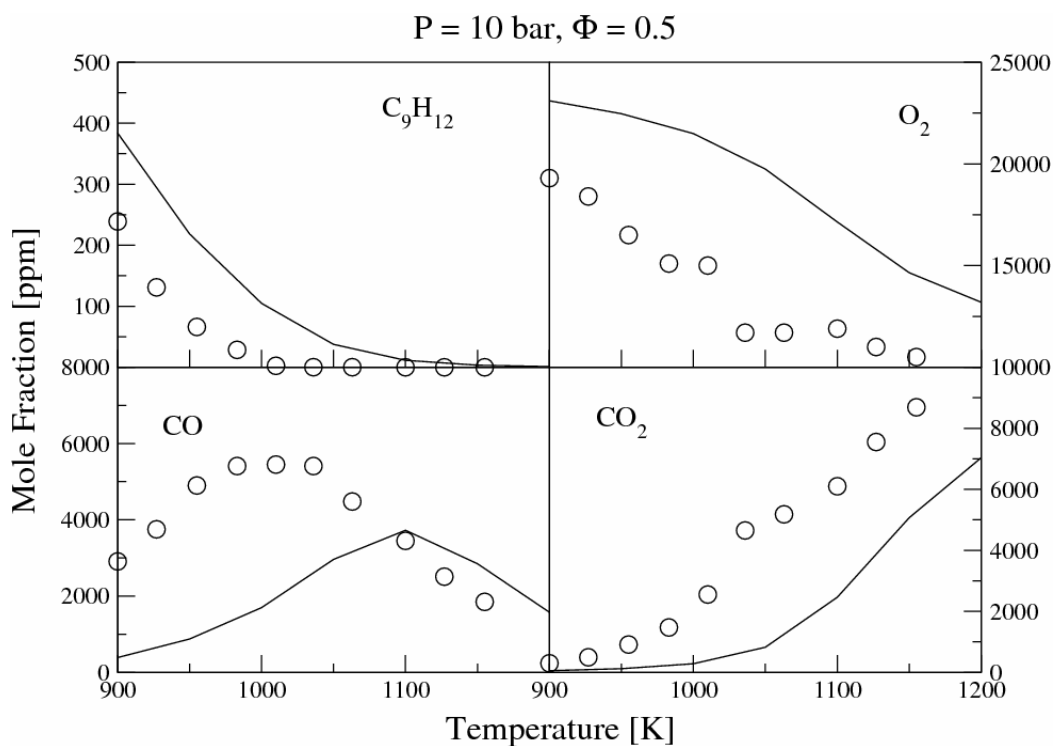


Figure 5.13 Concentration profiles of intermediate species during *n*-propyl benzene oxidation in a jet-stirred reactor with  $\Phi = 0.5$ ,  $P = 10 \text{ atm}$ ,  $T = 900 - 1200 \text{ K}$ . The circles are measurements [114] and the solid lines the current computations.

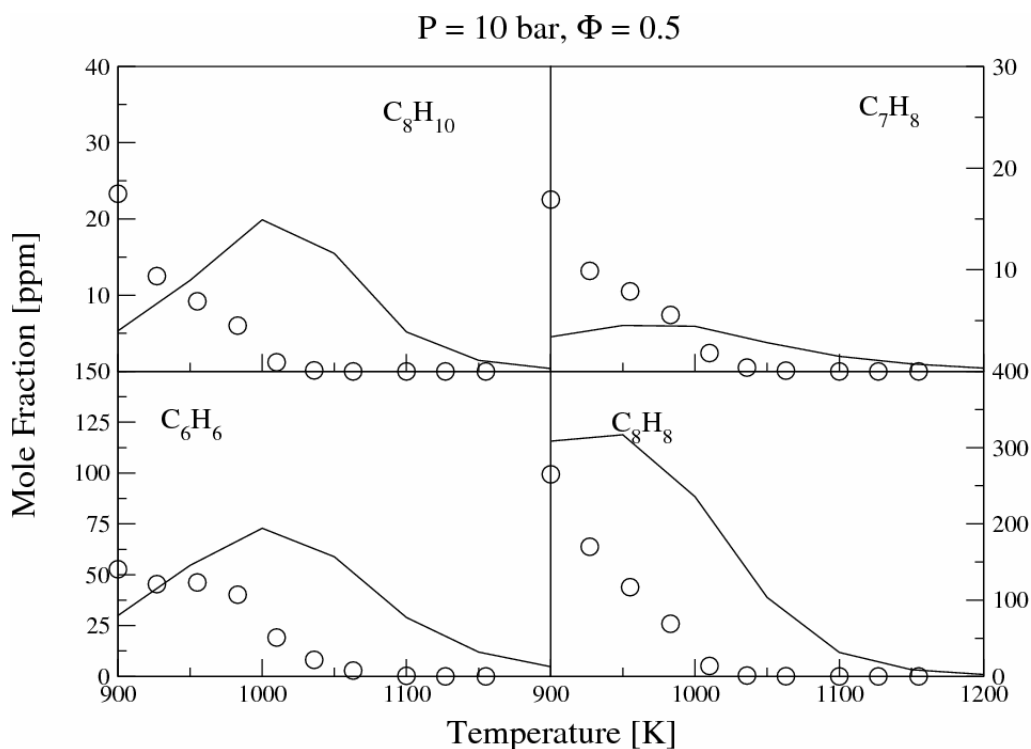


Figure 5.14 Concentration profiles of intermediate species during *n*-propyl benzene oxidation in a jet-stirred reactor with  $\Phi = 0.5$ ,  $P = 10 \text{ atm}$ ,  $T = 900 - 1200 \text{ K}$ . The circles are measurements [114] and the solid lines the current computations.

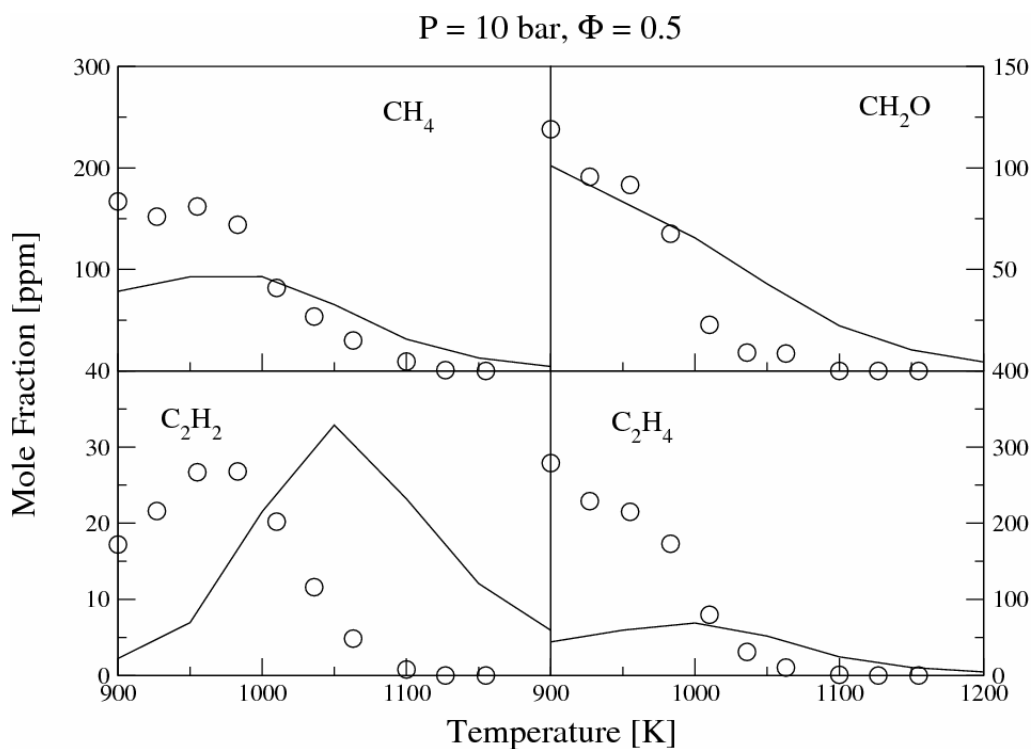


Figure 5.15 Concentration profiles of intermediate species during *n*-propyl benzene oxidation in a jet-stirred reactor with  $\Phi = 0.5$ ,  $P = 10 \text{ atm}$ ,  $T = 900 - 1200 \text{ K}$ . The circles are measurements [114] and the solid lines current computations.

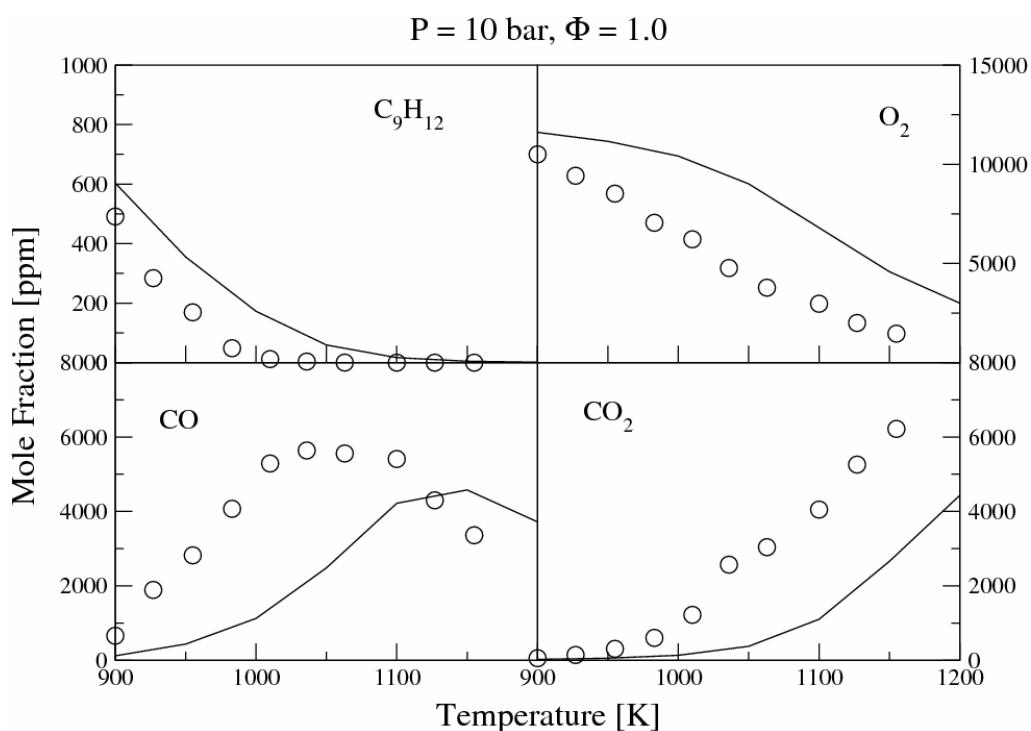


Figure 5.16 Concentration profiles of intermediate species during *n*-propyl benzene oxidation in a jet-stirred reactor with  $\Phi = 1.0$ ,  $P = 10 \text{ atm}$ ,  $T = 900 - 1200 \text{ K}$ . The circles are measurements [114] and the solid lines the current computations.

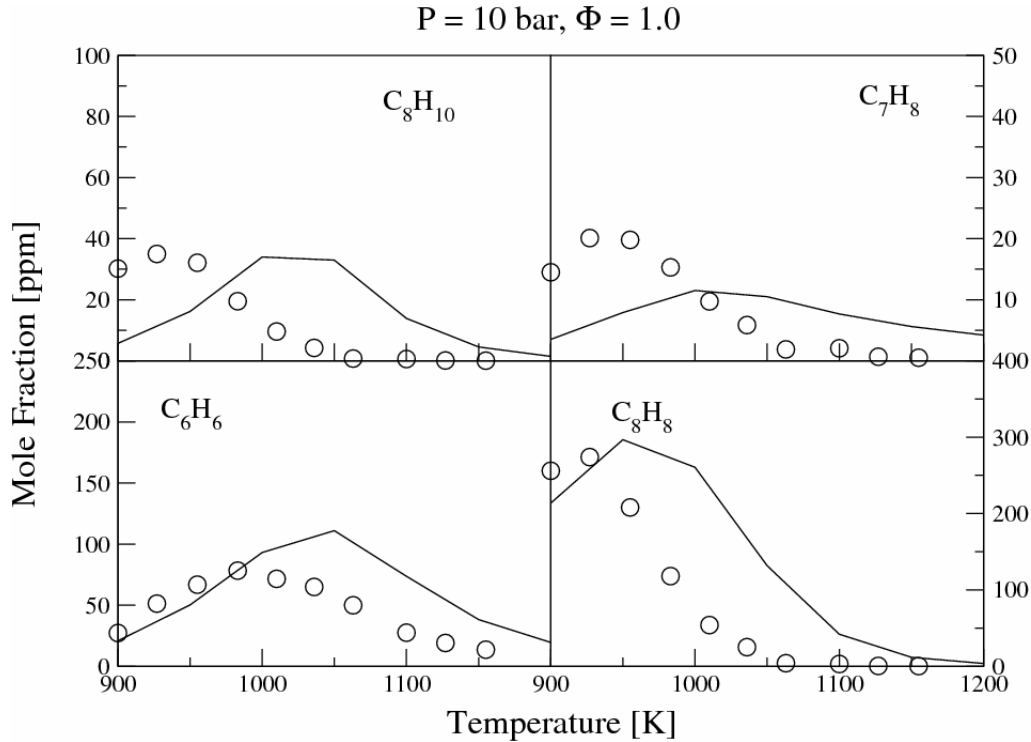


Figure 5.17 Concentration profiles of intermediate species during *n*-propyl benzene oxidation in a jet-stirred reactor with  $\Phi = 1.0$ ,  $P = 10 \text{ atm}$ ,  $T = 900 - 1200 \text{ K}$ . The circles are measurements [114] and the solid lines the current computations.

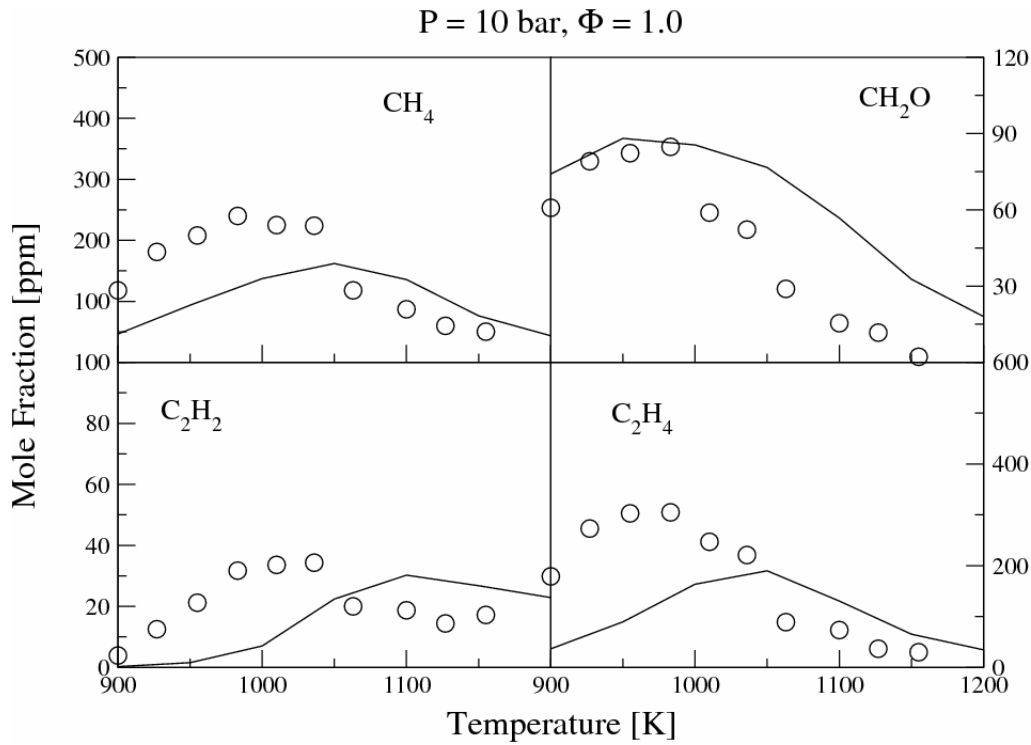


Figure 5.18 Concentration profiles of intermediate species during *n*-propyl benzene oxidation in a jet-stirred reactor with  $\Phi = 1.0$ ,  $P = 10 \text{ atm}$ ,  $T = 900 - 1200 \text{ K}$ . The circles are measurements [114] and the solid lines the current computations.



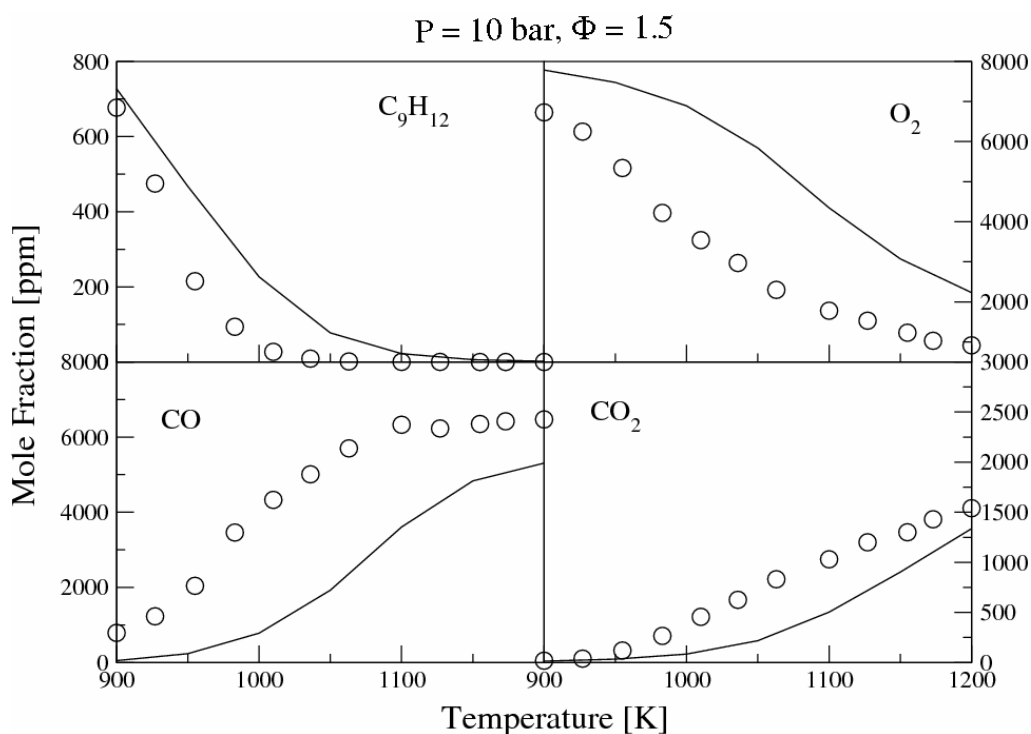


Figure 5.19 Concentration profiles of intermediate species during *n*-propyl benzene oxidation in a jet-stirred reactor with  $\Phi = 1.5$ ,  $P = 10$  atm,  $T = 900 - 1200$  K. The circles are measurements [114] and the solid lines the current computations.

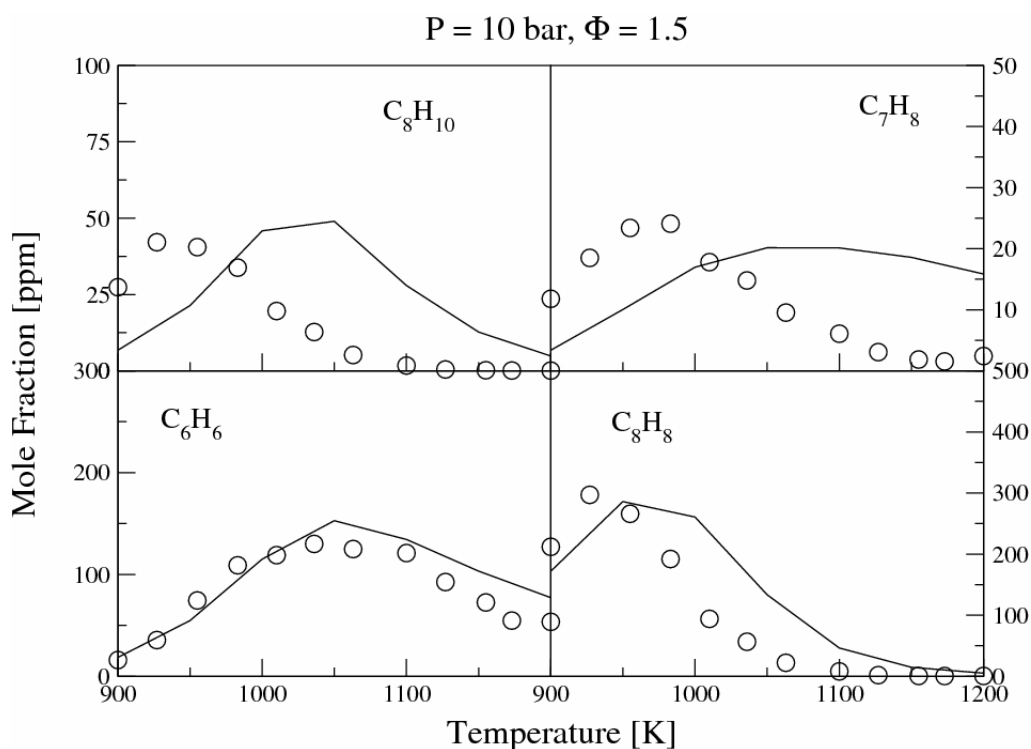


Figure 5.20 Concentration profiles of intermediate species during *n*-propyl benzene oxidation in a jet-stirred reactor with  $\Phi = 1.5$ ,  $P = 10$  atm,  $T = 900 - 1200$  K. The circles are measurements [114] and the solid lines the current computations.

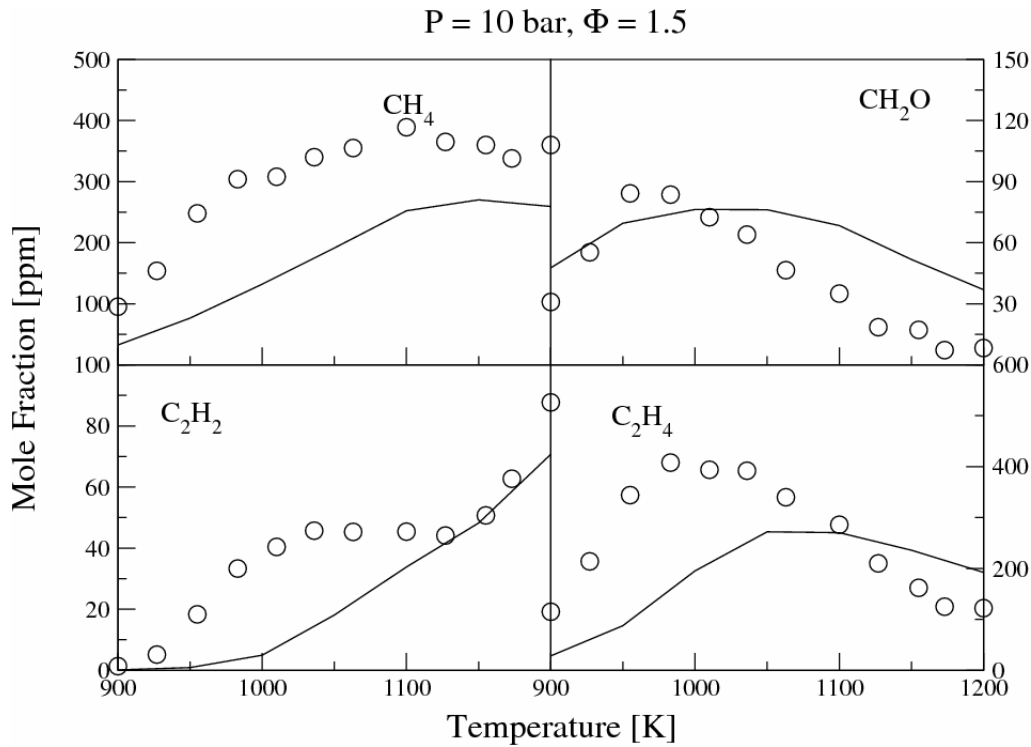


Figure 5.21 Concentration profiles of intermediate species during *n*-propyl benzene oxidation in a jet-stirred reactor with  $\Phi = 1.5$ ,  $P = 10 \text{ atm}$ ,  $T = 900 - 1200 \text{ K}$ . The circles are measurements [114] and the solid lines the current computations.

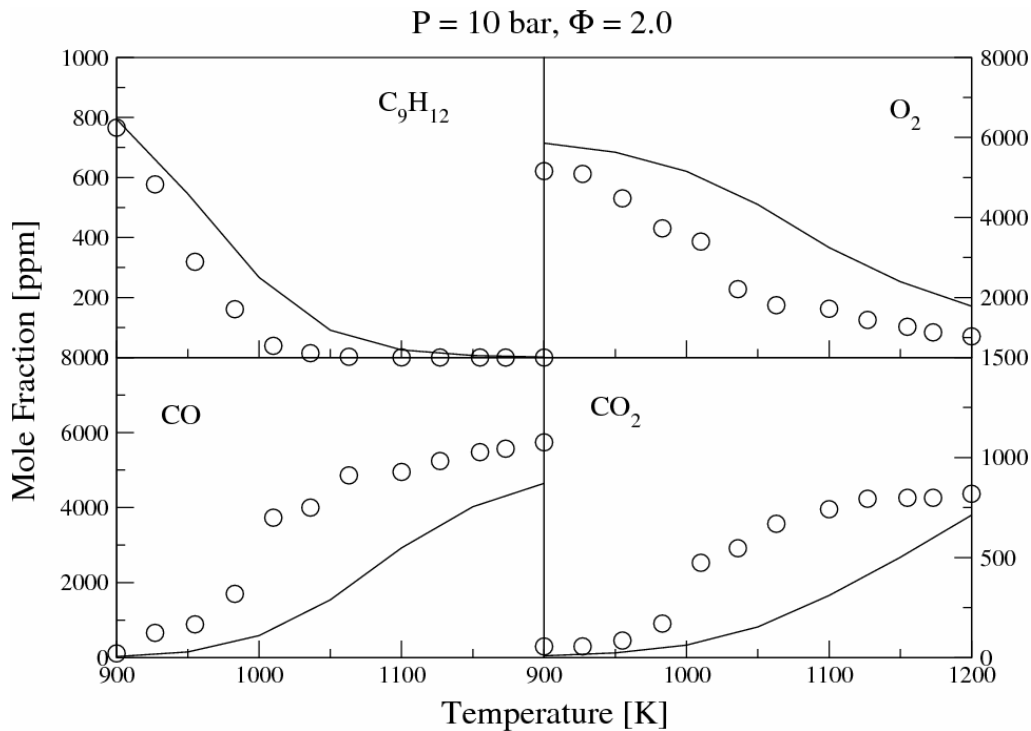


Figure 5.22 Concentration profiles of intermediate species during *n*-propyl benzene oxidation in a jet-stirred reactor with  $\Phi = 2.0$ ,  $P = 10 \text{ atm}$ ,  $T = 900 - 1200 \text{ K}$ . The circles are measurements [114] and the solid lines the current computations.

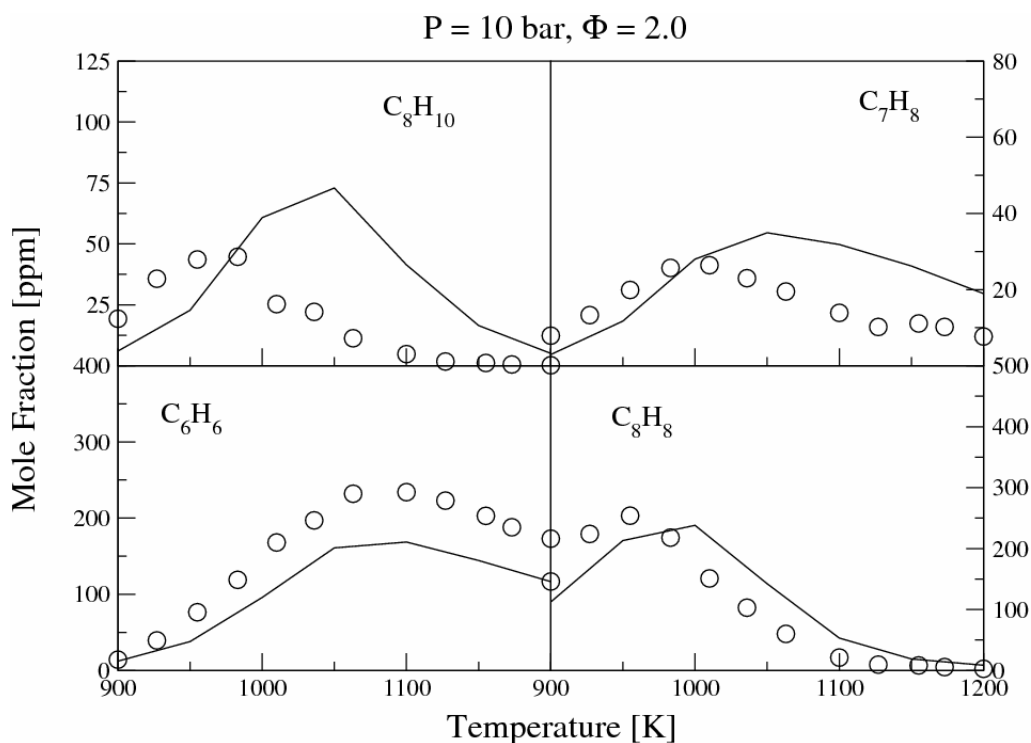


Figure 5.23 Concentration profiles of intermediate species during *n*-propyl benzene oxidation in a jet-stirred reactor with  $\Phi = 2.0$ ,  $P = 10 \text{ atm}$ ,  $T = 900 - 1200 \text{ K}$ . The circles are measurements [114] and the solid lines the current computations.

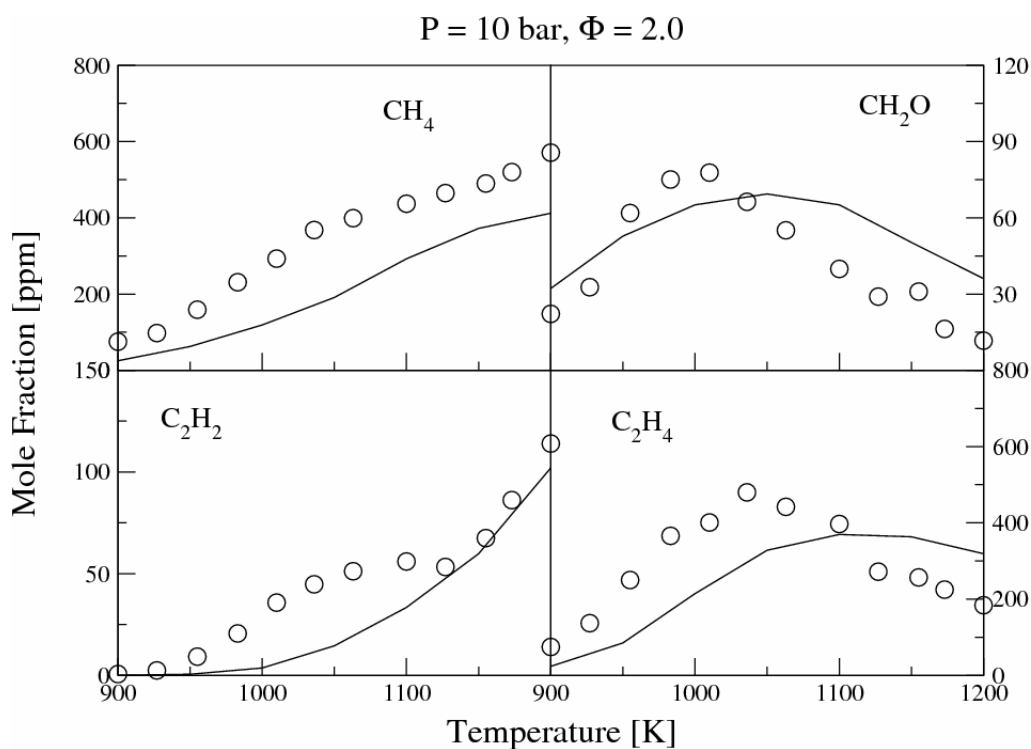
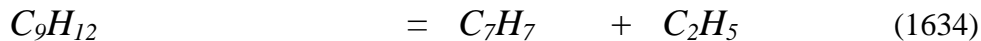


Figure 5.24 Concentration profiles of intermediate species during *n*-propyl benzene oxidation in a jet-stirred reactor with  $\Phi = 2.0$ ,  $P = 10 \text{ atm}$ ,  $T = 900 - 1200 \text{ K}$ . The circles are measurements [114] and the solid lines the current computations.

## 5.6 Rate Analysis for Fuel Oxidations at High Pressures

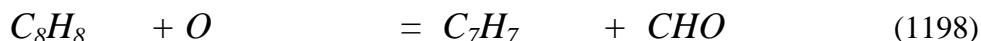
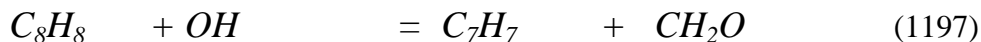
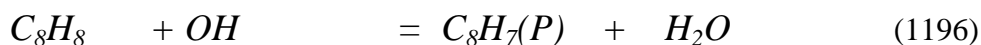
A reaction rate analysis was performed for a fuel rich mixture ( $\Phi = 1.5$ ) that was tested under oxidation conditions in a jet-stirred reactor at a temperature of 1050 K and at a pressure of 10 atm.

The fuel is decomposed through the same reaction steps as at low pressures. The *C-C* scission proceeds through a homolytic reaction (25%) that leads to the formation of benzyl and ethyl radicals (1634) plays a significant role. However, the impact of the step is reduced as compared to the contribution of 35% at low pressures. The other two major products of the fuel consumption,  $1C_9H_{11}$  (23%) and  $2C_9H_{11}$  (16%), are produced through hydrogen abstraction reactions. However, at high pressures the dominant fuel consumption channel that leads to the formation of  $1C_9H_{11}$  (1602) occurs via *OH* attack (15%) compared to the hydrogen atom attack which is favoured at atmospheric pressures. The same applies to the formation of the  $2C_9H_{11}$  radical (1605), which is mostly produced via *OH* attack which is responsible for 12% of the total fuel breakdown.



The  $1C_9H_{11}$  decomposition follows the same route as at lower pressures by producing  $C_8H_8$  (100%). Styrene is further decomposed via three reaction channels (1196, 1197, 1198). Reaction (1196) shows an increased impact as the pressure increases. At the 10 atm the step contributes 35% compared to 21% for the low pressure. Reaction (1197) also plays a significant role in the styrene consumption (15%), and the impact is increased by a factor of 2 compared to the low pressure case. A rate suggested by Maurice [112] was tested but caused toluene and phenyl acetylene overproduction as it was found to be faster than that proposed by Rizos [72] by a factor of 2. The rate proposed by Rizos [72] was also tested and found to produce satisfactory results that improve the profiles of  $C_8H_8$ ,  $C_7H_8$  and  $C_8H_6$ . The atomic oxygen attack on styrene leading to *C-C* scission and production of benzyl

and formyl radical shows a reduction to 11% as compared to 19% at atmospheric pressures.



The benzyl radical, which is one of the major products (1634) follows a different route at higher pressures. Although it is decomposed via three major pathways, only two of these are identical at low and high pressures. Moreover, the impact of the two identical consumption routes is also different. More specifically, the benzyl radical reacts with the methyl radical leading to the formation of ethyl benzene (1063) contributing 20%, as compared to 34% at atmospheric pressures. A big difference is also noted for the hydrogen recombination reaction with  $C_7H_7$  leading to the formation of toluene (1078), which is responsible for only 13% of the benzyl radical consumption compared to 35% at atmospheric pressure. A major difference at 10 atm is that the benzyl radical does not recombine with itself to the formation of  $C_{14}H_{14}$ , as at 1 atm, but it is being oxidized to  $C_7H_7O$  via  $HO_2$  via reaction (1064), which contributes up to 47% to the benzyl radical consumption. The rate assigned to reaction (1064) follows the suggestions by Rizos [72] and is based on suggestions of Ellis *et al.*[115].



Ethyl benzene is consumed (29%) to  $C_8H_9$ , and subsequently recycles back. The rate assigned to (1206) was adopted from Maurice [112]. An additional 43% of  $C_8H_{10}$  reacts with atomic hydrogen leading to  $C_6H_6$  and  $C_2H_5$  in a similar manner to the lower pressure case. The rate used for reaction (1207) was adopted from Robaugh *et al.* [116].



Benzene is predominantly formed (30%) from the thermal decomposition of  $C_7H_7O$ , which is produced (90%) from the benzyl radical and 16% from the primary C-C scission of propyl benzene via hydrogen attack. Whereas, at low pressures benzene is formed by the primary C-C scission of the fuel (65%). Benzene is oxidized via two major reaction routes, the impact of which is reversed compared to the low pressure case. Reaction (957) is responsible for 34% of the benzene oxidation versus 59% and reaction (959) is responsible for 56% of the consumption versus 33% at atmospheric pressure.



As mentioned above, ethyl benzene is responsible for the production of the ethyl radical which leads to the formation of ethylene (60%). Acetylene is formed (56%) from  $C_4H_4$ . At low pressures, acetylene is produced via thermal decomposition of  $C_3H_5(S)$  (27%) and  $C_5H_5$  (41%). Hence, at high pressures acetylene follows a different formation route.

The production of methane is also interesting. At high pressures, methane is produced via three major channels (80, 81, 106) that do not directly involve the fuel.



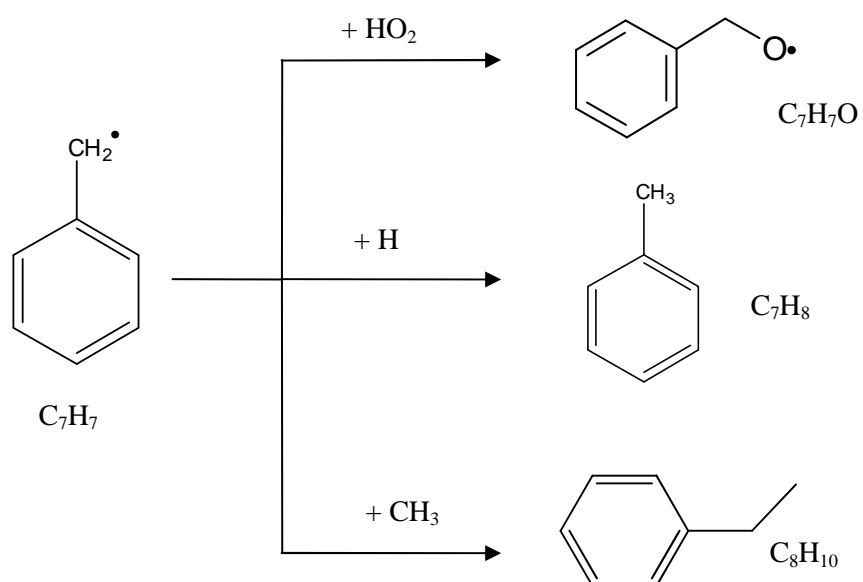


Figure 5.25 Benzyl radical consumption paths for  $\Phi = 1.5$ ,  $T = 1050$  K and  $P = 10$  atm in a jet-stirred reactor

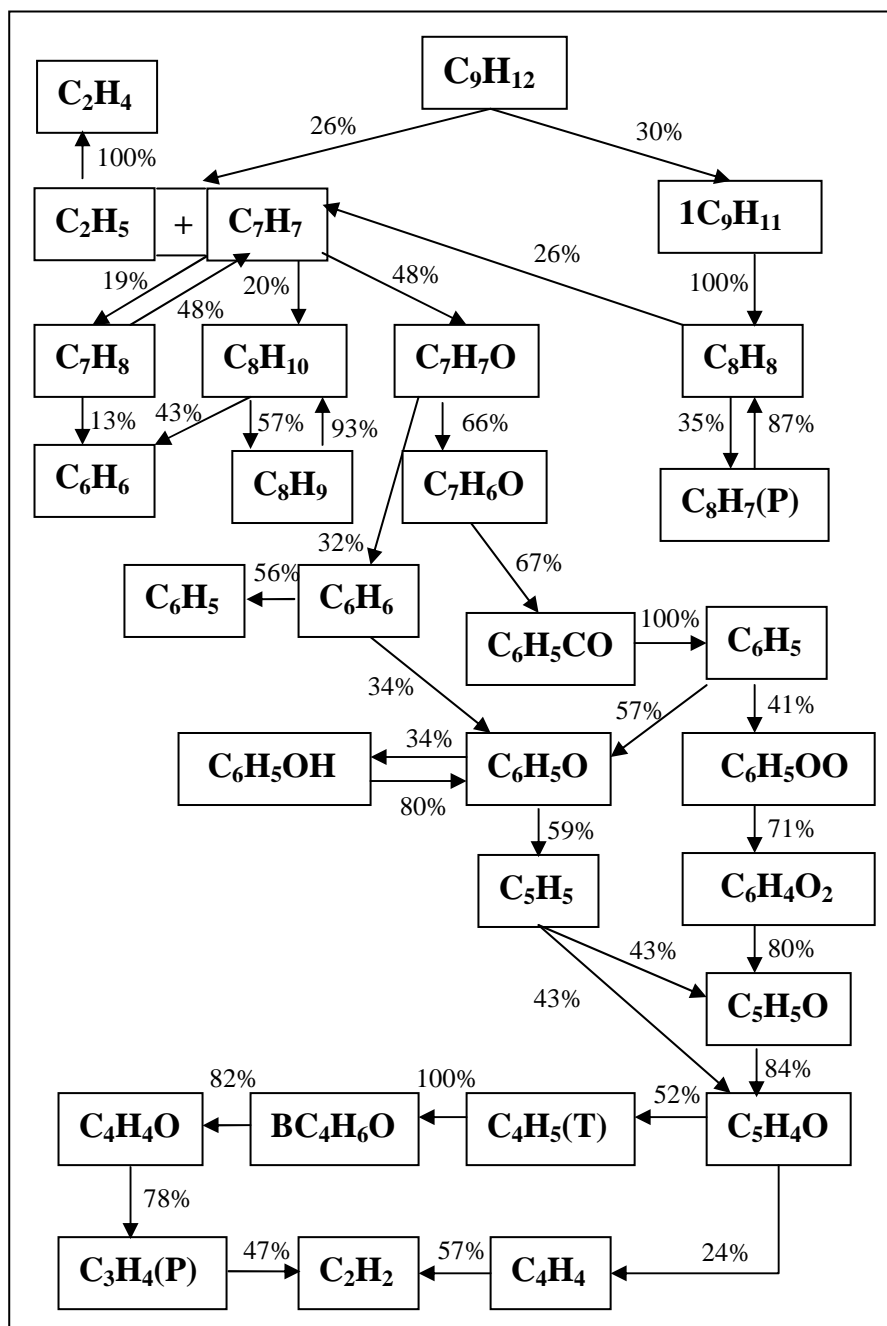


Figure 5.26  $N$ -propyl benzene oxidation for  $\Phi = 1.5$ ,  $T = 1050$  K and  $P = 10$  atm in a jet-stirred reactor



## 5.7 N-Propyl benzene Ignition Delay Times

Ignition delay times for *n*-propyl benzene were computed and validated against measurements obtained by Eberius *et al.* [117] as shown in Figure 5.27. The data were obtained in *n*-propyl benzene/ $O_2$ /Ar mixtures for a temperature range of 1400 – 1760 K, a pressure range of 5 atm and stoichiometries from 0.8 – 1.142. The ignition delay time was defined by Eberius *et al.* [117] as the time needed for the CH-emission signal to reach its peak value. Low dilution conditions were responsible for difficulties in evaluating the measured data by Eberius *et al.* [117] due to the change in density during the progress of reaction. Hence, a series of experiments for fuel/ $O_2$  mixtures diluted in Argon were used. The set of conditions computed are shown in Table 5.3.

	[ $C_9H_{12}$ ] (ppm)	[ $O_2$ ] (ppm)	[Ar] (ppm)	$\Phi$	P (atm)	T (K)
1	537	8057	991406	0.800	5	1437
2	545	8057	991398	0.812	5	1416
3	537	8057	991406	0.800	5	1569
4	545	6289	993166	1.040	5	1468
5	544	6289	993167	1.038	5	1631
6	541	6289	993170	1.032	5	1549
7	598	6284	993118	1.142	5	1558
8	536	6284	993180	1.024	5	1555
9	542	6284	993174	1.035	5	1478
10	536	6284	993180	1.024	5	1759
11	538	6295	993167	1.026	5	1448
12	537	6295	993168	1.024	5	1606
13	553	6295	993152	1.054	5	1550

Table 5.3 Experimental and modelling conditions for *n*-propyl benzene ignition delay times in a shock tube

As can be seen in Figure 5.27 the current *n*-propyl benzyl chemical model provides very satisfactory predictions of the ignition delay times at intermediate temperatures.

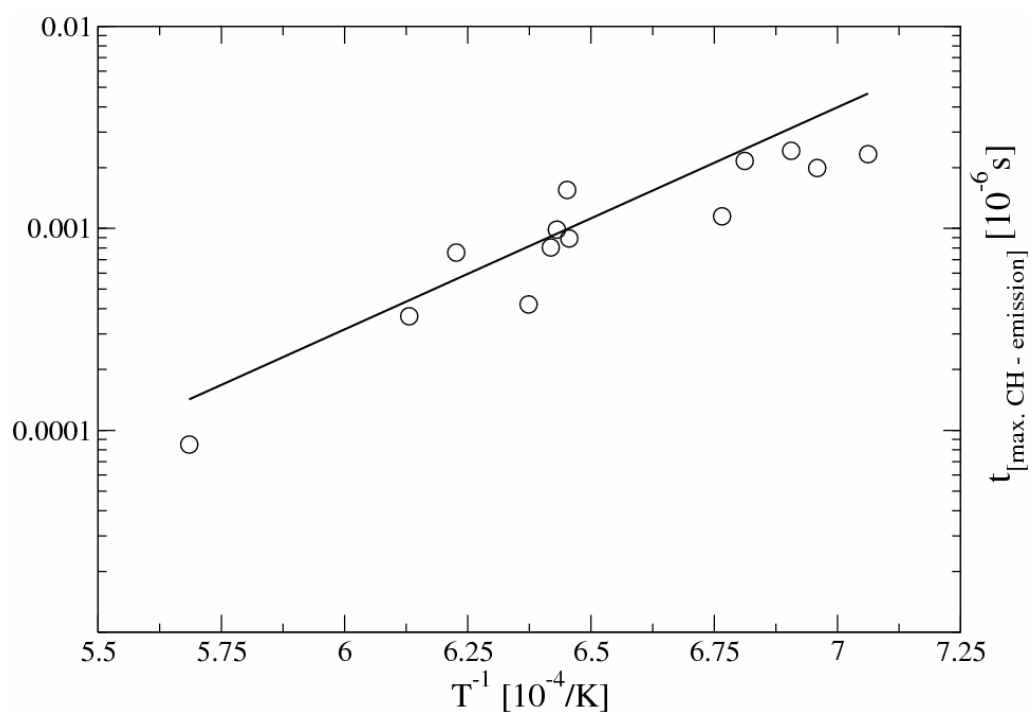
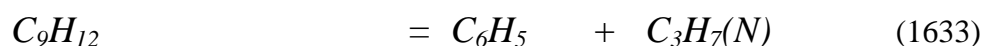


Figure 5.27 Ignition delay times of *n*-propyl benzene at  $P = 5$  atm,  $0.71 < \Phi < 1.18$ . The circles are the measurements [117] and the solid line is the current simulation

## 5.8 Rate Analysis for Auto-ignition of N-Propyl benzene

A reaction rate analysis was performed at 1148 K (Case 11 - Table 5.2) and major reaction channels for the fuel breakdown were identified corresponding to Figure 5.28. The fuel is solely decomposed via thermal breakdown to phenyl (46%) and benzyl (51%) radicals. The rates assigned to the thermal decomposition steps (1633) and (1634) were based on the approach of Dean [13].

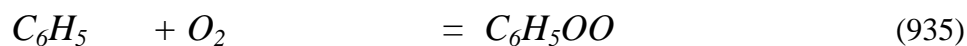


The benzyl radical is predominantly (65%) consumed via hydrogen recombination to toluene. Under jet stirred reactor conditions the formation of toluene is responsible for 35% of the benzyl radical consumption. Most of the toluene (47%) recycles back to benzyl radical via hydrogen abstraction reactions with  $H$  (1080) and  $OH$  radical attack (1083), while 14% produces benzene via  $C-C$  scission (1081) and 12% is oxidized to  $OC_7H_7$  (1091). The rate assigned to reaction (1080) was adopted from Oehlschlaeger *et al.* [90] and the second benzyl radical formation channel (1083) used a rate proposed by Baulch *et al.* [101]. The rate proposed by Oehlschlaeger *et al.* [90] was used for reaction (1081) while the toluene oxidation channel (1091) was assigned a rate suggested by Hoffman *et al.* [118].



Most of the benzene is consumed via hydrogen abstraction with  $H$  (21%) and  $OH$  (42%) radicals leading to the phenyl radical. An additional 32% of the former is oxidized to phenoxy via reaction with atomic oxygen. The phenyl radical constitutes the second major direct product from the fuel consumption. However, the

production comes predominantly from the decomposition of benzene. Once the phenyl radical is formed, 71% is oxidised to  $C_6H_5O$  (934) and 22% to  $C_6H_5OO$  (935) respectively.



The phenoxy radical is further decomposed to cyclopentadienyl radical (80%), which subsequently is thermally decomposed (73%) to the propargyl radical and acetylene. Approximately 34% of  $C_6H_5OO$ , is converted to  $C_6H_5O$  and the dominant consumption channel of  $C_6H_5OO$  leads to  $C_6H_4O_2$  formation. The latter goes through the sequence of reaction steps illustrated in Figure 5.28 that lead to the formation of acetylene.

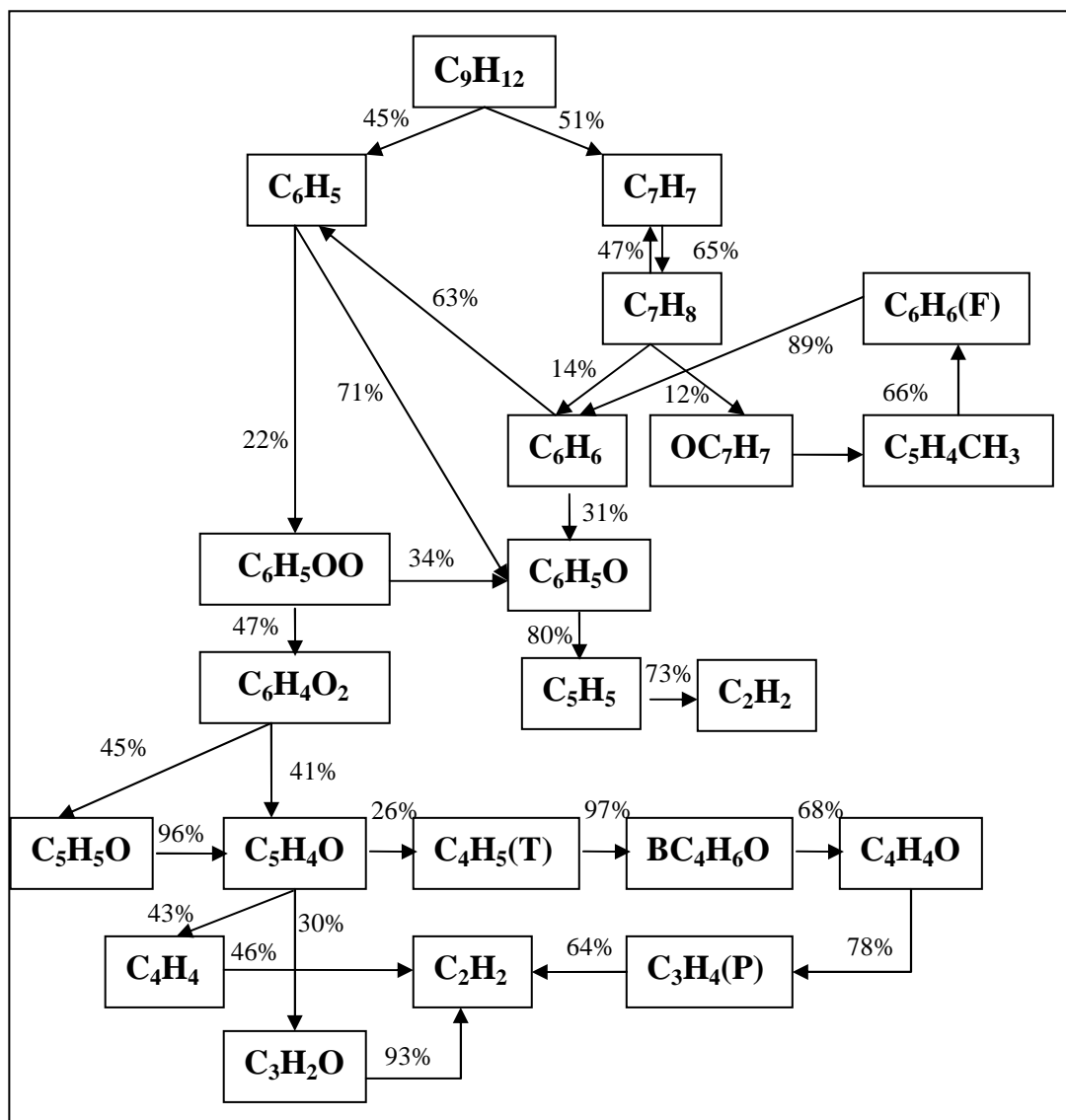


Figure 5.28 Reaction pathways for the oxidation of *n*-propyl benzene in a shock tube at T = 1448 K,  $\Phi = 1.026$  and P = 5.06 bar

## 5.9 Conclusions

In the present chapter, a detailed chemical mechanism for *n*-propyl benzene oxidation featuring 1683 reversible reactions and 269 species was proposed and validated under oxidation conditions in jet-stirred reactors and shock tubes. New reaction rates were evaluated and further updates applied. The validation was performed via comparisons with ignition delay times and measured species concentrations obtained by Eberius *et al.* [117], Dagaut *et al.* [36] and Dagaut [114].

The *n*-propyl benzene chemistry was partly developed based on chemical structure similarities with toluene and propane for reactions occurring at the *n*-propyl benzene branch. Extensive comparisons between computed results and the measurements for a pressure range of  $1 \leq P$  (atm)  $\leq 10$ , temperatures of  $900 \leq T$  (K)  $\leq 1250$  and for various stoichiometries between  $0.5 \leq \Phi \leq 2.0$  illustrate the ability of the model to predict the oxidation of *n*-propyl benzene.

Important reaction paths were identified, including the generation of styrene. The significance of the thermal breakdown of the fuel at the primary and secondary carbon atom was also noted as small rate changes could lead to large discrepancies in the intermediate species concentrations. On the other hand, under shock tube conditions it was shown that the hydrogen abstraction reactions do not play any significant role. The only reaction steps that initiate the fuel breakdown and can affect the evolution of the rest of the intermediate species are the thermal decomposition channels that occur via C-C rupture to the primary and secondary carbon atom. The dominant homolytic reaction step in both jet stirred and shock tube reactors is predicted to lead to benzyl radical formation.

The prediction and measurement of large early concentrations of specific species such as styrene, ethyl benzene or toluene is a clear indication that abstraction and homolytic reactions occur at the beginning of the fuel oxidation and promote the fuel decay.

The results presented here are encouraging and suggest that the current reaction class based approach can be applied also to other alkyl substituted aromatic fuel compounds that form part of real and surrogate fuel formulations. It must also be noted that as the chain increases in length, new categories of reaction steps are

likely to occur such as radical isomerisations, cyclic transition states and group shifts along the chain that should be taken into account.

## Chapter 6

### Naphthalene

#### 6.1 Introduction

One of the central subjects of research in the area of combustion is the formation of polycyclic aromatic hydrocarbons. Many studies in the literature have addressed the formation and growth of the aromatic compounds, which act as precursors to soot. The control and prediction of the combustion of aromatics is of high importance for both environmental and health reasons as PAHs are associated with tumorigenic effects. Hence, the ability to reproduce the chemical properties of aromatic hydrocarbon fuels is highly required.

The formation of benzene has received particular attention and has been subject to a number of studies [45, 73, 119-122]. A number of growth mechanisms, specifically reaction routes that proceed via acetylene addition to alkadienyl radicals have been reported in the literature [45, 47, 123]. Moreover, Marinov *et al.* [58] and Castaldi *et al.* [124] suggested that naphthalene is produced by the recombination of two cyclopentadienyl radicals releasing two hydrogen atoms. The cyclopentadienyl recombination leading to naphthalene formation was also studied by Melius *et al.* [42] and Dean [125]. Moreover, Marinov *et al.* [126] and Richter *et al.* [127] highlighted the role of cyclopentadienyl radical in premixed flames. A recent study of Lindstedt *et al.* [61] proposed a two-step mechanism involving the cyclopentadienyl route with energy barriers that are in accordance with Melius *et al.* [42].

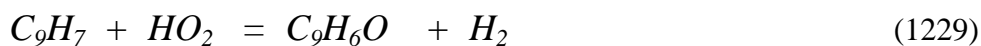
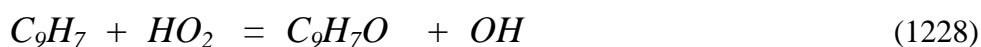
The naphthalene formation and oxidation pathways are presented in this study and compared with plug flow reactor data obtained by Shaddix [24].



## 6.2 Modelling Approach

The derived reaction mechanism for naphthalene oxidation was based on the reactions steps and reaction classes derived from the oxidation of benzene and cyclopentadiene with parameters adjusted according to molecular size and reactive site differences [70].

The studies by Lindstedt *et al.* [61] Maurice [112] and Potter [75] identified the importance of the linkages between aromatic  $C_5$  and  $C_6$  structures and the key role of the indene/indenyl system. In particular, the oxidation of indenyl was found to exert a strong influence on the overall oxidation kinetics of larger aromatic species such as naphthalene and 1-methyl naphthalene and on the subsequent product distribution of single ring aromatics. The studies identified possible reaction channels featuring molecular oxygen (1232, 1233, 1234) though estimates of the rates of reaction proved problematic [75]. In the current study, the aforementioned channels were considered along with  $HO_2$  channels (1228, 1229). For this set of reactions, DFT and composite quantum mechanical methods were used to calculate the PES. Both RRKM/ME theory and VTST were used to derive estimates of the rate constants [70].

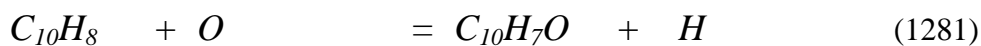
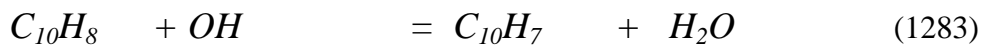


The reaction mechanism used here consists of 1431 reversible reactions and 269 species. The reverse rates were computed via chemical equilibrium. The rates of consumption and productions were also calculated for each species. The thermochemical data was obtained from literature sources [71] and when not available were calculated with quantum mechanical methods using Gaussian-03 by Robinson [15].

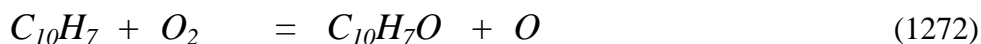
### 6.3 Oxidation of Naphthalene and Reaction Analysis

The naphthalene mechanism was validated under plug flow reactor conditions and compared with measurements by Shaddix [24]. The computations correspond to conditions of  $\Phi = 1.1$ ,  $T = 1197$  K and  $P = 1$  atm. An offset of 32 ms in the temporal evolution of the experimental data was also reported by Shaddix [24]. Predictions of reactants and major species are presented in Figure 6.1 to Figure 6.3.

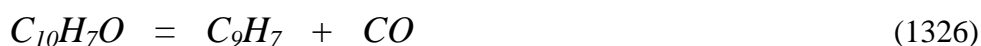
A reaction rate analysis was performed in order to identify major channels during the oxidation of naphthalene. The measured naphthalene concentrations show considerable scatter with the trend in reasonable agreement with computations. The fuel is decomposed via two major channels that involve  $H$  abstraction with the  $OH$  radical (49%) and  $O$  addition to the ring forming the naphthoxy radical (44%). The rate assigned to reaction (1283) was based on the reaction rate of the hydrogen atom abstraction from the benzene ring as discussed by Leung and Lindstedt [73]. Relative adjustments according to the benzene chemistry were applied to reaction (1281) based on a rate proposed by DiNaro *et al.* [91].



The naphthyl radical is further decomposed (67%) to naphthoxy (1272), which is the other major product of the fuel decay, with a rate assigned based on the kinetics of benzene as proposed by Frank *et al.* [105].



The naphthoxy radical decomposes thermally via one major pathway leading to the formation of the indenyl radical and  $CO$ . The rate assigned to reaction (1326) was based on suggestions of Potter [75] and adjusted from benzene kinetics. The reaction is also the major indenyl radical production channel (69%).



The indenyl radical is consumed via three major pathways. Most (33%) recombines with the hydrogen atom to indene (1222) with a reaction rate assigned based on suggestions of Potter [75]. The second route (19%) involves  $CO$  abstraction via oxygen attack leading to the formation of  $C_8H_7$  (1224). The rate assigned to this channel was based on suggestions of Maurice [112]. A further 17% of the indenyl concentration reacts with  $HO_2$  forming the naphthoxy radical (1228) with a rate proposed by Lindstedt *et al.* [70] as mentioned in Section 6.2.



Indene is solely formed via the indenyl radical with hydrogen addition via reactions with  $H_2$ ,  $OH$  and  $H_2O$ . Once it is formed, it recycles back to the indenyl radical.

The  $C_8H_7$  radical decomposes (100%) to phenyl acetylene with a rate adopted from Wang and Frenklach [119]. A schematic representation of the naphthalene and indene oxidation channels is shown in Figure 6.4.



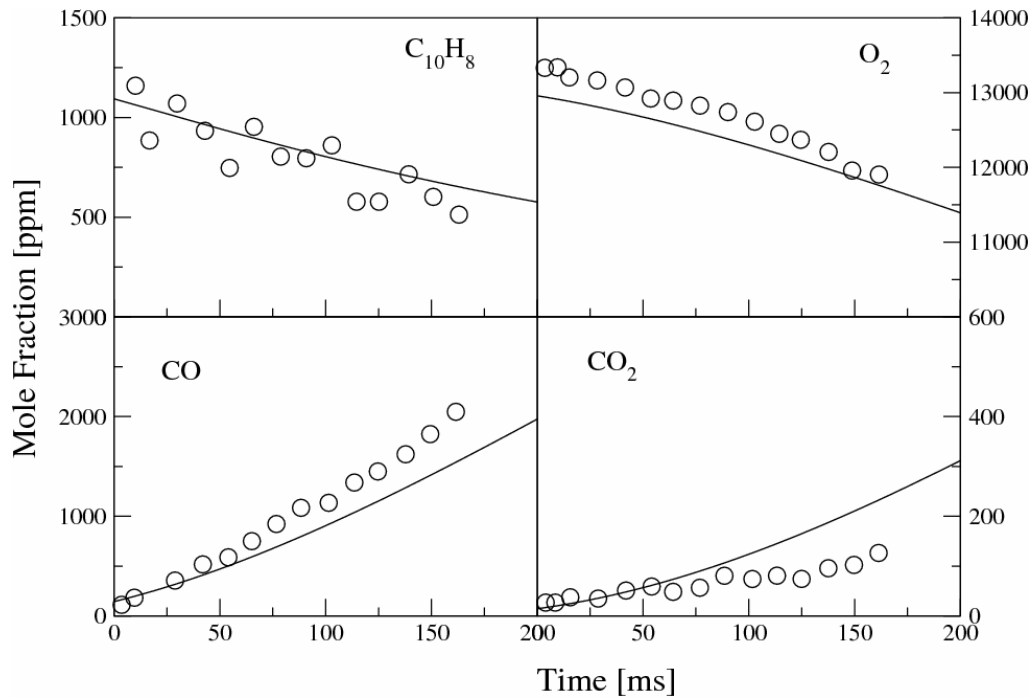


Figure 6.1 Concentration profiles of major species during naphthalene oxidation in a plug flow reactor for  $\Phi = 1.1$ ,  $T = 1197$  and  $P = 1$  atm. The solid lines indicate the current computations and the circles indicate the measurements [24].

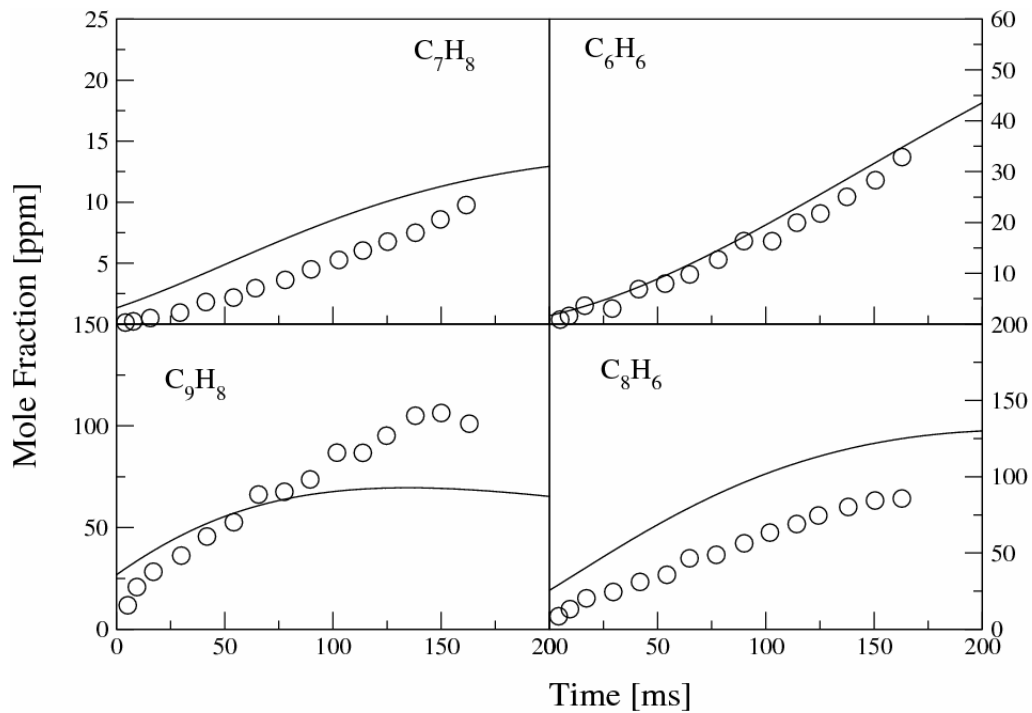


Figure 6.2 Concentration profiles of major species during naphthalene oxidation in a plug flow reactor for  $\Phi = 1.1$ ,  $T = 1197$  and  $P = 1$  atm. The solid lines indicate the current computations and the circles indicate the measurements [24].

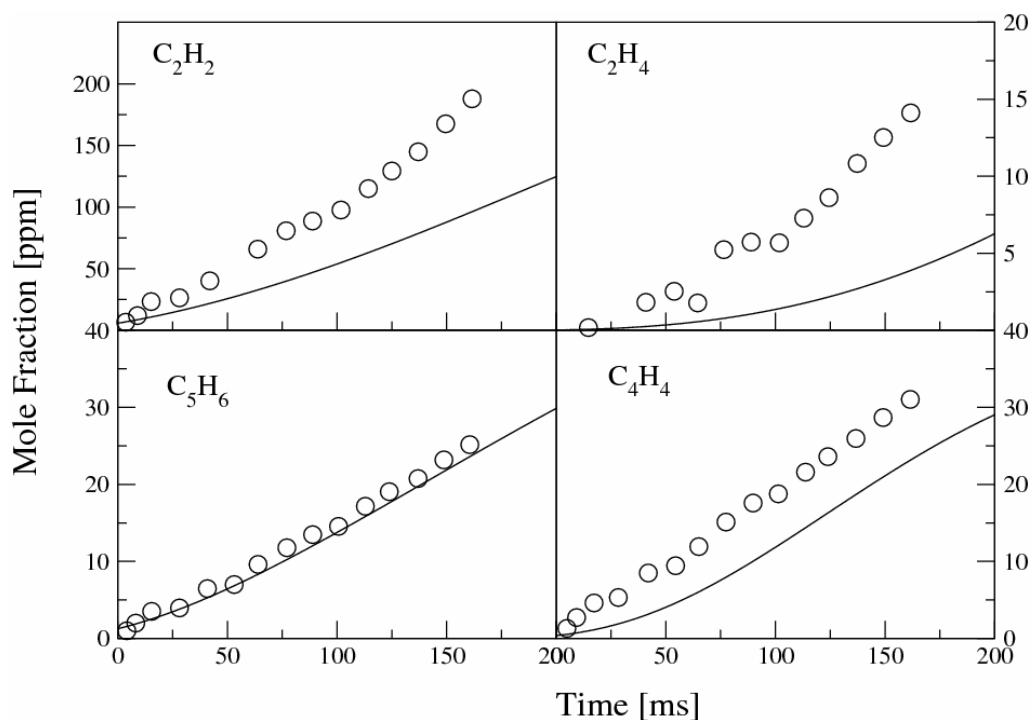


Figure 6.3 Concentration profiles of major species during naphthalene oxidation in a plug flow reactor for  $\Phi = 1.1$ ,  $T = 1197$  and  $P = 1$  atm. The solid lines indicate the current computations and the circles indicate the measurements [24].

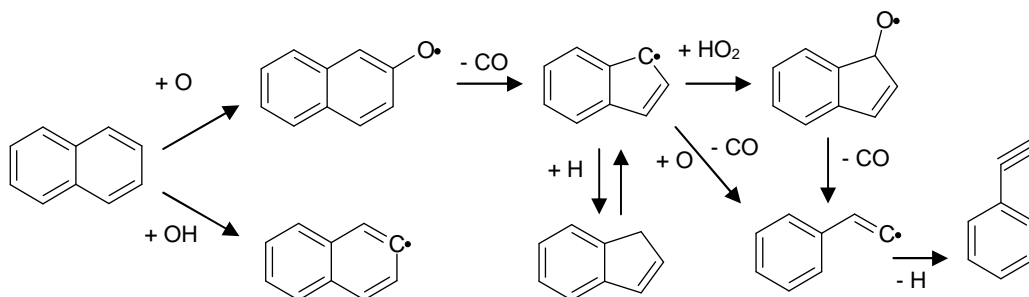
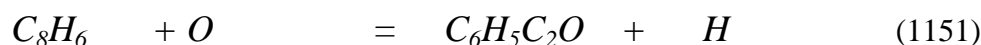
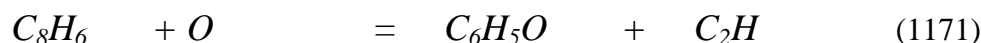
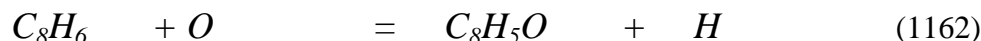
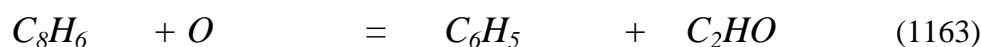


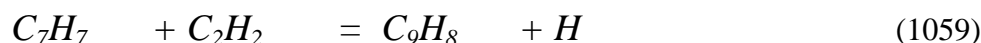
Figure 6.4 Naphthalene and indene oxidation pathways

Reaction (1187) is also the major phenyl acetylene formation channel (75%). Phenyl acetylene is oxidised via the five major reaction routes shown below.



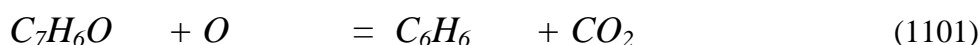
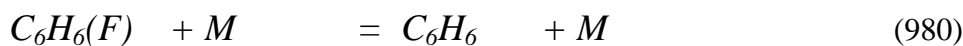
The major phenyl acetylene consumption channel (33%) occurs via oxygen attack that removes the side chain via *C-C* cleavage (1163). The rate assigned to reaction (1163) was adopted from suggestions of Lindstedt *et al.* [61]. The second major consumption channel (1154) occurs via *H* abstraction by *OH* attack, which is responsible for 19% of *C<sub>8</sub>H<sub>6</sub>* consumption and utilizes a rate recommended by Frenklach and Wang [119]. Reactions (1162), (1171) and (1151) are responsible for 11%, 11% and 10% of the phenyl acetylene consumption respectively.

Toluene is formed via the benzyl radical, which is formed via three major pathways. The oxidation of the indenyl radical with molecular oxygen (1232) constitutes the dominant formation channel for the benzyl radical. The rate assigned to reaction (1232) was calculated through DFT and composite quantum mechanical methods were used to calculate the PES with RRKM/ME theory and VTST used to derive an estimate of the rate constant [70]. Approximately 20% of the benzyl radical is formed via *C<sub>8</sub>H<sub>8</sub>* oxidation with *OH* (1197). The rate assigned to reaction (1197) was adopted from Maurice [112]. A further 11% of benzyl radical is formed via reaction (1059) with a rate adopted from Colket *et al.* [74].



Benzene is formed (32%) through hydrogen assisted isomerization (980) and (24%) from benzaldehyde via oxygen addition and *CO<sub>2</sub>* abstraction (1101). Benzene

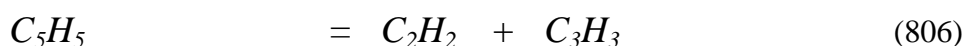
is a precursor to the cyclopentadienyl radical from which cyclopentadiene is formed (92%). Benzene is consumed (47%) to the phenyl radical via *H* abstraction via *OH* attack and (40%) to phenoxy radical via *O* addition and hydrogen abstraction. The phenyl radical is predominantly consumed (66%) to the phenoxy radical.



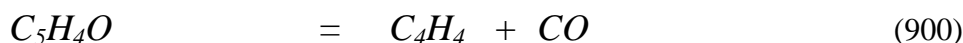
The phenoxy radical is responsible (77%) for cyclopentadienyl radical production via *CO* thermal abstraction (994) with a rate proposed by Leung and Lindstedt [73]. The cyclopentadienyl radical recombines with the *H* atom (92%) to the cyclopentadiene (832) with a rate adopted from Kern *et al.* [52].



Acetylene is also formed (44%) via the thermal breakdown of  $C_5H_5$  that leads to  $C_2H_2$  and  $C_3H_3$ . The rate used for reaction (806) was proposed by Kern *et al.* [52] and was reduced by a factor of 2 due to acetylene overproduction. The evolution of  $C_2H_4$  is also affected by  $C_5H_5$  via reaction channels that include  $C_2H_2$  and  $C_2H_2O$ .



Vinyl acetylene production is initially controlled by phenyl acetylene consumption through  $C_8H_5O$ , which thermally decomposed to  $C_7H_5$  leading to  $C_4H_4$  via  $C_5H_4O$ . A rate by Ristori *et al.* [128] was assigned to reaction (900), which is responsible for 94% of the  $C_4H_4$  production.



## 6.4 Conclusions

In the present chapter, a detailed chemical sub-mechanism of naphthalene was developed and evaluated. Computations were performed under PFR conditions and concentration profiles for reactants and major intermediate species were obtained. Reaction rate estimates for the  $C_9H_7 + O_2/HO_2$  were computed from Potential Energy Surfaces using the Rice-Ramsperger-Kassel-Marcus/Master Equation (RRKM/ME) approach and Variable Transition State Theory (VTST) by Lindstedt *et al.* [70] and the resulting mechanism was evaluated against the species profiles obtained from Shaddix [24].

It was shown that the naphthalene oxidation is controlled by two major channels that involve  $H$  abstraction via  $OH$  radical and  $O$  addition to the ring. Most of its structure and oxidation process is assumed to follow similar behaviour to the benzene chemistry. From the comparison between the computations and the measurements is shown that the main oxidation channels are well represented and that the  $C_9H_7 + O_2/HO_2$  reactions have an important role in determining the product distribution of single ring aromatics. Accurate thermodynamic data computed in our group were also utilized for the  $C_{10}$  species.

Experimental data of measurements of intermediate species concentration profiles over a wider range of conditions are essential in order to refine the current predictive methods.



## Chapter 7

### 1-Methyl naphthalene

#### 7.1 Introduction

While extensive work has been performed on the development of chemical mechanisms for major oxidative pathways of aliphatic hydrocarbons and simple aromatic compounds such as benzene and toluene, very few studies on the combustion of polycyclic aromatic fuels have been reported in the literature. In this study, a mechanism for 1-methyl naphthalene is developed on the basis of reaction classes determined with toluene as a reference fuel. The choice is natural since 1-methyl naphthalene is the corresponding bicyclic analog.

Shaddix *et al.* [21, 22, 24] studied the oxidation of 1-methyl naphthalene in a plug flow reactor and obtained species profiles under atmospheric pressure conditions for a temperature range of 1165 – 1200 K and for equivalence ratios of 0.6, 1.0 and 1.6. The study arguably contains the first reported species profiles for the oxidation of a polycyclic hydrocarbon fuel. Based on the obtained profiles, a chemical mechanism for 1-methyl naphthalene was proposed. Elevated pressure ( $P = 13$  atm) ignition delay times were measured by Pfahl *et al.* [129] under shock tube conditions for a temperature range of 840 – 1300 K. A more recent study on 1-methyl naphthalene was performed by Mati *et al.* [35], who studied the oxidation under jet stirred reactor conditions for a temperature range of  $800 < T < 1421$  K, a pressure range of  $1 < P < 13$  atm and equivalence ratios of  $0.5 < \Phi < 1.5$ . Major species concentration profiles were obtained by on-line GC-MS and off-line GC-TCD-FID and GC-MS analyses. New data covering a wide range of conditions were provided and a kinetic model was proposed and validated.

Important reactions pathways were identified in the above studies. More specifically, Shaddix *et al.* [22] highlighted the fuel consumption paths that occur via i) abstractions of the benzylic hydrogen atom by  $H/O$  radicals or molecular

oxygen, ii) homolysis from  $C-H$  fission forming the 1-naphthyl methyl radical, iii) displacement of the methyl group by the hydrogen atom leading to the formation of naphthalene and iv) addition of an oxygen atom leading to the formation of 1-methyl-4-naphthol or 1-methyl naphthoxy radical.

In this study, the oxidation of 1-methyl naphthalene is studied under jet stirred reactor conditions and compared against data from Mati *et al.* [35] and Shaddix [24] featuring concentrations profiles for various species.

## 7.2 Modelling Approach

The starting point is the detailed scheme for 1-methyl naphthalene derived by Potter [75] on the basis of the chemistry of toluene. Modifications and updates were applied as appropriate. The reaction steps and reaction rates were analysed at conditions corresponding to the JSR experiments of Mati *et al.* [35] and plug flow reactor conditions of Shaddix [24] and Shaddix *et al.* [21, 22].

The reaction mechanism used here consists of 1431 reversible reactions involving 269 species. The reverse rates were computed using chemical equilibrium. The rates of consumption and production were also calculated for each species. The thermochemical data were obtained from literature sources [71] and when not available, were calculated with quantum mechanical methods using Gaussian-03 [15].

## 7.3 Oxidation in Jet-Stirred Reactors

The 1-methyl naphthalene mechanism was initially validated under jet-stirred reactor conditions using species data from Mati *et al.* [35]. The measurements were aimed at clarifying the decomposition channels of the fuel. Three different stoichiometries were tested at atmospheric pressure over a temperature range of 1090–1450 K and at a fixed residence time  $\tau$  of 0.1 s. The conditions are listed in Table 7.1 and the species profiles for all stoichiometries are shown in Figure 7.1 to Figure 7.12.

$\Phi$	P (atm)	T (K)	$X_{O_2}$	$X_{C_{11}H_{10}}$
0.5	1.0	1097-1290	0.0270	0.001
1.0	1.0	1094-1400	0.0135	0.001
1.5	1.0	1147-1440	0.0090	0.001

Table 7.1 Experimental and modelling conditions for the oxidation of 1-methyl naphthalene in a jet-stirred reactor. The species concentrations correspond to mole fractions.

According to the measurements, the major species detected, besides  $CO$  and  $CO_2$ , were formaldehyde, methane, acetylene, ethylene, cyclopentadiene, benzene, toluene, styrene, naphthalene, indene and ethane. As can be seen from Figure 7.1 to Figure 7.12, the current 1-methyl naphthalene model reproduces the experimental data well as compared to other studies [35, 130]. It is shown that the fuel consumption is in excellent agreement with measurements for all the three stoichiometries. The prediction of intermediate species shows that the associated decomposition pathways are also well represented.

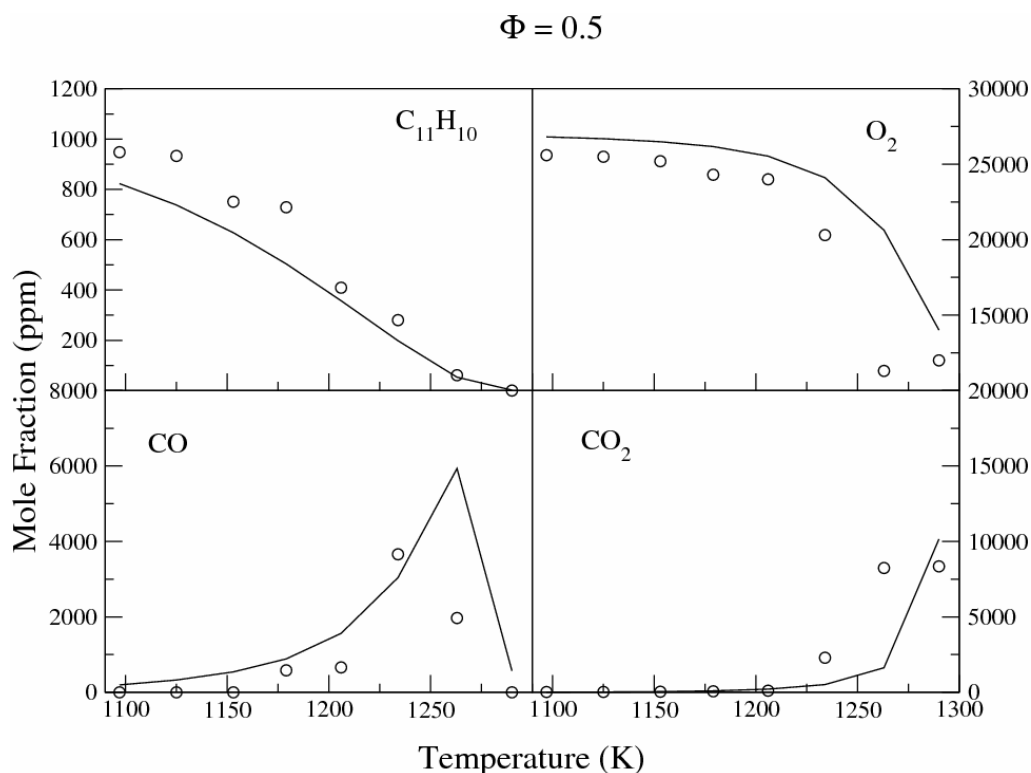


Figure 7.1 Concentration profiles of intermediate species during 1-methyl naphthalene oxidation in a jet-stirred reactor with  $\Phi = 0.5$ ,  $P = 1$  atm and  $T = 1097 - 1290$  K. Circles are experimental data [35] and the solid lines the current simulations.

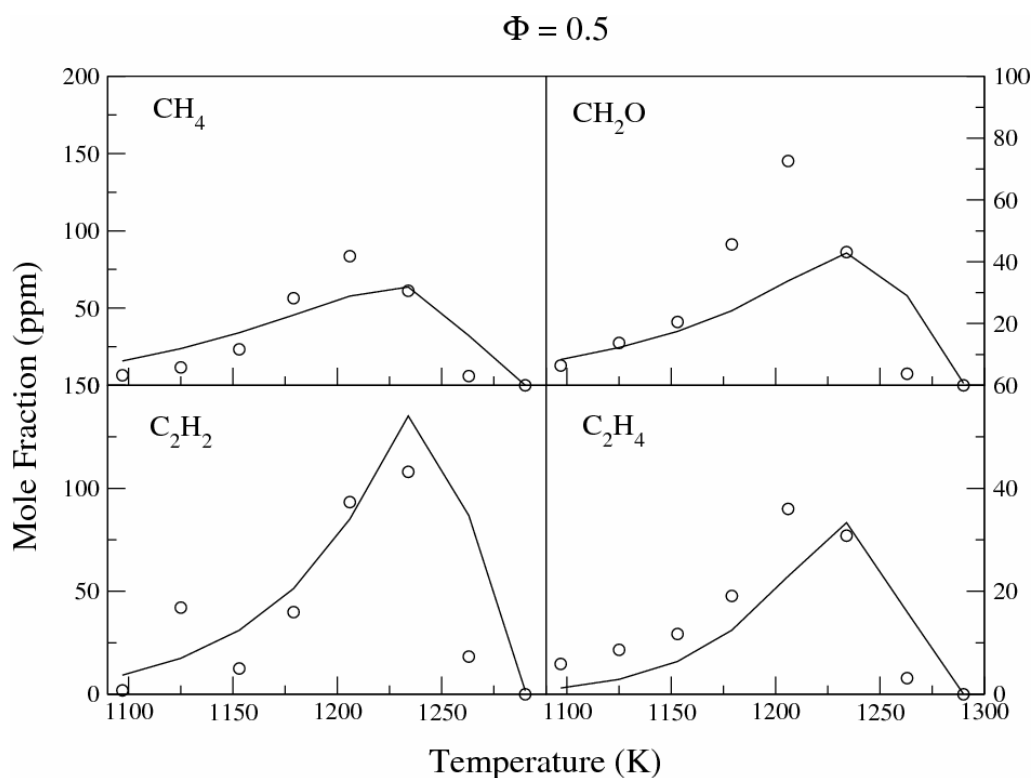


Figure 7.2 Concentration profiles of intermediate species during 1-methyl naphthalene oxidation in a jet-stirred reactor with  $\Phi = 0.5$ ,  $P = 1$  atm and  $T = 1097 - 1290$  K. Circles are experimental data [35] and the solid lines the current simulations.

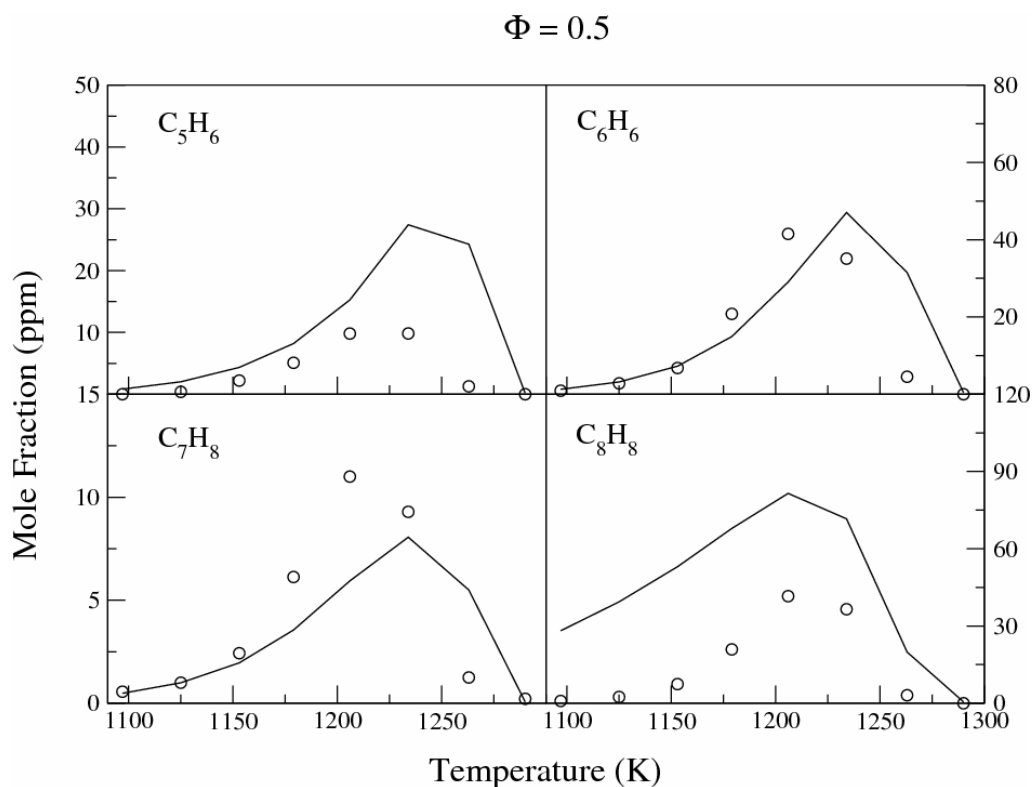


Figure 7.3 Concentration profiles of intermediate species during 1-methyl naphthalene oxidation in a jet-stirred reactor with  $\Phi = 0.5$ ,  $P = 1$  atm and  $T = 1097 - 1290$  K. Circles are experimental data [35] and the solid lines the current simulations.

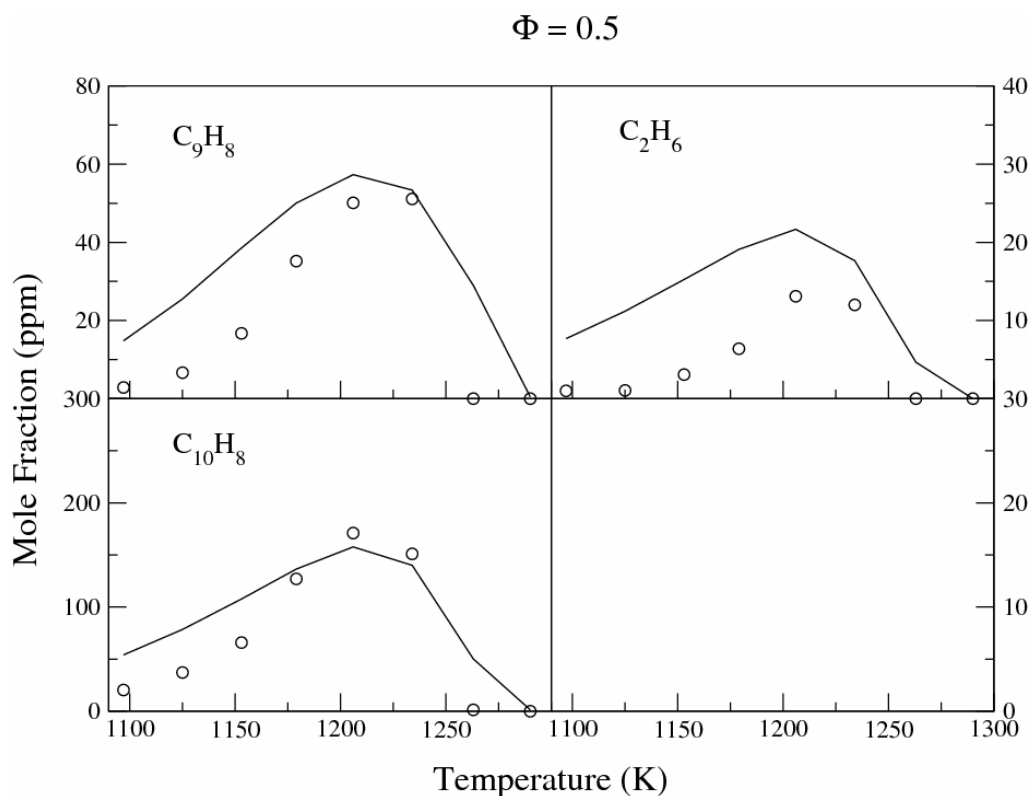


Figure 7.4 Concentration profiles of intermediate species during 1-methyl naphthalene oxidation in a jet-stirred reactor with  $\Phi = 0.5$ ,  $P = 1$  atm and  $T = 1097 - 1290$  K. Circles are experimental data [35] and the solid lines the current simulations.

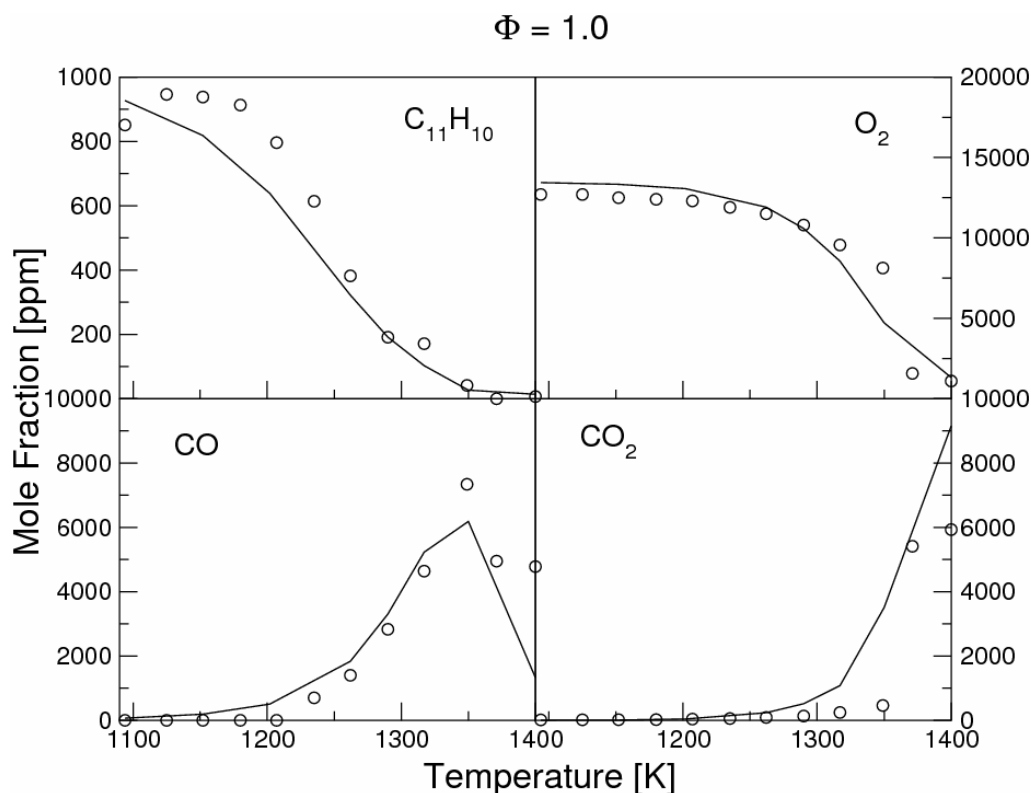


Figure 7.5 Concentration profiles of intermediate species during 1-methyl naphthalene oxidation in jet-stirred reactor.  $\Phi = 1.0$ ,  $P = 1$  atm and  $T = 1094 - 1400$  K. Circles are experimental data [35] and the solid lines the current simulations.

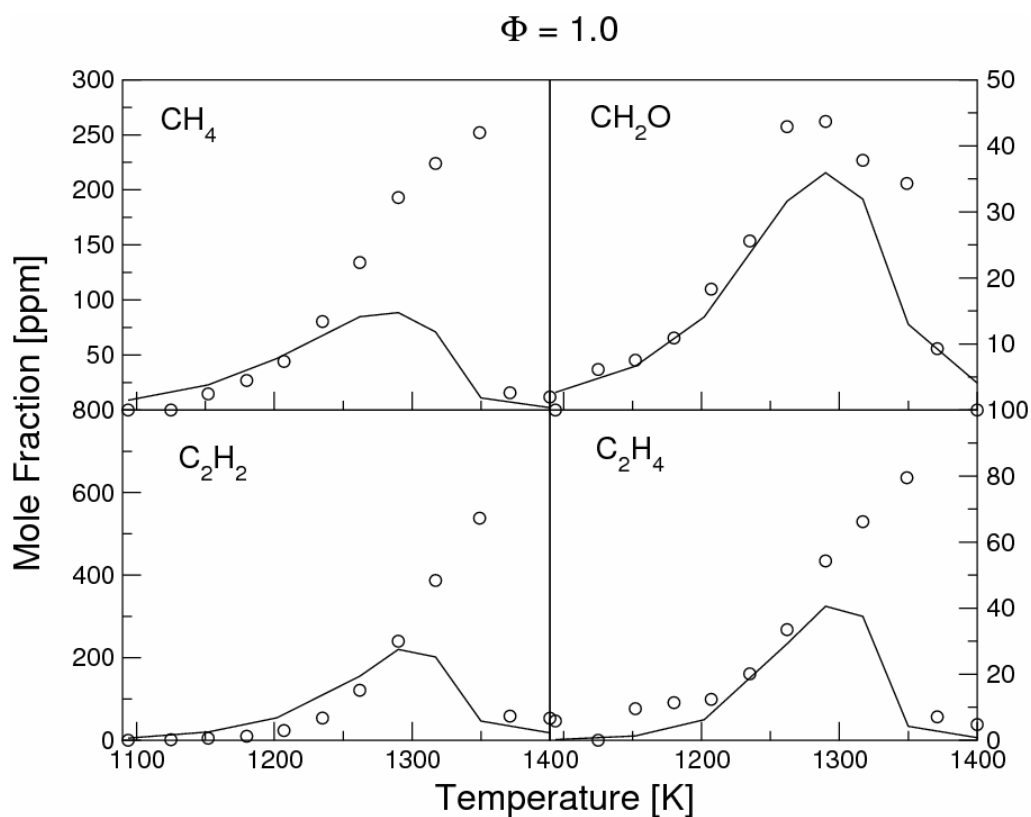


Figure 7.6 Concentration profiles of intermediate species during 1-methyl naphthalene oxidation in jet-stirred reactor.  $\Phi = 1.0$ ,  $P = 1$  atm and  $T = 1094 - 1400$  K. Circles are experimental data [35] and the solid lines the current simulations.

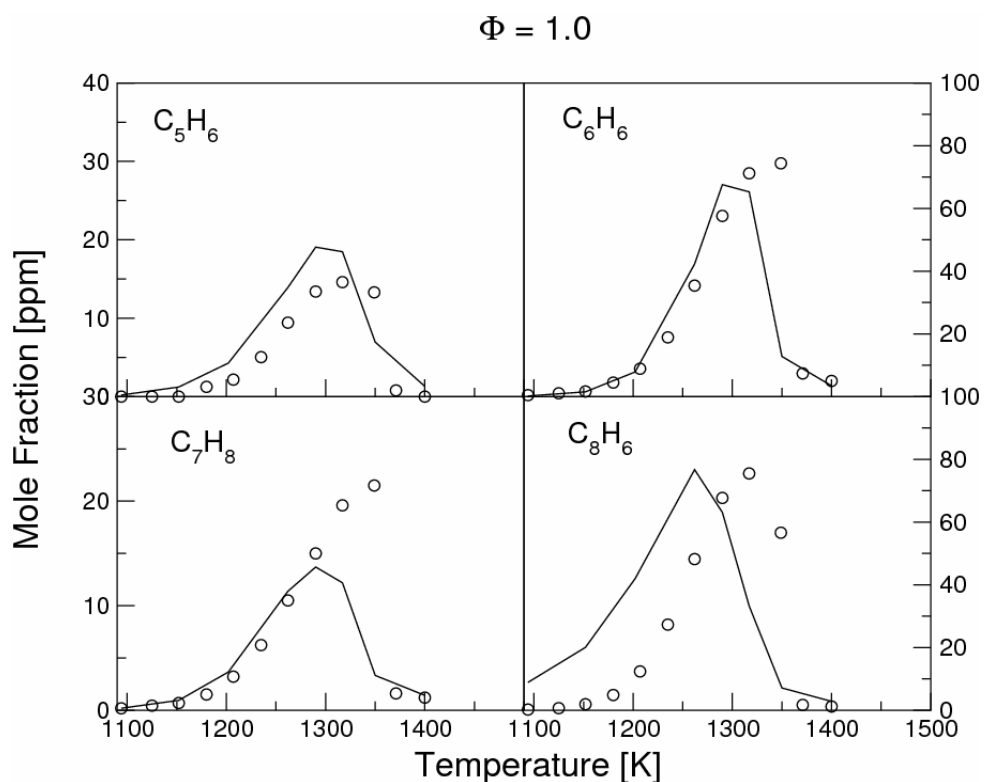


Figure 7.7 Concentration profiles of intermediate species during 1-methyl naphthalene oxidation in jet-stirred reactor.  $\Phi = 1.0$ ,  $P = 1$  atm and  $T = 1094 - 1400$  K. Circles are experimental data [35] and the solid lines the current simulations.

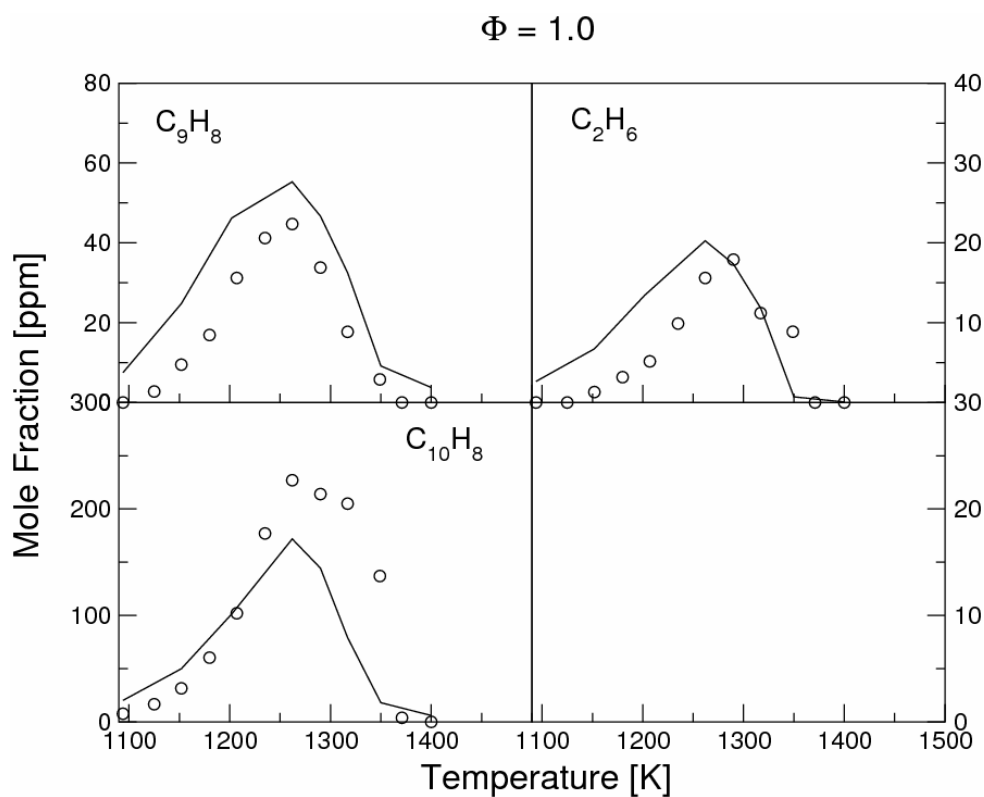


Figure 7.8 Concentration profiles of intermediate species during 1-methyl naphthalene oxidation in jet-stirred reactor.  $\Phi = 1.0$ ,  $P = 1$  atm and  $T = 1094 - 1400$  K. Circles are experimental data [35] and the solid lines the current simulations.

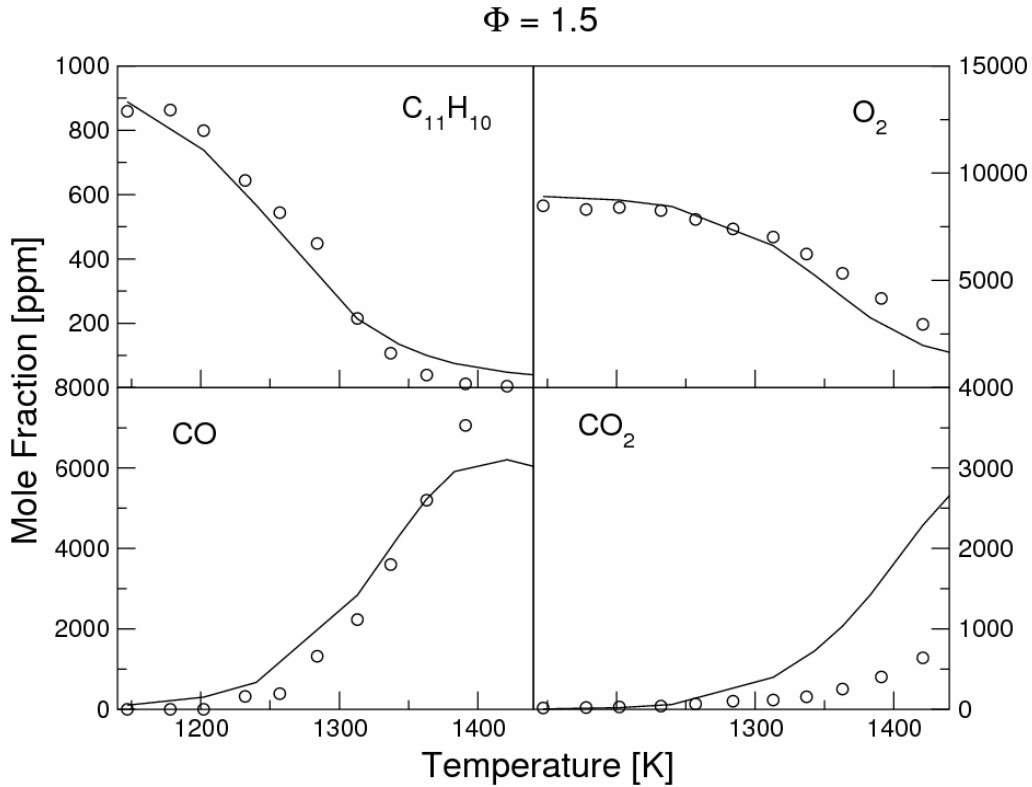


Figure 7.9 Concentration profiles of intermediate species during 1-methyl naphthalene oxidation in jet-stirred reactor.  $\Phi = 1.5$ ,  $P = 1$  atm and  $T = 1147 - 1440$  K. Circles are experimental data [35] and the solid lines the current simulations.

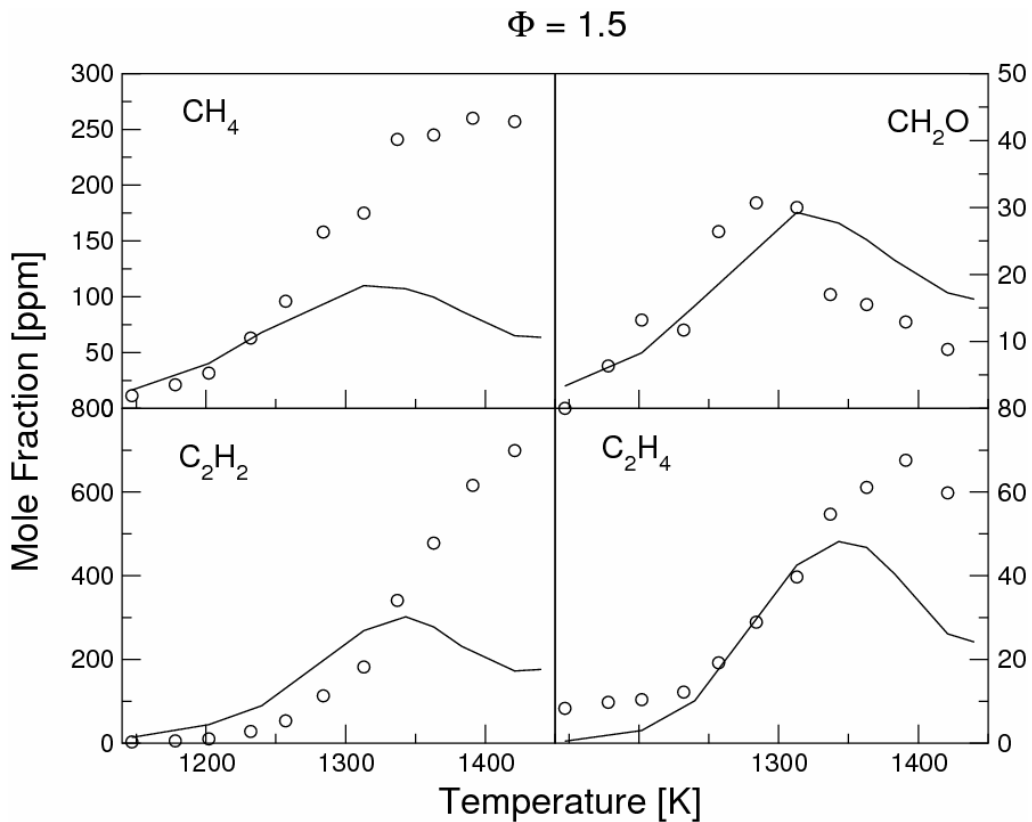


Figure 7.10 Concentration profiles of intermediate species during 1-methyl naphthalene oxidation in jet-stirred reactor.  $\Phi = 1.5$ ,  $P = 1$  atm and  $T = 1147 - 1440$  K. Circles are experimental data [35] and the solid lines the current simulations.



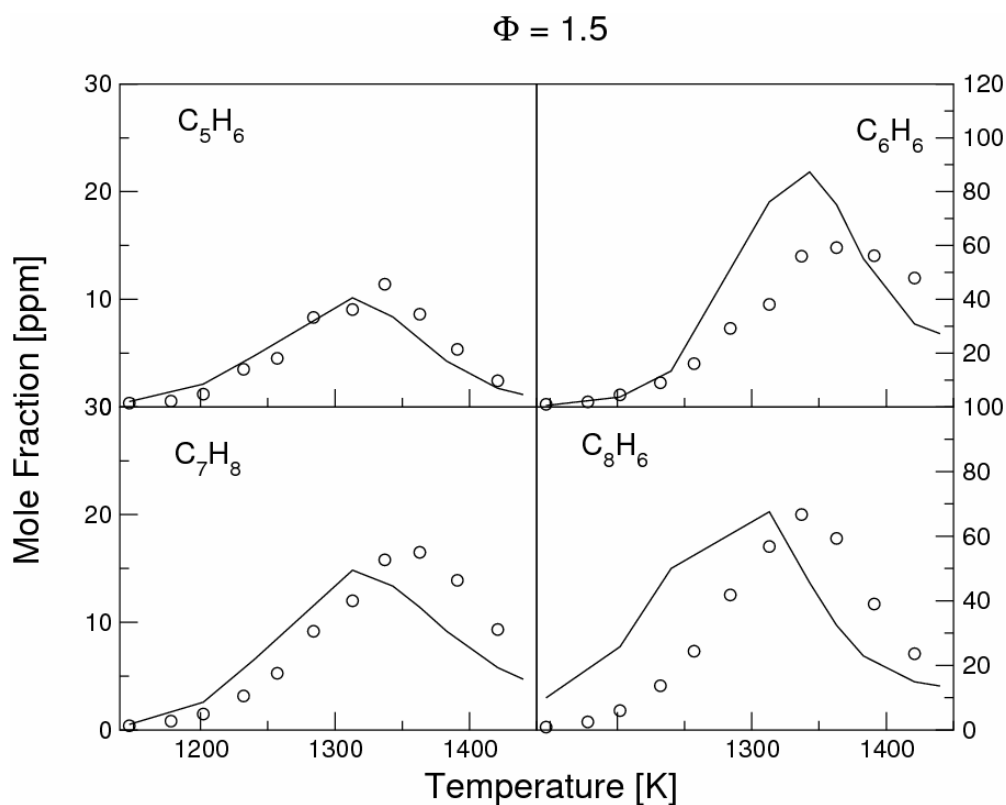


Figure 7.11 Concentration profiles of intermediate species during 1-methyl naphthalene oxidation in jet-stirred reactor.  $\Phi = 1.5$ ,  $P = 1$  atm and  $T = 1147 - 1440$  K. Circles are experimental data [35] and the solid lines the current simulations.

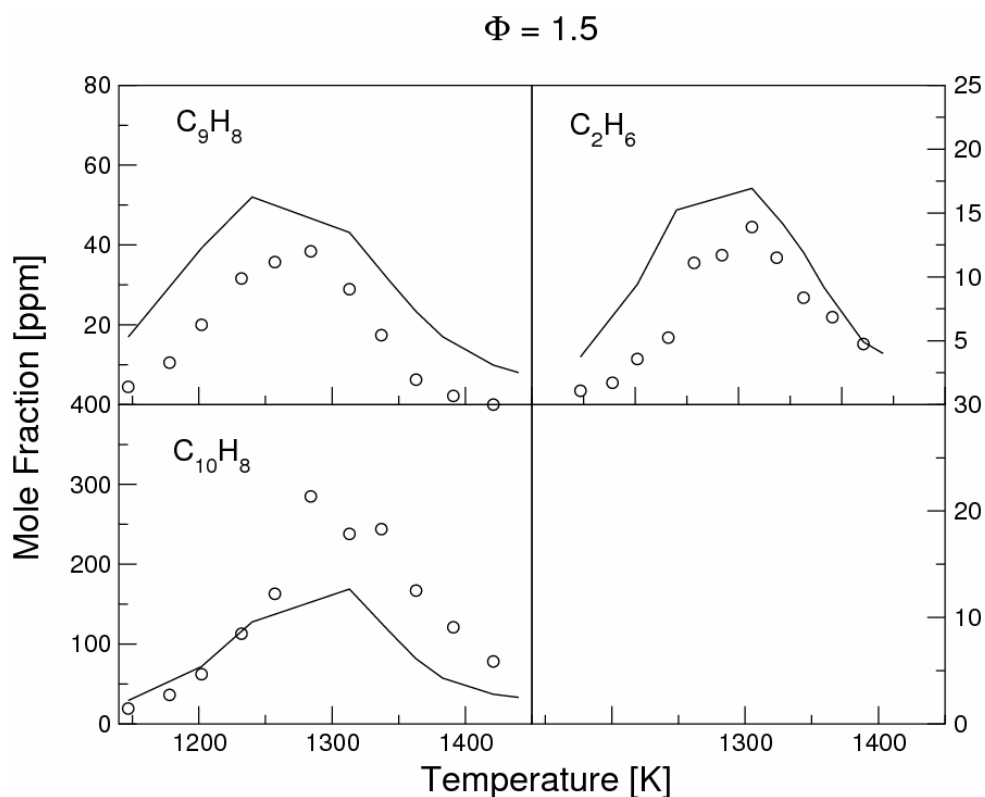
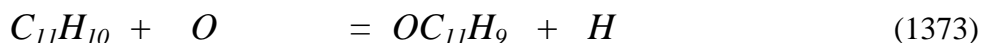
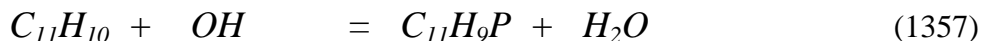
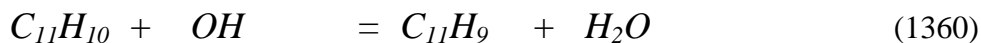


Figure 7.12 Concentration profiles of intermediate species during 1-methyl naphthalene oxidation in jet-stirred reactor.  $\Phi = 1.5$ ,  $P = 1$  atm and  $T = 1147 - 1440$  K. Circles are experimental data [35] and the solid lines the current simulations.

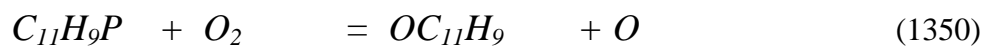
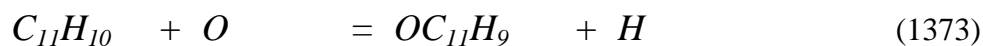
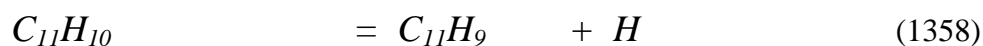
## 7.4 Fuel Lean Mixtures

A reaction rate analysis was performed for a fuel lean mixture ( $\Phi = 0.5$ ) at a temperature of 1206 K at atmospheric pressure.

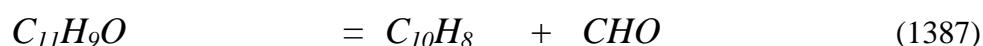
The computations show the major fuel decomposition pathways to occur via hydrogen abstraction by *OH* attack and oxygen addition. The rates assigned to the reactions were adopted from Potter [75] and determined on the basis of the toluene chemistry. The *OH* attack on the methyl branch (1360) is responsible for 31% of the fuel consumption, whereas the hydrogen abstraction from the ring (1357) is responsible for 19%. The oxygen addition to the branch (1372) accounts for 12% of the 1-methyl naphthalene consumption, whereas the oxygen addition to the ring (1373) accounts for 23%.



The fuel is formed from the 1-methylnaphthyl radical (82%) (-1358). The reaction rate was adopted by Potter [75] and was based on the toluene kinetics as proposed by Maurice [112]. The formation from  $HOC_{11}H_9$  (1369) also makes a contribution (17%) via *OH* replacement. The  $HOC_{11}H_9$  is formed by the  $OC_{11}H_9$  radical (100%) with the addition of atomic hydrogen to the oxygenated radical (1396). The  $OC_{11}H_9$  radical is formed from 1-methyl naphthalene by the replacement of a hydrogen atom on the ring (1373) with an oxygen atom (52%) with a rate that stems from the kinetics of toluene proposed by Hoffman *et al.* [118] and from oxygen addition to the 1-methyl-4-naphthyl radical ( $C_{11}H_9P$ ) via molecular oxygen attack (1350) (32%) that was assigned a rate based on the toluene kinetics proposed by Maurice [112]. The reaction rates were adopted from Potter [75]. The major 1-methyl naphthalene decomposition and formation pathways are shown in Figure 7.13 and Figure 7.14.



Naphthalene is formed via thermal decomposition of the  $C_{11}H_9O$  radical (1387) (65%), which is formed from oxygen attack on 1-methyl naphthalene (1372) (Figure 7.15).



Once naphthalene is formed, hydrogen abstraction via  $OH$  radical attack (1283), leading to the formation of the naphthyl radical contributes 49% to consumption of the former. Moreover, 43% of the naphthalene forms naphthaldehyde (1281) by oxygen addition and hydrogen abstraction. The naphthalene decomposition channels were assigned rates based on the corresponding benzene decomposition channels. The naphthaldehyde thermally decomposes by  $CO$  abstraction leading to the formation of the indenyl radical and indene.

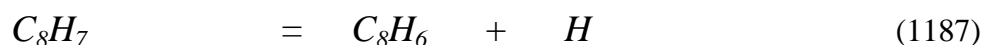
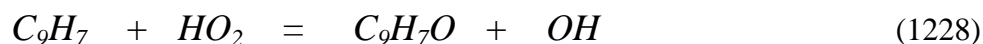


The formation of indene occurs (98%) from the indenyl radical. The indenyl radical is oxidized in a sequence of reaction steps initiated by the formation of the  $OC_{11}H_9$  radical. The latter thermally decomposes via  $CO$  expulsion from the ring leading to the formation of  $C_9H_6CH_3$ . The latter species recombines with a hydrogen atom leading to the formation of  $C_9H_7CH_3$ , which thermally decomposes to indenyl and methyl (50%). The rates of these last two steps were assigned from suggestions proposed by Laskin and Lifshitz [131]. In addition to this reaction

sequence, the indenyl radical, as mentioned above, is formed by the thermal decomposition of the naphthaldehyde (16%). A more direct link to the fuel is provided by the indenyl radical and acetylene formation from the 1-methylnaphthyl radical (1347) (12%). The reverse reaction step was also tested with a rate relative to the benzyl radical formation channel proposed by Colket and Seery [77], but found to lead to excessive acetylene and indene concentrations. By contrast, the use of the 1-methyl naphthyl radical thermal decomposition channel (1347) with a rate relative to the benzyl radical thermal decomposition proposed by Braun-Unkhoff [28] leads to excellent agreement between computed and measured concentration profiles for both acetylene and indene. A schematic representation of the indene formation channels is shown in Figure 7.16.



The further oxidation of the indenyl radical by  $HO_2$  is responsible for  $C_9H_7O$  formation (1228). Density Functional Theory and composite quantum mechanical methods were used to calculate the potential energy surfaces for this oxidation channel. Both RRKM/ME theory and VTST were used to derive an estimate of the rate constant [70]. The species is a precursor to phenyl acetylene ( $C_8H_6$ ) through  $C_8H_7$ . A rate proposed by Pitch [130] was adopted for the  $CO$  abstraction from  $C_9H_7O$  (1263). The thermal decomposition of  $C_8H_7$  is responsible for 71% of the phenyl acetylene formation (1187) with a rate based on suggestions of Wang and Frenklach [119].



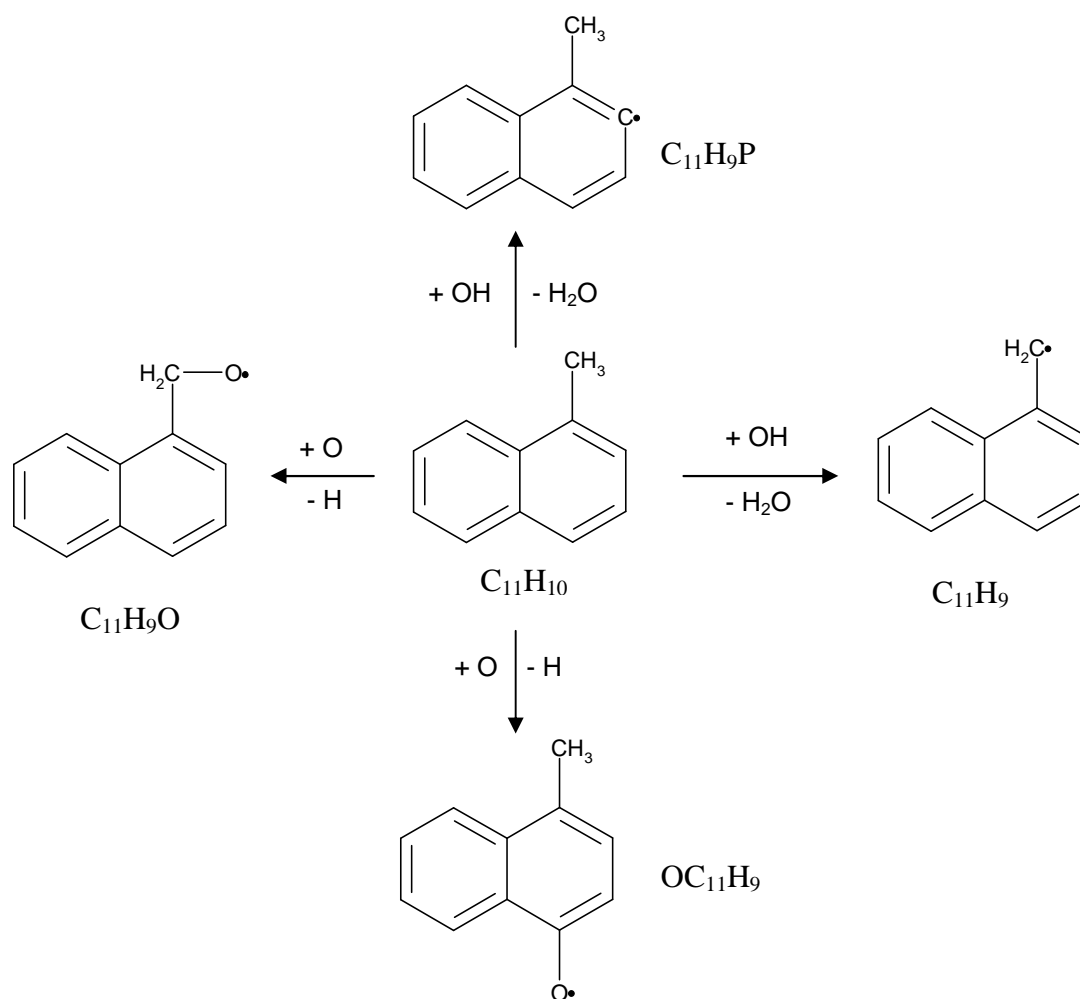


Figure 7.13 Major 1-methyl naphthalene decomposition pathways.

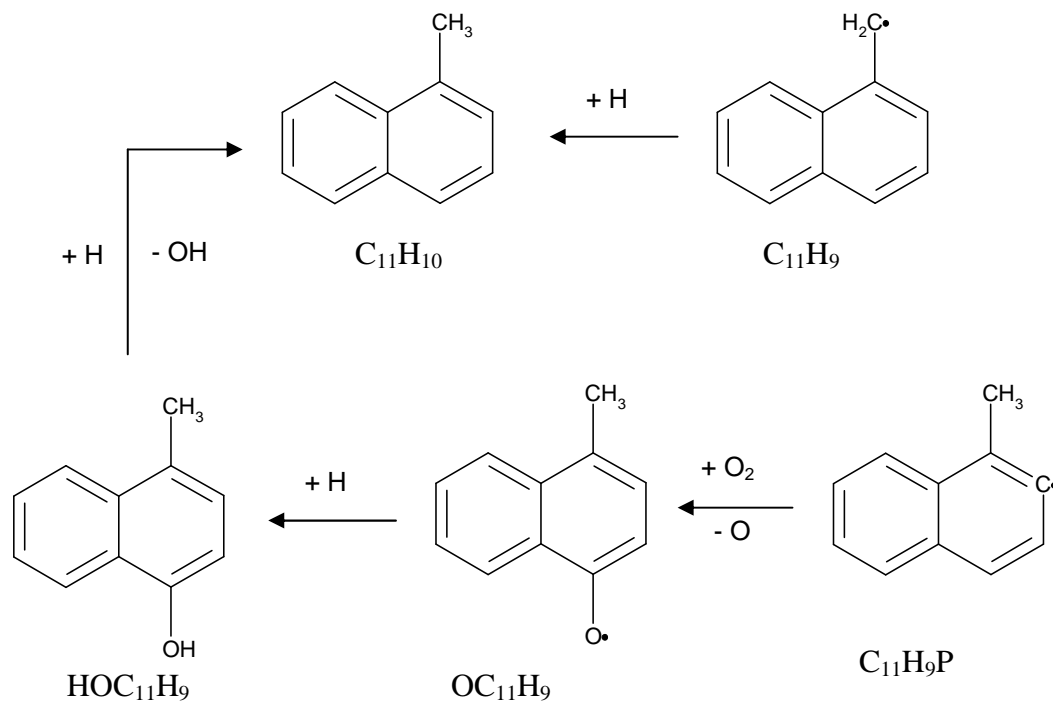


Figure 7.14 Major 1-methyl naphthalene formation pathways.

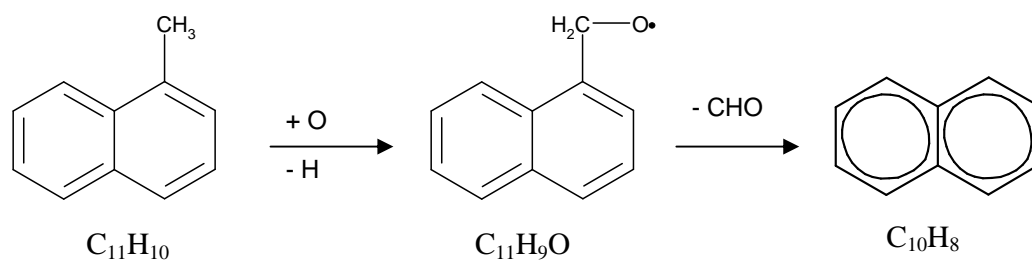


Figure 7.15 Naphthalene formation pathways

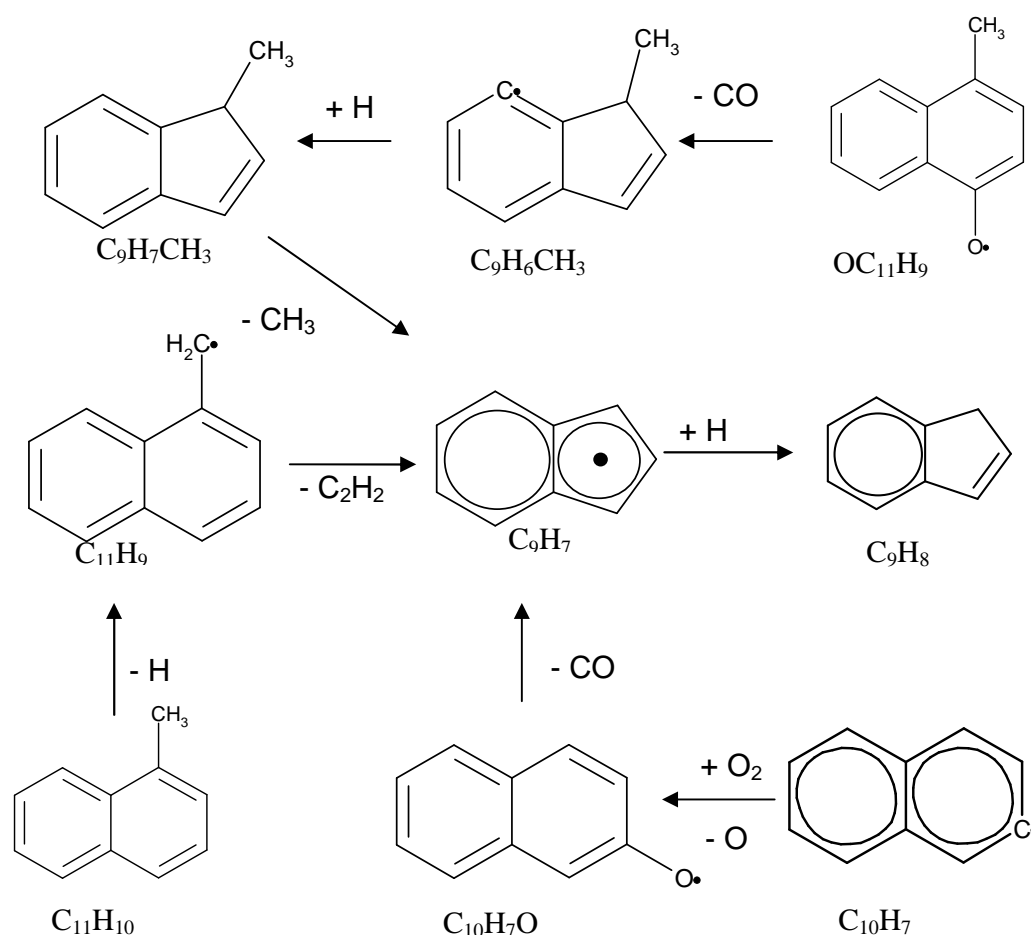
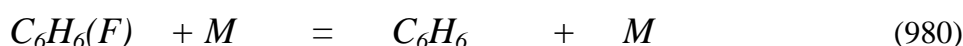
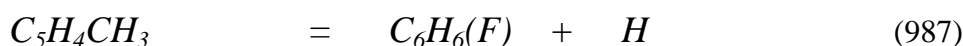


Figure 7.16 Major indene formation pathways

Computations show that another important indenyl oxidation step is via molecular oxygen which is responsible for 50% of the benzyl radical via (1232). Lindstedt *et al.* [70] used Density Functional Theory and composite quantum mechanical methods to calculate the potential energy surfaces for the channel and RRKM/ME and VTST approach to derive an estimate of the rate constant. The benzyl radical leads (97%) to toluene. The rate determined by Oehlschlaeger *et al.* [90] is used for reaction (1078).



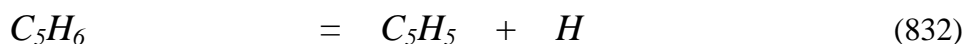
Benzene is mostly formed (35%) from fulvene via isomerization (980) assigned a rate proposed by Marinov *et al.* [78]. Fulvene is produced (100%) by the methyl cyclopentadienyl radical after thermal decomposition (987) and assigned a rate proposed by Lindstedt and Rizos [62]. In addition to the fulvene reaction sequence, 25% of benzene is formed from benzaldehyde. A rate proposed by Potter [75] was used for reaction (1101).



Benzene is consumed by reactions leading to phenyl (42%) and phenoxy (48%) radicals. The phenyl radical also predominantly (65%) leads to phenoxy which in turn leads to the formation of the cyclopentadienyl radical (80%) by CO expulsion. The cyclopentadienyl radical follows two major decomposition routes; 28% thermally decomposes to acetylene and the propargyl radical and 25% recombines with hydrogen leading to cyclopentadiene.

Cyclopentadiene is predominantly (90%) produced by the recombination of the cyclopentadienyl radical with atomic hydrogen. A rate proposed by Kern *et al.* [52] was applied to this channel. Kern *et al.* [52] proposed that the cyclopentadienyl dissociation occurs after a 1,2 *H*-atom shift that controls the rate of the reaction. Cyclopentadiene then recycles back to cyclopentadienyl radical.





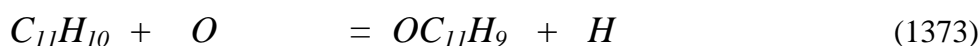
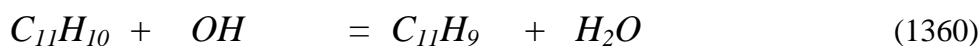
Acetylene is formed via two major thermal decomposition channels. The dominant (39%) is the thermal decomposition of the 1-methyl naphthyl radical that forms acetylene and the indenyl radical (1347) and the second major channel is (21%) via the thermal breakdown of cyclo pentadienyl radical (806). The rate of Kern *et al.* [52] was applied to reaction channel (806) but found to produce excessive acetylene concentrations, hence an adjustment was made by reducing the rate by 50%.



## 7.5 Fuel Rich Mixtures

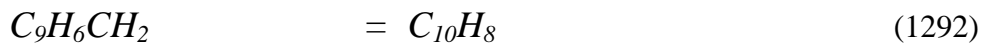
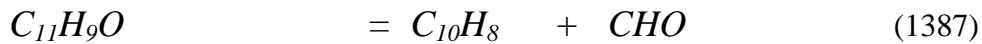
A reaction rate analysis was performed for a fuel rich mixture ( $\Phi = 1.5$ ) under jet-stirred reactor conditions at a temperature of 1240 K and at atmospheric pressure.

The fuel decomposes via four major oxidation channels. The hydrogen abstraction via *OH* attack on the methyl branch (1360) contributes 21% and the hydrogen abstraction from the ring (1357) is responsible for 14%. It is evident that in fuel rich mixtures the impact (21%) of reaction (1360) is reduced compared to lean mixtures (31%). The oxygen addition reactions either to the branch (10%) or to the ring (20%) make similar contribution to the fuel lean case.



The 1-methyl naphthyl radical recombines (90%) with the hydrogen atom leading to the formation of 1-methyl naphthalene.

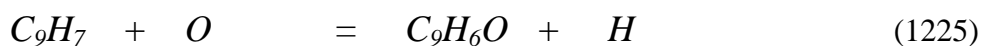
Naphthalene is formed from the thermal breakdown of  $C_{11}H_9O$  leading to naphthalene and  $CHO$  (48%). The impact is reduced from 65% for the same reaction in lean mixtures. The isomerization channel from  $C_9H_6CH_2$  contributes 28% compared to only 8% of the  $C_{10}H_8$  formation in lean mixtures. Reaction (1292) was assigned a rate proposed by Laskin and Lifshitz [131].

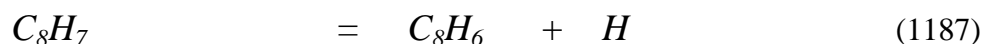
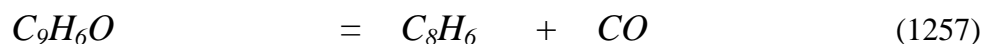
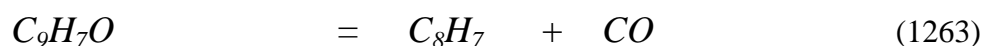
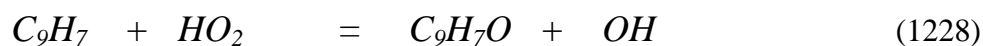


Two major species, naphthaldehyde and the naphthyl radical, which leads to naphthaldehyde, are produced from naphthalene decomposition. The subsequent consumption of naphthaldehyde leads to the indenyl radical (20%). The indenyl radical pool is also formed by the thermal decomposition of  $C_9H_7CH_3$  (-1221) which accounts for 31% of the formation as compared to 50% in lean mixtures. The 1-methyl naphthyl radical consumption leading to the formation of acetylene and indenyl radical is responsible for 28% of the formation compared to 12% in fuel lean mixtures.

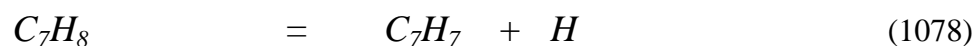
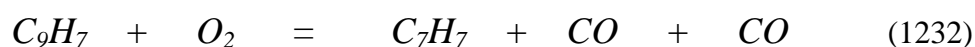


The further oxidation of the indenyl radical leads to the formation of phenyl acetylene via the formation of  $C_9H_6O$  and  $C_9H_7O$ . Phenyl acetylene is formed 50% via  $C_9H_6O$  through  $CO$  (1257) expulsion and 50% via  $C_8H_7$  formed from  $C_9H_7O$ . The dominant path for  $C_9H_6O$  formation is via reaction (1225) with a reaction rate based on a suggestion by Potter [75]. The subsequent decomposition to phenyl acetylene (1257), was assigned a rate proposed by Maurice [112]. The contribution of reaction (1187) reduced to 50%, compared to the 71% in lean mixtures, and reaction (1257) is equally important.





The molecular oxygen oxidation of indenyl radical is responsible for 60% of the production of the benzyl radical, which recombines with atomic hydrogen leading to toluene (98%).



Benzene is formed through a sequence of reactions that initiate from toluene  $\rightarrow OC_7H_7 \rightarrow C_5H_4CH_3 \rightarrow C_6H_6(F) \rightarrow C_6H_6$ . The isomerization that converts fulvene to benzene is responsible for 45% of the formation, compared to 35% in lean mixtures. Once benzene is formed, it follows a decomposition route through the phenoxy (41%) and phenyl (38%) radicals. The phenyl radical is oxidized to phenoxy and also leads to the formation of the cyclopentadienyl radical via thermal CO expulsion (994). The rate proposed by Leung and Lindstedt [73] was used for reaction (994).



Cyclopentadiene recycles back to the cyclopentadienyl radical, which is one of the main reactants for the formation of acetylene via the thermal decomposition to acetylene and the propargyl radical (806). Moreover, it is quite interesting to note that the thermal decomposition of the 1-methylnaphthyl radical ( $C_{11}H_9$ ) to the indenyl radical and acetylene (1347) contributes 60% of the acetylene production compared to 39% in fuel lean mixtures.





## 7.6 Oxidation in Turbulent Flow Reactors

Shaddix [24] performed gas-phase sampling to study the oxidation of 1-methyl naphthalene in the Princeton turbulent flow reactor and obtained concentration profiles for major species at atmospheric pressure and at a temperature of approximately 1170 K. Major fuel consumption routes and reaction classes were identified. In the current study, computations were performed corresponding to the experimental conditions for stoichiometric and fuel rich mixtures as shown in Table 7.2.

$\Phi$	T (K)	P (atm)	[O <sub>2</sub> ] (ppm)	[C <sub>11</sub> H <sub>10</sub> ] (ppm)
1.0	1169	1.0	14850	1100
1.5	1166	1.0	9900	1100
1.5	1198	1.0	9900	1100

Table 7.2 Experimental and modelling conditions for the oxidation of 1-methyl naphthalene in a turbulent flow reactor.

In Figure 7.17 to Figure 7.28, it can be seen that only partial conversion of *CO* to *CO*<sub>2</sub> occurs. The fuel profile is again well reproduced, suggesting that the 1-methyl naphthalene sub-mechanism is adequate. Moreover, naphthalene and indene, which are two of the major initial products of the fuel decomposition process, are very well reproduced for all the three test cases leading to good agreement between computations and measurements for the next direct products such as phenyl acetylene, styrene and toluene. The profiles of aliphatic hydrocarbons such as acetylene, ethane and methane are also well predicted implying that the reaction channels leading to lower hydrocarbons are well represented. The large measured concentrations of acetylene agree with the computations and are an indication of the sooting tendency of 1-methyl naphthalene.

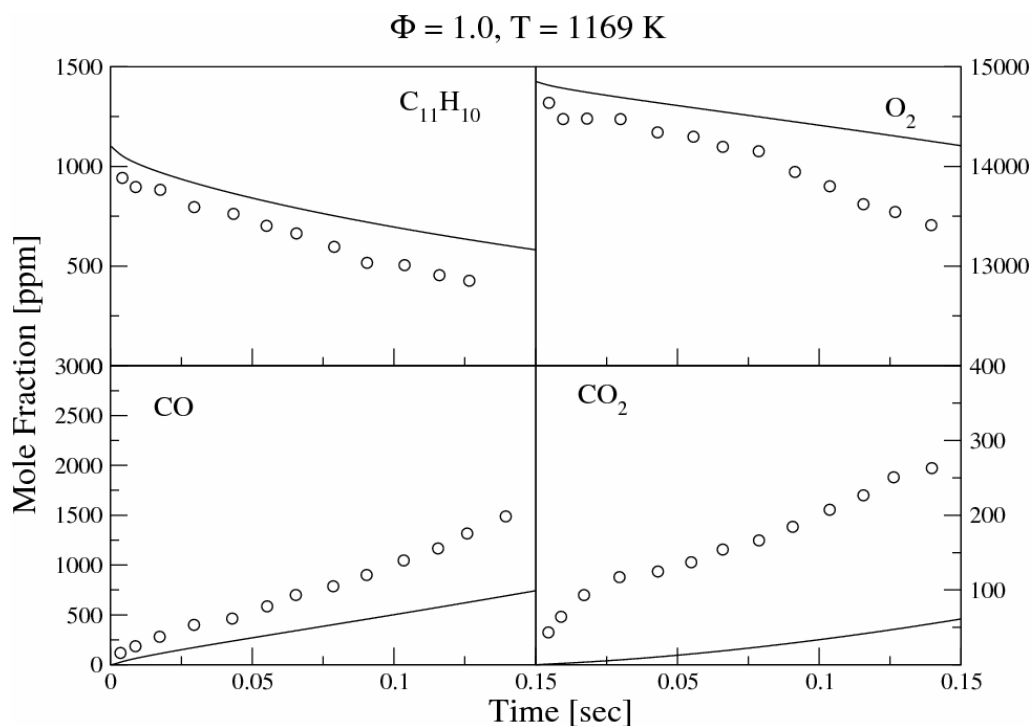


Figure 7.17 Concentration profiles of major species during 1-methyl naphthalene oxidation in a flow reactor ( $\Phi = 1.0, P = 1 \text{ atm}, T = 1169 \text{ K}$ ). Circles indicate measurements [24] and solid lines the current computations.

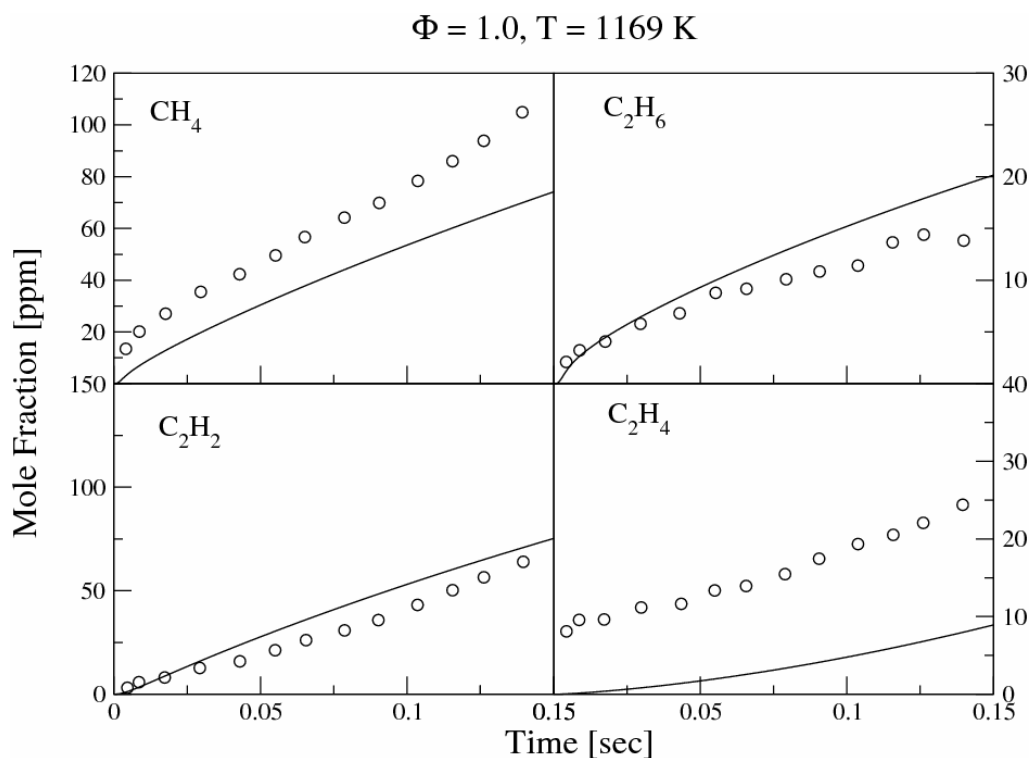


Figure 7.18 Concentration profiles of major species during 1-methyl naphthalene oxidation in a flow reactor ( $\Phi = 1.0, P = 1 \text{ atm}, T = 1169 \text{ K}$ ). Circles indicate measurements [24] and solid lines the current computations.

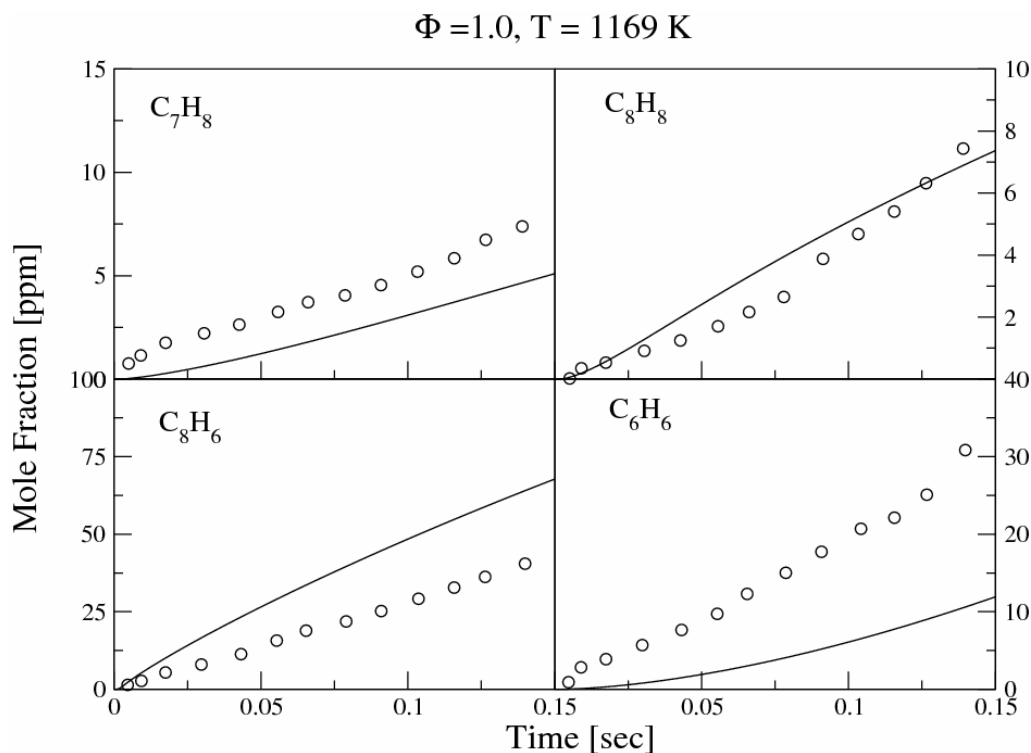


Figure 7.19 Concentration profiles of major species during 1-methyl naphthalene oxidation in a flow reactor ( $\Phi = 1.0, P = 1 \text{ atm}, T = 1169 \text{ K}$ ). Circles indicate measurements [24] and solid lines the current computations.

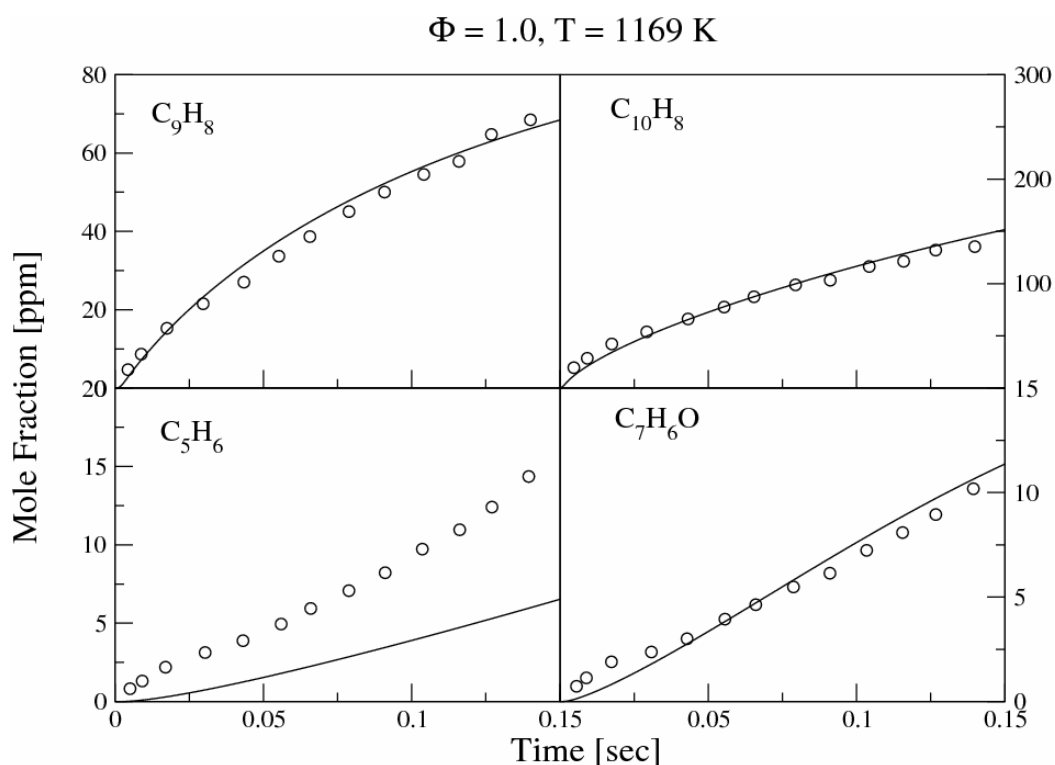


Figure 7.20 Concentration profiles of major species during 1-methyl naphthalene oxidation in a flow reactor ( $\Phi = 1.0, P = 1 \text{ atm}, T = 1169 \text{ K}$ ). Circles indicate measurements [24] and solid lines the current computations.

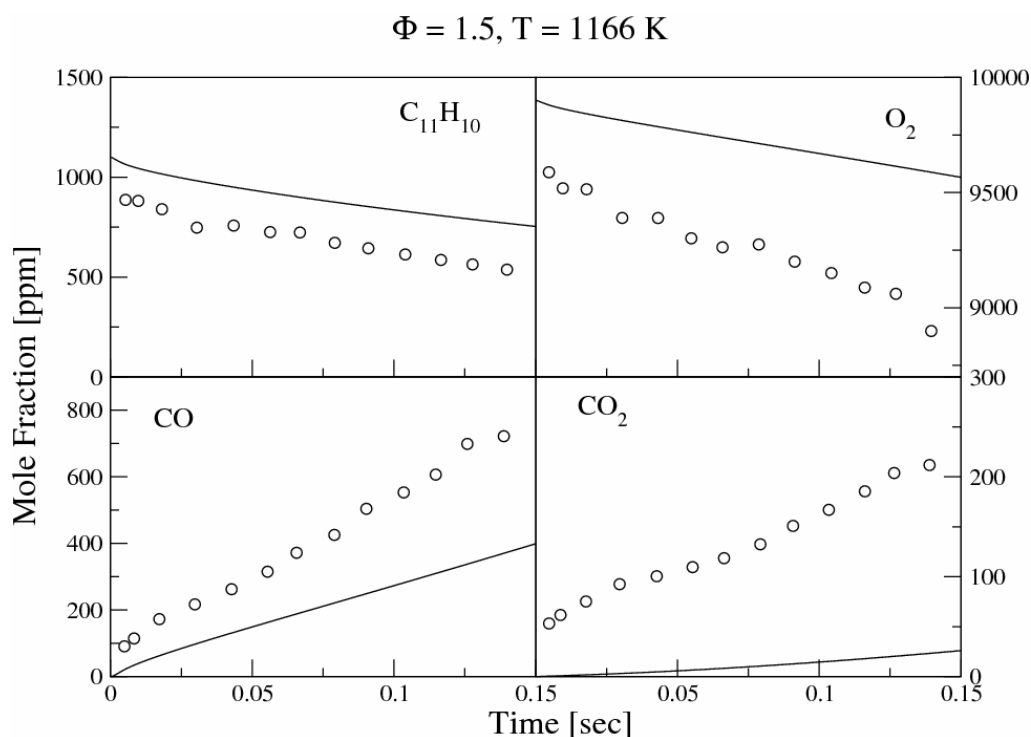


Figure 7.21 Concentration profiles of major species during 1-methyl naphthalene oxidation in a flow reactor ( $\Phi = 1.5, P = 1 \text{ atm}, T = 1166 \text{ K}$ ). Circles indicate measurements [24] and solid lines the current computations.

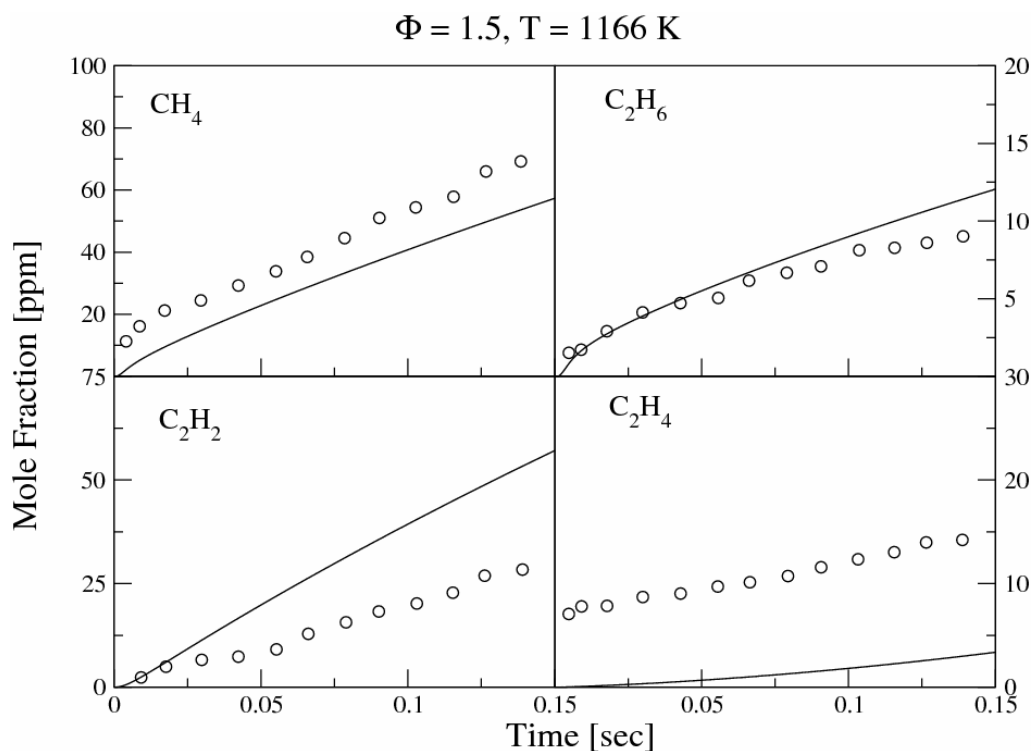


Figure 7.22 Concentration profiles of major species during 1-methyl naphthalene oxidation in a flow reactor ( $\Phi = 1.5, P = 1 \text{ atm}, T = 1166 \text{ K}$ ). Circles indicate measurements [24] and solid lines the current computations.

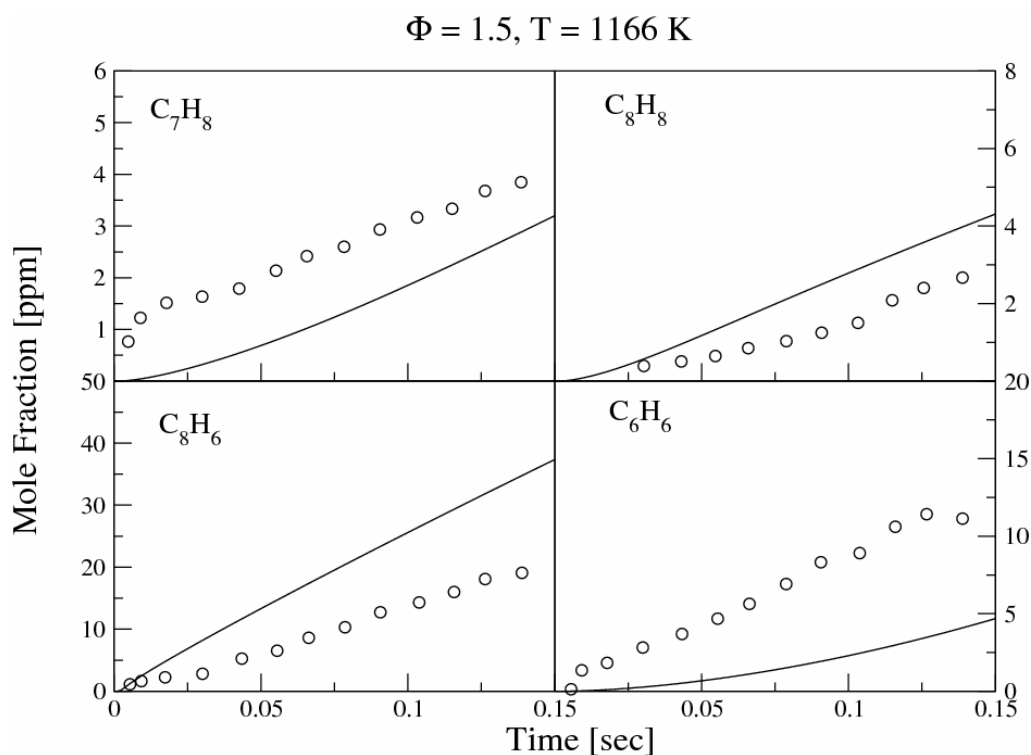


Figure 7.23 Concentration profiles of major species during 1-methyl naphthalene oxidation in a flow reactor ( $\Phi = 1.5$ ,  $P = 1 \text{ atm}$ ,  $T = 1166 \text{ K}$ ). Circles indicate measurements [24] and solid lines the current computations.

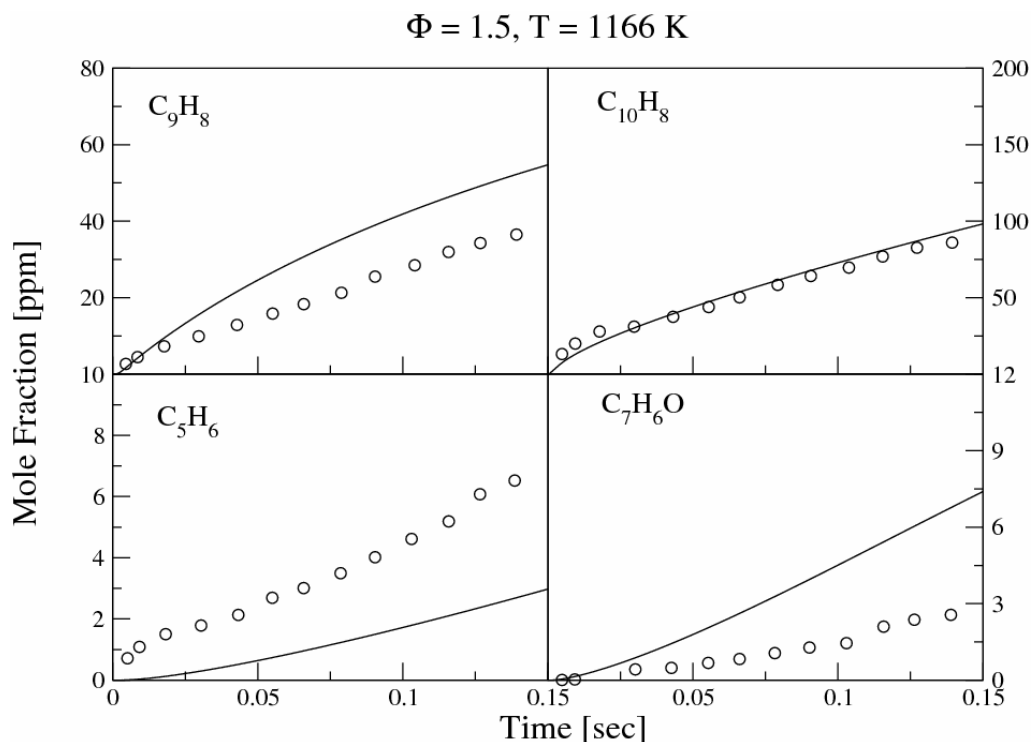


Figure 7.24 Concentration profiles of major species during 1-methyl naphthalene oxidation in a flow reactor ( $\Phi = 1.5$ ,  $P = 1 \text{ atm}$ ,  $T = 1166 \text{ K}$ ). Circles indicate measurements [24] and solid lines the current computations.



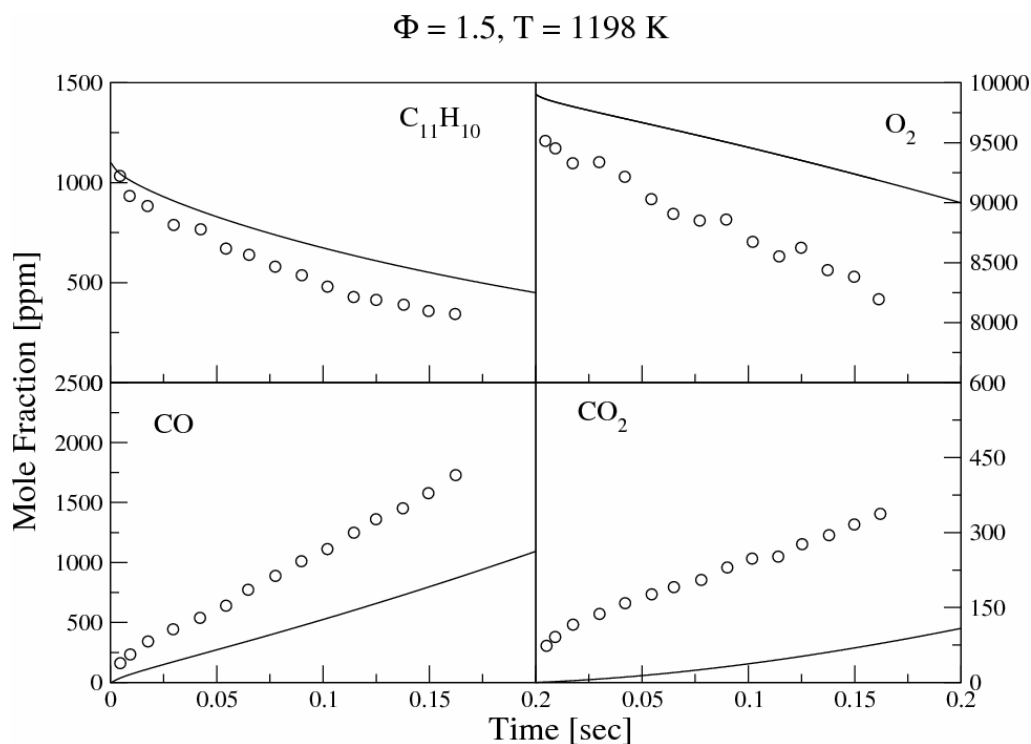


Figure 7.25 Concentration profiles of major species during 1-methyl naphthalene oxidation in a flow reactor ( $\Phi = 1.5, P = 1 \text{ atm}, T = 1198 \text{ K}$ ). Circles indicate measurements [24] and solid lines the current computations.

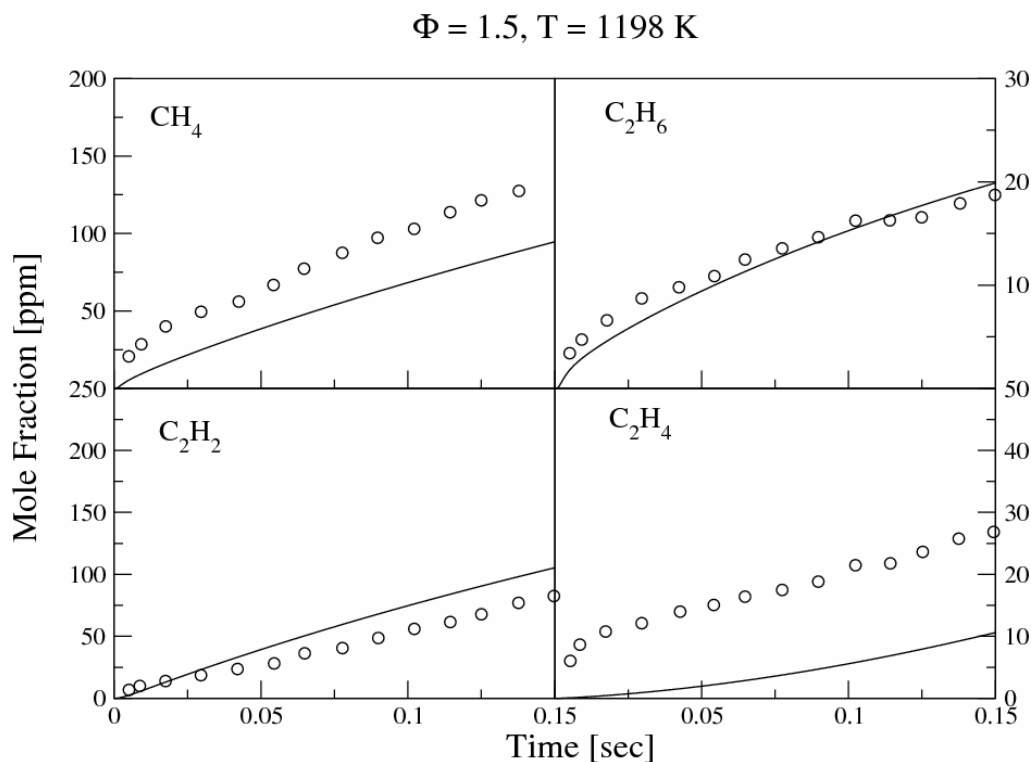


Figure 7.26 Concentration profiles of major species during 1-methyl naphthalene oxidation in a flow reactor ( $\Phi = 1.5, P = 1 \text{ atm}, T = 1198 \text{ K}$ ). Circles indicate measurements [24] and solid lines the current computations.

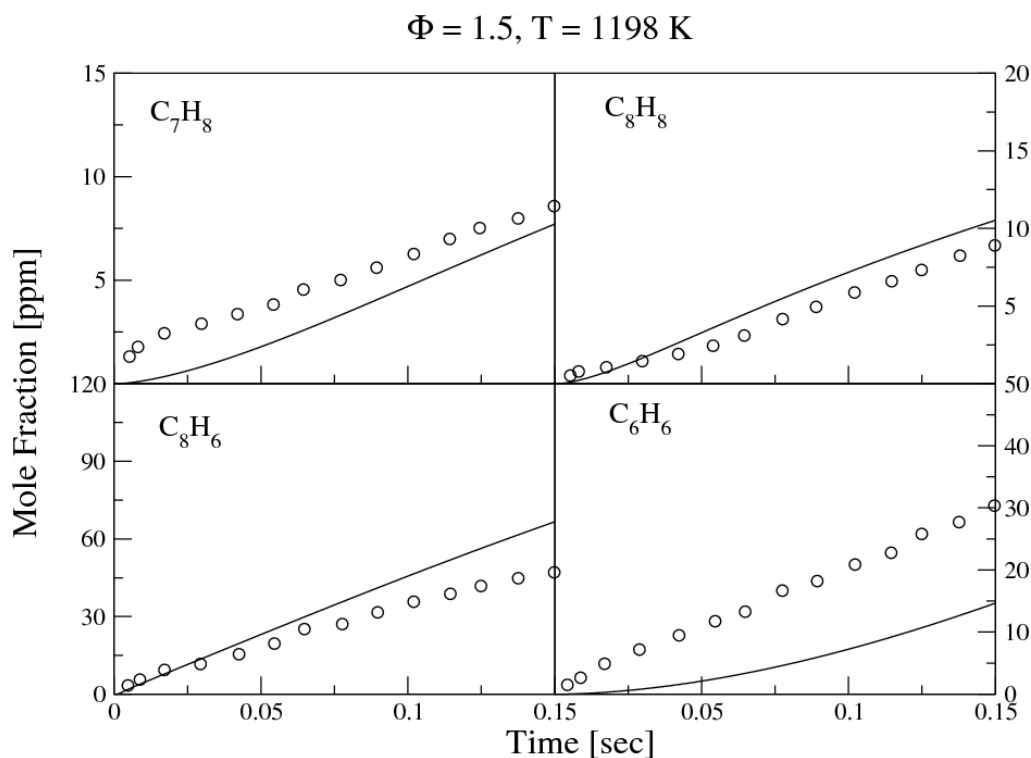


Figure 7.27 Concentration profiles of major species during 1-methyl naphthalene oxidation in a flow reactor ( $\Phi = 1.5, P = 1 \text{ atm}, T = 1198 \text{ K}$ ). Circles indicate measurements [24] and solid lines the current computations.

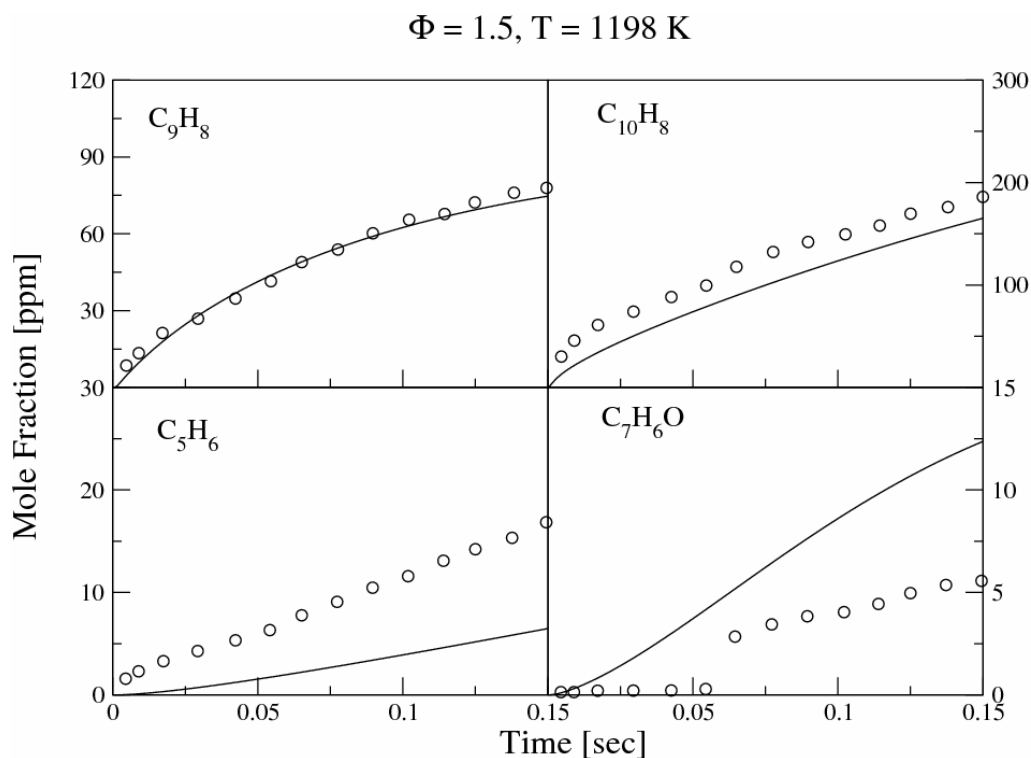
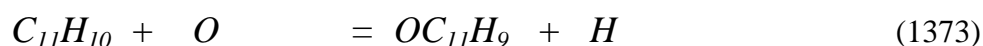
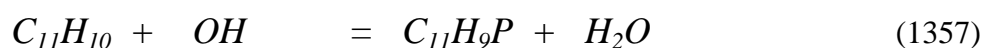
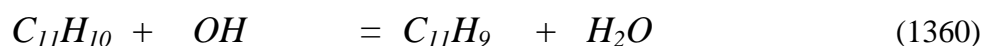


Figure 7.28 Concentration profiles of major species during 1-methyl naphthalene oxidation in a flow reactor ( $\Phi = 1.5, P = 1 \text{ atm}, T = 1198 \text{ K}$ ). Circles indicate measurements [24] and solid lines the current computations.

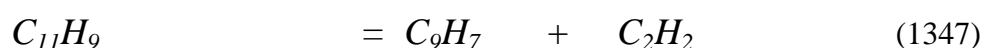
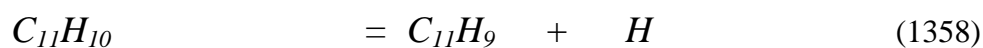
## 7.7 Further Analysis of Reaction Paths

Computations and rate analyses were performed at atmospheric pressure for both stoichiometric and rich fuel mixtures under plug flow reactor conditions. Significant oxidation pathways were identified for the initial fuel decay and the formation and decomposition of important intermediate species. Stoichiometric and rich mixtures show similar behaviour and there are no qualitative changes in either the species growth or the mechanisms under the current conditions. Consequently, a rate analysis is only presented for the stoichiometric case.

The 1-methyl naphthalene fuel decomposition is mainly controlled by hydrogen atom abstraction reactions either from the ring (1357) 15% or from the methyl branch (1360) 25%. Oxygen addition reactions also take place and account for 22% of the fuel decay by replacing a hydrogen atom from the ring and 12% by replacing a ‘benzylic’ hydrogen. The direct removal of the methyl group, either via a pyrolytic reaction or displacement via  $H$  attack, is found to be a minor route that does not exceed 6% of the total fuel consumption.

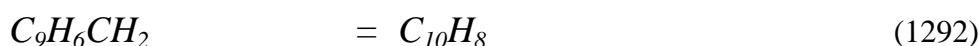
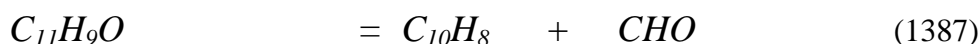


The 1-methyl naphthyl radical which is formed by the ‘benzylic’ hydrogen removal from 1-methyl naphthalene forms  $C_{11}H_{10}$  via  $H$  recombination contributing 36% to the  $C_{11}H_9$  consumption. The second major  $C_{11}H_9$  decomposition channel is via thermal decomposition leading to the formation of the indenyl radical and acetylene (30%). Approximately 11% of  $C_{11}H_9$  forms  $C_{11}H_9O$  via oxygen addition. Reaction rates applied to reactions (1358) and (1343) were based on the relevant kinetics of benzene as proposed by Potter [75].

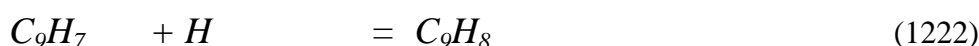
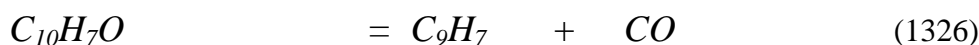
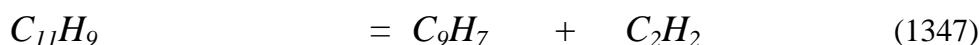




The decomposition of  $C_{11}H_9O$  leads essentially (98%) to the formation of naphthalene via reaction (1387), which contributes 66% of the total formation of naphthalene. Naphthalene is also formed from the isomerization of  $C_9H_6CH_2$  (11%), which is formed after a sequence of reactions that initiate from  $OC_{11}H_9$ , a major initial product. Added to this, the  $C_{11}H_9P$  radical, which is produced from one of the four major fuel oxidation pathways also leads to the formation of  $OC_{11}H_9$ . The  $OC_{11}H_9$  radical leads (95%) to the formation of  $C_9H_6CH_3$  via  $CO$  expulsion. Approximately 43% of  $C_9H_6CH_3$  converts to  $C_9H_6CH_2$  via thermal decomposition and subsequently leads to  $C_{10}H_8$ .

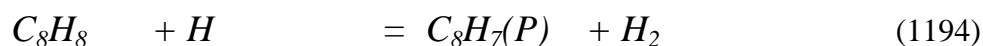
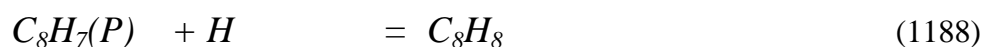


Naphthalene decomposes via two major channels to  $C_{10}H_7$  (44%) and  $C_{10}H_7O$  (46%). The  $C_{10}H_7$  radical is predominantly oxidized to  $C_{10}H_7O$  (65%). Following  $CO$  expulsion,  $C_{10}H_7O$  breaks down to the indenyl radical (1326) and contributes 12% of the total indenyl formation. A major (45%) indenyl formation pathway is via thermal decomposition of the  $C_9H_7CH_3$  (1347) to  $C_9H_7$  and  $CH_3$  radicals (1221). The thermal decay of the 1-methyl naphthyl radical leads to  $C_9H_7$  and  $C_2H_2$  and plays an important (28%) role in the formation of the indenyl radical. The formation channels of  $C_9H_7$  are of key importance in the oxidation chain and also leads to indene via (1222).

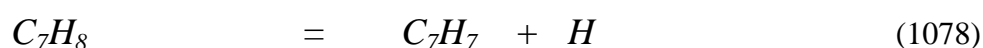
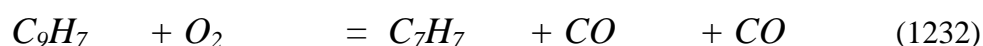


Further oxidation of  $C_9H_7$  produces  $C_8H_7(P)$  and approximately 42% leads to styrene via reactions (1188) and (1194), which are responsible for 60% and 28%

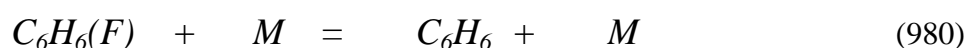
respectively. The reaction rates applied to these channels were adopted from Maurice [112].



Approximately 65% of the styrene leads to the benzyl radical and formaldehyde via *OH* attack, but this channel constitutes only 9% of the total benzyl formation. The major benzyl radical formation channel is reaction (1232) (83%). The benzyl radical recombines with hydrogen (37%) leading to toluene. The channel is solely responsible for the toluene formation.



Phenyl acetylene is produced via a reaction sequence through the indenyl radical  $C_9H_7 \rightarrow C_9H_7O \rightarrow C_8H_7 \rightarrow C_8H_6$ . The dominant consumption pathway of  $C_8H_6$  (36%) leads to the formation of the phenyl radical and  $C_2HO$ . As mentioned earlier, the phenyl radical is an important intermediate specie for the formation of cyclopentadienyl radical which occurs from the conversion of  $C_6H_5$  to  $C_6H_5O$  (65%) via molecular oxygen attack. The phenoxy radical leads (98%) to  $C_5H_5$ . The channel is also the dominant  $C_5H_5$  formation pathway (87%). The cyclopentadienyl radical recombines with  $CH_3$  leading to the formation of  $C_5H_4CH_3$  which is converted to fulvene via hydrogen abstraction and subsequently to benzene via isomerization.



The cyclopentadienyl radical recombines (24%) with atomic hydrogen to the formation of cyclopentadiene which is the main formation channel for  $C_5H_6$  (95%). The predominant consumption step for  $C_5H_5$  (41%) is through thermal decomposition to acetylene and the propargyl radical. However, this step constitutes a secondary formation channel for acetylene (14%). The dominant  $C_2H_2$  formation

step is via thermal decomposition of the  $C_{11}H_9$  radical to indenyl and acetylene (70%).

Methane is produced from direct fuel consumption pathways that occur via hydrogen abstraction via methyl radicals either from the branch (1365) of 1-methyl naphthalene (62%), which is the dominant formation channel, or (22%) from the ring (1370).



The major methyl radical formation channel is the thermal decomposition of  $C_9H_7CH_3$  (73%).

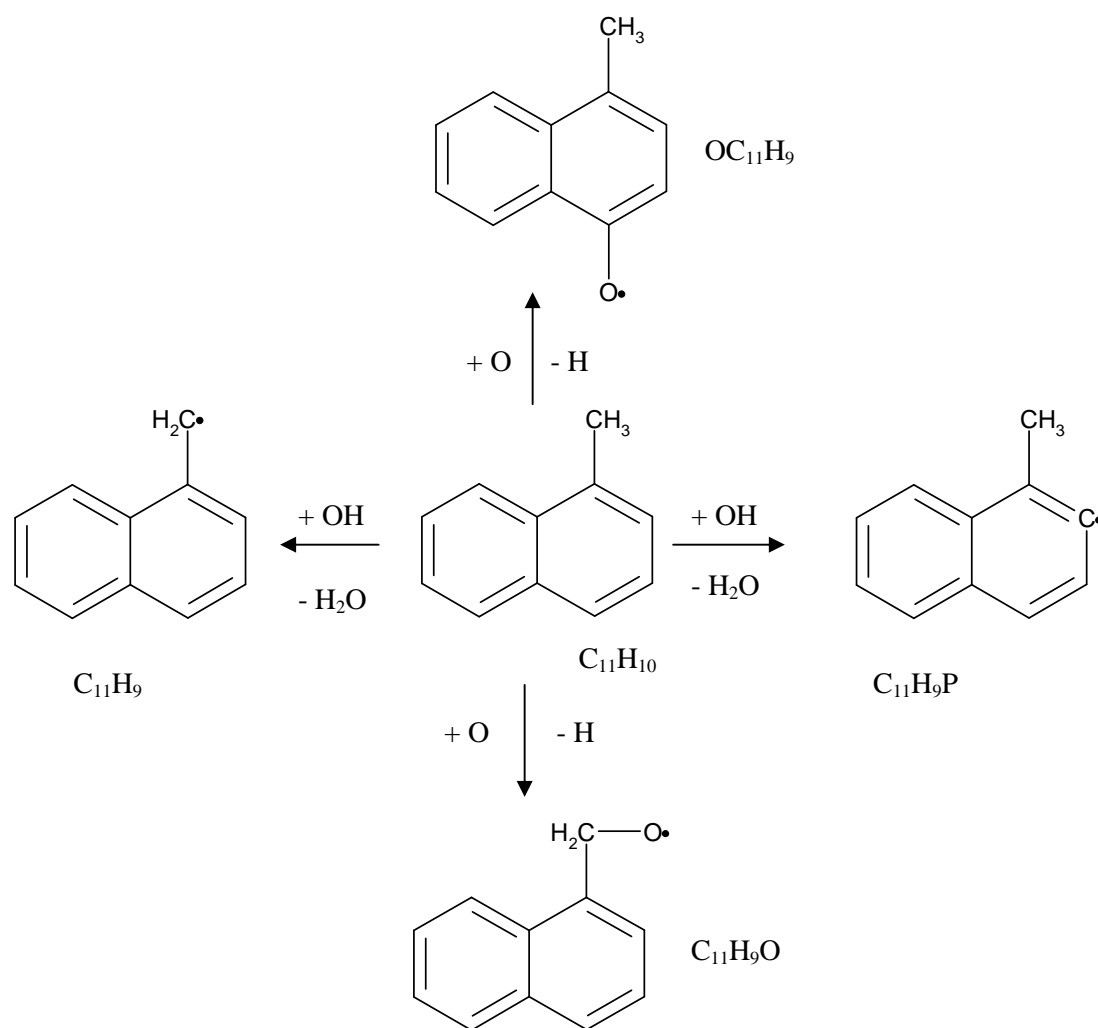


Figure 7.29 Major 1-methyl naphthalene decomposition pathways under plug flow reactor conditions

## 7.8 Conclusions

In the present work, a detailed chemical sub-mechanism for 1-methyl naphthalene was developed and validated under oxidation conditions in jet-stirred and flow reactors. A reaction rate analysis has shown that the ‘benzylic’ hydrogen abstraction is the dominant fuel decomposition process. The contribution of this channel reduces as the equivalence ratio increases. The second main fuel decay path is predicted to occur via oxygen atom addition to the bicyclic ring, which contributes 20-23% of the fuel consumption. Hydrogen abstraction from the ring via *OH* attack is less favoured.

The removal of the methyl group, either by replacement or via thermal decomposition, is a minor process contributing approximately 3% to the fuel breakdown. Once the 1-methylnaphthyl radical is formed, the proposed thermal decomposition channel leading to the indenyl radical and acetylene is important and affects the growth and evolution of major intermediate species such as indene, styrene, phenyl acetylene, toluene benzene, cyclopentadiene and acetylene. The rate from Braun-Unhoff *et al.* [28] was adjusted to the 1-methyl naphthalene from toluene and resulted in good agreement for species concentrations in both reactors and for all the tested equivalence ratios.

The level of agreement obtained between the computed concentrations and measurements for the naphthalene and indene species also implies that the accuracy of the fuel decay paths that involve oxygen addition to the fuel and lead to the formation of  $C_{11}H_9O$  and  $OC_{11}H_9$  is adequate. The further decomposition of the oxygenated species leads to the formation of  $C_{10}H_8$  and significant amounts of  $C_9H_7$ . The branching ratios between abstraction and addition pathways are also important for 1-methyl naphthalene combustion at intermediate temperatures.

This current study presents a detailed chemical mechanism that captures the fuel profile decay and the growth of the rest of the major intermediate species in both jet-stirred and flow reactor conditions.



## Chapter 8

### Conclusions and Future Work

#### 8.1 Conclusions

The main objective of the present work has been the development, update and validation of detailed gas phase chemical kinetic mechanisms for aromatic components of aviation fuels and surrogates. A broad range of reactors and conditions has been used for the computational validation of the fuels and a reaction class based approach was used for the generation of the chemical mechanisms. The mechanisms feature molecules up to  $C_{11}$  that involve aliphatic compounds and a submechanism of mono-substituted and polyaromatic hydrocarbons. The starting point for this work was the development and validation of a mechanism for cyclopentadiene, which constitutes a major intermediate component in the combustion of single-ring aromatics such as benzene. The work was extended to two single-ring aromatics, toluene and *n*-propyl benzene, and to two-ring aromatics, naphthalene and 1-methyl naphthalene.

Cyclopentadiene is responsible for the production of the cyclopentadienyl radical that has high sooting tendencies, hence a detailed analysis of the cyclopentadienyl mechanism was performed. The oxidation of  $C_5H_6$  was studied under plug flow reactor conditions and concentration profiles were computed and compared with measurements of Butler [20]. Reaction rates for channels featuring  $O$ ,  $HO_2$  and  $OH$  were also updated and validated. A variety of cases varying from stoichiometric to fuel rich at atmospheric pressure were tested and reaction rate analyses were performed for representative cases. The pyrolysis of cyclopentadiene was also studied for a variety of fuel concentrations. The detection of high concentrations of species such as naphthalene, toluene, benzene and acetylene suggest pathways leading to PAH. During oxidation conditions, cyclopentadiene is mainly consumed via hydrogen abstraction reactions by  $H$ ,  $OH$ ,  $O$  radicals leading

to  $C_5H_5$ . Naphthalene is a two ring aromatic compound that plays a significant role in aromatic growth and is formed via  $C_5H_5$  through  $C_{10}H_9F$  formation. Temperature perturbations affect the fuel consumption pathways and promote soot formation. Especially when the temperature rises, thermal decomposition pathways start to play significant role in the evolution of species such as  $C_5H_5$  leading to acetylene and propargyl radical. Both the latter species were shown to facilitate soot growth. The prediction of excessive concentrations of all the intermediate species during pyrolytic studies lead to the replacement of the reaction rate of the  $C_5H_5$  thermal decomposition channel to acetylene and propargyl radical with a rate proposed by Robinson [15]. The modification was responsible for the refinement of the predicted species concentrations. However, some species still showed overprediction tendencies and a reaction rate analysis was performed and important pathways affecting the evolution of these species were identified. The pathways are mostly acetylene recombination reactions with  $C_3H_3$ ,  $C_3H_5(A)$ ,  $C_5H_5$  and  $C_7H_7$ , as well as, recombination of cyclopentadiene with the cyclopentadienyl radical leading to formation of indene.

The combustion of toluene was further validated and analysed under shock tube conditions. Tests involved pyrolytic and oxidation conditions, similar to those obtained by Braun-Unkloff *et al.* [28], Vasudevan *et al.* [26] and Burcat *et al.* [25]. Reaction rates were updated and new reaction pathways were added to the starting mechanism. Hydrogen atom profiles were calculated under pyrolytic conditions and managed to capture the measured profiles of Braun-Unkloff *et al.* [28] reasonably well. The result that the branching ratio of the toluene thermal decomposition to benzyl radical or phenyl and methyl radicals utilised in this study is arguably correct. Time resolved  $OH$  profile was also computed under shock tube conditions and compared against experimental data of Vasudevan *et al.* [26]. Sensitivity analysis that was performed identified the chain branching reaction  $O + H_2 \leftrightarrow OH + H$  as an important pathway to the determination of the  $OH$  concentration. A rate of Li *et al.* [98], adopted from Sutherland *et al.* [99], applied to the scheme was found responsible for the current excellent prediction of the slope of the  $OH$  profile as compared to the measurements. A rate of Sun *et al.* [96] adopted from Baulch *et al.* [97] was also tested to the current mechanism and was found problematic causing delays to the ignition. The step that involves acetylene recombination with the cyclopentadienyl radical was identified as significant for the accurate prediction of

the *OH* profile. The absence of this step is responsible for delay in the ignition by 20%. Toluene ignition delay times were also computed and showed excellent agreement with experimental data obtained from Vasudevan *et al.* [26] and Burcat *et al.* [25]. A reaction rate analysis was performed for both pyrolytic and oxidation conditions and important pathways were identified. The analyses highlight the toluene thermal decomposition to the benzyl radical and phenyl and methyl radicals, as well as hydrogen assisted reactions leading to the production of the benzyl radical and benzene. The results suggest that the reaction class based approach can also be applied to other methyl-substituted aromatic fuel components that form part of real and surrogate fuel formulations.

*N*-propyl benzene follows the behaviour of benzene, toluene and propane. The mechanism was validated under jet-stirred reactor conditions for both low and high pressures for a wide range of stoichiometries and against ignition delay times. Reaction rates were updated and a rate analysis performed highlights the importance of the hydrogen abstraction reactions, which generate styrenes and promote the fuel consumption. The thermal breakdown of the *n*-propyl benzene chain to the primary and secondary site is significant and small rate changes can cause big discrepancies in the intermediate species concentrations. Large early concentrations of styrene, ethyl benzene and toluene is a clear indication that homolytic reactions occur and promote the fuel decay. The results presented in this work are very encouraging and suggest that the reaction class based approach can be applied to other alkyl substituted aromatic fuel components. However, as the chain increases in length, new categories of reaction steps such as radical isomerisations, cyclic transition states and group shifts along the chain are likely to occur and should be taken into account.

The mechanism was expanded to two-ring aromatic compounds such as naphthalene and tested under plug flow reactor conditions at atmospheric pressure and compared to measurements obtained by Shaddix [24]. Reaction rates for the  $C_9H_7 + O_2/HO_2$  were obtained by Lindstedt *et al.* [70] and a reaction rate analysis performed in this work showed that the aforementioned channels play a significant role to the product distribution of single ring aromatics. Moreover, it was shown that hydrogen abstraction reaction via *OH* and oxygen addition to the ring constitute major fuel consumption pathways. However, due to limited availability of experimental data in the literature only a single test case was analysed in this work.

Hence, measurements of wider range of conditions are essential for the further refinements.

The 1-methyl naphthalene submechanism is based on the toluene chemistry due to structural similarities. Reaction rates were updated and reaction steps were proposed to the scheme. Validation was performed under plug flow and jet stirred reactor conditions at atmospheric pressure for a variety of stoichiometries. Results were compared against measurements obtained by Shaddix and co-workers [21, 24] and Mati *et al.* [35]. A reaction rate analysis was performed for both plug flow and jet stirred reactor conditions and showed that the fuel decomposes via *OH* hydrogen abstraction from the chain and the ring and oxygen addition to both the chain and the ring. However, the attack on the chain side dominates the consumption of the fuel. The proposed thermal decomposition of the 1-methylnaphthyl radical to the indenyl radical and acetylene, was shown to constitute major channel for the evolution of the produced intermediate species. Moreover, the reaction sequence of  $C_9H_7 + O_2/HO_2$  is also important for the distribution of single-ring aromatics. The good agreement between the computations and the measurements for the current 1-methyl naphthalene is encouraging.

## 8.2 Suggestions for Future Work

The present work has identified some significant aspects of the chemical kinetic modelling of the studied fuel components that will need further investigation. A summary of the suggestions for future work is outlined below.

1. The chemical kinetic analysis of the fuels studied here has revealed that pathways that involve acetylene recombination with radicals such as  $C_3H_3$ ,  $C_3H_4(A)$ ,  $C_5H_5$ ,  $C_7H_7$  and  $C_{11}H_9$  play a significant role in the evolution of intermediate species. There is need for further refinement of the reaction rates of the relevant reaction steps in order to minimize concentration discrepancies as compared to measurements.
2. The present toluene chemistry manages to capture the high temperature regimes very well. However, uncertainties in the low

temperature reaction suggest potential problems under such conditions.

3. The present oxidation mechanism for naphthalene highlights some key reaction steps that occur under oxidation conditions. The model may need further refinement in order to capture the behaviour of the fuel under wider range of conditions. Hence, measurements for a variety of stoichiometries tested under wider pressure and temperature conditions are essential in order to reduce uncertainties in the concentrations of intermediate species.
4. The present 1-methyl naphthalene chemical scheme manages to simulate the behaviour of fuel oxidation in good agreement with the measurements under atmospheric pressure. Further work is essential for refinement of the model at higher pressures.
5. The current refinement of the models can provide insight of relevance to the aviation industry and the next step should target systematic reductions leading to more acceptable computational costs for practical applications to the current combustor configurations.

## References

- [1] J. P. Longwell, The Formation of Polycyclic Aromatic Hydrocarbons by Combustion, *Nineteenth Symposium (International) on Combustion* (1) 19 (1982), 1339-1350.
- [2] W. J. Pitz, C. K. Westbrook, A. E. Lutz, R. J. Kee, S. M. Senkan and J. G. Seebold, Numerical Modeling Capabilities for the Simulation of toxic By-Products Formation in Combustion Processes, *Combust. Sci. and Tech.* 101 (1994), 383-396.
- [3] J. B. Howard, J. P. Longwell, J. A. Marr, C. J. Pope, W. F. Busby, A. L. Lafleur and K. Taghizadeh, Effects of PAH Isomerizations on Mutagenicity of Combustion Products, *Combust. Flame* (3) 101 (1995), 262-270.
- [4] D. R. Ballal, S. P. Heneghan, W. J. Schmoll, F. Tanakashi and M. D. Vangness, Combustion and Heat Transfer Studies Utilising Advanced Diagnostics: Combustion Studies. Report Number: A352062, (1992).
- [5] T. Edwards, L. Q. Maurice, H. Lander and W. E. Harisson, Advances in Aviation Fuels: A Look Ahead via a Historical Perspective, *Fuel* 80 (2001), 747-756.
- [6] P. Dagaut and M. Cathonnet, The Ignition, Oxidation and Combustion of Kerosene: A Review of Experimental and Kinetic Modeling, *Prog. Energy Combust. Sci.* (1) 32 (2006), 48-92.
- [7] A. F. Sarofim, E. G. Eddings, S. Yan, A. Violi, S. Granata, T. Faravelli and E. Ranzi, Experimental Formulation and Kinetic Modeling for JP-8 Surrogate Mixtures, *Second Mediterranean Combustion Symposium, Sharm el Sheick, Egypt* (2002).
- [8] P. Lindstedt, Modeling of the Chemical Complexities of Flames, *Twenty-Seventh Symposium (International) on Combustion, The Combustion Institute* (1) 27

(1998), 269-285.

[9] M. Bernabei, R. Reda, R. Galiero and G. Bocchinfuso, Determination of Total and Polycyclic Aromatic Hydrocarbons in Aviation Jet Fuel, *Journal of Chromatography A* (1-2) 985 (2003), 197-203.

[10] C. K. Westbrook and F. L. Dryer, Chemical Kinetic Modeling of Hydrocarbon Combustion, *Prog. Energy Combust. Sci.* (1) 10 (1984), 1-57.

[11] S. W. Benson, *Thermochemical Kinetics*, (John Wiley & Sons, INC, 1976).

[12] J. Troe, Towards a Quantitative Understanding of Elementary Combustion Reactions, *Twenty-Second Symposium (International) on Combustion*, *The Combustion Institute* (1) 22 (1989), 843-862.

[13] A. M. Dean, Predictions of Pressure and Temperature Effects upon Radical Addition and Recombination Reactions, *J. Phys. Chem.* 89 (1985), 4600-4608.

[14] A. Burcat and B. Ruscic, Third Millennium Ideal Gas and Condensed Phase Thermochemical Database for Combustion with Updates from Active Thermochemical Tables, (2005), ANL-05/20 and TAE 960 Technion-IIT, Aerospace Engineering and Argonne National Laboratory, Chemistry Division, September 2005.

[15] R. Robinson, Private Communication, (2009).

[16] J. A. Miller, R. J. Kee and C. K. Westbrook, Chemical Kinetics and Combustion Modeling, *Annu. Rev. Phys. Chem.* (1) 41 (1990), 345-387.

[17] W. P. Jones and R. P. Lindstedt, Global Reaction Schemes for Hydrocarbon Combustion, *Combust. Flame* (3) 73 (1988), 233-249.

[18] G. Dixon-Lewis, T. David, P. H. Gaskell, S. Fukutani, H. Jinno, J. A. Miller, R. J. Kee, M. D. Smooke, N. Peters, E. Effelsberg, J. Warnatz and F. Behrendt, Calculation of the Structure and Extinction Limit of a Methane-Air Counterflow

Diffusion Flame in the Forward Stagnation Region of a Porous Cylinder, *Twentieth Symposium (International) on Combustion, The Combustion Institute* (1) 20 (1985), 1893-1904.

[19] R. J. Kee, J. A. Miller and T. H. Jefferson, A General purpose Problem-Independent Transortable Fortran Chemical Kinetics Code Package, (1980), Sandia National Laboratories Report SAND80-8003.

[20] R. G. Butler, Combustion Chemistry of 1-3 Cyclopentadiene, In *Department of Chemistry*, (Princeton University, PhD Thesis, 2001).

[21] C. R. Shaddix, K. Brezinsky and I. Glassman, Oxidation of 1-Methylnaphthalene, *Twenty-Fourth Symposium (International) on Combustion, The Combustion Institute* (1) 24 (1992), 683-690.

[22] C. R. Shaddix, K. Brezinsky and I. Glassman, Analysis of Fuel Decay Routes in the High-Temperature Oxidation of 1-Methylnaphthalene, *Combust. Flame* (1-2) 108 (1997), 139-157.

[23] R. G. Butler and I. Glassman, Cyclopentadiene Combustion in a Plug Flow Reactor near 1150 K, *Thirty-Second Symposium (International) on Combustion, The Combustion Institute* 32 (2009), 395-402.

[24] C. R. Shaddix, An Experimental Study of the High Temperature Oxidation of 1-Methylnaphthalene, (PhD Thesis, Princeton University, USA, 1993).

[25] A. Burcat, C. Snyder and T. Brabbs, Ignition Delay Times of Benzene and Toluene With Oxygen in Argon Mixtures., In *Technical Memorandum 87312*, (NASA, 1986).

[26] V. Vasudevan, D. F. Davidson and R. K. Hanson, Shock tube measurements of toluene ignition times and OH concentration time histories, *Thirtieth Symposium (International) on Combustion, The Combustion Institute* 30 (2005), 1155-1163.

[27] V. S. Rao and G. B. Skinner, Formation of H and D Atoms in the Pyrolysis



of Toluene-d, and Toluene- $\alpha,\alpha,\alpha$ -d<sub>3</sub> behind Shock Waves, *J. Phys. Chem.* 93 (1989), 1864-1869.

[28] M. Braun-Unkloff, P. Frank and T. Just, A Shock Tube Study on the Thermal Decomposition of Toluene and of the Phenyl Radical at High Temperatures, *Twenty-Second Symposium (International) on Combustion, The Combustion Institute* (1) 22 (1989), 1053-1061.

[29] D. F. Davidson, B. M. Gauthier and R. K. Hanson, Shock tube ignition measurements of iso-octane/air and toluene/air at high pressures, *Thirtieth Symposium (International) on Combustion, The Combustion Institute* 30 (2005), 1175-1182.

[30] W. Tsang and A. Lifshitz, Shock Tube Techniques in Chemical Kinetics, *Annu. Rev. Phys. Chem.* (1) 41 (1990), 559-599.

[31] R. L. Belford and R. A. Strehlow, Shock Tube Technique in Chemical Kinetics, *Annu. Rev. Phys. Chem.* (1) 20 (1969), 247-272.

[32] K. A. Bhaskaran and P. Roth, The Shock Tube as Wave Reactor for Kinetic Studies and Material Systems, *Prog. Energy Combust. Sci.* (2) 28 (2002), 151-192.

[33] R. Atkinson, D. L. Baulch, R. A. Cox, R. F. Hampson, J. A. Kerr and J. Troe, Evaluated Kinetic and Photochemical Data for Atmospheric Chemistry: Supplement III. IUPAC Subcommittee on Gas Kinetic Data Evaluation for Atmospheric Chemistry, *J. Phys. Chem. Ref. Data* 18 (1989), 881-1097.

[34] P. Dagaut, M. Cathonnet, J. P. Rouan, R. Foulatier, A. Quilgars, J. C. Boettner, F. Gaillard and H. James, A Jet-Stirred Reactor for Kinetic Studies of Homogeneous Gas-Phase Reactions at Pressures up to Ten Atmospheres (~1 MPa), *J. Phys. E: Sci. Instrum.* (3) 19 (1986), 207-209.

[35] K. Mati, A. Ristori, G. Pengloan and P. Dagaut, Oxidation of 1-Methylnaphthalene at 1–13 atm: Experimental Study in a JSR and Detailed Chemical Kinetic Modelling, *Combust. Sci. and Tech.* 179 (2007), 1261-1285.

- [36] P. Dagaut, A. Ristori, A. E. Bakali and M. Cathonnet, Experimental and Kinetic Modelling Study of the Oxidations of n-Propylbenzene, *Fuel* 81 (2002), 173-184.
- [37] J. Warnatz, J. Maas and R. W. Dibble, *Combustion. Physical and Chemical Fundamentals, Modelling and Simulation, Experiments, Pollutant Formation*, no. 3rd Edition (2001).
- [38] S. Arrhenius, Uber die Reaktionsgeschwindigkeit bei der Inversion von Rohrzucker durch Sauren, *Z. Phys. Chem.* 4 (1889), 226-248.
- [39] F. A. Lindemann, Discussion on "The radiation Theory of Chemical Action" *Trans. Faraday Soc.* 17 (1922), 598-606.
- [40] M. J. Pilling and P. W. Seakins, *Reaction Kinetics*, (Oxford University Press Inc., New York, 1995).
- [41] D. Wang, A. Violi, D. H. Kim and J. A. Mullholland, Formation of Naphthalene, Indene, and Benzene from Cyclopentadiene Pyrolysis: A DFT Study, *J. Phys. Chem. A* (14) 110 (2006), 4719-4725.
- [42] C. F. Melius, M. E. Colvin, N. M. Marinov, W. J. Pitt and S. M. Senkan, Reaction Mechanisms in Aromatic Hydrocarbon Formation Involving the C<sub>5</sub>H<sub>5</sub> Cyclopentadienyl Moiety, *Twenty-Sixth Symposium (International) on Combustion, The Combustion Institute* (1) 26 (1996), 685-692.
- [43] C. F. Melius, J. A. Miller and E. M. Evleth, Unimolecular Reaction Mechanisms Involving C<sub>3</sub>H<sub>4</sub>, C<sub>4</sub>H<sub>4</sub>, and C<sub>6</sub>H<sub>6</sub> Hydrocarbon Species, *Twenty-Fourth Symposium (International) on Combustion, The Combustion Institute* (1) 24 (1992), 621-628.
- [44] M. Frenklach, D. W. Clary, W. C. Gardiner Jr and S. E. Stein, Effect of Fuel Structure on Pathways to Soot, *Twenty-First Symposium (International) on Combustion* (1) 21 (1986), 1067-1076.

- [45] M. Frenklach and J. Warnatz, Detailed Modeling of PAH Profiles in a Sooting Low-Pressure Acetylene Flame, *Combust. Sci. and Tech.* (4) 51 (1987), 265-283.
- [46] M. Frenklach, D. W. Clary, T. Yuan, W. C. Gardiner and S. E. Stein, *Combust. Sci. and Tech.* (1) 50 (1986), 79-115.
- [47] M. Frenklach, D. W. Clary, J. W. C. Gardiner and S. E. Stein, Detailed Kinetic Modeling of Soot Formation in Shock-Tube Pyrolysis of Acetylene, *Twentieth Symposium (International) on Combustion, The Combustion Institute* (1) 20 (1985), 887-901.
- [48] A. Burcat and M. Dvinyaninov, Detailed Kinetics of Cyclopentadiene Decomposition Studied in a Shock Tube, *Int. J. Chem. Kinet.* (7) 29 (1997), 505-514.
- [49] K. Roy, M. Braun-Unkhoff, P. Frank and T. Just, Kinetics of the Cyclopentadiene Decay and the Recombination of Cyclopentadienyl Radicals with H-Atoms: Enthalpy of Formation of the Cyclopentadienyl Radical, *Int. J. Chem. Kinet.* (3) 34 (2002), 209-222.
- [50] K. Roy, C. Horn, P. Frank, V. G. Slutsky and T. Just, High-Temperature Investigations of the Pyrolysis of Cyclopentadiene, *Twenty-Seventh Symposium (International) on Combustion, The Combustion Institute* 27 (1998), 329-336.
- [51] M. B. Colket, The Pyrolysis of Cyclopentadiene, *Eastern States Section Annual Meeting of the Combustion Institute, Orland, FL* (1990).
- [52] R. D. Kern, Q. Zhang, J. Yao, B. S. Jursic, R. S. Tranter, M. A. Greybill and J. H. Kiefer, Pyrolysis of Cyclopentadiene: Rates for Initial C-H Bond Fission and the Decomposition of c-C<sub>5</sub>H<sub>5</sub>, *Twenty-Seventh Symposium (International) on Combustion, The Combustion Institute* 27 (1998), 143-150.
- [53] X. Zhong and J. W. Bozzelli, Thermochemical and Kinetic Analysis of the H, OH, HO<sub>2</sub>, O, and O<sub>2</sub> Association Reactions with Cyclopentadienyl Radical, *J.*

*Phys. Chem. A* (20) 102 (1998), 3537-3555.

[54] A. B. Lovell, K. Brezinsky and I. Glassman, Benzene Oxidation Perturbed by NO<sub>2</sub> Addition, *Twenty-Second Symposium (International) on Combustion*, *The Combustion Institute* (1) 22 (1989), 1063-1074.

[55] J. L. Emdee, K. Brezinsky and I. Glassman, A Kinetic Model for the Oxidation of Toluene near 1200 K, *J. Phys. Chem.* 96 (1992), 2151-2161.

[56] L. V. Moskaleva and M. C. Lin, Computational Study of the Kinetics and Mechanisms for the Reaction of H atoms with *c*-C<sub>5</sub>H<sub>6</sub>, *Twenty-Ninth Symposium (International) on Combustion*, *The Combustion Institute* (1) 29 (2002), 1319-1327.

[57] G. B. Bacskay and J. C. Mackie, The Pyrolysis of Cyclopentadiene: Quantum Chemical and Kinetic Modelling Studies of the Acetylene Plus Propyne/Allene Decomposition Channels, *Phys. Chem. Chem. Phys.* 3 (2001), 2467-2473.

[58] N. M. Marinov, W. J. Pitz, C. K. Westbrook, M. J. Castaldi and S. M. Senkan, Modelling of Aromatic and Polycyclic Aromatic Hydrocarbon Formation in Premixed Methane and Ethane Flames, *Combust. Sci. and Tech.* 116-117 (1996), 211-287.

[59] V. V. Kislov and A. M. Mebel, The Formation of Naphthalene, Azulene, and Fulvalene from Cyclic C<sub>5</sub> Species in Combustion: An Ab Initio/RRKM Study of 9-H-Fulvalenyl (C<sub>5</sub>H<sub>5</sub>-C<sub>5</sub>H<sub>4</sub>) Radical Rearrangements, *J. Phys. Chem. A* (38) 111 (2007), 9532-9543.

[60] M. Lu and J. A. Mulholland, Aromatic Hydrocarbon Growth from Indene, *Chemosphere* (5-7) 42 (2001), 625-633.

[61] P. Lindstedt, L. Maurice and M. Meyer, Thermodynamic and Kinetic Issues in the Formation and Oxidation of Aromatic Species, *Faraday Discuss.* 119 (2001), 409-432.

- [62] R. P. Lindstedt and K. A. Rizos, The Formation and Oxidation of Aromatics in Cyclopentene and Methyl-Cyclopentadiene Mixtures, *Twenty-Ninth Symposium (International) on Combustion, The Combustion Institute* 29 (2002), 2291-2298.
- [63] C. S. McEnally and L. Pfefferle, The Use of Carbon-13-Labeled Fuel Dopants For Identifying Naphthalene Formation Pathways in Non-Premixed Flames, *Twenty-Eighth Symposium (International) on Combustion, The Combustion Institute* 28 (2000), 2569-2576.
- [64] J. A. Mulholland, M. Lu and D.-H. Kim, Pyrolytic Growth of Polycyclic Aromatic Hydrocarbons by Cyclopentadienyl Moieties, *Twenty-Eighth Symposium (International) on Combustion, The Combustion Institute* (2) 28 (2000), 2593-2599.
- [65] A. D'Anna and A. Violi, A Kinetic Model for the Formation of Aromatic Hydrocarbons in Premixed Laminar Flames, *Twenty-Seventh Symposium (International) on Combustion, The Combustion Institute* (1) 27 (1998), 425-433.
- [66] A. Violi, A. F. Sarofim and T. N. Truong, Quantum Mechanical Study of Molecular Weight Growth Process by Combination of Aromatic Molecules, *Combust. Flame* (1-2) 126 (2001), 1506-1515.
- [67] A. Violi, A. F. Sarofim and T. N. Truong, Mechanistic Pathways to Explain H/C Ratio of Soot Precursors, *Combust. Sci. and Tech.* (11) 174 (2002), 205 - 222.
- [68] V. V. Kislov and A. M. Mebel, An Ab Initio G3-Type/Statistical Theory Study of the Formation of Indene in Combustion Flames. II. The Pathways Originating from Reactions of Cyclic C5 Species Cyclopentadiene and Cyclopentadienyl Radicals, *J. Phys. Chem. A* (4) 112 (2008), 700-716.
- [69] L. V. Moskaleva, A. M. Mebel and M. C. Lin, The CH<sub>3</sub>+C<sub>5</sub>H<sub>5</sub> Reaction: A Potential Source of Benzene at High Temperatures, *Twenty-Sixth Symposium (International) on Combustion* (1) 26 (1996), 521-526.
- [70] R. P. Lindstedt, V. Markaki and R. Robinson, Oxidation of Two-Ringed Aromatic Species as Models for Soot Surface Reactions, *Proc. of Anacapri*

*Workshop on Fine Carbon Based Particles* (2009), 483-506.

[71] A. Burcat and B. Ruscic, Third Millennium Ideal Gas and Condensed Phase Thermochemical Database for Combustion with Updates from Active Thermochemical Tables, (Techion-IIT, Aerospace Engineering and Argonne National Laboratory, 2005).

[72] K. A. Rizos, Detailed Chemical Kinetic Modelling of Homogeneous Systems, (PhD Thesis, Imperial College of Science, Technology and Medicine, England, UK, 2003).

[73] K. M. Leung and R. P. Lindstedt, Detailed Kinetic Modelling of C1-C2 Alkane Diffusion Flames, *Combust. Flame* 102 (1995), 129-160.

[74] M. B. Colket, R. J. Hall and M. D. Smooke, Mechanistic Models of Soot Formation, In *Final Report on AFOSR Contract.* , (F49620-91-C-0056, 1994).

[75] M. L. Potter, Detailed Chemical Kinetic Modelling of Propulsion Fuels, (PhD Thesis, Imperial College London, 2003).

[76] M. Frenklach and H. Wang, *Detailed Mechanism and Modelling of Soot Particle Formation in Soot Formation in Combustion: Mechanisms and models*, (Springer-Verlag, first edition, 1994).

[77] M. B. Colket and D. J. Seery, Reaction Mechanisms for Toluene Pyrolysis, *Twenty-Fifth Symposium (International) on Combustion* (1) 25 (1994), 883-891.

[78] N. M. Marinov, M. J. Castaldi, C. F. Melius and W. Tsang, Aromatic and Polycyclic Aromatic Hydrocarbon Formation in a Premixed Propane Flame, *Combust. Sci. and Tech.* (1) 128 (1997), 295 - 342.

[79] H. Richter, O. A. Mazyar, R. Sumathi, W. H. Green, J. B. Howard and J. W. Bozzelli, Detailed Kinetic Study of the Growth of Small Polycyclic Aromatic Hydrocarbons. 1. 1-Naphthyl + Ethyne, *J. Phys. Chem. A* 105 (2001), 1561-1573.

- [80] S. D. Klotz, K. Brezinsky and I. Glassman, Modeling the Combustion of Toluene-Butane Blends, *Twenty-Seventh Symposium (International) on Combustion, The Combustion Institute* (1) 27 (1998), 337-344.
- [81] P. Dagaut, G. Pengloan and A. Ristori, Oxidation, Ignition and Combustion of Toluene: Experimental and Detailed Chemical and Kinetic Modelling., *Phys. Chem. Chem. Phys.* 4 (2002), 1846-1854.
- [82] P. Lindstedt and L. Q. Maurice, Detailed Kinetic Modelling of Toluene Combustion, *Combust. Sci. and Tech.* 120 (1996), 119-167.
- [83] R. Sivaramakrishnan, R. S. Tranter and K. Brezinsky, A high pressure model for the oxidation of toluene, *Thirtieth Symposium (International) on Combustion, The Combustion Institute* 30 (2005), 1165-1173.
- [84] W. J. Pitz, R. Seiser, J. W. Bozzelli, I. Da Costa, R. Fournet, F. Billaud, F. Battin-Leclerc, K. Seshadri and C. K. Westbrook, Chemical Kinetic Characterization of Combustion of Toluene, (Lawrence Livermore National Laboratory, 2001).
- [85] K. M. Pamidimukkala, R. D. Kern, M. R. Patel, H. C. Wei and J. H. Kiefer, High-Temperature Pyrolysis of Toluene, *J. Phys. Chem.* 91 (1987), 2148-2154.
- [86] W. Muller-Markgraf and J. Troe, Thermal Decomposition of Ethylbenzene, Styrene, and Bromophenylethane: UV Absorption Study in Shock Waves, *J. Phys. Chem.* 92 (1988), 4914-4922.
- [87] L. D. Brouwer, W. Muller-Markgraf and J. Troe, Thermal Decomposition of Toluene: A comparison of Thermal and Laser-Photochemical Activation Experiments, *J. Phys. Chem.* 92 (1988), 4905-4914.
- [88] H. Hippler and J. Troe, Thermodynamic Properties of Benzyl Radicals: Enthalpy of Formation from Toluene, Benzyl Iodide, and Dibenzyl Dissociation Equilibria, *J. Phys. Chem.* 94 (1990), 3803-3806.

- [89] R. A. Eng, A. Gebert, E. Goos, H. Hippler and C. Kachiani, Incubation Times, Fall-Off and Branching Ratios in the Thermal Decomposition of Toluene: Experiments and Theory, *Phys. Chem. Chem. Phys.* 4 (2002), 3989-3996.
- [90] M. A. Oehlschlaeger, D. F. Davidson and R. K. Hanson, Thermal decomposition of toluene: Overall rate and branching ratio, *Thirty-First Symposium (International) on Combustion, The Combustion Institute* (1) 31 (2007), 211-219.
- [91] J. L. DiNaro, J. B. Howard, W. H. Green, J. W. Tester and J. W. Bozzelli, Elementary Reaction Mechanism for Benzene Oxidation in Supercritical Water, *J. Phys. Chem. A* 104 (2000), 10576-10586.
- [92] T. B. Hunter, T. A. Litzinger, H. Wang and M. Frenklach, Ethane Oxidation at Elevated Pressures in the Intermediate Temperature Regime: Experiments and Modelling, *Combust. Flame* 104 (1996), 505-523.
- [93] R. Zellner and F. Ewig, Computational Study of the  $\text{CH}_3 + \text{O}_2$  Chain Branching Reaction, *J. Phys. Chem.* 92 (1988), 2971-2974.
- [94] S. P. Walch, Characterization of the Potential Energy Surface for  $\text{CH}_3 + \text{O}_2 = \text{Products}$ , *Chem. Phys. Lett.* (1) 215 (1993), 81-86.
- [95] P. Q. Clothier, D. Shen and H. O. Pritchard, Stimulation of Diesel-Fuel Ignition by Benzyl Radicals, *Combust. Flame* 101 (1995), 383-386.
- [96] H. Sun, S. I. Yang, G. Jomaas and C. K. Law, High-Pressure Laminar Flame Speeds and Kinetic Modelling of Carbon Monoxide / Hydrogen Combustion, *Thirty-First Symposium (International) on Combustion, The Combustion Institute* 31 (2007), 439-446.
- [97] D. L. Baulch, C. T. Bowman, C. J. Cobos, R. A. Cox, T. Just, J. A. Kerr, M. J. Pilling, D. Stocker, J. Troe, W. Tsang, R. W. Walker and J. Warnatzota, Evaluated Kinetic Data for Combustion Modelling: Supplement II, *J. Phys. Chem. Ref. Data* (3) 34 (2005), 757-1397.



- [98] J. Li, Z. Zhao, A. Kazakov and F. L. Dryer, An Updated Comprehensive Kinetic Model of Hydrogen Combustion, *Int. J. Chem. Kinet.* (10) 36 (2004), 566-575.
- [99] J. W. Sutherland, J. V. Michael, A. N. Pirraglia, F. L. Nesbitt and R. B. Klemm, Rate Constant for the Reaction of O(3P) with H<sub>2</sub> by the Flash Photolysis--Shock Tube and Flash Photolysis--Resonance Fluorescence Techniques; 504K<T<2495K, *Symposium (International) on Combustion* (1) 21 (1986), 929-941.
- [100] K. Gkagkas and R. P. Lindstedt, The Impact of Reduced Chemistry on Auto-ignition of H<sub>2</sub> in Turbulent Flows, *Combust. Theor. Model.* (4) 13 (2009), 607-643.
- [101] D. L. Baulch, C. J. Cobos, R. A. Cox, C. Esser, P. Frank, T. Just, J. A. Kerr, M. J. Pilling, J. Troe, R. W. Walker and J. Warnatz, Evaluated Kinetic Data for Combustion Modelling, *J. Phys. Chem. Ref. Data* (3) 21 (1992), 411-734.
- [102] C. L. Yu, M. Frenklach, D. A. Masten, R. K. Hanson and C. T. Bowman, Reexamination of Shock-Tube Measurements of the Rate Coefficient of H + O<sub>2</sub> = OH + O, *The Journal of Physical Chemistry* (17) 98 (1994), 4770-4771.
- [103] W. J. Pitz, R. Seiser, J. W. Bozzelli, D. C. I., R. Fournet, F. Billaud, F. Battin-Leclerc, K. Seshadri and C. K. Westbrook, *Second Joint Meeting, US Sections of the Combustion Institute Paper* 253 (2001).
- [104] K. Luther, J. Troe and K. M. Weitzel, Carbon-Carbon and Carbon-Hydrogen Bond Splits of Laser-Excited Aromatic Molecules. 2. In Situ Measurements of Branching Ratios, *J. Phys. Chem.* (16) 94 (1990), 6316-6320.
- [105] P. Frank, J. Herzler, T. Just and C. Wahl, High-Temperature Reactions of Phenyl Oxidation, *Twenty-Fifth Symposium (International) on Combustion, The Combustion Institute* (1) 25 (1994), 833-840.
- [106] K. Brezinsky, G. T. Linteris, T. A. Litzinger and I. Glassman, High Temperature Oxidation of N-Alkyl Benzenes, *Twenty-first Symposium*

(*International*) on Combustion, *The Combustion Institute* (1) 21 (1986), 833-840.

[107] T. A. Litzinger, K. Brezinsky and I. Glassman, Gas-Phase Oxidation of Isopropylbenzene at High Temperature, *J. Phys. Chem.* (3) 90 (1986), 508-513.

[108] T. A. Litzinger, K. Brezinsky and I. Glassman, The Oxidation of Ethylbenzene Near 1060K, *Combust. Flame* (1-2) 63 (1986), 251-267.

[109] T. A. Litzinger, K. Brezinsky and I. Glassman, Reactions of N-Propylbenzene During Gas Phase Oxidation, *Combust. Sci. and Tech.* (1) 50 (1986), 117-133.

[110] A. Roubaud, R. Minetti and L. R. Sochet, Oxidation and Combustion of Low Alkylbenzenes at High Pressure: Comparative Reactivity and Auto-ignition, *Combust. Flame* (3) 121 (2000), 535-541.

[111] F. H. Seubold, The Rearrangement of the Neophyl Radical, *J.A.C.S.* (10) 75 (1953), 2532-2533.

[112] L. Q. Maurice, Detailed Chemical Kinetic Models for Aviation Fuels, (PhD Thesis, Imperial College of Science, Technology and Medicine, England, UK, 1996).

[113] W. Tsang, Chemical Kinetic Data Base for Combustion Chemistry. Part 3. Propane, *J. Phys. Chem. Ref. Data* 17 (1988), 887-951.

[114] P. Dagaut, Computational Fluid Dynamics for Combustion. Final Report on Chemical Delay Measurements. Project No: GRD1-1999-10325, (2001).

[115] C. Ellis, M. S. Scott and R. W. Walker, Addition of Toluene and Ethylbenzene to Mixtures of H<sub>2</sub> and O<sub>2</sub> at 772 K: Part 2: Formation of Products and Determination of Kinetic Data for H<sup>+</sup> additive and for other Elementary Reactions Involved, *Combust. Flame* (3) 132 (2003), 291-304.

[116] D. Robaugh, W. Tsang, A. Fahr and S. E. Stein, Ethylbenzene Pyrolysis:

Benzyl C-C or C-H Bond Homolysis, *Ber. Bunsenges. Phys. Chemistry* 90 (1986), 77.

[117] H. Eberius, P. Frank and C. Wahl, Computational Fluid Dynamics For Combustion, (DLR Institute for Combustion Technology, Stuttgart, 2001).

[118] A. Hoffman, M. Klatt and H. G. Wagner, An Investigation of the Reaction Between O(3P) and Toluene at High Temperatures, *Z. Phys. Chem ( Neue Folge)* 168 (1990), 1-12.

[119] H. Wang and M. Frenklach, A Detailed Kinetic Modelling Study of Aromatics Formation in Laminar Premixed Acetylene and Ethylene Flames, *Combust. Flame* 110 (1997), 173-221.

[120] J. A. Miller and C. F. Melius, Kinetic and Thermodynamic Issues in the Formation of Aromatic Compounds in Flames of Aliphatic Fuels, *Combust. Flame* (1) 91 (1992), 21-39.

[121] P. Dagaut and M. Cathonnet, A Comparative Study of the Kinetics of Benzene Formation from Unsaturated C2 to C4 Hydrocarbons, *Combust. Flame* (4) 113 (1998), 620-623.

[122] H. Richter and J. B. Howard, Formation of Polycyclic Aromatic Hydrocarbons and their Growth to Soot - A Review of Chemical Reaction Pathways, *Prog. Energy Combust. Sci.* 26 (2000), 565-608.

[123] F. C. Stehling, J. D. Frazee and R. C. Anderson, Carbon Formation from Acetylene, *Sixth Symposium (International) on Combustion, The Combustion Institute* (1) 6 (1957), 247-254.

[124] M. J. Castaldi, N. M. Marinov, C. F. Melius, J. Huang, S. M. Senkan, W. J. Pit and C. K. Westbrook, Experimental and Modeling Investigation of Aromatic and Polycyclic Aromatic Hydrocarbon Formation in a Premixed Ethylene Flame, *Twenty-Sixth Symposium (International) on Combustion, The Combustion Institute* (1) 26 (1996), 693-702.

- [125] A. M. Dean, Detailed Kinetic Modelling of Autocatalysis in Methane Pyrolysis, *J. Phys. Chem.* 94 (1990), 1432-1439.
- [126] N. M. Marinov, W. J. Pitz, C. K. Westbrook, A. M. Vincitore, M. J. Castaldi, S. M. Senkan and C. F. Melius, Aromatic and Polycyclic Aromatic Hydrocarbon Formation in a Laminar Premixed n-Butane Flame, *Combust. Flame* 114 (1998), 192-213.
- [127] H. Richter, W. J. Grieco and J. B. Howard, Formation Mechanism of Polycyclic Aromatic Hydrocarbons and Fullerenes in Premixed Benzene Flames, *Combust. Flame* 119 (1999), 1-22.
- [128] A. Ristori, P. Dagaut, A. E. Bakali, G. Pengloan and M. Cathonnet, Benzene Oxidation: Experimental Results in a JDR and Comprehensive Kinetic Modelling in JSR, Shock-Tube and Flame, *Combust. Sci. and Tech.* 167 (2001), 223-256.
- [129] U. Pfahl, K. Fieweger and G. Adomeit, Self-Ignition of Diesel-Relevant Hydrocarbon-air Mixtures Under Engine Conditions, *Twenty-Sixth Symposium (International) on Combustion, The Combustion Institute* 26 (1996), 781-789.
- [130] H. Pitsch, Detailed Kinetic Reaction Mechanism For Ignition and Oxidation of  $\alpha$ -Methylnaphthalene, *Twenty-Sixth Symposium (International) on Combustion, The Combustion Institute* 26 (1996), 721-728.
- [131] A. Laskin and A. Lifshitz, Thermal Decomposition of Indene. Experimental Results and Kinetic Modelling, *Twenty-Seventh Symposium (International) on Combustion, The Combustion Institute* 27 (1998), 313-320.
- [132] R. Atkinson, D. L. Baulch, R. A. Cox, R. F. Hampson, J. A. Kerr, M. J. Rossi and J. Troe, Evaluated Kinetic and Photochemical and Heterogeneous Data for Atmospheric Chemistry: Supplement V - IUPAC Subcommittee on Gas Kinetic Data Evaluation for Atmospheric Chemistry, *J. Phys. Chem. Ref. Data* (3) 26 (1997), 521-1011.
- [133] R. P. Lindstedt and G. Skevis, A Study of Acetylene Chemistry in Flames,

*Combust. Sci. and Tech.* (1) 125 (1997), 73 - 137.

[134] A. J. Dean, D. F. Davidson and R. K. Hanson, A Shock Tube Study of Reactions of Carbon Atoms with Hydrogen and Oxygen Using Excimer Photolysis of C<sub>3</sub>O<sub>2</sub> and Carbon Atom Atomic Resonance Absorption Spectroscopy, *J. Phys. Chem.* (1) 95 (1991), 183-191.

[135] M. W. Slack, Kinetics and Thermodynamics of the CN Molecule. III. Shock Tube Measurement of CN Dissociation Rates, *J. Chem. Phys.* (1) 64 (1976), 228-236.

[136] R. P. Lindstedt and G. Skevis, Molecular Growth and Oxygenated Species Formation in Laminar Flames, *Twenty-Eighth Symposium (International) on Combustion, The Combustion Institute* 28 (2000), 1801-1807.

[137] T. Bohland and F. Temps, Direct Determination of the Rate Constant for the Reaction CH<sub>2</sub> + H = CH + H<sub>2</sub>, *Ber. Bunsenges. Phys. Chem.* 88 (1984), 459-461.

[138] J. Peeters, W. Boullart and K. Devriendt, CH(a<sup>4</sup>.SIGMA.- and/or X<sup>2</sup>.PI.) Formation in the Reaction Between Ketenyl Radicals and Oxygen Atoms. Determination of the CH-yield between 405 and 960 K, *J. Phys. Chem.* (11) 99 (1995), 3583-3591.

[139] C. Dombrowsky and H. G. Wagner, Investigation of the CH<sub>2</sub>(T) + O<sub>2</sub> Reaction in Shock Waves, *Ber. Bunsenges. Phys. Chem.* 96 (1992), 1048-1055.

[140] D. L. Baulch, C. J. Cobos, R. A. Cox, P. Frank, G. Hayman, T. Just, J. A. Kerr, T. Murrells, M. J. Pilling, J. Troe, R. W. Walker and J. Warnatz, Evaluated Kinetic Data for Combustion Modelling Supplement I, *J. Phys. Chem. Ref. Data* (6) 23 (1994), 847-1033.

[141] C. L. Yu, C. Wang and M. Frenklach, Chemical Kinetics of Methyl Oxidation by Molecular Oxygen, *J. Phys. Chem.* 99 (1995), 14377-14387.

[142] R. I. Quiceno, J. PÈrez-RamÈrez, J. r. Warnatz and O. Deutschmann,

Modeling the High-Temperature Catalytic Partial Oxidation of Methane over Platinum Gauze: Detailed Gas-Phase and Surface Chemistries Coupled with 3D Flow Field Simulations, *Appl. Catal. A-Gen* (2) 303 (2006), 166-176.

[143] M. J. Rabinowitz, J. W. Sutherland, P. M. Patterson and R. B. Klemm, Direct Rate Constant Measurements OF  $H + CH_4 = CH_3 + H_2$  at 897-1729 K, Using the Flash Photolysis-Shock Tube Technique, *J. Phys. Chem.* (2) 95 (1991), 674-681.

[144] C. C. Hsu, A. M. Mebel and M. C. Lin, Ab Initio Molecular Orbital Study of the HCO+O Reaction: Direct versus Indirect Abstraction Channels, *J. Chem. Phys.* (6) 105 (1996), 2346-2352.

[145] Y. Hidaka, T. Oki, H. Kawano and T. Higashihara, Thermal Decomposition of Methanol in Shock Waves, *J. Phys. Chem.* (20) 93 (1989), 7134-7139.

[146] T. J. Held and F. L. Dryer, An Experimental and Computational Study of Methanol Oxidation in the Intermediate-and High-Temperature Regimes, *Twenty-Fifth Symposium (International) on Combustion* (1) 25 (1994), 901-908.

[147] W. Tsang and V. Mokrushin, Mechanism and Rate Constants for 1,3-Butadiene Decomposition, *Twenty-Eighth Symposium (International) on Combustion, The Combustion Institute* (2) 28 (2000), 1717-1723.

[148] I. A. B. Reid, C. Robinson and D. B. Smith, Spontaneous Ignition of Methane: Measurement and Chemical Model, *Twentieth Symposium (International) on Combustion, The Combustion Institute* (1) 20 (1985), 1833-1843.

[149] P. D. Lightfoot, R. A. Cox, J. N. Crowley, M. Destriau, G. D. Hayman, M. E. Jenkin, G. K. Moortgat and F. Zabel, Organic Peroxy Radicals: Kinetics, Spectroscopy and Tropospheric Chemistry, *Atmos. Environ. Part A* (10) 26 (1992), 1805-1961.

[150] W. Tsang and R. F. Hampson, Chemical Kinetic Data Base for Combustion Chemistry. Part I, Methane and Related Compounds, *J. Phys. Chem. Ref. Data* (3)

15 (1986), 1087-1280.

[151] A. R. Fairbairn, The Dissociation of Carbon Monoxide, *Proc. Roy. Soc. London A* 312 (1969), 207-227.

[152] S. L. Baughcum and R. C. Oldenborg, Measurement of the  $C_2(a^3\Pi)$  and  $C_2(x^1\Sigma_g^+)$  Disappearance Rates with  $O_2$  from 298-1300K, *The Chemistry of Combustion Processes, ACS Symp. Ser. (Ed. T.M. Sloane)* 249 (1984), 257-266.

[153] A. Laskin and H. Wang, On Initiation Reactions of Acetylene Oxidation in Shock Tubes A Quantum Mechanical and Kinetic Modelling Study, *Chem. Phys. Lett.* 303 (1999), 43-49.

[154] B. Eiteneer and M. Frenklach, Experimental and Modeling Study of Shock-Tube Oxidation of Acetylene, *Int. J. Chem. Kinet.* (9) 35 (2003), 391-414.

[155] A. M. Dean and P. R. Westmoreland, Bimolecular QRRK Analysis of Methyl Radical Reactions, *Int. J. Chem. Kinet.* (3) 19 (1987), 207-228.

[156] S. G. Davis, C. K. Law and H. Wang, Propene Pyrolysis and Oxidation Kinetics in a Flow Reactor and Laminar Flames, *Combust. Flame* 119 (1999), 375-399.

[157] H. Wang and M. Frenklach, Calculations of Rate Coefficients for the Chemically Activated Reactions of Acetylene with Vinylic and Aromatic Radicals, *J. Phys. Chem.* 98 (1994), 11465-11489.

[158] R. P. Duran, V. T. Amorebieta and A. J. Colussi, Is the Homogeneous Thermal Dimerization of Acetylene a Free-Radical Chain Reaction? Kinetic and Thermochemical Analysis, *J. Phys. Chem.* (3) 92 (1988), 636-640.

[159] V. D. Knyazev, A. Bencsura, S. I. Stoliarov and I. R. Slagle, Kinetics of the  $C_2H_3 + H_2 = H + C_2H_4$  and  $CH_3 + H_2 = H + CH_4$  Reactions, *J. Phys. Chem.* (27) 100 (1996), 11346-11354.

- [160] T. B. Hunters, T. A. Litzinger, H. Wang and M. Frenklach, Ethane Oxidation at Elevated Pressures in the Intermediate Temperature Regime: Experiments and Modelling, *Combust. Flame* 104 (1996), 505-523.
- [161] Y. Hidaka, T. Nishimori, K. Sato, Y. Henmi, R. Okuda and K. Inami, Shock-Tube and Modelling Study of Ethylene Pyrolysis and Oxidation, *Combust. Flame* 117 (1999), 755-776.
- [162] M. Frenklach, H. Wang and M. J. Rabinowitz, Optimization and Analysis of Large Chemical Kinetic Mechanisms Using the Solution Mapping Method-Combustion of Methane, *Prog. Energy Combust. Sci.* (1) 18 (1992), 47-73.
- [163] H.-H. Carstensen, C. V. Naik and A. M. Dean, Detailed Modelling of the Reaction of C<sub>2</sub>H<sub>5</sub> + O<sub>2</sub>, *J. Phys. Chem. A* 109 (2005), 2264-2281.
- [164] E. V. Shafir, I. R. Slagle and V. D. Knyazev, Kinetics of the Self-Reaction of C<sub>2</sub>H<sub>5</sub> Radicals, *J. Phys. Chem. A* (35) 107 (2003), 6804-6813.
- [165] S. J. Klippenstein, J. A. Miller and L. B. Harding, Resolving the Mystery of Prompt CO<sub>2</sub>: The HCCO + O<sub>2</sub> Reaction, *Twenty-Ninth Symposium (International) on Combustion, The Combustion Institute* 29 (2002), 1209-1217.
- [166] Y. Hidaka, K. Kimura and H. Kawano, High-Temperature Pyrolysis of Ketene in Shock Waves, *Combust. Flame* (1) 99 (1994), 18-28.
- [167] J. Warnatz, *Combustion Chemistry*, (Springer-Verlag, 1984).
- [168] C. E. Canosa-Mas, H. M. Frey and R. Walsh, Studies of Methylene Chemistry by Pulsed Laser-Induced Decomposition of ketene, *J. Chem. Soc. Faraday Trans 2* 80 (1984), 561-578.
- [169] P. R. Westmoreland, A. M. Dean, J. B. Howard and J. P. Longwell, Forming Benzene in Flames by Chemically Activated Isomerization, *J. Phys. Chem.* (25) 93 (1989), 8171-8180.



- [170] P. Dagaut, M. Cathonnet and J.-C. Boettner, A Kinetic Modeling Study of Propene Oxidation in JSR and Flame, *Combust. Sci. and Tech.* (4) 83 (1992), 167 - 185.
- [171] C. Horn, K. Roy, P. Frank and T. Just, Shock-Tube Study on the High Temperature Pyrolysis of Phenol, *Twenty-Seventh Symposium (International) on Combustion, The Combustion Institute* 27 (1998), 321-328.
- [172] W. Tsang, Chemical Kinetic Data Base for Combustion Chemistry Part V. Propene, *J. Phys. Chem. Ref. Data* (2) 20 (1991), 221-273.
- [173] P. Dagaut and M. Cathonnet, Isobutene Oxidation and Ignition: Experimental and Detailed Kinetic Modeling Study, *Combust. Sci. and Tech.* (1) 137 (1988), 237 - 275.
- [174] W. J. Pitz, C. K. Westbrook, W. M. Proscia and F. L. Dryer, A comprehensive Chemical Kinetic Reaction Mechanism for the Oxidation of N-Butane, *Twentieth Symposium (International) on Combustion, The Combustion Institute* (1) 20 (1985), 831-843.
- [175] Y. Hidaka, T. Nakamura, H. Tanaka, A. Jinno and H. Kawano, Shock Tube and Modelling Study of Propene Pyrolysis, *Int. J. Chem. Kinet.* (9) 24 (1992), 761-780.
- [176] R. D. Wilk, N. P. Cernansky, W. J. Pitz and C. K. Westbrook, Propene Oxidation at Low and Intermediate Temperatures: A Detailed Chemical Kinetic Study, *Combust. Flame* (2) 77 (1989), 145-170.
- [177] A. Bencsura, V. D. Knyazev, S.-B. Xing, I. R. Slagle and D. Gutman, Kinetics of the Thermal Decomposition of the N-Propyl Radical, *Twenty-Fourth Symposium (International) on Combustion, The Combustion Institute* (1) 24 (1992), 629-635.
- [178] D. L. Baulch, C. J. Cobos, R. A. Cox, P. Frank, G. Hayman, T. Just, J. A. Kerr, T. Murrells, M. J. Pilling, J. Troe, R. W. Walker and J. Warnatz, Summary

Table of Evaluated Kinetic Data for Combustion Modeling: Supplement 1, *Combust. Flame* (1-2) 98 (1994), 59-79.

[179] S. W. Benson, The Kinetics and Thermochemistry of Chemical Oxidation with Application to Combustion and Flames, *Prog. Energy Combust. Sci.* (2) 7 (1981), 125-134.

[180] R. D. Wilk, N. P. Cernansky and R. S. Cohen, The Oxidation of Propane at Low and Transition Temperatures, *Combust. Sci. and Tech.* 49 (1986), 41-78.

[181] K. H. Homann, Reaktionen des Butadiins ii. Die Reaction mit Sauerstoffatomen., *Ber. Bunsenges. Phys. Chem.* 79 (1975), 536-540.

[182] A. Laskin, H. Wang and C. K. Law, Detailed Kinetic Modeling of 1,3-Butadiene Oxidation at High Temperatures, *Int. J. Chem. Kinet.* (10) 32 (2000), 589-614.

[183] R. D. Kern, H. J. Singh and C. H. Wu, Thermal Decomposition of 1,2-Butadiene, *Int. J. Chem. Kinet.* (9) 20 (1988), 731-747.

[184] J. A. Cole, J. D. Bittner, J. P. Longwell and J. B. Howard, Formation Mechanisms of Aromatic Compounds in Aliphatic Flames, *Combust. Flame* (1) 56 (1984), 51-70.

[185] Y. Hidaka, T. Higashihara, N. Ninomiya, H. Oshita and H. Kawano, Thermal Isomerization and Decomposition of 2-Butyne in Shock Waves, *J. Phys. Chem.* (42) 97 (1993), 10977-10983.

[186] P. Dagaut and M. Cathonnet, The Oxidation of 1,3-Butadiene: Experimental Results and Kinetic Modeling, *Combust. Sci. and Tech.* (1) 140 (1998), 225 - 257.

[187] A. Chakir, M. Cathonnet, J. C. Boettner and F. Gaillard, Kinetic Study of N-Butane oxidation, *Combust. Sci. and Tech.* (4) 65 (1989), 207 - 230.

[188] W. Tsang, Pyrolysis of 2,4-Dimethylhexene-1 and the Stability of Isobutenyl

Radicals, *Int. J. Chem. Kinet.* (6) 5 (1973), 929-946.

[189] J. Gang, M. J. Pilling and S. H. Robertson, Asymmetric Internal Rotation: Application to the 2-C<sub>4</sub>H<sub>9</sub>CH<sub>3</sub>+C<sub>3</sub>H<sub>6</sub> Reaction, *J. Chem. Soc. Faraday Trans.* 93 (1997), 1481-1491.

[190] R. R. Baker, R. R. Baldwin, A. R. Fuller and R. W. Walker, Addition of n-C<sub>4</sub>H<sub>10</sub> and C<sub>4</sub>H<sub>8</sub> to Slowly Reacting Mixtures of Hydrogen and Oxygen at 480°C, *Faraday Discuss.* 71 (1975), 736-755.

[191] J. A. Kerr and A. F. Trotman-Dickenson, The Reactions of Alkyl Radicals. Part III. n-Butyl Radicals from the Photolysis of n-Valeraldehyde, *J. Chem. Soc.* (1960), 1602-1608.

[192] W. Tsang, Chemical Kinetic Data Base for Combustion Chemistry Part 4. Isobutane, *J. Phys. Chem. Ref. Data* (1) 19 (1990), 1-68.

[193] W. J. Pitz and C. K. Westbrook, Chemical Kinetics of the High Pressure Oxidation of n-Butane and its Relation to Engine Knock, *Combust. Flame* (1-2) 63 (1986), 113-133.

[194] S. Kojima, Detailed Modeling of n-Butane Autoignition Chemistry, *Combust. Flame* (1) 99 (1994), 87-136.

[195] A. C. Lloyd, Evaluated and Estimated Kinetic Data for Phase Reactions of the Hydroperoxyl Radical, *Int. J. Chem. Kinet.* (2) 6 (1974), 169-228.

[196] M. U. Alzueta, P. Glarborg and K. Dam-Johansen, Experimental and Kinetic Modelling Study of the Oxidation of Benzene, *Int. J. Chem. Kinet.* (8) 32 (2000), 498-522.

[197] J. S. Gaffney, R. Atkinson and J. N. Pitts, Temperature Dependence of the Relative Rate Constants for the Reaction of O(3P) Atoms with Selected Olefins, Monoterpenes and Unsaturated Aldehydes, *J. Am. Chem. Soc.* 97 (1975), 6481-6483.

- [198] A. Fahr and S. E. Stein, Reactions of Vinyl and Phenyl Radicals with Ethyne, Ethene and Benzene *Twenty-Second Symposium (International) on Combustion, The Combustion Institute 22* (1989), 1023-1029.
- [199] E. Ikeda, R. S. Tranter, J. H. Kiefer, R. D. Kern, H. J. Singh and Q. Zhang, The Pyrolysis of Methylcyclopentadiene: Isomerization and Formation of Aromatics, *Twenty-Eighth Symposium (International) on Combustion, The Combustion Institute 28* (2000), 1725-1732.
- [200] H. Richter and J. B. Howard, Formation and Consumption of Single-Ring Aromatic Hydrocarbons and Their Precursors in Premixed Acetylene, Ethylene and Benzene Flames, *Phys. Chem. Chem. Phys.* 4 (2002), 2038-2055.
- [201] M. Braun-Unkhoff, P. Frank and T. Just, High Temperature Reactions of Benzyl Radicals, *Ber. Bunsenges. Phys. Chem.* 94 (1990), 1417-1425.
- [202] H. Hippler, C. Reihls and J. Troe, Shock Tube UV Absorption Study of the Oxidation of Benzyl Radicals, *Twenty-Third Symposium (International) on Combustion, The Combustion Institute (1) 23* (1991), 37-43.
- [203] A. Fahr and S. E. Stein, Gas-Phase Reactions of Phenyl Radicals with Aromatic Molecules, *J. Phys. Chem.* (17) 92 (1988), 4951-4955.
- [204] M. A. Grela and A. J. Colussi, Kinetics and Mechanism of the Thermal Decomposition of Unsaturated Aldehydes: Benzaldehyde, 2-Butenal, and 2-Furaldehyde, *J. Phys. Chem.* (3) 90 (1986), 434-437.
- [205] Y. Z. He, W. G. Mallard and W. Tsang, Kinetics of Hydrogen and Hydroxyl Radical Attack on Phenol at High Temperatures, *J. Phys. Chem.* 92 (1988), 2196-2201.
- [206] R. K. Solly and S. W. Benson, Kinetics of the Gas-Phase Unimolecular Decomposition of the Benzoyl Radical, *J. Am. Chem. Soc.* (9) 93 (1971), 2127-2131.

- [207] R. Buth, K. Hoyer mann and G. Rohde, Mechanisms and Rates of Benzoyl Reactions: The Reactions  $C_6H_5CHO+Cl$ ,  $C_6H_5CO+O$ , and  $C_6H_5CO+H$ , *Twenty-Fourth Symposium (International) on Combustion, The Combustion Institute* (1) 24 (1992), 669-674.
- [208] I. W. C. E. Arends, R. Louw and P. Mulder, Kinetic Study of the Thermolysis of Anisole in a Hydrogen Atmosphere, *J. Phys. Chem.* 97 (1993), 7914-7925.
- [209] M. Koch, F. Temps, R. Wagener and H. G. Wagner, Kinetics of the Reactions of  $CH_2(a-1A_1)$  with  $CH_3C_2H$ ,  $HCN$ ,  $CO_2$ ,  $N_2O$  and  $COS$ , *Ber. Bunsenges. Phys. Chem.* 94 (1990), 645.
- [210] R. A. Perry, R. Atkinson and J. N. Pitts, Kinetics and Mechanism of the Gas Phase Reaction of Hydroxyl Radicals with Methoxybenzene and o-Cresol over the Temperature Range 299-435 K, *J. Phys. Chem.* (17) 81 (1977), 1607-1611.
- [211] M. F. R. Mulcahy, B. G. Tucker, D. J. Williams and J. R. Wilmshurst, Reactions of Free Radicals with Aromatic Compounds in the Gaseous Phase, *Aust. J. Chem.* 20 (1967), 1155-1171.
- [212] M. Eichholtz, A. Schneider, D. V. Stucken, J. T. Vollmer and H. G. Wagner, The Reactions of Phenylacetylene With  $O(3)$  in the Gas Phase, *Twenty-Fifth Symposium (International) on Combustion, The Combustion Institute* 25 (1994), 859-866.
- [213] C. K. Westbrook, J. r. Warnatz and W. J. Pitz, A Detailed Chemical Kinetic Reaction Mechanism for the Oxidation of Iso-Octane and n-Heptane over an Extended Temperature Range and its Application to Analysis of Engine Knock, *Twenty-Second Symposium (International) on Combustion, The Combustion Institute* (1) 22 (1989), 893-901.
- [214] W. Tsang, Thermal Decomposition of Cyclopentane and Related Compounds, *Int. J. Chem. Kinet.* (6) 10 (1978), 599-617.

- [215] A. Chakir, M. Bellimam, J. C. Boettner and M. Cathonnet, Kinetic Study of n-Heptane Oxidation, *Int. J. Chem. Kinet.* (4) 24 (1992), 385-410.
- [216] W. Tsang and J. A. Walker, Hydrogen-Atom Attack on 1-Phenylpropene at High Temperatures, *Twenty-Fifth Symposium (International) on Combustion, The Combustion Institute* (1) 25 (1994), 867-874.
- [217] N. Cohen, Are Reaction Rate Coefficients Additive? Revised Transition State Theory Calculations for OH + Alkane Reactions, *Int. J. Chem. Kinet.* (5) 23 (1991), 397-417.
- [218] L. V. Gurvich, I. V. Veyts and C. B. Alcock, Thermodynamic Properties of Individual Substances, In *4th Ed.*, (Begel House, New York, 1996).
- [219] R. O. Foelsche, J. M. Keen and W. C. Solomon, A Non-Equilibrium Computational Method for Predicting Fuel Rich Gas Generator Performance and Exhaust Properties Volume II: Reaction Kinetics and Computational Results, (University of Illinois, 1993).
- [220] A. Burcat and B. J. McBride, Ideal Gas Thermodynamic Data for Combustion and Air Pollution Use, (TAE697, 1994).
- [221] A. Burcat, R. C. Farmer, R. L. Espinoza and R. A. Matula, Comparative Ignition Delay Times For Selected Ring-Structured Hydrocarbons, *Combust. Flame* 36 (1979), 313-316.
- [222] B. R. Stanmore, J. F. Brilhac and P. Gilot, The Oxidation of Soot: A Review of Experiments, Mechanisms and Models, *Carbon* (15) 39 (2001), 2247-2268.

## Appendix A

### Reaction Mechanisms

The detailed chemical reaction mechanism that was developed and utilized in the present work is shown in Table A.1. Reaction rates are expressed in the form:

$$k = AT^n \exp(-E_a / RT) \quad (\text{A.1})$$

where A = frequency factor, (kmol/m<sup>3</sup>)<sup>(1-m)</sup>/s, m is the order of the reaction

n = temperature dependence exponent

E<sub>a</sub> = activation energy, kJ/mole

R = ideal gas constant, 8.314 kJ/K/kmol

T = temperature, K

Unimolecular and recombination reactions generally exhibit complex pressure dependence. Troe [12] proposed a generalised expression for the fall-off behaviour of such reactions:

$$k = \frac{k_o k_\infty [M]}{k_o [M] + k_\infty} F \quad (\text{A.2})$$

where k<sub>∞</sub> is the high pressure limit rate constant, k<sub>o</sub> is the low pressure limit, [M] is the concentration of the third body collision partner and F is the broadening factor which is defined as :

$$\log F = \frac{\log F_c}{1 + \left\{ \log(k_o [M] / k_\infty) / N \right\}^2} \quad (\text{A.3})$$

where  $N = 0.75 - 1.27 \log F_c \quad (\text{A.4})$

and F<sub>c</sub> is a temperature dependent parameter specifically defined for a particular reaction. The reaction mechanism follows.

**TABLE A.1**  
**Elementary reactions**  
 (units are kmole, m<sup>3</sup>, s, K and kJ/mole)

No	Reaction	A	n	Ea	Ref
1	H + O <sub>2</sub> = OH + O	3.5500E+12	-0.41	69.50	[98]
2	O + H <sub>2</sub> = OH + H	5.1200E+01	2.67	26.30	[98]
3	OH + H <sub>2</sub> = H <sub>2</sub> O + H	1.0000E+05	1.60	13.80	[73]
4	OH + OH = H <sub>2</sub> O + O	3.5700E+01	2.40	-8.84	[73]
5	O <sub>2</sub> + H = HO <sub>2</sub> <sup>a,1</sup>	k <sub>∞</sub> = 4.6500E+09 k <sub>0</sub> = 2.6500E+13	0.40 -1.30	0.00 0.00	[96]
6	O <sub>2</sub> + H = HO <sub>2</sub> <sup>b,2</sup>	k <sub>∞</sub> = 4.6500E+09 k <sub>0</sub> = 3.6300E+13	0.40 -1.00	0.00 0.00	[96]
7	O <sub>2</sub> + H = HO <sub>2</sub> <sup>c,3</sup>	k <sub>∞</sub> = 4.6500E+09 k <sub>0</sub> = 6.8900E+12	0.40 -1.20	0.00 0.00	[96]
8	O <sub>2</sub> + H = HO <sub>2</sub> <sup>d,3</sup>	k <sub>∞</sub> = 4.6500E+09 k <sub>0</sub> = 6.8900E+12	0.40 -1.20	0.00 0.00	[96]
9	HO <sub>2</sub> + H = OH + OH	6.0000E+10	0.00	1.23	[96]
10	HO <sub>2</sub> + H = H <sub>2</sub> + O <sub>2</sub>	1.6600E+10	0.00	3.43	[73]
11	HO <sub>2</sub> + OH = H <sub>2</sub> O + O <sub>2</sub>	2.8900E+10	0.00	-2.08	[73]
12	HO <sub>2</sub> + H = H <sub>2</sub> O + O	3.0000E+10	0.00	7.20	[73]
13	HO <sub>2</sub> + O = OH + O <sub>2</sub>	3.1900E+10	0.00	0.00	[73]
14	HO <sub>2</sub> + HO <sub>2</sub> = H <sub>2</sub> O <sub>2</sub> + O <sub>2</sub>	1.8600E+09	0.00	6.44	[73]
15	H <sub>2</sub> O <sub>2</sub> + H = H <sub>2</sub> O + OH	1.0000E+10	0.00	15.00	[73]
16	H <sub>2</sub> O <sub>2</sub> + H = HO <sub>2</sub> + H <sub>2</sub>	4.8200E+10	0.00	33.27	[73]
17	H <sub>2</sub> O <sub>2</sub> + O = HO <sub>2</sub> + OH	6.6000E+08	0.00	16.60	[73]
18	H <sub>2</sub> O <sub>2</sub> + OH = H <sub>2</sub> O + HO <sub>2</sub>	1.7500E+09	0.00	1.33	[132]
19	H <sub>2</sub> O <sub>2</sub> = OH + OH <sup>e,4</sup>	k <sub>∞</sub> = 2.9500E+14 k <sub>0</sub> = 1.2000E+14	0.00 0.00	202.64 190.37	[98]
20	H + H + M = H <sub>2</sub> + M <sup>f</sup>	6.5300E+11	-1.00	0.00	[73]
21	H + H + M = H <sub>2</sub> + M <sup>g</sup>	9.2000E+10	-0.60	0.00	[73]
22	H + H + M = H <sub>2</sub> + M <sup>h</sup>	6.0000E+13	-1.25	0.00	[73]
23	H + H + M = H <sub>2</sub> + M <sup>i</sup>	5.4900E+14	-2.00	0.00	[73]
24	H + OH + M = H <sub>2</sub> O + M <sup>j</sup>	2.2000E+16	-2.00	0.00	[73]
25	O + O + M = O <sub>2</sub> + M <sup>k</sup>	1.0000E+11	-1.00	0.00	[73]
26	C <sub>1</sub> + OH = CO + H	5.0000E+10	0.00	0.00	[133]
27	C <sub>1</sub> + O <sub>2</sub> = CO + O	1.2000E+11	0.00	16.71	[134]
28	C <sub>1</sub> + C <sub>1</sub> + M = C <sub>2</sub> + M	1.8000E+15	-1.60	0.00	[135]
29	CH + M = C <sub>1</sub> + H + M	1.0000E+11	0.00	267.65	[136]



No	Reaction	A	n	Ea	Ref
30	$\text{CH} + \text{H} = \text{C}_1 + \text{H}_2$	3.0000E+10	0.00	0.00	[72]
31	$\text{CH} + \text{O} = \text{CO} + \text{H}$	4.0000E+10	0.00	0.00	[73]
32	$\text{CH} + \text{OH} = \text{C}_1 + \text{H}_2\text{O}$	4.0000E+04	2.00	12.55	[133]
33	$\text{CH} + \text{OH} = \text{CHO} + \text{H}$	3.0000E+10	0.00	0.00	[73]
34	$\text{CH} + \text{O}_2 = \text{CHO} + \text{O}$	7.5000E+10	0.00	0.00	[133]
35	$\text{CH} + \text{H}_2\text{O} = \text{CH}_2\text{OH}$	5.7300E+09	0.00	-3.15	[133]
36	$\text{CH} + \text{CO}_2 = \text{CO} + \text{CHO}$	3.4000E+09	0.00	2.90	[73]
37	$\text{CH}_2(\text{S}) + \text{M} = \text{CH}_2(\text{T}) + \text{M}'$	1.0000E+10	0.00	0.00	[73]
38	$\text{CH}_2(\text{S}) + \text{H} = \text{CH} + \text{H}_2$	7.0000E+10	0.00	0.00	[73]
39	$\text{CH}_2(\text{S}) + \text{O} = \text{CO} + \text{H} + \text{H}$	1.5000E+10	0.00	0.00	[73]
40	$\text{CH}_2(\text{S}) + \text{O} = \text{CO} + \text{H}_2$	1.5000E+10	0.00	0.00	[73]
41	$\text{CH}_2(\text{S}) + \text{OH} = \text{CH}_2\text{O} + \text{H}$	3.0000E+10	0.00	0.00	[73]
42	$\text{CH}_2(\text{S}) + \text{H}_2 = \text{CH}_3 + \text{H}$	7.2300E+10	0.00	0.00	[73]
43	$\text{CH}_2(\text{S}) + \text{O}_2 = \text{CO} + \text{OH} + \text{H}$	3.0000E+10	0.00	0.00	[73]
44	$\text{CH}_2(\text{S}) + \text{CO}_2 = \text{CH}_2\text{O} + \text{CO}$	3.0000E+09	0.00	0.00	[73]
45	$\text{CH}_2(\text{T}) + \text{M} = \text{C}_1 + \text{H}_2 + \text{M}$	1.1148E+11	0.00	233.70	[136]
46	$\text{CH}_2(\text{T}) + \text{H} = \text{CH} + \text{H}_2$	1.1000E+11	0.00	0.00	[137]
47	$\text{CH}_2(\text{T}) + \text{O} = \text{CO} + \text{H} + \text{H}$	4.8800E+10	0.00	0.00	[138]
48	$\text{CH}_2(\text{T}) + \text{O} = \text{CO} + \text{H}_2$	3.2500E+10	0.00	0.00	[138]
49	$\text{CH}_2(\text{T}) + \text{OH} = \text{CH} + \text{H}_2\text{O}$	1.1300E+04	2.00	12.56	[73]
50	$\text{CH}_2(\text{T}) + \text{OH} = \text{CH}_2\text{O} + \text{H}$	2.5000E+10	0.00	0.00	[73]
51	$\text{CH}_2(\text{T}) + \text{C}_1 = \text{C}_2\text{H} + \text{H}$	5.0000E+10	0.00	0.00	[133]
52	$\text{CH}_2(\text{T}) + \text{CH} = \text{C}_2\text{H}_2 + \text{H}$	4.0000E+10	0.00	0.00	[73]
53	$\text{CH}_2(\text{T}) + \text{CH}_2(\text{T}) = \text{C}_2\text{H}_2 + \text{H} + \text{H}$	1.2000E+11	0.00	3.32	[73]
54	$\text{CH}_2(\text{T}) + \text{H}_2 = \text{CH}_3 + \text{H}$	3.0000E+06	0.00	0.00	[73]
55	$\text{CH}_2(\text{T}) + \text{O}_2 = \text{CO} + \text{H} + \text{OH}$	1.6400E+18	-3.30	12.00	[139]
56	$\text{CH}_2(\text{T}) + \text{O}_2 = \text{CO} + \text{H}_2\text{O}$	2.2400E+19	-3.30	12.00	[139]
57	$\text{CH}_2(\text{T}) + \text{O}_2 = \text{CO}_2 + \text{H} + \text{H}$	3.2850E+18	-3.30	12.00	[139]
58	$\text{CH}_2(\text{T}) + \text{O}_2 = \text{CO}_2 + \text{H}_2$	2.6300E+18	-3.30	12.00	[139]
59	$\text{CH}_2(\text{T}) + \text{O}_2 = \text{CH}_2\text{O} + \text{O}$	3.2850E+18	-3.30	12.00	[139]
60	$\text{CH}_2(\text{T}) + \text{CO} = \text{C}_2\text{H}_2\text{O}$	6.0300E+05	0.00	0.00	[72]
61	$\text{CH}_2(\text{T}) + \text{CO}_2 = \text{CH}_2\text{O} + \text{CO}$	1.1000E+08	0.00	4.18	[73]
62	$\text{CH}_3 + \text{M} = \text{CH}_2(\text{S}) + \text{H} + \text{M}$	1.9000E+13	0.00	382.44	[73]
63	$\text{CH}_3 + \text{H} = \text{CH}_4^{m,4}$	2.1000E+11	0.00	0.00	[73]
		$k_\infty =$ $k_0 =$ 6.3000E+17	-1.80	0.00	
64	$\text{CH}_3 + \text{O} = \text{CH}_2\text{O} + \text{H}$	8.4300E+10	0.00	0.00	[73]

No	Reaction	A	n	Ea	Ref
65	CH <sub>3</sub> + OH = CH <sub>2</sub> (S) + H <sub>2</sub> O	4.0000E+10	0.00	10.47	[73]
66	CH <sub>3</sub> + OH = CH <sub>2</sub> O + H <sub>2</sub>	1.0240E+09	0.00	0.00	[73]
67	CH <sub>3</sub> + OH = CH <sub>2</sub> OH + H	1.5000E+11	0.00	34.46	[73]
68	CH <sub>3</sub> + OH = CH <sub>3</sub> O + H	5.7400E+09	-0.23	58.28	[73]
69	CH <sub>3</sub> + OH = CH <sub>3</sub> OH <sup>5</sup>	k <sub>∞</sub> = 6.0000E+10 k <sub>0</sub> = 1.5950E+18	0.00 -8.20	0.00 0.00	[140]
70	CH <sub>3</sub> + HO <sub>2</sub> = CH <sub>3</sub> O + OH	1.8000E+10	0.00	0.00	[101]
71	CH <sub>3</sub> + C <sub>1</sub> = C <sub>2</sub> H <sub>2</sub> + H	5.0000E+10	0.00	0.00	[133]
72	CH <sub>3</sub> + CH = C <sub>2</sub> H <sub>3</sub> + H	3.0000E+10	0.00	0.00	[73]
73	CH <sub>3</sub> + CH <sub>2</sub> (S) = C <sub>2</sub> H <sub>4</sub> + H	1.8000E+10	0.00	0.00	[73]
74	CH <sub>3</sub> + CH <sub>2</sub> (T) = C <sub>2</sub> H <sub>4</sub> + H	4.0000E+10	0.00	0.00	[101]
75	CH <sub>3</sub> + CH <sub>3</sub> = C <sub>2</sub> H <sub>5</sub> + H	5.0000E+09	0.10	44.36	[101]
76	CH <sub>3</sub> + CH <sub>3</sub> = C <sub>2</sub> H <sub>6</sub> <sup>6</sup>	k <sub>∞</sub> = 3.6000E+10 k <sub>0</sub> = 1.2750E+35	0.00 -7.00	0.00 11.55	[73]
77	CH <sub>3</sub> + O <sub>2</sub> = CH <sub>2</sub> O + OH	1.8500E+09	0.00	85.01	[141]
78	CH <sub>3</sub> + O <sub>2</sub> = CH <sub>3</sub> O + O	1.3200E+11	0.00	131.36	[73]
79	CH <sub>3</sub> + O <sub>2</sub> = CH <sub>3</sub> OO <sup>6</sup>	k <sub>∞</sub> = 2.0600E+06 k <sub>0</sub> = 5.3100E+19	1.10 -3.30	0.00 0.00	[132]
80	CH <sub>3</sub> + HO <sub>2</sub> = CH <sub>4</sub> + O <sub>2</sub>	3.6000E+09	0.00	0.00	[142]
81	CH <sub>4</sub> + H = CH <sub>3</sub> + H <sub>2</sub>	3.8600E+03	2.11	32.42	[143]
82	CH <sub>4</sub> + O = CH <sub>3</sub> + OH	9.0330E+05	1.56	35.55	[101]
83	CH <sub>4</sub> + OH = CH <sub>3</sub> + H <sub>2</sub> O	1.5600E+04	1.83	11.60	[101]
84	CH <sub>4</sub> + HO <sub>2</sub> = CH <sub>3</sub> + H <sub>2</sub> O <sub>2</sub>	9.0330E+09	0.00	103.09	[73]
85	CH <sub>4</sub> + CH = C <sub>2</sub> H <sub>4</sub> + H	6.0000E+10	0.00	0.00	[73]
86	CH <sub>4</sub> + CH <sub>2</sub> (S) = CH <sub>3</sub> + CH <sub>3</sub>	4.2700E+10	0.00	0.00	[73]
87	CO + O + M = CO <sub>2</sub> + M <sup>n</sup>	3.0000E+08	0.00	12.55	[96]
88	CO + OH = CO <sub>2</sub> + H	1.0000E+10	0.00	66.92	[96]
89	CO + OH = CO <sub>2</sub> + H	9.0000E+08	0.00	19.12	[96]
90	CO + OH = CO <sub>2</sub> + H	1.0100E+08	0.00	0.249	[96]
91	CO + HO <sub>2</sub> = CO <sub>2</sub> + OH	1.1500E+02	0.00	73.40	[96]
92	CO + O <sub>2</sub> = CO <sub>2</sub> + O	2.5000E+09	0.00	200.00	[73]
93	CHO + M = CO + H + M <sup>o</sup>	1.8600E+14	-1.00	71.13	[73]
94	CHO + H = CO + H <sub>2</sub>	1.1100E+11	0.00	0.00	[96]
95	CHO + O = CO + OH	3.0000E+10	0.00	0.00	[73]
96	CHO + O = CO <sub>2</sub> + H	3.0000E+10	0.00	0.00	[73]
97	CHO + OH = CO + H <sub>2</sub> O	1.0000E+11	0.00	0.00	[73]
98	CHO + CH <sub>3</sub> = CO + CH <sub>4</sub>	1.2000E+11	0.00	0.00	[73]
99	CHO + O <sub>2</sub> = CO + HO <sub>2</sub>	1.2000E+07	0.81	-3.04	[144]

No	Reaction	A	n	Ea	Ref
100	$\text{CH}_2\text{O} + \text{M} = \text{CHO} + \text{H} + \text{M}$	1.2600E+13	0.00	326.00	[73]
101	$\text{CH}_2\text{O} + \text{H} = \text{CHO} + \text{H}_2$	1.2600E+05	1.62	9.06	[140]
102	$\text{CH}_2\text{O} + \text{O} = \text{CHO} + \text{OH}$	4.1500E+08	0.57	11.56	[73]
103	$\text{CH}_2\text{O} + \text{OH} = \text{CHO} + \text{H}_2\text{O}$	3.4300E+06	1.18	-1.87	[101]
104	$\text{CH}_2\text{O} + \text{HO}_2 = \text{CHO} + \text{H}_2\text{O}_2$	2.0000E+09	0.00	48.97	[73]
105	$\text{CH}_2\text{O} + \text{CH} = \text{C}_2\text{H}_2\text{O} + \text{H}$	9.4600E+10	0.00	-2.16	[73]
106	$\text{CH}_2\text{O} + \text{CH}_3 = \text{CHO} + \text{CH}_4$	4.0900E+09	0.00	37.00	[73]
107	$\text{CH}_2\text{O} + \text{O}_2 = \text{CHO} + \text{HO}_2$	6.0000E+10	0.00	170.00	[73]
108	$\text{CH}_2\text{OH} + \text{M} = \text{CH}_2\text{O} + \text{H} + \text{M}$	4.4000E+12	0.00	125.52	[145]
109	$\text{CH}_2\text{OH} + \text{H} = \text{CH}_2\text{O} + \text{H}_2$	3.0000E+10	0.00	0.00	[73]
110	$\text{CH}_2\text{OH} + \text{O} = \text{CH}_2\text{O} + \text{OH}$	4.2200E+10	0.00	0.00	[73]
111	$\text{CH}_2\text{OH} + \text{OH} = \text{CH}_2\text{O} + \text{H}_2\text{O}$	2.4000E+10	0.00	0.00	[73]
112	$\text{CH}_2\text{OH} + \text{O}_2 = \text{CH}_2\text{O} + \text{HO}_2$	4.5600E-09	5.94	-18.99	[73]
113	$\text{CH}_3\text{O} + \text{M} = \text{CH}_2\text{O} + \text{H} + \text{M}$	5.4500E+10	0.00	56.50	[73]
114	$\text{CH}_3\text{O} + \text{M} = \text{CH}_2\text{OH} + \text{M}^P$	3.0100E+08	0.00	17.04	[73]
115	$\text{CH}_3\text{O} + \text{H} = \text{CH}_2\text{O} + \text{H}_2$	2.0000E+10	0.00	0.00	[73]
116	$\text{CH}_3\text{O} + \text{O} = \text{CH}_2\text{O} + \text{OH}$	6.0000E+09	0.00	0.00	[73]
117	$\text{CH}_3\text{O} + \text{OH} = \text{CH}_2\text{O} + \text{H}_2\text{O}$	1.8000E+10	0.00	0.00	[73]
118	$\text{CH}_3\text{O} + \text{O}_2 = \text{CH}_2\text{O} + \text{HO}_2$	6.6000E+07	0.00	10.88	[73]
119	$\text{CH}_3\text{OH} + \text{M} = \text{CH}_2(\text{S}) + \text{H}_2\text{O} + \text{M}$	7.0000E+12	0.00	277.99	[73]
120	$\text{CH}_3\text{OH} + \text{M} = \text{CH}_2\text{OH} + \text{H} + \text{M}$	2.0000E+14	0.00	315.89	[73]
121	$\text{CH}_3\text{OH} + \text{H} = \text{CH}_2\text{OH} + \text{H}_2$	1.4400E+10	0.00	25.50	[146]
122	$\text{CH}_3\text{OH} + \text{H} = \text{CH}_3\text{O} + \text{H}_2$	4.0000E+09	0.00	25.50	[73]
123	$\text{CH}_3\text{OH} + \text{O} = \text{CH}_2\text{OH} + \text{OH}$	3.8800E+02	2.50	12.90	[73]
124	$\text{CH}_3\text{OH} + \text{O} = \text{CH}_3\text{O} + \text{OH}$	1.0000E+10	0.00	19.59	[73]
125	$\text{CH}_3\text{OH} + \text{OH} = \text{CH}_2\text{OH} + \text{H}_2\text{O}$	3.0000E+01	2.65	-3.70	[73]
126	$\text{CH}_3\text{OH} + \text{OH} = \text{CH}_3\text{O} + \text{H}_2\text{O}$	5.3000E+00	2.65	-3.70	[73]
127	$\text{CH}_3\text{OH} + \text{CH}_3 = \text{CH}_2\text{OH} + \text{CH}_4$	3.1900E-02	3.20	30.00	[73]
128	$\text{CH}_3\text{OH} + \text{O}_2 = \text{CH}_2\text{OH} + \text{HO}_2$	2.0500E+10	0.00	188.00	[147]
129	$\text{CH}_3\text{OH} + \text{HO}_2 = \text{CH}_2\text{OH} + \text{H}_2\text{O}_2$	3.9800E+10	0.00	81.22	[146]
130	$\text{CH}_3\text{OO} + \text{CH}_4 = \text{CH}_3\text{OOH} + \text{CH}_3$	3.0000E+09	0.00	95.00	[148]
131	$\text{CH}_3\text{OO} + \text{CH}_2\text{O} = \text{CH}_3\text{OOH} + \text{CHO}$	3.0000E+09	0.00	52.00	[72]
132	$\text{CH}_3\text{OO} + \text{HO}_2 = \text{CH}_3\text{OOH} + \text{O}_2$	2.4700E+08	0.00	-6.56	[149]
133	$\text{CH}_3\text{OO} + \text{CH}_3\text{OO} = \text{CH}_3\text{O} + \text{CH}_3\text{O} + \text{O}_2$	5.4800E+07	0.00	-3.49	[140]
134	$\text{CH}_3\text{OO} + \text{CH}_3 = \text{CH}_3\text{O} + \text{CH}_3\text{O}$	1.0000E+10	0.00	0.00	[72]

No	Reaction	A	n	Ea	Ref
135	$\text{CH}_3\text{OO} + \text{C}_2\text{H}_6 = \text{CH}_3\text{OOH} + \text{C}_2\text{H}_5$	3.0000E+08	0.00	62.50	[150]
136	$\text{CH}_3\text{OOH} = \text{CH}_3\text{O} + \text{OH}$	6.0000E+14	0.00	177.09	[148]
137	$\text{C}_2 + \text{O} = \text{CO} + \text{C}_1$	3.6100E+11	0.00	0.00	[151]
138	$\text{C}_2 + \text{O}_2 = \text{CO} + \text{CO}$	8.9700E+09	0.00	4.10	[152]
139	$\text{C}_2\text{H} + \text{O} = \text{CO} + \text{CH}$	1.0000E+10	0.00	0.00	[73]
140	$\text{C}_2\text{H} + \text{OH} = \text{C}_2\text{HO} + \text{H}$	2.0000E+10	0.00	0.00	[73]
141	$\text{C}_2\text{H} + \text{H}_2 = \text{C}_2\text{H}_2 + \text{H}$	5.6700E+07	0.90	8.34	[73]
142	$\text{C}_2\text{H} + \text{O}_2 = \text{CO} + \text{CO} + \text{H}$	9.0400E+09	0.00	-1.91	[73]
143	$\text{C}_2\text{H} + \text{H}_2\text{O} = \text{C}_2\text{H}_2\text{O} + \text{H}$	1.1400E+10	0.00	1.66	[73]
144	$\text{C}_2\text{H} + \text{H} = \text{C}_2 + \text{H}_2$	3.6100E+10	0.00	118.25	[73]
145	$\text{C}_2\text{H} + \text{C}_2\text{H} = \text{C}_2\text{H}_2 + \text{C}_2$	1.8100E+09	0.00	0.00	[150]
146	$\text{C}_2\text{H} + \text{CH}_3 = \text{C}_3\text{H}_3 + \text{H}$	2.4100E+10	0.00	0.00	[73]
147	$\text{C}_2\text{H} + \text{C}_2\text{H} = \text{C}_4\text{H} + \text{H}$	1.0000E+11	0.00	0.00	[73]
148	$\text{C}_2\text{H}_2 + \text{M} = \text{C}_2\text{H} + \text{H} + \text{M}$	4.2000E+13	0.00	448.00	[73]
149	$\text{C}_2\text{H}_2 + \text{M} = \text{H}_2\text{C}_2 + \text{M}^q$	2.5000E+12	-0.64	207.95	[153]
150	$\text{C}_2\text{H}_2 + \text{O} = \text{CO} + \text{CH}_2(\text{T})$	1.2500E+04	2.00	7.94	[154]
151	$\text{C}_2\text{H}_2 + \text{O} = \text{C}_2\text{HO} + \text{H}$	9.0400E+09	0	19.00	[150]
152	$\text{C}_2\text{H}_2 + \text{OH} = \text{C}_2\text{H} + \text{H}_2\text{O}$	3.3700E+04	2.00	58.57	[73]
153	$\text{C}_2\text{H}_2 + \text{OH} = \text{C}_2\text{H}_2\text{O} + \text{H}$	3.7500E+03	1.70	4.18	[133]
154	$\text{C}_2\text{H}_2 + \text{HO}_2 = \text{C}_2\text{H}_2\text{O} + \text{OH}$	6.0000E+06	0.00	33.52	[150]
155	$\text{C}_2\text{H}_2 + \text{O}_2 = \text{C}_2\text{H} + \text{HO}_2$	1.2000E+10	0.00	311.70	[73]
156	$\text{C}_2\text{H}_2 + \text{CH} = \text{C}_3\text{H} + \text{H}_2$	3.1500E+10	0.00	-0.51	[133]
157	$\text{C}_2\text{H}_2 + \text{CH} = \text{C}_3\text{H}_2 + \text{H}$	1.7850E+11	0.00	-0.51	[133]
158	$\text{C}_2\text{H}_2 + \text{CH}_2(\text{S}) = \text{C}_3\text{H}_3 + \text{H}$	8.0000E+10	0.00	0.00	[133]
159	$\text{C}_2\text{H}_2 + \text{CH}_2(\text{S}) = \text{C}_3\text{H}_4(\text{B})$	8.0000E+10	0.00	0.00	[133]
160	$\text{C}_2\text{H}_2 + \text{CH}_2(\text{T}) = \text{C}_3\text{H}_4(\text{B})$	1.2000E+10	0.00	27.70	[73]
161	$\text{C}_2\text{H}_2 + \text{CH}_3 = \text{C}_3\text{H}_4(\text{A}) + \text{H}$	9.6800E+10	0.00	117.13	[8]
162	$\text{C}_2\text{H}_2 + \text{CH}_3 = \text{C}_3\text{H}_5(\text{S})$	1.6100E+37	-8.58	85.06	[155]
163	$\text{C}_2\text{H}_2 + \text{CH}_3 = \text{C}_3\text{H}_5(\text{A})$	2.6800E+50	-12.82	150.00	[156]
164	$\text{C}_2\text{H}_2 + \text{CH}_3 = \text{C}_2\text{H} + \text{CH}_4$	1.8100E+08	0.00	72.33	[150]
165	$\text{C}_2\text{H}_2 + \text{C}_2\text{H}_2 = \text{C}_4\text{H}_3(\text{N}) + \text{H}$	1.0000E+09	0.00	276.14	[73]
166	$\text{C}_2\text{H}_2 + \text{C}_2\text{H}_2 = \text{C}_4\text{H}_3(\text{I}) + \text{H}$	2.0000E+09	0.00	268.00	[73]
167	$\text{C}_2\text{H}_2 + \text{C}_2\text{H} = \text{C}_4\text{H}_2 + \text{H}$	1.2000E+11	0.00	0.00	[73]
168	$\text{H}_2\text{C}_2 + \text{O}_2 = \text{CH}_2(\text{T}) + \text{CO}_2$	5.0000E+10	0.00	0.00	[153]
169	$\text{H}_2\text{C}_2 + \text{O} = \text{CH}_2(\text{T}) + \text{CO}$	3.0000E+10	0.00	0.00	[153]

No	Reaction	A	n	Ea	Ref
170	$\text{H}_2\text{C}_2 + \text{OH} = \text{CH}_2(\text{T}) + \text{CHO}$	2.0000E+10	0.00	0.00	[153]
171	$\text{H}_2\text{C}_2 + \text{O}_2 = \text{CHO} + \text{CHO}$	1.0000E+10	0.00	0.00	[72]
172	$\text{C}_2\text{H}_3 = \text{C}_2\text{H}_2 + \text{H}^{r,7}$	$k_\infty = 2.0000\text{E}+14$ $k_0 = 4.1600\text{E}+38$	0.00 -7.50	166.28 190.40	[101]
173	$\text{C}_2\text{H}_3 + \text{H} = \text{C}_2\text{H}_2 + \text{H}_2$	3.0000E+10	0.00	0.00	[101]
174	$\text{C}_2\text{H}_3 + \text{O} = \text{C}_2\text{H}_2\text{O} + \text{H}$	3.0000E+10	0.00	0.00	[73]
175	$\text{C}_2\text{H}_3 + \text{OH} = \text{C}_2\text{H}_2 + \text{H}_2\text{O}$	2.0000E+10	0.00	0.00	[73]
176	$\text{C}_2\text{H}_3 + \text{HO}_2 = \text{CH}_3\text{CO} + \text{OH}$	3.0000E+10	0.00	0.00	[150]
177	$\text{C}_2\text{H}_3 + \text{CH} = \text{C}_2\text{H}_2 + \text{CH}_2(\text{T})$	5.0000E+10	0.00	0.00	[73]
178	$\text{C}_2\text{H}_3 + \text{C}_2\text{H} = \text{C}_2\text{H}_2 + \text{C}_2\text{H}_2$	3.0000E+10	0.00	0.00	[73]
179	$\text{C}_2\text{H}_3 + \text{O}_2 = \text{CH}_2\text{O} + \text{CHO}$	1.6400E+18	-2.78	1.06	[157]
180	$\text{C}_2\text{H}_3 + \text{O}_2 = \text{C}_2\text{H}_2 + \text{HO}_2$	1.6600E+11	-0.83	10.62	[136]
181	$\text{C}_2\text{H}_3 + \text{O}_2 = \text{CH}_2\text{CHO} + \text{O}$	2.5000E+09	0.06	3.97	[136]
182	$\text{C}_2\text{H}_3 + \text{O}_2 = \text{CH}_3\text{CO} + \text{O}$	1.5000E+08	0.00	-1.00	[133]
183	$\text{C}_2\text{H}_3 + \text{C}_2\text{H} = \text{C}_4\text{H}_4$	1.0000E+11	0.00	0.00	[158]
184	$\text{C}_2\text{H}_3 + \text{C}_2\text{H}_2 = \text{C}_4\text{H}_4 + \text{H}$	4.6800E+09	0.00	21.70	[133]
185	$\text{C}_2\text{H}_3 + \text{C}_2\text{H}_3 = \text{C}_4\text{H}_6(\text{T})$	1.0000E+10	0.00	0.00	[73]
186	$\text{C}_2\text{H}_3 + \text{CH} = \text{C}_3\text{H}_2 + \text{H}_2$	3.1500E+10	0.00	-0.51	[72]
187	$\text{C}_2\text{H}_3 + \text{CH} = \text{C}_3\text{H}_3 + \text{H}$	1.7885E+11	0.00	-0.51	[72]
188	$\text{C}_2\text{H}_3 + \text{CH}_2(\text{S}) = \text{C}_3\text{H}_3 + \text{H}_2$	8.0000E+10	0.00	0.00	[72]
189	$\text{C}_2\text{H}_3 + \text{CH}_2(\text{S}) = \text{C}_3\text{H}_4(\text{B}) + \text{H}$	8.0000E+10	0.00	0.00	[72]
190	$\text{C}_2\text{H}_3 + \text{CH}_2(\text{T}) = \text{C}_3\text{H}_4(\text{B}) + \text{H}$	1.2000E+10	0.00	27.70	[72]
191	$\text{C}_2\text{H}_4 + \text{M} = \text{C}_2\text{H}_3 + \text{H} + \text{M}$	2.6000E+14	0.00	404.00	[73]
192	$\text{C}_2\text{H}_4 + \text{H} = \text{C}_2\text{H}_3 + \text{H}_2$	5.0700E+04	1.93	54.19	[159]
193	$\text{C}_2\text{H}_4 + \text{H} = \text{C}_2\text{H}_5^{r,7}$	$k_\infty = 3.9700\text{E}+06$ $k_0 = 4.7140\text{E}+12$	1.28 0.00	5.40 3.16	[140]
194	$\text{C}_2\text{H}_4 + \text{O} = \text{CHO} + \text{CH}_3$	8.1000E+03	1.88	0.76	[136]
195	$\text{C}_2\text{H}_4 + \text{O} = \text{CH}_2\text{CHO} + \text{H}$	4.7000E+03	1.88	0.76	[140]
196	$\text{C}_2\text{H}_4 + \text{O} = \text{C}_2\text{H}_2\text{O} + \text{H}_2$	6.7500E+02	1.88	0.76	[136]
197	$\text{C}_2\text{H}_4 + \text{OH} = \text{C}_2\text{H}_3 + \text{H}_2\text{O}$	2.0500E+10	0.00	24.86	[101]
198	$\text{C}_2\text{H}_4 + \text{HO}_2 = \text{C}_2\text{H}_3 + \text{H}_2\text{O}_2$	1.1200E+10	0.00	127.30	[160]
199	$\text{C}_2\text{H}_4 + \text{HO}_2 = \text{CH}_3\text{CHO} + \text{OH}$	6.0300E+06	0.00	33.25	[150]
200	$\text{C}_2\text{H}_4 + \text{HO}_2 = \text{C}_2\text{H}_4\text{O} + \text{OH}$	2.2300E+09	0.00	71.90	[101]
201	$\text{C}_2\text{H}_4 + \text{O}_2 = \text{C}_2\text{H}_3 + \text{HO}_2$	4.2200E+10	0.00	241.11	[150]
202	$\text{C}_2\text{H}_4 + \text{C}_2\text{H}_4 = \text{C}_2\text{H}_3 + \text{C}_2\text{H}_5$	5.0100E+11	0.00	271.00	[161]
203	$\text{C}_2\text{H}_4 + \text{CH}_2(\text{S}) = \text{C}_3\text{H}_6$	6.6000E+10	0.00	0.00	[73]
204	$\text{C}_2\text{H}_4 + \text{CH}_2(\text{T}) = \text{C}_3\text{H}_6$	1.8000E+07	0.00	0.00	[73]

No	Reaction	A	n	Ea	Ref
205	$C_2H_4 + CH = C_3H_3 + H_2$	3.1500E+10	0.00	-0.51	[72]
206	$C_2H_4 + CH = C_3H_4(B) + H$	1.7850E+11	0.00	-0.51	[72]
207	$C_2H_4 + CH_2(S) = C_3H_4(B) + H_2$	8.0000E+10	0.00	0.00	[72]
208	$C_2H_4 + CH_2(S) = C_3H_5(B) + H$	8.0000E+10	0.00	0.00	[72]
209	$C_2H_4 + CH_2(T) = C_3H_5(B) + H$	1.2000E+10	0.00	27.70	[72]
210	$C_2H_4 + C_2H = C_4H_4 + H$	1.2100E+10	0.00	0.00	[150]
211	$C_2H_5 + H = C_2H_4 + H_2$	4.5000E+10	0.00	0.00	[162]
212	$C_2H_5 + O = CH_2O + CH_3$	6.6000E+10	0.00	0.00	[73]
213	$C_2H_5 + O = C_2H_4 + OH$	3.0600E+10	0.00	0.00	[162]
214	$C_2H_5 + O = CH_3CHO + H$	6.6000E+10	0.00	0.00	[133]
215	$C_2H_5 + O_2 = CH_3CHO + OH$	1.9462E+09	-0.47	32.47	[163]
216	$C_2H_5 + O_2 = C_2H_4 + HO_2$	1.0200E+17	-2.97	36.13	[163]
217	$C_2H_5 + O_2 = C_2H_4O + OH$	1.9390E+17	-3.08	36.13	[163]
218	$C_2H_5 + O_2 = C_2H_4OOH$	8.8400E+34	-9.33	42.48	[163]
219	$C_2H_5 + O_2 = C_2H_5OO$	9.4200E+33	-8.01	25.50	[163]
220	$C_2H_5 + C_2H_5 = C_4H_{10}(N)$	1.7200E+14	-1.66	4.59	[164]
221	$C_2H_6 = C_2H_5 + H^{s,8}$	8.8500E+20	-1.23	427.70	[73]
		4.9000E+39	-6.43	448.40	
222	$C_2H_6 + H = C_2H_5 + H_2$	1.4450E+06	1.50	31.00	[73]
223	$C_2H_6 + O = C_2H_5 + OH$	1.0000E+06	1.50	24.30	[73]
224	$C_2H_6 + OH = C_2H_5 + H_2O$	7.2260E+03	2.00	3.61	[73]
225	$C_2H_6 + CH_2(S) = C_2H_5 + CH_3$	1.1400E+11	0.00	0.00	[73]
226	$C_2H_6 + O_2 = C_2H_5 + HO_2$	6.0230E+10	0.00	216.99	[101]
227	$C_2H_6 + HO_2 = C_2H_5 + H_2O_2$	1.3200E+10	0.00	85.63	[101]
228	$C_2H_6 + CH_3 = C_2H_5 + CH_4$	1.5000E-10	6.00	25.26	[101]
229	$C_2O + H = CO + CH$	5.0000E+10	0.00	0.00	[73]
230	$C_2O + O = CO + CO$	5.0000E+10	0.00	0.00	[73]
231	$C_2O + OH = CO + CO + H$	2.0000E+10	0.00	0.00	[73]
232	$C_2O + O_2 = CO + CO + O$	2.0000E+10	0.00	0.00	[73]
233	$C_2HO + H = CH_2(S) + CO$	1.0000E+11	0.00	0.00	[73]
234	$C_2HO + O = CO + CO + H$	9.6350E+10	0.00	0.00	[73]
235	$C_2HO + OH = C_2O + H_2O$	3.0000E+10	0.00	0.00	[73]
236	$C_2HO + CH = C_2H_2 + CO$	5.0000E+10	0.00	0.00	[73]
237	$C_2HO + CH_2(T) = C_2H_3 + CO$	3.0000E+10	0.00	0.00	[73]
238	$C_2HO + C_2HO = C_2H_2 + CO + CO$	1.0000E+10	0.00	0.00	[73]
239	$C_2HO + O_2 = CO + CO + OH$	1.9092E+08	-0.02	4.28	[165]

No	Reaction	A	n	Ea	Ref
240	$C_2HO + O_2 = CO_2 + CO + H$	4.7800E+09	-0.14	4.81	[165]
241	$C_2HO + C_2H_2 = C_3H_3 + CO$	1.0000E+08	0.00	12.60	[73]
242	$C_2H_2O + H = CO + CH_3$	1.1100E+04	2.00	8.36	[166]
243	$C_2H_2O + H = C_2HO + H_2$	1.8000E+11	0.00	35.98	[166]
244	$C_2H_2O + O = CO_2 + CH_2(T)$	2.0000E+10	0.00	9.60	[167]
245	$C_2H_2O + O = C_2HO + OH$	2.0000E+04	2.00	41.68	[136]
246	$C_2H_2O + OH = CH_2OH + CO$	1.0200E+10	0.00	0.00	[101]
247	$C_2H_2O + CH_2(S) = C_2H_4 + CO$	1.2600E+11	0.00	0.00	[168]
248	$C_2H_2O + CH_3 = C_2H_5 + CO$	9.0000E+07	0.00	0.00	[133]
249	$C_2H_2O + CH_3 = C_2HO + CH_4$	7.5000E+09	0.00	54.39	[133]
250	$C_2H_2O + OH = C_2HO + H_2O$	1.0000E+04	2.00	12.56	[136]
251	$CHCH_2O = CH_3CO$	8.5000E+14	0.00	58.60	[160]
252	$CHCH_2O = CH_2CHO$	1.0000E+14	0.00	58.60	[160]
253	$CH_2CHO = CH_3CO$	1.0000E+13	0.00	184.10	[136]
254	$CH_2CHO = C_2H_2O + H$	1.5800E+13	0.00	196.65	[136]
255	$CH_2CHO + OH = C_2H_2O + H_2O$	1.0000E+10	0.00	0.00	[136]
256	$CH_2CHO + O = C_2H_2O + OH$	1.0000E+11	0.00	0.00	[136]
257	$CH_2CHO + O_2 = CH_2O + CO + OH$	1.8100E+07	0.00	0.00	[101]
258	$CH_2CHO + CH_3 = C_2H_6 + CO$	6.1000E+09	0.00	0.00	[136]
259	$CH_3CHO + M = CHO + CH_3 + M$	7.0800E+15	0.00	342.15	[101]
260	$CH_3CHO + H = CH_3CO + H_2$	2.1000E+06	1.16	10.09	[133]
261	$CH_3CHO + O = CH_3CO + OH$	5.0000E+09	0.00	7.50	[167]
262	$CH_3CHO + OH = CH_3CO + H_2O$	2.3000E+07	0.73	-4.66	[133]
263	$CH_3CHO + HO_2 = CH_3CO + H_2O_2$	3.0000E+09	0.00	49.87	[101]
264	$CH_3CHO + CH_2(T) = CH_3CO + CH_3$	2.5000E+09	0.00	15.89	[133]
265	$CH_3CHO + CH_3 = CH_3CO + CH_4$	2.0000E-09	5.64	10.31	[101]
266	$CH_3CHO + O_2 = CH_3CO + HO_2$	4.0000E+10	0.00	164.19	[133]
267	$CH_3CO = CH_3 + CO$	$k_{\infty} = 2.8000E+13$ $k_0 = 6.0300E+12$	0.00 0.00	71.75 58.86	[136]
268	$CH_3CO + H = C_2H_2O + H_2$	1.1500E+10	0.00	0.00	[72]
269	$CH_3CO + H = CH_3 + CHO$	2.1500E+10	0.00	0.00	[72]
270	$CH_3CO + OH = C_2H_2O + H_2O$	1.2100E+10	0.00	0.00	[150]
271	$CH_3CO + O = CH_3 + CO_2$	1.5400E+11	0.00	0.00	[72]
272	$CH_3CO + O = C_2H_2O + OH$	3.8600E+10	0.00	0.00	[72]
273	$CH_3CO + CH_3 = C_2H_6 + CO$	5.0000E+10	0.00	0.00	[133]

No	Reaction	A	n	Ea	Ref
274	$C_2H_4O = CH_3 + CHO$	3.4000E+13	0.00	241.90	[160]
275	$C_2H_4O = CH_3CHO$	5.8400E+11	0.00	219.10	[160]
276	$C_2H_4O + H = CHCH_2O + H_2$	7.9000E+10	0.00	41.00	[160]
277	$C_2H_4O + OH = CHCH_2O + H_2O$	1.7800E+10	0.00	15.10	[160]
278	$C_2H_4O + HO_2 = CHCH_2O + H_2O_2$	1.1200E+10	0.00	127.30	[160]
279	$C_2H_4O + HO_2 = CH_3 + CO + H_2O_2$	4.0000E+09	0.00	71.20	[101]
280	$C_2H_4O + CH_3 = CHCH_2O + CH_4$	1.0700E+09	0.00	49.50	[160]
281	$C_2H_4O + CH_3O = CHCH_2O + CH_3OH$	1.2000E+08	0.00	28.30	[160]
282	$C_2H_4O + CH_3OO = CHCH_2O + CH_3OOH$	1.1200E+10	0.00	127.30	[160]
283	$C_2H_4OOH = C_2H_4O + OH$	1.4900E+41	-9.51	94.46	[163]
284	$C_2H_4OOH = C_2H_4 + HO_2$	6.5800E+41	-9.70	96.28	[163]
285	$C_2H_4OOH = C_2H_4 + HO_2$	5.6500E+41	-10.9	110.78	[163]
286	$C_2H_4OOH = CH_3CHO + OH$	3.1000E+37	-10.1	119.55	[163]
287	$C_2H_5O = CH_2O + CH_3$	1.0000E+15	0.00	90.40	[160]
288	$C_2H_5O = CH_3CHO + H$	2.5100E+14	0.00	97.90	[160]
289	$C_2H_5O + O_2 = CH_3CHO + HO_2$	6.0300E+07	0.00	6.90	[160]
290	$C_2H_5OO = C_2H_4OOH$	4.5540E+51	-13.30	184.53	[163]
291	$C_2H_5OO = C_2H_4 + HO_2$	6.4630E+30	-6.06	146.98	[163]
292	$C_2H_5OO = C_2H_4 + HO_2$	4.4700E+42	-10.10	128.07	[163]
293	$C_2H_5OO = C_2H_4O + OH$	3.0150E+42	-10.00	188.65	[163]
294	$C_2H_5OO = CH_3CHO + OH$	2.1340E+41	-9.81	192.03	[163]
295	$C_2H_5OO + HO_2 = C_2H_5OOH + O_2$	1.6300E+08	0.00	-8.31	[160]
296	$C_2H_5OO + CH_2O = C_2H_5OOH + CHO$	2.0000E+09	0.00	48.80	[160]
297	$C_2H_5OO + CH_4 = C_2H_5OOH + CH_3$	1.1200E+10	0.00	103.20	[160]
298	$C_2H_5OO + C_2H_4 = C_2H_4O + C_2H_5O$	2.8200E+09	0.00	71.60	[160]
299	$C_2H_5OO + C_2H_4 = C_2H_5OOH + C_2H_3$	1.1200E+10	0.00	127.30	[160]
300	$C_2H_5OO + C_2H_6 = C_2H_5OOH + C_2H_5$	1.7000E+10	0.00	85.60	[160]
301	$C_2H_5OO + C_2H_4O = CHCH_2O + C_2H_5OOH$	1.1200E+10	0.00	127.30	[160]
302	$C_2H_5OOH = C_2H_5O + OH$	4.0000E+15	0.00	179.60	[160]
303	$C_2H_5OOH + CH_2OH = C_2H_5OO + CH_3OH$	3.0160E+06	0.00	10.80	[160]
304	$C_3H + O = C_2H + CO$	6.8000E+10	0.00	0.00	[73]
305	$C_3H + OH = C_2H_2 + CO$	6.8000E+10	0.00	0.00	[73]
306	$C_3H + O_2 = C_2H + CO_2$	9.0400E+09	0.00	-1.91	[72]
307	$C_3H + H_2O = C_3H_2O + H$	1.1500E+10	0.00	1.66	[133]
308	$C_3H + CH = C_4H + H$	7.0000E+10	0.00	0.00	[133]



No	Reaction	A	n	Ea	Ref
309	$C_3H + CH_2(S) = C_4H_2 + H$	8.0000E+10	0.00	0.00	[133]
310	$C_3H + CH_2(T) = C_4H_2 + H$	8.0000E+10	0.00	0.00	[133]
311	$C_3H + CH_3 = C_4H_3(l) + H$	4.0000E+10	0.00	0.00	[133]
312	$C_3H_2 = C_3H_2L$	1.0000E+13	0.00	272.00	[133]
313	$C_3H_2 + H = C_3H + H_2$	1.0000E+11	0.00	0.00	[133]
314	$C_3H_2 + H_2O = C_3H_2O + H_2$	5.7300E+09	0.00	-3.16	[133]
315	$C_3H_2 + CH_3 = C_4H_4 + H$	4.0000E+10	0.00	0.00	[133]
316	$C_3H_2 + CH_2(S) = C_4H_3(l) + H$	8.0000E+10	0.00	0.00	[133]
317	$C_3H_2 + CH = C_4H_2 + H$	7.0000E+10	0.00	0.00	[133]
318	$C_3H_2 + O = C_2H + CO + H$	1.4000E+11	0.00	0.00	[133]
319	$C_3H_2 + OH = C_3H + H_2O$	6.0000E+10	0.00	0.00	[133]
320	$C_3H_2 + O_2 = C_2H_2 + CO_2$	2.0000E+09	0.00	0.00	[73]
321	$C_3H_2 + O_2 = C_3H_2O + O$	2.0000E+09	0.00	0.00	[72]
322	$C_3H_2 + CH_2(T) = C_4H_3(l) + H$	8.0000E+10	0.00	0.00	[133]
323	$C_3H_2L + H = C_3H + H_2$	1.0000E+11	0.00	0.00	[133]
324	$C_3H_2L + OH = C_3H + H_2O$	2.0000E+10	0.00	0.00	[133]
325	$C_3H_3 + C_3H_2 = C_6H_4L + H$	1.0000E+10	0.00	0.00	[73]
326	$C_3H_3 + C_3H_3 = C_6H_6(A)$	1.0000E+10	0.00	0.00	[73]
327	$C_3H_3 + C_3H_3 = C_6H_6(B)$	1.0000E+10	0.00	0.00	[73]
328	$C_3H_3 + C_3H_3 = C_6H_6(S)$	1.0000E+10	0.00	0.00	[73]
329	$C_3H_3 + C_3H_4(A) = C_6H_7(L)$	3.0000E+08	0.00	12.56	[169]
330	$C_3H_3 + CH = C_4H_3(N) + H$	7.0000E+10	0.00	0.00	[73]
331	$C_3H_3 + CH = C_4H_3(l) + H$	7.0000E+10	0.00	0.00	[73]
332	$C_3H_3 + CH_2(T) = C_4H_4 + H$	8.0000E+10	0.00	0.00	[73]
333	$C_3H_3 + CH_2(S) = C_4H_4 + H$	8.0000E+10	0.00	0.00	[133]
334	$C_3H_3 + H = C_3H_2L + H_2$	1.0000E+10	0.00	9.00	[133]
335	$C_3H_3 + O = C_3H_2O + H$	2.5000E+10	0.00	0.00	[72]
336	$C_3H_3 + OH = C_3H_2O + H_2$	4.0000E+09	0.00	0.00	[72]
337	$C_3H_3 + O_2 = C_2H_2O + CHO$	3.0000E+07	0.00	12.00	[73]
338	$C_3H_3 + H_2O = C_3H_4O + H$	1.1500E+10	0.00	100.66	[72]
339	$C_3H_3 + C_3H_3 = C_6H_5 + H$	4.0000E+09	0.00	0.00	[131]
340	$C_3H_4(A) + H = C_3H_5(T)$	8.5000E+09	0.00	8.37	[73]
341	$C_3H_4(A) + H = C_3H_5(A)$	1.5200E+56	-13.54	112.83	[156]
342	$C_3H_4(A) + H = C_3H_3 + H_2$	1.0000E+09	0.00	6.28	[145]
343	$C_3H_4(A) + O = C_2H_3 + CHO$	1.1000E-05	4.61	-17.80	[73]

No	Reaction	A	n	Ea	Ref
344	$C_3H_4(A) + OH = C_2H_2O + CH_3$	3.1200E+09	0.00	-1.66	[73]
345	$C_3H_4(A) + OH = C_3H_3 + H_2O$	1.0000E+09	0.00	6.27	[73]
346	$C_3H_4(A) + O_2 = C_3H_3 + HO_2$	4.0000E+10	0.00	257.50	[73]
347	$C_3H_4(A) + CH_3 = C_3H_3 + CH_4$	2.0000E+09	0.00	32.20	[73]
348	$C_3H_4(A) + C_2H = C_3H_3 + C_2H_2$	1.0000E+10	0.00	0.00	[73]
349	$C_3H_4(A) + C_3H_4(A) = C_3H_5(A) + C_3H_3$	5.0000E+11	0.00	270.88	[73]
350	$C_3H_4(A) + M = C_3H_3 + H + M$	2.0000E+15	0.00	334.71	[73]
351	$C_3H_4(A) + CH = C_4H_4 + H$	2.7700E+11	0.00	0.00	[133]
352	$C_3H_4(A) + CH_2(S) = C_4H_6(B)$	1.6000E+11	0.00	0.00	[133]
353	$C_3H_4(A) + CH_2(T) = C_4H_6(B)$	1.6000E+10	0.00	0.00	[133]
354	$C_3H_4(B) = C_3H_4(A)$	1.5130E+14	0.00	211.00	[73]
355	$C_3H_4(B) = C_3H_4(P)$	7.0800E+13	0.00	182.96	[73]
356	$C_3H_4(P) + H = C_3H_5(T)$	6.5000E+09	0.00	8.37	[73]
357	$C_3H_4(P) + H = C_3H_5(S)$	5.8000E+09	0.00	12.98	[73]
358	$C_3H_4(P) + H = C_3H_3 + H_2$	1.0000E+09	0.00	6.28	[145]
359	$C_3H_4(P) + O = C_2H_2O + CH_2(T)$	6.4000E+09	0.00	8.41	[73]
360	$C_3H_4(P) + CH_2(S) = C_4H_6(B)$	1.6000E+11	0.00	0.00	[73]
361	$C_3H_4(P) = C_3H_4(A)$	5.1500E+60	-13.93	381.48	[156]
362	$C_3H_4(P) + M = C_3H_4(A) + M$	6.2700E+14	-0.91	42.19	[156]
363	$C_3H_4(P) + M = C_3H_3 + H + M$	4.7000E+15	0.00	334.17	[73]
364	$C_3H_4(P) + O = C_2H_3 + CHO$	3.2000E+09	0.00	8.41	[73]
365	$C_3H_4(P) + O = C_2HO + CH_3$	6.3000E+09	0.00	8.41	[73]
366	$C_3H_4(P) + OH = C_2H_4 + CHO$	5.0000E-07	4.50	-4.19	[73]
367	$C_3H_4(P) + OH = C_3H_3 + H_2O$	3.0000E+00	3.00	0.84	[170]
368	$C_3H_4(P) + O_2 = C_2HO + CH_2(T) + OH$	6.1500E+04	1.50	126.00	[72]
369	$C_3H_4(P) + O_2 = C_3H_3 + HO_2$	5.0000E+09	0.00	231.00	[73]
370	$C_3H_4(P) + CH = C_4H_4 + H$	2.7700E+11	0.00	0.00	[133]
371	$C_3H_4(P) + CH_2(T) = C_4H_6(B)$	1.6000E+10	0.00	0.00	[133]
372	$C_3H_4(P) + CH_3 = C_3H_3 + CH_4$	2.0000E+09	0.00	32.20	[145]
373	$C_3H_4(P) + C_2H = C_3H_3 + C_2H_2$	1.0000E+10	0.00	0.00	[73]
374	$C_3H_4(P) + H = CH_3 + C_2H_2$	1.0000E+11	0.00	16.62	[171]
375	$C_3H_5(A) + H = C_3H_4(A) + H_2$	1.8100E+10	0.00	0.00	[172]
376	$C_3H_5(A) + O = C_3H_4O + H$	6.0000E+09	0.00	0.00	[172]
377	$C_3H_5(A) + O_2 = C_3H_4(A) + HO_2$	1.2100E+09	0.00	56.70	[172]
378	$C_3H_5(A) + O_2 = C_3H_4O + OH$	8.4200E+05	0.00	-9.62	[133]

No	Reaction	A	n	Ea	Ref
379	$C_3H_5(A) + O_2 = CH_3CO + CH_2O$	1.1900E+12	-1.01	84.27	[156]
380	$C_3H_5(A) + CH_3 = C_3H_4(A) + CH_4$	3.0000E+09	-0.32	-0.55	[73]
381	$C_3H_5(A) + HO_2 = OH + C_2H_3 + CH_2O$	6.6000E+09	0.00	0.00	[156]
382	$C_3H_5(A) + C_2H_3 = C_2H_4 + C_3H_4(A)$	2.4100E+09	0.00	0.00	[73]
383	$C_3H_5(A) + C_2H_5 = C_2H_6 + C_3H_4(A)$	9.6000E+08	0.00	-0.55	[73]
384	$C_3H_5(A) + C_3H_5(A) = C_3H_4(A) + C_3H_6$	8.4000E+07	0.00	-1.09	[73]
385	$C_3H_5(A) + H = C_3H_6^9$	$k_\infty = 2.0000E+11$ $k_0 = 1.3300E+54$	0.00 -12.00	0.00 24.87	[156]
386	$C_3H_5(A) + OH = C_2H_2 + CH_2O + H_2$	1.5000E+10	0.00	0.00	[172]
387	$C_3H_5(A) + HO_2 = C_3H_5O + OH$	4.4500E+09	0.00	0.00	[72]
388	$C_3H_5(A) + C_2H_4 = C_5H_8 + H$	1.2046E+07	0.00	48.02	[172]
389	$C_3H_5(A) + C_2H_2 = C_5H_6 + H$	4.0000E+10	0.00	90.00	[72]
390	$C_3H_5(A) + C_6H_4 = C_9H_8 + H$	2.0000E+10	0.00	90.00	[72]
391	$C_3H_5(S) + H = C_3H_4(A) + H_2$	1.8000E+10	0.00	0.00	[136]
392	$C_3H_5(S) + O = C_2H_2O + CH_3$	1.8000E+11	0.00	0.00	[73]
393	$C_3H_5(S) + O_2 = C_3H_4O + OH$	2.1700E+09	0.00	0.00	[133]
394	$C_3H_5(S) + CH_3 = C_3H_4(A) + CH_4$	1.0000E+08	0.00	0.00	[73]
395	$C_3H_5(S) + C_2H_3 = C_2H_4 + C_3H_4(A)$	1.0000E+08	0.00	0.00	[73]
396	$C_3H_5(S) + C_2H_5 = C_2H_6 + C_3H_4(A)$	1.0000E+08	0.00	0.00	[73]
397	$C_3H_5(S) + O_2 = CH_3CO + CH_2O$	2.1700E+09	0.00	0.00	[133]
398	$C_3H_5(T) + O_2 = CH_3CO + CH_2O$	2.1700E+09	0.00	0.00	[133]
399	$C_3H_5(T) + O_2 = C_3H_4O + OH$	2.1700E+09	0.00	0.00	[133]
400	$C_3H_5(T) + H = C_3H_4(A) + H_2$	1.8100E+10	0.00	0.00	[156]
401	$C_3H_5(T) + O = C_2HO + CH_3 + H$	1.8000E+11	0.00	0.00	[73]
402	$C_3H_5(T) + CH_3 = C_3H_4(A) + CH_4$	1.0000E+08	0.00	0.00	[73]
403	$C_3H_5(T) + C_2H_3 = C_2H_4 + C_3H_4(A)$	1.0000E+08	0.00	0.00	[73]
404	$C_3H_5(T) + C_2H_3 = C_5H_8(l)$	2.5000E+10	0.00	0.00	[173]
405	$C_3H_5(T) + C_2H_5 = C_2H_6 + C_3H_4(A)$	1.0000E+08	0.00	0.00	[73]
406	$C_3H_5(B) = C_3H_5(A)$	1.0000E+10	0.00	0.00	[136]
407	$C_3H_5(B) + H = C_3H_4(B) + H_2$	1.0000E+11	0.00	0.00	[136]
408	$C_3H_5(B) + OH = C_3H_4(B) + H_2O$	2.0000E+10	0.00	0.00	[136]
409	$C_3H_5(B) + O = C_3H_4(B) + OH$	3.6700E+10	0.00	0.00	[136]
410	$C_3H_5(B) + O = C_2H_4 + CHO$	1.1000E+11	0.00	0.00	[136]
411	$C_3H_6 + OH = CH_3CHO + CH_3$	3.4600E+08	0.00	0.00	[174]
412	$C_3H_6 + HO_2 = C_3H_5(A) + H_2O_2$	9.6400E+00	2.60	58.20	[156]
413	$C_3H_6 = C_2H_3 + CH_3^{10}$	$k_\infty = 1.1000E+21$ $k_0 = 2.0000E+11$	-1.20 0.00	408.84 0.00	[73]

No	Reaction	A	n	Ea	Ref
414	$C_3H_6 = C_3H_5(S) + H$	7.5900E+14	0.00	424.12	[73]
415	$C_3H_6 = C_3H_5(T) + H$	1.4500E+15	0.00	410.56	[73]
416	$C_3H_6 + H = C_3H_5(A) + H_2$	1.7200E+02	2.50	10.42	[172]
417	$C_3H_6 + H = C_3H_5(S) + H_2$	4.1000E+02	2.50	40.98	[172]
418	$C_3H_6 + H = C_3H_5(T) + H_2$	8.0360E+02	2.50	51.39	[172]
419	$C_3H_6 + O = C_2H_5 + CHO$	5.2170E+04	1.57	-2.63	[73]
420	$C_3H_6 + O = C_2H_4 + CH_2O$	3.4840E+04	1.57	-2.63	[73]
421	$C_3H_6 + O = CH_3 + CH_3 + CO$	6.9600E+04	1.57	-2.63	[73]
422	$C_3H_6 + OH = C_3H_5(A) + H_2O$	3.1000E+03	2.00	-1.25	[156]
423	$C_3H_6 + OH = C_3H_5(S) + H_2O$	4.1000E+09	0.00	28.87	[73]
424	$C_3H_6 + OH = C_3H_5(T) + H_2O$	4.1000E+09	0.00	28.87	[73]
425	$C_3H_6 + O_2 = C_3H_5(A) + HO_2$	1.9500E+09	0.00	163.28	[73]
426	$C_3H_6 + O_2 = C_3H_5(S) + HO_2$	2.0000E+10	0.00	199.29	[73]
427	$C_3H_6 + O_2 = C_3H_5(T) + HO_2$	2.0000E+10	0.00	184.22	[73]
428	$C_3H_6 + CH_3 = C_3H_5(A) + CH_4$	2.2100E-03	3.50	23.74	[73]
429	$C_3H_6 + CH_3 = C_3H_5(S) + CH_4$	8.4200E-04	3.50	48.77	[73]
430	$C_3H_6 + CH_3 = C_3H_5(T) + CH_4$	1.3510E-03	3.50	53.60	[73]
431	$C_3H_6 + C_2H_5 = C_3H_5(A) + C_2H_6$	2.2200E-03	3.50	27.77	[73]
432	$C_3H_6 + H = C_2H_4 + CH_3$	2.6000E+05	1.50	8.36	[175]
433	$C_3H_6 + HO_2 = C_3H_6O + OH$	1.2900E+09	0.00	62.38	[133]
434	$C_3H_6 + OH = C_3H_6OH$	2.7500E+09	0.00	-4.35	[133]
435	$C_3H_6 + H = C_3H_7(N)$	7.2300E+09	0.00	12.14	[73]
436	$C_3H_6(B) = C_3H_6$	8.0400E+14	0.00	267.50	[136]
437	$C_3H_6(B) + H = C_3H_5(B) + H_2$	1.6200E+11	0.00	49.00	[136]
438	$C_3H_6(B) + OH = C_3H_5(B) + H_2O$	7.0400E+04	1.50	4.33	[136]
439	$C_3H_6(B) + O = C_2H_6 + CO$	6.3000E+05	1.45	-3.59	[136]
440	$C_3H_7(N) + H = C_3H_6 + H_2$	1.8100E+09	0.00	0.00	[113]
441	$C_3H_7(N) + OH = C_3H_6 + H_2O$	2.4100E+10	0.00	0.00	[113]
442	$C_3H_7(N) + O = PC_3H_6O + H$	8.3000E+10	0.00	0.00	[136]
443	$C_3H_7(N) + O = CH_2O + C_2H_5$	1.4000E+10	0.00	0.00	[136]
444	$C_3H_7(N) + O_2 = C_3H_7OO(N)$	1.0000E+09	0.00	0.00	[176]
445	$C_3H_7(N) + H = C_3H_8$	2.0000E+10	0.00	0.00	[73]
446	$C_3H_7(N) + O_2 = C_3H_6 + HO_2$	1.0000E+09	0.00	20.91	[73]
447	$C_3H_7(N) = C_2H_4 + CH_3^{11}$	$k_{\infty} =$ 1.2300E+13 $k_0 =$ 5.4000E+46	-0.10 -12.00	126.37 149.65	[177]
448	$C_3H_7(I) + H = C_3H_8$	2.0000E+10	0.00	0.00	[73]

No	Reaction	A	n	Ea	Ref
449	$C_3H_7(l) + O_2 = C_3H_6 + HO_2$	1.0000E+09	0.00	12.50	[73]
450	$C_3H_7(l) = C_2H_4 + CH_3$	2.0000E+10	0.00	123.50	[73]
451	$C_3H_7(l) = C_3H_6 + H^{\cdot}$	8.7600E+07	1.76	148.57	[178]
	$k_{\infty} =$	2.6100E+14	0.00	118.06	
	$k_0 =$				
452	$C_3H_7(l) + O_2 = C_3H_7OO(l)$	6.6200E+09	0.00	0.00	[72]
453	$C_3H_7(l) + OH = C_3H_6 + H_2O$	2.4100E+10	0.00	0.00	[113]
454	$C_3H_7(l) + H = C_3H_6 + H_2$	3.6100E+09	0.00	0.00	[113]
455	$C_3H_7(l) + O = AC_3H_6O + H$	4.8200E+10	0.00	0.00	[113]
456	$C_3H_7(l) + O = CH_3CHO + CH_3$	4.8200E+10	0.00	0.00	[113]
457	$C_3H_8 + O_2 = C_3H_7(l) + HO_2$	3.9700E+10	0.00	199.54	[113]
458	$C_3H_8 + O_2 = C_3H_7(N) + HO_2$	3.9700E+10	0.00	212.84	[113]
459	$C_3H_8 = C_2H_5 + CH_3^{12}$	1.1000E+17	0.00	353.00	[73]
	$k_{\infty} =$	7.8220E+15	0.00	217.19	
	$k_0 =$				
460	$C_3H_8 + H = C_3H_7(N) + H_2$	1.3000E+11	0.00	40.60	[73]
461	$C_3H_8 + H = C_3H_7(l) + H_2$	1.0000E+11	0.00	34.90	[73]
462	$C_3H_8 + O = C_3H_7(N) + OH$	3.0000E+10	0.00	24.10	[73]
463	$C_3H_8 + O = C_3H_7(l) + OH$	2.6000E+10	0.00	18.70	[73]
464	$C_3H_8 + OH = C_3H_7(N) + H_2O$	5.7500E+05	1.40	3.55	[73]
465	$C_3H_8 + OH = C_3H_7(l) + H_2O$	4.7800E+05	1.40	3.55	[73]
466	$C_3H_8 + CH_3 = C_3H_7(N) + CH_4$	9.0300E-04	3.65	29.9	[113]
467	$C_3H_8 + CH_3 = C_3H_7(l) + CH_4$	1.5055E-03	3.46	22.9	[113]
468	$C_3H_2O = C_2H_2 + CO$	8.5100E+14	0.00	297.00	[73]
469	$C_3H_2O + O = CHO + C_2HO$	1.0000E+10	0.00	0.00	[73]
470	$C_3H_2O + OH = CHO + C_2H_2O$	1.0000E+10	0.00	0.00	[73]
471	$C_3H_3O = C_2H_3 + CO$	1.0000E+12	0.00	138.27	[133]
472	$C_3H_3O + H = C_3H_2O + H_2$	6.0000E+10	0.00	0.00	[133]
473	$C_3H_3O + O = C_3H_2O + OH$	7.8300E+10	0.00	0.00	[133]
474	$C_3H_4O = C_2H_3 + CHO$	1.0000E+14	0.00	422.00	[133]
475	$C_3H_4O + H = C_3H_3O + H_2$	3.9800E+10	0.00	17.58	[133]
476	$C_3H_4O + O = C_3H_3O + OH$	5.0000E+09	0.00	7.50	[133]
477	$C_3H_4O + OH = C_3H_3O + H_2O$	1.0000E+10	0.00	0.00	[133]
478	$C_3H_4O + HO_2 = C_3H_3O + H_2O_2$	1.6900E+09	0.00	44.80	[133]
479	$C_3H_5O = C_2H_2O + CH_3$	1.5100E+14	0.00	250.62	[133]
480	$C_3H_5O = C_2H_4 + CHO$	2.4500E+14	0.00	244.76	[133]
481	$C_3H_5O = C_2H_3 + CH_2O$	3.2400E+13	0.00	246.00	[133]
482	$C_3H_5O = PC_3H_5O$	1.8400E+14	0.00	244.76	[133]
483	$C_3H_5O = TC_3H_5O$	1.8400E+14	0.00	244.76	[133]

No	Reaction	A	n	Ea	Ref
484	$\text{PC}_3\text{H}_5\text{O} = \text{C}_2\text{H}_2\text{O} + \text{CH}_3$	8.0000E+13	0.00	125.52	[133]
485	$\text{TC}_3\text{H}_5\text{O} = \text{C}_2\text{H}_4 + \text{CHO}$	8.0000E+13	0.00	83.68	[133]
486	$\text{TC}_3\text{H}_5\text{O} + \text{O}_2 = \text{C}_3\text{H}_4\text{O} + \text{HO}_2$	1.7300E+08	0.00	7.32	[133]
487	$\text{AC}_3\text{H}_5\text{O} = \text{C}_2\text{H}_2\text{O} + \text{CH}_3$	8.0000E+13	0.00	108.78	[133]
488	$\text{C}_3\text{H}_6\text{O} = \text{C}_3\text{H}_5\text{O} + \text{H}$	8.0000E+14	0.00	383.92	[133]
489	$\text{C}_3\text{H}_6\text{O} = \text{CH}_3\text{CO} + \text{CH}_3$	8.0000E+15	0.00	384.92	[133]
490	$\text{C}_3\text{H}_6\text{O} + \text{H} = \text{C}_3\text{H}_5\text{O} + \text{H}_2$	5.0000E+09	0.00	6.27	[133]
491	$\text{C}_3\text{H}_6\text{O} + \text{OH} = \text{C}_3\text{H}_5\text{O} + \text{H}_2\text{O}$	2.0000E+10	0.00	12.80	[133]
492	$\text{C}_3\text{H}_6\text{O} + \text{O} = \text{C}_3\text{H}_5\text{O} + \text{OH}$	3.0000E+10	0.00	21.75	[133]
493	$\text{C}_3\text{H}_6\text{O} = \text{AC}_3\text{H}_6\text{O}$	1.0100E+14	0.00	250.62	[133]
494	$\text{C}_3\text{H}_6\text{O} = \text{PC}_3\text{H}_6\text{O}$	1.8400E+14	0.00	244.76	[133]
495	$\text{C}_3\text{H}_6\text{O} + \text{HO}_2 = \text{C}_3\text{H}_5\text{O} + \text{H}_2\text{O}_2$	3.2400E+08	0.00	62.34	[133]
496	$\text{AC}_3\text{H}_6\text{O} + \text{M} = \text{CH}_3\text{CO} + \text{CH}_3 + \text{M}$	2.4800E+16	0.00	340.57	[133]
497	$\text{AC}_3\text{H}_6\text{O} + \text{H} = \text{AC}_3\text{H}_5\text{O} + \text{H}_2$	2.0000E+11	0.00	37.65	[133]
498	$\text{AC}_3\text{H}_6\text{O} + \text{OH} = \text{AC}_3\text{H}_5\text{O} + \text{H}_2\text{O}$	1.0200E+09	0.00	4.98	[133]
499	$\text{AC}_3\text{H}_6\text{O} + \text{O} = \text{AC}_3\text{H}_5\text{O} + \text{OH}$	1.0000E+10	0.00	24.94	[133]
500	$\text{AC}_3\text{H}_6\text{O} + \text{CH}_3 = \text{AC}_3\text{H}_5\text{O} + \text{CH}_4$	5.0000E+09	0.00	33.47	[133]
501	$\text{PC}_3\text{H}_6\text{O} + \text{M} = \text{C}_2\text{H}_5 + \text{CHO} + \text{M}$	7.2500E+16	0.00	344.76	[133]
502	$\text{PC}_3\text{H}_6\text{O} + \text{M} = \text{CH}_3\text{CO} + \text{CH}_3 + \text{M}$	4.7800E+16	0.00	351.46	[133]
503	$\text{PC}_3\text{H}_6\text{O} + \text{H} = \text{PC}_3\text{H}_5\text{O} + \text{H}_2$	1.0000E+11	0.00	37.65	[133]
504	$\text{PC}_3\text{H}_6\text{O} + \text{H} = \text{TC}_3\text{H}_5\text{O} + \text{H}_2$	1.0000E+11	0.00	37.65	[133]
505	$\text{PC}_3\text{H}_6\text{O} + \text{O} = \text{PC}_3\text{H}_5\text{O} + \text{OH}$	5.6800E+09	0.00	6.45	[133]
506	$\text{PC}_3\text{H}_6\text{O} + \text{O} = \text{TC}_3\text{H}_5\text{O} + \text{OH}$	5.6800E+09	0.00	6.45	[133]
507	$\text{PC}_3\text{H}_6\text{O} + \text{OH} = \text{PC}_3\text{H}_5\text{O} + \text{H}_2\text{O}$	1.2100E+10	0.00	0.00	[133]
508	$\text{PC}_3\text{H}_6\text{O} + \text{OH} = \text{TC}_3\text{H}_5\text{O} + \text{H}_2\text{O}$	1.2100E+10	0.00	0.00	[133]
509	$\text{PC}_3\text{H}_6\text{O} + \text{CH}_3 = \text{PC}_3\text{H}_5\text{O} + \text{CH}_4$	5.0000E+09	0.00	33.47	[133]
510	$\text{PC}_3\text{H}_6\text{O} + \text{CH}_3 = \text{TC}_3\text{H}_5\text{O} + \text{CH}_4$	5.0000E+09	0.00	33.47	[133]
511	$\text{C}_3\text{H}_6\text{OH} = \text{C}_2\text{H}_5 + \text{CH}_2\text{O}$	1.4100E+09	0.00	72.00	[133]
512	$\text{C}_3\text{H}_6\text{OH} = \text{CH}_3\text{CHO} + \text{CH}_3$	1.0000E+09	0.00	72.00	[133]
513	$\text{C}_3\text{H}_6\text{OH} + \text{O}_2 = \text{CH}_3\text{CHO} + \text{CH}_2\text{O} + \text{OH}$	1.0000E+09	0.00	-4.60	[133]
514	$\text{C}_3\text{H}_6\text{OOH} = \text{C}_3\text{H}_6\text{O} + \text{OH}$	3.9800E+15	0.00	179.91	[179]
515	$\text{C}_3\text{H}_7\text{O}(\text{N}) + \text{O}_2 = \text{C}_3\text{H}_6\text{O} + \text{HO}_2$	3.1600E+08	0.00	16.73	[180]
516	$\text{C}_3\text{H}_7\text{O}(\text{N}) + \text{O}_2 = \text{PC}_3\text{H}_6\text{O} + \text{HO}_2$	3.1600E+08	0.00	16.73	[180]
517	$\text{C}_3\text{H}_7\text{O}(\text{N}) = \text{C}_2\text{H}_5 + \text{CH}_2\text{O}$	3.9800E+14	0.00	71.96	[180]
518	$\text{C}_3\text{H}_7\text{O}(\text{I}) + \text{O}_2 = \text{PC}_3\text{H}_6\text{O} + \text{HO}_2$	3.1600E+08	0.00	16.73	[180]

No	Reaction	A	n	Ea	Ref
519	$C_3H_7O(l) + O_2 = AC_3H_6O + HO_2$	3.1600E+08	0.00	16.73	[180]
520	$C_3H_7O(l) = CH_3CHO + CH_3$	3.9800E+14	0.00	71.96	[180]
521	$C_3H_7OO(l) = CH_3CHO + CH_3O$	1.0000E+13	0.00	104.60	[180]
522	$C_3H_7OO(l) + C_3H_8 = C_3H_7OOH(l) + C_3H_7(l)$	1.0000E+09	0.00	71.54	[180]
523	$C_3H_7OO(l) + C_3H_8 = C_3H_7OOH(l) + C_3H_7(N)$	1.0000E+09	0.00	81.16	[180]
524	$C_3H_7OO(l) + CH_3CHO = C_3H_7OOH(l) + CH_3CO$	1.0000E+09	0.00	37.65	[180]
525	$C_3H_7OO(N) = C_3H_6OOH$	1.2500E+12	0.00	158.99	[180]
526	$C_3H_7OO(N) + C_3H_8 = C_3H_7OOH(N) + C_3H_7(N)$	1.0000E+09	0.00	81.16	[180]
527	$C_3H_7OO(N) + C_3H_8 = C_3H_7OOH(N) + C_3H_7(l)$	1.0000E+09	0.00	71.54	[180]
528	$C_3H_7OO(N) + CH_3CHO = C_3H_7OOH(N) + CH_3CO$	1.0000E+09	0.00	37.65	[180]
529	$C_3H_7OOH(N) = C_3H_7O(N) + OH$	3.9800E+15	0.00	179.91	[180]
530	$C_3H_7OOH(l) = C_3H_7O(l) + OH$	3.9800E+15	0.00	179.91	[180]
531	$C_4H + C_2H_2 = C_6H_2 + H$	1.2000E+11	0.00	0.00	[73]
532	$C_4H + C_4H_2 = C_8H_2 + H$	1.2000E+11	0.00	0.00	[73]
533	$C_4H + H_2 = C_4H_2 + H$	4.0740E+02	2.40	0.84	[73]
534	$C_4H_2 = C_4H + H$	7.8000E+14	0.00	502.40	[73]
535	$C_4H_2 + O = C_3H_2 + CO$	9.0000E+08	0.00	0.00	[73]
536	$C_4H_2 + OH = C_4H_2O + H$	6.6900E+09	0.00	-1.71	[73]
537	$C_4H_2 + C_2H = C_6H_2 + H$	1.2000E+11	0.00	0.00	[73]
538	$C_4H_2 + C_4H_2 = C_8H_2 + H + H$	1.5000E+11	0.00	234.50	[73]
539	$C_4H_2 + C_2H_2 = C_6H_2 + H + H$	1.5000E+11	0.00	234.50	[73]
540	$C_4H_2 + CH_2(S) = C_5H_3(L) + H$	3.0000E+10	0.00	0.00	[73]
541	$C_4H_2 + CH_2(T) = C_5H_3(L) + H$	7.0000E+10	0.00	0.00	[73]
542	$C_4H_2 + CH = C_5H_2 + H$	8.0000E+10	0.00	0.00	[133]
543	$C_4H_3(N) = C_4H_2 + H$	1.0000E+14	0.00	150.72	[73]
		$k_{\infty} =$ $k_0 =$ 1.0000E+10	0.00	125.50	
544	$C_4H_3(N) + H = C_4H_2 + H_2$	8.1300E+10	0.00	0.00	[73]
545	$C_4H_3(N) + OH = C_4H_2 + H_2O$	3.0000E+10	0.00	0.00	[73]
546	$C_4H_3(N) + C_2H_2 = C_6H_5(B)$	4.1200E+03	1.65	10.46	[73]
547	$C_4H_3(N) + CH = C_5H_3(L) + H$	1.6000E+11	0.00	0.00	[133]
548	$C_4H_3(N) + CH_2(S) = C_5H_4(L) + H$	1.6000E+11	0.00	0.00	[133]
549	$C_4H_3(N) + CH_2(T) = C_5H_4(L) + H$	1.6000E+11	0.00	0.00	[133]
550	$C_4H_3(l) + CH = C_5H_3(L) + H$	1.6000E+11	0.00	0.00	[133]
551	$C_4H_3(l) + CH_2(T) = C_5H_4(L) + H$	1.6000E+11	0.00	0.00	[133]
552	$C_4H_3(l) + CH_2(S) = C_5H_4(L) + H$	1.6000E+11	0.00	0.00	[133]
553	$C_4H_3(l) = C_4H_3(N)$	1.5000E+13	0.00	284.45	[73]

No	Reaction		A	n	Ea	Ref
554	$C_4H_3(l) = C_4H_2 + H$	$k_\infty =$ $k_0 =$	1.0000E+14 1.0000E+11	0.00 0.00	150.62 125.50	[73]
555	$C_4H_3(l) + H = C_4H_2 + H_2$		8.1300E+10	0.00	0.00	[73]
556	$C_4H_3(l) + O = C_4H_2 + OH$		2.0000E+10	0.00	0.00	[73]
557	$C_4H_3(l) + OH = C_4H_2 + H_2O$		3.0000E+10	0.00	0.00	[73]
558	$C_4H_3(l) + O_2 = C_4H_2 + HO_2$		1.0000E+09	0.00	12.55	[73]
559	$C_4H_4 + CH_2(S) = C_5H_6$		7.0000E+10	0.00	0.00	[133]
560	$C_4H_4 + CH_2(T) = C_5H_6$		7.0000E+10	0.00	0.00	[133]
561	$C_4H_4 + C_2H_3 = C_6H_6 + H$		1.9000E+09	0.00	10.50	[136]
562	$C_4H_4 + CH = C_5H_5$		8.0000E+10	0.00	0.00	[133]
563	$C_4H_4 + CH_3 = C_5H_7(l)$		2.5000E+10	0.00	0.00	[173]
564	$C_4H_4 = C_4H_3(l) + H$		8.6300E+09	0.00	246.86	[73]
565	$C_4H_4 + H = C_4H_3(N) + H_2$		2.0000E+04	2.00	25.17	[73]
566	$C_4H_4 + O = C_3H_4(A) + CO$		2.9500E+09	0.00	0.00	[181]
567	$C_4H_4 + OH = C_4H_3(N) + H_2O$		1.0000E+04	2.00	12.60	[73]
568	$C_4H_4 + C_2H = C_4H_3(l) + C_2H_2$		3.9800E+10	0.00	0.00	[73]
569	$C_4H_5(S) = C_4H_4 + H$	$k_\infty =$ $k_0 =$	1.0000E+14 2.0000E+12	0.00 0.00	209.20 175.73	[73]
570	$C_4H_5(S) + H = C_4H_4 + H_2$		1.0000E+11	0.00	0.00	[73]
571	$C_4H_5(S) + OH = C_4H_4 + H_2O$		2.0000E+04	2.00	4.18	[73]
572	$C_4H_5(S) = C_4H_5(T)$		1.5000E+13	0.00	283.45	[73]
573	$C_4H_5(S) + O_2 = C_3H_3O + CH_2O$		4.1500E+07	0.00	10.50	[133]
574	$C_4H_5(S) + O = C_2H_2O + C_2H_3$		1.8070E+11	0.00	0.00	[133]
575	$C_4H_5(T) = C_4H_4 + H$	$k_\infty =$ $k_0 =$	1.0000E+14 1.0000E+11	0.00 0.00	154.90 125.50	[73]
576	$C_4H_5(T) = C_2H_3 + C_2H_2$		1.0000E+14	0.00	183.75	[13]
577	$C_4H_5(T) + O_2 = YC_4H_5O + O$		3.0000E+08	0.29	0.04	[182]
578	$C_4H_5(T) + H = C_4H_4 + H_2$		1.0000E+11	0.00	0.00	[73]
579	$C_4H_5(T) + OH = C_4H_4 + H_2O$		2.0000E+04	2.00	4.18	[73]
580	$C_4H_5(T) + O_2 = CH_3CO + C_2H_2O$		2.0000E+09	0.00	0.00	[136]
581	$C_4H_5(T) + O_2 = C_3H_4O + CHO$		5.0000E+08	0.00	0.00	[133]
582	$C_4H_5(T) + O = C_3H_4(A) + CHO$		1.8070E+11	0.00	0.00	[133]
583	$C_4H_5(T) + O_2 = C_4H_4O + OH$		5.0000E+08	0.00	0.00	[133]
584	$C_4H_5(T) + O_2 = C_4H_4 + HO_2$		1.0000E+10	0.00	0.00	[72]
585	$C_4H_5(T) + HO_2 = C_3H_4(A) + CHO + OH$		8.9100E+09	0.00	0.00	[133]
586	$C_4H_5(T) + C_3H_4(A) = C_7H_8 + H$		2.0000E+08	0.00	15.48	[183]
587	$C_4H_5(T) + C_3H_4(P) = C_7H_8 + H$		3.1600E+08	0.00	15.48	[184]
588	$C_4H_5(T) + C_4H_2 = C_8H_6 + H$		1.0000E+10	0.00	0.00	[72]



No	Reaction	A	n	Ea	Ref
589	$C_4H_5(T) + C_2H_2 = C_6H_7(L)$	1.7250E+03	1.79	9.37	[73]
590	$C_4H_5(T) + C_4H_4 = C_8H_8 + H$	3.1600E+08	0.00	2.51	[184]
591	$C_4H_5(l) + O_2 = C_4H_4 + HO_2$	1.0000E+09	0.00	0.00	[72]
592	$C_4H_5(l) + O_2 = CH_3CO + C_2H_2O$	4.1500E+07	0.00	10.50	[133]
593	$C_4H_5(l) + O = C_2H_2O + C_2H_3$	1.8070E+11	0.00	0.00	[133]
594	$C_4H_5(l) = C_4H_5(T)$	1.5000E+13	0.00	283.45	[73]
595	$C_4H_5(l) = C_4H_4 + H$	$k_{\infty} = 1.0000E+14$ $k_0 = 2.0000E+12$	0.00 0.00	209.34 175.73	[73]
596	$C_4H_5(l) + H = C_4H_4 + H_2$	1.0000E+11	0.00	0.00	[73]
597	$C_4H_5(l) + OH = C_4H_4 + H_2O$	2.0000E+04	2.00	4.18	[73]
598	$C_4H_6(T) + C_2H_3 = C_6H_8 + H$	5.6000E+08	0.00	6.90	[133]
599	$C_4H_6(T) = C_4H_5(l) + H$	4.4000E+15	0.00	397.92	[73]
600	$C_4H_6(T) + H = C_4H_5(T) + H_2$	6.3000E+07	0.70	25.10	[73]
601	$C_4H_6(T) + H = C_2H_4 + C_2H_3$	2.0000E+10	0.00	20.92	[185]
602	$C_4H_6(T) + OH = C_4H_5(T) + H_2O$	2.0000E+04	2.00	20.93	[120]
603	$C_4H_6(T) + O_2 = C_4H_5(T) + HO_2$	4.0000E+10	0.00	242.00	[73]
604	$C_4H_6(T) + C_2H_3 = C_4H_5(T) + C_2H_4$	6.3100E+10	0.00	60.70	[73]
605	$C_4H_6(T) + C_3H_3 = C_4H_5(T) + C_3H_4(A)$	2.0000E+09	0.00	75.31	[72]
606	$C_4H_6(T) + C_3H_3 = C_4H_5(T) + C_3H_4(P)$	1.0000E+10	0.00	75.31	[133]
607	$C_4H_6(T) + H = C_3H_4(A) + CH_3$	6.0000E+09	0.00	29.71	[133]
608	$C_4H_6(T) + OH = C_3H_5(A) + CH_2O$	2.8100E+09	0.00	-3.66	[133]
609	$C_4H_6(T) + OH = C_3H_4O + CH_3$	2.8100E+09	0.00	-3.66	[133]
610	$C_4H_6(T) + OH = CH_3CO + C_2H_4$	2.8100E+09	0.00	-3.66	[133]
611	$C_4H_6(T) + O = C_2H_2O + C_2H_4$	1.0000E+09	0.00	0.00	[72]
612	$C_4H_6(T) + O = C_3H_4(P) + CH_2O$	1.0000E+09	0.00	0.00	[72]
613	$C_4H_6(T) + HO_2 = C_3H_4O + CH_2O + H$	1.3000E+09	0.00	62.60	[133]
614	$C_4H_6(T) + O = C_4H_5(T) + OH$	2.2700E+12	-0.48	29.42	[186]
615	$C_4H_6(T) = C_4H_5(T) + H$	7.0000E+14	0.00	397.46	[185]
616	$C_4H_6(T) + O_2 = C_4H_5(l) + HO_2$	1.4000E+09	0.00	211.85	[186]
617	$C_4H_6(T) + O = C_4H_5(l) + OH$	4.5300E+12	-0.47	29.42	[186]
618	$C_4H_6(T) + OH = C_4H_5(l) + H_2O$	3.1000E+03	2.00	1.80	[182]
619	$C_4H_6(T) + H = C_4H_5(l) + H_2$	6.6500E+02	2.53	38.68	[119]
620	$C_4H_6(T) + O = XC_4H_5O + H$	1.5000E+05	1.45	-3.60	[182]
621	$C_4H_6(T) = C_4H_6(M)$	2.1000E+13	0.00	304.29	[147]
622	$C_4H_6(T) = C_4H_6(S)$	2.1877E+75	-17.56	484.45	[147]
623	$C_4H_6(T) = C_4H_6(B)$	2.1878E+11	-17.56	484.46	[147]

No	Reaction	A	n	Ea	Ref
624	$C_4H_6(S) = C_4H_6(M)$	7.0000E+12	0.00	263.72	[147]
625	$C_4H_6(S) = C_3H_3 + CH_3$	2.0000E+11	0.00	248.95	[133]
626	$C_4H_6(S) = C_4H_5(l) + H$	4.2000E+15	0.00	387.10	[73]
627	$C_4H_6(S) + H = C_2H_3 + C_2H_4$	4.0000E+08	0.00	0.00	[73]
628	$C_4H_6(S) + H = C_4H_5(S) + H_2$	1.0000E+11	0.00	60.71	[73]
629	$C_4H_6(S) + OH = C_4H_5(S) + H_2O$	1.6200E+10	0.00	0.00	[73]
630	$C_4H_6(S) + CH_3 = C_4H_5(S) + CH_4$	7.0000E+10	0.00	25.00	[73]
631	$C_4H_6(S) + C_3H_3 = C_4H_5(S) + C_3H_4(A)$	1.0000E+10	0.00	25.00	[133]
632	$C_4H_6(S) + C_3H_3 = C_4H_5(S) + C_3H_4(P)$	1.0000E+10	0.00	25.00	[133]
633	$C_4H_6(S) + H = C_3H_4(A) + CH_3$	6.0000E+09	0.00	8.78	[133]
634	$C_4H_6(S) + O = C_3H_3O + CH_3$	3.5800E+09	0.00	0.00	[133]
635	$C_4H_6(B) = C_4H_6(S)$	3.0000E+13	0.00	183.00	[73]
636	$C_4H_6(B) = C_4H_6(M)$	5.2500E+12	0.00	158.00	[73]
637	$C_4H_6(B) = C_2H_4 + C_2H_2$	1.4000E+15	0.00	301.79	[147]
638	$C_4H_6(M) + H = C_3H_4(P) + CH_3$	6.5000E+01	2.50	4.18	[133]
639	$C_4H_6(M) + O = C_3H_6 + CO$	6.0000E+10	0.00	7.48	[133]
640	$C_4H_6(F) = C_4H_6(S)$	2.5000E+13	0.00	271.96	[133]
641	$C_4H_6(F) + H = C_3H_4(A) + CH_3$	1.3000E+02	2.50	4.18	[133]
642	$C_4H_6(F) + H = C_2H_5 + C_2H_2$	6.5000E+01	2.50	4.18	[133]
643	$C_4H_6(F) = C_3H_3 + CH_3$	3.0000E+13	0.00	317.14	[133]
644	$C_4H_6(F) + O = C_3H_6 + CO$	2.0000E+10	0.00	6.94	[133]
645	$C_4H_7(N) + O_2 = C_4H_6(T) + HO_2$	1.0000E+08	0.00	0.00	[187]
646	$C_4H_7(N) = C_2H_4 + C_2H_3$	5.0000E+13	0.00	159.10	[186]
647	$C_4H_7(N) + H = C_4H_6(T) + H_2$	3.1600E+09	0.00	0.00	[72]
648	$C_4H_7(N) = C_4H_6(T) + H$	2.4800E+53	-12.30	217.57	[186]
649	$C_4H_7(N) + OH = C_4H_6(T) + H_2O$	4.0000E+10	0.00	0.00	[72]
650	$C_4H_7(N) + O = C_4H_6(T) + OH$	4.0000E+10	0.00	0.00	[72]
651	$C_4H_7(N) + H = C_4H_8(N)^{t,13}$	$k_{\infty} = 3.6000E+10$ $k_0 = 3.0100E+42$	0.00 -9.32	0.00 24.41	[131]
652	$C_4H_7(l) + HO_2 = C_4H_7O(X) + OH$	4.5000E+09	0.00	0.00	[173]
653	$C_4H_7(l) + CH_3OO = C_4H_7O(X) + CH_3O$	2.0000E+09	0.00	-5.02	[173]
654	$C_4H_7(l) = C_3H_4(A) + CH_3$	2.0000E+13	0.00	209.52	[188]
655	$C_4H_7(l) + CH_3 = C_5H_{10}(A)$	7.0000E+09	0.00	0.00	[173]
656	$C_4H_7(l) + C_4H_7(l) = C_3H_4(A) + C_5H_{10}(A)$	5.0000E+07	0.00	26.35	[173]
657	$C_4H_7(S) + H = C_4H_6(S) + H_2$	3.1600E+09	0.00	0.00	[186]
658	$C_4H_7(S) + OH = C_4H_6(S) + H_2O$	4.0000E+10	0.00	0.00	[186]

No	Reaction	A	n	Ea	Ref
659	$C_4H_7(S) + O = C_4H_6(S) + OH$	4.0000E+10	0.00	0.00	[186]
660	$C_4H_8(l) + CH_3 = C_5H_{11}(T)$	1.7000E+08	0.00	267.77	[173]
661	$C_4H_8(l) + CH_3 = C_5H_{10}(B) + H$	1.5500E+04	1.86	59.33	[173]
662	$C_4H_8(l) = C_3H_5(T) + CH_3$	3.3000E+21	-1.20	408.86	[173]
663	$C_4H_8(l) = C_4H_7(l) + H$	1.0600E+47	-9.30	437.44	[173]
664	$C_4H_8(l) + O_2 = C_4H_7(l) + HO_2$	1.4400E+10	0.00	161.21	[173]
665	$C_4H_8(l) + HO_2 = C_4H_7(l) + H_2O_2$	3.0000E+08	0.00	59.37	[173]
666	$C_4H_8(l) + HO_2 = C_4H_8O(X) + OH$	1.0200E+09	0.00	62.60	[173]
667	$C_4H_8(l) + OH = C_4H_7(l) + H_2O$	6.0000E+03	2.00	-0.25	[173]
668	$C_4H_8(l) + OH = C_4H_8OH(l)$	3.4000E+20	-3.58	8.71	[173]
669	$C_4H_8(l) + O = C_4H_7(l) + OH$	3.0000E+05	1.28	-4.51	[173]
670	$C_4H_8(l) + O = C_3H_7(l) + CHO$	5.0000E+05	1.28	-4.51	[173]
671	$C_4H_8(l) + O = C_4H_8O(X)$	1.0000E+05	1.28	-4.51	[173]
672	$C_4H_8(l) + H = C_4H_7(l) + H_2$	1.7200E+11	0.00	33.47	[173]
673	$C_4H_8(l) + H = C_3H_6 + CH_3$	1.7200E+10	0.00	15.06	[173]
674	$C_4H_8(l) + CH_3 = C_4H_7(l) + CH_4$	4.4200E-03	3.50	18.49	[173]
675	$C_4H_8(l) + CHO = C_4H_7(l) + CH_2O$	3.3000E+08	0.00	25.98	[173]
676	$C_4H_8(l) + C_2H_3 = C_4H_7(l) + C_2H_4$	1.0000E+10	0.00	54.39	[173]
677	$C_4H_8(l) + C_3H_5(A) = C_4H_7(l) + C_3H_6$	7.9400E+08	0.00	85.77	[173]
678	$C_4H_8(l) + C_3H_5(S) = C_4H_7(l) + C_3H_6$	7.9400E+08	0.00	85.77	[173]
679	$C_4H_8(l) + C_3H_5(T) = C_4H_7(l) + C_3H_6$	7.9400E+08	0.00	85.77	[173]
680	$C_4H_8(l) + CH_3OO = C_4H_8O(X) + CH_3O$	4.0000E+08	0.00	50.20	[173]
681	$C_4H_8(N) + O_2 = C_4H_7(N) + HO_2$	1.4400E+10	0.00	250.21	[72]
682	$C_4H_8(N) + HO_2 = C_4H_7(N) + H_2O_2$	3.0000E+08	0.00	148.34	[72]
683	$C_4H_8(N) = C_3H_5(A) + CH_3$	1.0000E+16	0.00	305.42	[13]
684	$C_4H_8(N) + OH = C_4H_7(N) + H_2O$	6.0000E+03	2.00	-0.25	[72]
685	$C_4H_8(N) + O = C_4H_7(N) + OH$	3.0000E+05	1.28	-4.51	[72]
686	$C_4H_8(N) + O = C_3H_7(N) + CHO$	5.0000E+05	1.28	-4.51	[72]
687	$C_4H_8(N) + H = C_4H_7(N) + H_2$	1.7200E+11	0.00	88.47	[72]
688	$C_4H_8(N) + H = C_3H_6 + CH_3$	1.7200E+10	0.00	32.06	[72]
689	$C_4H_8(N) + CH_3 = C_4H_7(N) + CH_4$	4.4200E-03	3.50	73.49	[72]
690	$C_4H_8(N) + CHO = C_4H_7(N) + CH_2O$	3.3000E+08	0.00	80.98	[72]
691	$C_4H_8(N) + C_2H_3 = C_4H_7(N) + C_2H_4$	1.0000E+10	0.00	109.92	[72]
692	$C_4H_8(N) + C_3H_5(A) = C_4H_7(N) + C_3H_6$	7.9400E+08	0.00	140.77	[72]
693	$C_4H_8(N) + C_3H_5(S) = C_4H_7(N) + C_3H_6$	7.9400E+08	0.00	140.77	[72]

No	Reaction	A	n	Ea	Ref
694	$C_4H_8(N) + C_3H_5(T) = C_4H_7(N) + C_3H_6$	7.9400E+08	0.00	140.77	[72]
695	$C_4H_8(S) + O_2 = C_4H_7(S) + HO_2$	1.4400E+10	0.00	250.21	[72]
696	$C_4H_8(S) + HO_2 = C_4H_7(S) + H_2O_2$	3.0000E+08	0.00	148.37	[72]
697	$C_4H_8(S) = C_4H_7(S) + H$	3.9800E+15	0.00	356.05	[13]
698	$C_4H_8(S) = C_3H_5(S) + CH_3$	3.1600E+17	0.00	415.45	[13]
699	$C_4H_8(S) + OH = C_4H_7(S) + H_2O$	6.0000E+03	2.00	-0.25	[72]
700	$C_4H_8(S) + O = C_4H_7(S) + OH$	3.0000E+05	1.28	-4.51	[72]
701	$C_4H_8(S) + O = C_3H_7(l) + CHO$	5.0000E+05	1.28	-4.51	[72]
702	$C_4H_8(S) + H = C_4H_7(S) + H_2$	1.7200E+11	0.00	88.47	[72]
703	$C_4H_8(S) + H = C_3H_6 + CH_3$	1.7200E+10	0.00	32.06	[72]
704	$C_4H_8(S) + CH_3 = C_4H_7(S) + CH_4$	4.4200E-03	3.50	73.49	[72]
705	$C_4H_8(S) + CHO = C_4H_7(S) + CH_2O$	3.3000E+08	0.00	80.98	[72]
706	$C_4H_8(S) + C_2H_3 = C_4H_7(S) + C_2H_4$	1.0000E+10	0.00	109.92	[72]
707	$C_4H_8(S) + C_3H_5(A) = C_4H_7(S) + C_3H_6$	7.9400E+08	0.00	140.77	[72]
708	$C_4H_8(S) + C_3H_5(S) = C_4H_7(S) + C_3H_6$	7.9400E+08	0.00	140.77	[72]
709	$C_4H_8(S) + C_3H_5(T) = C_4H_7(S) + C_3H_6$	7.9400E+08	0.00	140.77	[72]
710	$C_4H_9(S) = C_3H_6 + CH_3$ <sup>14</sup>	2.6700E+10 2.3000E+60	1.06 -14.30	129.47 153.80	[189]
711	$C_4H_9(S) = C_4H_8(S) + H$	3.1600E+12	0.00	154.38	[13]
712	$C_4H_9(S) = C_4H_8(N) + H$	1.5800E+13	0.00	165.67	[13]
713	$C_4H_9(S) + O_2 = C_4H_8(N) + HO_2$	5.1100E+07	0.00	0.00	[190]
714	$C_4H_9(S) + O_2 = C_4H_8(S) + HO_2$	7.8000E+07	0.00	0.00	[190]
715	$C_4H_9(S) + OH = C_4H_8(N) + H_2O$	1.8000E+10	0.00	0.00	[72]
716	$C_4H_9(S) + OH = C_4H_8(S) + H_2O$	1.8000E+10	0.00	0.00	[72]
717	$C_4H_9(S) + H = C_4H_8(N) + H_2$	5.4000E+09	0.00	0.00	[72]
718	$C_4H_9(S) + H = C_4H_8(S) + H_2$	5.4000E+09	0.00	0.00	[72]
719	$C_4H_9(S) + O = C_4H_8(N) + OH$	4.1600E+11	0.00	0.00	[72]
720	$C_4H_9(S) + O = C_4H_8(S) + OH$	4.1600E+11	0.00	0.00	[72]
721	$C_4H_9(S) + CH_3 = C_4H_8(N) + CH_4$	1.2600E+10	0.00	-2.49	[72]
722	$C_4H_9(S) + CH_3 = C_4H_8(S) + CH_4$	1.2600E+10	0.00	-2.49	[72]
723	$C_4H_9(l) = C_3H_6 + CH_3$	2.0000E+13	0.00	125.31	[72]
724	$C_4H_9(l) = C_4H_8(l) + H$	1.9100E+29	-5.24	166.34	[72]
725	$C_4H_9(l) + O_2 = C_4H_8(l) + HO_2$	2.4000E+07	0.00	0.00	[72]
726	$C_4H_9(l) + HO_2 = C_3H_7(l) + CH_2O + OH$	2.4100E+10	0.00	0.00	[72]
727	$C_4H_9(T) = C_4H_8(l) + H$	2.9000E+51	-11.53	220.16	[173]
728	$C_4H_9(T) + CH_3OO = AC_3H_6O + CH_3 + CH_3O$	1.3000E+10	0.00	0.00	[147]

No	Reaction	A	n	Ea	Ref
729	$C_4H_9(T) = C_3H_6 + CH_3$	3.0000E+14	0.00	193.71	[173]
730	$C_4H_9(T) + O_2 = C_4H_8(I) + HO_2$	4.8000E+08	0.00	0.00	[173]
731	$C_4H_9(T) + HO_2 = AC_3H_6O + CH_3 + OH$	1.8000E+10	0.00	0.00	[173]
732	$C_4H_9(T) + OH = C_4H_8(I) + H_2O$	1.8000E+10	0.00	0.00	[173]
733	$C_4H_9(T) + H = C_4H_8(I) + H_2$	5.4000E+09	0.00	0.00	[173]
734	$C_4H_9(T) + O = C_4H_8(I) + OH$	4.1600E+11	0.00	0.00	[173]
735	$C_4H_9(T) + O = AC_3H_6O + CH_3$	1.0400E+11	0.00	0.00	[173]
736	$C_4H_9(T) + CH_3 = C_4H_8(I) + CH_4$	1.2600E+10	0.00	-2.49	[173]
737	$C_4H_9(N) + OH = C_4H_8(N) + H_2O$	1.8000E+10	0.00	0.00	[72]
738	$C_4H_9(N) = C_3H_6 + CH_3$	1.2600E+12	0.00	113.38	[191]
739	$C_4H_9(N) = C_4H_8(N) + H$	1.0000E+14	0.00	160.24	[13]
740	$C_4H_9(N) + O_2 = C_4H_8(N) + HO_2$	2.7000E+08	0.00	0.00	[190]
741	$C_4H_9(N) + H = C_4H_8(N) + H_2$	5.4000E+09	0.00	0.00	[72]
742	$C_4H_9(N) + O = C_4H_8(N) + OH$	4.1600E+11	0.00	0.00	[72]
743	$C_4H_9(N) + CH_3 = C_4H_8(N) + CH_4$	1.2600E+10	0.00	-2.49	[72]
744	$C_4H_{10}(I) = C_3H_7(I) + CH_3$	1.1000E+26	-2.61	377.98	[192]
745	$C_4H_{10}(I) + H = C_4H_9(I) + H_2$	1.8100E+03	2.54	28.26	[192]
746	$C_4H_{10}(I) + H = C_4H_9(T) + H_2$	6.0200E+02	2.40	10.80	[192]
747	$C_4H_{10}(I) + OH = C_4H_9(I) + H_2O$	2.2900E+05	1.53	3.24	[192]
748	$C_4H_{10}(I) + OH = C_4H_9(T) + H_2O$	5.7300E+07	0.51	0.26	[192]
749	$C_4H_{10}(I) + O = C_4H_9(I) + OH$	4.2800E+02	2.50	15.24	[192]
750	$C_4H_{10}(I) + O = C_4H_9(T) + OH$	1.5600E+02	2.50	4.65	[192]
751	$C_4H_{10}(I) + HO_2 = C_4H_9(I) + H_2O_2$	3.0100E+01	2.55	64.85	[192]
752	$C_4H_{10}(I) + HO_2 = C_4H_9(T) + H_2O_2$	3.6100E+00	2.55	44.06	[192]
753	$C_4H_{10}(N) = C_4H_9(N) + H$	1.5800E+16	0.00	410.00	[13]
754	$C_4H_{10}(N) = C_4H_9(S) + H$	1.0000E+16	0.00	397.46	[13]
755	$C_4H_{10}(N) = C_3H_7(N) + CH_3$	1.0000E+17	0.00	354.37	[13]
756	$C_4H_{10}(N) + H = C_4H_9(N) + H_2$	5.6200E+04	2.00	32.21	[193]
757	$C_4H_{10}(N) + H = C_4H_9(S) + H_2$	2.0000E+11	0.00	34.90	[194]
758	$C_4H_{10}(N) + OH = C_4H_9(N) + H_2O$	4.1300E+04	1.73	3.15	[194]
759	$C_4H_{10}(N) + OH = C_4H_9(S) + H_2O$	2.5700E+06	1.25	2.92	[2]
760	$C_4H_{10}(N) + O = C_4H_9(N) + OH$	3.0000E+10	0.00	24.00	[194]
761	$C_4H_{10}(N) + O = C_4H_9(S) + OH$	5.2000E+10	0.00	18.60	[194]
762	$C_4H_{10}(N) + HO_2 = C_4H_9(N) + H_2O_2$	1.1200E+10	0.00	81.16	[193]
763	$C_4H_{10}(N) + HO_2 = C_4H_9(S) + H_2O_2$	5.0000E+08	0.00	43.92	[195]

No	Reaction	A	n	Ea	Ref
764	$C_4H_{10}(N) + O_2 = C_4H_9(N) + HO_2$	2.5100E+10	0.00	205.00	[126]
765	$C_4H_{10}(N) + O_2 = C_4H_9(S) + HO_2$	3.9800E+10	0.00	199.00	[126]
766	$C_4H_2O + OH = C_2H_2 + CO + CO + H$	1.0000E+12	0.00	0.00	[73]
767	$C_4H_4O = C_3H_4(P) + CO$	1.7800E+15	0.00	324.25	[133]
768	$C_4H_4O = C_2H_2O + C_2H_2$	5.0100E+14	0.00	324.25	[133]
769	$XC_4H_5O = C_3H_5(S) + CO$	1.0000E+14	0.00	125.60	[182]
770	$YC_4H_5O = C_3H_5(A) + CO$	1.0000E+14	0.00	104.67	[182]
771	$AC_4H_6O = BC_4H_6O$	1.3500E+14	0.00	211.70	[133]
772	$AC_4H_6O = CH_3CO + C_2H_3$	1.0000E+16	0.00	284.51	[133]
773	$BC_4H_6O = C_3H_6 + CO$	1.0900E+16	0.00	305.43	[73]
774	$BC_4H_6O = C_4H_5(T) + OH$	5.3000E+12	0.00	203.05	[72]
775	$BC_4H_6O = C_4H_4O + H_2$	5.3000E+13	0.00	203.05	[75]
776	$C_4H_7O(M) + M = C_3H_7(I) + CO + M$	8.6400E+12	0.00	60.25	[173]
777	$C_4H_8O(X) = C_4H_8O(M)$	4.0000E+13	0.00	239.32	[173]
778	$C_4H_8O(X) = C_3H_7(I) + CHO$	6.0000E+13	0.00	239.32	[173]
779	$C_4H_8O(M) = C_3H_7(I) + CHO$	2.4400E+16	0.00	351.99	[173]
780	$C_4H_8O(M) + O_2 = C_4H_7O(M) + HO_2$	3.0100E+10	0.00	163.79	[173]
781	$C_4H_8O(M) + HO_2 = C_4H_7O(M) + H_2O_2$	3.0100E+09	0.00	49.88	[173]
782	$C_4H_8O(M) + OH = C_4H_7O(M) + H_2O$	3.3700E+09	0.00	-2.57	[173]
783	$C_4H_8O(M) + O = C_4H_7O(M) + OH$	5.0000E+09	0.00	7.49	[173]
784	$C_4H_8O(M) + H = C_4H_7O(M) + H_2$	4.0000E+10	0.00	17.60	[173]
785	$C_4H_8OH(I) + O_2 = O_2C_4H_9O$	3.2500E+23	-4.68	17.96	[173]
786	$O_2C_4H_9O = AC_3H_6O + CH_2O + OH$	1.0000E+16	0.00	104.60	[173]
787	$C_5H + O = C_4H + CO$	6.8000E+10	0.00	0.00	[133]
788	$C_5H + OH = C_4H_2 + CO$	6.8000E+10	0.00	0.00	[133]
789	$C_5H + O_2 = C_3H + CO + CO$	3.2900E+18	-3.30	12.00	[133]
790	$C_5H_2 + H = C_5H + H_2$	1.0000E+11	0.00	0.00	[133]
791	$C_5H_2 + OH = C_4H_2 + CHO$	1.0000E+10	0.00	0.00	[133]
792	$C_5H_3(L) + H = C_5H_4(L)$	1.0000E+10	0.00	0.00	[73]
793	$C_5H_3(L) + H = C_5H_2 + H_2$	1.0000E+10	0.00	0.00	[73]
794	$C_5H_3(L) + O = C_4H_3(I) + CO$	1.0000E+11	0.00	0.00	[73]
795	$C_5H_3(L) + CH_2(S) = C_6H_4L + H$	7.0000E+10	0.00	0.00	[133]
796	$C_5H_3(L) + CH_2(T) = C_6H_4L + H$	7.0000E+10	0.00	0.00	[133]
797	$C_5H_3(L) + OH = C_5H_2 + H_2O$	1.0000E+10	0.00	0.00	[73]
798	$C_5H_4(L) + H = C_5H_3(L) + H_2$	1.0000E+10	0.00	0.00	[73]

No	Reaction	A	n	Ea	Ref
799	$C_5H_4(L) + CH = C_6H_4L + H$	8.0000E+10	0.00	0.00	[133]
800	$C_5H_4(L) + OH = C_5H_3(L) + H_2O$	1.0000E+10	0.00	83.68	[73]
801	$C_5H_5 + CH_3 = C_5H_4CH_3 + H$	2.0000E+10	0.00	26.00	[62]
802	$C_5H_5 + C_3H_5(A) = C_8H_9(F) + H$	2.0000E+10	0.00	42.30	[72]
803	$C_5H_5 + C_5H_5 = C_{10}H_{10}K$	1.0000E+10	0.00	0.00	[112]
804	$C_5H_5 + O_2 = C_5H_5O + O$	9.5100E+01	1.80	218.53	[15]
805	$C_5H_5 + C_2H_2 = C_7H_7$	3.7200E+08	0.00	34.72	[91]
806	$C_5H_5 = C_3H_3 + C_2H_2$	3.1500E+13	0.075	260.66	Adj.[52]
807	$C_5H_5 + O = C_4H_5(T) + CO$	2.1260E+53	-12.56	89.96	[15]
808	$C_5H_5 + O = C_5H_5O$	2.1260E+53	-12.56	89.96	[15]
809	$C_5H_5 + OH = C_5H_4OH + H$	2.2370E+60	-14.75	102.01	[15]
810	$C_5H_5 + C_{10}H_7OH = C_5H_6 + C_{10}H_7O$	2.6700E+11	0.00	105.62	[75]
811	$C_5H_5 + HO_2 = C_5H_5O + OH$	6.2480E+62	-16.16	82.82	[15]
812	$C_5H_5 + O_2 = C_5H_5OO$	2.2580E+09	-1.52	5.07	[15]
813	$C_5H_5 + C_5H_5 = C_{10}H_9F + H$	2.0000E+10	0.00	34.00	[61]
814	$C_5H_5 + O = C_5H_4O + H$	2.1260E+53	-12.56	89.96	[15]
815	$C_5H_5 + OH = C_5H_5OH$	2.2370E+60	-14.75	102.01	[15]
816	$C_5H_5 + OH = C_5H_5O + H$	1.3250E+45	-9.27	517.43	[15]
817	$C_5H_5 + HO_2 = C_5H_4O + H_2O$	6.2480E+62	-16.16	82.82	[15]
818	$C_5H_5 + OH = C_4H_6(T) + CO$	2.2370E+60	-14.75	102.02	[15]
819	$C_5H_5 = C_5H_5(L)$	1.0740E+38	-7.49	307.55	[15]
820	$C_5H_5(L) = C_3H_3 + C_2H_2$	3.3140E+42	-9.46	148.23	[15]
821	$C_5H_5(L) + H = C_5H_4(L) + H_2$	1.0000E+10	0.00	0.00	[73]
822	$C_5H_5(L) + O = C_4H_5(I) + CO$	1.0000E+11	0.00	0.00	[73]
823	$C_5H_5(L) + OH = C_5H_4(L) + H_2O$	1.0000E+10	0.00	0.00	[73]
824	$C_5H_5(L) + O_2 = C_2H_3 + C_2HO + CHO$	1.0000E+09	0.00	155.00	[73]
825	$C_5H_5(L) + H = C_5H_6(L)$	1.0000E+10	0.00	0.00	[73]
826	$C_5H_6 + H = C_5H_5 + H_2$	3.4970E+04	18.56	18.74	[15]
827	$C_5H_6 + O = C_5H_5 + OH$	1.8100E+10	0.00	12.87	[73]
828	$C_5H_6 + OH = C_5H_5 + H_2O$	1.1430E+06	1.18	-1.87	[72]
829	$C_5H_6 + HO_2 = C_5H_5 + H_2O_2$	2.0000E+09	0.00	48.78	[73]
830	$C_5H_6 = C_5H_6(L)$	1.0000E+14	0.00	235.00	[73]
831	$C_5H_6 + C_5H_5 = C_9H_8 + CH_3$	3.0000E+13	0.00	177.10	[41]
832	$C_5H_6 = C_5H_5 + H^{15}$	1.0000E+19	-0.65	368.19	[52]
833	$C_5H_6 + CH_3 = C_5H_5 + CH_4$	1.0000E+10	0.00	58.57	[131]

No	Reaction	A	n	Ea	Ref
834	$C_5H_6(L) + H = C_5H_5(L) + H_2$	1.0000E+09	0.00	0.00	[73]
835	$C_5H_6(L) + O = C_3H_2O + C_2H_3 + H$	2.0000E+10	0.00	126.00	[73]
836	$C_5H_6(L) + OH = C_5H_5(L) + H_2O$	1.0000E+10	0.00	0.00	[73]
837	$C_5H_7 = C_5H_6 + H$	3.1600E+15	0.00	185.40	[62]
838	$C_5H_7 + H = C_5H_6 + H_2$	3.6000E+09	0.00	0.00	[196]
839	$C_5H_7 + OH = C_5H_6 + H_2O$	2.4000E+10	0.00	0.00	[196]
840	$C_5H_7 + O = C_5H_6 + OH$	1.0000E+10	0.00	0.00	[196]
841	$C_5H_7 + O_2 = C_5H_6 + HO_2$	1.3000E+08	0.00	0.00	Present Work
842	$C_5H_7 = C_3H_4(A) + C_2H_3$	3.1600E+14	0.00	327.00	[128]
843	$C_5H_7 + O_2 = C_3H_4O + CH_2CHO$	4.0000E+07	0.00	20.92	[128]
844	$C_5H_7 + HO_2 = C_5H_6 + H_2O_2$	2.6500E+09	0.00	0.00	[128]
845	$C_5H_8 + O = C_5H_7 + OH$	2.7800E+08	0.00	10.49	[128]
846	$C_5H_8 + O_2 = C_5H_7 + HO_2$	1.2800E+08	0.00	104.60	[128]
847	$C_5H_8 + HO_2 = C_5H_7 + H_2O_2$	1.6000E+08	0.00	71.37	[128]
848	$C_5H_8 + O = C_3H_4O + C_2H_4$	5.6000E+09	0.00	-1.79	[197]
849	$C_5H_8 + H = C_5H_7 + H_2$	2.8000E+09	0.00	9.45	[62]
850	$C_5H_8 + OH = C_5H_7 + H_2O$	3.4300E+06	1.18	-1.87	[62]
851	$C_5H_8(l) + HO_2 = C_5H_7(l) + H_2O_2$	2.0000E+02	2.60	58.19	[173]
852	$C_5H_8(l) + OH = C_5H_7(l) + H_2O$	2.0000E+04	2.00	20.92	[173]
853	$C_5H_9(A) = C_5H_8(l) + H$	1.2000E+08	2.50	188.28	[173]
854	$C_5H_9(A) + O_2 = C_5H_8(l) + HO_2$	1.0000E+08	0.00	154.80	[173]
855	$C_5H_9(A) + HO_2 = C_5H_8(l) + H_2O_2$	1.0000E+09	0.00	0.00	[173]
856	$C_5H_9(A) + OH = C_5H_8(l) + H_2O$	1.8000E+10	0.00	0.00	[173]
857	$C_5H_9(A) + O = C_5H_8(l) + OH$	1.8000E+10	0.00	0.00	[173]
858	$C_5H_9(A) + H = C_5H_8(l) + H_2$	3.6000E+09	0.00	0.00	[173]
859	$C_5H_9(A) + CH_3 = C_5H_8(l) + CH_4$	1.0000E+10	0.00	0.00	[173]
860	$C_5H_9(A) + C_4H_7(l) = C_5H_8(l) + C_4H_8(l)$	4.0000E+10	0.00	0.00	[173]
861	$C_5H_9(B) = C_5H_8(l) + H$	1.2000E+08	2.50	188.28	[173]
862	$C_5H_9(B) + O_2 = C_5H_8(l) + HO_2$	1.0000E+08	0.00	154.80	[173]
863	$C_5H_9(B) + HO_2 = C_5H_8(l) + H_2O_2$	1.0000E+09	0.00	0.00	[173]
864	$C_5H_9(B) + OH = C_5H_8(l) + H_2O$	1.8000E+10	0.00	0.00	[173]
865	$C_5H_9(B) + O = C_5H_8(l) + OH$	1.8000E+10	0.00	0.00	[173]
866	$C_5H_9(B) + H = C_5H_8(l) + H_2$	3.6000E+09	0.00	0.00	[173]
867	$C_5H_9(B) + CH_3 = C_5H_8(l) + CH_4$	1.0000E+10	0.00	0.00	[173]
868	$C_5H_9(B) + C_4H_7(l) = C_5H_8(l) + C_4H_8(l)$	4.0000E+10	0.00	0.00	[173]



No	Reaction	A	n	Ea	Ref
869	$C_5H_{10}(A) + H = C_3H_6 + C_2H_5$	1.7000E+09	0.00	12.13	[173]
870	$C_5H_{10}(A) + CH_3 = C_2H_4 + C_2H_4 + C_2H_5$	1.7000E+08	0.00	30.96	[173]
871	$C_5H_{10}(A) = C_5H_{10}(B)$	3.5000E+12	0.00	251.04	[173]
872	$C_5H_{10}(A) = C_3H_5(T) + C_2H_5$	3.3000E+21	-1.20	408.86	[173]
873	$C_5H_{10}(A) = C_5H_9(A) + H$	4.0700E+18	-1.00	407.31	[173]
874	$C_5H_{10}(A) + O_2 = C_5H_9(A) + HO_2$	4.0000E+09	0.00	167.36	[173]
875	$C_5H_{10}(A) + HO_2 = C_5H_9(A) + H_2O_2$	1.0000E+08	0.00	71.37	[173]
876	$C_5H_{10}(A) + OH = C_5H_9(A) + H_2O$	6.2700E+03	2.00	-2.27	[173]
877	$C_5H_{10}(A) + O = C_5H_9(A) + OH$	1.3000E+09	0.00	18.82	[173]
878	$C_5H_{10}(A) + H = C_5H_9(A) + H_2$	1.9500E+10	0.00	18.59	[173]
879	$C_5H_{10}(A) + CH_3 = C_5H_9(A) + CH_4$	1.0000E+08	0.00	30.54	[173]
880	$C_5H_{10}(B) = C_5H_9(A) + H$	2.1300E+47	-9.30	437.44	[173]
881	$C_5H_{10}(B) = C_5H_9(B) + H$	1.0600E+47	-9.30	437.44	[173]
882	$C_5H_{10}(B) + O_2 = C_5H_9(A) + HO_2$	4.8000E+09	0.00	161.21	[173]
883	$C_5H_{10}(B) + O_2 = C_5H_9(B) + HO_2$	2.4000E+09	0.00	161.21	[173]
884	$C_5H_{10}(B) + HO_2 = C_5H_9(A) + H_2O_2$	3.0000E+08	0.00	59.37	[173]
885	$C_5H_{10}(B) + HO_2 = C_5H_9(B) + H_2O_2$	1.5000E+08	0.00	59.37	[173]
886	$C_5H_{10}(B) + OH = C_5H_9(A) + H_2O$	9.0000E+03	2.00	-0.25	[173]
887	$C_5H_{10}(B) + OH = C_5H_9(B) + H_2O$	3.0000E+03	2.00	-0.25	[173]
888	$C_5H_{10}(B) + OH = C_2H_4O + C_3H_7(I)$	2.0000E+07	0.00	16.37	[173]
889	$C_5H_{10}(B) + O = C_5H_9(A) + OH$	3.5000E+08	0.70	24.61	[173]
890	$C_5H_{10}(B) + O = C_5H_9(B) + OH$	1.7500E+08	0.70	24.61	[173]
891	$C_5H_{10}(B) + O = C_2H_4O + C_3H_6$	7.2300E+02	2.34	-4.39	[173]
892	$C_5H_{10}(B) + H = C_5H_9(A) + H_2$	1.2900E+10	0.00	18.59	[173]
893	$C_5H_{10}(B) + H = C_5H_9(B) + H_2$	6.4500E+09	0.00	18.59	[173]
894	$C_5H_{10}(B) + CH_3 = C_5H_9(A) + CH_4$	3.2000E+08	0.00	36.81	[173]
895	$C_5H_{10}(B) + CH_3 = C_5H_9(B) + CH_4$	1.6000E+08	0.00	36.81	[173]
896	$C_5H_{11}(T) = C_5H_{10}(A) + H$	1.6000E+13	0.00	150.62	[173]
897	$C_5H_{11}(T) = C_5H_{10}(B) + H$	5.3000E+12	0.00	138.07	[173]
898	$C_5H_{11}(T) + O_2 = C_5H_{10}(A) + HO_2$	2.0000E+09	0.00	20.92	[173]
899	$C_5H_{11}(T) + O_2 = C_5H_{10}(B) + HO_2$	4.0000E+08	0.00	20.92	[173]
900	$C_5H_4O = C_4H_4 + CO$	2.5000E+11	0.00	221.90	Adj. [128]
901	$C_5H_4O + O = C_4H_4 + CO_2$	1.0000E+10	0.00	8.37	[91]
902	$C_5H_4O + H = C_4H_5(T) + CO$	9.4730E+10	0.00	23.40	[75]
903	$C_5H_4O = C_3H_2O + C_2H_2$	1.0000E+15	0.00	326.57	[72]

No	Reaction	A	n	Ea	Ref
904	$C_5H_5O = C_4H_5(T) + CO$	6.5420E+60	-14.09	281.43	[15]
905	$C_5H_5O = C_5H_4O + H$	7.5040E+13	-1.45	25.81	[15]
906	$C_5H_4OH = C_5H_4O + H$	2.2880E+63	-15.10	245.37	[15]
907	$C_5H_5OH = C_5H_4OH + H$	4.7250E+56	-12.18	402.90	[15]
908	$C_5H_5OH = C_5H_5O + H$	1.7580E+43	-7.84	509.36	[15]
909	$C_5H_5OO = C_5H_4O + OH$	1.3200E+51	-11.54	221.57	[15]
910	$C_5H_5OO = C_5H_5O + O$	6.6940E+61	-14.02	344.67	[15]
911	$C_6H_2 + C_2H = C_8H_2 + H$	1.2000E+11	0.00	0.00	[73]
912	$C_6H_2 + C_2H_2 = C_8H_2 + H + H$	1.5000E+11	0.00	234.50	[73]
913	$C_6H_3 + H = C_6H_2 + H_2$	1.0000E+11	0.00	0.00	[73]
914	$C_6H_3 + O = C_6H_2 + OH$	2.0000E+10	0.00	0.00	[73]
915	$C_6H_3 + OH = C_6H_2 + H_2O$	2.0000E+10	0.00	0.00	[73]
916	$C_6H_4 = C_6H_4L$	1.0000E+12	0.00	138.07	[73]
917	$C_6H_4L + H = C_6H_3 + H_2$	1.0000E+11	0.00	0.00	[73]
918	$C_6H_4L + O = C_6H_3 + OH$	2.0000E+10	0.00	0.00	[73]
919	$C_6H_4L + OH = C_6H_3 + H_2O$	2.0000E+10	0.00	0.00	[73]
920	$C_6H_5 + C_2H_4 = C_8H_8 + H$	2.5100E+09	0.00	25.93	[198]
921	$C_6H_5 + C_4H_3(N) = C_{10}H_8J$	1.0000E+10	0.00	0.00	[61]
922	$C_6H_5 + C_4H_5(T) = C_{10}H_9M + H$	1.0000E+10	0.00	0.00	[61]
923	$C_6H_5 + C_3H_3 = C_9H_8(S)$	1.0000E+10	0.00	0.00	[61]
924	$C_6H_5 + C_3H_3 = C_9H_8(T)$	1.0000E+10	0.00	0.00	[61]
925	$C_6H_5 + C_3H_4(A) = C_9H_9(I)$	1.0000E+10	0.00	0.00	[61]
926	$C_6H_5 = C_6H_5(B)$	4.0000E+13	0.00	303.40	[73]
927	$C_6H_5 = C_6H_4 + H$	3.0000E+13	0.00	372.36	[73]
928	$C_6H_5 + H = C_6H_4 + H_2$	1.5000E+11	0.00	0.00	[73]
929	$C_6H_5 + H = C_6H_6$	7.8300E+10	0.00	0.00	[101]
930	$C_6H_5 + O = C_6H_4 + OH$	2.0000E+10	0.00	0.00	[73]
931	$C_6H_5 + OH = C_6H_4 + H_2O$	2.0000E+10	0.00	0.00	[73]
932	$C_6H_5 + HO_2 = C_6H_5O + OH$	5.0000E+10	0.00	4.18	[73]
933	$C_6H_5 + C_2H_3 = C_8H_8$	5.0000E+09	0.00	0.00	[112]
934	$C_6H_5 + O_2 = C_6H_5O + O$	2.6000E+10	0.00	25.61	[105]
935	$C_6H_5 + O_2 = C_6H_5OO$	3.0800E+09	-0.15	0.66	[75]
936	$C_6H_5 + C_2H_2 = C_8H_7$	2.6000E+09	0.00	42.30	[61]
937	$C_6H_5 + C_2H_2 = C_8H_6 + H$	1.8000E+13	-0.62	73.00	[79]
938	$C_6H_5 + C_4H_4 = C_{10}H_9B$	2.8000E+10	0.00	42.30	[61]

No	Reaction	A	n	Ea	Ref
939	$C_6H_5 + C_6H_5 = C_{12}H_{10}$	3.1600E+09	0.00	0.00	[112]
940	$C_6H_5 + C_4H_4 = C_{10}H_8G + H$	2.8000E+09	0.00	42.30	[61]
941	$C_6H_5 + C_4H_4 = C_{10}H_8J + H$	2.8000E+09	0.00	42.30	[61]
942	$C_6H_5 + C_3H_5(A) = C_9H_9(I) + H$	1.0000E+10	0.00	0.00	[61]
943	$C_6H_5(A) = C_6H_4L + H$	6.0000E+11	0.00	188.00	[73]
944	$C_6H_5(A) + H = C_6H_4L + H_2$	1.0000E+11	0.00	0.00	[73]
945	$C_6H_5(A) + O = C_6H_4L + OH$	2.0000E+10	0.00	0.00	[73]
946	$C_6H_5(A) + OH = C_6H_4L + H_2O$	2.0000E+10	0.00	0.00	[73]
947	$C_6H_5(B) = C_6H_4L + H$	2.5900E+58	-13.8	208.00	[73]
948	$C_6H_5(B) + H = C_6H_4L + H_2$	1.0000E+11	0.00	0.00	[73]
949	$C_6H_5(B) + O = C_6H_4L + OH$	2.0000E+10	0.00	0.00	[73]
950	$C_6H_5(B) + OH = C_6H_4L + H_2O$	2.0000E+10	0.00	0.00	[73]
951	$C_6H_5(B) = C_6H_5(A)$	1.0000E+11	0.00	0.00	[73]
952	$C_6H_5(B) = C_4H_3(I) + C_2H_2$	5.0000E+14	0.00	159.00	[73]
953	$C_6H_6 + C_2H_3 = C_8H_8 + H$	7.4900E+08	0.00	26.77	[61]
954	$C_6H_6 + C_6H_5 = C_{12}H_{10} + H$	2.0000E+09	0.00	16.72	[112]
955	$C_6H_6 + CH_2(S) = C_7H_7 + H$	4.0000E+10	0.00	36.33	[72]
956	$C_6H_6 + H = C_6H_5 + H_2$	2.5000E+11	0.00	66.94	[73]
957	$C_6H_6 + O = C_6H_5O + H$	2.4000E+10	0.00	19.53	[91]
958	$C_6H_6 + O = C_6H_5 + OH$	2.0000E+10	0.00	61.52	[73]
959	$C_6H_6 + OH = C_6H_5 + H_2O$	1.6300E+05	1.42	6.10	[73]
960	$C_6H_6 + OH = C_6H_5OH + H$	1.3200E+10	0.00	44.31	[73]
961	$C_6H_6 + H = C_6H_7$	4.0000E+10	0.00	18.04	[73]
962	$C_6H_6 + O_2 = C_6H_5 + HO_2$	6.3000E+10	0.00	251.04	[73]
963	$C_6H_6 + HO_2 = C_6H_5 + H_2O_2$	1.5200E+08	0.00	71.40	[128]
964	$C_6H_6 + CH_3 = C_6H_5 + CH_4$	4.3650E-07	5.00	51.49	[73]
965	$C_6H_6(A) = C_6H_6(S)$	5.4000E+11	0.00	149.66	[73]
966	$C_6H_6(A) = C_6H_5(A) + H$	1.4000E+15	0.00	326.60	[73]
967	$C_6H_6(A) + H = C_6H_5(A) + H_2$	1.0000E+11	0.00	0.00	[73]
968	$C_6H_6(A) + O = C_6H_5(A) + OH$	2.0000E+10	0.00	0.00	[73]
969	$C_6H_6(A) + OH = C_6H_5(A) + H_2O$	2.0000E+10	0.00	0.00	[73]
970	$C_6H_6(B) = C_6H_6(F)$	5.0000E+11	0.00	144.00	[73]
971	$C_6H_6(B) = C_6H_6(D)$	1.0000E+12	0.00	224.00	[73]
972	$C_6H_6(B) = C_6H_5(A) + H$	7.0000E+14	0.00	326.60	[73]
973	$C_6H_6(B) + H = C_6H_5(A) + H_2$	1.0000E+11	0.00	0.00	[73]

No	Reaction	A	n	Ea	Ref
974	$C_6H_6(B) + O = C_6H_5(A) + OH$	2.0000E+10	0.00	0.00	[73]
975	$C_6H_6(B) + OH = C_6H_5(A) + H_2O$	2.0000E+10	0.00	0.00	[73]
976	$C_6H_6(D) = C_6H_6$	5.0000E+11	0.00	200.00	[73]
977	$C_6H_6(D) + H = C_6H_5(B) + H_2$	1.0000E+11	0.00	46.00	[73]
978	$C_6H_6(D) + O = C_6H_5(B) + OH$	2.0000E+10	0.00	0.00	[73]
979	$C_6H_6(D) + OH = C_6H_5(B) + H_2O$	2.0000E+10	0.00	12.60	[73]
980	$C_6H_6(F) + M = C_6H_6 + M$	3.0000E+09	0.500	8.37	[78]
981	$C_6H_6(F) = C_6H_6(D)$	1.0000E+13	0.00	342.00	[73]
982	$C_6H_6(F) = C_6H_6$	7.5800E+13	0.00	309.00	[73]
983	$C_6H_6(M) = C_6H_6(F)$	4.2600E+13	0.00	206.00	[73]
984	$C_6H_6(S) = C_6H_6(M)$	5.0000E+11	0.00	92.00	[73]
985	$C_6H_6(S) = C_6H_6(F)$	5.0000E+11	0.00	132.40	[73]
986	$C_6H_7 = C_6H_7(L)$	3.0000E+14	0.00	209.20	[73]
987	$C_5H_4CH_3 = C_6H_6(F) + H$	1.0000E+14	0.00	217.00	[62]
988	$C_6H_8 = C_6H_6 + H_2$	1.0000E+06	0.00	0.00	[133]
989	$C_6H_8 = C_6H_7 + H$	5.0100E+15	0.00	303.74	[133]
990	$C_5H_5CH_3 = CH_3 + C_5H_5$	1.5200E+84	-20.29	437.22	[199]
991	$C_5H_5CH_3 + CH_3 = CH_4 + H + C_6H_6$	4.4200E-03	3.50	23.76	[199]
992	$C_6H_5O + O = C_6H_4O_2 + H$	3.0000E+10	0.00	0.00	[91]
993	$C_6H_5O + OH = C_6H_5OOH$	1.0000E+09	0.00	0.00	[91]
994	$C_6H_5O = C_5H_5 + CO$	4.5000E+11	0.00	126.68	[73]
995	$C_6H_5O + H = C_6H_5OH$	2.5000E+11	0.00	0.00	[91]
996	$C_6H_5O + HO_2 = C_6H_5OH + O_2$	1.2500E+10	0.00	0.00	[75]
997	$C_6H_3O_2 + H = C_2H_2 + C_2H_2 + CO + CO$	1.0000E+11	0.00	0.00	[91]
998	$C_6H_3O_2 + O = C_2H_2 + C_2HO + CO + CO$	1.0000E+11	0.00	0.00	[91]
999	$C_6H_3O_3 = C_2H_2 + C_2HO + CO + CO$	1.0000E+12	0.00	209.00	[91]
1000	$C_6H_4O_2 = C_5H_4O + CO$	3.7000E+11	0.00	247.00	[91]
1001	$C_6H_4O_2 + H = C_5H_5O + CO$	2.5000E+10	0.00	19.67	[91]
1002	$C_6H_4O_2 + H = C_6H_3O_2 + H_2$	2.0000E+09	0.00	33.90	[91]
1003	$C_6H_4O_2 + OH = C_6H_3O_2 + H_2O$	1.0000E+03	2.00	16.74	[91]
1004	$C_6H_4O_2 + O = C_6H_3O_3 + H$	1.5000E+10	0.00	18.96	[91]
1005	$C_6H_4O_2 + O = C_6H_3O_2 + OH$	1.4000E+10	0.00	61.55	[91]
1006	$C_6H_5OO = C_6H_5O + O$	4.2700E+15	-0.70	138.27	[91]
1007	$C_6H_5OO + H = C_6H_5OOH$	2.5000E+11	0.00	0.00	[91]
1008	$C_6H_5OO + C_6H_5OH = C_6H_5OOH + C_6H_5O$	3.1600E+08	0.00	29.14	[91]

No	Reaction	A	n	Ea	Ref
1009	$C_6H_5OO + HO_2 = C_6H_5OOH + O_2$	1.8700E+09	0.00	6.44	[91]
1010	$C_6H_5OO = C_6H_4O_2 + H$	4.0000E+08	0.00	0.00	[91]
1011	$C_6H_5OO = C_5H_5 + CO_2$	1.6000E+08	0.00	0.00	[91]
1012	$C_6H_5OH + C_5H_5 = C_6H_5O + C_5H_6$	2.6700E+11	0.00	105.59	[54]
1013	$C_6H_5OH + H = C_6H_5O + H_2$	1.1500E+11	0.00	51.92	[200]
1014	$C_6H_5OH + O = C_6H_5O + OH$	2.8100E+10	0.00	30.78	[200]
1015	$C_6H_5OH + OH = C_6H_5O + H_2O$	6.0000E+09	0.00	0.00	[128]
1016	$C_6H_5OH + C_7H_7 = C_6H_5O + C_7H_8$	1.0500E+08	0.00	39.76	[55]
1017	$C_6H_5OH = C_5H_6 + CO$	1.0000E+12	0.00	254.00	[171]
1018	$C_6H_5OH + HO_2 = C_6H_5O + H_2O_2$	3.0000E+10	0.00	62.76	[91]
1019	$C_7H_5 + OH = C_5H_4O + C_2H_2$	2.0000E+10	0.00	0.00	[75]
1020	$C_7H_5 + O = C_5H_4O + C_2H$	2.0000E+10	0.00	0.00	[75]
1021	$C_7H_5 + O_2 = C_5H_4O + C_2HO$	1.0800E+05	1.50	125.94	[75]
1022	$C_7H_5 + O = C_5H_4(L) + C_2HO$	2.0000E+10	0.00	0.00	[75]
1023	$C_7H_6 + H = C_5H_5 + C_2H_2$	2.0000E+10	0.00	20.00	[201]
1024	$C_7H_6 + H = C_4H_4 + C_3H_3$	6.0000E+10	0.00	61.92	[201]
1025	$C_7H_6 + H = C_7H_5 + H_2$	2.8000E+10	0.00	9.45	[75]
1026	$C_7H_6 + O = C_7H_5 + OH$	1.8100E+10	0.00	12.87	[75]
1027	$C_7H_6 + OH = C_7H_5 + H_2O$	1.1433E+06	1.18	-1.87	[75]
1028	$C_7H_6 + HO_2 = C_7H_5 + H_2O_2$	2.0000E+09	0.00	48.78	[75]
1029	$C_7H_6 + O = C_6H_6(F) + CO$	1.5550E+03	2.09	6.53	[75]
1030	$C_7H_6 + O = C_5H_5 + C_2HO$	2.3320E+03	2.09	6.53	[75]
1031	$C_7H_6 = C_5H_4(L) + C_2H_2$	1.0000E+14	0.00	294.00	Est.(1160)
1032	$C_6H_5C + O = C_6H_5 + CO$	1.5800E+10	0.00	0.00	[75]
1033	$C_6H_5C + O_2 = C_6H_5CO + O$	2.9700E+10	0.00	0.00	[75]
1034	$C_6H_5C + CH_4 = C_8H_8 + H$	2.3700E+10	0.00	0.00	[75]
1035	$C_6H_5C + CH_3 = C_8H_7 + H$	1.8900E+10	0.00	0.00	[75]
1036	$C_6H_5C + H_2O = C_7H_7O$	2.2700E+09	0.00	-3.15	[75]
1037	$C_6H_5CH + OH = C_7H_6O + H$	1.1400E+10	0.00	0.00	[75]
1038	$C_6H_5CH + OH = C_6H_5C + H_2O$	4.4810E+03	2.00	12.56	[75]
1039	$C_6H_5CH + CH_2(T) = C_8H_8$	1.0000E+10	0.00	0.00	[75]
1040	$C_6H_5CH + CH_2(S) = C_8H_8$	1.0000E+10	0.00	0.00	[75]
1041	$C_6H_5CH + CH_3 = C_8H_8 + H$	1.0000E+10	0.00	0.00	[75]
1042	$C_6H_5CH + CH_4 = C_8H_9 + H$	1.0000E+10	0.00	0.00	[75]
1043	$C_6H_5CH + C_3H_3 = C_9H_6CH_2 + H$	1.0000E+10	0.00	0.00	[75]

No	Reaction	A	n	Ea	Ref
1044	$C_6H_5CH + C_2H_2 = C_9H_8(T)$	3.3333E+09	0.00	0.00	[75]
1045	$C_6H_5CH + HO_2 = C_7H_7 + O_2$	1.0000E+10	0.00	0.00	[75]
1046	$C_6H_5CH + C_7H_7 = C_8H_8 + C_6H_5$	1.0000E+10	0.00	0.00	[75]
1047	$C_6H_5CH + O_2 = C_6H_6 + CO_2$	5.3300E+10	-3.30	12.00	[75]
1048	$C_6H_5CH + O_2 = C_7H_6O + O$	8.0000E+18	-3.30	12.00	[75]
1049	$C_6H_5CH + H = C_7H_7$	1.0000E+11	0.00	0.00	[75]
1050	$C_6H_5CH + H = C_6H_5C + H_2$	4.3620E+10	0.00	0.00	[75]
1051	$C_6H_5CH + O = C_7H_6O$	1.0000E+10	0.00	0.00	[75]
1052	$C_7H_7 + H = C_6H_5CH + H_2$	6.0300E+10	0.00	63.20	[200]
1053	$C_7H_7 + OH = C_7H_7O + H$	4.5920E+09	-0.23	58.28	[75]
1054	$C_7H_7 = C_7H_7L$	3.1600E+15	0.00	356.67	[201]
1055	$C_7H_7 + CH_3 = C_8H_9 + H$	3.5000E+09	0.10	44.36	[75]
1056	$C_7H_7 + C_7H_7 = C_{14}H_{14}$	5.0100E+09	0.00	1.89	[90]
1057	$C_7H_7 + O = C_6H_6 + CHO$	3.5000E+10	0.00	0.00	[202]
1058	$C_7H_7 + O = C_7H_6O + H$	3.5000E+10	0.00	0.00	[202]
1059	$C_7H_7 + C_2H_2 = C_9H_8 + H$	1.0000E+09	0.00	20.92	[74]
1060	$C_7H_7 + O_2 = C_7H_7O + O$	8.6400E+10	0.00	131.36	[75]
1061	$C_7H_7 + O_2 = C_7H_7OO^6$	$k_\infty = 1.3400E+06$ $k_0 = 5.3100E+19$	1.10 -3.30	0.00 0.00	[75]
1062	$C_7H_7 + CH_2(S) = C_8H_8 + H$	2.4000E+11	0.00	0.00	[72]
1063	$C_7H_7 + CH_3 = C_8H_{10}$	1.4600E+10	0.00	0.00	[61]
1064	$C_7H_7 + HO_2 = C_7H_7O + OH$	1.0000E+10	0.00	0.00	[72]
1065	$C_7H_7 + C_3H_3 = C_{10}H_{10}$	3.0000E+10	0.00	0.00	[112]
1066	$C_7H_7 + CH_2(T) = C_8H_8 + H$	7.0000E+10	0.00	37.50	[72]
1067	$C_7H_7 + C_2H_2 = C_9H_9(P)$	1.0000E+09	0.00	20.92	[61]
1068	$C_7H_7 = C_7H_6 + H$	8.2000E+14	0.00	337.52	[90]
1069	$C_7H_7 = C_4H_4 + C_3H_3$	2.0000E+14	0.00	349.78	[28]
1070	$C_7H_7L = C_7H_6 + H$	5.0000E+15	0.00	165.00	[28]
1071	$C_7H_7L = C_4H_4 + C_3H_3$	2.0000E+15	0.00	349.78	[28]
1072	$C_7H_7P + C_3H_3 = C_{10}H_{10}F$	3.0000E+10	0.00	0.00	[61]
1073	$C_7H_7P + C_2H_2 = C_9H_9(F)$	1.0000E+09	0.00	20.92	[61]
1074	$C_7H_7P = C_4H_3(N) + C_3H_4(P)$	2.5000E+14	0.00	408.00	[112]
1075	$C_7H_7P = C_2H_2 + C_2H_2 + C_3H_3$	2.5000E+14	0.00	347.00	[85]
1076	$C_7H_7P + O_2 = OOC_7H_7P$	3.8000E+09	-0.15	0.66	[72]
1077	$C_7H_7P + O_2 = OC_7H_7 + O$	2.6000E+10	0.00	25.61	[72]
1078	$C_7H_8 = C_7H_7 + H$	2.0900E+15	0.00	366.14	[90]

No	Reaction	A	n	Ea	Ref
1079	$C_7H_8 = C_6H_5 + CH_3$	2.6600E+16	0.00	409.52	[90]
1080	$C_7H_8 + H = C_7H_7 + H_2$	1.2600E+12	0.00	61.99	[90]
1081	$C_7H_8 + H = C_6H_6 + CH_3$	5.7800E+10	0.00	33.84	[90]
1082	$C_7H_8 + H = C_7H_7P + H_2$	2.5000E+11	0.00	66.94	[72]
1083	$C_7H_8 + OH = C_7H_7 + H_2O$	5.1900E+06	1.00	3.65	[101]
1084	$C_7H_8 + OH = C_7H_7O + H_2$	2.2900E+09	0.00	35.00	[75]
1085	$C_7H_8 + OH = HOC_7H_7 + H$	2.2900E+09	0.00	-1.49	[112]
1086	$C_7H_8 + OH = C_7H_7OH + H$	6.6000E+09	0.00	44.31	[112]
1087	$C_7H_8 + O_2 = C_7H_7 + HO_2$	1.8100E+09	0.00	166.28	[101]
1088	$C_7H_8 + C_6H_5 = C_6H_6 + C_7H_7$	2.1000E+10	0.00	18.42	[203]
1089	$C_7H_8 + CH_3 = CH_4 + C_7H_7$	3.1600E+09	0.00	0.00	[90]
1090	$C_7H_8 + CH_3 = C_7H_7P + CH_4$	1.0000E+10	0.00	66.94	[112]
1091	$C_7H_8 + O = OC_7H_7 + H$	3.1000E+10	0.00	16.62	[118]
1092	$C_7H_8 + O = C_7H_7 + OH$	6.3000E+08	0.00	0.00	[118]
1093	$C_7H_8 + O = C_7H_7O + H$	1.5500E+10	0.00	16.62	[112]
1094	$C_7H_8 + O = C_7H_8OA$	3.1000E+09	0.00	16.62	[118]
1095	$C_7H_8 + O = C_7H_7P + OH$	1.8400E+10	0.00	61.52	[75]
1096	$C_7H_8 + C_2H_3 = C_7H_7 + C_2H_4$	3.9800E+09	0.00	33.47	[112]
1097	$C_7H_8 + C_3H_5(A) = C_7H_7 + C_3H_6$	5.0000E+09	0.00	58.57	[112]
1098	$C_7H_8 + HO_2 = C_7H_7 + H_2O_2$	3.9750E+08	0.00	58.86	[178]
1099	$C_7H_8 + HO_2 = C_7H_7P + H_2O_2$	5.4800E+09	0.00	120.55	[178]
1100	$C_7H_8 + OH = C_7H_7P + H_2O$	1.5000E+05	1.42	6.10	[75]
1101	$C_7H_6O + O = C_6H_6 + CO_2$	2.0000E+10	0.00	0.00	[75]
1102	$C_7H_6O = C_6H_5CO + H$	3.9800E+15	0.00	350.19	[204]
1103	$C_7H_6O + O_2 = C_6H_5CO + HO_2$	1.0200E+10	0.00	163.04	[55]
1104	$C_7H_6O + OH = C_6H_5CO + H_2O$	1.7100E+06	1.18	-1.87	[55]
1105	$C_7H_6O + H = C_6H_5CO + H_2$	5.0000E+10	0.00	20.62	[55]
1106	$C_7H_6O + H = C_6H_6 + CHO$	6.3000E+04	1.62	9.06	[55]
1107	$C_7H_6O + O = C_6H_5CO + OH$	9.0400E+09	0.00	12.89	[55]
1108	$C_7H_6O + HO_2 = C_6H_5CO + H_2O_2$	1.9900E+09	0.00	48.80	[112]
1109	$C_7H_6O + CH_3 = C_6H_5CO + CH_4$	2.7700E+00	2.81	24.16	[55]
1110	$C_7H_6O + C_6H_5 = C_6H_5CO + C_6H_6$	7.0100E+08	0.00	18.41	[55]
1111	$C_7H_7O = C_6H_5 + CH_2O$	2.5000E+12	0.00	135.00	[75]
1112	$C_7H_7O + H = C_7H_6O + H_2$	3.0000E+10	0.00	0.00	[112]
1113	$C_7H_7O + H = C_7H_7OH$	2.5300E+11	0.00	0.00	[112]

No	Reaction	A	n	Ea	Ref
1114	$C_7H_7O + O = C_7H_6O + OH$	4.2000E+10	0.00	0.00	[112]
1115	$C_7H_7O + OH = C_7H_6O + H_2O$	2.4000E+10	0.00	0.00	[112]
1116	$C_7H_7O + O_2 = C_7H_6O + HO_2$	1.0000E+10	0.00	21.00	[112]
1117	$C_7H_7O = C_7H_6O + H$	3.0000E+12	0.00	68.00	[75]
1118	$C_7H_7O + M = C_7H_6O + H + M$	2.5000E+08	0.00	0.00	[118]
1119	$OC_7H_7 + H = HOC_7H_7$	2.5000E+11	0.00	0.00	[55]
1120	$OC_7H_7 = C_5H_4CH_3 + CO$	2.5100E+11	0.00	189.00	[72]
1121	$OC_7H_7 + H_2O = HOC_7H_7 + OH$	6.8800E+09	0.36	136.18	[55]
1122	$HOC_7H_7 + C_7H_7 = OC_7H_7 + C_7H_8$	1.0500E+08	0.00	39.76	[55]
1123	$HOC_7H_7 + H = OC_7H_7 + H_2$	1.1500E+11	0.00	51.90	[205]
1124	$HOC_7H_7 + H = C_6H_5OH + CH_3$	1.2000E+10	0.00	21.55	[55]
1125	$C_7H_7OH + O_2 = C_7H_6O + HO_2 + H$	2.0000E+11	0.00	173.30	[55]
1126	$C_7H_7OH + OH = C_7H_7O + H_2O$	5.0000E+09	0.00	0.00	[88]
1127	$C_7H_7OH + H = C_7H_7O + H_2$	8.0000E+10	0.00	34.45	[75]
1128	$C_7H_7OH + H = C_6H_6 + CH_2OH$	1.2000E+10	0.00	21.55	[55]
1129	$C_7H_7OH + C_6H_5 = C_7H_6O + C_6H_6 + H$	1.4000E+09	0.00	18.41	[55]
1130	$C_7H_7OO = C_7H_6O + OH$	1.0000E+10	0.00	121.00	[112]
1131	$C_7H_7OO = C_7H_7O + O$	7.8300E+16	0.00	244.78	Est.(1006)
1132	$OOC_7H_7P = OC_7H_7 + O$	4.2700E+15	-0.70	138.27	[75]
1133	$OOC_7H_7P = C_5H_4CH_3 + CO_2$	1.5060E+08	0.00	0.00	[75]
1134	$C_6H_5CO = C_6H_5 + CO$	3.9800E+14	0.00	123.00	[206]
1135	$C_6H_5CO + H = C_6H_6 + CO$	3.0000E+10	0.00	0.00	[207]
1136	$C_7H_8OA = C_6H_5O + CH_3$	2.0000E+15	0.00	266.09	[208]
1137	$C_7H_8OA + H = C_6H_5OH + CH_3$	7.0800E+09	0.00	22.54	[208]
1138	$C_7H_8OA + O = C_7H_7OA + OH$	1.6700E+10	0.00	12.29	[209]
1139	$C_7H_8OA + OH = C_7H_7OA + H_2O$	1.2000E+09	0.00	-2.09	[210]
1140	$C_7H_8OA + CH_3 = C_7H_7OA + CH_4$	5.0100E+08	0.00	43.92	[211]
1141	$C_7H_7OA = C_7H_6O + H$	3.1600E+12	0.00	87.85	[211]
1142	$C_8H_5 + H = C_8H_6$	2.0000E+11	0.00	0.00	[75]
1143	$C_8H_5 + C_2H_2 = C_{10}H_7L$	4.0000E+10	0.00	42.30	[76]
1144	$C_8H_5 + O_2 = C_8H_5OO$	1.6490E+10	-0.15	0.66	[75]
1145	$C_8H_5 + O_2 = C_8H_5O + O$	2.2700E+10	0.00	25.61	[75]
1146	$C_8H_5(S) + H = C_8H_6$	1.8100E+11	0.00	0.00	[112]
1147	$C_8H_5(S) + O_2 = C_6H_4 + CHO + CO$	1.8800E+09	0.00	31.25	[112]
1148	$C_8H_5(S) + C_2H_2 = C_{10}H_7M$	4.0000E+10	0.00	42.30	[76]



No	Reaction	A	n	Ea	Ref
1149	$C_8H_6 + H = C_8H_5 + H_2$	2.5000E+11	0.00	66.94	[119]
1150	$C_8H_6 + H = C_8H_5(S) + H_2$	3.0150E+10	0.00	116.40	[112]
1151	$C_8H_6 + O = C_6H_5C_2O + H$	2.1900E+03	2.09	6.53	[75]
1152	$C_8H_6 + OH = C_6H_6 + C_2HO$	2.4400E+00	3.02	46.34	[112]
1153	$C_8H_6 + OH = C_7H_7 + CO$	6.1000E+00	3.02	46.34	[112]
1154	$C_8H_6 + OH = C_8H_5 + H_2O$	2.1000E+10	0.00	19.10	[76]
1155	$C_8H_6 + OH = C_8H_5(S) + H_2O$	1.6850E+04	2.00	58.57	[112]
1156	$C_8H_6 + CH_2(S) = C_9H_8(S)$	1.2000E+10	0.00	0.00	[112]
1157	$C_8H_6 + CH_2(T) = C_9H_8(T)$	1.2000E+10	0.00	0.00	[112]
1158	$C_8H_6 + CH_3 = C_9H_8(S) + H$	4.0000E+16	-2.08	132.18	[112]
1159	$C_8H_6 + CH_3 = C_9H_8(T) + H$	1.6000E+15	-1.96	86.16	[112]
1160	$C_8H_6 = C_6H_4 + C_2H_2$	1.0000E+14	0.00	398.70	[75]
1161	$C_8H_6 + O = C_6H_5CH + CO$	1.4600E+03	2.09	6.53	[212]
1162	$C_8H_6 + O = C_8H_5O + H$	2.4000E+10	0.00	19.53	[75]
1163	$C_8H_6 + O = C_6H_5 + C_2HO$	6.5100E+03	2.09	6.54	[61]
1164	$C_8H_6 + O = C_8H_5 + OH$	2.0000E+10	0.00	61.52	[75]
1165	$C_8H_6 + OH = C_2H + C_6H_5OH$	3.3700E+04	2.00	58.57	[75]
1166	$C_8H_6 + OH = C_2H_2O + C_6H_5$	3.7500E+03	1.70	4.18	[75]
1167	$C_8H_6 + HO_2 = C_2H_2O + C_6H_5O$	6.0000E+06	0.00	33.52	[75]
1168	$C_8H_6 + HO_2 = C_8H_5 + H_2O_2$	1.0000E+09	0.00	101.00	[75]
1169	$C_8H_6 + M = C_6H_5CHC + M$	1.3400E+12	-0.64	207.00	[75]
1170	$C_8H_6 + CH_2(T) = C_9H_8$	7.0000E+10	0.00	0.00	Adj.(560)
1171	$C_8H_6 + O = C_6H_5O + C_2H$	2.2000E+10	0.00	18.95	est.
1172	$C_6H_5CHC + O_2 = C_6H_5CH + CO_2$	2.6800E+10	0.00	0.00	[75]
1173	$C_6H_5CHC + H = C_8H_7$	1.0750E+11	0.00	0.00	[75]
1174	$C_8H_7 + M = C_8H_6 + H + M$	2.0000E+14	0.00	166.28	[112]
1175	$C_8H_7 + H = C_8H_6 + H_2$	9.6400E+10	0.00	0.00	[112]
1176	$C_8H_7 + H = C_8H_8$	1.2000E+11	0.00	0.00	[112]
1177	$C_8H_7 + OH = C_8H_6 + H_2O$	2.0000E+10	0.00	0.00	[112]
1178	$C_8H_7 + OH = C_6H_5 + CH_3CO$	3.0000E+10	0.00	0.00	[112]
1179	$C_8H_7 + O = C_6H_5 + C_2H_2O$	3.0000E+10	0.00	0.00	[112]
1180	$C_8H_7 + O = C_7H_7 + CO$	3.0000E+10	0.00	0.00	[112]
1181	$C_8H_7 + O_2 = C_8H_6 + HO_2$	8.4900E+10	-0.83	10.63	[75]
1182	$C_8H_7 + O_2 = C_7H_6O + CHO$	8.3900E+17	-2.78	10.56	[75]
1183	$C_8H_7 + O_2 = C_6H_6 + C_2HO + O$	2.5000E+09	0.06	43.97	[75]

No	Reaction	A	n	Ea	Ref
1184	$C_8H_7 + C_2H_2 = C_{10}H_9A$	4.0000E+10	0.00	42.30	[112]
1185	$C_8H_7 + HO_2 = C_8H_6 + H_2O_2$	2.0000E+10	0.00	0.00	[75]
1186	$C_8H_7 + HO_2 = C_7H_7 + CO + OH$	3.0000E+10	0.00	0.00	[75]
1187	$C_8H_7 = C_8H_6 + H$	1.3000E+41	-8.65	46.10	[119]
1188	$C_8H_7(P) + H = C_8H_8$	7.8300E+10	0.00	0.00	[112]
1189	$C_8H_7(P) + O = C_7H_7P + CO$	3.0000E+10	0.00	0.00	[112]
1190	$C_8H_7(P) + O = C_6H_5O + C_2H_2$	3.0000E+10	0.00	0.00	[112]
1191	$C_8H_7(P) + OH = C_6H_5O + C_2H_3$	3.0000E+10	0.00	0.00	[112]
1192	$C_8H_7(P) + C_2H_2 = C_{10}H_9P$	1.0000E+10	0.00	20.92	Est.(1073)
1193	$C_8H_8 + H = C_8H_7 + H_2$	6.6200E+02	2.53	51.21	[112]
1194	$C_8H_8 + H = C_8H_7(P) + H_2$	2.7000E+10	0.00	40.58	[112]
1195	$C_8H_8 + OH = C_8H_7 + H_2O$	7.8500E+00	2.75	17.46	[112]
1196	$C_8H_8 + OH = C_8H_7(P) + H_2O$	2.1000E+10	0.00	19.10	[112]
1197	$C_8H_8 + OH = C_7H_7 + CH_2O$	3.0000E+10	0.00	0.00	[112]
1198	$C_8H_8 + O = C_7H_7 + CHO$	4.2020E+03	1.88	0.76	[72]
1199	$C_8H_8 + O = C_6H_5 + CH_3CO$	2.5000E+03	1.88	0.76	[75]
1200	$C_8H_8 + O = C_6H_6 + C_2H_2O$	3.3000E+02	1.88	0.76	[75]
1201	$C_8H_8 + O = C_8H_7 + OH$	7.5500E+03	1.91	15.63	[61]
1202	$C_8H_9 = C_8H_8 + H$	3.1600E+13	0.00	211.99	[86]
1203	$C_8H_9 = C_6H_5 + C_2H_4$	8.9100E+12	0.00	303.75	[112]
1204	$C_8H_9(F) = C_8H_8 + H$	3.0000E+13	0.00	172.40	[61]
1205	$C_8H_{10} = C_8H_9 + H$	2.5000E+15	0.00	339.99	[86]
1206	$C_8H_{10} + H = C_8H_9 + H_2$	1.2600E-01	3.44	13.05	[112]
1207	$C_8H_{10} + H = C_6H_6 + C_2H_5$	1.2000E+10	0.00	21.33	[116]
1208	$C_8H_{10} + O = C_8H_9 + OH$	2.2000E+09	0.00	15.89	[112]
1209	$C_8H_{10} + OH = C_8H_9 + H_2O$	5.0000E+08	0.00	0.00	[101]
1210	$C_8H_{10} + HO_2 = C_8H_9 + H_2O_2$	2.6500E+08	0.00	47.21	[178]
1211	$C_8H_{10} + C_6H_5 = C_8H_9 + C_6H_6$	5.0000E+08	0.00	0.00	[112]
1212	$C_8H_5O = C_7H_5 + CO$	4.0100E+11	0.00	183.68	[75]
1213	$C_8H_5OO = C_8H_5O + O$	3.8060E+14	-0.70	138.20	[75]
1214	$C_8H_5OO = C_7H_5 + CO_2$	1.7825E+07	0.00	0.00	[75]
1215	$C_6H_5C_2O + O_2 = C_6H_5CO + CO_2$	1.1839E+10	0.00	0.00	[75]
1216	$C_6H_5C_2O + O_2 = C_6H_5 + CO + CO_2$	1.0000E+10	0.00	0.00	[75]
1217	$C_6H_5C_2O + O_2 = C_6H_5O + CO + CO$	1.0000E+10	0.00	0.00	[75]
1218	$C_9H_7L + O = C_6H_5 + C_2H_2 + CO$	8.2000E+10	0.00	0.00	[112]

No	Reaction	A	n	Ea	Ref
1219	$C_9H_7L + OH = C_6H_5 + C_2H_2 + CHO$	3.5000E+10	0.00	26.00	[112]
1220	$C_9H_7L + O_2 = C_6H_5 + C_2HO + CHO$	1.7000E+07	0.00	12.00	[112]
1221	$C_9H_7 + CH_3 = C_9H_7CH_3$	2.0000E+10	0.00	0.00	[131]
1222	$C_9H_7 + H = C_9H_8$	2.0000E+11	0.00	0.00	[75]
1223	$C_9H_7 + O = C_8H_7(P) + CO$	4.5000E+10	0.00	0.00	[75]
1224	$C_9H_7 + O = C_8H_7 + CO$	1.0000E+11	0.00	0.00	[112]
1225	$C_9H_7 + O = C_9H_6O + H$	5.8100E+10	-0.02	0.08	[75]
1226	$C_9H_7 + OH = C_8H_7(P) + CHO$	1.0000E+11	0.00	97.00	[75]
1227	$C_9H_7 + O = C_9H_7O$	7.5000E+09	0.00	0.00	[130]
1228	$C_9H_7 + HO_2 = C_9H_7O + OH$	8.5770E+65	-16.69	101.78	[70]
1229	$C_9H_7 + HO_2 = C_9H_6O + H_2O$	1.9600E+30	-6.14	228.50	[70]
1230	$C_9H_7 + O_2 = C_9H_6O + OH$	1.9325E+12	-0.73	203.92	[75]
1231	$C_9H_7 + O_2 = C_9H_7O + O$	1.9325E+12	-0.73	203.92	[75]
1232	$C_9H_7 + O_2 = C_7H_7 + CO + CO$	1.7420E+09	0.31	123.10	[70]
1233	$C_9H_7 + O_2 = C_6H_5O + C_3H_2O$	1.8760E+10	-0.05	124.68	[70]
1234	$C_9H_7 + O_2 = C_7H_6O + C_2HO$	1.7420E+09	0.31	123.10	[70]
1235	$C_9H_7 + CH_2(S) = C_{10}H_9T$	1.0000E+11	0.00	0.00	[112]
1236	$C_9H_8 + CH_3 = C_9H_7 + CH_4$	7.5400E+09	0.00	58.57	[131]
1237	$C_9H_8 + H = C_9H_7 + H_2$	2.1120E+10	0.00	9.45	[75]
1238	$C_9H_8 + O = C_9H_7 + OH$	1.3650E+10	0.00	12.87	[75]
1239	$C_9H_8 + HO_2 = C_9H_7 + H_2O_2$	1.5086E+09	0.00	48.78	[75]
1240	$C_9H_8 + OH = C_9H_7 + H_2O$	8.6230E+05	1.18	-1.87	[75]
1241	$C_9H_8(S) + H = C_9H_7L + H_2$	1.2000E+11	0.00	62.84	[112]
1242	$C_9H_8(S) + O = C_8H_7 + CHO$	6.5000E-06	4.61	-17.80	[112]
1243	$C_9H_8(S) + OH = C_9H_7L + H_2O$	5.9000E+08	0.00	6.27	[112]
1244	$C_9H_8(T) + H = C_9H_7L + H_2$	1.2000E+11	0.00	62.84	[112]
1245	$C_9H_8(T) + O = C_8H_8 + CO$	1.3690E+03	2.09	6.53	[112]
1246	$C_9H_8(T) + OH = C_8H_8 + CHO$	3.0000E-07	4.50	-4.19	[112]
1247	$C_9H_8(T) + OH = C_9H_7L + H_2O$	1.8000E+00	3.00	0.83	[112]
1248	$C_9H_9(S) = C_9H_8 + H$	1.0000E+13	0.00	137.00	[112]
1249	$C_9H_9(l) = C_9H_8(T) + H$	1.0000E+13	0.00	150.00	[112]
1250	$C_9H_9(l) = C_9H_9(N)$	1.0000E+13	0.00	17.00	[112]
1251	$C_9H_9(l) = C_9H_8(S) + H$	1.0000E+13	0.00	138.00	[112]
1252	$C_9H_9(N) = C_9H_9(S)$	1.0000E+10	0.00	0.00	[112]
1253	$C_9H_9(C) = C_9H_9(P)$	1.0000E+14	0.00	334.00	[112]

No	Reaction	A	n	Ea	Ref
1254	$C_9H_9(C) = C_9H_8 + H$	1.0000E+13	0.00	90.00	[112]
1255	$C_9H_9(P) = C_9H_8(T) + H$	1.0000E+13	0.00	137.00	[112]
1256	$C_9H_9(F) = C_9H_9(S)$	1.0000E+09	0.00	0.00	[112]
1257	$C_9H_6O = C_8H_6 + CO$	1.8825E+11	0.00	183.68	[112]
1258	$C_9H_6O = CO + C_2H_2 + C_6H_4$	1.0000E+15	0.00	326.57	[112]
1259	$C_9H_6O + O = C_8H_6 + CO_2$	1.0000E+10	0.00	8.37	[112]
1260	$C_9H_6O + H = C_8H_7 + CO$	1.2500E+10	0.00	19.67	[112]
1261	$C_9H_6O + H = C_8H_7(P) + CO$	1.2500E+10	0.00	16.67	[112]
1262	$C_9H_7O = C_9H_6O + H$	2.0000E+14	0.00	242.00	[112]
1263	$C_9H_7O = C_8H_7 + CO$	2.0000E+14	0.00	155.00	[130]
1264	$C_{10}H_7L = C_{10}H_7$	1.0000E+10	0.00	0.00	[61]
1265	$C_{10}H_7L = C_{10}H_6 + H$	1.0000E+13	0.00	138.00	[75]
1266	$C_{10}H_7L + H = C_{10}H_6 + H_2$	1.0000E+10	0.00	0.00	[112]
1267	$C_{10}H_7L + H = C_{10}H_8L$	1.0000E+11	0.00	0.00	[112]
1268	$C_{10}H_7L + OH = C_{10}H_6 + H_2O$	1.0000E+10	0.00	0.00	[112]
1269	$C_{10}H_7M = C_{10}H_7$	1.6600E+11	0.00	68.41	[112]
1270	$C_{10}H_7M = C_{10}H_6 + H$	1.0000E+13	0.00	141.00	[112]
1271	$C_{10}H_7 + H = C_{10}H_8$	1.1300E+10	0.00	0.00	[75]
1272	$C_{10}H_7 + O_2 = C_{10}H_7O + O$	2.1500E+10	0.00	25.61	[75]
1273	$C_{10}H_7 + O_2 = C_{10}H_7OO$	2.5000E+09	-0.15	0.66	[75]
1274	$C_{10}H_7 + HO_2 = C_{10}H_7O + OH$	4.0700E+10	0.00	4.18	[75]
1275	$C_{10}H_7 + H_2 = C_{10}H_8 + H$	4.4400E+01	2.43	26.29	Est.[196]
1276	$C_{10}H_7 + OH = C_{10}H_7O + H$	5.0000E+10	0.00	0.00	[112]
1277	$C_{10}H_7 + C_2H_4 = 1C_{12}H_{10} + H$	2.0160E+09	0.00	25.93	Est.(920)
1278	$C_{10}H_7 + C_2H_2 = AC_{12}H_8 + H$	3.5700E+21	-3.17	62.20	[200]
1279	$C_{10}H_8 + C_2H_3 = 1C_{12}H_{10} + H$	7.9400E+08	0.00	26.70	[75]
1280	$C_{10}H_8 + HO_2 = C_{10}H_7 + H_2O_2$	1.2160E+08	0.00	71.70	[75]
1281	$C_{10}H_8 + O = C_{10}H_7O + H$	2.5000E+10	0.00	19.54	[75]
1282	$C_{10}H_8 + O = C_{10}H_7 + OH$	2.0000E+10	0.00	61.52	[75]
1283	$C_{10}H_8 + OH = C_{10}H_7 + H_2O$	1.7000E+05	1.42	6.07	[75]
1284	$C_{10}H_8 + OH = C_{10}H_7OH + H$	1.0300E+10	0.00	44.31	[75]
1285	$C_{10}H_8 + H = C_{10}H_9T$	4.0000E+10	0.00	18.04	[112]
1286	$C_{10}H_8 + H = C_{10}H_9$	4.0000E+10	0.00	18.04	[112]
1287	$C_{10}H_8 + O_2 = C_{10}H_7 + HO_2$	5.0400E+10	0.00	251.04	[75]
1288	$C_{10}H_8 + CH_3 = C_{10}H_7 + CH_4$	4.3600E-07	5.00	51.49	Adj.(964)

No	Reaction	A	n	Ea	Ref
1289	$C_{10}H_8L + H = C_{10}H_7L + H_2$	1.0000E+10	0.00	24.00	[112]
1290	$C_{10}H_8L + OH = C_{10}H_7L + H_2O$	1.0000E+10	0.00	0.00	[112]
1291	$C_{10}H_8K = C_{10}H_8$	8.5100E+12	0.00	263.00	[112]
1292	$C_9H_6CH_2 = C_{10}H_8$	8.0000E+13	0.00	305.60	[131]
1293	$C_{10}H_8G + H = C_{10}H_9T$	2.0000E+11	0.00	0.00	[61]
1294	$C_{10}H_8J + H = C_{10}H_9T$	2.0000E+11	0.00	0.00	[61]
1295	$C_{10}H_9 + O_2 = C_6H_5 + C_4H_4O + O$	1.6000E+09	0.00	31.25	[112]
1296	$C_{10}H_9 = C_{10}H_9A$	3.0000E+14	0.00	209.20	[112]
1297	$C_{10}H_9A = C_{10}H_8L + H$	1.0000E+13	0.00	146.00	[112]
1298	$C_{10}H_9P = C_{10}H_9T$	1.0000E+10	0.00	0.00	[112]
1299	$C_{10}H_9P = C_{10}H_8L + H$	1.0000E+13	0.00	135.00	[112]
1300	$C_{10}H_9B = C_{10}H_9L$	1.0000E+13	0.00	36.00	[61]
1301	$C_{10}H_9B = C_{10}H_8L + H$	1.0000E+13	0.00	166.00	[112]
1302	$C_{10}H_9L = C_{10}H_9M$	1.0000E+10	0.00	0.00	[112]
1303	$C_{10}H_9M = C_{10}H_9T$	1.0000E+10	0.00	0.00	[112]
1304	$C_{10}H_9D = C_{10}H_9$	1.0000E+10	0.00	0.00	[112]
1305	$C_{10}H_9D = C_{10}H_8L + H$	1.0000E+13	0.00	70.00	[112]
1306	$C_{10}H_9E = C_{10}H_9T$	1.0000E+10	0.00	0.00	[112]
1307	$C_{10}H_9E = C_{10}H_8L + H$	1.0000E+13	0.00	90.00	[112]
1308	$C_{10}H_9F = C_{10}H_8 + H$	3.0000E+13	0.00	197.00	[112]
1309	$C_9H_6CH_3 = C_9H_6CH_2 + H$	5.0000E+14	0.00	213.50	[131]
1310	$C_{10}H_9K = C_{10}H_8K + H$	1.0000E+13	0.00	210.40	[112]
1311	$C_{10}H_9T + O_2 = C_6H_5 + C_4H_4O + O$	1.6000E+09	0.00	31.25	[112]
1312	$C_{10}H_{10}F = C_{10}H_9E + H$	1.0000E+13	0.00	459.00	[112]
1313	$C_{10}H_{10}F + H = C_{10}H_9E + H_2$	1.0000E+10	0.00	23.00	[112]
1314	$C_{10}H_{10}F + O = C_{10}H_9E + OH$	1.0000E+10	0.00	31.00	[112]
1315	$C_{10}H_{10}F + OH = C_{10}H_9E + H_2O$	1.0000E+10	0.00	0.00	[112]
1316	$C_{10}H_{10}K = C_{10}H_9K + H$	1.0000E+13	0.00	266.00	[112]
1317	$C_{10}H_{10}K + H = C_{10}H_9K + H_2$	1.0000E+11	0.00	0.00	[112]
1318	$C_{10}H_{10}K + O = C_{10}H_9K + H_2O$	1.0000E+11	0.00	0.00	[112]
1319	$C_{10}H_{10}K + O = C_{10}H_9K + OH$	1.0000E+11	0.00	000	[112]
1320	$C_{10}H_{10} = C_{10}H_9D + H$	1.0000E+13	0.00	459.00	[112]
1321	$C_{10}H_{10} + H = C_{10}H_9D + H_2$	1.0000E+10	0.00	24.00	[112]
1322	$C_{10}H_{10} + O = C_{10}H_9D + OH$	1.0000E+10	0.00	31.00	[112]
1323	$C_{10}H_{10} + OH = C_{10}H_9D + H_2O$	1.0000E+10	0.00	0.00	[112]

No	Reaction	A	n	Ea	Ref
1324	$C_9H_7CH_3 = C_9H_6CH_3 + H$	5.0000E+15	0.00	314.00	[131]
1325	$C_{10}H_7O + O = C_{10}H_6O_2 + H$	3.0000E+10	0.00	0.00	[75]
1326	$C_{10}H_7O = C_9H_7 + CO$	1.8000E+11	0.00	183.68	[75]
1327	$C_{10}H_7O + H = C_{10}H_7OH$	2.5000E+11	0.00	0.00	[75]
1328	$C_{10}H_6O_2 = C_9H_6O + CO$	2.9600E+11	0.00	247.00	[75]
1329	$C_{10}H_6O_2 + H = C_9H_7O + CO$	2.5000E+10	0.00	19.67	[75]
1330	$C_{10}H_7OO = C_{10}H_7O + O$	3.5300E+15	-0.70	138.27	[75]
1331	$C_{10}H_7OO = C_{10}H_6O_2 + H$	2.2720E+08	0.00	0.00	[75]
1332	$C_{10}H_7OO = C_9H_7 + CO_2$	2.2720E+08	0.00	0.00	[75]
1333	$C_{10}H_7OH + H = C_{10}H_7O + H_2$	9.0000E+10	0.00	51.88	[75]
1334	$C_{10}H_7OH + O = C_{10}H_7O + OH$	2.2300E+10	0.00	30.76	[75]
1335	$C_{10}H_7OH + OH = C_{10}H_7O + H_2O$	4.8000E+09	0.00	0.00	[75]
1336	$C_{10}H_7OH = C_9H_8 + CO$	4.0350E+11	0.00	254.00	[75]
1337	$C_{10}H_7OH + HO_2 = C_{10}H_7O + H_2O_2$	2.4490E+10	0.00	62.80	[75]
1338	$C_{10}H_7OH + O_2 = C_{10}H_7O + HO_2$	8.0000E+09	0.00	159.00	[75]
1339	$C_{11}H_9 + CH_3 = C_{12}H_{11} + H$	2.4500E+07	0.100	44.36	[75]
1340	$C_{11}H_9 + OH = C_{11}H_9O + H$	3.2100E+09	-0.23	58.28	[75]
1341	$C_{11}H_9 + O = C_{11}H_8O + H$	2.8000E+10	0.00	0.00	[75]
1342	$C_{11}H_9 + O = C_{10}H_8 + CHO$	2.8000E+10	0.00	0.00	[75]
1343	$C_{11}H_9 + O_2 = C_{11}H_9O + O$	6.6000E+10	0.00	131.36	[75]
1344	$C_{11}H_9 + O_2 = C_{11}H_8O + OH$	4.1827E+03	0.20	0.00	[75]
1345	$C_{11}H_9 + HO_2 = C_{11}H_9O + OH$	4.0000E+09	0.00	0.00	[75]
1346	$C_{11}H_9 + CH_3 = C_{12}H_{12}$	7.3000E+08	0.00	0.00	[72]
1347	$C_{11}H_9 = C_9H_7 + C_2H_2$	8.0000E+09	0.00	186.60	Adj.[28]
1348	$C_{11}H_9P = C_3H_3 + C_8H_6$	1.0000E+14	0.00	298.17	[75]
1349	$C_{11}H_9P = C_8H_5 + C_3H_4(P)$	2.0000E+14	0.00	408.00	[75]
1350	$C_{11}H_9P + O_2 = OC_{11}H_9 + O$	1.9575E+10	0.00	25.61	[75]
1351	$C_{11}H_9P + O_2 = OOC_{11}H_9P$	2.5000E+09	-0.15	0.66	[75]
1352	$C_{11}H_9P + H_2 = C_{11}H_{10} + H$	4.4400E+01	2.43	26.29	[75]
1353	$C_{11}H_9P + H = C_{11}H_{10}$	7.8300E+10	0.00	0.00	[75]
1354	$C_{11}H_{10} + O_2 = C_{11}H_9P + HO_2$	5.0400E+10	0.00	251.00	[75]
1355	$C_{11}H_{10} + O = C_{11}H_9P + OH$	2.0000E+10	0.00	61.52	[75]
1356	$C_{11}H_{10} = C_{10}H_7 + CH_3$	7.1280E+12	0.00	303.76	[75]
1357	$C_{11}H_{10} + OH = C_{11}H_9P + H_2O$	1.7000E+05	1.42	6.07	[75]
1358	$C_{11}H_{10} = C_{11}H_9 + H$	4.4800E+15	0.00	381.30	[75]

No	Reaction	A	n	Ea	Ref
1359	$C_{11}H_{10} + O_2 = C_{11}H_9 + HO_2$	1.2670E+09	0.00	166.28	[75]
1360	$C_{11}H_{10} + OH = C_{11}H_9 + H_2O$	4.1520E+06	1.00	3.66	[75]
1361	$C_{11}H_{10} + H = C_{11}H_9 + H_2$	1.6860E+11	0.00	61.99	Adj.[90]
1362	$C_{11}H_{10} + H = C_{10}H_8 + CH_3$	7.7356E+09	0.00	33.84	Adj.[90]
1363	$C_{11}H_{10} + O = C_{11}H_9 + OH$	5.0400E+08	0.00	0.00	[75]
1364	$C_{11}H_{10} + HO_2 = C_{11}H_9 + H_2O_2$	3.1800E+08	0.00	58.76	[75]
1365	$C_{11}H_{10} + CH_3 = C_{11}H_9 + CH_4$	1.5000E-10	6.00	25.26	Adj.[90]
1366	$C_{11}H_{10} + C_{10}H_7 = C_{11}H_9 + C_{10}H_8$	1.6800E+09	0.00	18.42	[75]
1367	$C_{11}H_{10} + HO_2 = C_{11}H_9P + H_2O_2$	4.3840E+09	0.00	120.55	[75]
1368	$C_{11}H_{10} + OH = C_{11}H_9O + H_2$	1.7760E+09	0.00	35.00	[75]
1369	$C_{11}H_{10} + OH = HOC_{11}H_9 + H$	1.8320E+09	0.00	-1.49	[75]
1370	$C_{11}H_{10} + CH_3 = CH_4 + C_{11}H_9P$	1.0000E+10	0.00	66.94	Present Work
1371	$C_{11}H_{10} + OH = C_{11}H_{10}O + H$	5.2800E+09	0.00	44.31	[75]
1372	$C_{11}H_{10} + O = C_{11}H_9O + H$	1.2420E+10	0.00	16.62	[75]
1373	$C_{11}H_{10} + O = OC_{11}H_9 + H$	2.4000E+10	0.00	16.54	[75]
1374	$C_{11}H_{10} + O = AC_{11}H_{10}O$	2.1700E+08	0.00	16.62	[75]
1375	$C_{11}H_7O = C_{10}H_7 + CO$	3.1840E+14	0.00	123.06	[75]
1376	$C_{11}H_7O + H = C_{10}H_8 + CO$	2.4000E+10	0.00	0.00	[75]
1377	$C_{11}H_8O = C_{11}H_7O + H$	3.1840E+14	0.00	350.20	Adj.[204]
1378	$C_{11}H_8O + O_2 = C_{11}H_7O + HO_2$	8.1600E+09	0.00	163.05	[75]
1379	$C_{11}H_8O + OH = C_{11}H_7O + H_2O$	1.3680E+06	1.18	-1.87	[75]
1380	$C_{11}H_8O + H = C_{11}H_7O + H_2$	4.0000E+10	0.00	20.63	[75]
1381	$C_{11}H_8O + H = C_{10}H_8 + CHO$	5.0000E+04	1.62	9.06	[75]
1382	$C_{11}H_8O + O = C_{11}H_7O + OH$	7.2320E+09	0.00	12.89	[75]
1383	$C_{11}H_8O + HO_2 = C_{11}H_7O + H_2O_2$	1.6000E+09	0.00	48.81	[75]
1384	$C_{11}H_8O + CH_3 = C_{11}H_7O + CH_4$	2.2160E+00	2.81	24.17	[75]
1385	$C_{11}H_8O + C_{10}H_7 = C_{11}H_7O + C_{10}H_8$	5.6080E+08	0.00	18.42	[75]
1386	$C_{11}H_8O + O = C_{10}H_8 + CO_2$	1.6000E+10	0.00	0.00	[75]
1387	$C_{11}H_9O = C_{10}H_8 + CHO$	4.0000E+12	0.00	79.00	[75]
1388	$C_{11}H_9O = C_{10}H_7 + CH_2O$	2.0000E+13	0.00	135.39	[75]
1389	$C_{11}H_9O + M = C_{11}H_8O + H + M$	2.0000E+08	0.00	0.00	[75]
1390	$C_{11}H_9O + H = C_{11}H_8O + H_2$	2.4000E+10	0.00	0.00	[75]
1391	$C_{11}H_9O + O = C_{11}H_8O + OH$	3.3600E+10	0.00	0.00	[75]
1392	$C_{11}H_9O + OH = C_{11}H_8O + H_2O$	1.9200E+10	0.00	0.00	[75]
1393	$C_{11}H_9O + O_2 = C_{11}H_8O + HO_2$	8.0000E+09	0.00	21.00	[75]

No	Reaction	A	n	Ea	Ref
1394	$C_{11}H_9O + H = C_{11}H_{10}O$	2.0240E+11	0.00	0.00	[75]
1395	$AC_{11}H_9O = C_{11}H_8O + H$	2.5280E+12	0.00	87.86	[75]
1396	$OC_{11}H_9 + H = HOC_{11}H_9$	2.0000E+11	0.00	0.00	[75]
1397	$OC_{11}H_9 + H_2O = HOC_{11}H_9 + OH$	5.5040E+09	0.36	136.25	[75]
1398	$OC_{11}H_9 = C_{10}H_9 + CO$	1.0080E-11	0.00	129.56	[72]
1399	$OC_{11}H_9 = C_9H_6CH_3 + CO$	3.3750E+11	0.00	183.74	[75]
1400	$OOC_{11}H_9P = C_9H_6CH_3 + CO_2$	1.2048E+08	0.00	0.00	[75]
1401	$OOC_{11}H_9P = OC_{11}H_9 + O$	1.0000E+10	0.00	0.00	[72]
1402	$C_{11}H_9OO = C_{11}H_8O + OH$	8.0000E+09	0.00	121.00	[75]
1403	$HOC_{11}H_9 + H = OC_{11}H_9 + H_2$	9.2000E+10	0.00	51.91	[75]
1404	$HOC_{11}H_9 + H = C_{10}H_7OH + CH_3$	9.6000E+09	0.00	21.55	[75]
1405	$C_{11}H_{10}O + H = C_{10}H_8 + CH_2OH$	9.0000E+07	0.00	21.55	Adj.[55]
1406	$AC_{11}H_{10}O = C_{10}H_7O + CH_3$	1.6000E+15	0.00	266.10	[75]
1407	$AC_{11}H_{10}O + H = C_{10}H_7OH + CH_3$	5.6640E+09	0.00	22.55	[75]
1408	$AC_{11}H_{10}O + O = AC_{11}H_9O + OH$	1.3360E+10	0.00	12.30	[75]
1409	$AC_{11}H_{10}O + OH = AC_{11}H_9O + H_2O$	9.6000E+08	0.00	-2.10	[75]
1410	$AC_{11}H_{10}O + CH_3 = AC_{11}H_9O + CH_4$	4.0080E+08	0.00	43.92	[75]
1411	$C_{11}H_{10}O + H = C_{11}H_9O + H_2$	5.6000E+10	0.00	34.00	[75]
1412	$C_{11}H_{10}O + O = C_{11}H_9O + OH$	4.0000E+09	0.00	8.00	[72]
1413	$C_{11}H_{10}O + OH = C_{11}H_9O + H_2O$	4.0000E+09	0.00	0.00	[72]
1414	$C_{11}H_{10}O + O_2 = C_{11}H_8O + HO_2 + H$	1.4000E+10	0.00	173.30	[75]
1415	$C_{11}H_{10}O + HO_2 = C_{11}H_9O + H_2O_2$	3.0000E+10	0.00	69.60	[72]
1416	$1C_{12}H_{10} + OH = C_{11}H_9 + CH_2O$	3.3750E+03	1.88	0.76	[75]
1417	$1C_{12}H_{10} + O = C_{11}H_9 + CHO$	3.3750E+03	1.88	0.76	[75]
1418	$1C_{12}H_{10} + O = C_{10}H_7 + CH_3CO$	2.0080E+03	1.88	0.76	[75]
1419	$C_{12}H_{11} = 1C_{12}H_{10} + H$	2.5380E+13	0.00	211.99	[75]
1420	$C_{12}H_{12} = C_{12}H_{11} + H$	1.2255E+15	0.00	330.00	[75]
1421	$C_{12}H_{12} + H = C_{12}H_{11} + H_2$	6.3000E-02	3.44	13.05	[75]
1422	$C_{12}H_{12} + H = C_{10}H_8 + C_2H_5$	6.0000E+09	0.00	21.33	[75]
1423	$C_{12}H_{12} + O = C_{12}H_{11} + OH$	1.1000E+09	0.00	15.89	[75]
1424	$C_{12}H_{12} + OH = C_{12}H_{11} + H_2O$	2.5000E+08	0.00	0.00	[75]
1425	$C_{12}H_{12} + HO_2 = C_{12}H_{11} + H_2O_2$	1.3250E+09	0.00	47.21	[75]
1426	$AC_{14}H_{10} = PC_{14}H_{10}$	7.4900E+09	0.00	271.90	[75]



**TABLE A.2**  
***n*-Propyl benzene Detailed Kinetic Sub-Mechanism**  
 (units are kmole, m<sup>3</sup>, s, K and kJ/mole)

No	Reaction	A	n	Ea	Ref
1427	C <sub>5</sub> H <sub>9</sub> = C <sub>3</sub> H <sub>5</sub> (A) + C <sub>2</sub> H <sub>4</sub>	2.5000E+13	0.00	125.52	[213]
1428	C <sub>5</sub> H <sub>9</sub> = C <sub>2</sub> H <sub>3</sub> + C <sub>3</sub> H <sub>6</sub>	2.5000E+13	0.00	125.52	[213]
1429	C <sub>5</sub> H <sub>9</sub> = C <sub>4</sub> H <sub>6</sub> (S) + CH <sub>3</sub>	1.0000E+14	0.00	133.89	[112]
1430	1C <sub>5</sub> H <sub>10</sub> = C <sub>2</sub> H <sub>5</sub> + C <sub>3</sub> H <sub>5</sub> (A)	1.0000E+16	0.00	298.80	[214]
1431	1C <sub>5</sub> H <sub>10</sub> = C <sub>3</sub> H <sub>6</sub> + C <sub>2</sub> H <sub>4</sub>	3.1600E+12	0.00	237.99	[214]
1432	1C <sub>5</sub> H <sub>10</sub> + H = C <sub>5</sub> H <sub>9</sub> + H <sub>2</sub>	2.8000E+10	0.00	16.74	[213]
1433	1C <sub>5</sub> H <sub>10</sub> + O = C <sub>5</sub> H <sub>9</sub> + OH	2.5400E+02	2.56	-4.73	[112]
1434	1C <sub>5</sub> H <sub>10</sub> + O = C <sub>4</sub> H <sub>9</sub> (N) + CHO	1.0000E+08	0.00	0.00	[112]
1435	1C <sub>5</sub> H <sub>10</sub> + O = C <sub>3</sub> H <sub>7</sub> (N) + CH <sub>3</sub> CO	1.0000E+08	0.00	0.00	[112]
1436	1C <sub>5</sub> H <sub>10</sub> + O = C <sub>4</sub> H <sub>8</sub> (N) + CH <sub>2</sub> O	8.5100E+09	0.00	0.00	[112]
1437	1C <sub>5</sub> H <sub>10</sub> + O = CH <sub>3</sub> CHO + C <sub>3</sub> H <sub>6</sub>	8.5100E+09	0.00	0.00	[213]
1438	1C <sub>5</sub> H <sub>10</sub> + O = C <sub>3</sub> H <sub>5</sub> (S) + C <sub>2</sub> H <sub>4</sub> + OH	2.0000E+10	0.00	29.30	[112]
1439	1C <sub>5</sub> H <sub>10</sub> + O = C <sub>3</sub> H <sub>6</sub> + C <sub>2</sub> H <sub>3</sub> + OH	1.0000E+10	0.00	29.30	[112]
1440	1C <sub>5</sub> H <sub>10</sub> + OH = C <sub>5</sub> H <sub>9</sub> + H <sub>2</sub> O	6.8000E+10	0.00	12.80	[112]
1441	1C <sub>5</sub> H <sub>10</sub> + OH = C <sub>4</sub> H <sub>9</sub> (N) + CH <sub>2</sub> O	1.0000E+08	0.00	0.00	[112]
1442	1C <sub>5</sub> H <sub>10</sub> + OH = C <sub>3</sub> H <sub>7</sub> (N) + CH <sub>3</sub> CHO	1.0000E+08	0.00	0.00	[112]
1443	1C <sub>5</sub> H <sub>10</sub> + OH = C <sub>3</sub> H <sub>5</sub> (S) + C <sub>2</sub> H <sub>4</sub> + H <sub>2</sub> O	2.0000E+06	1.20	0.50	[112]
1444	1C <sub>5</sub> H <sub>10</sub> + OH = C <sub>3</sub> H <sub>6</sub> + C <sub>2</sub> H <sub>3</sub> + H <sub>2</sub> O	1.0000E+06	1.20	0.50	[112]
1445	1C <sub>5</sub> H <sub>10</sub> + O <sub>2</sub> = C <sub>5</sub> H <sub>9</sub> + HO <sub>2</sub>	4.0000E+09	0.00	167.44	[112]
1446	1C <sub>5</sub> H <sub>10</sub> + CH <sub>3</sub> = C <sub>5</sub> H <sub>9</sub> + CH <sub>4</sub>	1.0000E+08	0.00	30.55	[112]
1447	1C <sub>5</sub> H <sub>11</sub> = C <sub>3</sub> H <sub>7</sub> (N) + C <sub>2</sub> H <sub>4</sub>	3.2000E+13	0.00	118.82	[112]
1448	1C <sub>5</sub> H <sub>11</sub> = 1C <sub>5</sub> H <sub>10</sub> + H	1.3000E+13	0.00	161.50	[112]
1449	C <sub>6</sub> H <sub>11</sub> = C <sub>3</sub> H <sub>6</sub> + C <sub>3</sub> H <sub>5</sub> (A)	5.0400E+13	0.00	125.58	[215]
1450	C <sub>6</sub> H <sub>11</sub> = C <sub>2</sub> H <sub>5</sub> + C <sub>4</sub> H <sub>6</sub> (T)	5.0000E+12	0.00	133.88	[215]
1451	1C <sub>6</sub> H <sub>12</sub> = C <sub>3</sub> H <sub>6</sub> + C <sub>3</sub> H <sub>6</sub>	3.9800E+12	0.00	241.41	[214]
1452	1C <sub>6</sub> H <sub>12</sub> + H = C <sub>6</sub> H <sub>11</sub> + H <sub>2</sub>	5.0000E+09	0.00	14.23	[112]
1453	1C <sub>6</sub> H <sub>12</sub> + O = C <sub>6</sub> H <sub>11</sub> + OH	4.0000E+10	0.00	16.74	[215]
1454	1C <sub>6</sub> H <sub>12</sub> + OH = C <sub>6</sub> H <sub>11</sub> + H <sub>2</sub> O	2.0000E+09	0.00	10.88	[112]
1455	1C <sub>6</sub> H <sub>12</sub> + CH <sub>3</sub> = C <sub>6</sub> H <sub>11</sub> + CH <sub>4</sub>	2.0000E+08	0.00	28.46	[215]
1456	1C <sub>6</sub> H <sub>12</sub> + HO <sub>2</sub> = C <sub>6</sub> H <sub>11</sub> + H <sub>2</sub> O <sub>2</sub>	1.0000E+08	0.00	71.41	[215]
1457	1C <sub>6</sub> H <sub>12</sub> + O = C <sub>2</sub> H <sub>3</sub> + C <sub>4</sub> H <sub>8</sub> (N) + OH	2.8200E+10	0.00	21.76	[215]

No	Reaction	A	n	Ea	Ref
1458	$1\text{C}_6\text{H}_{12} + \text{O} = \text{C}_3\text{H}_5(\text{A}) + \text{C}_3\text{H}_6 + \text{OH}$	2.8200E+10	0.00	21.76	[215]
1459	$1\text{C}_6\text{H}_{12} + \text{O} = \text{C}_4\text{H}_7(\text{N}) + \text{C}_2\text{H}_4 + \text{OH}$	5.0100E+10	0.00	32.86	[215]
1460	$1\text{C}_6\text{H}_{12} + \text{O} = \text{CHO} + 1\text{C}_5\text{H}_{11}$	1.0000E+08	0.00	0.00	[215]
1461	$1\text{C}_6\text{H}_{12} + \text{O} = \text{CH}_3 + \text{CO} + \text{C}_4\text{H}_9(\text{N})$	1.0000E+08	0.00	0.00	[215]
1462	$1\text{C}_6\text{H}_{12} + \text{OH} = \text{C}_2\text{H}_3 + \text{C}_4\text{H}_8(\text{N}) + \text{H}_2\text{O}$	2.1700E+05	1.25	2.93	[215]
1463	$1\text{C}_6\text{H}_{12} + \text{OH} = \text{C}_3\text{H}_5(\text{A}) + \text{C}_3\text{H}_6 + \text{H}_2\text{O}$	2.1700E+05	1.25	2.93	[215]
1464	$1\text{C}_6\text{H}_{12} + \text{OH} = \text{C}_4\text{H}_7(\text{N}) + \text{C}_2\text{H}_4 + \text{H}_2\text{O}$	7.1700E+05	1.05	7.57	[215]
1465	$1\text{C}_6\text{H}_{12} + \text{OH} = \text{CH}_2\text{O} + 1\text{C}_5\text{H}_{11}$	1.0000E+08	0.00	0.00	[215]
1466	$1\text{C}_6\text{H}_{12} + \text{OH} = \text{CH}_3\text{CHO} + \text{C}_4\text{H}_9(\text{N})$	1.0000E+08	0.00	0.00	[215]
1467	$1\text{C}_6\text{H}_{12} = \text{C}_3\text{H}_7(\text{N}) + \text{C}_3\text{H}_5(\text{A})$	7.9400E+15	0.00	297.64	[214]
1468	$1\text{C}_6\text{H}_{13} = 2\text{C}_6\text{H}_{13}$	2.0000E+11	0.00	75.76	[215]
1469	$1\text{C}_6\text{H}_{13} = \text{C}_2\text{H}_4 + \text{C}_4\text{H}_9(\text{N})$	2.5200E+13	0.00	120.55	[213]
1470	$2\text{C}_6\text{H}_{13} = \text{C}_3\text{H}_7(\text{N}) + \text{C}_3\text{H}_6$	1.6000E+13	0.00	118.46	[213]
1471	$\text{C}_7\text{H}_{13} = \text{C}_3\text{H}_5(\text{A}) + \text{C}_4\text{H}_8(\text{N})$	2.5200E+13	0.00	125.58	[215]
1472	$\text{C}_7\text{H}_{13} = \text{C}_3\text{H}_4(\text{A}) + \text{C}_4\text{H}_9(\text{N})$	1.0000E+13	0.00	125.58	[215]
1473	$\text{C}_7\text{H}_{13} = \text{C}_4\text{H}_6(\text{S}) + \text{C}_3\text{H}_7(\text{N})$	1.0000E+13	0.00	133.95	[213]
1474	$1\text{C}_7\text{H}_{14} = \text{C}_3\text{H}_5(\text{A}) + \text{C}_4\text{H}_9(\text{N})$	2.5200E+16	0.00	297.62	[215]
1475	$1\text{C}_7\text{H}_{14} + \text{H} = \text{C}_7\text{H}_{13} + \text{H}_2$	8.0000E+10	0.00	14.23	[215]
1476	$1\text{C}_7\text{H}_{14} + \text{OH} = \text{C}_7\text{H}_{13} + \text{H}_2\text{O}$	2.0000E+10	0.00	10.88	[215]
1477	$1\text{C}_7\text{H}_{14} + \text{OH} = \text{C}_2\text{H}_3 + 1\text{C}_5\text{H}_{10} + \text{H}_2\text{O}$	1.2900E+06	1.25	2.93	[215]
1478	$1\text{C}_7\text{H}_{14} + \text{OH} = \text{C}_3\text{H}_5(\text{A}) + \text{C}_4\text{H}_8(\text{N}) + \text{H}_2\text{O}$	1.2900E+06	1.25	2.93	[215]
1479	$1\text{C}_7\text{H}_{14} + \text{OH} = \text{C}_4\text{H}_7(\text{N}) + \text{C}_3\text{H}_6 + \text{H}_2\text{O}$	1.2900E+06	1.25	2.93	[215]
1480	$1\text{C}_7\text{H}_{14} + \text{OH} = \text{C}_5\text{H}_9 + \text{C}_2\text{H}_4 + \text{H}_2\text{O}$	4.2700E+06	1.05	7.56	[215]
1481	$1\text{C}_7\text{H}_{14} + \text{CH}_3 = \text{C}_7\text{H}_{13} + \text{CH}_4$	2.0000E+08	0.00	28.46	[215]
1482	$1\text{C}_7\text{H}_{14} + \text{HO}_2 = \text{C}_7\text{H}_{13} + \text{H}_2\text{O}_2$	5.0000E+09	0.00	0.00	[215]
1483	$1\text{C}_7\text{H}_{14} + \text{O} = \text{C}_7\text{H}_{13} + \text{OH}$	4.0000E+10	0.00	16.74	[215]
1484	$1\text{C}_7\text{H}_{14} + \text{O} = \text{C}_2\text{H}_3 + 1\text{C}_5\text{H}_{10} + \text{OH}$	2.8200E+10	0.00	21.76	[215]
1485	$1\text{C}_7\text{H}_{14} + \text{O} = \text{C}_3\text{H}_5(\text{A}) + \text{C}_4\text{H}_8(\text{N}) + \text{OH}$	2.8200E+10	0.00	21.76	[215]
1486	$1\text{C}_7\text{H}_{14} + \text{O} = \text{C}_4\text{H}_7(\text{N}) + \text{C}_3\text{H}_6 + \text{OH}$	2.8200E+10	0.00	21.76	[215]
1487	$1\text{C}_7\text{H}_{14} + \text{O} = \text{C}_5\text{H}_9 + \text{C}_2\text{H}_4 + \text{OH}$	5.0000E+10	0.00	32.86	[215]
1488	$2\text{C}_7\text{H}_{14} = \text{C}_3\text{H}_7(\text{N}) + \text{C}_4\text{H}_7(\text{N})$	1.6000E+16	0.00	290.00	[213]
1489	$2\text{C}_7\text{H}_{14} + \text{H} = \text{C}_7\text{H}_{13} + \text{H}_2$	1.6000E+11	0.00	14.23	[215]
1490	$2\text{C}_7\text{H}_{14} + \text{O} = \text{C}_7\text{H}_{13} + \text{OH}$	8.0000E+10	0.00	16.74	[215]
1491	$2\text{C}_7\text{H}_{14} + \text{O} = \text{C}_3\text{H}_5(\text{T}) + \text{C}_4\text{H}_8(\text{N}) + \text{OH}$	2.8200E+10	0.00	21.76	[215]
1492	$2\text{C}_7\text{H}_{14} + \text{O} = \text{C}_4\text{H}_7(\text{N}) + \text{C}_3\text{H}_6 + \text{OH}$	2.8200E+10	0.00	21.76	[215]

No	Reaction	A	n	Ea	Ref
1493	$2C_7H_{14} + O = C_5H_9 + C_2H_4 + OH$	5.0000E+10	0.00	32.86	[215]
1494	$2C_7H_{14} + OH = C_7H_{13} + H_2O$	4.0000E+10	0.00	10.88	[215]
1495	$2C_7H_{14} + OH = C_3H_5(A) + C_4H_8(N) + H_2O$	1.1600E+06	1.25	2.93	[215]
1496	$2C_7H_{14} + OH = C_4H_7(N) + C_3H_6 + H_2O$	1.1600E+06	1.25	2.93	[215]
1497	$2C_7H_{14} + OH = C_5H_9 + C_2H_4 + H_2O$	4.2700E+06	1.05	7.57	[215]
1498	$2C_7H_{14} + CH_3 = C_7H_{13} + CH_4$	4.0000E+08	0.00	28.46	[112]
1499	$2C_7H_{14} + HO_2 = C_7H_{13} + H_2O_2$	5.0000E+09	0.00	0.00	[215]
1500	$3C_7H_{14} = C_2H_5 + C_5H_9$	3.6000E+15	0.00	297.20	[215]
1501	$3C_7H_{14} = C_6H_{11} + CH_3$	5.3000E+16	0.00	305.57	[215]
1502	$3C_7H_{14} + H = C_7H_{13} + H_2$	1.6000E+11	0.00	14.23	[215]
1503	$3C_7H_{14} + O = C_7H_{13} + OH$	8.0000E+10	0.00	16.74	[215]
1504	$3C_7H_{14} + O = C_4H_7(N) + C_3H_6 + OH$	2.8200E+10	0.00	21.76	[215]
1505	$3C_7H_{14} + O = C_5H_9 + C_2H_4 + OH$	5.0000E+10	0.00	32.86	[215]
1506	$3C_7H_{14} + OH = C_7H_{13} + H_2O$	4.0000E+10	0.00	10.88	[215]
1507	$3C_7H_{14} + OH = C_4H_7(N) + C_3H_6 + H_2O$	1.1600E+06	1.25	2.93	[215]
1508	$3C_7H_{14} + OH = C_5H_9 + C_2H_4 + H_2O$	4.2700E+06	1.05	2.93	[215]
1509	$3C_7H_{14} + CH_3 = C_7H_{13} + CH_4$	4.0800E+08	0.00	28.46	[215]
1510	$3C_7H_{14} + HO_2 = C_7H_{13} + H_2O_2$	5.0000E+09	0.00	0.00	[215]
1511	$1C_7H_{15} = C_2H_4 + 1C_5H_{11}$	2.5200E+13	0.00	120.55	[213]
1512	$1C_7H_{15} = 2C_7H_{15}$	2.0000E+11	0.00	46.46	[215]
1513	$1C_7H_{15} = 3C_7H_{15}$	2.0000E+11	0.00	75.76	[215]
1514	$1C_7H_{15} = 4C_7H_{15}$	2.0000E+11	0.00	83.72	[215]
1515	$1C_7H_{15} = 1C_7H_{14} + H$	1.0000E+13	0.00	169.11	[215]
1516	$1C_7H_{15} + O_2 = 1C_7H_{14} + HO_2$	1.0000E+09	0.00	8.37	[215]
1517	$2C_7H_{15} = 3C_7H_{15}$	2.0000E+11	0.00	83.72	[215]
1518	$2C_7H_{15} + O_2 = 1C_7H_{14} + HO_2$	1.0000E+09	0.00	18.83	[215]
1519	$2C_7H_{15} + O_2 = 2C_7H_{14} + HO_2$	2.0000E+09	0.00	17.79	[215]
1520	$2C_7H_{15} = C_3H_6 + C_4H_9(N)$	1.6000E+13	0.00	118.46	[213]
1521	$2C_7H_{15} = 1C_7H_{14} + H$	1.0000E+13	0.00	169.11	[215]
1522	$2C_7H_{15} = 2C_7H_{14} + H$	1.0000E+13	0.00	169.11	[215]
1523	$3C_7H_{15} = C_3H_7(N) + C_4H_8(N)$	5.0000E+12	0.00	121.81	[213]
1524	$3C_7H_{15} = 2C_7H_{14} + H$	1.0000E+13	0.00	169.11	[215]
1525	$3C_7H_{15} = 3C_7H_{14} + H$	1.0000E+13	0.00	169.11	[215]
1526	$3C_7H_{15} + O_2 = 2C_7H_{14} + HO_2$	2.0000E+09	0.00	17.79	[215]
1527	$3C_7H_{15} + O_2 = 3C_7H_{14} + HO_2$	2.0000E+09	0.00	17.79	[215]

No	Reaction	A	n	Ea	Ref
1528	$4C_7H_{15} = 3C_7H_{14} + H$	1.0000E+13	0.00	169.11	[215]
1529	$4C_7H_{15} + O_2 = 3C_7H_{14} + HO_2$	4.0000E+09	0.00	17.79	[215]
1530	$C_7H_{16} = 1C_6H_{13} + CH_3$	4.1750E+12	0.00	261.90	[112]
1531	$C_7H_{16} = 1C_7H_{15} + H$	1.0000E+15	0.00	418.60	[215]
1532	$C_7H_{16} = 2C_7H_{15} + H$	1.0000E+15	0.00	418.60	[215]
1533	$C_7H_{16} = 3C_7H_{15} + H$	1.0000E+15	0.00	418.60	[215]
1534	$C_7H_{16} = 4C_7H_{15} + H$	1.0000E+15	0.00	418.60	[215]
1535	$C_7H_{16} + H = 1C_7H_{15} + H_2$	5.6200E+04	2.00	32.23	[215]
1536	$C_7H_{16} + H = 2C_7H_{15} + H_2$	1.8200E+03	2.00	20.93	[215]
1537	$C_7H_{16} + H = 3C_7H_{15} + H_2$	1.8200E+03	2.00	20.93	[215]
1538	$C_7H_{16} + H = 4C_7H_{15} + H_2$	9.0000E+03	2.00	20.93	[215]
1539	$C_7H_{16} + O = 1C_7H_{15} + OH$	2.3000E+03	2.40	6.65	[215]
1540	$C_7H_{16} + O = 2C_7H_{15} + OH$	6.4000E+02	2.50	20.93	[215]
1541	$C_7H_{16} + O = 3C_7H_{15} + OH$	6.4000E+02	2.50	20.93	[215]
1542	$C_7H_{16} + O = 4C_7H_{15} + OH$	3.2000E+02	2.50	20.93	[215]
1543	$C_7H_{16} + OH = 1C_7H_{15} + H_2O$	5.2500E+06	0.97	6.65	[215]
1544	$C_7H_{16} + OH = 2C_7H_{15} + H_2O$	2.3500E+04	1.61	0.00	[215]
1545	$C_7H_{16} + OH = 3C_7H_{15} + H_2O$	2.3500E+04	1.61	0.00	[215]
1546	$C_7H_{16} + OH = 4C_7H_{15} + H_2O$	1.1750E+04	1.61	0.00	[215]
1547	$C_7H_{16} + CH_3 = 1C_7H_{15} + CH_4$	3.0000E+09	0.00	48.55	[215]
1548	$C_7H_{16} + CH_3 = 2C_7H_{15} + CH_4$	1.6000E+09	0.00	39.76	[215]
1549	$C_7H_{16} + CH_3 = 3C_7H_{15} + CH_4$	1.6000E+09	0.00	39.76	[215]
1550	$C_7H_{16} + CH_3 = 4C_7H_{15} + CH_4$	8.0000E+08	0.00	39.76	[215]
1551	$C_7H_{16} + O_2 = 1C_7H_{15} + HO_2$	2.5100E+10	0.00	205.11	[215]
1552	$C_7H_{16} + O_2 = 2C_7H_{15} + HO_2$	3.9800E+10	0.00	199.25	[215]
1553	$C_7H_{16} + O_2 = 3C_7H_{15} + HO_2$	4.0000E+10	0.00	199.25	[215]
1554	$C_7H_{16} + O_2 = 4C_7H_{15} + HO_2$	2.0000E+10	0.00	199.25	[215]
1555	$C_7H_{16} = C_3H_7(N) + C_4H_9(N)$	2.5000E+13	0.00	261.90	[112]
1556	$C_7H_{16} = C_2H_5 + 1C_5H_{11}$	1.2500E+13	0.00	261.90	[112]
1557	$C_8H_{16} + O = 1C_7H_{15} + CHO$	1.0000E+08	0.00	0.00	[213]
1558	$C_8H_{16} + OH = 1C_7H_{15} + CH_2O$	1.0000E+08	0.00	0.00	[213]
1559	$C_8H_{16} = 1C_5H_{11} + C_3H_5(A)$	2.0000E+15	0.00	297.48	[213]
1560	$C_8H_{16} = C_4H_9(N) + C_4H_7(N)$	1.0000E+16	0.00	342.25	[213]
1561	$C_8H_{16} + O = 1C_6H_{13} + CH_3CO$	1.0000E+08	0.00	0.00	[213]
1562	$C_8H_{16} + OH = 1C_6H_{13} + CH_3CHO$	1.0000E+08	0.00	0.00	[213]

No	Reaction	A	n	Ea	Ref
1563	$C_8H_{17} = 1C_7H_{14} + CH_3$	7.9400E+13	0.00	138.07	[213]
1564	$C_8H_{17} = 1C_5H_{11} + C_3H_6$	1.5800E+13	0.00	118.41	[213]
1565	$C_8H_{17} = C_4H_9(N) + C_4H_8(N)$	5.0100E+12	0.00	121.75	[213]
1566	$C_8H_{17} = C_8H_{16} + H$	2.0000E+13	0.00	158.99	[112]
1567	$C_8H_{17} = 1C_5H_{10} + C_3H_7(N)$	5.0100E+12	0.00	121.75	[213]
1568	$C_8H_{17} = 1C_6H_{13} + C_2H_4$	2.5100E+13	0.00	120.50	[213]
1569	$C_8H_{17} + O_2 = C_8H_{16} + HO_2$	4.0000E+09	0.00	8.36	[112]
1570	$1C_9H_{10} + H = C_6H_5 + C_3H_6$	1.0000E+10	0.00	44.57	[216]
1571	$1C_9H_{10} + H = C_8H_8 + CH_3$	3.9800E+10	0.00	9.97	[216]
1572	$1C_9H_{10} + H = C_6H_6 + C_3H_5(S)$	1.5848E+11	0.00	52.35	[216]
1573	$1C_9H_{10} + H = C_9H_9(T) + H_2$	1.5848E+11	0.00	46.53	[216]
1574	$1C_9H_{10} + O = C_7H_6O + C_2H_4$	5.2300E+04	1.57	-2.63	[75]
1575	$1C_9H_{10} + O_2 = C_9H_9(T) + HO_2$	2.0000E+10	0.00	184.10	[75]
1576	$1C_9H_{10} + O_2 = C_7H_6O + CH_3CHO$	1.0000E+10	0.00	0.00	[75]
1577	$1C_9H_{10} + HO_2 = C_7H_6O + C_2H_4 + OH$	1.0000E+09	0.00	0.00	[75]
1578	$1C_9H_{10} + OH = C_7H_6O + C_2H_5$	1.0000E+10	0.00	0.00	[75]
1579	$2C_9H_{10} + H = 3C_9H_{11}$	7.2300E+09	0.00	12.14	[75]
1580	$2C_9H_{10} + H = C_6H_5 + C_3H_6$	1.0000E+11	0.00	44.57	[75]
1581	$2C_9H_{10} + H = C_7H_7 + C_2H_4$	2.6000E+05	1.50	8.36	Present Work
1582	$2C_9H_{10} + H = C_6H_6 + C_3H_5(S)$	1.5848E+11	0.00	52.35	[75]
1583	$2C_9H_{10} + O = C_8H_8 + CH_2O$	5.2300E+04	1.57	2.63	[75]
1584	$1C_9H_{11} = 1C_9H_{10} + H$	6.3000E+13	0.00	154.39	[75]
1585	$1C_9H_{11} = C_7H_7 + C_2H_4$	2.0000E+10	0.00	123.50	[75]
1586	$2C_9H_{11} = 2C_9H_{10} + H$	3.1500E+13	0.00	154.39	[75]
1587	$2C_9H_{11} = C_8H_8 + CH_3$	2.0000E+10	0.00	123.43	[75]
1588	$2C_9H_{11} = 1C_9H_{10} + H$	3.1500E+13	0.00	154.39	[75]
1589	$2C_9H_{11} = C_6H_6 + C_3H_5(S)$	4.0000E+13	0.00	197.75	[75]
1590	$2C_9H_{11} = C_6H_6 + C_3H_5(A)$	0.00	0.00	0.00	[75]
1591	$3C_9H_{11} + HO_2 = C_8H_{10} + CHO + OH$	2.5000E+09	0.00	0.00	[75]
1592	$3C_9H_{11} + HO_2 = C_8H_9 + CH_2O + OH$	2.5000E+09	0.00	0.00	[75]
1593	$3C_9H_{11} = C_8H_8 + CH_3$	2.0000E+13	0.00	113.10	[75]
1594	$1C_9H_{11} = C_8H_8 + CH_3$	1.0000E+14	0.00	145.81	[36]
1595	$1C_9H_{11} + O = C_7H_6O + C_2H_5$	1.6000E+10	0.00	0.00	[36]
1596	$1C_9H_{11} + OH = C_7H_6O + C_2H_6$	1.6000E+10	0.00	0.00	[36]
1597	$2C_9H_{11} + OH = C_7H_8 + CH_3CHO$	2.0000E+10	0.00	16.73	[36]

No	Reaction	A	n	Ea	Ref
1598	$2C_9H_{11} = C_6H_5 + C_3H_6$	1.0000E+14	0.00	145.60	[36]
1599	$3C_9H_{11} = C_7H_7 + C_2H_4$	1.2300E+13	-0.10	126.37	Present Work
1600	$C_9H_{12} + H = 1C_9H_{11} + H_2$	1.0100E+01	2.90	8.07	[36]
1601	$C_9H_{12} + O = 1C_9H_{11} + OH$	4.7700E+01	2.70	4.62	Adj.[113]
1602	$C_9H_{12} + OH = 1C_9H_{11} + H_2O$	7.0800E+03	1.90	-4.84	[36]
1603	$C_9H_{12} + H = 2C_9H_{11} + H_2$	1.0100E+01	2.90	12.26	[36]
1604	$C_9H_{12} + O = 2C_9H_{11} + OH$	4.7700E+01	2.70	8.81	Adj.[113]
1605	$C_9H_{12} + OH = 2C_9H_{11} + H_2O$	4.7865E+03	1.40	3.56	[75]
1606	$C_9H_{12} + H = 3C_9H_{11} + H_2$	1.3300E+03	2.50	28.26	[36]
1607	$C_9H_{12} + O = 3C_9H_{11} + OH$	1.9300E+02	2.70	15.54	[36]
1608	$C_9H_{12} + OH = 3C_9H_{11} + H_2O$	3.1600E+04	1.80	3.90	Adj.[217]
1609	$C_9H_{12} + HO_2 = 1C_9H_{11} + H_2O_2$	9.6400E+00	2.60	54.01	[36]
1610	$C_9H_{12} + CH_3 = 1C_9H_{11} + CH_4$	1.5000E-03	3.46	22.90	Adj.[113]
1611	$C_9H_{12} + HO_2 = 2C_9H_{11} + H_2O_2$	9.6400E+00	2.60	58.20	Adj.[113]
1612	$C_9H_{12} + HO_2 = 3C_9H_{11} + H_2O_2$	4.7600E+01	2.50	69.01	Adj.[113]
1613	$C_9H_{12} + CH_3 = 3C_9H_{11} + CH_4$	9.0300E-04	3.65	29.90	Adj.[113]
1614	$C_9H_{12} + CH_3 = 2C_9H_{11} + CH_4$	1.5055E-03	3.46	22.90	Adj.[113]
1615	$C_9H_{12} + C_2H_5 = 1C_9H_{11} + C_2H_6$	1.2100E-03	3.46	31.26	Adj.[113]
1616	$C_9H_{12} + C_2H_5 = 2C_9H_{11} + C_2H_6$	1.2100E-03	3.46	31.26	Adj.[113]
1617	$C_9H_{12} + C_2H_5 = 3C_9H_{11} + C_2H_6$	9.0400E-04	3.65	38.24	Adj.[113]
1618	$C_9H_{12} + C_2H_3 = 1C_9H_{11} + C_2H_4$	1.0000E+00	3.10	36.94	Adj.[113]
1619	$C_9H_{12} + C_2H_3 = 2C_9H_{11} + C_2H_4$	1.0000E+00	3.10	36.94	Adj.[113]
1620	$C_9H_{12} + C_2H_3 = 3C_9H_{11} + C_2H_4$	6.0000E-01	3.30	43.94	Adj.[113]
1621	$C_9H_{12} + C_3H_5(A) = 1C_9H_{11} + C_3H_6$	7.9400E+08	0.00	67.82	[36]
1622	$C_9H_{12} + C_3H_5(A) = 2C_9H_{11} + C_3H_6$	7.9400E+08	0.00	67.78	[36]
1623	$C_9H_{12} + C_3H_5(A) = 3C_9H_{11} + C_3H_6$	7.9400E+08	0.00	85.77	[36]
1624	$C_9H_{12} + C_6H_5 = 1C_9H_{11} + C_6H_6$	7.9400E+08	0.00	67.78	[36]
1625	$C_9H_{12} + C_6H_5 = 2C_9H_{11} + C_6H_6$	7.9400E+08	0.00	67.68	[36]
1626	$C_9H_{12} + C_6H_5 = 3C_9H_{11} + C_6H_6$	7.9400E+08	0.00	85.77	[36]
1627	$C_9H_{12} + C_7H_7 = 1C_9H_{11} + C_7H_8$	7.9400E+08	0.00	67.78	[36]
1628	$C_9H_{12} + C_7H_7 = 2C_9H_{11} + C_7H_8$	7.9400E+08	0.00	67.68	[36]
1629	$C_9H_{12} + C_7H_7 = 3C_9H_{11} + C_7H_8$	7.9400E+08	0.00	85.84	[36]
1630	$C_9H_{12} + O_2 = 1C_9H_{11} + HO_2$	4.0000E+10	0.00	149.78	[36]
1631	$C_9H_{12} + O_2 = 2C_9H_{11} + HO_2$	4.0000E+10	0.00	207.10	[36]
1632	$C_9H_{12} + O_2 = 3C_9H_{11} + HO_2$	4.0000E+10	0.00	211.71	[36]

No	Reaction	A	n	Ea	Ref
1633	$C_9H_{12} = C_6H_5 + C_3H_7(N)$	1.0000E+16	0.00	305.43	Adj.[13]
1634	$C_9H_{12} = C_7H_7 + C_2H_5$	1.0000E+16	0.00	305.43	Adj.[13]
1635	$C_9H_{12} = C_8H_9 + CH_3$	8.0000E+16	0.00	353.13	Adj.[13]
1636	$C_9H_{12} + H = C_3H_7(N) + C_6H_6$	5.7800E+10	0.00	33.84	Adj.[90]
1637	$C_9H_{12} = 3C_9H_{11} + H$	8.0000E+15	0.00	419.27	[36]
1638	$C_9H_{12} = 2C_9H_{11} + H$	8.0000E+15	0.00	414.00	[36]
1639	$C_9H_{12} = 1C_9H_{11} + H$	8.0000E+15	0.00	360.70	[36]
1640	$C_9H_{12} + C_3H_5(T) = 1C_9H_{11} + C_3H_6$	7.9400E+08	0.00	67.78	[36]
1641	$C_9H_{12} + C_3H_5(S) = 1C_9H_{11} + C_3H_6$	7.9400E+08	0.00	67.78	[36]
1642	$C_9H_{12} + C_3H_5(T) = 2C_9H_{11} + C_3H_6$	7.9400E+08	0.00	67.78	[36]
1643	$C_9H_{12} + C_3H_5(S) = 2C_9H_{11} + C_3H_6$	7.9400E+08	0.00	67.78	[36]
1644	$C_9H_{12} + C_3H_5(T) = 3C_9H_{11} + C_3H_6$	7.9400E+08	0.00	85.77	[36]
1645	$C_9H_{12} + C_3H_5(S) = 3C_9H_{11} + C_3H_6$	7.9400E+08	0.00	85.77	[36]
1646	$1C_{10}H_{21} = C_8H_{17} + C_2H_4$	2.1000E+13	0.00	121.00	[112]
1647	$1C_{10}H_{21} = 4C_{10}H_{21}$	2.0000E+11	0.00	84.00	[112]
1648	$1C_{10}H_{21} = 5C_{10}H_{21}$	2.0000E+11	0.00	84.00	[112]
1649	$2C_{10}H_{21} = 1C_7H_{15} + C_3H_6$	2.1000E+13	0.00	121.00	[112]
1650	$2C_{10}H_{21} = 5C_{10}H_{21}$	2.0000E+11	0.00	84.00	[112]
1651	$2C_{10}H_{21} = 4C_{10}H_{21}$	2.0000E+11	0.00	84.00	[112]
1652	$3C_{10}H_{21} = 1C_6H_{13} + C_4H_8(N)$	2.1000E+13	0.00	121.00	[112]
1653	$3C_{10}H_{21} = 5C_{10}H_{21}$	2.0000E+11	0.00	84.00	[112]
1654	$3C_{10}H_{21} = 4C_{10}H_{21}$	2.0000E+11	0.00	84.00	[112]
1655	$4C_{10}H_{21} = 1C_5H_{11} + 1C_5H_{10}$	2.1000E+13	0.00	121.00	[112]
1656	$4C_{10}H_{21} = C_8H_{16} + C_2H_5$	2.1000E+13	0.00	121.00	[75]
1657	$5C_{10}H_{21} = C_4H_9(N) + 1C_6H_{12}$	2.1000E+13	0.00	121.00	[75]
1658	$5C_{10}H_{21} = C_3H_7(N) + 1C_7H_{14}$	2.1000E+13	0.00	121.00	[75]
1659	$C_{10}H_{22} = 1C_7H_{15} + C_3H_7(N)$	3.1420E+14	0.00	283.90	[75]
1660	$C_{10}H_{22} = 1C_5H_{11} + 1C_5H_{11}$	3.1420E+14	0.00	283.90	[75]
1661	$C_{10}H_{22} = 1C_6H_{13} + C_4H_9(N)$	3.1420E+14	0.00	283.90	[75]
1662	$C_{10}H_{22} = 1C_{10}H_{21} + H$	8.0000E+14	0.00	424.00	[112]
1663	$C_{10}H_{22} = 2C_{10}H_{21} + H$	8.0000E+14	0.00	424.00	[112]
1664	$C_{10}H_{22} = 3C_{10}H_{21} + H$	8.0000E+14	0.00	424.00	[112]
1665	$C_{10}H_{22} = 4C_{10}H_{21} + H$	8.0000E+14	0.00	424.00	[112]
1666	$C_{10}H_{22} = 5C_{10}H_{21} + H$	8.0000E+14	0.00	424.00	[112]
1667	$C_{10}H_{22} + H = 1C_{10}H_{21} + H_2$	4.7000E+04	2.00	32.20	[112]

No	Reaction	A	n	Ea	Ref
1668	$C_{10}H_{22} + H = 2C_{10}H_{21} + H_2$	1.5000E+04	2.00	20.92	[112]
1669	$C_{10}H_{22} + H = 3C_{10}H_{21} + H_2$	1.5000E+04	2.00	20.92	[112]
1670	$C_{10}H_{22} + H = 4C_{10}H_{21} + H_2$	1.5000E+04	2.00	20.92	[112]
1671	$C_{10}H_{22} + H = 5C_{10}H_{21} + H_2$	1.5000E+04	2.00	20.92	[112]
1672	$C_{10}H_{22} + OH = 1C_{10}H_{21} + H_2O$	4.4000E+06	0.97	6.65	[112]
1673	$C_{10}H_{22} + OH = 2C_{10}H_{21} + H_2O$	1.9600E+04	1.61	0.00	[112]
1674	$C_{10}H_{22} + OH = 3C_{10}H_{21} + H_2O$	1.9600E+04	1.61	0.00	[112]
1675	$C_{10}H_{22} + OH = 4C_{10}H_{21} + H_2O$	1.9600E+04	1.61	0.00	[112]
1676	$C_{10}H_{22} + OH = 5C_{10}H_{21} + H_2O$	1.9600E+04	1.61	0.00	[112]
1677	$C_{10}H_{22} + O = 1C_{10}H_{21} + OH$	1.9200E+03	2.40	6.65	[112]
1678	$C_{10}H_{22} + O = 2C_{10}H_{21} + OH$	5.3300E+02	2.50	20.92	[112]
1679	$C_{10}H_{22} + O = 3C_{10}H_{21} + OH$	5.3300E+02	2.50	20.92	[112]
1680	$C_{10}H_{22} + O = 4C_{10}H_{21} + OH$	5.3300E+02	2.50	20.92	[112]
1681	$C_{10}H_{22} + O = 5C_{10}H_{21} + OH$	5.3300E+02	2.50	20.92	[112]
1682	$C_{10}H_{22} + CH_3 = 1C_{10}H_{21} + CH_4$	2.5000E+09	0.00	48.53	[112]
1683	$C_{10}H_{22} + CH_3 = 2C_{10}H_{21} + CH_4$	1.3300E+09	0.00	39.75	[112]
1684	$C_{10}H_{22} + CH_3 = 3C_{10}H_{21} + CH_4$	1.3300E+09	0.00	39.75	[112]
1685	$C_{10}H_{22} + CH_3 = 4C_{10}H_{21} + CH_4$	1.3300E+09	0.00	39.75	[112]
1686	$C_{10}H_{22} + CH_3 = 5C_{10}H_{21} + CH_4$	1.3300E+09	0.00	39.75	[112]
1687	$C_{10}H_{22} + O_2 = 1C_{10}H_{21} + HO_2$	2.0900E+10	0.00	218.12	[112]
1688	$C_{10}H_{22} + O_2 = 2C_{10}H_{21} + HO_2$	3.3000E+10	0.00	204.00	[112]
1689	$C_{10}H_{22} + O_2 = 3C_{10}H_{21} + HO_2$	3.3000E+10	0.00	204.00	[112]
1690	$C_{10}H_{22} + O_2 = 4C_{10}H_{21} + HO_2$	3.3000E+10	0.00	204.00	[112]
1691	$C_{10}H_{22} + O_2 = 5C_{10}H_{21} + HO_2$	3.3000E+10	0.00	204.00	[112]



**Enhanced Collision Efficiencies**

Unless otherwise specified, collision efficiencies are set equal to 1.

- a* CO = 1.9; CO<sub>2</sub> = 2.4; H<sub>2</sub> = 1.49; H<sub>2</sub>O = 0.0; Ar = 0.0; He = 0.0
- b* H<sub>2</sub>O = 1.0
- c* Ar = 1.0
- d* He = 1.0
- e* CO = 1.9; CO<sub>2</sub> = 3.8; H<sub>2</sub> = 2.5; H<sub>2</sub>O = 12.0
- f* CO = 0.0; CO<sub>2</sub> = 0.0; H<sub>2</sub>O = 0.0
- g* H<sub>2</sub> = 1.0
- h* H<sub>2</sub>O = 1.0
- i* CO<sub>2</sub> = 1.0
- j* CO = 2.0; CO<sub>2</sub> = 5.0; H<sub>2</sub> = 3.0; H<sub>2</sub>O = 12.0; O<sub>2</sub> = 2.5
- k* CO = 1.9; CO<sub>2</sub> = 3.8; H<sub>2</sub> = 2.5; H<sub>2</sub>O = 6.5
- l* C<sub>2</sub>H<sub>2</sub> = 5.0; C<sub>2</sub>H<sub>4</sub> = 1.4; C<sub>2</sub>H<sub>6</sub> = 2.2; CH<sub>4</sub> = 0.7; CO = 0.36; CO<sub>2</sub> = 0.36;  
H<sub>2</sub>O = 4.0; N<sub>2</sub> = 0.36
- m* H<sub>2</sub> = 2.0; O<sub>2</sub> = 1.5; CO = 1.5; H<sub>2</sub>O = 6.0; CO<sub>2</sub> = 3.0
- n* CO = 1.9; CO<sub>2</sub> = 3.8; H<sub>2</sub> = 2.5; H<sub>2</sub>O = 12.0
- o* CO = 2.5; CO<sub>2</sub> = 2.5; H<sub>2</sub> = 1.89; H<sub>2</sub>O = 12.0
- p* CH<sub>3</sub>OH = 1.0
- q* H<sub>2</sub>O = 6.5; Ar = 0.4
- r* CO = 2.0; CO<sub>2</sub> = 3.0; H<sub>2</sub> = 2.0; H<sub>2</sub>O = 5.0; O<sub>2</sub> = 1.5
- s* CO = 1.9; CO<sub>2</sub> = 3.3; H<sub>2</sub> = 1.1; H<sub>2</sub>O = 5.7; O<sub>2</sub> = 1.9; N<sub>2</sub> = 1.6
- t* H<sub>2</sub> = 2.0; H<sub>2</sub>O = 6.0; CH<sub>4</sub> = 2.0; CO = 1.5; CO<sub>2</sub> = 2.0; C<sub>2</sub>H<sub>6</sub> = 3.0

**Fall-off parameters for pressure dependent reactions**

Unless otherwise defined, third body collision efficiencies are 1.

\* Reactions in the Lindemann form

1  $F_c = 0.57$

2  $F_c = 0.81$

3  $F_c = 0.51$

4  $F_c = 0.5$

5  $F_c = 0.18\exp(-T/200.0) + 0.82\exp(-T/1438)$

6  $F_c = 0.27$

7  $F_c = 0.35$

8  $F_c = 47.6\exp(-16182.0/T) + \exp(-T/3371.0)$

9  $F_c = \exp(-T/1097.0) + \exp(6860.0/T)$

10  $F_c = \log(k/k_\infty) = -0.1155 + 8.8420\text{E-}4*T - 1.591\text{E-}6*T^2 + 2.874\text{E-}10*T^3$

11  $F_c = 2.17\exp(-T/251.0) + \exp(-1185.0/T)$

12  $F_c = 0.76\exp(-T/38.0) + 0.24\exp(-T/1946.0)$

13  $F_c = 1.0\exp(-T/1314.0) + 1.0\exp(-50000.0/T)$

14  $F_c = 1.01\exp(-T/206.0) + 0.196\exp(-278.0/T)$

## Appendix B

### Thermodynamic Properties

The thermodynamic data of the chemical species are essential for the predictions of the heat release and equilibrium constants.

$$\ln(K) = \frac{\Delta H}{RT} + \frac{\Delta S}{R} \quad (\text{B.1})$$

The thermodynamic data or commonly referred as JANAF polynomials can take the following forms:

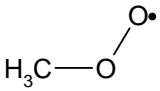
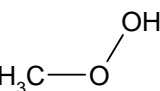
$$\frac{C_p}{R} = a_1 + a_2T + a_3T^2 + a_4T^3 + a_5T^4 \quad (\text{B.2})$$

$$\frac{H}{RT} = a_1 + \frac{a_2T}{2} + \frac{a_3T^2}{3} + \frac{a_4T^3}{4} + \frac{a_5T^4}{5} + \frac{a_6}{T} \quad (\text{B.3})$$

$$\frac{S}{R} = a_1 \ln(T) + a_2T + \frac{a_3T^2}{2} + \frac{a_4T^3}{3} + \frac{a_5T^4}{4} + a_7 \quad (\text{B.4})$$

The data for each species is represented by fourteen coefficients corresponding to temperature ranges above 1000 K (first set of seven coefficients) and below 1000 K (second set). The molecular structures, heats of formation and entropies at 298 K are found in Table B.1. The JANAF polynomials for the species utilized in the current chemical mechanism are grouped in Table B.2.

**Table B.1**  
**Species Structure and Thermodynamic Data**

Acronym	Structure	$\Delta_f H_{298}$ kJ/mol	$S_{298}$ J/mol/K	Reference
H <sub>2</sub>	H <sub>2</sub>	0.00	130.67	[71]
O <sub>2</sub>	O <sub>2</sub>	0.00	205.14	[71]
H	H	217.99	114.71	[71]
OH	OH	37.30	183.73	[71]
O	H	249.19	160.94	[71]
H <sub>2</sub> O	H <sub>2</sub> O	-241.81	188.82	[71]
HO <sub>2</sub>	HO—O•	12.55	229.09	[71]
H <sub>2</sub> O <sub>2</sub>	HO—OH	-135.87	234.53	[71]
CH <sub>4</sub>	CH <sub>4</sub>	-74.60	186.36	[71]
CH <sub>3</sub>	CH <sub>3</sub>	145.69	194.04	[71]
CH <sub>2</sub> (S)	C <sup>1</sup> H <sub>2</sub>	428.78	189.21	[71]
CH <sub>2</sub> (T)	C <sup>3</sup> H <sub>2</sub>	391.18	194.41	[71]
CH	CH	595.77	183.03	[71]
C1	C	716.63	158.09	[71]
CO	C≡O	-110.52	197.65	[71]
CO <sub>2</sub>	O=C=O	-393.49	213.77	[71]
CH <sub>2</sub> O	H <sub>2</sub> C=O	-108.57	218.75	[218]
CHO	HC•=O	42.30	224.27	[71]
CH <sub>2</sub> OH	H <sub>2</sub> C•—OH	-17.00	244.16	[71]
CH <sub>3</sub> OH	H <sub>3</sub> C—OH	-200.99	240.64	[71]
CH <sub>3</sub> O	H <sub>3</sub> C—O•	21.00	234.27	[71]
CH <sub>3</sub> OO		9.00	269.64	[71]
CH <sub>3</sub> OOH		-126.73	275.89	[71]
C <sub>2</sub>	C <sub>2</sub>	824.30	197.09	[71]
C <sub>2</sub> O	C•≡—O•	291.02	233.61	[71]
C <sub>2</sub> H	C•≡—H	569.10	213.29	[71]
C <sub>2</sub> H <sub>2</sub>	HC≡CH	228.19	200.90	[71]
H <sub>2</sub> C <sub>2</sub>	H <sub>2</sub> C=C:	414.76	221.01	[71]

Acronym	Structure	$\Delta_f H_{298}$ kJ/mol	$S_{298}$ J/mol/K	Reference
C <sub>2</sub> HO		178.26	249.24	[15]
C <sub>2</sub> H <sub>2</sub> O		-47.70	241.88	[71]
C <sub>2</sub> H <sub>3</sub>		296.56	233.65	[71]
CH <sub>3</sub> CHO		-165.13	265.42	[15]
CH <sub>3</sub> CO		-10.30	267.43	[71]
CH <sub>2</sub> CHO		25.34	268.96	[71]
C <sub>2</sub> H <sub>4</sub>		52.50	219.31	[71]
C <sub>2</sub> H <sub>5</sub>		118.65	247.10	[71]
C <sub>2</sub> H <sub>6</sub>		-83.85	229.21	[71]
CHCH <sub>2</sub> O		12.79	259.61	[15]
C <sub>2</sub> H <sub>4</sub> O		-52.63	242.86	[71]
C <sub>2</sub> H <sub>4</sub> OOH		28.80	324.79	[71]
C <sub>2</sub> H <sub>5</sub> O		-13.60	277.63	[71]
C <sub>2</sub> H <sub>5</sub> OO		-28.70	299.97	[71]
C <sub>2</sub> H <sub>5</sub> OOH		-162.23	324.50	[15]
C <sub>3</sub> H		719.35	247.78	[71]
C <sub>3</sub> H <sub>2</sub>		476.95	236.19	[71]
C <sub>3</sub> H <sub>2</sub> L		601.30	248.32	[15]
C <sub>3</sub> H <sub>3</sub>		345.98	256.64	[71]
C <sub>3</sub> H <sub>4</sub> (A)		190.91	243.42	[71]
C <sub>3</sub> H <sub>4</sub> (P)		185.42	248.28	[71]

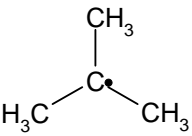
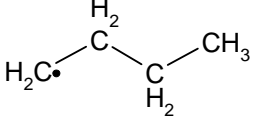
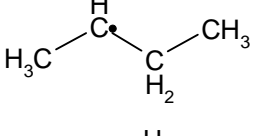
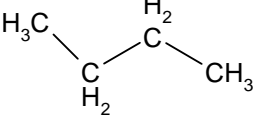
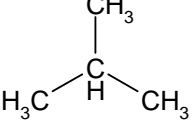
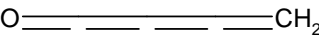
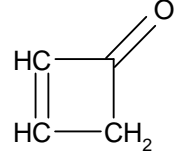
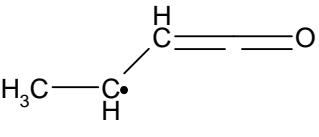
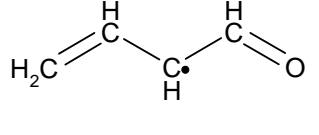
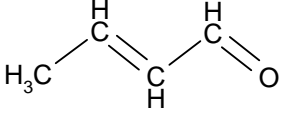
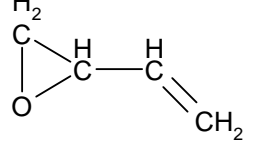
Acronym	Structure	$\Delta_f H_{298}$ kJ/mol	$S_{298}$ J/mol/K	Reference
$C_3H_4(B)$		277.08	243.59	[71]
$C_3H_5(A)$		167.79	258.98	[15]
$C_3H_5(S)$		265.52	271.29	[71]
$C_3H_5(T)$		250.67	276.03	[15]
$C_3H_5(B)$		279.89	251.47	[71]
$C_3H_6(B)$		56.20	237.89	[15]
$C_3H_6$		20.00	266.65	[71]
$C_3H_7(N)$		101.31	290.44	[71]
$C_3H_7(I)$		90.18	289.49	[15]
$C_3H_8$		-104.47	273.62	[15]
$C_3H_2O$		128.67	277.37	[15]
$C_3H_3O$		88.53	300.64	[71]
$C_3H_4O$		-68.06	297.01	[71]

Acronym	Structure	$\Delta_f H_{298}$ kJ/mol	$S_{298}$ J/mol/K	Reference
$C_3H_5O$		71.85	281.76	[15]
$PC_3H_5O$		-32.83	314.27	[71]
$TC_3H_5O$		21.78	321.38	[15]
$AC_3H_5O$		-33.34	307.50	[71]
$C_3H_6O$		-101.50	277.44	[71]
$AC_3H_6O$		-219.94	297.33	[15]
$PC_3H_6O$		-185.12	311.53	[15]
$C_3H_7O(I)$		-47.73	306.81	[15]
$C_3H_7O(N)$		-37.91	324.76	[15]
$C_3H_6OH$		-55.22	343.23	[15]
$C_3H_7OOH(I)$		-200.68	352.43	[15]

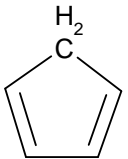
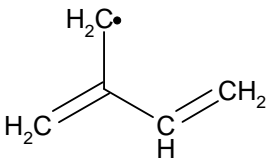
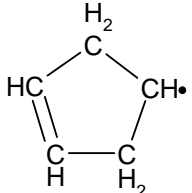
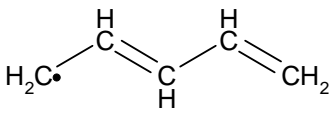
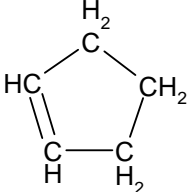
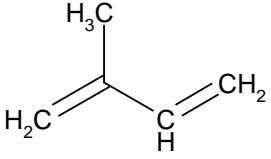
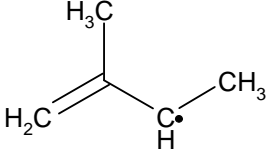
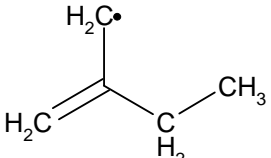
Acronym	Structure	$\Delta_f H_{298}$ kJ/mol	$S_{298}$ J/mol/K	Reference
$C_3H_7OOH(N)$		-181.90	371.12	[15]
$C_3H_7OO(I)$		-63.89	350.32	[15]
$C_3H_7OO(N)$		-42.43	365.55	[15]
$C_3H_6OOH$		16.38	391.26	[15]
$C_4H$		815.76	264.53	[15]
$C_4H_2$		458.27	249.60	[71]
$C_4H_3(N)$		543.50	284.36	[15]
$C_4H_3(I)$		501.80	305.35	[71]
$C_4H_4$		287.84	277.30	[71]
$C_4H_5(S)$		315.23	286.22	[15]
$C_4H_5(T)$		363.32	303.57	[71]
$C_4H_5(I)$		315.20	290.10	[71]
$C_4H_6(S)$		161.30	290.98	[71]

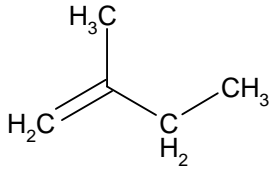
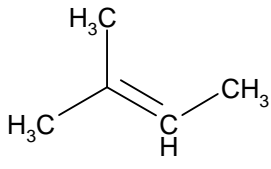
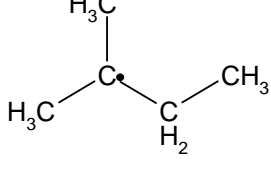
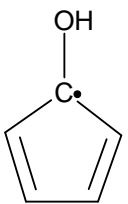
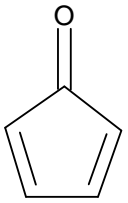
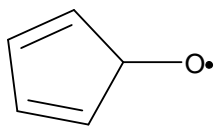
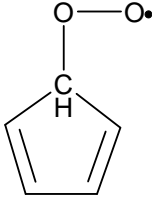
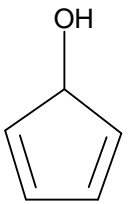


Acronym	Structure	$\Delta_f H_{298}$ kJ/mol	$S_{298}$ J/mol/K	Reference
C <sub>4</sub> H <sub>6</sub> (T)		110.83	293.31	[71]
C <sub>4</sub> H <sub>6</sub> (F)		165.91	291.69	[15]
C <sub>4</sub> H <sub>6</sub> (B)		255.04	285.28	[15]
C <sub>4</sub> H <sub>6</sub> (M)		146.31	291.89	[71]
C <sub>4</sub> H <sub>7</sub> (I)		135.63	301.70	[15]
C <sub>4</sub> H <sub>7</sub> (N)		204.58	317.33	[71]
C <sub>4</sub> H <sub>7</sub> (S)		136.32	304.16	[15]
C <sub>4</sub> H <sub>8</sub> (I)		-16.17	297.72	[15]
C <sub>4</sub> H <sub>8</sub> (N)		0.42	313.98	[15]
C <sub>4</sub> H <sub>8</sub> (S)		-10.48	301.07	[15]
C <sub>4</sub> H <sub>9</sub> (I)		73.78	304.64	[71]

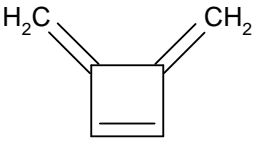
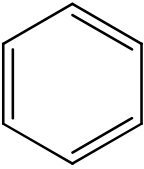
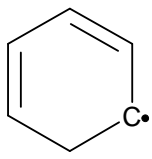
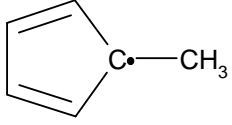
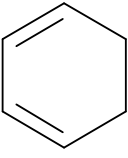
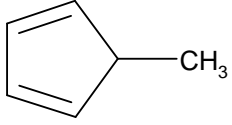
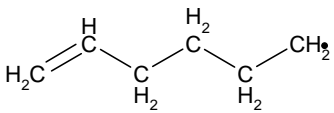
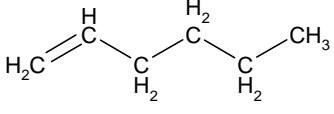
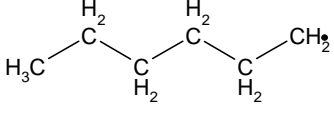
Acronym	Structure	$\Delta_f H_{298}$ kJ/mol	$S_{298}$ J/mol/K	Reference
$C_4H_9(T)$		55.04	322.37	[71]
$C_4H_9(N)$		81.80	307.61	[71]
$C_4H_9(S)$		70.22	321.63	[71]
$C_4H_{10}(N)$		-125.49	317.94	[15]
$C_4H_{10}(I)$		-134.98	295.48	[71]
$C_4H_2O$		216.65	292.39	[15]
$C_4H_4O$		41.80	285.52	[15]
$XC_4H_5O$		67.55	328.19	[15]
$YC_4H_5O$		35.07	311.37	[15]
$BC_4H_6O$		-105.21	305.99	[15]
$AC_4H_6O$		9.40	310.72	[15]

Acronym	Structure	$\Delta_f H_{298}$ kJ/mol	$S_{298}$ J/mol/K	Reference
C <sub>4</sub> H <sub>7</sub> O(X)		55.78	341.89	[15]
C <sub>4</sub> H <sub>7</sub> O(M)		-58.85	348.45	[15]
C <sub>4</sub> H <sub>8</sub> O(X)		-139.28	317.03	[15]
C <sub>4</sub> H <sub>8</sub> O(M)		-215.68	338.68	[15]
C <sub>4</sub> H <sub>8</sub> OH(I)		-77.91	366.98	[15]
O <sub>2</sub> C <sub>4</sub> H <sub>9</sub> O		-223.55	425.07	[15]
C <sub>5</sub> H	C=C=C=C=CH	778.23	260.40	[71]
C <sub>5</sub> H <sub>2</sub>	CH=C=C=C=CH	691.37	266.62	[71]
C <sub>5</sub> H <sub>3</sub> (L)	CH≡C-CH-C≡CH	560.97	295.18	[71]
C <sub>5</sub> H <sub>4</sub> (L)	CH <sub>2</sub> =C=CH=C≡CH	427.00	304.10	[15]
C <sub>5</sub> H <sub>5</sub>		266.09	279.47	[71]
C <sub>5</sub> H <sub>5</sub> (L)	CH <sub>2</sub> =C=CH=CH=CH	396.48	307.44	[71]
C <sub>5</sub> H <sub>6</sub> (L)		247.12	316.15	[15]

Acronym	Structure	$\Delta_f H_{298}$ kJ/mol	$S_{298}$ J/mol/K	Reference
$C_5H_6$		136.39	275.05	[15]
$C_5H_7(I)$		316.29	341.67	[15]
$C_5H_7$		172.65	292.49	[15]
$C_5H_7(L)$		221.74	312.11	[128]
$C_5H_8$		37.33	292.45	[15]
$C_5H_8(I)$		87.84	321.42	[15]
$C_5H_9$	$CH_3CH_2CHCHCH_2$	170.80	357.26	[219]
$C_5H_9(A)$		110.45	345.06	[15]
$C_5H_9(B)$		120.98	340.03	[15]

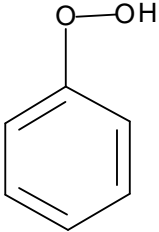
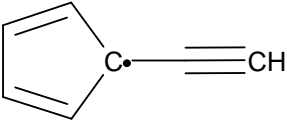
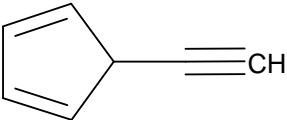
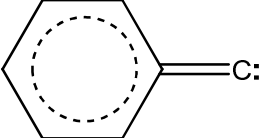
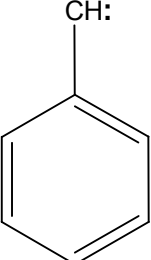
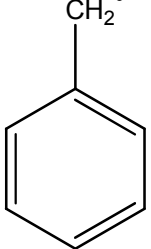
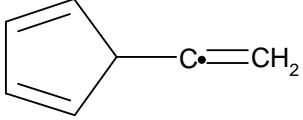
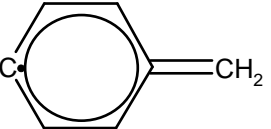
Acronym	Structure	$\Delta_f H_{298}$ kJ/mol	$S_{298}$ J/mol/K	Reference
$C_5H_{10}(A)$		-33.91	345.94	[15]
$C_5H_{10}(B)$		-39.79	337.91	[15]
$C_5H_{11}(T)$		36.75	375.81	[15]
$1C_5H_{11}$	$CH_3-3(CH_2)CH_2$	45.28	374.97	[220]
$1C_5H_{10}$	$CH_2CH-2(CH_2)CH_3$	-21.73	345.24	[220]
$C_5H_4OH$		90.83	309.17	[15]
$C_5H_4O$		54.75	291.42	[15]
$C_5H_5O$		103.29	307.79	[71]
$C_5H_5OO$		215.59	352.45	[15]
$C_5H_5OH$		-8.14	309.39	[15]

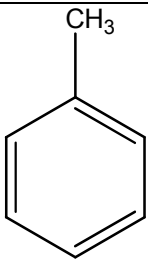
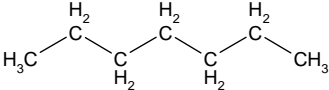
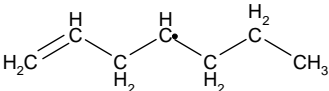
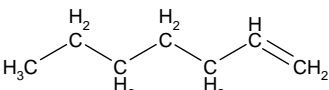
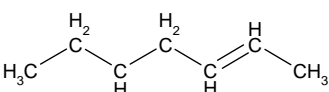
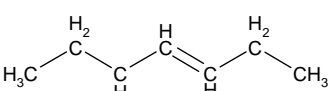
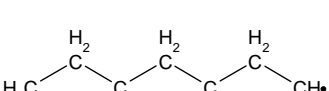
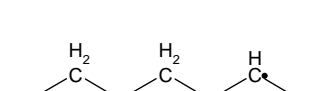
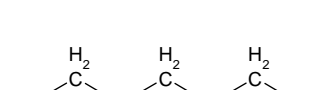
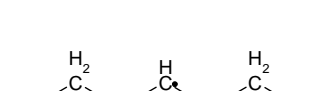
Acronym	Structure	$\Delta_f H_{298}$ kJ/mol	$S_{298}$ J/mol/K	Reference
$C_6H_2$		700.78	299.17	[73]
$C_6H_3$		752.48	352.48	[15]
$C_6H_4$		461.11	283.22	[71]
$C_6H_4L$		523.17	325.85	[15]
$C_6H_5(A)$		576.05	363.46	[15]
$C_6H_5(B)$	CH=C-CH=CH-CH=CH	605.93	342.09	[15]
$C_6H_5$		345.44	290.01	[15]
$C_6H_6(A)$		417.44	348.66	[15]
$C_6H_6(B)$		416.49	354.17	[15]
$C_6H_6(D)$		343.51	336.18	[15]
$C_6H_6(S)$		396.28	337.90	[15]
$C_6H_6(F)$		216.34	294.74	[15]

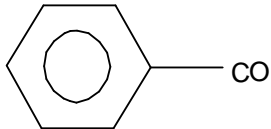
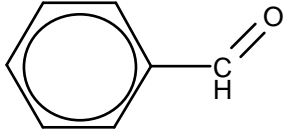
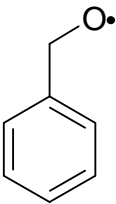
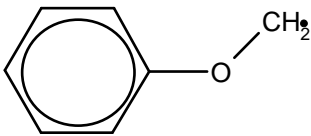
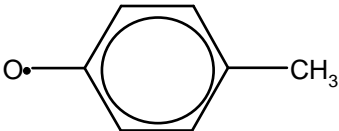
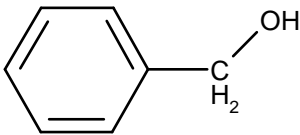
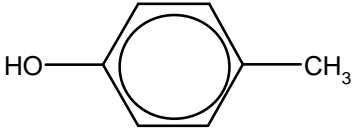
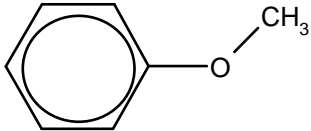
Acronym	Structure	$\Delta_f H_{298}$ kJ/mol	$S_{298}$ J/mol/K	Reference
$C_6H_6(M)$		339.99	305.15	[15]
$C_6H_6$		85.13	270.20	[15]
$C_6H_7$		210.86	302.72	[15]
$C_6H_7(L)$	$CH_2=CH-CH=CH-CH=CH$	428.53	346.54	[15]
$C_5H_4CH_3$		219.37	324.56	[15]
$C_6H_8$		109.16	299.54	[15]
$C_5H_5CH_3$		112.16	312.62	[15]
$C_6H_{11}$		142.25	394.95	[221]
$1C_6H_{12}$		-41.69	384.80	[221]
$1C_6H_{13}$		25.10	407.63	[126]

Acronym	Structure	$\Delta_f H_{298}$ kJ/mol	$S_{298}$ J/mol/K	Reference
$2C_6H_{13}$		75.35	378.93	[126]
$C_6H_3O_2$		147.09	341.81	[15]
$C_6H_3O_3$		-129.54	365.08	[15]
$C_6H_5OH$		-82.45	321.64	[15]
$C_6H_5O$		61.65	311.57	[15]
$C_6H_4O_2$		-121.32	323.52	[15]
$C_6H_5OO$		151.60	354.30	[15]



Acronym	Structure	$\Delta_f H_{298}$ kJ/mol	$S_{298}$ J/mol/K	Reference
$C_6H_5OOH$		-2.61	355.43	[15]
$C_7H_5$		476.46	326.03	[15]
$C_7H_6$		367.33	357.35	[71]
$C_6H_5C$		616.44	328.29	[15]
$C_6H_5CH$		474.03	320.41	[15]
$C_7H_7$		215.28	318.42	[15]
$C_7H_7L$		453.53	350.43	[15]
$C_7H_7P$		314.52	321.27	[15]

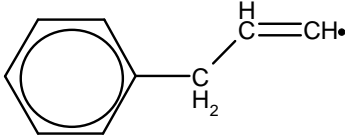
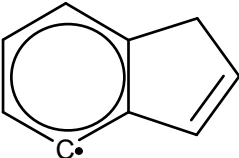
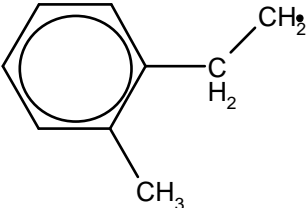
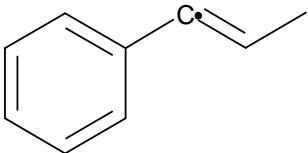
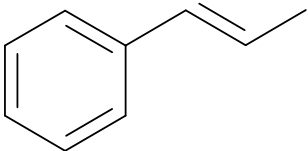
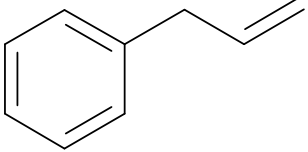
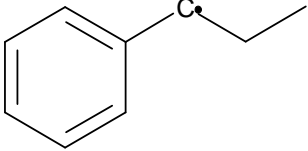
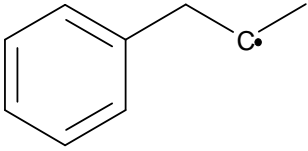
Acronym	Structure	$\Delta_f H_{298}$ kJ/mol	$S_{298}$ J/mol/K	Reference
$C_7H_8$		51.97	322.10	[15]
$C_7H_{16}$		-188.23	456.03	[15]
$C_7H_{13}$		145.06	458.15	[15]
$1C_7H_{14}$		-63.28	501.66	[15]
$2C_7H_{14}$		-73.07	436.49	[15]
$3C_7H_{14}$		-72.02	440.73	[15]
$1C_7H_{15}$		18.59	472.84	[15]
$2C_7H_{15}$		7.09	481.86	[15]
$3C_7H_{15}$		8.09	487.97	[15]
$4C_7H_{15}$		8.09	485.73	[15]

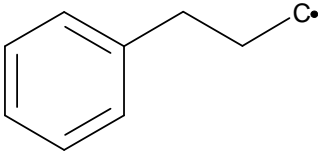
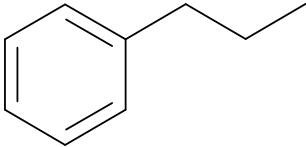
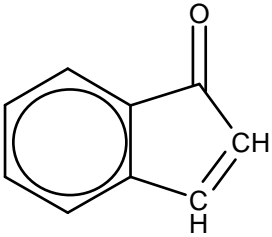
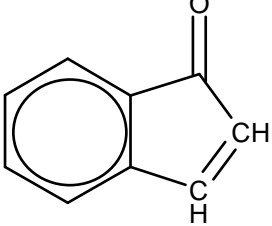
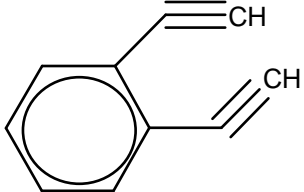
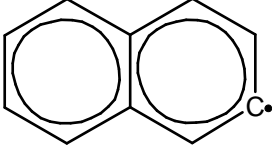
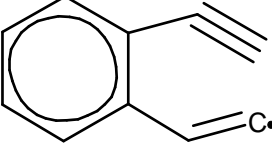
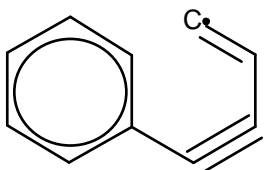
Acronym	Structure	$\Delta_f H_{298}$ kJ/mol	$S_{298}$ J/mol/K	Reference
$C_6H_5CO$		108.77	355.34	[55]
$C_7H_6O$		-39.04	342.33	[15]
$C_7H_7O$		126.00	359.06	[15]
$C_7H_7OA$		118.99	369.23	[15]
$OC_7H_7$		22.87	354.68	[15]
$C_7H_7OH$		-92.71	361.86	[15]
$HOC_7H_7$		-123.72	352.43	[15]
$C_7H_8OA$		-72.39	351.10	[15]

Acronym	Structure	$\Delta_f H_{298}$ kJ/mol	$S_{298}$ J/mol/K	Reference
$C_7H_7OO$		119.20	403.25	[15]
$OOC_7H_7P$		117.94	385.43	[15]
$C_8H_2$		908.89	352.66	[15]
$C_8H_5(S)$		555.46	326.08	[126]
$C_8H_5$		624.12	342.36	[15]
$C_8H_6$		317.78	331.20	[15]
$C_6H_5CHC$		519.80	351.11	[15]
$C_8H_7$		411.51	359.34	[15]

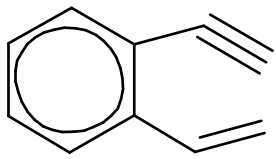
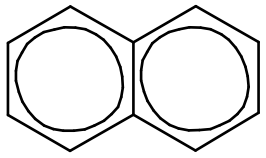
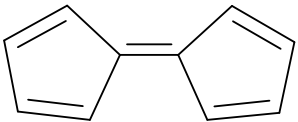
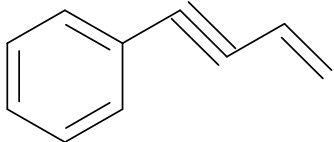
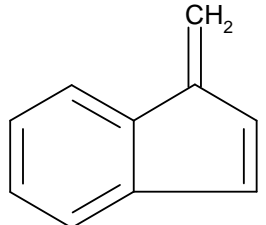
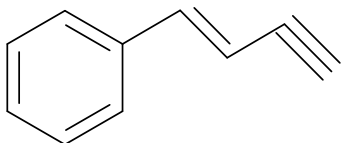
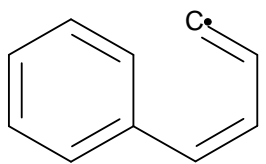
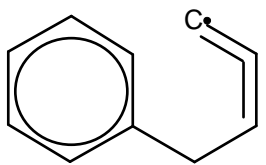
Acronym	Structure	$\Delta_f H_{298}$ kJ/mol	$S_{298}$ J/mol/K	Reference
$C_8H_7(F)$		480.56	364.00	[15]
$C_8H_7(P)$		397.09	368.11	[126]
$C_8H_8$		149.14	345.99	[15]
$C_8H_9(F)$		366.22	393.84	[15]
$C_8H_9$		185.64	354.34	[15]
$C_8H_{10}$		30.29	365.14	[15]
$C_8H_{16}$	$CH_2CH-5(CH_2)CH_3$	-82.90	462.37	[221]
$C_8H_{17}$	$CH_3-6(CH_2)CH_2$	-16.32	486.80	[221]
$C_6H_5C_2O$		249.20	368.19	[15]
$C_8H_5O$		287.26	358.29	[15]

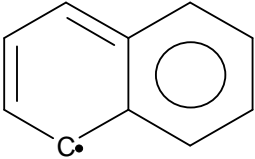
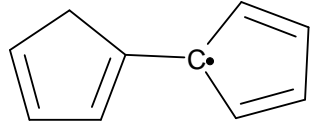
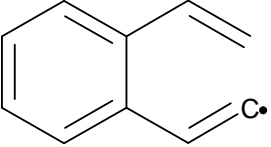
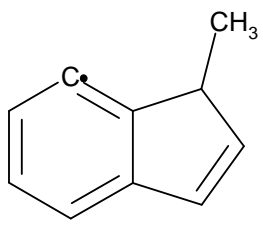
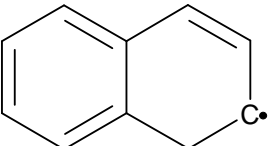
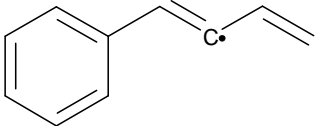
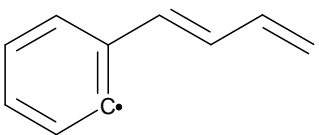
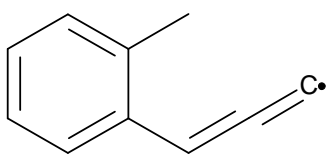
Acronym	Structure	$\Delta_f H_{298}$ kJ/mol	$S_{298}$ J/mol/K	Reference
$C_8H_5OO$		375.82	396.28	[15]
$C_9H_7$		285.58	342.82	[126]
$C_9H_7L$		531.47	370.08	[126]
$C_9H_8$		164.13	335.83	[221]
$C_9H_8(S)$		286.30	376.70	[15]
$C_9H_8(T)$		305.78	380.15	[15]
$C_9H_9(N)$		394.26	407.04	[15]
$C_9H_9(I)$		365.57	415.19	[15]
$C_9H_9(S)$		214.35	356.69	[15]

Acronym	Structure	$\Delta_f H_{298}$ kJ/mol	$S_{298}$ J/mol/K	Reference
$C_9H_9(P)$		381.09	399.98	[15]
$C_9H_9(C)$		315.29	353.21	[15]
$C_9H_9(F)$		378.85	391.22	[15]
$C_9H_9(T)$		377.28	394.43	[126]
$1C_9H_{10}$		117.00	380.36	[222]
$2C_9H_{10}$		117.00	380.36	[222]
$1C_9H_{11}$		147.18	397.42	[36]
$2C_9H_{11}$		204.21	403.43	[36]

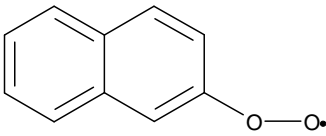
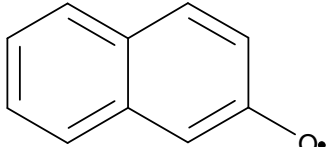
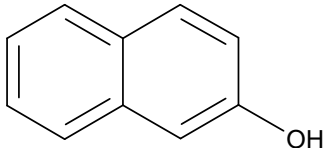
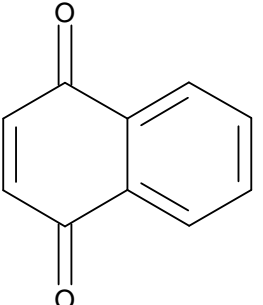
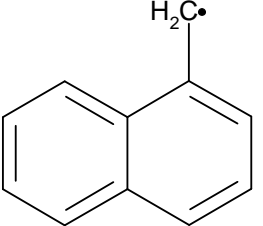
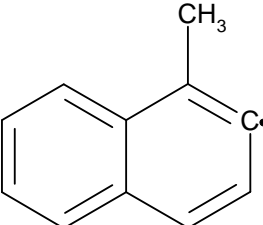
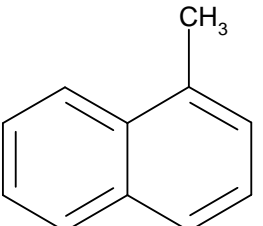
Acronym	Structure	$\Delta_f H_{298}$ kJ/mol	$S_{298}$ J/mol/K	Reference
$3C_9H_{11}$		209.22	403.43	[36]
$C_9H_{12}$		7.74	408.34	[15]
$C_9H_6O$		54.97	352.13	[15]
$C_9H_7O$		131.92	342.22	est. [221]
$C_{10}H_6$		554.44	381.76	[15]
$C_{10}H_7$		401.66	352.22	[15]
$C_{10}H_7L$		650.04	394.28	[15]
$C_{10}H_7M$		635.52	406.56	[15]

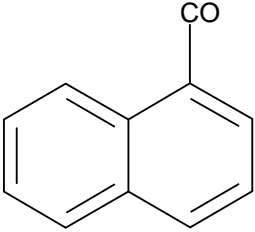
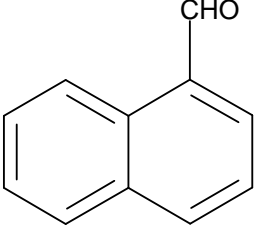
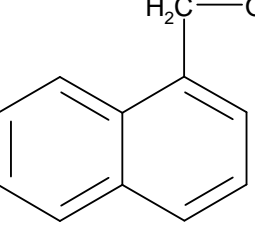
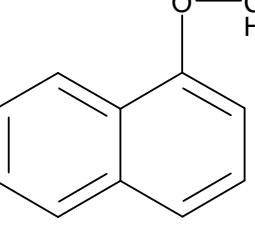
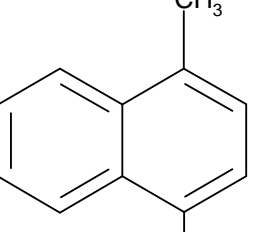
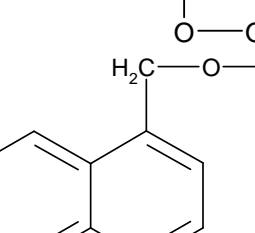


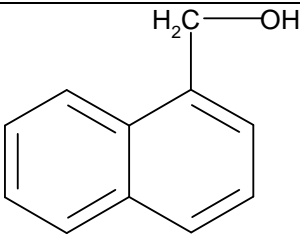
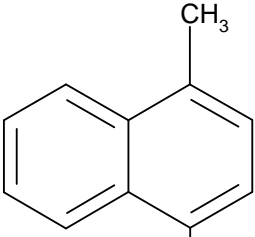
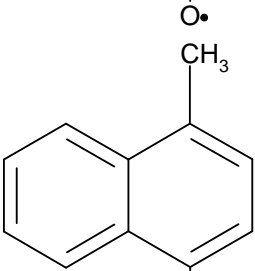
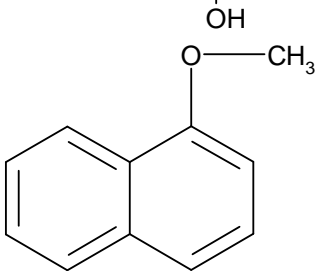
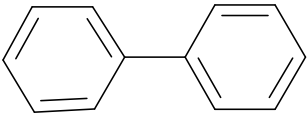
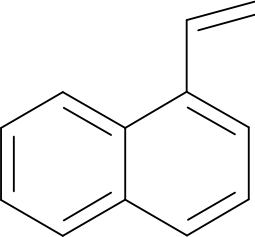
Acronym	Structure	$\Delta_f H_{298}$ kJ/mol	$S_{298}$ J/mol/K	Reference
$C_{10}H_8L$		375.14	393.20	[126]
$C_{10}H_8$		147.64	335.46	[15]
$C_{10}H_8K$		360.22	368.63	[15]
$C_{10}H_8G$		375.49	402.18	[15]
$C_9H_6CH_2$		238.45	355.60	[131]
$C_{10}H_8J$		381.95	403.90	[15]
$C_{10}H_9A$		475.08	408.21	[15]
$C_{10}H_9D$		433.78	428.40	[15]

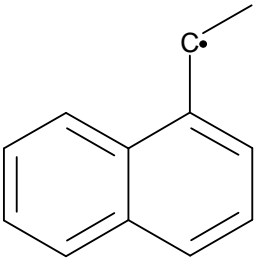
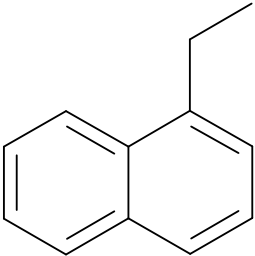
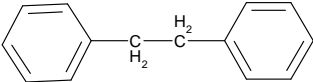
Acronym	Structure	$\Delta_f H_{298}$ kJ/mol	$S_{298}$ J/mol/K	Reference
$C_{10}H_9$		249.25	366.87	[15]
$C_{10}H_9F$		361.64	380.29	[15]
$C_{10}H_9P$		485.87	416.74	[15]
$C_9H_6CH_3$		255.55	347.44	[131]
$C_{10}H_9T$		249.22	366.74	[15]
$C_{10}H_9B$		424.68	408.01	[15]
$C_{10}H_9L$		453.42	421.82	[126]
$C_{10}H_9E$		403.44	405.78	[15]

Acronym	Structure	$\Delta_f H_{298}$ kJ/mol	$S_{298}$ J/mol/K	Reference
$C_{10}H_{10}K$		264.39	367.18	[126]
$C_{10}H_9K$		460.09	398.36	[15]
$C_{10}H_9M$		472.83	419.40	[15]
$C_9H_7CH_3$		147.10	390.12	[131]
$C_{10}H_{10}$		279.36	414.96	[126]
$C_{10}H_{10}F$		256.27	410.98	[15]
$1C_{10}H_{21}$	$CH_3-8(CH_2)CH_2$	-57.75	565.99	[126]
$2C_{10}H_{21}$	$CH_3-7(CH_2)CHCH_3$	-58.99	566.73	[126]
$3C_{10}H_{21}$	$CH_3-6(CH_2)CHCH_2CH_3$	-58.99	566.73	[126]
$4C_{10}H_{21}$	$CH_2-5(CH_2)CH-2(CH_2)CH_3$	-58.99	566.73	[126]
$5C_{10}H_{21}$	$CH_3-4(CH_2)CH-3(CH_2)CH_3$	-58.99	566.73	[126]
$C_{10}H_{22}$	$CH_3-8(CH_2)CH_3$	-250.13	544.19	[126]

Acronym	Structure	$\Delta_f H_{298}$ kJ/mol	$S_{298}$ J/mol/K	Reference
$C_{10}H_7OO$		220.99	402.03	[15]
$C_{10}H_7O$		123.14	374.07	[15]
$C_{10}H_7OH$		-30.79	368.69	[126]
$C_{10}H_6O_2$		-103.86	388.72	[15]
$C_{11}H_9$		272.79	375.72	[221]
$C_{11}H_9P$		357.02	375.81	[11]
$C_{11}H_{10}$		116.10	381.96	[221]

Acronym	Structure	$\Delta_f H_{298}$ kJ/mol	$S_{298}$ J/mol/K	Reference
$C_{11}H_7O$		174.92	415.82	[221]
$C_{11}H_8O$		30.54	415.68	[221]
$C_{11}H_9O$		189.23	375.81	est. [11]
$AC_{11}H_9O$		155.20	375.81	est. [11]
$OOC_{11}H_9P$		284.20	465.62	est. [11]
$C_{11}H_9OO$		254.99	415.78	est. [126]

Acronym	Structure	$\Delta_f H_{298}$ kJ/mol	$S_{298}$ J/mol/K	Reference
$C_{11}H_{10}O$		-28.47	452.86	est. [11]
$OC_{11}H_9$		85.22	375.81	est. [11]
$HOC_{11}H_9$		-58.77	375.81	est. [11]
$AC_{11}H_{10}O$		0.48	452.76	Est.[11, 15]
$C_{12}H_{10}$		182.14	388.84	[221]
$1C_{12}H_{10}$		215.04	400.83	[221]

Acronym	Structure	$\Delta_f H_{298}$ kJ/mol	$S_{298}$ J/mol/K	Reference
$C_{12}H_{11}$		220.45	426.59	[221]
$C_{12}H_{12}$		96.90	406.30	[221]
$C_{14}H_{14}$		143.14	483.24	[221]

**Table B.2**  
**Polynomials for species**

H2	REF : BURCAT 20/09/06				
0.29328305E+01	0.82659802E-03	-0.14640057E-06	0.15409851E-10	-0.68879615E-15	
-0.81305582E+03	-0.10243164E+01	0.23443029E+01	0.79804248E-02	-0.19477917E-04	
0.20156967E-07	-0.73760289E-11	-0.91792413E+03	0.68300218E+00		
O2	REF : BURCAT 20/09/06				
3.66096083E+00	6.56365523E-04	-1.41149485E-07	2.05797658E-11	-1.29913248E-15	
-1.21597725E+03	3.41536184E+00	3.78245636E+00	-2.99673415E-03	9.84730200E-06	
-9.68129508E-09	3.24372836E-12	-1.06394356E+03	3.65767573E+00		
H	REF : BURCAT 20/09/06				
0.25000000E+01	0.00000000E+00	0.00000000E+00	0.00000000E+00	0.00000000E+00	
0.25473660E+05	-0.44668285E+00	0.25000000E+01	0.00000000E+00	0.00000000E+00	
0.00000000E+00	0.00000000E+00	0.25473660E+05	-0.44668285E+00		
OH	REF : BURCAT 20/09/06				
2.83853033E+00	1.10741289E-03	-2.94000209E-07	4.20698729E-11	-2.42289890E-15	
3.69780808E+03	5.84494652E+00	3.99198424E+00	-2.40106655E-03	4.61664033E-06	
-3.87916306E-09	1.36319502E-12	3.36889836E+03	-1.03998477E-01	4.48615380E+03	
O	REF : BURCAT 20/09/06				
0.25420597E+01	-0.27550619E-04	-0.31028033E-08	0.45510674E-11	-0.43680515E-15	
0.29230803E+05	0.49203081E+01	0.29464288E+01	-0.16381665E-02	0.24210317E-05	
-0.16028432E-08	0.38906963E-12	0.29147644E+05	0.29639949E+01		
H2O	REF : BURCAT 20/09/06				
0.26770389E+01	0.29731816E-02	-0.77376889E-06	0.94433514E-10	-0.42689991E-14	
-0.29885894E+05	0.68825500E+01	0.41986352E+01	-0.20364017E-02	0.65203416E-05	
-0.54879269E-08	0.17719680E-11	-0.30293726E+05	-0.84900901E+00		
HO2	REF : BURCAT 20/09/06				
0.41722659E+01	0.18812098E-02	-0.34629297E-06	0.19468516E-10	0.17609153E-15	
0.61818851E+02	0.29577974E+01	0.43017880E+01	-0.47490201E-02	0.21157953E-04	
-0.24275961E-07	0.92920670E-11	0.29480876E+03	0.37167010E+01		
H2O2	REF : BURCAT 20/09/06				
4.57977305E+00	4.05326003E-03	-1.29844730E-06	1.98211400E-10	-1.13968792E-14	
-1.80071775E+04	6.64970694E-01	4.31515149E+00	-8.47390622E-04	1.76404323E-05	
-2.26762944E-08	9.08950158E-12	-1.77067437E+04	3.27373319E+00	-1.63425145E+04	
C2H6	REF : BURCAT 20/09/06				
4.04666411E+00	1.53538802E-02	-5.47039485E-06	8.77826544E-10	-5.23167531E-14	
-1.24473499E+04	-9.68698313E-01	4.29142572E+00	-5.50154901E-03	5.99438458E-05	
-7.08466469E-08	2.68685836E-11	-1.15222056E+04	2.66678994E+00		
C2H5	REF : BURCAT 20/09/06				
0.42878814E+01	0.12433893E-01	-0.44139119E-05	0.70654102E-09	-0.42035136E-13	
0.12056455E+05	0.84602583E+00	0.43058580E+01	-0.41833638E-02	0.49707270E-04	
-0.59905874E-07	0.23048478E-10	0.12841714E+05	0.47100236E+01		
C2H4	REF : BURCAT 20/09/06				
3.99182724E+00	1.04833908E-02	-3.71721342E-06	5.94628366E-10	-3.53630386E-14	
4.26865851E+03	-2.69081762E-01	3.95920063E+00	-7.57051373E-03	5.70989993E-05	
-6.91588352E-08	2.69884190E-11	5.08977598E+03	4.09730213E+00		
C2H2	REF : BURCAT 20/09/06				
4.65878489E+00	4.88396667E-03	-1.60828888E-06	2.46974544E-10	-1.38605959E-14	
2.57594042E+04	-3.99838194E+00	8.08679682E-01	2.33615762E-02	-3.55172234E-05	
2.80152958E-08	-8.50075165E-12	2.64289808E+04	1.39396761E+01		
CH4	ANHARMONIC REF : BURCAT 20/09/06				
1.65326226E+00	1.00263099E-02	-3.31661238E-06	5.36483138E-10	-3.14696758E-14	
-1.00095936E+04	9.90506283E+00	5.14911468E+00	-1.36622009E-02	4.91453921E-05	
-4.84246767E-08	1.66603441E-11	-1.02465983E+04	-4.63848842E+00	-8.97226656E+03	
CH3	REF : BURCAT 20/09/06				
0.28440516E+01	0.61379741E-02	-0.22303452E-05	0.37851608E-09	-0.24521590E-13	
0.16437808E+05	0.54526973E+01	0.24304428E+01	0.11124099E-01	-0.16802203E-04	
0.16218287E-07	-0.58649526E-11	0.16423781E+05	0.67897939E+01		
CH2(S)	REF : BURCAT 20/09/06				
3.13501686E+00	2.89593926E-03	-8.16668090E-07	1.13572697E-10	-6.36262835E-15	
5.05040504E+04	4.06030621E+00	4.19331325E+00	-2.33105184E-03	8.15676451E-06	
-6.62985981E-09	1.93233199E-12	5.03662246E+04	-7.46734310E-01		
CH2(T)	REF : BURCAT 20/09/06				
3.14631886E+00	3.03671259E-03	-9.96474439E-07	1.50483580E-10	-8.57335515E-15	
4.60412605E+04	4.72341711E+00	3.71757846E+00	1.27391260E-03	2.17347251E-06	



-3.48858500E-09	1.65208866E-12	4.58723866E+04	1.75297945E+00		
CH				REF :	BURCAT 20/09/06
0.25209369E+01	0.17653639E-02	-0.46147660E-06	0.59289675E-10	-0.33474501E-14	
0.70946769E+05	0.74051829E+01	0.34897583E+01	0.32432160E-03	-0.16899751E-05	
0.31628420E-08	-0.14061803E-11	0.70612646E+05	0.20842841E+01		
C1					
0.26055830E+01	-0.19593434E-03	0.10673722E-06	-0.16423940E-10	0.81870580E-15	
0.85411742E+05	0.41923868E+01	0.25542395E+01	-0.32153772E-03	0.73379223E-06	
-0.73223487E-09	0.26652144E-12	0.85442681E+05	0.45313085E+01		
CO				REF :	BURCAT 20/09/06
0.30484859E+01	0.13517281E-02	-0.48579405E-06	0.78853644E-10	-0.46980746E-14	
-0.14266117E+05	0.60170977E+01	0.35795335E+01	-0.61035369E-03	0.10168143E-05	
0.90700586E-09	-0.90442449E-12	-0.14344086E+05	0.35084093E+01		
CO2				REF :	BURCAT 20/09/06
0.46365111E+01	0.27414569E-02	-0.99589759E-06	0.16038666E-09	-0.91619857E-14	
-0.49024904E+05	-0.19348955E+01	0.23568130E+01	0.89841299E-02	-0.71220632E-05	
0.24573008E-08	-0.14288548E-12	-0.48371971E+05	0.99009035E+01		
CH2O					
0.31694807E+01	0.61932742E-02	-0.22505981E-05	0.36598245E-09	-0.22015410E-13	
-0.14478425E+05	0.60423533E+01	0.47937036E+01	-0.99081518E-02	0.37321459E-04	
-0.37927902E-07	0.13177015E-10	-0.14308955E+05	0.60288702E+00		
CHO				REF :	BURCAT 20/09/06
3.92001542E+00	2.52279324E-03	-6.71004164E-07	1.05615948E-10	-7.43798261E-15	
3.65342928E+03	3.58077056E+00	4.23754610E+00	-3.32075257E-03	1.40030264E-05	
-1.34239995E-08	4.37416208E-12	3.87241185E+03	3.30834869E+00		
CH3OH				REF :	BURCAT 20/09/06
3.52726795E+00	1.03178783E-02	-3.62892944E-06	5.77448016E-10	-3.42182632E-14	
-2.60028834E+04	5.16758693E+00	5.65851051E+00	-1.62983419E-02	6.91938156E-05	
-7.58372926E-08	2.80427550E-11	-2.56119736E+04	-8.97330508E-01		
CH3O				REF :	BURCAT 20/09/06
4.75779238E+00	7.44142474E-03	-2.69705176E-06	4.38090504E-10	-2.63537098E-14	
3.78111940E+02	-1.96680028E+00	3.71180502E+00	-2.80463306E-03	3.76550971E-05	
-4.73072089E-08	1.86588420E-11	1.29569760E+03	6.57240864E+00		
CH2OH				REF :	BURCAT 20/09/06
5.09314370E+00	5.94761260E-03	-2.06497460E-06	3.23008173E-10	-1.88125902E-14	
-4.03409640E+03	-1.84691493E+00	4.47834367E+00	-1.35070310E-03	2.78484980E-05	
-3.64869060E-08	1.47907450E-11	-3.50072890E+03	3.30913500E+00		
C2O				REF :	BURCAT 20/09/06
5.42468378E+00	1.85393945E-03	-5.17932956E-07	6.77646230E-11	-3.53315237E-15	
3.31537194E+04	-3.69608405E+00	2.86278214E+00	1.19701204E-02	-1.80851222E-05	
1.52777730E-08	-5.20063163E-12	3.37501779E+04	8.89759099E+00		
C2H					
0.36646060E+01	0.38218694E-02	-0.13650743E-05	0.21324828E-09	-0.12309430E-13	
0.67297055E+05	0.39134973E+01	0.29018020E+01	0.13285982E-01	-0.28050886E-04	
0.28930184E-07	-0.10744742E-10	0.67190326E+05	0.61723506E+01		
C2HO				REF :	R.ROBINSON 22/09/06
5.80668033E+00	3.63140881E-03	-1.28197024E-06	2.04562706E-10	-1.21475486E-14	
1.94243191E+04	-4.44501759E+00	2.50499402E+00	1.94889354E-02	-3.30041888E-05	
2.96410713E-08	-1.02822778E-11	2.00662139E+04	1.11211692E+01		
C2H2O				REF :	BURCAT 20/09/06
0.57577901E+01	0.63496507E-02	-0.22584407E-05	0.36208462E-09	-0.21569030E-13	
-0.79786113E+04	-0.61064037E+01	0.21401165E+01	0.18088368E-01	-0.17324216E-04	
0.92767477E-08	-0.19915011E-11	-0.70430509E+04	0.12198699E+02		
C2H3				REF :	BURCAT 20/09/06
4.15026763E+00	7.54021341E-03	-2.62997847E-06	4.15974048E-10	-2.45407509E-14	
3.38566380E+04	1.72812235E+00	3.36377642E+00	2.65765722E-04	2.79620704E-05	
-3.72986942E-08	1.51590176E-11	3.44749589E+04	7.91510092E+00		
CH3CHO				REF :	UNPUBLISHED R.ROBINSON IMPERIAL 20/09/06
5.25190093E+00	1.18574124E-02	-4.27442759E-06	6.91482701E-10	-4.14491372E-14	
-2.24327033E+04	-2.48438587E+00	5.08801432E+00	-6.39393756E-03	5.50299788E-05	
-6.47002177E-08	2.44610814E-11	-2.14638582E+04	2.91845026E+00		
CH3CO				REF :	BURCAT 20/09/06
0.53137165E+01	0.91737793E-02	-0.33220386E-05	0.53947456E-09	-0.32452368E-13	
-0.36450414E+04	-0.16757558E+01	0.40358705E+01	0.87729487E-03	0.30710010E-04	
-0.39247565E-07	0.15296869E-10	-0.26820738E+04	0.78617682E+01	-0.12388039E+04	
C2				REF :	BURCAT 20/09/06
4.12492246E+00	1.08348338E-04	1.57252585E-07	-4.24046828E-11	3.25059373E-15	

9.81882961E+04	7.97432262E-01	-1.96261001E+00	5.76822247E-02	-1.58039636E-04
1.72462711E-07	-6.57913199E-11	9.82538219E+04	2.33201223E+01	
CH2CHO				
0.59756699E+01	0.81305914E-02	-0.27436245E-05	0.40703041E-09	-0.21760171E-13
0.49032178E+03	-0.50320879E+01	0.34090624E+01	0.10738574E-01	0.18914925E-05
0.71585831E-08	0.28673851E-11	0.15214766E+04	0.95714535E+01	
H2C2				
0.42780340E+01	0.47562804E-02	-0.16301009E-05	0.25462806E-09	-0.14886379E-13
0.48316688E+05	0.64023701E+00	0.32815483E+01	0.69764791E-02	-0.23855244E-05
-0.12104432E-08	0.98189545E-12	0.48621794E+05	0.59203910E+01	
CH3OO				
5.92505819E+00	9.00194542E-03	-3.24254309E-06	5.24362718E-10	-3.14263003E-14
-1.53258958E+03	-4.93669747E+00	4.76597792E+00	-3.51077148E-03	4.54394152E-05
-5.66763729E-08	2.21591482E-11	-4.82401289E+02	4.76095141E+00	
CH3OOH				
7.76538058E+00	8.61499712E-03	-2.98006935E-06	4.68638071E-10	-2.75339255E-14
-1.82979984E+04	-1.43992663E+01	2.90540897E+00	1.74994735E-02	5.28243630E-06
-2.52827275E-08	1.34368212E-11	-1.68894632E+04	1.13741987E+01	
CHCH2O				
6.23101359E+00	8.68490881E-03	-3.11847314E-06	5.03260099E-10	-3.01192222E-14
-1.14930996E+03	-7.80034154E+00	2.49418731E+00	1.16640629E-02	1.21136016E-05
-2.54818477E-08	1.14805860E-11	2.14716931E+02	1.32015748E+01	
C2H4O				
0.54887641E+01	0.12046190E-01	-0.43336931E-05	0.70028311E-09	-0.41949088E-13
-0.91804251E+04	-0.70799605E+01	0.37590532E+01	-0.94412180E-02	0.80309721E-04
-0.10080788E-06	0.40039921E-10	-0.75608143E+04	0.78497475E+01	
C2H4OOH				
9.74660000E+00	0.01084240E+00	-3.13022000E-06	3.83694000E-10	-1.60474000E-14
-3.94819063E+02	-2.07656245E+01	2.10863000E+00	0.03341860E+00	-2.66198000E-05
1.03835000E-08	-1.41770000E-12	1.56528996E+03	1.81813376E+01	
C2H5O				
0.66889982E+01	0.13125676E-01	-0.47038840E-05	0.75858552E-09	-0.45413306E-13
-0.47457832E+04	-0.96983755E+01	0.43074268E+01	0.64147205E-02	0.31139714E-04
-0.43314083E-07	0.17276184E-10	-0.34027524E+04	0.59025837E+01	
C2H5OO				
8.05957692E+00	1.52921019E-02	-5.54442603E-06	9.00496195E-10	-5.41302799E-14
-7.31028500E+03	-1.59992904E+01	5.21694144E+00	1.24160003E-04	6.15529492E-05
-7.94505636E-08	3.12101317E-11	-5.41455775E+03	4.22381533E+00	
C2H5OOH				
8.99519146E+00	1.52768090E-02	-5.42345537E-06	8.64392953E-10	-5.12061321E-14
-2.34335955E+04	-1.78995702E+01	6.95135129E+00	2.46459348E-03	5.06621132E-05
-6.73457524E-08	2.69294264E-11	-2.20224273E+04	-3.02023422E+00	
C3H				
6.14184491E+00	3.39661013E-03	-1.21915444E-06	1.97782838E-10	-1.18312807E-14
8.44225753E+04	-6.44480148E+00	3.34917187E+00	1.65822626E-02	-2.77115653E-05
2.51382364E-08	-8.85285352E-12	8.49863168E+04	6.80362439E+00	
C3H2				
5.69445684E+00	6.53821901E-03	-2.35907266E-06	3.82037384E-10	-2.29227460E-14
5.49264274E+04	-6.96163733E+00	3.18167129E+00	-3.37611741E-04	3.95343765E-05
-5.49792422E-08	2.28335240E-11	5.61816758E+04	9.06482468E+00	
C3H2L				
6.42557170E+00	5.57113530E-03	-1.93729414E-06	3.05883061E-10	-1.80270714E-14
6.99539184E+04	-8.83877867E+00	2.51874113E+00	1.96318981E-02	-2.17479988E-05
1.29990854E-08	-3.05445698E-12	7.08679212E+04	1.05212804E+01	
C3H3				
7.14221880E+00	7.61902005E-03	-2.67459950E-06	4.24914801E-10	-2.51475415E-14
3.89087427E+04	-1.25848435E+01	1.35110927E+00	3.27411223E-02	-4.73827135E-05
3.76309808E-08	-1.18540923E-11	4.01057783E+04	1.52058924E+01	
C3H4(A)				
0.63168722E+01	0.11133728E-01	-0.39629378E-05	0.63564238E-09	-0.37875540E-13
0.20117495E+05	-0.10995766E+02	0.26130445E+01	0.12122575E-01	0.18539880E-04
-0.34525149E-07	0.15335079E-10	0.21541567E+05	0.10226139E+02	
C3H4(P)				
0.60252400E+01	0.11336542E-01	-0.40223391E-05	0.64376063E-09	-0.38299635E-13
0.19620942E+05	-0.86043785E+01	0.26803869E+01	0.15799651E-01	0.25070596E-05
-0.13657623E-07	0.66154285E-11	0.20802374E+05	0.98769351E+01	
C3H4(B)				

6.28078872E+00	1.12393798E-02	-4.01957416E-06	6.46920405E-10	-3.86433056E-14
3.03415080E+04	-1.11420363E+01	2.24666571E+00	5.76237942E-03	4.42080338E-05
-6.62906810E-08	2.81824735E-11	3.21284389E+04	1.33451493E+01	
C3H5(A)			REF : R.ROBINSON 20/09/06	
7.05019790E+00	1.30417133E-02	-4.62341683E-06	7.39605232E-10	-4.39893394E-14
1.69162444E+04	-1.41334291E+01	1.36322505E+00	2.00030606E-02	1.22366530E-05
-3.34032456E-08	1.59644171E-11	1.88365517E+04	1.71382540E+01	
C3H5(S)			REF : BURCAT 20/09/06	
6.05091412E+00	1.34052084E-02	-4.73450586E-06	7.55380897E-10	-4.48421084E-14
2.90860210E+04	-6.73692060E+00	3.33277282E+00	1.06102499E-02	2.17559727E-05
-3.47145235E-08	1.44476835E-11	3.03404530E+04	9.78922358E+00	
C3H5(T)			REF : R.ROBINSON 20/09/06	
6.17467558E+00	1.35842068E-02	-4.86523676E-06	7.83574439E-10	-4.68222090E-14
2.72013596E+04	-7.02846541E+00	4.82883324E+00	8.99954001E-04	4.44768198E-05
-5.67019197E-08	2.21267105E-11	2.83786431E+04	3.89995688E+00	
C3H5(B)			REF : BURCAT 20/09/06	
6.62512238E+00	1.36577057E-02	-4.90066661E-06	7.90436486E-10	-4.72860275E-14
3.03239999E+04	-1.31845240E+01	2.15143774E+00	3.80171682E-03	6.14538989E-05
-8.83383102E-08	3.70565687E-11	3.24689062E+04	1.48309194E+01	
C3H6(B)			REF : R.ROBINSON 20/09/06	
6.33778554E+00	1.64174480E-02	-5.85359278E-06	9.40111948E-10	-5.60727359E-14
3.28971390E+03	-1.41848666E+01	2.57234000E+00	-2.50916956E-03	8.62737013E-05
-1.16111392E-07	4.75602007E-11	5.54899161E+03	1.18019800E+01	
C3H6			REF : BURCAT 20/09/06	
6.03870234E+00	1.62963931E-02	-5.82130800E-06	9.35936829E-10	-5.58603143E-14
-7.41715057E+02	-8.43825992E+00	3.83464468E+00	3.29078952E-03	5.05228001E-05
-6.66251176E-08	2.63707473E-11	7.88717123E+02	7.53408013E+00	
C3H7(N)			REF : BURCAT 20/09/06	
6.49636579E+00	1.77337992E-02	-6.24898046E-06	9.95389495E-10	-5.90199770E-14
8.85973885E+03	-8.56389710E+00	4.08211458E+00	5.23240341E-03	5.13554466E-05
-6.99343598E-08	2.81819493E-11	1.04074558E+04	8.39534919E+00	
C3H7(I)			REF : R.ROBINSON 20/09/06	
6.10103510E+00	1.85252265E-02	-6.63451675E-06	1.06844391E-09	-6.38396464E-14
7.53376696E+03	-6.77594633E+00	7.17878202E+00	-1.63182405E-02	9.96703136E-05
-1.15074793E-07	4.35402866E-11	8.75779397E+03	-4.71632586E+00	
C3H8			REF : R.ROBINSON 20/09/06	
6.46876392E+00	2.07740138E-02	-7.41974628E-06	1.19269771E-09	-7.11713650E-14
-1.61396855E+04	-1.15613433E+01	4.34772075E+00	3.58595707E-03	6.14128031E-05
-7.96781660E-08	3.12762429E-11	-1.44205640E+04	4.98218695E+00	
C3H2O			REF : R.ROBINSON 20/09/06	
8.31837925E+00	6.29241735E-03	-2.23673278E-06	3.58419038E-10	-2.13415819E-14
1.24699728E+04	-1.64469649E+01	3.31113539E-01	4.22486648E-02	-6.51735418E-05
4.99681989E-08	-1.46632942E-11	1.39839966E+04	2.13631640E+01	
C3H3O			REF : BURCAT 20/09/06	
6.90703955E+00	1.02341927E-02	-3.65649593E-06	5.87914100E-10	-3.51359226E-14
7.62708561E+03	-7.29856114E+00	4.11237192E+00	5.05829116E-03	3.17832265E-05
-4.55489258E-08	1.86325507E-11	8.99713585E+03	1.01743843E+01	
C3H4O			REF : BURCAT 20/09/06	
7.31820729E+00	1.27398510E-02	-4.60112009E-06	7.44735077E-10	-4.46993049E-14
-1.16137229E+04	-1.11884734E+01	3.98487241E+00	3.40751550E-03	4.81227535E-05
-6.61399005E-08	2.67817331E-11	-9.83297241E+03	1.03960574E+01	
C3H5O			REF : R.ROBINSON 20/09/06	
8.79584189E+00	1.43678209E-02	-5.15086817E-06	8.30425063E-10	-4.96670802E-14
4.54840599E+03	-2.22910017E+01	1.70176691E+00	1.81714690E-02	3.24069942E-05
-6.06152090E-08	2.71285315E-11	7.14713827E+03	1.78178812E+01	
PC3H5O			REF : BURCAT 20/09/06	
6.52325448E+00	1.54211952E-02	-5.50898157E-06	8.85889862E-10	-5.28846399E-14
-7.19631634E+03	-5.19862218E+00	6.25722402E+00	-9.17612184E-03	7.61190493E-05
-9.05514997E-08	3.46198215E-11	-5.91616484E+03	2.23330599E+00	
TC3H5O			REF : R.ROBINSON 05/10/06	
8.19121321E+00	1.40061388E-02	-5.00831912E-06	8.03961104E-10	-4.79449403E-14
-1.02130206E+03	-1.33490112E+01	7.54792894E+00	-7.02219530E-03	6.80989676E-05
-8.26664815E-08	3.19868293E-11	2.27709482E+02	-4.61588282E+00	
AC3H5O			REF : BURCAT 20/09/06	
7.54410697E+00	1.43443222E-02	-5.08381081E-06	8.13200521E-10	-4.83673315E-14
-7.48672286E+03	-1.14792587E+01	4.70187196E+00	5.51653762E-03	4.27505858E-05
-5.94680816E-08	2.40685378E-11	-5.92845491E+03	7.12932590E+00	

C3H6O				REF : BURCAT 20/09/06
8.95739587E+00	1.60217198E-02	-5.65131014E-06	9.01550505E-10	-5.35370086E-14
-1.65852904E+04	-2.45939234E+01	2.12818440E+00	8.44261433E-03	6.99012101E-05
-1.04542243E-07	4.42460530E-11	-1.36496693E+04	1.64564771E+01	
AC3H6O			REF : R.ROBINSON 20/09/06	
7.34483390E+00	1.74962257E-02	-6.28532764E-06	1.01447594E-09	-6.07151779E-14
-3.01532755E+04	-1.27759736E+01	5.14509588E+00	4.67026325E-04	6.25054589E-05
-7.97481327E-08	3.11400443E-11	-2.84186997E+04	4.17376406E+00	
PC3H6O			REF : R.ROBINSON 20/09/06	
7.49953799E+00	1.74385179E-02	-6.27541492E-06	1.01203640E-09	-6.05432962E-14
-2.60089832E+04	-1.19306739E+01	5.53463757E+00	-4.31251930E-04	6.31224828E-05
-7.93331121E-08	3.07213777E-11	-2.43119275E+04	3.89943422E+00	
C3H7O(I)			REF : R.ROBINSON 05/10/06	
8.80421897E+00	1.88114477E-02	-6.74383714E-06	1.08690817E-09	-6.49826929E-14
-9.96635265E+03	-2.04194805E+01	4.06975593E+00	1.57818571E-02	3.26769683E-05
-5.24145601E-08	2.17797338E-11	-7.85093901E+03	7.97686302E+00	
C3H7O(N)			REF : R.ROBINSON 05/10/06	
8.83565525E+00	1.89091891E-02	-6.80731617E-06	1.09639726E-09	-6.54627942E-14
-8.79968060E+03	-1.84611914E+01	5.11003655E+00	9.85648839E-03	4.56472212E-05
-6.46689824E-08	2.60236989E-11	-6.80904476E+03	5.49940565E+00	
C3H6OH			REF : R.ROBINSON 20/09/06	
8.30739359E+00	1.86672380E-02	-6.65912831E-06	1.06610221E-09	-6.33929131E-14
-1.06259963E+04	-1.29498986E+01	8.01766675E+00	-6.97669884E-03	7.66310473E-05
-9.03375783E-08	3.39837757E-11	-9.23620653E+03	-4.99358603E+00	
C3H7OOH(I)			REF : R.ROBINSON 20/09/06	
1.20456150E+01	2.00609758E-02	-7.14988442E-06	1.14410241E-09	-6.79756845E-14
-2.93586148E+04	-3.37253315E+01	5.33794019E+00	2.76687712E-02	1.27589136E-05
-3.73171105E-08	1.75843187E-11	-2.70062593E+04	3.45478108E+00	
C3H7OOH(N)			REF : R.ROBINSON 20/09/06	
1.13659898E+01	2.09104854E-02	-7.54558182E-06	1.21408112E-09	-7.23348512E-14
-2.69948187E+04	-2.79668904E+01	7.72592798E+00	7.00071376E-03	6.31053345E-05
-8.74966515E-08	3.55373150E-11	-2.48944233E+04	-3.57008863E+00	
C3H7OO(I)			REF : R.ROBINSON 05/10/06	
1.01751084E+01	1.99154854E-02	-7.17577191E-06	1.15641116E-09	-6.90571155E-14
-1.24254561E+04	-2.34403543E+01	6.27854157E+00	9.67831116E-03	4.97219807E-05
-6.92781488E-08	2.76014913E-11	-1.03016894E+04	1.82502336E+00	
C3H7OO(N)			REF : R.ROBINSON 05/10/06	
1.00126671E+01	2.02489787E-02	-7.37478477E-06	1.19344117E-09	-7.13933622E-14
-9.88113441E+03	-2.09357644E+01	7.01899874E+00	-3.60956122E-04	7.97640943E-05
-1.03233840E-07	4.08206117E-11	-7.70037244E+03	1.37035175E+00	
C3H6OOH			REF : R.ROBINSON 05/10/06	
1.12645108E+01	1.83702458E-02	-6.64465781E-06	1.07024893E-09	-6.38038186E-14
-2.96405270E+03	-2.41355971E+01	1.08227752E+01	-1.44735606E-02	1.06410370E-04
-1.29121248E-07	5.03582068E-11	-1.32195120E+03	-1.39762404E+01	
C4H			REF : R.ROBINSON 20/09/06	
6.80958026E+00	5.53720360E-03	-1.99731156E-06	3.23402907E-10	-1.94028936E-14
9.55410750E+04	-9.27742185E+00	1.61853523E+00	2.42334896E-02	-2.92435255E-05
1.90475677E-08	-5.00259472E-12	9.67816455E+04	1.65122775E+01	
C4H2			REF : BURCAT 20/09/06	
8.68978130E+00	6.69732229E-03	-2.34774865E-06	3.72759231E-10	-2.20554548E-14
5.19942624E+04	-2.20010465E+01	-5.84768273E-01	5.33506727E-02	-9.50805952E-05
8.37959674E-08	-2.80912179E-11	5.36111160E+04	2.09878997E+01	
C4H3(N)			REF : R.ROBINSON 20/09/06	
8.67518979E+00	8.99760032E-03	-3.18870421E-06	5.10080852E-10	-3.03404906E-14
6.19699844E+04	-1.87973407E+01	7.12909471E-01	3.86307007E-02	-4.72486887E-05
3.09706868E-08	-8.10178201E-12	6.38015128E+04	2.04653602E+01	
C4H3(I)			REF : BURCAT 20/09/06	
8.51181244E+00	9.03337808E-03	-3.17602594E-06	5.05276458E-10	-2.99379699E-14
5.71046116E+04	-1.51017769E+01	3.37964170E+00	2.70498840E-02	-2.90761572E-05
1.83027765E-08	-4.81164203E-12	5.83688723E+04	1.05464883E+01	
C4H4			REF : BURCAT 20/09/06	
7.98456038E+00	1.20558816E-02	-4.23587475E-06	6.73646140E-10	-3.99059864E-14
3.11993029E+04	-1.67958975E+01	1.37368786E+00	2.88801256E-02	-1.46863874E-05
-3.91045446E-09	4.78133572E-12	3.30633344E+04	1.75941274E+01	
C4H5(S)			REF : R.ROBINSON 20/09/06	
9.07499704E+00	1.40412416E-02	-5.01355646E-06	8.05965772E-10	-4.81032062E-14
3.39249544E+04	-2.28554397E+01	1.70299608E+00	2.89781109E-02	-4.25871048E-06

-1.81301166E-08	1.05682649E-11	3.61876524E+04	1.64121819E+01	
C4H5(T)			REF : BURCAT 20/09/06	
8.11183574E+00	1.42276370E-02	-5.02419535E-06	8.00816580E-10	-4.75459802E-14
4.00134524E+04	-1.52704514E+01	3.28605952E+00	1.43352325E-02	2.78456642E-05
-4.84612551E-08	2.10628469E-11	4.19222504E+04	1.26653969E+01	
C4H5(I)			REF : BURCAT 20/09/06	
8.58761100E+00	1.42683804E-02	-5.04812095E-06	8.06555355E-10	-4.79335634E-14
3.40836919E+04	-1.96196761E+01	2.00881066E+00	2.50340684E-02	4.47930427E-06
-2.63989791E-08	1.34432880E-11	3.62069792E+04	1.59913722E+01	
C4H6(S)			REF : BURCAT 20/09/06	
8.13872997E+00	1.68655431E-02	-5.97324908E-06	9.54915173E-10	-5.67693708E-14
1.55467985E+04	-1.77959041E+01	2.90828336E+00	1.79025349E-02	2.61486503E-05
-4.81598832E-08	2.11295844E-11	1.75928783E+04	1.23118106E+01	
C4H6(T)			REF : BURCAT 20/09/06	
7.62637466E+00	1.72523403E-02	-6.09184911E-06	9.70800102E-10	-5.76169721E-14
9.55306395E+03	-1.48325259E+01	4.10599669E+00	5.05575563E-03	5.83885454E-05
-8.05950198E-08	3.27447711E-11	1.15092468E+04	8.42978067E+00	
C4H6(F)			REF : R.ROBINSON 20/09/06	
8.69736431E+00	1.65073792E-02	-5.87610730E-06	9.42570499E-10	-5.61671362E-14
1.59826676E+04	-2.07144041E+01	2.11600152E+00	2.84863898E-02	-2.01729179E-06
-1.84254439E-08	1.00553840E-11	1.81079466E+04	1.47677382E+01	
C4H6(B)			REF : R.ROBINSON 20/09/06	
8.43096095E+00	1.68899025E-02	-6.04874596E-06	9.74340249E-10	-5.82343628E-14
2.66115375E+04	-2.04239627E+01	2.94003921E+00	1.44314059E-02	3.92545706E-05
-6.34679968E-08	2.70302044E-11	2.89234985E+04	1.20214885E+01	
C4H6(M)			REF : BURCAT 20/09/06	
7.26055302E+00	1.80160845E-02	-6.47062409E-06	1.04411453E-09	-6.24741250E-14
1.39644246E+04	-1.29484347E+01	5.39211846E+00	2.98346178E-03	5.22542032E-05
-6.64726627E-08	2.56305331E-11	1.55148209E+04	1.71080366E+00	
C4H7(I)			REF : R.ROBINSON 05/10/06	
8.97924987E+00	1.89314502E-02	-6.74883879E-06	1.08370764E-09	-6.46277001E-14
1.19605358E+04	-2.22521993E+01	1.01003603E+00	3.02533518E-02	9.27971616E-06
-3.58385260E-08	1.74763632E-11	1.46483074E+04	2.13831640E+01	
C4H7(N)			REF : BURCAT 05/10/06	
8.49073768E+00	1.91056974E-02	-6.74370664E-06	1.07343267E-09	-6.36251837E-14
2.04659294E+04	-1.74555814E+01	5.07355313E+00	5.27619329E-03	6.23441322E-05
-8.54203458E-08	3.45890031E-11	2.24615054E+04	5.60318035E+00	
C4H7(S)			REF : R.ROBINSON 05/10/06	
8.77047624E+00	1.92187729E-02	-6.87542705E-06	1.10663532E-09	-6.61028746E-14
1.20695085E+04	-2.08842606E+01	4.16630233E+00	8.96330982E-03	5.79781450E-05
-8.30895850E-08	3.41361824E-11	1.43921546E+04	8.26375850E+00	
C4H8(I)			REF : R.ROBINSON 05/10/06	
8.06269034E+00	2.20765179E-02	-7.90114313E-06	1.27198170E-09	-7.59864193E-14
-6.16389292E+03	-1.83725208E+01	5.16031440E+00	5.63178326E-03	6.25749118E-05
-8.20550258E-08	3.21220767E-11	-4.13902874E+03	2.60924249E+00	
C4H8(N)			REF : R.ROBINSON 05/10/06	
8.37176539E+00	2.17689316E-02	-7.77572559E-06	1.24747571E-09	-7.43321930E-14
-4.28560037E+03	-1.81843440E+01	5.48963814E+00	1.37802066E-03	7.79778572E-05
-1.01585586E-07	4.02781850E-11	-2.15478324E+03	3.42836316E+00	
C4H8(S)			REF : R.ROBINSON 05/10/06	
7.88750247E+00	2.22988814E-02	-7.99637187E-06	1.28899533E-09	-7.70725949E-14
-5.45955297E+03	-1.70739220E+01	6.85844649E+00	-6.51094213E-03	9.08047195E-05
-1.09617044E-07	4.18667549E-11	-3.62153801E+03	-4.07345440E+00	
C4H9(I)			REF : BURCAT 05/10/06	
9.61250942E+00	2.28581786E-02	-8.06391309E-06	1.28556553E-09	-7.62730799E-14
4.15218608E+03	-2.66485099E+01	3.34476784E+00	2.31869650E-02	3.28261040E-05
-5.96398514E-08	2.58980820E-11	6.66201200E+03	9.68860372E+00	
C4H9(T)			REF : BURCAT 05/10/06	
6.72557390E+00	2.53649194E-02	-9.05306262E-06	1.45474620E-09	-8.67934112E-14
2.57430692E+03	-8.89920414E+00	6.45910754E+00	-1.02015930E-02	1.06310577E-04
-1.25717030E-07	4.75543216E-11	4.43420391E+03	1.30648608E+00	
C4H9(N)			REF : BURCAT 05/10/06	
8.97401527E+00	2.39704154E-02	-8.48703645E-06	1.35644127E-09	-8.06234913E-14
5.19161526E+03	-2.31075609E+01	4.73737837E+00	9.69051565E-03	6.63846383E-05
-9.24799302E-08	3.74006099E-11	7.57382332E+03	4.91063455E+00	
C4H9(S)			REF : BURCAT 05/10/06	
7.72287211E+00	2.43427284E-02	-8.65476475E-06	1.38712529E-09	-8.26084187E-14
4.15004489E+03	-1.43949625E+01	5.42089393E+00	-9.12146870E-04	8.84998581E-05

-1.12115531E-07	4.38222782E-11	6.28927311E+03	5.04210029E+00	
C4H10(N)			REF : R.ROBINSON 05/10/06	
8.92213454E+00	2.62597428E-02	-9.42142441E-06	1.51500444E-09	-9.03538061E-14
-1.98790900E+04	-2.23198916E+01	6.84977207E+00	-1.75116891E-03	9.48605428E-05
-1.19284063E-07	4.65100207E-11	-1.76822354E+04	-3.51832851E+00	
C4H10(I)			REF : BURCAT 05/10/06	
9.76991697E+00	2.54997141E-02	-9.14142587E-06	1.47328201E-09	-8.80799697E-14
-2.14052667E+04	-3.00329670E+01	4.45479140E+00	8.26058864E-03	8.29886433E-05
-1.14647616E-07	4.64569994E-11	-1.84593929E+04	4.92740653E+00	
C4H2O			REF : R.ROBINSON 20/09/06	
9.40908701E+00	8.64021882E-03	-3.12908612E-06	5.07868742E-10	-3.05160749E-14
2.24615264E+04	-2.18745001E+01	2.15973548E+00	3.72020987E-02	-5.14278090E-05
4.03137307E-08	-1.28501835E-11	2.41419803E+04	1.37260239E+01	
C4H4O			REF : R.ROBINSON 20/09/06	
9.61322922E+00	1.39225141E-02	-5.05874715E-06	8.23043284E-10	-4.95420588E-14
5.87078239E+02	-2.66451271E+01	1.78782779E+00	1.73722022E-02	3.80649464E-05
-6.80589897E-08	3.00845106E-11	3.50676877E+03	1.78264604E+01	
XC4H5O			REF : R.ROBINSON 05/10/06	
1.00109193E+01	1.56609245E-02	-5.64859331E-06	9.14217653E-10	-5.48218361E-14
3.70525874E+03	-2.37578616E+01	5.01239905E+00	1.50193265E-02	2.82372524E-05
-4.74581120E-08	2.00717803E-11	5.79705805E+03	5.56182744E+00	
YC4H5O			REF : R.ROBINSON 05/10/06	
1.05082001E+01	1.56939134E-02	-5.67000455E-06	9.18897935E-10	-5.51590124E-14
-5.18511078E+02	-2.90238850E+01	3.28894051E+00	1.95544826E-02	2.97994330E-05
-5.57675403E-08	2.45205321E-11	2.20378942E+03	1.20012623E+01	
BC4H6O			REF : R.ROBINSON 05/10/06	
1.04017539E+01	1.91801473E-02	-7.15850045E-06	1.17439803E-09	-7.08810109E-14
-1.75011636E+04	-3.00059373E+01	3.94073764E+00	2.32480563E-02	1.80932390E-05
-3.81207793E-08	1.63656642E-11	-1.49548630E+04	6.92065946E+00	
AC4H6O			REF : R.ROBINSON 20/09/06	
1.06955708E+01	1.76034072E-02	-6.31551730E-06	1.01520407E-09	-6.05533529E-14
-3.74306952E+03	-3.07187354E+01	2.43462425E+00	2.77197540E-02	1.56055031E-05
-4.30249223E-08	2.02031524E-11	-8.90012699E+02	1.48831206E+01	
C4H7O(X)			REF : R.ROBINSON 05/10/06	
1.03519991E+01	2.03385849E-02	-7.35907392E-06	1.18946887E-09	-7.11844228E-14
1.75561028E+03	-2.59117862E+01	4.80290347E+00	1.26829060E-02	5.37008113E-05
-7.94047836E-08	3.26679573E-11	4.37998505E+03	8.22571029E+00	
C4H7O(M)			REF : R.ROBINSON 05/10/06	
9.95812346E+00	2.00549144E-02	-7.19396488E-06	1.15740437E-09	-6.91060030E-14
-1.17601480E+04	-2.24695101E+01	4.68146299E+00	1.86787473E-02	2.95246310E-05
-4.97395546E-08	2.07620847E-11	-9.47693435E+03	8.75509363E+00	
C4H8O(X)			REF : R.ROBINSON 05/10/06	
1.01453808E+01	2.30313259E-02	-8.27843616E-06	1.33674487E-09	-8.00286667E-14
-2.18459352E+04	-2.86842582E+01	4.91524246E+00	1.07110614E-02	6.48871041E-05
-9.10021090E-08	3.66436878E-11	-1.91042078E+04	4.78044074E+00	
C4H8O(M)			REF : R.ROBINSON 05/10/06	
9.74197781E+00	2.30221779E-02	-8.28513329E-06	1.33580581E-09	-7.98631500E-14
-3.08246201E+04	-2.35538706E+01	6.85713509E+00	1.73287406E-03	7.75498242E-05
-9.87341435E-08	3.83292752E-11	-2.85711183E+04	-1.49989282E+00	
C4H8OH(I)			REF : R.ROBINSON 05/10/06	
1.20408349E+01	2.27109222E-02	-8.09318390E-06	1.29534127E-09	-7.69845061E-14
-1.47279195E+04	-3.27518521E+01	3.50432963E+00	4.36215967E-02	-2.32342059E-05
1.29922560E-09	2.68598392E-12	-1.21533089E+04	1.21840368E+01	
O2C4H9O			REF : R.ROBINSON 05/10/06	
1.58754061E+01	2.45143718E-02	-9.02792662E-06	1.47136702E-09	-8.84192089E-14
-3.37499714E+04	-4.87350426E+01	1.20350104E+01	4.07786695E-03	8.13917304E-05
-1.106870642E-07	4.21108331E-11	-3.11855572E+04	-2.14156628E+01	
C5H			REF : BURCAT 24/09/07	
0.86957493E+01	0.60543008E-02	-0.20160105E-05	0.28928926E-09	-0.14700995E-13
0.90310687E+05	-0.21029110E+02	0.16348248E+01	0.25095381E-01	-0.12066364E-04
-0.10465111E-07	0.88099883E-11	0.92124875E+05	0.15135100E+02	
C5H2			REF : BURCAT 24/09/07	
0.11329175E+02	0.74240565E-02	-0.26281887E-05	0.40825410E-09	-0.23013326E-13
0.78787062E+05	-0.36184340E+02	0.30623217E+01	0.27099982E-01	-0.10091697E-04
-0.12727451E-07	0.91672191E-11	0.81149687E+05	0.70842413E+01	
C5H3(L)			REF : BURCAT 24/09/07	
0.10296658E+02	0.10470124E-01	-0.37746103E-05	0.61077326E-09	-0.36621089E-13
0.63439389E+05	-0.27338507E+02	0.15946538E+01	0.43378369E-01	-0.56253789E-04

0.41304029E-07	-0.12456939E-10	0.65491079E+05	0.15644812E+02	
C5H4(L)		200K-6000K REF	: G3MP2B3 R.ROBINSON	30-Oct-07
1.05272273E+01	1.27467546E-02	-4.54905408E-06	7.31127121E-10	-4.36321667E-14
4.70599415E+04	-2.84644483E+01	5.99684934E-01	4.72382712E-02	-5.23129053E-05
3.15166007E-08	-7.62922870E-12	4.94837602E+04	2.11375685E+01	
C5H5	G3withG3B3HeatofFormation	200K-6000K REF	:	R.ROBINSON 22-Apr-08
1.08491980E+01	1.53713657E-02	-5.55119834E-06	8.99523521E-10	-5.39951842E-14
2.64320961E+04	-3.52284407E+01	-1.12762243E+00	3.43596094E-02	1.73763744E-05
-5.81600874E-08	2.90666197E-11	3.02130502E+04	2.94588572E+01	
C5H5(I)		200K-6000K REF	: CBS-QB3 R.ROBINSON	24-Apr-08
1.23767441E+01	1.33125781E-02	-4.74652058E-06	7.58879775E-10	-4.50797047E-14
5.69143625E+04	-3.79040748E+01	4.02036903E-01	4.74761735E-02	-3.30601849E-05
4.06793719E-10	6.43178251E-12	6.00378092E+04	2.33056553E+01	
C5H6(L)		200K-6000K REF	: G3B3 R.ROBINSON	07-Aug-07
9.59529027E+00	1.86098051E-02	-6.68618072E-06	1.07930396E-09	-6.46016547E-14
2.52114864E+04	-2.38846887E+01	4.10249044E+00	1.70779364E-02	3.34941096E-05
-5.56537037E-08	2.35127842E-11	2.75445653E+04	8.51660798E+00	
C5H6		200K-6000K REF	: G3B3 R.ROBINSON	13-Mar-07
1.01131403E+01	1.87180456E-02	-6.75847566E-06	1.09493046E-09	-6.57129588E-14
1.13288676E+04	-3.27694463E+01	5.92562815E-01	1.81067404E-02	6.35718117E-05
-1.04819105E-07	4.56499177E-11	1.50470513E+04	2.23183055E+01	
C5H7(I)		200K-6000K REF	: G3B3 R.ROBINSON	07-Aug-07
7.17295000E+00	2.74828000E-02	-1.25234000E-05	2.51195000E-09	-1.83816000E-13
3.43404120E+04	-8.47072535E+00	2.70639000E+00	3.76025000E-02	-1.95473000E-05
3.85395000E-09	-6.81935000E-14	3.57297975E+04	1.52991891E+01	
C5H7		200K-6000K REF	: G3B3 R.ROBINSON	15-Mar-07
1.05539442E+01	2.10410274E-02	-7.60264581E-06	1.23216241E-09	-7.39648585E-14
1.53795928E+04	-3.40182093E+01	1.51100557E+00	1.47703124E-02	7.75539517E-05
-1.19683376E-07	5.09986302E-11	1.91867221E+04	1.96776449E+01	
C5H7(L)				
0.18941353E+02	0.85102411E-02	-0.14014643E-05	0.00000000E+00	0.00000000E+00
0.18109184E+05	-0.78403470E+02	-0.56457147E+00	0.48115796E-01	-0.23131123E-04
0.00000000E+00	0.00000000E+00	0.24904574E+05	0.27439042E+02	
C5H8		200K-6000K REF	: G3B3 R.ROBINSON	13-Mar-07
9.86592030E+00	2.44020184E-02	-8.82789062E-06	1.43181832E-09	-8.59919666E-14
-9.59855751E+02	-3.13231941E+01	2.50933871E+00	3.82798417E-03	1.11024150E-04
-1.53500143E-07	6.29245445E-11	2.86394578E+03	1.60336382E+01	
C5H8(I)		200K-6000K REF	: G3B3 R.ROBINSON	29-May-07
1.26178849E+01	2.04825855E-02	-7.27655362E-06	1.16254450E-09	-6.90540663E-14
4.78553010E+03	-4.17166324E+01	2.51337826E+00	2.62954561E-02	4.80576980E-05
-9.15599235E-08	4.16107984E-11	8.38349742E+03	1.50903564E+01	
C5H9(A)		200K-6000K REF	: G3B3 R.ROBINSON	29-May-07
1.02387504E+01	2.62103815E-02	-9.61636547E-06	1.56028890E-09	-9.34073089E-14
8.03598745E+03	-2.67338239E+01	4.25891338E+00	1.73539089E-02	5.87298434E-05
-8.88205873E-08	3.67775696E-11	1.08830148E+04	1.01660095E+01	
C5H9(B)		200K-6000K REF	: G3B3 R.ROBINSON	29-May-07
1.16475532E+01	2.42158386E-02	-8.73709605E-06	1.40732927E-09	-8.39543416E-14
9.02167848E+03	-3.46927661E+01	4.24094102E+00	2.53634639E-02	3.72604538E-05
-6.82161902E-08	2.98010023E-11	1.19508500E+04	8.06049917E+00	
C5H10(A)		200K-6000K REF	: G3B3 R.ROBINSON	06-Jun-07
1.05001829E+01	2.75643169E-02	-9.91309486E-06	1.59706130E-09	-9.53724218E-14
-9.52157434E+03	-2.86285984E+01	4.70682242E+00	1.70738409E-02	6.06846510E-05
-8.91019491E-08	3.62897286E-11	-6.61782541E+03	7.71884933E+00	
C5H10(B)		200K-6000K REF	: G3B3 R.ROBINSON	06-Jun-07
9.93522662E+00	2.80726324E-02	-1.00775991E-05	1.62568308E-09	-9.72552799E-14
-1.00942898E+04	-2.65246769E+01	6.85180867E+00	2.28456171E-03	9.11518952E-05
-1.15578710E-07	4.47491318E-11	-7.52818050E+03	-2.19532254E+00	
C5H11(T)		200K-6000K REF	: G3B3 R.ROBINSON	06-Jun-07
1.01825195E+01	3.02340266E-02	-1.09144648E-05	1.76329609E-09	-1.05510064E-13
-1.17151228E+03	-2.42477873E+01	9.30810413E+00	-1.62593976E-02	1.46448111E-04
-1.76147687E-07	6.78107372E-11	1.38991968E+03	-8.07080433E+00	
C5H4OH		200K-6000K REF	: G3B3 R.ROBINSON	29-Mar-07
1.36752494E+01	1.52162113E-02	-5.52789930E-06	8.99389731E-10	-5.41428455E-14
4.95232766E+03	-4.79581152E+01	-1.20148288E+00	4.86464089E-02	-1.30026599E-05
-2.83448443E-08	1.81113865E-11	9.28350067E+03	3.03205893E+01	
C5H4O		200K-6000K REF	: G3B3 R.ROBINSON	13-Mar-07
1.16281545E+01	1.47998088E-02	-5.37621419E-06	8.74710788E-10	-5.26577627E-14
1.35657386E+03	-3.80263557E+01	-2.83091176E-03	3.43473269E-02	1.05744670E-05

-4.66599559E-08	2.36147951E-11	5.04708261E+03	2.47228122E+01		
C5H5O				BURCAT	13-Mar-07
0.12711510E+02	0.16650171E-01	-0.60741189E-05	0.99090150E-09	-0.59758183E-13	
0.66172961E+04	-0.43161680E+02	0.45438248E-01	0.33871750E-01	0.25637288E-04	
-0.67844135E-07	0.32508364E-10	0.10797244E+05	0.26058142E+02		
C5H5O		200K-6000K REF	: G3B3	R.ROBINSON	15-Mar-07
1.42226314E+01	1.75152612E-02	-6.40305264E-06	1.04200860E-09	-6.26515921E-14	
1.96213722E+04	-4.66729070E+01	4.03772698E+00	1.80835145E-02	6.44483027E-05	
-1.06778175E-07	4.65228276E-11	2.35429815E+04	1.19816804E+01		
C5H5OH		200K-6000K REF	: G3B3	R.ROBINSON	15-Mar-07
1.38018850E+01	1.72092529E-02	-6.11269503E-06	9.79577036E-10	-5.83486016E-14	
-7.03744252E+03	-4.91661999E+01	-1.13448598E+00	4.58163497E-02	1.04750370E-05	
-6.34680356E-08	3.41308062E-11	-2.65979172E+03	3.00448818E+01		
C6H2		200K-6000K REF	: G3	R.ROBINSON	04-Jun-08
1.11167234E+01	9.69979976E-03	-3.49004981E-06	5.64122418E-10	-3.38030377E-14	
7.86280484E+04	-3.13759648E+01	-4.73261257E-01	5.61811081E-02	-7.90149003E-05	
5.80414115E-08	-1.68775653E-11	8.11517592E+04	2.50177740E+01		
C6H3		200K-6000K REF	: G3B3	R.ROBINSON	25-May-07
1.29646245E+01	1.05759186E-02	-3.77023128E-06	6.05639149E-10	-3.61341970E-14	
8.56896329E+04	-3.56595296E+01	1.36849693E+00	6.19812015E-02	-9.82993088E-05	
8.23077695E-08	-2.70183424E-11	8.80637205E+04	1.98144459E+01		
C6H4		o-BENZYNE	200K-6000K REF	: G3B3	BURCAT
1.05707063E+01	1.56860613E-02	-5.68267148E-06	9.22956737E-10	-5.54966417E-14	
5.04976657E+04	-3.32563927E+01	7.21604591E-01	2.47976151E-02	3.16372209E-05	
-6.53230986E-08	2.96082142E-11	5.39797980E+04	2.16733825E+01		
C6H4L		200K-6000K REF	: G3B3	R.ROBINSON	08-Aug-07
1.26801074E+01	1.34374251E-02	-4.78401266E-06	7.67759645E-10	-4.57749413E-14	
5.78931791E+04	-3.84682066E+01	1.36749388E-01	6.13125097E-02	-7.95470793E-05	
5.62489114E-08	-1.60955867E-11	6.07596914E+04	2.32034252E+01		
C6H5(A)		200K-6000K REF	: G3B3	R.ROBINSON	06-Jun-07
1.33608611E+01	1.49335995E-02	-5.38331240E-06	8.70337474E-10	-5.21352783E-14	
6.39400509E+04	-3.83416826E+01	1.55766331E+00	5.78077255E-02	-7.01319214E-05	
4.82579599E-08	-1.37620769E-11	6.67841381E+04	2.03237088E+01		
C6H5(B)		200K-6000K REF	: G3B3	R.ROBINSON	06-Jun-07
1.48931797E+01	1.37493189E-02	-4.90394555E-06	7.85066443E-10	-4.67065445E-14	
6.69001550E+04	-4.98647517E+01	7.53536133E-01	5.37019231E-02	-3.68463678E-05	
-1.38310583E-09	8.25092729E-12	7.05934868E+04	2.24753680E+01		
C6H5		200K-6000K REF	: G3B3	R.ROBINSON	19-Mar-07
1.14565087E+01	1.77093641E-02	-6.44201438E-06	1.04899091E-09	-6.31832290E-14	
3.60343704E+04	-3.85283667E+01	-6.64246625E-03	2.64038690E-02	4.48459620E-05	
-8.64753186E-08	3.89417961E-11	4.01343585E+04	2.57413079E+01		
C6H6(A)		200K-6000K REF	: G3B3	R.ROBINSON	29-May-07
1.36500711E+01	1.74518735E-02	-6.31301878E-06	1.02314365E-09	-6.13964652E-14	
4.44410108E+04	-4.30034010E+01	1.74187936E+00	4.95354683E-02	-3.29381168E-05	
3.46367151E-09	3.94777069E-12	4.77704725E+04	1.86686267E+01		
C6H6(B)		200K-6000K REF	: G3B3	R.ROBINSON	06-Jun-07
1.27658744E+01	1.82379363E-02	-6.59535455E-06	1.06869756E-09	-6.41213620E-14	
4.45731479E+04	-3.74802751E+01	2.19981510E+00	4.34694277E-02	-2.01332649E-05	
-7.63977524E-09	7.51682971E-12	4.76970262E+04	1.80525270E+01		
C6H6(D)		200K-6000K REF	: G3B3	R.ROBINSON	29-Oct-07
1.48965378E+01	1.64872725E-02	-5.90741622E-06	9.49118132E-10	-5.66082426E-14	
3.49812229E+04	-5.19034433E+01	2.28698860E+00	3.70898548E-02	1.51535445E-05	
-5.64718054E-08	2.83103215E-11	3.89510057E+04	1.61157498E+01		
C6H6(S)		200K-6000K REF	: G3B3	R.ROBINSON	29-May-07
1.46022188E+01	1.67304256E-02	-6.08012037E-06	9.88196740E-10	-5.94101913E-14	
4.14784695E+04	-4.99135626E+01	1.15004104E+00	4.70506058E-02	-1.23493573E-05	
-2.70994349E-08	1.74294560E-11	4.53844375E+04	2.08155548E+01		
C6H6(F)		200K-6000K REF	: G3B3	R.ROBINSON	19-Mar-07
1.21895898E+01	1.95046414E-02	-7.03416458E-06	1.13879769E-09	-6.83157498E-14	
2.02202826E+04	-4.26337898E+01	-2.35057858E-01	3.38024640E-02	3.30290867E-05	
-7.69207160E-08	3.60547717E-11	2.44318628E+04	2.58522534E+01		
C6H6(M)		200K-6000K REF	: G3B3	R.ROBINSON	19-Mar-07
1.25877237E+01	1.90952438E-02	-6.87307907E-06	1.11119217E-09	-6.65937919E-14	
3.51088063E+04	-4.32640698E+01	2.56250451E-01	3.90023715E-02	1.29479000E-05	
-5.29412523E-08	2.65892171E-11	3.90616716E+04	2.34546412E+01		



C6H6		200K-6000K REF	: G3B3	R.ROBINSON	15-Mar-07
1.13666933E+01	2.04079721E-02	-7.39919697E-06	1.20214373E-09	-7.22929443E-14	
4.52666630E+03	-4.14111483E+01	9.69438736E-02	2.29318584E-02	6.33937535E-05	
-1.08316455E-07	4.73992187E-11	8.82216986E+03	2.31554832E+01		
C6H7		200K-6000K REF	: G3B3	R.ROBINSON	15-Mar-07
1.23338010E+01	2.22625674E-02	-8.07486797E-06	1.31213477E-09	-7.89120659E-14	
1.92360666E+04	-4.36413477E+01	2.42231177E-01	2.86715106E-02	5.46203889E-05	
-1.00348133E-07	4.45687256E-11	2.37102853E+04	2.48525327E+01		
C6H7(L)		200K-6000K REF	: G3B3	R.ROBINSON	29-Oct-07
1.68702156E+01	1.72634805E-02	-6.25732251E-06	1.00976679E-09	-6.03669209E-14	
4.43145917E+04	-6.27561110E+01	2.07404306E+00	3.61323587E-02	3.88002702E-05	
-9.20661197E-08	4.38852212E-11	4.91369816E+04	1.80934521E+01		
C5H4CH3		200K-6000K REF	: G3B3	R.ROBINSON	29-Mar-07
1.24476217E+01	2.15029689E-02	-7.75134839E-06	1.25437737E-09	-7.52224739E-14	
2.04084826E+04	-4.11056808E+01	8.36909343E-01	3.18167267E-02	3.84022363E-05	
-8.02365832E-08	3.65591080E-11	2.45236619E+04	2.37127995E+01		
C6H8		200K-6000K REF	: G3B3	R.ROBINSON	15-Mar-07
1.18161918E+01	2.54108479E-02	-9.20915524E-06	1.49551515E-09	-8.98979453E-14	
6.94418806E+03	-4.21338291E+01	1.28995501E+00	2.03667087E-02	7.93314916E-05	
-1.24246815E-07	5.26821611E-11	1.13601162E+04	2.00737498E+01		
C5H5CH3		200K-6000K REF	: G3B3	R.ROBINSON	19-Mar-07
1.28684461E+01	2.38025614E-02	-8.57820021E-06	1.38790503E-09	-8.32166735E-14	
7.12182042E+03	-4.59786731E+01	1.28310910E+00	2.47381989E-02	7.05624489E-05	
-1.19384342E-07	5.21980809E-11	1.15959246E+04	2.07311292E+01		
C6H3O2		200K-6000K REF	: G3B3	R.ROBINSON	29-Mar-07
1.51915951E+01	1.46748024E-02	-5.42163659E-06	8.92003180E-10	-5.41138909E-14	
1.12656245E+04	-5.25491166E+01	3.18403948E-01	5.12223736E-02	-2.75750371E-05	
-7.51782629E-09	8.83473610E-12	1.55741843E+04	2.53014412E+01		
C6H3O3		200K-6000K REF	: G3B3	R.ROBINSON	19-Mar-07
1.74177458E+01	1.54590628E-02	-5.72711684E-06	9.43993385E-10	-5.73410135E-14	
-2.28280418E+04	-6.29444157E+01	7.76897049E-01	5.80164093E-02	-3.67022863E-05	
-7.28416129E-10	6.67374018E-12	-1.80689237E+04	2.38114327E+01		
C6H5OH		200K-6000K REF	: G3B3	R.ROBINSON	07-Aug-07
1.46414690E+01	1.94932405E-02	-7.02116352E-06	1.13603259E-09	-6.81317840E-14	
-1.65950023E+04	-5.37200677E+01	-5.64771978E-01	4.33464039E-02	2.07605251E-05	
-6.99372749E-08	3.45765647E-11	-1.17365183E+04	2.86068445E+01		
C6H5O		200K-6000K REF	: G3B3	R.ROBINSON	15-Mar-07
1.37326455E+01	1.84244924E-02	-6.71682550E-06	1.09539441E-09	-6.60492978E-14	
1.07830189E+03	-4.93708126E+01	-9.78096054E-02	3.71196938E-02	2.68005407E-05	
-7.12459156E-08	3.38931483E-11	5.68218891E+03	2.63366728E+01		
C6H4O2		200K-6000K REF	: G3B3	R.ROBINSON	19-Mar-07
1.50535698E+01	1.74168758E-02	-6.39478550E-06	1.04778871E-09	-6.33840383E-14	
-2.12124800E+04	-5.50096707E+01	4.98149162E-01	4.66938856E-02	-6.41492151E-06	
-3.18237578E-08	1.81067093E-11	-1.67049843E+04	2.26833299E+01		
C6H5O2		200K-6000K REF	: G3B3	R.ROBINSON	29-Mar-07
1.63022037E+01	1.85033368E-02	-6.79432980E-06	1.10923299E-09	-6.68544424E-14	
1.09994191E+04	-5.92010142E+01	8.78266943E-01	3.92775211E-02	3.25262349E-05	
-8.33110188E-08	3.96825851E-11	1.60845838E+04	2.51120238E+01		
C6H5OOH		200K-6000K REF	: G3B3	R.ROBINSON	04-Oct-07
1.70218621E+01	1.96332619E-02	-7.09504317E-06	1.14641152E-09	-6.86057418E-14	
-7.70247401E+03	-6.32603258E+01	-1.06714347E-01	5.42672219E-02	-8.24717731E-07	
-5.13970113E-08	2.86991080E-11	-2.59867312E+03	2.76131116E+01		
C7H5		200K-6000K REF	: G3B3	R.ROBINSON	29-Mar-07
1.49448053E+01	1.69815759E-02	-6.11230385E-06	9.88416374E-10	-5.92520096E-14	
5.09198929E+04	-5.35861988E+01	-1.76307160E+00	6.38163332E-02	-4.60335922E-05	
4.31530589E-09	6.40826637E-12	5.53922611E+04	3.22277699E+01		
C7H6					
0.98222523E+01	0.33532158E-01	-0.18960140E-04	0.51221400E-08	-0.52916027E-12	
0.39350844E+05	-0.23534618E+02	0.10617721E+01	0.60266692E-01	-0.48446786E-04	
0.18895387E-07	-0.27898133E-11	0.41581770E+05	0.20963522E+02		
C6H5C		200K-6000K REF	: G3B3	R.ROBINSON	29-Mar-07
1.41262353E+01	1.80237245E-02	-6.56048441E-06	1.06877362E-09	-6.43967261E-14	
6.77605763E+04	-4.93634930E+01	1.92634259E+00	2.85073680E-02	4.37838991E-05	
-8.70786602E-08	3.94549028E-11	7.20701846E+04	1.87571979E+01		
C6H5CH		200K-6000K REF	: G3B3	R.ROBINSON	01-Nov-07
1.39987971E+01	2.10115301E-02	-7.74130392E-06	1.26828964E-09	-7.66390696E-14	
5.04105003E+04	-5.07316398E+01	-1.42752653E-01	3.86171141E-02	3.12258253E-05	

-7.78471033E-08	3.66075904E-11	5.52022173E+04	2.70663171E+01	
C7H7		200K-6000K REF	: G3B3	R.ROBINSON 01-Mar-07
1.44185062E+01	2.32955544E-02	-8.54365127E-06	1.39475899E-09	-8.40514185E-14
1.90472689E+04	-5.40649462E+01	-8.88621147E-01	4.67433711E-02	1.94036631E-05
-6.85453132E-08	3.37680170E-11	2.40293208E+04	2.91018098E+01	
C7H7L		200K-6000K REF	: G3B3	R.ROBINSON 04-Dec-07
1.46529322E+01	2.23127123E-02	-8.06039662E-06	1.30477447E-09	-7.82841066E-14
4.77231917E+04	-5.11565691E+01	1.78224005E+00	3.21036329E-02	4.97938535E-05
-9.78136681E-08	4.42656799E-11	5.23244914E+04	2.09864666E+01	
C7H7P		200K-6000K REF	:	R.ROBINSON 03-Oct-07
1.33211864E+01	2.36827436E-02	-8.60327957E-06	1.39947590E-09	-8.42275079E-14
3.12684833E+04	-4.76131212E+01	1.24576524E+00	2.84214251E-02	5.73365370E-05
-1.01673075E-07	4.43852462E-11	3.58688678E+04	2.13324917E+01	
C7H8		200K-6000K REF	: G3B3	R.ROBINSON 01-Mar-07
1.32565954E+01	2.63599691E-02	-9.55302770E-06	1.55145524E-09	-9.32680913E-14
-5.15601767E+02	-4.81552995E+01	1.28570757E+00	2.53359931E-02	7.52284706E-05
-1.23066209E-07	5.27377613E-11	4.29498473E+03	2.15013550E+01	
C6H5CO		200K-6000K REF	: G3MP2	R.ROBINSON 02-May-08
1.50802910E+01	2.01206682E-02	-7.37900571E-06	1.20800427E-09	-7.30282061E-14
7.49341908E+03	-5.42585042E+01	1.29243926E+00	3.59691923E-02	3.34213989E-05
-7.75153854E-08	3.57892845E-11	1.22652588E+04	2.20114271E+01	
C7H6O		200K-6000K REF	: G3B3	R.ROBINSON 08-May-07
1.53113995E+01	2.20764479E-02	-8.06352686E-06	1.31293198E-09	-7.90305224E-14
-1.18489313E+04	-5.61277803E+01	1.16187164E+00	3.53975987E-02	4.45580684E-05
-9.26018106E-08	4.20424938E-11	-6.84612985E+03	2.27562799E+01	
C7H7O		200K-6000K REF	: G3B3	R.ROBINSON 01-Mar-07
1.58869165E+01	2.43099288E-02	-8.90170362E-06	1.45158328E-09	-8.74320865E-14
7.64485078E+03	-5.82334053E+01	1.34875562E+00	3.62538213E-02	5.07399910E-05
-1.01179022E-07	4.54957471E-11	1.28715161E+04	2.32423194E+01	
C7H7OA		200K-6000K REF	: G3B3	R.ROBINSON 28-Mar-07
1.63642524E+01	2.30069915E-02	-8.31828902E-06	1.34493299E-09	-8.05414900E-14
7.05523453E+03	-5.85875486E+01	1.33751930E+00	5.60429555E-02	-1.89546627E-05
-1.94032242E-08	1.32947585E-11	1.16214229E+04	2.10678967E+01	
OC7H7		200K-6000K REF	: G3B3	R.ROBINSON 28-Mar-07
1.55885621E+01	2.44114513E-02	-8.88432600E-06	1.44703270E-09	-8.71687304E-14
-4.63475079E+03	-5.69949856E+01	1.30109345E+00	3.78573405E-02	4.26663785E-05
-9.00408613E-08	4.06916002E-11	4.62424782E+02	2.27793822E+01	
C7H7OH		200K-6000K REF	: G3B3	R.ROBINSON 29-Mar-07
1.55570133E+01	2.64742745E-02	-9.61492723E-06	1.56021335E-09	-9.36632967E-14
-1.85951846E+04	-5.64807692E+01	4.57952512E+00	1.99720826E-02	8.62270226E-05
-1.32663415E-07	5.57676957E-11	-1.39302817E+04	8.70611961E+00	
HOC7H7		200K-6000K REF	: G3B3	R.ROBINSON 05-Dec-07
1.62209484E+01	2.57279235E-02	-9.27769536E-06	1.50201883E-09	-9.01081430E-14
-2.24968087E+04	-6.12270691E+01	6.18655473E-01	4.67674565E-02	2.70020458E-05
-7.68288867E-08	3.65238162E-11	-1.72475878E+04	2.43271696E+01	
C7H8OA		200K-6000K REF	: G3B3	R.ROBINSON 14-May-07
1.61455922E+01	2.60503227E-02	-9.47230904E-06	1.53776710E-09	-9.23380319E-14
-1.63397736E+04	-6.11038338E+01	9.17201862E-01	4.26156233E-02	4.04519700E-05
-9.27459204E-08	4.29301602E-11	-1.10690376E+04	2.32349913E+01	
C7H7OO		200K-6000K REF	: G3B3	R.ROBINSON 01-Mar-07
1.75384010E+01	2.50464937E-02	-9.26566669E-06	1.52026888E-09	-9.19216824E-14
6.21200901E+03	-6.27388490E+01	3.43834939E+00	3.01848465E-02	7.00879785E-05
-1.22437556E-07	5.34739568E-11	1.15679497E+04	1.77734871E+01	
OC7H7P		200K-6000K REF	: G3B3	R.ROBINSON 24-May-07
1.81925301E+01	2.44591365E-02	-8.95127578E-06	1.45924431E-09	-8.78792315E-14
5.89545445E+03	-6.84482373E+01	2.19445974E+00	4.08471616E-02	4.62775588E-05
-9.99260531E-08	4.56786288E-11	1.14829234E+04	2.04135472E+01	
C8H2		200K-6000K REF	: G3B3	R.ROBINSON 24-May-07
1.51207039E+01	1.15836375E-02	-4.19394867E-06	6.80845141E-10	-4.09238459E-14
1.03629939E+05	-4.86456518E+01	-1.11492303E+00	8.37576243E-02	-1.36625122E-04
1.14597154E-07	-3.74644192E-11	1.06927919E+05	2.89314564E+01	
C8H5(S)				
-0.18226665E+02	0.98105334E-01	-0.71376540E-04	0.23047990E-07	-0.27072450E-11
0.70338272E+05	0.12116527E+03	-0.10600960E+02	0.12687966E+00	-0.19579499E-03
0.15129409E-06	-0.42934854E-10	0.65782034E+05	0.69241891E+02	
C8H5		200K-6000K REF	: G3B3	R.ROBINSON 16-May-07
1.59141211E+01	1.90512856E-02	-6.91841357E-06	1.12540152E-09	-6.77403364E-14
6.81007829E+04	-5.81811951E+01	-1.13488264E+00	6.07145806E-02	-2.90528278E-05

-1.47803066E-08	1.33580907E-11	7.29875380E+04	3.09385073E+01	
C8H6		200K-6000K REF	: G3B3	R.ROBINSON 28-Mar-07
1.58841649E+01	2.16827507E-02	-7.84831056E-06	1.27381396E-09	-7.65525168E-14
3.10445790E+04	-6.03434222E+01	-1.15774739E+00	5.83055920E-02	-1.28838641E-05
-3.44192242E-08	2.10711101E-11	3.61473155E+04	2.98836364E+01	
C6H5CHC		200K-6000K REF	: G3B3	R.ROBINSON 01-Nov-07
1.60987575E+01	2.12246579E-02	-7.71771138E-06	1.25489588E-09	-7.55314844E-14
5.52793982E+04	-5.90713760E+01	8.74638267E-01	4.62530440E-02	1.31075596E-05
-5.90928872E-08	2.96427137E-11	6.01908641E+04	2.33384585E+01	
C8H7		200K-6000K REF	: G3B3	R.ROBINSON 06-Jun-07
1.62024214E+01	2.37169830E-02	-8.59466428E-06	1.39261244E-09	-8.35582353E-14
4.19911173E+04	-5.96757392E+01	5.98199404E-01	4.40312910E-02	3.19607403E-05
-8.36468343E-08	3.96903979E-11	4.72247875E+04	2.59253903E+01	
C8H7(F)		200K-6000K REF	: G3B3	R.ROBINSON 19-Oct-07
1.70920957E+01	2.32185495E-02	-8.38554563E-06	1.35891114E-09	-8.15767381E-14
5.01059137E+04	-6.39311685E+01	1.88585454E-01	5.32872069E-02	9.17657942E-06
-6.13342150E-08	3.18842773E-11	5.54011643E+04	2.68906693E+01	
C8H7(P)		200K-6000K REF	: G3B3	R.ROBINSON 09-May-08
1.63560947E+01	2.37093009E-02	-8.62640748E-06	1.40109008E-09	-8.41885947E-14
4.11114604E+04	-6.17370864E+01	5.63912682E-01	4.11827962E-02	4.23434307E-05
-9.54358236E-08	4.41015736E-11	4.65490247E+04	2.56255584E+01	
C8H8		200K-6000K REF	: G3B3	R.ROBINSON 16-May-07
1.62750706E+01	2.63964230E-02	-9.57863609E-06	1.55335595E-09	-9.32416572E-14
1.00959790E+04	-6.29161344E+01	5.95011053E-01	3.80448247E-02	6.03961301E-05
-1.17000056E-07	5.25170617E-11	1.57432079E+04	2.51273231E+01	
C8H9(F)		200K-6000K REF	: G3B3	R.ROBINSON 31-Oct-07
1.68344671E+01	2.79084466E-02	-1.01238931E-05	1.64223501E-09	-9.85715951E-14
3.61377855E+04	-6.03841052E+01	5.44310351E+00	2.04252993E-02	9.47478839E-05
-1.46919245E-07	6.24656421E-11	4.09409910E+04	7.23134573E+00	
C8H9		200K-6000K REF	: G3B3	R.ROBINSON 03-Oct-07
1.70077836E+01	2.85107743E-02	-1.03611087E-05	1.68579546E-09	-1.01474435E-13
1.40901227E+04	-6.68746601E+01	1.20030068E+00	3.91799992E-02	6.16792669E-05
-1.17564426E-07	5.22466290E-11	1.98924692E+04	2.22931985E+01	
C8H10		200K-6000K REF	: G3B3	R.ROBINSON 07-Aug-07
1.55887664E+01	3.19611997E-02	-1.16287800E-05	1.88981260E-09	-1.13573824E-13
-4.28458286E+03	-5.83661343E+01	3.39486331E+00	2.28588681E-02	1.01068868E-04
-1.54540904E-07	6.49157293E-11	9.96421839E+02	1.45061179E+01	
C6H5C2O		200K-6000K REF	: G3B3	R.ROBINSON 15-Oct-07
1.71311590E+01	2.09165892E-02	-7.65442484E-06	1.25139872E-09	-7.55835919E-14
2.23670210E+04	-6.29702618E+01	6.88575892E-01	5.16059386E-02	1.11467607E-06
-4.67425909E-08	2.49025388E-11	2.75447687E+04	2.52906444E+01	
C8H5O		200K-6000K REF	: G3B3	R.ROBINSON 28-Mar-07
1.81825231E+01	1.97889516E-02	-7.20508244E-06	1.17413394E-09	-7.07633472E-14
2.67589710E+04	-6.96738502E+01	-1.09646467E+00	7.05298740E-02	-4.51376296E-05
-1.29231576E-09	8.86629889E-12	3.21408799E+04	3.03139151E+01	
C8H50O		200K-6000K REF	: G3B3	R.ROBINSON 24-May-07
2.05521332E+01	2.00445657E-02	-7.33413614E-06	1.19500584E-09	-7.19472479E-14
3.65926838E+04	-7.89142990E+01	1.99509144E-01	7.21815780E-02	-4.20268840E-05
-7.95299583E-09	1.19844141E-11	4.23167792E+04	2.69212527E+01	
C9H7		200K-6000K REF	: G3B3	R.ROBINSON 09-May-07
1.78551775E+01	2.55569711E-02	-9.31059993E-06	1.51771688E-09	-9.14866981E-14
2.53861457E+04	-7.29344363E+01	-2.10502145E+00	5.40482794E-02	3.51502447E-05
-9.95706637E-08	4.80049399E-11	3.19332187E+04	3.58960228E+01	
C9H7L		200K-6000K REF	: G3B3	R.ROBINSON 19-Jun-07
1.73899530E+01	2.56207079E-02	-9.35120219E-06	1.52234845E-09	-9.16292324E-14
7.18886856E+04	-6.37763834E+01	2.32219368E+00	3.45034586E-02	6.40157037E-05
-1.17798121E-07	5.20469433E-11	7.74618372E+04	2.14806537E+01	
C9H8		200K-6000K REF	: G3B3	R.ROBINSON 09-May-07
1.74713086E+01	2.86713708E-02	-1.04526480E-05	1.70450761E-09	-1.02766685E-13
1.07722661E+04	-7.22017233E+01	-9.86208045E-01	4.46571876E-02	6.38460940E-05
-1.28213551E-07	5.79882498E-11	1.73319384E+04	3.09463621E+01	
C9H8(S)		200K-6000K REF	: G3B3	R.ROBINSON 30-May-07
1.79363817E+01	2.74951917E-02	-1.00445999E-05	1.63921965E-09	-9.88557024E-14
2.59928036E+04	-6.91184788E+01	2.41274408E+00	3.68385244E-02	6.56609310E-05
-1.22373357E-07	5.43884946E-11	3.17152719E+04	1.86346007E+01	
C9H8(T)		200K-6000K REF	: G3B3	R.ROBINSON 19-Jun-07
1.84716616E+01	2.68726914E-02	-9.78675620E-06	1.59388623E-09	-9.59868825E-14

2.83514107E+04	-7.12401639E+01	2.22172745E+00	4.86449880E-02	2.80106646E-05
-7.97385688E-08	3.79166848E-11	3.38466357E+04	1.79470475E+01	
C9H9(N)		200K-6000K REF	: G3B3	R.ROBINSON 19-Jun-07
1.81928310E+01	2.95786006E-02	-1.08194577E-05	1.76277892E-09	-1.06103115E-13
3.87738812E+04	-6.76043726E+01	4.02079723E+00	2.91381348E-02	8.79576149E-05
-1.44921842E-07	6.24139447E-11	4.44076026E+04	1.46093595E+01	
C9H9(I)		200K-6000K REF	: G3B3	R.ROBINSON 18-May-07
1.81016326E+01	2.95750815E-02	-1.07844213E-05	1.75590613E-09	-1.05736838E-13
3.53174008E+04	-6.61691485E+01	5.29905239E+00	1.92041567E-02	1.11981782E-04
-1.69167614E-07	7.12250848E-11	4.08480913E+04	1.03975671E+01	
C9H9(S)		200K-6000K REF	: G3B3	R.ROBINSON 30-May-07
1.80310429E+01	3.08549384E-02	-1.12389309E-05	1.83155488E-09	-1.10374070E-13
1.68565437E+04	-7.37394814E+01	-1.67306559E-01	4.22231459E-02	7.63992304E-05
-1.42403222E-07	6.33163838E-11	2.35314116E+04	2.90045443E+01	
C9H9(P)		200K-6000K REF	: G3B3	R.ROBINSON 30-May-07
1.85560305E+01	2.91794143E-02	-1.06454331E-05	1.73195284E-09	-1.04178066E-13
3.71145562E+04	-7.03815823E+01	2.09658023E+00	4.39112247E-02	5.28195952E-05
-1.09993507E-07	4.98838938E-11	4.29868426E+04	2.15967500E+01	
C9H9(C)		200K-6000K REF	: G3B3	R.ROBINSON 16-May-07
1.84920702E+01	3.04579694E-02	-1.10995700E-05	1.80942158E-09	-1.09064739E-13
2.88684041E+04	-7.67019087E+01	-9.78555510E-01	4.85483215E-02	6.35762462E-05
-1.31511465E-07	5.99162791E-11	3.57270679E+04	3.18021083E+01	
C9H9(F)		200K-6000K REF	: G3B3	R.ROBINSON 30-May-07
1.84884580E+01	2.92919169E-02	-1.06058128E-05	1.71829897E-09	-1.03102152E-13
3.69222518E+04	-7.09394144E+01	3.39687672E+00	3.85992795E-02	6.12333521E-05
-1.15853351E-07	5.14136016E-11	4.25033352E+04	1.43939647E+01	
C9H6O		200K-6000K REF	: G3MP2B3	R.ROBINSON 23-May-07
1.89691541E+01	2.47818525E-02	-9.08390735E-06	1.48682032E-09	-8.98777623E-14
-2.14760016E+03	-7.74939321E+01	-9.70808676E-01	5.55808772E-02	2.49057709E-05
-8.50465645E-08	4.15947668E-11	4.35937475E+03	3.08758874E+01	
C9H7O		200K-6000K REF	: CBS-QB3	R.ROBINSON 30-Apr-08
1.98149165E+01	2.66922030E-02	-9.76836131E-06	1.59708554E-09	-9.64679926E-14
2.76549520E+04	-8.16307465E+01	-4.91651031E-01	5.20289871E-02	4.64077741E-05
-1.12441821E-07	5.27360863E-11	3.45109648E+04	3.00220310E+01	
C10H6		200K-6000K REF	: G3B3	R.ROBINSON 23-May-07
2.03945148E+01	2.29843220E-02	-8.31173559E-06	1.34829347E-09	-8.10008039E-14
5.80398517E+04	-8.05122711E+01	-2.34461417E+00	9.28838499E-02	-8.68597641E-05
3.69340876E-08	-4.27916532E-12	6.39550773E+04	3.51261635E+01	
C10H7		200K-6000K REF	: G3B3	R.ROBINSON 09-May-07
1.91497125E+01	2.73037655E-02	-9.99294685E-06	1.63389295E-09	-9.86950716E-14
3.92300112E+04	-7.95973962E+01	-1.74709178E+00	5.65867963E-02	3.58370225E-05
-1.00865176E-07	4.81841784E-11	4.61768363E+04	3.46502365E+01	
C10H7L		200K-6000K REF	: G3B3	R.ROBINSON 16-Oct-07
2.24638279E+01	2.33461601E-02	-8.44005656E-06	1.36505447E-09	-8.17822119E-14
6.86149398E+04	-9.15971151E+01	-1.60155935E+00	8.17909513E-02	-3.34045862E-05
-3.29260130E-08	2.47944110E-11	7.53769696E+04	3.38894723E+01	
C10H7M		200K-6000K REF	: G3B3	R.ROBINSON 19-Jun-07
2.01585376E+01	2.61331590E-02	-9.50512984E-06	1.54759668E-09	-9.32061993E-14
6.74419179E+04	-7.77106181E+01	8.40106188E-01	6.12918902E-02	5.53646468E-06
-6.20566266E-08	3.26291228E-11	7.35237090E+04	2.60776758E+01	
C10H8L				
0.20179207E+02	0.29670304E-01	-0.11986855E-04	0.22532105E-08	-0.15916158E-12
0.36023766E+05	-0.80279839E+02	-0.27711501E+01	0.98102115E-01	-0.93714450E-04
0.50875709E-07	-0.12535519E-10	0.42320391E+05	0.37574230E+02	
C10H8		200K-6000K REF	: G3B3	R.ROBINSON 09-May-07
1.90700871E+01	2.99951680E-02	-1.09479895E-05	1.78674993E-09	-1.07789182E-13
8.47476587E+03	-8.21752689E+01	-1.70336697E+00	5.33574054E-02	5.41019138E-05
-1.22619765E-07	5.66600389E-11	1.56318632E+04	3.27123601E+01	
C10H8K		200K-6000K REF	: G3MP2B3	R.ROBINSON 01-Nov-07
2.03900746E+01	2.85301415E-02	-1.03537922E-05	1.68348737E-09	-1.01302082E-13
3.38045415E+04	-8.51027336E+01	-1.05459566E+00	5.65513917E-02	4.74179342E-05
-1.19663649E-07	5.68975279E-11	4.09183627E+04	3.23240253E+01	
C10H8G		200K-6000K REF	: G3B3	R.ROBINSON 29-Oct-07
1.94150861E+01	2.90026607E-02	-1.05308167E-05	1.70876070E-09	-1.02612470E-13
3.61820040E+04	-7.49948493E+01	2.06153655E+00	4.84901972E-02	4.32807233E-05
-1.01207981E-07	4.68686020E-11	4.21895477E+04	2.10486943E+01	
C9H6CH2				
0.19196302E+02	0.31294353E-01	-0.11452624E-04	0.20944079E-08	-0.15138942E-12

0.22725338E+05	-0.82727289E+02	-0.67796676E+01	0.99132130E-01	-0.77043901E-04
0.31111080E-07	-0.54388908E-11	0.30449510E+05	0.53315855E+02	
C10H8J		200K-6000K REF	: G3B3	R.ROBINSON 19-Oct-07
2.01059079E+01	2.83480509E-02	-1.03369605E-05	1.68270688E-09	-1.01253068E-13
3.68183988E+04	-7.84540589E+01	3.54764062E+00	4.32006001E-02	5.50173036E-05
-1.13961268E-07	5.18941762E-11	4.26775448E+04	1.39458527E+01	
C10H9A		200K-6000K REF	: G3B3	R.ROBINSON 19-Oct-07
2.28669724E+01	2.83091966E-02	-1.04039005E-05	1.70107940E-09	-1.02684204E-13
4.68026622E+04	-9.45859608E+01	6.45528245E-01	5.79537252E-02	4.65853370E-05
-1.19991015E-07	5.71770878E-11	5.41724986E+04	2.70192785E+01	
C10H9D		200K-6000K REF	: G3B3	R.ROBINSON 19-Oct-07
2.16097416E+01	2.84473467E-02	-1.03397395E-05	1.68222254E-09	-1.01248424E-13
4.26242097E+04	-8.40595232E+01	1.11809534E-01	7.88412797E-02	-3.41993081E-05
-2.00348144E-08	1.65793561E-11	4.89715031E+04	2.90476430E+01	
C10H9		200K-6000K REF	: G3B3	R.ROBINSON 19-Oct-07
1.98957312E+01	3.19619669E-02	-1.16609266E-05	1.90243854E-09	-1.14736441E-13
2.02993377E+04	-8.38097392E+01	-1.04738447E+00	5.38670055E-02	5.90433326E-05
-1.29056526E-07	5.91780458E-11	2.76030323E+04	3.24328027E+01	
C10H9F		200K-6000K REF	: G3B3	R.ROBINSON 26-Oct-07
2.10483105E+01	3.06628768E-02	-1.11305804E-05	1.80996266E-09	-1.08915680E-13
3.35684775E+04	-8.83295990E+01	-5.93555383E-01	5.44304345E-02	6.23536974E-05
-1.38057443E-07	6.41485208E-11	4.09471695E+04	3.12155273E+01	
C10H9P		200K-6000K REF	: G3B3	R.ROBINSON 16-Oct-07
2.11712464E+01	2.95760474E-02	-1.07264003E-05	1.73492056E-09	-1.03868341E-13
4.89011343E+04	-8.34394739E+01	5.25278518E+00	3.73495403E-02	7.47364782E-05
-1.35966596E-07	6.02797378E-11	5.47938808E+04	6.82103263E+00	
C9H6CH3		200K-6000K REF	: G3	R.ROBINSON 09-May-08
1.95402271E+01	3.19082520E-02	-1.16574967E-05	1.90347271E-09	-1.14860486E-13
1.94504304E+04	-8.02533927E+01	4.69536362E-01	4.85000051E-02	6.23857388E-05
-1.26955691E-07	5.71800051E-11	2.62999839E+04	2.64982394E+01	
C10H9T		200K-6000K REF	: G3B3	R.ROBINSON 19-Oct-07
1.98990021E+01	3.19590476E-02	-1.16598773E-05	1.90226923E-09	-1.14726315E-13
2.02955018E+04	-8.38426896E+01	-1.06814137E+00	5.40198750E-02	5.86876924E-05
-1.28708105E-07	5.90543947E-11	2.76018112E+04	3.25031057E+01	
C10H9B		200K-6000K REF	: G3B3	R.ROBINSON 19-Oct-07
2.16506089E+01	2.94452290E-02	-1.07362554E-05	1.75062691E-09	-1.05534492E-13
4.11748845E+04	-8.77141335E+01	7.41778612E-01	5.93020333E-02	3.35408171E-05
-9.94256386E-08	4.78456845E-11	4.81001111E+04	2.64612257E+01	
C10H9L		200K-6000K REF	: G3	R.ROBINSON 09-May-08
2.46488052E+01	2.69281063E-02	-9.97295235E-06	1.63836311E-09	-9.91943546E-14
4.59391590E+04	-1.05186933E+02	2.05861761E+00	5.43928401E-02	5.51868671E-05
-1.28249685E-07	5.97544880E-11	5.35783154E+04	1.91485057E+01	
C10H9E		200K-6000K REF	: G3B3	R.ROBINSON 29-Oct-07
2.11567465E+01	3.01287315E-02	-1.10361445E-05	1.79894691E-09	-1.08280140E-13
3.89281463E+04	-8.49248325E+01	1.65289299E-02	7.22740207E-02	-8.70756093E-06
-4.98720547E-08	2.82290663E-11	4.54698059E+04	2.79363669E+01	
C10H10K		200K-6000K REF	: G3B3	R.ROBINSON 02-May-08
2.09911209E+01	3.33899968E-02	-1.21115160E-05	1.96841287E-09	-1.18403555E-13
2.64315799E+04	-8.95090652E+01	-2.05618726E-01	4.59091076E-02	9.74273950E-05
-1.79429042E-07	8.04177688E-11	3.40979229E+04	2.99560338E+01	
EC10H9		200K-6000K REF	: G3B3	R.ROBINSON 29-Oct-07
2.11567465E+01	3.01287315E-02	-1.10361445E-05	1.79894691E-09	-1.08280140E-13
3.89281463E+04	-8.49248325E+01	1.65289299E-02	7.22740207E-02	-8.70756093E-06
-4.98720547E-08	2.82290663E-11	4.54698059E+04	2.79363669E+01	
GC10H9				
0.19929077E+02	0.32680734E-01	-0.12861148E-04	0.23499754E-08	-0.16510897E-12
0.18696181E+05	-0.15099373E+02	-0.11953660E+01	0.87286167E-01	-0.65343927E-04
0.25376810E-07	-0.41583087E-11	0.25054098E+05	0.24035862E+02	
C10H9K		200K-6000K REF	: G3B3	R.ROBINSON 30-Oct-07
2.15323912E+01	2.96025034E-02	-1.07916786E-05	1.75863733E-09	-1.05953365E-13
4.53865005E+04	-8.84454524E+01	-8.97421771E-01	6.11060586E-02	4.28921687E-05
-1.18183167E-07	5.70782617E-11	5.27185282E+04	3.38332754E+01	
C10H9M		200K-6000K REF	: G3	R.ROBINSON 05-Feb-08
2.19149977E+01	2.94389622E-02	-1.07769075E-05	1.76113517E-09	-1.06308668E-13
4.69078750E+04	-8.78033814E+01	1.19474282E+00	5.85700725E-02	3.53025398E-05
-1.01796708E-07	4.89612314E-11	5.37787117E+04	2.54086306E+01	
C9H7CH3		200K-6000K REF	: G3	R.ROBINSON 30-Apr-08
2.01180990E+01	3.40764215E-02	-1.24393729E-05	2.03000712E-09	-1.22447963E-13

6.14160687E+03	-8.58609871E+01	1.59612349E-01	4.73821231E-02	7.98260414E-05
-1.50801211E-07	6.70961412E-11	1.34561914E+04	2.67080379E+01	
GC10H10				
0.18912177E+02	0.34327266E-01	-0.13514685E-04	0.24029682E-08	-0.16235052E-12
0.70698054E+04	-0.15099373E+02	-0.11953660E+01	0.87286167E-01	-0.65343927E-04
0.25376810E-07	-0.41583087E-11	0.13030043E+05	0.24035862E+02	
EC10H10				
0.18912177E+02	0.34327266E-01	-0.13514685E-04	0.24029682E-08	-0.16235052E-12
0.66488284E+04	-0.15099373E+02	-0.11953660E+01	0.87286167E-01	-0.65343927E-04
0.25376810E-07	-0.41583087E-11	0.12609066E+05	0.24035862E+02	
C10H10				
2.07237519E+01	3.20420615E-02	-1.16635294E-05	1.89942575E-09	-1.14395965E-13
2.34021253E+04	-8.08334078E+01	3.02911361E+00	4.54157069E-02	6.41302895E-05
-1.26124981E-07	5.64371843E-11	2.98411201E+04	1.86631755E+01	
200K-6000K REF : G3B3 R.ROBINSON 30-Apr-08				
C10H10F				
2.07741646E+01	3.25954531E-02	-1.18965594E-05	1.94064254E-09	-1.17010422E-13
2.10532336E+04	-8.32029885E+01	4.16133760E+00	3.98020647E-02	7.53399313E-05
-1.34798392E-07	5.87917489E-11	2.73869314E+04	1.15819865E+01	
200K-6000K REF : G3B3 R.ROBINSON 01-Nov-07				
C10H70O				
2.38458193E+01	2.82830183E-02	-1.04366366E-05	1.71179015E-09	-1.03540228E-13
1.58145756E+04	-1.01211526E+02	-5.92153711E-01	6.74448059E-02	2.74306631E-05
-1.00787983E-07	4.98051184E-11	2.36924331E+04	3.11940000E+01	
200K-6000K REF : G3B3 R.ROBINSON 05-Feb-08				
C10H7O				
2.13897470E+01	2.80525216E-02	-1.02801736E-05	1.68233474E-09	-1.01684503E-13
4.91393515E+03	-9.02166334E+01	-1.45929061E+00	6.44203495E-02	2.48698363E-05
-9.28973133E-08	4.58091634E-11	1.23251313E+04	3.37249315E+01	
200K-6000K REF : G3 R.ROBINSON 09-May-08				
C10H7OH				
2.21393483E+01	2.93982444E-02	-1.07158216E-05	1.74762148E-09	-1.05386549E-13
-1.38716461E+04	-9.47546215E+01	-1.93343217E+00	6.96713698E-02	2.09740134E-05
-9.29937128E-08	4.67457679E-11	-6.18360395E+03	3.52838683E+01	
200K-6000K REF : G3B3 R.ROBINSON 23-May-07				
C10H6O2				
2.25799298E+01	2.71712679E-02	-1.00063568E-05	1.64285532E-09	-9.95210613E-14
-2.26918741E+04	-9.49418759E+01	-3.40769476E-01	6.68991807E-02	1.20446767E-05
-7.58721745E-08	3.85572616E-11	-1.53380749E+04	2.88094233E+01	
C11H9				
0.23571720E+02	0.29080150E-01	-0.94253200E-05	0.14375044E-08	-0.86432991E-13
0.21835987E+05	-0.10355592E+03	-0.55627434E+01	0.10663281E+00	-0.86584861E-04
0.36316999E-07	-0.62652074E-11	0.30429877E+05	0.48643127E+02	
C11H9P				
0.23571720E+02	0.29080150E-01	-0.94253200E-05	0.14375044E-08	-0.86432991E-13
0.31963483E+05	-0.10355592E+03	-0.55627434E+01	0.10663281E+00	-0.86584861E-04
0.36316999E-07	-0.62652074E-11	0.40557373E+05	0.48643127E+02	
C11H10				
0.20618816E+02	0.35127148E-01	-0.11830690E-04	0.18073995E-08	-0.10553787E-12
0.37591297E+04	-0.87356517E+02	-0.58980299E+01	0.10341065E+00	-0.76758084E-04
0.29731117E-07	-0.48860931E-11	0.11751871E+05	0.51882836E+02	
C11H7O				
0.27231269E+02	0.26040644E-01	-0.10377854E-04	0.18715858E-08	-0.12636018E-12
0.81121090E+04	-0.12050997E+03	-0.31465258E+01	0.10679716E+00	-0.10968916E-03
0.69037351E-07	-0.18363943E-10	0.18071491E+05	0.40402345E+02	
C11H8O				
0.21204625E+02	0.40753532E-01	-0.17960043E-04	0.35348363E-08	-0.25728495E-12
-0.64059942E+04	-0.87076491E+02	-0.44640862E+01	0.10410496E+00	-0.54663804E-04
-0.13750550E-07	0.16040985E-10	0.88328263E+03	0.46924361E+02	
C11H9O				
0.23571720E+02	0.29080150E-01	-0.94253200E-05	0.14375044E-08	-0.86432991E-13
0.11781769E+05	-0.10355592E+03	-0.55627434E+01	0.10663281E+00	-0.86584861E-04
0.36316999E-07	-0.62652074E-11	0.20375631E+05	0.48643127E+02	
AC11H9O				
0.23571720E+02	0.29080150E-01	-0.94253200E-05	0.14375044E-08	-0.86432991E-13
0.76891553E+04	-0.10355592E+03	-0.55627434E+01	0.10663281E+00	-0.86584861E-04
0.36316999E-07	-0.62652074E-11	0.16283017E+05	0.48643127E+02	
BC11H9O				
0.23571720E+02	0.29080150E-01	-0.94253200E-05	0.14375044E-08	-0.86432991E-13
0.11334813E+05	-0.10355592E+03	-0.55627434E+01	0.10663281E+00	-0.86584861E-04
0.36316999E-07	-0.62652074E-11	0.19928675E+05	0.48643127E+02	
EC11H9O				

0.23571720E+02	0.29080150E-01	-0.94253200E-05	0.14375044E-08	-0.86432991E-13
-0.12317013E+04	-0.10355592E+03	-0.55627434E+01	0.10663281E+00	-0.86584861E-04
0.36316999E-07	-0.62652074E-11	0.73621602E+04	0.48643127E+02	
OOC11H9P				
0.72920350E 01	0.92502000E-01	-0.51686410E-04	0.13627090E-07	-0.13811480E-11
2.73164660E 04	-1.27437380E 01	-0.13889580E 02	0.17209840E 00	-0.17006600E-03
0.96018880E-07	-0.23732530E-10	0.31998940E 05	0.90588360E 02	
C11H9O0				
0.21204625E+02	0.40753532E-01	-0.17960043E-04	0.35348363E-08	-0.25728495E-12
0.20586909E+05	-0.87076491E+02	-0.44640862E+01	0.10410496E+00	-0.54663804E-04
-0.13750550E-07	0.16040985E-10	0.27876186E+05	0.46924361E+02	
C11H100				
0.22727753E+02	0.43812073E-01	-0.17862083E-04	0.32897970E-08	-0.22638566E-12
-0.14723957E+05	-0.93448156E+02	-0.49985988E+01	0.11278945E+00	-0.72481576E-04
0.11138080E-07	0.52180972E-11	-0.63307633E+04	0.52433847E+02	
OC11H9				
0.23571720E+02	0.29080150E-01	-0.94253200E-05	0.14375044E-08	-0.86432991E-13
-0.72797280E+03	-0.10355592E+03	-0.55627434E+01	0.10663281E+00	-0.86584861E-04
0.36316999E-07	-0.62652074E-11	0.78658888E+04	0.48643127E+02	
HOC11H9				
0.23571720E+02	0.29080150E-01	-0.94253200E-05	0.14375044E-08	-0.86432991E-13
-0.18046832E+05	-0.10355592E+03	-0.55627434E+01	0.10663281E+00	-0.86584861E-04
0.36316999E-07	-0.62652074E-11	-0.94529708E+04	0.48643127E+02	
AC11H100				
0.22727753E+02	0.43812073E-01	-0.17862083E-04	0.32897970E-08	-0.22638566E-12
-0.11238992E+05	-0.93448156E+02	-0.49985988E+01	0.11278945E+00	-0.72481576E-04
0.11138080E-07	0.52180972E-11	-0.28457983E+04	0.52433847E+02	
AC12H8				
1.93183637E+01	3.90205238E-02	-1.63352587E-05	3.10041991E-09	-2.19199281E-13
2.15445149E+04	-8.32372261E+01	-2.81264181E+00	7.04681002E-02	3.15341955E-05
-1.05176189E-07	5.08713845E-11	2.88462829E+04	3.75755975E+01	3.12345526E+04
4C12H9				
0.27231269E+02	0.26040644E-01	-0.10377854E-04	0.18715858E-08	-0.12636018E-12
4.31301090E+04	-0.11857997E+03	-0.31465258E+01	0.10679716E+00	-0.10968916E-03
0.69037351E-07	-0.18363943E-10	0.53089491E+05	0.42322345E+02	
C12H10				
0.24289017E 02	0.34006648E-01	-0.11722408E-04	0.17729298E-08	-0.96812532E-13
0.10287000E 05	-0.10802374E 03	-0.40739527E 01	0.86973310E-01	-0.42353613E-05
-0.64564460E-07	0.34150169E-10	0.19405965E 05	0.44741348E 02	
1C12H10				
2.35491970E+01	3.62502472E-02	-1.32050239E-05	2.14808308E-09	-1.29217696E-13
1.53538069E+04	-1.00965903E+02	1.35063575E+00	6.20091845E-02	5.01436081E-05
-1.20331553E-07	5.54414104E-11	2.30624723E+04	2.18769600E+01	
C12H11				
2.35238553E+01	3.63051378E-02	-1.32336643E-05	2.15367986E-09	-1.29592424E-13
1.49809324E+04	-1.01219624E+02	4.09837637E-01	6.49785912E-02	4.77231657E-05
-1.20899622E-07	5.64074436E-11	2.28951982E+04	2.61779929E+01	
C12H12				
2.53697727E+01	4.04594180E-02	-1.49784208E-05	2.46402471E-09	-1.49382751E-13
-8.20299732E+02	-1.14459910E+02	1.98405802E-02	6.20844325E-02	7.79624479E-05
-1.55438421E-07	6.85371120E-11	8.47514808E+03	2.80182938E+01	1.16544980E+04
C14H14				
0.72920350E 01	0.92502000E-01	-0.51686410E-04	0.13627090E-07	-0.13811480E-11
0.10316730E 05	-0.11327380E 02	-0.13889580E 02	0.17209840E 00	-0.17006600E-03
0.96018880E-07	-0.23732530E-10	0.15032340E 05	0.92707360E 02	0.17216410E+05
AC14H10				
0.26567127E+02	0.39790904E-01	-0.14577610E-04	0.23850396E-08	-0.14413090E-12
0.14850923E+05	-0.12283160E+03	-0.15665980E+01	0.69536302E-01	0.78609880E-04
-0.17056214E-06	0.78003880E-10	0.24656643E+05	0.33282196E+02	0.27674511E+05
PC14H10				
0.26602474E+02	0.39769744E-01	-0.14572026E-04	0.23843296E-08	-0.14409548E-12
0.12132838E+05	-0.12266672E+03	-0.33646717E+01	0.85073271E-01	0.37531110E-04
-0.12664499E-06	0.61445705E-10	0.22019878E+05	0.40596218E+02	0.24908263E+05
C7H16				
1.71920296E+01	4.14539747E-02	-1.51651024E-05	2.47160939E-09	-1.48771543E-13
-3.13651815E+04	-5.89840908E+01	1.49411476E+01	-1.83441607E-02	1.92992088E-04
-2.33818731E-07	9.00333961E-11	-2.75648103E+04	-3.14981036E+01	
C7H13				
		200K-6000K REF : G3B3	R.ROBINSON 01-Mar-07	

1.66403664E+01	3.43972231E-02	-1.25294440E-05	2.03134169E-09	-1.21742286E-13
9.46402139E+03	-5.30039257E+01	9.66695103E+00	1.25596990E-02	1.03972230E-04
-1.43656988E-07	5.78758528E-11	1.33448708E+04	-7.18321426E+00	
1C7H14		200K-6000K REF : G3B3	R.ROBINSON 01-Mar-07	
2.04869566E+01	3.76992169E-02	-1.37946056E-05	2.24153654E-09	-1.34500804E-13
-1.68911870E+04	-7.06200500E+01	1.60772494E+01	1.61146132E-03	1.31069585E-04
-1.68141995E-07	6.58823035E-11	-1.33331433E+04	-3.62129019E+01	
2C7H14		200K-6000K REF : G3B3	R.ROBINSON 01-Mar-07	
1.62946407E+01	3.75501193E-02	-1.37047240E-05	2.22982210E-09	-1.34055742E-13
-1.69494880E+04	-5.48434002E+01	1.10167077E+01	2.81865403E-04	1.41659750E-04
-1.82794411E-07	7.20718900E-11	-1.30107170E+04	-1.51754558E+01	
3C7H14		200K-6000K REF : G3B3	R.ROBINSON 01-Mar-07	
1.57526847E+01	3.81420729E-02	-1.39355391E-05	2.26856281E-09	-1.36423158E-13
-1.66980330E+04	-5.14409888E+01	1.00522701E+01	2.98530045E-03	1.37335816E-04
-1.79230419E-07	7.09483902E-11	-1.26852346E+04	-9.81436803E+00	
1C7H15		200K-6000K REF : G3B3	R.ROBINSON 02-Mar-07	
1.87757382E+01	3.72035123E-02	-1.36134958E-05	2.21954080E-09	-1.33647354E-13
-6.95510130E+03	-6.52269276E+01	1.25072516E+01	-1.29516508E-02	1.96884688E-04
-2.52881776E-07	1.00893135E-10	-2.20512181E+03	-1.72426086E+01	
2C7H15		200K-6000K REF : G3B3	R.ROBINSON 02-Mar-07	
1.91986718E+01	3.68720501E-02	-1.35092395E-05	2.20449215E-09	-1.32823611E-13
-8.36338230E+03	-6.62409810E+01	1.54320320E+01	-2.35043255E-02	2.12832009E-04
-2.63880433E-07	1.03753869E-10	-4.11174461E+03	-3.02929014E+01	
3C7H15		200K-6000K REF : G3B3	R.ROBINSON 02-Mar-07	
1.81495153E+01	3.80195319E-02	-1.39431440E-05	2.27524196E-09	-1.37046980E-13
-7.95284499E+03	-5.97896206E+01	1.43358024E+01	-1.98137038E-02	2.03162883E-04
-2.52433995E-07	9.91131117E-11	-3.76391235E+03	-2.40746635E+01	
4C7H15		200K-6000K REF : G3B3	R.ROBINSON 02-Mar-07	
1.89373102E+01	3.72576526E-02	-1.36618760E-05	2.22933930E-09	-1.34285083E-13
-8.11716615E+03	-6.42462492E+01	1.55726284E+01	-2.23878814E-02	2.07190459E-04
-2.56411153E-07	1.00664088E-10	-4.04671392E+03	-3.07705801E+01	
C5H9				
0.37042289E+01	0.39042108E-01	-0.18223191E-04	0.38031742E-08	-0.29095449E-12
0.17857311E+05	0.11002142E+02	0.37042289E+01	0.39042108E-01	-0.18223191E-04
0.38031742E-08	-0.29095449E-12	0.17857311E+05	0.11002142E+02	
1C5H11		200K-6000K REF : G3B3	R.ROBINSON 19-Jun-08	
1.21220106E+01	2.84364383E-02	-1.02910526E-05	1.66173552E-09	-9.93163072E-14
1.22077977E+03	-3.36590974E+01	6.93079867E+00	1.07381051E-02	8.20981999E-05
-1.14226471E-07	4.62891827E-11	4.15909261E+03	7.36508569E-01	
1C5H10				
-0.26194715E+00	0.52521653E-01	-0.27921931E-04	0.52903104E-08	0.22517016E-12
-0.46336323E+04	0.28551981E+02	-0.26194715E+00	0.52521653E-01	-0.27921931E-04
0.52903104E-08	0.22517016E-12	-0.46336323E+04	0.28551981E+02	
C6H11		200K-6000K REF : G3B3	R.ROBINSON 12-May-08	
1.40490015E+01	2.93908111E-02	-1.06889547E-05	1.73012907E-09	-1.03556777E-13
1.27697251E+04	-4.32903166E+01	7.39110577E+00	1.01303849E-02	9.86631131E-05
-1.38582018E-07	5.67748444E-11	1.63095012E+04	-1.63694229E-01	
C6H12		200K-6000K REF : G3B3	R.ROBINSON 12-May-08	
1.37740168E+01	3.23524115E-02	-1.17758412E-05	1.90845558E-09	-1.14354808E-13
-1.19910313E+04	-4.51639875E+01	9.47768743E+00	-1.45943889E-03	1.27633398E-04
-1.64725402E-07	6.52184443E-11	-8.66661827E+03	-1.21673450E+01	
C6H13		200K-6000K REF : G3B3	R.ROBINSON 12-May-08	
1.45710701E+01	3.39665373E-02	-1.23992076E-05	2.01336857E-09	-1.20773917E-13
-2.44926920E+03	-4.61250074E+01	9.96221886E+00	1.76854348E-03	1.23676086E-04
-1.61529444E-07	6.41535906E-11	9.30978164E+02	-1.16821636E+01	
2C6H13		200K-6000K REF : G3B3	R.ROBINSON 04-Jun-08	
1.43598724E+01	3.35491015E-02	-1.21943169E-05	1.97936223E-09	-1.18824899E-13
-3.55655231E+03	-4.31834609E+01	1.06700712E+01	-7.08820296E-03	1.44732473E-04
-1.82081962E-07	7.13428152E-11	-1.34025754E+02	-1.20329429E+01	
C8H16		200K-6000K REF : G3B3	R.ROBINSON 19-Jun-08	
1.98020647E+01	4.13898968E-02	-1.51156295E-05	2.46028532E-09	-1.47971777E-13
-1.98180374E+04	-7.40219156E+01	1.46318153E+01	-7.23507470E-03	1.74473079E-04
-2.18240351E-07	8.47591774E-11	-1.53378090E+04	-3.21363886E+01	
C8H17		200K-6000K REF : G3B3	R.ROBINSON 04-Jun-08	
1.99038919E+01	4.45230697E-02	-1.64031177E-05	2.67992936E-09	-1.61438565E-13
-1.00772766E+04	-6.81527405E+01	1.54466788E+01	-8.75522049E-03	1.86131548E-04
-2.33509059E-07	9.12283870E-11	-5.72319179E+03	-2.94702395E+01	
1C10H21		200K-6000K REF : G3MP2B3	R.ROBINSON 19-Jun-08	



2.69792643E+01	5.09002132E-02	-1.85904821E-05	3.03114872E-09	-1.82621083E-13
-1.83058146E+04	-1.03958658E+02	2.15565615E+01	-1.97079655E-02	2.43572172E-04
-2.98314579E-07	1.15031334E-10	-1.26729329E+04	-5.53280156E+01	
2C10H21				
0.13470533E+02	0.80290854E-01	-0.39518403E-04	0.97089403E-08	-0.96419151E-12
-0.15685746E+05	-0.33952385E+02	0.29079616E+00	0.10640167E+00	-0.45561803E-04
-0.35957344E-08	0.54528122E-11	-0.11504166E+05	0.36831581E+02	
3C10H21				
0.13470533E+02	0.80290854E-01	-0.39518403E-04	0.97089403E-08	-0.96419151E-12
-0.15685746E+05	-0.33952385E+02	0.29079616E+00	0.10640167E+00	-0.45561803E-04
-0.35957344E-08	0.54528122E-11	-0.11504166E+05	0.36831581E+02	
4C10H21				
0.13470533E+02	0.80290854E-01	-0.39518403E-04	0.97089403E-08	-0.96419151E-12
-0.15685746E+05	-0.33952385E+02	0.29079616E+00	0.10640167E+00	-0.45561803E-04
-0.35957344E-08	0.54528122E-11	-0.11504166E+05	0.36831581E+02	
5C10H21		200K-6000K REF : G3MP2B3 R.ROBINSON 19-Jun-08		
2.53320576E+01	5.19816695E-02	-1.88999290E-05	3.07318111E-09	-1.84823104E-13
-1.90309455E+04	-9.44791611E+01	2.00541677E+01	-1.82264070E-02	2.42000562E-04
-2.97642453E-07	1.15116287E-10	-1.34971611E+04	-4.68496909E+01	
C10H22		200K-6000K REF : G3MP2B3 R.ROBINSON 19-Jun-08		
2.44359479E+01	5.37798374E-02	-1.92747269E-05	3.10516936E-09	-1.85568963E-13
-4.21122175E+04	-8.75997433E+01	2.21829472E+01	-2.08434192E-02	2.38368120E-04
-2.89524082E-07	1.11677093E-10	-3.76437569E+04	-5.66573146E+01	
1C9H11		200K-6000K REF : G3 R.ROBINSON 01-May-08		
2.01253464E+01	3.39544364E-02	-1.24488961E-05	2.03581310E-09	-1.22932424E-13
9.80808429E+03	-8.18509643E+01	1.91621566E+00	4.66715275E-02	6.75582623E-05
-1.30639887E-07	5.80376488E-11	1.65264254E+04	2.08976724E+01	
2C9H11		200K-6000K REF : G3 R.ROBINSON 22-Apr-08		
1.83794491E+01	3.45999957E-02	-1.27298452E-05	2.08359251E-09	-1.25822741E-13
1.74790161E+04	-6.69259597E+01	5.36291665E+00	1.81280438E-02	1.30279878E-04
-1.91020800E-07	7.94573309E-11	2.34210842E+04	1.24284940E+01	
3C9H11		200K-6000K REF : G3B3 R.ROBINSON 20-Jun-07		
1.89656331E+01	3.37869607E-02	-1.23636786E-05	2.01605387E-09	-1.21416680E-13
1.66970707E+04	-7.11059151E+01	3.88078214E+00	3.30048899E-02	9.39094121E-05
-1.55591844E-07	6.70803124E-11	2.27102222E+04	1.64776031E+01	
1C9H10		200K-6000K REF : G3B3 R.ROBINSON 22-Apr-08		
1.81249058E+01	3.24696892E-02	-1.18413013E-05	1.92769396E-09	-1.15997421E-13
5.25365017E+03	-7.09920747E+01	3.08905449E+00	3.38417912E-02	8.53571547E-05
-1.43596366E-07	6.18733556E-11	1.11871094E+04	1.59112579E+01	
C9H9 (T)		200K-6000K REF : G3B3 R.ROBINSON 12-May-08		
1.81120956E+01	3.01382784E-02	-1.09325842E-05	1.77664313E-09	-1.06854228E-13
3.21311876E+04	-6.88060877E+01	1.96017972E+00	4.28462408E-02	5.64127943E-05
-1.12860281E-07	5.06286454E-11	3.79927940E+04	2.19151760E+01	
2C9H10		200K-6000K REF : G3B3 R.ROBINSON 22-Apr-08		
1.82404720E+01	3.21597958E-02	-1.17387160E-05	1.91040340E-09	-1.14909287E-13
7.33725444E+03	-7.03367784E+01	2.71720641E+00	3.40273426E-02	8.86276170E-05
-1.49886221E-07	6.49711012E-11	1.34032564E+04	1.91708004E+01	
C9H12		200K-6000K REF : G3B3 R.ROBINSON 12-Nov-07		
1.86522630E+01	3.68024836E-02	-1.34769018E-05	2.19971236E-09	-1.32590770E-13
-8.42809806E+03	-7.27057393E+01	4.82394371E+00	2.42161569E-02	1.21943162E-04
-1.84028759E-07	7.70904630E-11	-2.33412955E+03	1.04635945E+01	
N2		REF : BURCAT 20/09/06		
2.95257637E+00	1.39690040E-03	-4.92631603E-07	7.86010195E-11	-4.60755204E-15
-9.23948688E+02	5.87188762E+00	3.53100528E+00	-1.23660988E-04	-5.02999433E-07
2.43530612E-09	-1.40881235E-12	-1.04697628E+03	2.96747038E+00	
AR				
0.25000000E+01	0.00000000E+00	0.00000000E+00	0.00000000E+00	0.00000000E+00
-0.74537502E 03	0.43660006E 01	0.25000000E+01	0.00000000E+00	0.00000000E+00
0.00000000E+00	0.00000000E+00	-0.74537502E 03	0.43660006E 01	

